



**HAL**  
open science

# Functional study of key fish interferon-stimulated genes using an in vitro knock-out approach in fish cell lines : from comparative immunology to interest for vaccine production

Lise Chaumont

## ► To cite this version:

Lise Chaumont. Functional study of key fish interferon-stimulated genes using an in vitro knock-out approach in fish cell lines: from comparative immunology to interest for vaccine production. Biotechnology. Université Paris-Saclay, 2024. English. NNT : 2024UPASL038 . tel-04702655

**HAL Id: tel-04702655**

**<https://theses.hal.science/tel-04702655v1>**

Submitted on 19 Sep 2024

**HAL** is a multi-disciplinary open access archive for the deposit and dissemination of scientific research documents, whether they are published or not. The documents may come from teaching and research institutions in France or abroad, or from public or private research centers.

L'archive ouverte pluridisciplinaire **HAL**, est destinée au dépôt et à la diffusion de documents scientifiques de niveau recherche, publiés ou non, émanant des établissements d'enseignement et de recherche français ou étrangers, des laboratoires publics ou privés.

Functional study of key fish interferon-stimulated genes using an *in vitro* knock-out approach in fish cell lines: from comparative immunology to interest for vaccine production

*Étude fonctionnelle de gènes stimulés par l'interféron par une approche in vitro d'invalidation génique en lignées cellulaires de poisson : de l'immunologie comparée à l'intérêt pour la production de vaccins*

**Thèse de doctorat de l'université Paris-Saclay**

École doctorale n°577, structure et dynamique des systèmes vivants (SDSV)  
Spécialité de doctorat : Biotechnologies  
Graduate School : Life Sciences and Health  
Réfèrent : Université de Versailles-Saint-Quentin-en-Yvelines

Thèse préparée dans l'unité de recherche **VIM** (Université Paris-Saclay, UVSQ, INRAE)  
sous la direction de **Bertrand COLLET**, directeur de recherche  
et la co-direction de **Pierre BOUDINOT**, directeur de recherche

**Thèse soutenue à Jouy-en-Josas, le 04 septembre 2024, par**

**Lise CHAUMONT**

**Composition du Jury**

**Karim BENIHOUD**

Professeur des Universités, Université Paris-Saclay, CNRS, Institut Gustave Roussy

Président du Jury

**Stephanie DEWITTE-ORR**

Maîtresse de Conférences, Wilfrid Laurier University

Rapporteuse & Examinatrice

**Georges LUTFALLA**

Directeur de recherche, Université de Montpellier, CNRS

Rapporteur & Examineur

**Øystein EVENSEN**

Professeur des Universités, Norwegian University of Life Sciences

Examineur

**Jean-Pierre LEVRAUD**

Directeur de recherche, Université Paris-Saclay, Institut des Neurosciences Paris-Saclay, CNRS, Institut Pasteur

Examineur

**Title:** Functional study of key fish interferon-stimulated genes using an *in vitro* knock-out approach in fish cell lines: from comparative immunology to interest for vaccine production

**Keywords:** interferon response, PKR, Viperin, cell lines, CRISPR/Cas9, fish viruses

**Abstract:** In jawed vertebrates, innate antiviral defenses are primarily based on type I interferons (IFNs). These master cytokines are secreted following virus recognition and induce the expression of hundreds of IFN-stimulated genes (ISGs). ISGs encode proteins with diverse functions, including enhancers of the type I IFN pathway and antiviral effectors, which all work towards establishing an antiviral state refractory to viral infection. Overall, the type I IFN system is well-conserved between mammals and fish but the ISG repertoire is more diverse in fish, largely due to their complex evolutionary history and physiological specificities. Consequently, most mammalian ISGs have one or more orthologs in fish. However, it is still unclear whether fish ISGs are true functional homologs and their mechanisms of action remain to be explored in detail.

In this context, my thesis aimed to functionally characterize two key fish ISGs, namely dsRNA-dependent protein kinase (*pkcr*) and virus inhibitory protein endoplasmic reticulum-associated, interferon-inducible (*viperin*), by using an *in vitro* knock-out approach. In mammals, both proteins are primarily regarded as antiviral effectors: PKR is involved in host translation inhibition and apoptosis, while Viperin operates by generating antiviral ribonucleotides and modulating metabolic pathways exploited during viral replication cycles. However, the extent to which these functions are conserved in fish remains largely unknown. The objectives of my thesis were articulated along three axes: (1) to develop and validate *pkcr*<sup>-/-</sup> and *viperin*<sup>-/-</sup> fish cell lines using the CRISPR/Cas9 technology; (2) to functionally characterize these cell lines, in order to identify the mechanisms of action of fish PKR and Viperin and their role in regulating the type I IFN response through feedback loops; (3) to assess their permissivity to viral infections and their ability to produce viral particles at higher yields than their wild-type counterparts.

Using complementary overexpression and knockout approaches, I first studied the molecular mechanisms of action of PKR in Chinook salmon (*Oncorhynchus tshawytscha*) CHSE-EC cells. Our findings show that salmonid PKR has conserved molecular functions, including apoptosis activation and inhibition of host protein synthesis. However, endogenous PKR did not play a major antiviral role during viral hemorrhagic septicemia virus (VHSV) infection. In fact, our results suggest that VHSV has evolved strategies to subvert PKR antiviral action, by limiting early induction of *pkcr* expression, evading PKR-mediated translational arrest and taking advantage of PKR-mediated apoptosis at a late infection stage to favor viral spread.

In parallel, we conducted a comparative RNA-seq analysis of the *viperin*<sup>-/-</sup> and wild-type fathead minnow (*Pimephales promelas*) EPC-EC cell lines with or without stimulation with recombinant type I IFN to have a global overview of the regulatory role of fish Viperin. Our data show that cyprinid Viperin is not involved in the regulation of the canonical type I IFN but negatively regulates specific inflammatory pathways. Our analysis further indicates that it plays a regulatory role in other metabolic processes, even in non-induced conditions, including extracellular matrix organization, cell adhesion and one carbon metabolism.

During the development process of initial *pkcr*<sup>-/-</sup> cell lines, two CHSE-EC cell lines were found to be persistently infected with infectious pancreatic necrosis virus (IPNV), presumably due to inadvertent contamination. I set out to characterize these persistently IPNV-infected cell lines over the course of 40 passages. A striking feature in both cell lines was the periodic oscillatory pattern of extracellular titers and intracellular viral RNA levels over passages. We further showed that the type I IFN response was not triggered during persistent infection, suggesting that persistent IPNV is able to evade the host innate immune response.

**Titre :** Étude fonctionnelle de gènes stimulés par l'interféron par une approche in vitro d'inactivation génique en lignées cellulaires de poisson : de l'immunologie comparée à l'intérêt pour la production de vaccins

**Mots clés :** réponse à l'interféron, PKR, Viperin, lignées cellulaires, CRISPR/Cas9, virus de poisson

**Résumé :** Chez les vertébrés à mâchoires, les défenses antivirales innées sont principalement basées sur les interférons (IFN) de type I. Ces cytokines sont sécrétées en cas d'infection virale et induisent l'expression de gènes stimulés par l'IFN (*ISGs*). Les *ISGs* codent des protéines aux fonctions diverses dont l'expression conduit à l'établissement d'un état réfractaire à l'infection. Le système IFN de type I est globalement bien conservé entre les mammifères et les poissons, mais le répertoire des *ISGs* est plus diversifié chez ces derniers, en raison de leur histoire évolutive complexe et de leurs spécificités physiologiques. Par conséquent, la plupart des *ISGs* de mammifères ont un ou plusieurs orthologues chez les poissons. Il reste, cependant, à déterminer si les *ISGs* de poisson ont les mêmes fonctions et mécanismes d'action que leurs homologues mammaliens.

Dans ce contexte, ma thèse avait pour but de caractériser fonctionnellement deux *ISGs* de poisson, *pkcr* et *viperin*, en utilisant une approche in vitro d'inactivation génique. Chez les mammifères, la PKR est principalement impliquée dans l'inhibition de la traduction et l'apoptose, tandis que la Viperin agit en générant des ribonucléotides antiviraux et en modulant certaines voies métaboliques exploitées par les virus. Chez les poissons, ces fonctions restent à explorer en détail. Les objectifs de ma thèse s'articulaient autour de trois axes : (1) développer des lignées cellulaires de poisson *pkcr*<sup>-/-</sup> et *viperin*<sup>-/-</sup> en utilisant la technologie CRISPR/Cas9 ; (2) caractériser fonctionnellement ces lignées, afin d'identifier les mécanismes d'action de la PKR et de la Viperin de poisson et leur rôle dans la régulation de la réponse IFN; (3) évaluer leur perméabilité aux infections virales et leur capacité à produire des virus à plus hauts rendements que ceux obtenus en cellules sauvages.

En utilisant des approches complémentaires de surexpression et d'inactivation génique, j'ai tout d'abord étudié les mécanismes d'action de la PKR en cellules de saumon Chinook (*Oncorhynchus tshawytscha*).

Nos résultats montrent que la PKR de salmonidés a des fonctions moléculaires conservées : elle est impliquée dans l'activation de l'apoptose et l'inhibition de la synthèse des protéines de l'hôte. Cependant, la PKR n'a pas de rôle majeur lors de l'infection par le virus de la septicémie hémorragique virale (VSHV) : nos résultats suggèrent que le VSHV a développé des stratégies pour échapper aux effets antiviraux de la PKR, en limitant l'expression précoce de *pkcr*, en évitant l'inhibition de la traduction et en tirant partie de l'apoptose médiée par la PKR à un stade d'infection tardif pour favoriser la propagation du virus.

En parallèle, nous avons mené une analyse transcriptomique comparative des lignées cellulaires du poisson tête-de-boule (*Pimephales promelas*), sauvages ou *viperin*<sup>-/-</sup>, stimulées ou non par l'IFN de type I, dans le but d'avoir une vue d'ensemble du rôle régulateur de la Viperin chez les cyprinidés. Nos données montrent que la Viperin n'est pas impliquée dans la régulation de la réponse IFN de type I mais qu'elle régule négativement certaines voies inflammatoires. Notre analyse indique aussi que la Viperin a une fonction régulatrice dans d'autres processus métaboliques tels que l'organisation de la matrice extracellulaire, l'adhésion cellulaire et le métabolisme un-carbone.

Au cours du processus de développement de lignées cellulaires *pkcr*<sup>-/-</sup> initiales, deux lignées se sont révélées être infectées de façon persistante par le virus de la nécrose pancréatique infectieuse (IPNV). J'ai entrepris de caractériser ces lignées cellulaires infectées au cours de 40 passages. Nous avons ainsi observé la présence d'oscillations périodiques des titres viraux extracellulaires et des niveaux intracellulaires d'ARN viral au cours des passages. De plus, la réponse IFN de type I n'était pas déclenchée par l'infection, ce qui suggère que l'IPNV persistant est capable d'échapper à la réponse innée de l'hôte.

## FUNDING

---



This PhD project was funded by VIRBAC S.A., France, and the French Association for Research and Technology (ANRT) [Convention CIFRE #2020/0646] in collaboration with the Fish Infection and Immunity laboratory (Université Paris-Saclay, UVSQ, INRAE, VIM). This project was carried out under the supervision of **Dr. Bertrand COLLET** (main supervisor, INRAE) and **Dr. Pierre BOUDINOT** (co-supervisor, INRAE) and under the responsibility of **Dr. Jules MINKE** (Virbac).

## ACKNOWLEDGMENTS / REMERCIEMENTS

---

After almost 4 years of work on my thesis, it is time for me to thank all the great people I have worked with and with whom I have spent all these years.

Je voudrais tout d'abord remercier **Bertrand Collet**, mon directeur de thèse, pour m'avoir fait confiance alors que je n'avais presque aucune expérience de laboratoire et pour m'avoir donné une grande liberté durant toute la durée de la thèse. Un immense merci pour ta bienveillance dans ton encadrement, ton optimisme à toute épreuve ainsi que pour tous nos échanges qui m'ont aidée à progresser en tant que scientifique. Je remercie également **Pierre Boudinot**, mon co-directeur de thèse et directeur d'équipe, pour m'avoir poussée à être toujours plus rigoureuse ; j'ai énormément appris à vos côtés, et je vous remercie pour votre disponibilité malgré votre emploi du temps très chargé, vos conseils toujours avisés et vos connaissances sans fin en immunologie et sur bien d'autres sujets.

Je voudrais également remercier l'équipe encadrante de Virbac avec qui j'ai eu des réunions régulières tout au long de cette thèse : **Jules Minke, Jérôme Le Hir** et **Claudine Raffy**. Un très grand merci à tous les trois pour votre confiance, nos échanges qui m'ont souvent permis de voir mon sujet sous d'autres angles et votre indulgence face à tous les retards et problèmes de manips qui se sont accumulés. J'aimerais aussi tout particulièrement remercier **Jules** pour m'avoir permis de prolonger ma thèse de 8 mois afin que je puisse la terminer sereinement dans les meilleures conditions possibles.

Un grand merci également tous les autres membres passés et présents de l'équipe IIP pour toutes les interactions scientifiques et conviviales que nous avons eues : la branche bactério – **Eric, Tatiana, Bo, Benjamin, Jean-François, Pierre Lopez, Inès, Sacha, Yanis**, comme la branche immuno – **Maxence, Mathilde, Luc, Catherine, Thomas, Dean, Alex, Camille** et **Sophie**. Une mention spéciale à **Luc**, pour le traitement des données brutes de RNA-Seq, **Tatiana**, pour toutes tes remarques pertinentes sur mes présentations ; **Bo**, for your warm welcome when I arrived ; **Pierre Lopez**, pour ces quelques mois où tu étais là et ta sérénité d'esprit même en dernière année de thèse ; **Benjamin**, pour tous nos rires, ta bienveillance et tes petits gâteaux ; **Mathilde**, pour ton aide et tes conseils en qPCR et pour tous les chouettes moments passés ensemble au labo et en dehors ; **Dean**, for your unconditional support and for being an outstanding English grammar checker and dictionary on legs. Une pensée également pour **Valentin**, je lui souhaite bonne chance pour sa propre thèse !

Je remercie aussi tous les membres anciens et présents du bureau 567, en particulier **Alex, Maxime** et **Sophie** pour leur constante bonne humeur, et **Inès**, pour toutes nos discussions et pour m'avoir supportée durant ces derniers mois de rédaction, j'espère que la suite se passera bien pour toi !

Je voudrais aussi dire un grand merci à toute l'unité VIM, qui m'a chaleureusement accueillie et avec qui les échanges sont toujours très enrichissants. Merci particulièrement à **Jenna Fix** et **Marie**

**Galloux** de l'équipe BMP pour leur disponibilité et tous les conseils sur les western blots ; **Bernard Delmas** de l'équipe Corona, pour les discussions enrichissantes sur les infections persistantes ; **Stéphane Biacchesi** et **Emilie Mérour** de l'équipe VMP, pour tous les prêts de virus, anticorps et réactifs et pour avoir toujours pris le temps de répondre à mes questions, quand j'arrivais comme une fleur dans vos bureaux. Merci aussi à **Joël Albusquier**, notre informaticien de proximité, pour sa serviabilité et pour tous nos chaleureux échanges. Une pensée également pour toute l'équipe laverie, notamment **Cindy, Aurélie** et **Vincent**, qui font un travail de l'ombre tellement utile et qu'on oublie trop souvent ! Je souhaite également bon courage à tous les doctorants de l'unité, en début comme en fin de thèse, vous allez y arriver !

A big thanks to all the people who helped me in my quest for antibodies against my proteins of interest, which are rare and precious reagents in fish research: **Amr Gamil** and **Øystein Evensen** (NMBU), for the anti-PKR antiserum; **Jorunn Jorgensen** (UiT), **Jo-Ann Leong** (HIMB), **Peter Chiou** (NTOU) and **Marta Alonso-Hearn** (NEIKER-Tecnalia), for the anti-Mx antiserum.

J'aimerais aussi remercier les membres restants de mon comité de suivi de thèse : **François Huetz**, pour ses conseils, sa gentillesse et son aide dans l'obtention de clones triés au FACS ; **Catherine Mariojouis**, qui été bien plus qu'une tutrice de thèse au cours de ces 4 années : merci pour votre bienveillance et pour avoir pris toujours le temps de vous enquérir que tout allait bien.

Merci aussi à l'école doctorale SDSV, notamment mes interlocuteurs directs **Bernard Mignotte** et **Isabelle Guénal**, pour leur disponibilité et pour m'avoir aidée à naviguer dans les limbes administratifs de l'université Paris-Saclay.

I would also like to express my sincere gratitude to all the members of my thesis jury for having accepted to assess my work: **Stephanie DeWitte-Orr** and **Georges Lutfalla** as rapporteurs, **Karim Benihoud**, **Øystein Evensen** and **Jean-Pierre Levraud** as examiners.

Enfin, j'aimerais remercier mes ami(e)s qui ont été à mes côtés durant toute ma thèse, malgré mon manque de disponibilité – j'espère vous retrouver plus souvent maintenant que cette aventure se termine ! Une mention spéciale à **Maé, Clémentine, Olivia, Roma, Léo, Cage, Camille** et **Hugo** pour leur amitié indéfectible.

Je remercie aussi toute ma famille, mes parents et ma sœur, pour tout le soutien qu'ils m'ont apporté et pour avoir veillé sur moi durant ces quatre années de thèse et bien avant.

# TABLE OF CONTENTS

---

Funding.....	iii
Acknowledgments / Remerciements .....	iv
Table of contents .....	vi
List of figures .....	ix
List of tables .....	xi
Abbreviations .....	xii

## **INTRODUCTION..... 1**

## **CHAPTER 1 Overview of the type I IFN response in fish and mammals ..... 2**

1. Introduction .....	2
2. Fish immunology: a new and complex discipline .....	3
2. 1. Very brief history of fish immunology .....	3
2. 2. Challenges specific to fish immunology.....	3
3. Virus sensing and the subsequent signaling transduction pathways in mammals and fish .....	4
3. 1. Toll-like receptors (TLRs).....	5
3. 2. RIG-I-like receptors (RLRs) and related helicases .....	9
3. 3. Cytosolic nucleic acid sensors .....	12
3. 4. NOD-like receptors (NLRs).....	14
3. 5. C-type lectin receptors (CLRs).....	14
4. Early cytokine response: focus on the type I IFN response.....	15
4. 1. Transcription factors .....	15
4. 2. Interferons (IFNs) .....	16
4. 3. Type I IFN signaling pathway and other ISG induction pathways .....	22
4. 4. ISG diversity in fish and mammals.....	24
4. 5. Apoptosis: at the crossroad of type IFN cascade and TNF cascade.....	27
5. Viral subversion mechanisms of the type I IFN response .....	29
5. 1. VHSV and IHNV evasion strategies.....	29
5. 2. IPNV evasion strategies.....	30
5. 3. ISAV evasion strategies.....	30
6. Alternative antiviral system: RNA interference .....	30
7. Conclusion.....	31

## **CHAPTER 2 The role of PKR in antiviral defenses in fish and mammals..... 32**

1. Introduction .....	32
2. Brief overview of the historical discovery of PKR .....	32
3. Structure and evolution of PKR and PKZ .....	33
3. 1. eIF2 $\alpha$ kinase family .....	33
3. 2. Structure of PKR and PKZ .....	34
3. 3. Evolution of fish PKR and PKZ .....	38
4. Induction of PKR/PKZ and their antiviral activity.....	39
4. 1. Subcellular localization of PKR and PKZ .....	39
4. 2. Transcriptional regulation of PKR and PKZ.....	39
4. 3. Antiviral activity .....	40
5. Underlying molecular mechanisms of PKR/PKZ antiviral action .....	43
5. 1. Activation of PKR and PKZ .....	46

5. 2. Phosphorylation of eIF2 $\alpha$ and inhibition of protein synthesis .....	49
5. 3. PKR-mediated activation of apoptosis.....	51
5. 4. PKR as a transducer of the inflammatory and interferon responses .....	55
6. Modulation of PKR during viral infections.....	59
6. 1. Autoregulation of PKR .....	59
6. 2. Cellular inhibitors of PKR functions .....	59
6. 3. PKR modulation in stress granules (SGs).....	60
6. 4. Viral subversion of PKR and PKZ activation.....	60
7. Conclusion.....	61
<b>CHAPTER 3 The role of Viperin in antiviral defenses in fish and mammals .....</b>	<b>62</b>
1. Introduction .....	62
2. Brief overview of the historical discovery of Viperin .....	62
3. Structure and evolution of Viperin .....	63
3. 1. Radical SAM enzyme superfamily .....	63
3. 2. Structure of Viperin .....	63
3. 3. Radical SAM activity of Viperin: substrates and products .....	68
3. 4. Evolution of Viperin .....	71
4. Induction pathways and antiviral activity of Viperin .....	73
4. 1. Constitutive expression and inducers.....	73
4. 2. Transcriptional regulation of Viperin .....	77
4. 3. Subcellular localization of Viperin .....	78
4. 4. Viperin's antiviral activity .....	79
5. Underlying molecular mechanisms of Viperin's antiviral action.....	82
5. 1. Direct antiviral mechanisms .....	82
5. 2. Indirect antiviral mechanisms .....	86
6. Regulation of Viperin at the steady state and during viral infections.....	92
6. 1. Negative regulation of Viperin .....	92
6. 2. Viral subversion of Viperin activation.....	93
7. Emerging role of Viperin in regulating metabolic processes under non-pathological conditions.....	94
7. 1. Viperin-mediated regulation of lipid metabolism and thermogenesis .....	94
7. 2. Regulation of mitochondrial metabolism.....	95
7. 3. Bone metabolism .....	96
8. Conclusion.....	96
<b>CHAPTER 4 Development of <i>in vitro</i> fish models for the aquaculture sector.....</b>	<b>97</b>
1. Introduction .....	97
2. The importance of fish health in aquaculture .....	98
2. 1. Fish farming: a fast-growing sector .....	98
2. 2. Challenges of fish disease management .....	98
2. 3. Challenges of fish health research .....	101
3. <i>In vitro</i> fish cell lines for fish health research .....	101
3. 1. Uses .....	101
3. 2. From conventional to engineered cell lines .....	102
3. 3. Development of knockout fish cell lines.....	103
<b>OBJECTIVES .....</b>	<b>107</b>
<b>RESULTS .....</b>	<b>110</b>

<b>RESULTS 1 Characterization of the molecular functions of salmonid PKR using overexpression and knockout approaches.....</b>	<b>111</b>
1. Introduction .....	111
2. Article.....	111
3. Supplementary data .....	159
4. Summary and conclusion .....	160
<b>RESULTS 2 Characterization of cyprinid Viperin by transcriptomic study in <i>viperin</i><sup>-/-</sup> cell lines.....</b>	<b>161</b>
1. Introduction .....	161
2. Article.....	162
3. Summary and conclusion .....	223
<b>RESULTS 3 Characterization of cell lines persistently infected with IPNV.....</b>	<b>224</b>
1. Preamble.....	224
2. Introduction .....	224
3. Material and methods .....	226
4. Results .....	231
4. 1. Development of an initial <i>pkrr</i> <sup>-/-</sup> cell line and identification of a persistent IPNV infection.....	231
4. 2. Characterization of the persistent IPNV infection over the course of passages.....	233
4. 3. The innate immune response is dampened in persistently IPNV-infected cell lines.....	235
4. 4. Persistently IPNV-infected cells are refractory to acute IPNV infection but permissive to other viruses .....	239
5. Discussion .....	240
6. Conclusion and perspectives .....	242
7. Supplementary data .....	243
<b>GENERAL DISCUSSION .....</b>	<b>249</b>
1. Salmonid PKR.....	250
2. Cyprinid Viperin.....	252
3. Towards the use of knockout cell lines as virus production platforms?.....	254
4. Challenges and limitations for the development of knockout fish cell lines .....	258
5. Perspectives .....	261
6. Conclusion.....	262
<b>REFERENCES.....</b>	<b>263</b>
<b>SUPPLEMENTARY MATERIAL.....</b>	<b>289</b>
<b>APPENDIX 1 List of publications and presentations .....</b>	<b>290</b>
<b>APPENDIX 2 - RÉSUMÉ EN FRANÇAIS « Étude fonctionnelle de gènes stimulés par l'interféron par une approche in vitro d'invalidation génique en lignées cellulaires de poisson : de l'immunologie comparée à l'intérêt pour la production de vaccins » .....</b>	<b>291</b>
<b>APPENDIX 3 Development and validation of three Chinook salmon <i>mx</i> knockout cell lines .....</b>	<b>303</b>
<b>APPENDIX 4 Review article .....</b>	<b>330</b>

## LIST OF FIGURES

---

Figure 1: Time-calibrated phylogeny of fish species .....	4
Figure 2: TLR signaling pathway during viral infection in fish and mammals .....	7
Figure 3: RLR and CDS signaling pathways during viral infection in mammals .....	11
Figure 4: Phylogenetic tree analysis of fish type I IFNs and the resulting classification .....	19
Figure 5: Mechanisms leading to the expression of secreted and intracellular type I IFNs in zebrafish and rainbow trout .....	22
Figure 6: Ligand-receptor and downstream signaling pathway for type I IFNs in fish .....	23
Figure 7: Schematic representation of a “core ISG repertoire” conserved between zebrafish and mammals, classified by molecular functions .....	26
Figure 8: Mechanism of intrinsic and extrinsic pathways leading to apoptosis .....	28
Figure 9: Overall structure of mammalian and fish PKR and fish PKZ proteins .....	34
Figure 10: Sequence alignment of PKR dsRNA-binding motifs from vertebrate species .....	35
Figure 11: Sequence alignment of PKR kinase domain from vertebrate species .....	37
Figure 12: Promoter region and transcriptional regulation of the human <i>pkrr</i> gene .....	40
Figure 13: Overview of mammalian PKR mechanisms of action during viral infection .....	45
Figure 14: Molecular mechanism of inhibition of protein translation initiation via phosphorylation of eIF2 $\alpha$ in response to environmental stresses .....	50
Figure 15: Molecular structure Viperin proteins from vertebrates and lower eukaryotes .....	64
Figure 16: Characteristics of N-terminal amphipathic $\alpha$ -helices of Viperin proteins from vertebrates .....	66
Figure 17: Sequence alignment of a portion of the radical SAM domains of Viperin proteins from vertebrates and lower eukaryotes .....	67
Figure 18: Reaction mechanism of radical SAM enzymes .....	69
Figure 19: Proposed mechanism for the generation of ddhCTP catalyzed by Viperin .....	70
Figure 20: Synteny of fish <i>viperin</i> genes .....	72
Figure 21: Promoter region and transcriptional regulation of the human <i>Viperin</i> gene .....	78
Figure 22: Overview of mammalian Viperin’s mechanisms of action during viral infection and under non-pathological conditions .....	85
Figure 23: World capture fisheries and aquaculture production .....	97
Figure 24: Atlantic salmon production from 1990 to 2018 .....	99
Figure 25: Overview of CRISPR/Cas9-based genome editing .....	105
Figure 26: Workflow implemented in this project to develop fish knockout cell lines .....	109
Figure 27: PKR-ML and PKR-SL do not have a dominant negative effect .....	159
Figure 28: Model of PKR-mediated molecular functions in Chinook salmon CHSE-EC cells and PKR-dependent mechanisms activated during VHSV .....	160
Figure 29: Diagram of the different pathways regulated by Viperin in epithelial-like EPC-EC cells .....	223
Figure 30: Diagram illustrating the weekly protocol carried out on EC-PKR-C4 <sup>IPNV</sup> and EC <sup>IPNV</sup> .....	228
Figure 31: Validation of the PKR expression status in EC-PKR-C4-GFP(-) and EC-PKR-C4-GFP(+) and identification of a persistent IPNV infection in both cell lines .....	232

Figure 32: Extracellular viral titers from supernatants of EC <sup>IPNV</sup> and EC-PKR-C4 <sup>IPNV</sup> cells persistently infected IPNV. ....	234
Figure 33: Intracellular IPNV replication correlates with extracellular titers. ....	236
Figure 34: Persistent and acute IPNV infections dampen the innate immune response in infected cells. ....	237
Figure 35: IRF1 is induced in both in both acutely and persistently infected cells. ....	238
Figure 36: Comparison of permissivity to IPNV31.75 and IHNV25.70 of IPNV-free cell lines and persistently IPNV-infected cells. ....	239
Figure 37: Alignment of chromatograms from EC <sup>IPNV</sup> and EC-PKR-C4 <sup>IPNV</sup> with EC (WT) cell line. ....	243
Figure 38: Original full-length blots used in Figure 31 ....	244
Figure 39: Correlation between the number of cells per flask and the extracellular viral titers in the supernatants at each weekly sampling time point in EC <sup>IPNV</sup> and EC-PKR-C4 <sup>IPNV</sup> ....	245
Figure 40: IRF3 expression levels in persistently IPNV-infected cells. ....	246
Figure 41: Mx123 expression levels in persistently IPNV-infected cells. ....	247
Figure 42: PKR expression levels in persistently IPNV-infected cells. ....	248
Figure 43: Schéma simplifié de la réponse IFN de type I. ....	292
Figure 44: La PKR de saumon Chinook présente des fonctions moléculaires conservées ....	299
Figure 45 : Schéma-bilan des différentes voies régulées par la Viperin à l'échelle transcriptionnelle dans les cellules de poisson tête-de-boule de type épithélial. ....	301
Figure 46: Le niveau intracellulaire d'ARN viral dans les cellules infectées de façon persistante avec le VNPI corrèle avec les titres extracellulaires ....	302
Figure 47: Phylogenetic tree (A) and chromosome location (B) of salmonid mx genes from Wang <i>et al.</i> (2019). ....	304
Figure 48: mx1-3 genes are induced in EC cells following IFNA2 stimulation. ....	309
Figure 49: Development and validation of mx <sup>-/-</sup> cell lines ....	312
Figure 50: rVHSV-Tomato replicates better in mx1 <sup>-/-</sup> mx2 <sup>-/-</sup> mx3 <sup>-/-</sup> cell lines than WT EC cell line ....	312
Figure 51: Sequence alignment of the first coding exon from mx1 (LOC112247236), mx2a (LOC112247237), mx2b (LOC121839060) and mx3 (LOC112247235) ....	315
Figure 52: Genotype of EC cells (WT) and EC-Mx clones obtained from sequencing of purified PCR products amplified from genomic DNA from each cell line (A) and corresponding protein sequences (B) ....	317
Figure 53: Alignment of chromatograms from EC-Mx clones with EC (WT) cell line. ....	328
Figure 54: Original full-length blots used in Figure 49 ....	329

## LIST OF TABLES

---

Table I: Functions of PKR and PKZ described in fish .....	41
Table II: Antiviral activity of fish PKR and PKZ .....	44
Table III: Functions of Viperin described in fish.....	74
Table IV: Antiviral activity of fish Viperin .....	80
Table V: Viral diseases notifiable to WOAHA in 2023 .....	100
Table VI: Comparison of genome editing tools ZFNs, TALENs and CRISPR/Cas9.....	104
Table VII: non-exhaustive list of published fish knockout cell lines.....	106
Table VIII: qPCR primers used in this study .....	229
Table IX: Genotypes of EC-Mx clones isolated and characterized in this study.....	311
Table X: Primers used in this study .....	313

## ABBREVIATIONS

---

### Acronyms

5'-Ado <sup>•</sup>	5'-deoxyadenosyl radical
5'-dA	5'-deoxyadenosine
Ab	Antibody
ADAR	Adenosine deaminase RNA-specific binding protein
AIM	Absent in melanoma
ALDH	Aldehyde dehydrogenase
ALR	AIM2-like receptor
AP	Activator protein
APAF	Apoptotic peptidase activating factor
ATF	Activating transcription factor
BAK	BCL-2 homologous antagonist killer
BAX	BCL-2-associated X protein
BCL-2	B-cell lymphoma 2
best5	Bone-expressed sequence tag 5
BF	Bluegill fry
BFP	Blue fluorescent protein
BID	BH3 interacting-domain death agonist
BMDM	Bone marrow-derived macrophages
BMP	Bone morphogenetic protein
CaHV	Crucian carp herpes virus
CARD	Caspase recruitment domains
CDK5RAP	CDK5 regulatory subunit associated protein
CDS	Cytosolic DNA sensor
cFLIP	Cellular FADD-like IL-1 $\beta$ -converting enzyme inhibitory protein
cGAS	Cyclic GMP-AMP synthase
Ch25h	Cholesterol-25-hydroxylase
CHIKV	Chikungunya virus
CHOP	C/EBP homologous protein
CHSE	Chinook salmon embryo
CHSE-EC	CHSE expressing mEGFP and Cas9
CIAO	Cytosolic iron-sulfur assembly component
cig5	Cytomegalovirus-induced gene
CLR	C-type lectin receptor
CMPK2	Cytidine monophosphate kinase 2
co-IP	Co-immunoprecipitation
CPE	Cytopathic effect
CRFB	Cytokine receptor family B
CRISPR	Clustered regularly interspaced short palindromic repeats
crRNA	CRISPR RNA
CSV	Chum salmon virus
CXCL	C-X-C motif ligand
CyHV	Cyprinid herpes virus
DAI	dsRNA-activated inhibitor of translation
DAMP	Damage (or danger)-associated molecular pattern
ddhNTP	3'-deoxy-3',4'-didehydro-nucleoside triphosphate
DDX	DExD-box helicase
DEG	Differentially expressed gene
DENV	Dengue virus
DHX	DExH-box helicase
DIP	Defective interfering particle
DISC	Death-inducing signaling complex
DR	Death receptor
DSB	Double-strand break
dsRBM	dsRNA binding motif
dsRNA/DNA	double stranded RNA/DNA
ECM	Extracellular matrix
EHNV	Epizootic hematopoietic necrosis virus
EIF2AK	EIF2 $\alpha$ kinase
EIF2 $\alpha$	Eukaryotic translation initiation factor 2 alpha
ELP3	Elongator acetyltransferase complex subunit 3
EMCV	Encephalomyocarditis virus

EPC	Epithelioma papulosum cyprinid
EPC-EC	EPC expressing mEGFP and Cas9
ER	Endoplasmic reticulum
ERK	Extracellular signal-regulated kinase
FA	Fatty acid
FADD	FAS-associated death domain protein
FAO	Food and agriculture organization
FAS	FS-7-associated surface antigen
FASL	FAS ligand
FASR	FAS receptor
FBS	Fetal bovine serum
FHM	Fathead minnow
FPPS	Farnesyl-pyrophosphate synthase
GAPDH	Glyceraldehyde 3-phosphate dehydrogenase
GBF1	Golgi brefeldin A-resistant guanine nucleotide exchange factor 1
GCN2	General control non-derepressible 2
GCRV	Grass carp reovirus
GFP	Green fluorescent protein
GMEM	Glasgow's modified Eagle's medium
GO	Gene ontology
GSV	Golden shiner virus
HADHB	Hydroxyacyl-CoA dehydrogenase subunit beta
HCMV	Human cytomegalovirus
HCV	Hepatitis C virus
HDR	Homology directed repair
HGNC	HUGO gene nomenclature committee
hpi	Hours post-infection
HPLC	High performance liquid chromatography
hpt	Hours post-treatment
HRI	Heme-regulated inhibitor
HSMI	Heart and skeletal muscles inflammation
HSP	Heat-shock protein
HUGO	Human genome organization
IFI	IFN- $\gamma$ -inducible protein
IFN	Interferon
IFNAR	IFN- $\alpha/\beta$ receptor
IFNGR	IFN- $\gamma$ receptor
IFN- $\gamma$ -rel	IFN- $\gamma$ -related gene
IHNV	Infectious hematopoietic necrosis virus
IKK	I $\kappa$ B kinase
IL	Interleukin
IPNV	Infectious pancreatic necrosis virus
IRAK	IL-1 receptor associated kinase
IRF	IFN regulatory factor
IRF-E	IRF-binding element
ISAV	Infectious salmon anemia virus
ISG	IFN-stimulated gene
ISGF	ISG factor
ISKNV	Infectious spleen and kidney necrosis virus
ISR	Integrated stress response
ISRE	IFN-stimulated response element
I $\kappa$ B	Inhibitor of NF- $\kappa$ B
JAK	Janus kinase
JEV	Japanese encephalitis virus
JNK	c-Jun N-terminal kinase
KCS	Kinase-conserved sequence
KD	Kinase domain
KEGG	Kyoto encyclopedia of genes and genomes
KHV	Koi herpesvirus
KO	Knockout
LCBV	<i>Lates calcarifer</i> birnavirus
LC-MS	Liquid chromatography-mass spectrometry
LD	Lipid droplet
LDH	Lactate dehydrogenase
LGP	Laboratory of genetics and physiology
LIAS	Lipoic acid synthase
LOX	Lysyl oxidase
LRR	Leucine-rich repeat
LS	Lanosterol synthase

MAM	Mitochondria-associated ER membranes
MAPK	Mitogen-activated protein kinase
MAT	Methionine adenosyltransferase
MAVS	Mitochondrial antiviral-signaling protein
MDA	Melanoma differentiation associated gene
MDH	Malate dehydrogenase
MEF	Mouse embryonic fibroblast
MKK	MAPK kinase
MLS	Mitochondrial localization sequence
MOCS1	Molybdenum cofactor synthesis 1
MTHFD	Methylenetetrahydrofolate dehydrogenase
MyD88	Myeloid differentiation primary response 88
NA	Not applicable
NEMO	NF- $\kappa$ B essential modulator
NF- $\kappa$ B	Nuclear factor $\kappa$ B
NHEJ	Non-homologous end-joining
NK	Natural killer
NLR	NOD-like receptor
NLRB	Baculoviral inhibitory repeat-like domain-containing NLR
NLRC	CARD-containing NLR
NLRP	Pyrin domain-containing NLR
NMD	Non-sense mediated mRNA decay
NMR	Nuclear magnetic resonance
NNV	Nervous necrosis virus
NOD	Nucleotide-binding oligomerization domain
OAS	Oligoadenylate synthetase
ORF	Open reading frame
P/S	Penicillin/streptomycin
PACT	Protein activator of PKR
PAM	Protospacer adjacent motif
PAMP	Pathogen-associated molecular pattern
PERK	PKR-like ER kinase
PEX19	Peroxisomal biogenesis factor 19
PIAS	Protein inhibitor of activated STAT
PKR	dsRNA-dependent protein kinase
PKR-FL	PKR-full length
PKR-ML	PKR-medium length
PKR-SL	PKR-short length
PKZ	Z-DNA-dependent protein kinase
PMCV	Piscine myocarditis virus
Poly(I:C)	Polyinosinic:polycytidylic acid
PPM	Protein phosphatase, Mg <sup>2+</sup> /Mn <sup>2+</sup> -dependent
PRDI-BF1	Positive regulatory domain I binding factor 1
PRR	Pattern recognition receptor
PRRSV	Porcine reproductive and respiratory syndrome virus
PRV	Piscine orthoreovirus
PYD	Pyrin domain
RdRp	RNA-dependent RNA polymerase
RGNNV	Red-spotted grouper nervous necrosis virus
RIG-I	Retinoic acid inducible gene I
RIP	Receptor interacting protein kinase
RISC	RNA-induced silencing complex
RLR	RIG-I-like receptor
RNAi	RNA interference
RNase	Ribonuclease
RNF	Ring finger protein
RSAD2	Radical SAM domain-containing protein 2
RSV	Respiratory syncytial virus
RTG	Rainbow trout gonad
SAM	S-adenosyl-methionine
SAV	Salmonid alphavirus
SG	Stress granule
SGIV	Singapore grouper iridovirus
sgRNA	Single guide RNA
SHMT	Serine hydroxymethyl transferase
siRNA	Short interfering RNA
SM	Squalene monooxygenase
SMART	Simple modular architecture research tool
SMRV	<i>Scophthalmus maximus</i> rhabdovirus

SOCS	Suppressor of cytokine signaling
ssRNA/DNA	single stranded RNA/DNA
STAT	Signal transducer and activator of transcription
STING	Stimulator of IFN genes
SVCV	Spring viremia of carp virus
TAK	TGF- $\beta$ -activated kinase
TALEN	Transcription-activator like effector nuclease
TANK	TRAF family member-associated NF- $\kappa$ B activator
TBEV	Tick-borne encephalitis virus
TBK1	TANK-binding kinase
TCID50	Median tissue culture infectious dose
TFP	Trifunctional protein
TGF	Transforming growth factor
TiLV	Tilapia lake virus
TIR	Toll/IL-1 receptor
TIRAP	TIR domain-containing adaptor protein
TLR	Toll-like receptor
TNF	Tumor necrosis factor
TNFR	TNF receptor
tracrRNA	Transactivating crRNA
TRADD	TNFR1 associated death domain protein
TRAF	TNF receptor-associated factor
TRAIL	TNF related apoptosis inducing ligand
TRAM	TRIF-related adaptor molecule
TRBP	Transactivation response RNA-binding protein
TRIF	TIR domain-containing adaptor inducing IFN- $\beta$
TRIM	Tripartite motif
TYK	Tyrosine kinase
TYW1	tRNA-yW synthesizing protein
UTR	Untranslated region
VHSV	Viral hemorrhagic septicemia virus
vig-1	VHSV-induced gene 1
Viperin	Virus inhibitory protein, endoplasmic reticulum-associated, interferon-inducible
vMIA	Viral mitochondrial inhibitor of apoptosis
VP	Virus protein
WGD	Whole genome duplication
WNV	West Nile virus
WOAH	World organization for animal health
WT	Wild-type
ZFN	Zinc finger nuclease
ZIKV	Zika virus
$\beta$ -ME	$\beta$ -mercaptoethanol

## Species names

Latin name	Abbreviation	Common name
<i>Anguilla japonica</i>	Aj	Japanese eel
<i>Branchiostoma japonicus</i>	Bj	Amphoxius
<i>Carassius auratus</i>	Ca	Crucian carp
<i>Carcharodon carcharias</i>	Cac	Great white shark
<i>Crassostrea gigas</i>	Cg	Oyster
<i>Ctenopharyngodon idella</i>	Ci	Grass carp
<i>Cynoglossus semilaevis</i>	Cs	Tongue sole
<i>Cyprinus carpio</i>	Cyc	Common carp
<i>Danio rerio</i>	Dr	Zebrafish
<i>Dicentrarchus labrax</i>	Dl	European sea bass
<i>Epinephelus coioides</i>	Ec	Orange-spotted grouper
<i>Gadus morhua</i>	Gm	Atlantic cod
<i>Gallus gallus</i>	Gg	Chicken
<i>Gasterosteus aculeatus</i>	Ga	Three-spined stickleback
<i>Gobiocypris rarus</i>	Gr	Rare minnow
<i>Hippocampus abdominalis</i>	Ha	Big-belly seahorse
<i>Homo sapiens</i>	Hs	Human
<i>Ictalurus punctatus</i>	Ip	Channel catfish
<i>Labeo rohita</i>	Lr	Rohu
<i>Lacinutrix mariniflava</i>	Lm	Bacteria sp.
<i>Larimichthys crocea</i>	Lcr	Yellow croaker
<i>Lateolabrax japonicus</i>	Lj	Japanese seabass
<i>Lateolabrax maculatus</i>	Lm	Spotted seabass
<i>Lates calcarifer</i>	Lca	Barramundi / Asian seabass
<i>Liza haematocheila</i>	Lh	Redlip mullet
<i>Methanofollis liminatans</i>	Ml	Archaea sp.
<i>Nematostella vectensis</i>	Nv	Sea anemone
<i>Oncorhynchus kisutch</i>	Ok	Coho salmon
<i>Oncorhynchus mykiss</i>	Om	Rainbow trout
<i>Oncorhynchus nerka</i>	Onn	Sockeye salmon
<i>Oncorhynchus tshawytscha</i>	Ot	Chinook salmon
<i>Oplegnathus fasciatus</i>	Of	Rock bream
<i>Oreochromis niloticus</i>	On	Nile tilapia
<i>Oryzias latipes</i>	Ol	Japanese medaka
<i>Paralichthys olivaceus</i>	Po	Japanese flounder
<i>Petromyzon marinus</i>	Pm	Sea lamprey
<i>Pimephales promelas</i>	Pp	Fathead minnow
<i>Salmo salar</i>	Ss	Atlantic salmon
<i>Salmo trutta</i>	St	Brown trout
<i>Sciaenops ocellatus</i>	So	Red drum
<i>Sebastes schlegelii</i>	Ssc	Rockfish
<i>Shewanella baltica</i>	Sb	Bacteria sp.
<i>Siniperca chuatsi</i>	Sc	Mandarin fish
<i>Sparus aurata</i>	Sa	Gilthead seabream
<i>Takifugu obscurus</i>	To	Obscure pufferfish
<i>Takifugu rubripes</i>	Tr	Fugu
<i>Tetraodon nigroviridis</i>	Tn	Green spotted pufferfish
<i>Thielavia terrestris</i>	Tt	Fungus sp.
<i>Trachinotus ovatus</i>	To	Golden pompano
<i>Trichoderma virens</i>	Tvi	Fungus sp.
<i>Trichomonas vaginalis</i>	Tva	Protozoa sp.
<i>Xenopus laevis</i>	Xl	African clawed frog
<i>Xenopus tropicalis</i>	Xt	Western clawed frog

---

# **INTRODUCTION**

---

---

# CHAPTER 1

## Overview of the type I IFN response in fish and mammals

---

### 1. Introduction

During a microbial infection – caused by a virus, bacterium, fungus or parasite, vertebrates rely on immune responses to fight against the pathogen and eventually clear the infection (if possible). In fish, like in all vertebrates, this immune response has two arms: the innate immune response and the adaptive immune response. The innate immune response is the first line of defense against pathogens. It is a fast-acting response initiated by a specialized network of sensors, called host pattern recognition receptors (PRRs), which are sported by a wide range of host cells. During a viral infection, the detection of virus-specific pathogen-associated molecular patterns (PAMPs) by these sensors triggers a signaling cascade, resulting in the production of host defense molecules, primarily type I and II interferons (IFNs), but also pro-inflammatory cytokines and chemokines. Collectively, they elicit defense mechanisms, amplify the innate immune response and regulate the adaptive response in an autocrine and paracrine manner. IFNs induce the transcription of hundreds of IFN-stimulated genes (ISGs), including effector genes, which can have direct antiviral actions or modulate the cell physiology to limit viral replication and spread. Other cytokines and chemokines play a major role in regulating activation, proliferation, differentiation and/or recruitment of specific immune cells. They are also involved in triggering systemic reactions including adaptive responses. As a consequence, cytokines and chemokines secreted upon infection are at the interface of the innate and adaptive immune responses, as they initiate, coordinate and shape both types of response <sup>1</sup>.

Overall, innate immune mechanisms are relatively well conserved across jawed vertebrates. In fish, however, there are some specificities driven by anatomical and physiological differences. Another notable difference is the high number of paralogous genes, which are the result of whole genome duplication events giving rise to extended gene families (as discussed below).

The focus of this chapter is on molecular mechanisms. Nonetheless, it is important to bear in mind that, at the organism level, although most cell types can express PRRs and secrete cytokines, the innate immune response is primarily mediated by a network of specialized cells, including dendritic cells, granulocytes (neutrophils, eosinophils, basophils), macrophages and natural killer (NK) cells. The specific roles of these different cell types will not be presented in this manuscript, as it is beyond the scope of this project.

The following chapter provides an overview of the innate immune response in mammals and fish upon viral infection. For this purpose, it is divided as follows: (1) brief overview of fish immunology and the challenges associated with this discipline; (2) molecular mechanisms underlying virus sensing and the subsequent signal transduction pathways; (3) focus on the type I IFN response, signaling pathways and ISG diversity; (4) overview of viral subversion mechanisms of the type I IFN response.

## 2. Fish immunology: a new and complex discipline

### 2.1. Very brief history of fish immunology

Before diving into the molecular mechanisms of the innate immune response in fish and mammals, a few words on the fish immunology discipline and the associated research challenges are worth mentioning. Indeed, fish immunology is a relatively recent discipline, which has lagged far behind mammalian immunology for many years. For instance, mammalian IFNs were identified in 1957 by Isaacs and Lindenmann <sup>2</sup> and the gene encoding IFN- $\alpha$  in humans was cloned in 1980 <sup>3</sup>. In contrast, the identification of molecules with IFN-like activity produced by fish cells was reported in 1970s <sup>4</sup> but the first type I IFN genes were only cloned in 2003 from zebrafish (*Danio rerio*), green-spotted pufferfish (*Tetraodon nigroviridis*) and Atlantic salmon (*Salmo salar*) <sup>5-7</sup>. At that time, the identification of key fish immune genes was mainly carried out by homology cloning based on the sequences available from other animal species (mainly mammals) for highly conserved genes and comparison of amino acid sequences and gene structures for rapidly diverging genes. Later, the widespread sequencing of fish genomes paved the way for the identification of the homologs of mammalian cytokines, receptors and signaling pathways of the innate immune response in fish.

### 2.2. Challenges specific to fish immunology

The term “fish” refers to a large variety of species, belonging to different taxonomic classes. They are typically divided into three superclasses: Agnatha (jawless fish), Chondrichthyes (cartilaginous fish), and Osteichthyes (bony fish), which include Actinopterygii (ray-finned fish) and Sarcopterygii (lobe-finned fish) (**Figure 1**). Teleosts are the largest infraclass of ray-finned fish and comprise more than 27 000 species, that represent 96% of all fish species and over 50% of living vertebrate species <sup>8</sup>. Despite all this diversity, the fish immune system has primarily been studied in a few key model species, including carp and zebrafish (cyprinids), as well as trout and salmon (salmonids). However, it should be kept in mind that each species has its own specificities and the knowledge on one species cannot be systematically applied to another, especially if they belong to distinct families.

To add another layer of complexity, in addition to the two rounds of whole genome duplication (WGD) events that occurred during the early evolution of chordates / vertebrates (1R and 2R), the

genome of early teleost fish went through a 3<sup>rd</sup> whole genome duplication event (3R) 320-350 million years ago; while salmonid fish underwent an additional 4<sup>th</sup> genome duplication event (4R) ~80-100 million years ago<sup>9-11</sup> (**Figure 1**). As a consequence, for each gene in single copy in tetrapods, two copies can potentially be found in distinct loci in diploid cyprinids and up to four copies are potentially present in salmonids. In reality, duplicated genes can either be lost, pseudogenized, sub- or neo-functionalized, with additional tandem duplication events also being a common occurrence<sup>12</sup>. Although pseudogenization appears to be the most common fate of duplicate genes<sup>9</sup>, some gene families are prone to diversification and comprise several members<sup>13,14</sup>. For instance, while two *mx* genes are present in mammalian genomes, nine paralogous genes were found in rainbow trout (*Oncorhynchus mykiss*) and Atlantic salmon<sup>14</sup>. It has been suggested that this diversification was favored by the evolutionary pressure and the need to counteract viral inhibitors involved in immune evasion, as postulated by the Red Queen hypothesis<sup>15,16</sup>. As a consequence, due to neo- and sub-functionalization events, the precise functions of fish immune genes cannot be directly extrapolated from what is known about their mammalian counterparts and the mechanisms of action of many of them remain to be elucidated.

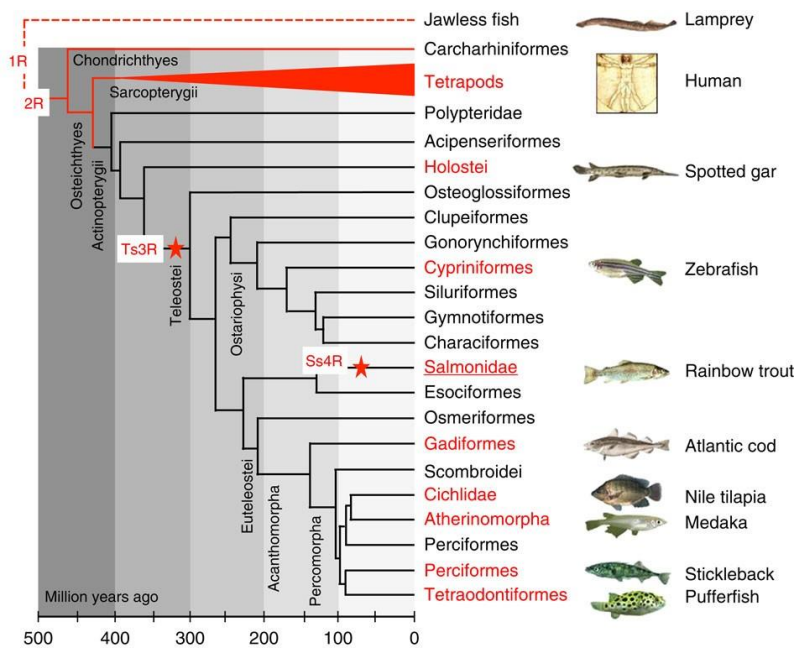


**Figure 1: Time-calibrated phylogeny of fish species**

Red stars indicate the position of teleost-specific WGD (Ts3R) salmonid-specific WGD (Ss4R). 1R and 2R correspond to the WGD events that occurred during early vertebrate evolution. Figure taken from Berthelot *et al.* (2014)<sup>9</sup>.

### 3. Virus sensing and the subsequent signaling transduction pathways in mammals and fish

In both mammals and fish, recognition of viruses by the host defense system is mediated by a subset of specialized sensors, referred to as pattern-recognition receptors (PRRs) and expressed by many

cell types in the host<sup>1</sup>. These receptors recognize conserved molecular motifs – the so-called PAMPs – present within one or several classes of microorganisms but absent from the host. Viral PAMPs include nucleic acids (single stranded (ss)/double stranded (ds) RNA or ss/dsDNA), derived from the viral genome and/or from the intermediate species produced during the virus replication cycle, as well as viral proteins (mainly surface glycoproteins and capsid proteins)<sup>1</sup>.

Virus-sensing PRRs can be divided into 5 main types based on their structures and functions, including: (1) Toll-like receptors (TLRs), (2) Retinoic acid inducible gene (RIG)-I-like receptors (RLRs) and related RNA helicases, (3) Nucleotide-binding oligomerization domain (NOD)-like receptors (NLRs), (4) C-type lectin receptors (CLRs) and (5) a heterogenous family of cytosolic nucleic acid sensors<sup>1,17,18</sup>. Members of these receptor families can be further classified in terms of ligand specificity and subcellular localization<sup>19</sup>. For instance, endosome-located TLRs recognize viral nucleic acids while TLRs and CLRs expressed on the cell surface mainly detect viral envelope proteins. In contrast, RLRs and NLRs exclusively bind to viral RNA in the cytoplasm of infected cells. As their name suggests, cytosolic nucleic acid sensors are specialized in detecting cytoplasmic nucleic acids from pathogens and/or DNA from damaged and dying cells called damage (or danger)-associated molecular patterns (DAMPs)<sup>17</sup>.

The recognition of viruses by PRRs in both mammalian models<sup>1,17,19</sup> and fish models<sup>18,20–23</sup> has been well documented over the years in several reviews. A comprehensive review of mammalian and fish PRRs and their downstream signaling pathways is beyond the scope of this chapter, which only gives a broad overview of the main activation cascades triggered upon viral sensing. Overall, PRRs are well conserved between fish and mammals, suggesting that the underlying mechanisms are similar<sup>21,22</sup>.

### **3. 1. Toll-like receptors (TLRs)**

TLRs are transmembrane glycoproteins with a tripartite structure: (1) a N-terminal extracellular domain containing multiple leucine-rich repeats (LRRs), which form a horseshoe structure and are responsible for binding PAMPs; (2) a transmembrane domain, and (3) a C-terminal cytoplasmic Toll/IL-1 receptor (TIR) domain, which interacts with adaptor molecules to initiate downstream signaling pathways<sup>24</sup>.

#### **3. 1. 1. Virus-sensing TLRs and their ligands**

*In mammals.* To date, 13 TLRs have been identified in mice and humans: TLR1-9 are conserved between the two species, TLR10 is only functional in humans, and TLR11-13 are specific to mice<sup>17</sup>. The TLR family recognizes a wide range of PAMPs including lipids, lipoproteins, glycans and

nucleic acids<sup>24</sup>. In humans, only a few TLRs can recognize virus-derived PAMPs, including TLR2, TLR3, TLR4, TLR7, TLR8 and TLR9<sup>1</sup>. Cell surface-expressed TLR2 and TLR4 are primarily known for sensing bacterial PAMPs but are also involved in the recognition of specific viral surface proteins during virus attachment<sup>1,19</sup>. TLR3 localizes to the endosomal membrane in most cell types but is also expressed on the cell surface in fibroblasts and epithelial cells<sup>25</sup>, while TLR7, TLR8, and TLR9 are exclusively expressed in the endosomal compartment. They all recognize specific viral nucleic acids: TLR3 detects dsRNA and ssRNA with internal loops, TLR7 and TLR8 sense ssRNA, TLR9 recognizes unmethylated CpG motifs present in viral DNA<sup>1</sup> (**Figure 2**). Importantly, some TLRs, including TLR3 and TLR4, are expressed by various cell types, including immune cells but also epithelial cells and fibroblasts at a lower level. In contrast, others are mainly expressed by immune cells or specific subsets of them: for instance, TLR2 is found in most immune cells, TLR7 and TLR9 are primarily expressed in plasmacytoid dendritic cells, and TLR8 is mainly present in monocytes/macrophages<sup>1,19</sup>.

***In fish.*** Many teleost fish species possess a higher number of *tlr* genes compared to mammals. To date, 21 TLRs (TLR1-5, 5S, TLR7-9, TLR13, 14, TLR18-23, and TLR25-28) have been reported in different fish species, as recently reviewed by Nie *et al.* (2018)<sup>22</sup>. However, for most of them, it is currently unclear whether there is a cell type-dependent expression profile similar to mammalian models<sup>20</sup>.

Some of these TLRs appear to be orthologs of their mammalian counterparts, while others are “teleost-specific”<sup>22,23</sup>. However, for many fish TLRs, including virus-sensing TLRs, evidence of direct recognition of viral PAMPs is still lacking<sup>23,26</sup>. Nonetheless, for nucleic acid-binding TLRs, including TLR3 and TLR7-9, structural similarities in terms of number of LRR modules and residues involved in nucleic acid binding in the N-terminal extracellular domain suggest that ligand specificity may be conserved<sup>27</sup>. In addition, a few studies have linked fish TLR2, TLR3, TLR4, TLR7, TLR8, TLR9, TLR19, TLR21 and TLR22 to viral infections<sup>23,26</sup>. For instance, expression of Japanese flounder (*Paralichthys olivaceus*) *tlr2* and Grass carp (*Ctenopharyngodon idella*) *tlr4* was induced upon infection with Viral hemorrhagic septicemia virus (VHSV) and Grass carp reovirus (GCRV), respectively<sup>28–30</sup>. Recently, it was also shown that *tlr2*<sup>-/-</sup> zebrafish larvae displayed lower nuclear factor κB (NF-κB) activity and lower expression of pro-inflammatory genes upon injection with the Spike protein of SARS-CoV-2<sup>31</sup>. *tlr3* knockdown in Japanese flounder cells reduced the immune response triggered by polyinosinic:polycytidylic acid (poly(I:C)), a synthetic analog of dsRNA<sup>32</sup>. In addition, Fugu (*Takifugu rubripes*) TLR22 and Grass carp TLR19 were found to be primarily expressed on the cell surface and in the endosome, respectively, and were both engaged upon poly(I:C) stimulation<sup>33,34</sup>. TLR7 and TLR8 have been identified in many fish species as reviewed by

Poynter *et al.* (2015) and Pietretti & Wiegertjes (2014)<sup>23,26</sup>, but to date, their ligand specificities remain poorly characterized experimentally. TLR9 and TLR21, which is present in chicken and binds CpG DNA<sup>35</sup>, are also expressed in fish<sup>36,37</sup>. Fish TLR9 was reported to localize to endosome-like vesicles<sup>36</sup> and there is also some evidence that both receptors are able to detect CpG DNA<sup>37</sup>. However, it is currently unclear whether they play a role during viral infections.

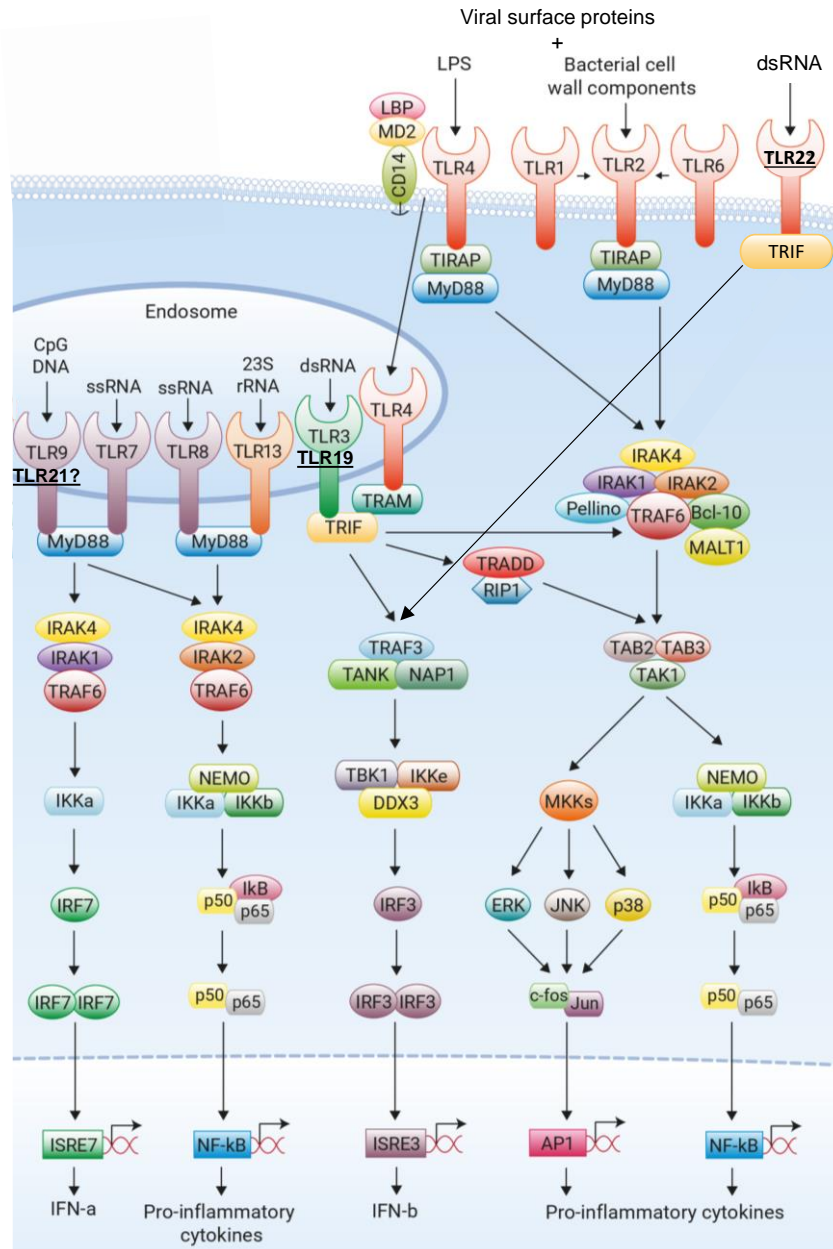


**Figure 2: TLR signaling pathway during viral infection in fish and mammals**

Figure adapted from Invivogen (2024)<sup>38</sup>. Fish-specific TLRs mentioned in the main text are underlined.

### 3. 1. 2. Downstream signaling pathways

In mammals, upon binding to their respective PAMP(s), TLRs trigger specific signal transduction pathways, that are primarily determined by the initial adaptor molecule that interacts with its

cytoplasmic domain. Two key adaptor molecules can be directly recruited by TLRs: Myeloid differentiation primary response 88 (MyD88) and TIR domain-containing adaptor inducing IFN- $\beta$  (TRIF). Most TLRs can signal *via* the MyD88-dependent pathway, while TLR3 exclusively signals *via* the TRIF-dependent pathway and TLR4 is able to signal through both <sup>17</sup> (**Figure 2**). Of note, additional adaptor molecules, TIR domain-containing adaptor protein (TIRAP) and TRIF-related adaptor molecule (TRAM), are required for linking MyD88 to TLR2 and TLR4 and TRIF to TLR4, respectively <sup>24</sup>.

### 3. 1. 2. 1. *MyD88-dependent pathway*

***In mammals.*** Upon recruitment, MyD88 interacts with different interleukin-1 receptor (IL-1R) associated kinase (IRAK) family members, including IRAK4 and IRAK1 or IRAK2, thereby forming a signaling oligomeric complex called Myddosome. IRAK1 or IRAK2 associate with the E3 ubiquitin ligase tumor necrosis factor (TNF) receptor-associated factor 6 (TRAF6), which is then recruited to the transforming growth factor (TGF)  $\beta$ -activated kinase 1 (TAK1) complex. In turn, the TAK1 complex activates two pathways, namely the NF- $\kappa$ B pathway and the mitogen-activated protein kinase (MAPK) pathway. TAK1 binds to the inhibitor of NF- $\kappa$ B (I $\kappa$ B) kinase (IKK) complex (composed of IKK $\alpha$ , IKK $\beta$ , and NF- $\kappa$ B essential modulator (NEMO)), which catalyzes the phosphorylation of NF- $\kappa$ B inhibitory protein I $\kappa$ B $\alpha$  leading to its proteasomal degradation. This allows NF- $\kappa$ B to translocate to the nucleus and induce the transcription of target genes. In parallel, TAK1 also activates MAPK family members, including extracellular signal-regulated kinases (ERKs), c-Jun N-terminal kinases (JNKs) and p38 thereby mediating activation of activator protein (AP)-1 family transcription factors <sup>17,24</sup>. NF- $\kappa$ B and AP-1 induce the transcription of their respective target genes. Of note, in plasmacytoid dendritic cells, engagement of TLR7 and TLR9 leads to MyD88 interaction with IRAK4/IRAK1 and triggers IRF7 activation, resulting in IFN- $\alpha$  expression <sup>17</sup>.

***In fish.*** Most – if not all – components of the downstream adaptor molecules involved in this pathway are also present and expressed in fish. However, several copies are often present in fish genomes, suggesting that their functions may be more complex. In particular, it was reported that *myd88* knockout in zebrafish impaired TLR-mediated immune response during bacterial infections, thereby highlighting a conserved central role of this adaptor protein in TLR signaling pathway <sup>39</sup>. In line with these results, overexpression of zebrafish IRAK4 and TRAF6 induced the expression of an NF- $\kappa$ B reporter gene <sup>40</sup>.

### 3. 1. 2. 2. *TRIF-dependent pathway*

***In mammals.*** TRIF is recruited upon engagement of TLR3 and TLR4 interacts with either ubiquitin ligases TRAF6 and TRAF3. TRAF6 recruits the receptor interacting protein kinase (RIP1), which

activates the TAK1 complex, leading to a signal transduction cascade similar to the MyD88-dependent pathway. On the other hand, TRAF3 recruits the TANK-binding kinase (TBK) 1 and NEMO kinases, resulting in IFN regulatory factor (IRF) 3 phosphorylation, dimerization and translocation into the nucleus, where it induces the expression of type I IFN genes<sup>17</sup>.

*In fish.* It was shown that Fugu TLR22 and TLR3 as well as Grass carp TLR19 could induce type I IFN *via* a TRIF-dependent pathway<sup>33,34</sup>, suggesting that this downstream cascade is conserved in fish.

### 3. 2. RIG-I-like receptors (RLRs) and related helicases

Viral replication often results in an accumulation of ssRNA or dsRNA in the cytoplasm, which can be detected by cytosolic RNA sensors called RLRs. RLRs belong to the DExD/H box helicase family and, unlike TLRs, they are constitutively expressed by almost all cell types and are specialized in recognizing viral RNA<sup>1,17</sup>. Over the past ten years, non-RLR helicases have also been identified as important viral RNA sensors<sup>41</sup>.

#### 3. 2. 1. Structure and ligands

Structurally, RLRs are composed of two N-terminal caspase recruitment domains (CARD) involved in signaling, a central DExD/H-Box helicase domain involved in viral RNA binding, and a C-terminal domain that is important for the recognition of specific RNA ligands<sup>24</sup>. The RLR family includes three members: Retinoic acid inducible I (RIG-I), melanoma differentiation associated gene 5 (MDA5), Laboratory of genetics and physiology 2 (LGP2). In contrast, non-RLR helicases comprise a central DExD/H-Box domain but typically lack the CARD domain and present an alternative C-terminal domain<sup>41</sup>.

*In mammals.* In mammals, it has been observed that RIG-I is primarily involved in sensing negative-strand RNA viruses (*e.g. Paramyxoviridae, Rhabdoviridae, Orthomyxoviridae*), while MDA5 detects positive-strand RNA viruses (*e.g. Picornaviridae, Arteriviridae*); nonetheless, some viruses are also detected by both, including some flaviviruses such as West Nile virus (WNV), Dengue virus (DENV) and Japanese encephalitis virus (JEV)<sup>17</sup>. In fact, RIG-I and MDA5 are activated by different viral RNA structures: RIG-I preferentially binds to short dsRNA (10–300 bp), 5'-mono/di/triphosphate dsRNA and 5'-triphosphate ssRNA, among others<sup>41–43</sup>. In contrast, MDA5 preferentially recognizes long dsRNA (>1,000 bp)<sup>41,42</sup>. LGP2 is also able to bind dsRNA but it lacks the N-terminal CARD domain involved in signal transduction; it functions as a modulator of RIG-I and MDA5 signaling, although its precise role is still unclear<sup>41</sup>. Several additional non-RLR members of the DExD/H box helicase family, such as DDX1, DDX3, DHX9, DHX15, DHX33, DDX60, SNRNP200, have

emerged as alternative viral RNA sensors. Because their precise ligands and functions are still not well understood <sup>41</sup>, they will not be further discussed in this chapter.

***In fish.*** In fish, RLR orthologs have been identified and cloned from various fish species, including cyprinids, salmonids and catfish, as recently reviewed by Chen *et al.* (2017) <sup>44</sup>. Interestingly, the *rig-I* gene was not found in the genomes of fish belonging to the superorder Acanthopterygii, including medaka (*Oryzias latipes*), fugu, green-spotted puffer fish, three-spined stickleback (*Gasterosteus aculeatus*), gilthead seabream (*Sparus aurata*), European sea bass (*Dicentrarchus labrax*) and mandarin fish (*Siniperca chuatsi*) <sup>44</sup>. In addition, constitutive expression of non-RLR DExD/H-box RNA helicases, including DDX1, DDX3, DHX9 was reported in various fish species, as recently reviewed in Mojzesz *et al.* (2020) <sup>18</sup>. In most cases, the RNA-binding activity of fish RLRs and related DExD/H-box RNA helicases is unknown. Nonetheless, it was demonstrated by pull-down assays that rainbow trout MDA5, LGP2, DDX3 and DHX9 were able to bind poly(I:C) <sup>45,46</sup>. Further studies are needed to determine whether fish RLRs can recognize different RNA structures, in a similar fashion to their mammalian counterparts.

### 3. 2. 2. Downstream signaling pathways

***In mammals.*** Upon ligand binding, RIG-I and MDA5 are ubiquitinated, thereby triggering their translocation to the mitochondria, where binding to mitochondrial antiviral-signaling protein (MAVS) occurs. Interactions with MAVS initiate downstream signaling *via* the TRAF3 axis leading to TBK1 phosphorylation and subsequent activation of IRF3 and IRF7 transcription factors. MAVS also recruits adaptor protein TRAF6, resulting in activation of the NF- $\kappa$ B pathway, as described for TLR signaling <sup>17</sup> (**Figure 3**). In addition, non-RLR DExD/H helicases potentiate type I IFN production but the precise signaling pathways are currently unclear <sup>41</sup>.

***In fish.*** In fish, signaling pathways downstream of RLRs are poorly described. However, several studies have shown *via* overexpression and knockdown approaches that fish RLRs are able to induce the expression of type I IFNs, ISGs and pro-inflammatory cytokines leading to an antiviral state <sup>18</sup>. For instance, knockdown of zebrafish *rig-I* resulted in reduced expression of group II type I IFNs (IFN $\phi$ 2 and IFN $\phi$ 3) upon Nervous necrosis virus (NNV) infection and in reduced inflammatory response <sup>47</sup>. Similarly, overexpression of Japanese eel (*Anguilla japonica*) *rig-I*, zebrafish *rig-I* isoform b, Crucian carp (*Carassius auratus*) *rig-I* resulted in the activation of type I IFNs <sup>48–50</sup>. Similar results were obtained upon overexpression of rainbow trout and Crucian carp *mda5* <sup>45,49</sup>. In addition, overexpression of Atlantic salmon MAVS induced the expression of ISGs and offered protection against various fish viruses, including VHSV, Infectious hematopoietic necrosis virus (IHNV), Spring viremia of carp virus (SVCV) and Epizootic hematopoietic necrosis virus (EHNV) <sup>51</sup>.

In line with these findings, fish IFN promoter activation was reduced in SVCV-infected EPC cells following transfection with dominant negative mutants of key signaling molecules, including MAVS, TBK1, IRF3 and IRF7<sup>52</sup>. Taken together, these results suggest that RLR-initiated transduction pathways are likely conserved in fish.

Concerning non-RLR DExD/H helicases, the downstream signaling pathways remain to be explored. Indeed, it was only reported that overexpression of DDX3 from Orange-spotted grouper (*Epinephelus coioides*) enhanced type I IFN and pro-inflammatory responses and inhibited replication of Red-spotted grouper nervous necrosis virus (RGNNV) but not Singapore grouper iridovirus (SGIV)<sup>53</sup>. Similarly, knockdown of rainbow trout DDX3 in RTG-2 cells resulted in increased IHNV replication<sup>54</sup>.

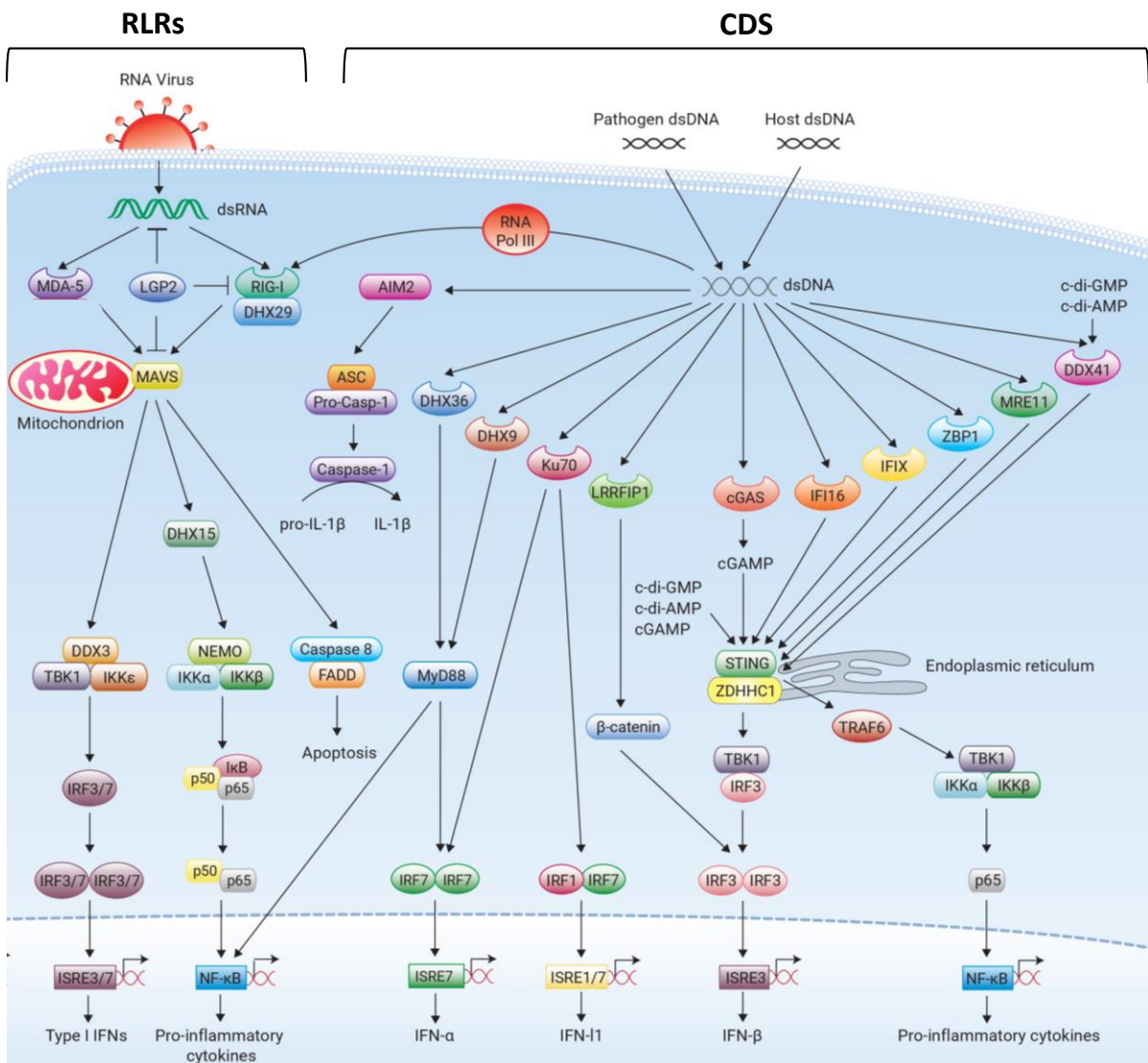


Figure 3: RLR and CDS signaling pathways during viral infection in mammals

Figure adapted from Invivogen (2024)<sup>55</sup>.

### 3. 3. Cytosolic nucleic acid sensors

This heterogeneous family includes sensors specific to viral nucleic acids, but with little or no structural similarities with one another, contrary to TLRs and NLRs. Sensors in this family can be classified as cytosolic DNA sensors (CDS) and cytosolic RNA sensors.

#### 3. 3. 1. Cytosolic DNA sensors (CDS)

Upon DNA virus infection, viral DNA is released into the host cell cytoplasm. As DNA of eukaryotic cells is located in the nucleus or mitochondrion, cytoplasmic DNA can be detected by several sensor molecules, forming an heterogeneous family. In mammals, this family comprises several members; the best-known are cyclic GMP–AMP synthase (cGAS)<sup>56</sup>, DDX41<sup>57</sup>, Absent in melanoma 2 (AIM2)<sup>58</sup> and IFN- $\gamma$ -inducible protein 16 (IFI16)<sup>59</sup>. Due to structural similarities, AIM2 and IFI16 form the subfamily of AIM2-like receptors (ALRs)<sup>1</sup> (**Figure 3**).

##### 3. 3. 1. 1. Ligands

**In mammals.** cGAS has been shown to recognize various DNA species, including dsDNA viruses, retroviruses, bacteria, parasites, fungi, as well as cytosolic self-DNA leaked from the nucleus and mitochondria<sup>60</sup>. Similarly, DDX41 can bind dsDNA of different origins, including synthetic repetitive dsDNA (poly(dA:dT) and poly(dG:dC)), *Listeria monocytogenes* DNA, vaccinia virus DNA as well as bacterial secondary messenger c-di-GMP<sup>57,61</sup>. AIM2 is also able to bind cytosolic DNA of synthetic, bacterial, fungal, viral and host origin<sup>17,58</sup>; in particular, AIM2 was reported to sense DNA viruses, including poxviruses and herpesviruses<sup>1</sup>. Last but not least, IFI16 can bind dsDNA genomic fragment from vaccinia virus, among others<sup>59</sup>.

**In fish.** Orthologs of *AIM2* and *IFI16* genes were not found in the genomes of fish, chicken and frog<sup>62</sup>. However, orthologs of *cGAS* and *DDX41* genes have been identified in several fish species, as recently reviewed by Mojzesz *et al.* (2020)<sup>18</sup>. In most cases, their specific ligands have not been studied. Recently, a study confirmed by pull-down assay that Mandarin fish DDX41 was able to bind dsDNA<sup>63</sup>.

##### 3. 3. 1. 2. Downstream signaling pathways

**In mammals.** Upon dsDNA binding, CDS proteins (except AIM2) signal through the adaptor Stimulator of interferon genes (STING) *via* direct interactions or production cGAMP from ATP and GTP for cGAS<sup>64</sup>. In both cases, STING translocates from the endoplasmic reticulum (ER) to the Golgi apparatus and activates the TBK1-IRF3 axis and/or the TRAF6-NF- $\kappa$ B axis<sup>64</sup>. Interestingly, cGAS-generated cGAMP can be transferred to neighboring cells through gap junctions, where it promotes STING activation and confers antiviral protection<sup>65</sup>. Concerning AIM2, dsDNA binding

results in the formation of AIM2 inflammasome, leading to Caspase-1 activation and cleavage of IL-1 $\beta$  into its active form<sup>17,58</sup>. This pathway can also be activated by IFI16 upon detection of viral DNA in the nucleus<sup>17</sup>.

***In fish.*** In fish, it was reported that overexpression of zebrafish paralogs, cGASa and cGASb, resulted in activation of NF- $\kappa$ B- and type I IFN-inducible reporter genes in a STING-dependent manner<sup>66</sup>. In contrast, Grass carp cGASb and Grouper cGAS were found to interact with STING but downregulated the transcription of genes encoding type I IFNs, ISGs and pro-inflammatory cytokines<sup>67,68</sup>. It was later discovered that Grass carp cGAS paralogs played opposite regulatory roles in the type I IFN response: cGASa potentiates the type I IFN response, while cGASb acts as a negative regulator<sup>69</sup>. Grass carp cGASb was reported to inhibit RIG-I-dependent signaling pathway by interacting with RIG-I and MAVS and promoting MAVS degradation through the autophagic pathway<sup>70</sup>. These results suggest that fish cGAS may play a more complex role than their mammalian counterparts, as specific paralogs act as negative regulators of the IFN response.

Co-immunoprecipitation (co-IP) assays also confirmed Mandarin fish DDX41 could interact with STING to activate the type I IFN cascade<sup>63</sup>. Furthermore, overexpression of Grouper DDX41<sup>71</sup>, Nile tilapia (*Oreochromis niloticus*) DDX41<sup>72</sup> and Mandarin fish DDX41<sup>63</sup> resulted in enhanced type I IFN and pro-inflammatory responses, suggesting that this pathway is also conserved in fish.

### 3. 3. 2. Miscellaneous cytosolic RNA sensors

***In mammals.*** A few additional cytosolic proteins are involved viral RNA sensing but can hardly be classified into any specific category, as they act as both viral RNA sensors and antiviral effectors. In mammals, the most well-known are the OAS/RNaseL system and the protein kinase R (PKR)<sup>41</sup>.

Oligoadenylate synthetases (OASs) share structural and functional similarities with cGAS<sup>73</sup>. They are both nucleotidyltransferases activated by double stranded nucleic acids and signal through second messenger molecules: OAS enzymes bind to cytosolic dsRNA and subsequently convert ATP into 2'-5'-oligoadenylates that activate the latent endoribonuclease RNaseL. Once activated, RNaseL cleaves viral ssRNAs, thereby inhibiting viral replication<sup>41</sup>. In addition, cleaved RNA species can also activate RIG-I and MDA5, thereby resulting in the production of type I IFNs<sup>41,74</sup>. On the other hand, PKR is directly activated *via* binding to dsRNA resulting in phosphorylation of eIF2 $\alpha$  and host translational arrest<sup>75</sup>. It is also involved in the potentiation of both type I IFN and inflammatory responses<sup>75</sup>. The underlying mechanisms of PKR activity will be described in details in **Chapter 2**.

***In fish.*** Contrary to mammals, genes encoding OAS and RNaseL have not been found in any ray-finned fish species but are still present in cartilaginous fish, indicating that this specific pathway was

lost during evolution of Actinopterygii <sup>76</sup>. In contrast, paralogs of the mammalian *pkr* gene have been identified in many fish species (refer to [Chapter 2](#) for more details).

### 3. 4. NOD-like receptors (NLRs)

NOD-like receptors (NLRs) are cytosolic proteins involved in the inflammatory and apoptotic responses. NLR family members have a similar domain structure characterized by: (1) a LRR-containing C-terminal domain, which acts as a sensor; (2) a central NACHT domain, mediating oligomerization and activation; (3) a N-terminal effector domain, involved in downstream signal transduction <sup>17</sup>.

*In mammals.* Humans and mice express 22 and 34 NLR genes, respectively. Based on the N-terminal structure, NLRs are classified into four subfamilies: (1) acidic transactivation domain-containing NLR (NLRA), (2) baculoviral inhibitory repeat-like domain-containing NLR (NLRB), (3) CARD-containing NLR (NLRC1-5 and NLRX1); and (4) pyrin domain-containing NLR (NLRP1-14). Many NLRs (primarily NLRP1, NLRP3 and NLRC4), can form inflammasomes, which are signaling platforms mediating Caspase-1 activation, leading to IL-1 $\beta$  and IL-18 cleavage into their active forms and pyroptosis, a form of programmed cell death. Others (including NLRC3, NLRC5, NLRX1) are involved in the downregulation of the inflammatory response <sup>17</sup>. NLRs were initially believed to exclusively detect bacterial PAMPs, but this hypothesis was later proven false, as some NLRs were shown to be involved virus sensing <sup>77,78</sup>. In particular, NLRC2 (*aka.* NOD2) was found to detect ssRNA species from Respiratory syncytial virus (RSV) and to induce the expression of IFN- $\beta$  *via* interaction with adaptor protein MAVS to activate both the IRF3 and NF- $\kappa$ B pathways <sup>78</sup>. Similarly, NLRP3 can be activated following dsRNA and ssRNA exposure as well as influenza virus infection leading to induction of pro-inflammatory cytokines <sup>77</sup>.

*In fish.* Contrary to mammals, fish NLRs have expanded into very large families of hundreds of proteins <sup>79</sup>. Interestingly, several of them are characterized by the presence of a C-terminal B30.2 domain, which is typically present in some tripartite motif containing (TRIM) and Pyrin proteins <sup>79,80</sup>. The functional role of fish NLRs during viral infection is still unclear and their large expansion makes their characterization even more challenging <sup>13,81</sup>.

### 3. 5. C-type lectin receptors (CLRs)

C-type lectin receptors (CLRs) are glycosylated transmembrane proteins with a C-terminal carbohydrate recognition domain. They form a large family comprising more than 1000 proteins, that are expressed by most cell types, but at higher levels in macrophages and dendritic cells. CLRs are primarily involved in recognition of glucans, high mannose and fucose structures expressed by fungi,

bacteria and/or parasites<sup>17</sup>. Nonetheless, a few CLRs are also involved in virus recognition due to specific glycan profiles of viral proteins compared to host cell proteins<sup>1</sup>. Mechanistically, CLRs trigger downstream activation of NF- $\kappa$ B and MAPK pathways, resulting in the induction of proinflammatory cytokines<sup>17</sup>. Engagement of specific CLRs can also positively or negatively modulate the type I IFN response, depending on the cell type and the viral pathogen<sup>82</sup>. The functional role of these receptors and the downstream signaling pathway will not be specifically discussed in this manuscript, as their role in virus sensing is thought to be relatively minor.

#### **4. Early cytokine response: focus on the type I IFN response**

Upon binding to their respective ligands, PRRs activate distinct but converging downstream signaling pathways, resulting in the expression of diverse cytokines. Most cytokines induced by viral infection are produced by immune cells; however, type I IFNs, TNFs, TGF- $\beta$ , IL-1, and IL-6 are also secreted by non-immune cells such as fibroblasts and epithelial cells. It should be kept in mind that each virus triggers the expression of a specific mix of cytokines, depending on its type, replication cycle and immune subversion strategies<sup>1</sup>. The early cytokine response following viral infection has three main functions: (1) to block viral spread; (2) to activate and/or recruit cells involved in the innate immune response, including macrophages, dendritic cells, natural killer cells and neutrophils; (3) to participate in activating adaptive T and B cell responses<sup>1</sup>. The following section aims to provide an overview of the signaling cascade triggered by type I IFNs and how they fulfill the first goal mentioned above.

##### **4. 1. Transcription factors**

In both mammals and fish, most viruses activate the NF- $\kappa$ B, IRF3/IRF7, IRF1 and AP-1 pathways, which result in the production of specific cytokines.

Under normal conditions, NF- $\kappa$ B dimers are held inactive in the cell cytosol through association with I $\kappa$ B, which blocks NF- $\kappa$ B nuclear localization signal<sup>83</sup>. Upon stress stimuli, the I $\kappa$ B kinase complex (IKK) is activated by phosphorylation, leading to phosphorylation, ubiquitination and subsequent degradation of I $\kappa$ B proteins *via* the proteasomal pathway. Released NF- $\kappa$ B translocates to the nucleus and binds specific regulatory elements, thereby inducing the transcription of its target genes<sup>83</sup>. Once activated, NF- $\kappa$ B drives the transcription of over 150 target genes including interleukins (IL-1, IL-2, IL-6, IL-8, IL-9, IL-11, IL-12, IL-15), IFNs (IFN- $\gamma$ , IFN- $\beta$ ) and IRF1, among others<sup>84</sup>.

IRF3 and IRF7 are both activated through phosphorylation, resulting in the formation of homo- or heterodimers. IRF3/7 dimers then translocate into the nucleus, where they induce the expression of multiple genes most notably type I IFNs<sup>85</sup>. Besides IRF3 and IRF7, IRF1 is also a key transcription

factor, which can be directly activated *via* interactions with MyD88; once translocated into the nucleus, IRF1 can bind directly to the promoters of type I IFNs as well as several ISGs<sup>17</sup>.

AP-1 is a generic term referring to dimeric transcription factors composed of subunits from the Jun, Fos and Activating transcription factor (ATF) families, which are all downstream targets of the MAPK pathway. AP-1 interacts with ~2000 target genes including proinflammatory cytokines<sup>86</sup>.

## 4. 2. Interferons (IFNs)

### 4. 2. 1. Types of IFNs

In the modern classification of cytokines, helical cytokines are divided into two classes (class I and class II) based on the structure of their receptors. Class II cytokines contain some interleukins, including IL-10, IL-19, IL-20, IL-22, IL-24, IL-26, IL-29 as well as IFNs<sup>87,88</sup>.

#### 4. 2. 1. 1. In mammals

In mammals, IFNs can be subdivided into three different families, based on sequence similarities, structural features, receptor types and biological functions<sup>89</sup>.

- **Type I IFNs**

Type I IFNs include IFN- $\alpha$  (13 subtypes in humans), IFN- $\beta$ , IFN- $\epsilon$ , IFN- $\kappa$ , and IFN- $\omega$  in humans as well as a few others in other mammals (*e.g.* IFN- $\delta$  in pig, IFN- $\tau$  in cattle, IFN- $\zeta$  in mouse)<sup>89,90</sup>. In mammals, type I IFN-encoding genes (except *IFNK*) are intronless and clustered together on a single locus located on Chr9 in humans and Chr4 in mouse. IFN- $\alpha/\beta$  can be produced by many cell types including non-immune cells, although plasmacytoid dendritic cells are major producers of IFN- $\alpha$ <sup>89</sup>. Mechanistically, they all bind a common heterodimeric receptor complex, composed of IFN- $\alpha/\beta$  receptor (IFNAR) 1 and IFNAR2 chains<sup>89,91</sup>.

- **Type II IFN**

Type II IFN include a single member called IFN- $\gamma$ . It forms a homodimer and binds the IFN- $\gamma$  receptor complex, composed of two IFN- $\gamma$  receptor (IFNGR) 1 and two IFNGR2<sup>92</sup>. IFN- $\gamma$  is mainly produced by NK and T helper 1 cells but most cell types are capable of responding to IFN- $\gamma$  due to the ubiquitous expression of IFNGR1/2<sup>93</sup>.

- **Type III IFNs**

Type III IFNs are also known as IFN- $\lambda$  and include four members: IFN- $\lambda$ 1 (IL-29), IFN- $\lambda$ 2 (*aka.* IL-28A) and IFN- $\lambda$ 3 (*aka.* IL-28B), and IFN- $\lambda$ 4<sup>94</sup>. They bind to a receptor complex formed by IL-28R1 and IL-10R2<sup>90</sup>. They are primarily produced by epithelial cells<sup>94</sup>.

During viral infections, both type I IFNs and type III IFNs are strongly induced and play a major role in the early innate response against viruses; for this reason, they are often called “virus-induced IFNs”. Type I and type III IFNs signal through the same JAK-STAT pathway and induce the expression of similar *ISGs* <sup>94</sup>. However, it was suggested that type III IFNs were involved in controlling local low-level infections at epithelial barriers while more severe infections trigger a type I IFN-driven systemic response <sup>94</sup>. In contrast, IFN- $\gamma$  is a regulatory cytokine playing a key role in bridging the innate and adaptive responses against viral and intracellular bacterial infections by promoting macrophage activation, enhancing antigen presentation and participating in the differentiation of naive CD4 T cells into T helper 1 effectors <sup>95</sup>.

#### 4. 2. 1. 2. *In fish*

Like mammals, fish also possess class II cytokines and their receptors <sup>88</sup>. Similar to mammals, all three types of IFNs have been identified in early finned fish and cartilaginous fish, but type III IFNs appear to be absent in teleost fish <sup>88,96,97</sup>. Recently, type IV IFNs have also been discovered in fish <sup>98</sup>.

- **Type I IFNs**

**Diversity.** In fish, the number of type I IFN genes greatly varies from one species to another <sup>88,99</sup>. For instance, 2 type I IFN genes were identified in Medaka <sup>100</sup>, 3 genes in Obscure pufferfish (*Takifugu obscurus*) <sup>101</sup>, 4 genes (*IFN $\phi$ 1-4*) in zebrafish <sup>5,102</sup>, 11 genes in Atlantic salmon <sup>103</sup>, 16 genes in channel catfish (*Ictalurus punctatus*) <sup>104</sup>, and at least 18 genes in rainbow trout <sup>105</sup>. Nonetheless, it should be noted that these studies were based on genome assemblies of uneven quality; it is therefore possible that more type I IFN genes are present in the genome of some of these fish species.

**Gene structure.** Contrary to mammals, teleost type I IFNs genes consist of 5 exons and 4 introns, which is similar to the gene structure of type III IFNs <sup>6</sup>. This feature, along with the fact that fish type I IFN receptors have common structural features with mammalian type III IFN receptors, led to the initial hypothesis that fish type I IFNs were possibly orthologs of mammalian type III IFNs <sup>106</sup>. However, this hypothesis was later refuted with a crystallography study: the structure of zebrafish IFN $\phi$ 1 and IFN $\phi$ 2 confirmed that fish type I IFNs belong to the type I IFN family <sup>107</sup>.

**Classification.** Based on structural features and phylogenetic analysis, fish type I IFNs can be further classified into three groups <sup>96,97</sup>. A criterion of structural distinction is the presence of 2 or 4 cysteines in the mature peptide sequence, which are predicted to be involved in the formation of 1 or 2 disulfide bridges <sup>108</sup>.

**Group I IFN** sequences comprise one pair of cysteines (C1/C3); they can be further divided into phylogenetic subgroups, including IFNa, IFNd and IFNe found in salmonids, as well IFNh identified in perciform species <sup>109</sup> (**Figure 4**). Of note, zebrafish IFN $\phi$ 1 belongs to subgroup a, while IFN $\phi$ 4

falls into subgroup d<sup>99</sup>. In zebrafish, group I IFNs signal through the heterodimeric receptor complex, which consists of long-chain cytokine receptor family B (CRFB) 1 and short-chain CRFB5<sup>102</sup>. Consistently, Nile tilapia IFNd, IFNh and yellow croaker (*Larimichthys crocea*) IFNd also preferentially bind to CRFB1 and CRFB5<sup>110,111</sup>.

**Group II IFN** sequences contain two conserved pairs of cysteines (C1/C3 and C2/C4). Like group I, they are divided into subgroups b and c in salmonids<sup>109</sup> (**Figure 4**). Zebrafish IFN $\phi$ 2 and IFN $\phi$ 3 both fall into subgroup c<sup>99</sup>. Interestingly, while group I IFNs seem to be present in all fish species, group II IFNs appear to be restricted to specific fish species, including cyprinids, salmonids and perciform fish<sup>88,105</sup>. In zebrafish, group II IFNs signal through a heterodimeric receptor CRFB2/CRFB5<sup>102</sup>. Similar findings were recently obtained with Nile tilapia and yellow croaker IFNc<sup>110,112</sup>.

**Group III IFNs** (*aka.* IFNf) also comprise four conserved cysteines and were initially grouped together with group II IFNs<sup>88</sup>. However, phylogenetic analysis revealed that IFNf is not a member of group II IFNs<sup>96,97</sup>. This is further supported by the observation that group III IFNs are found in cartilaginous and ray-finned fish, while group I and group II IFNs are specific to Actinopterygii<sup>97</sup>.

The expression profiles and functional roles of type I IFNs in fish will be discussed in **Section 4. 2. 2.**

- **Type II IFNs**

Contrary to mammals, which only express one type II IFN (IFN- $\gamma$ ), two paralogs encoding type II IFNs, called IFN- $\gamma$  and IFN- $\gamma$ -rel (standing for IFN- $\gamma$ -related gene), have been reported in several teleost groups, including tetraodontiforms<sup>101,113</sup>, catfish<sup>104,114</sup>, cyprinids<sup>113,115,116</sup> and salmonids<sup>117,118</sup>. Phylogenetic studies indicate that *ifn-y-rel* arose from a tandem duplication of IFN- $\gamma$  during teleost evolution<sup>97</sup>. Both genes have the canonical genomic structure of 4 exons and 3 introns found in all jawed vertebrates. The structure of IFN- $\gamma$  and IFN- $\gamma$ -rel receptors is not fully understood. In zebrafish, it appears that the type II IFNs use different receptor complexes: IFN $\gamma$ relR consists of CRFB6, CRFB13 and CRFB17, while IFN $\gamma$ R includes CRFB17, but not CRFB6 or CRFB13<sup>119</sup>. Furthermore, while IFN- $\gamma$  acts as a homodimer like its mammalian counterparts, IFN- $\gamma$ -rel functions both as a monomer and homodimer<sup>120</sup>. Functionally, fish IFN- $\gamma$  seems to exert similar functions as their mammalian counterparts although the precise roles of IFN- $\gamma$  and IFN- $\gamma$ -rel are currently unclear<sup>88</sup>.

- **Type III IFNs**

While type III IFNs appear to be absent in teleost fish<sup>99</sup>, IFN- $\lambda$ -encoding genes forming a clade with tetrapod IFN- $\lambda$ -encoding genes have recently been identified in cartilaginous fish, suggesting that

IFN- $\lambda$  existed in the jawed vertebrate ancestors<sup>97</sup>. However, functional analyses have yet to be performed to identify their precise role in fish.

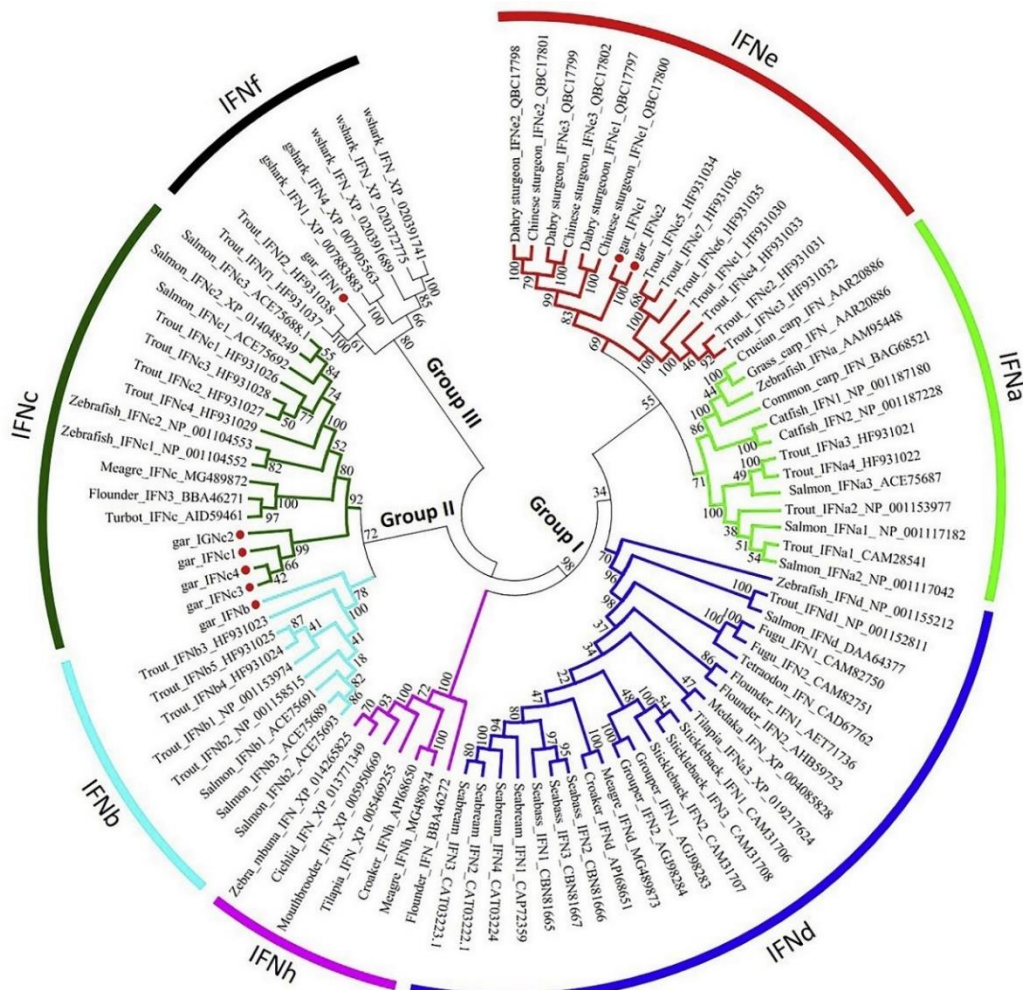


Figure 4: Phylogenetic tree analysis of fish type IFNs and the resulting classification

Figure taken from Liu *et al.* (2019)<sup>96</sup>

- **Type IV IFNs**

Recently, Chen *et al.* (2022) reported the identification of a novel class II cytokine, referred to as IFN- $\nu$  and its receptors, CRFB12 and CRFB4, in zebrafish<sup>98</sup>. Importantly, bioinformatic analysis revealed that IFN- $\nu$ -encoding genes were also present in the genome of other vertebrates including other teleost fish, cartilaginous fish, amphibians, reptiles, birds as well as a few mammals (platypus)<sup>98</sup>. Based on sequence features, phylogenetic analysis and receptor types, IFN- $\nu$  was proposed to be classified as a novel type IV IFN. Overexpression and knockout studies further revealed that zebrafish IFN- $\nu$  was able to modulate the expression of *ISGs* and to inhibit GCRV replication<sup>98</sup>. Similar properties were recently described for IFN- $\nu$  from Black carp (*Mylopharyngodon piceus*)<sup>121</sup> as well as African clawed frog (*Xenopus laevis*)<sup>122</sup> and mallard (*Anas platyrhynchos*)<sup>123</sup>.

Fish, even more so than mammals, have a wide range of IFN genes, particularly type I IFNs. This diversity stems from the WGD events along with local duplications and was likely fostered by the need to combat viral subversion strategies<sup>99</sup>. The following section focuses on the variations in expression and function between fish type I IFNs, which are the canonical virus-induced IFNs. Therefore, type II, III and IV IFNs will not be further discussed in this manuscript.

## 4. 2. 2. Spatio-temporal expression of type I IFNs

### 4. 2. 2. 1. *In mammals*

In mammals, the current view concerning the type I IFN response is that most cell types are capable of producing IFN- $\beta$  upon virus detection; in parallel, some immune cells, such as plasmacytoid dendritic cells can produce very high levels of IFN- $\alpha$ <sup>124</sup>. However, the ratio of IFN- $\alpha$  and IFN- $\beta$  produced following viral infection can greatly vary depending on the tissue studied, the virus type and the time post-infection<sup>89</sup>. Indeed, during a systemic infection there are two waves of IFN production: an early wave (IFN- $\alpha$ 4 and/or IFN- $\beta$ ) and a late wave (IFN- $\alpha$ 2,-5,-6,-8)<sup>125</sup>. The first wave is initiated by infected cells while the late wave results from the activation of a positive-feedback loop in both infected and non-infected cells<sup>124</sup>.

Molecularly, differences in expression dynamics are primarily due to two main factors: (1) differences in promoter structure and IRF binding site combinations between type I IFN genes; and (2) differences in IRF expression between cell types. For instance, the promoter of IFN- $\beta$  contains binding sites for IRF family members, including IRF3 and IRF7 which operate as homodimers (IRF3/3, IRF7/7) or heterodimers (IRF3/7), NF- $\kappa$ B and AP-1. In contrast, the promoters of IFN- $\alpha$ -encoding genes contain IRF-binding sites only and are preferentially activated by IRF7<sup>124</sup>. In mammals, IRF3 is ubiquitously and constitutively expressed. On the other hand, IRF7 is highly inducible but is poorly expressed by most cells at the steady state except by plasmacytoid dendritic cells. As a consequence, during the early phase of infection, IFN- $\beta$  and IFN- $\alpha$  can be rapidly transcribed in a IRF3-dependent manner in infected non-immune cells and in a IRF7-dependent manner in plasmacytoid dendritic cells, respectively. Activation of the type I IFN signaling pathway in infected and neighbouring cells induce high levels of IRF7, resulting in a second type I IFN wave<sup>124</sup>.

### 4. 2. 2. 2. *In fish*

The expression kinetics and tissue specificity of type I IFNs are unclear in fish. Nonetheless, a few studies provide some clues concerning the temporal and spatial expression dynamics.

## Temporal and spatial expression patterns

In salmonids, group I IFNs are induced in most fish cells (*e.g.* fibroblasts, macrophages, leukocytes) and tissues after viral infection or activation by viral PAMPs (*e.g.* poly(I:C)) and has been reported to upregulate a wide array of *ISGs*<sup>88,103,105,108</sup>. In contrast, group II IFNs appear to have a low basal expression but are strongly upregulated in lymphoid organs and head kidney leukocytes upon poly(I:C) stimulation and viral infection<sup>103,105,108</sup>. These results were further confirmed by qPCR and *in situ* hybridization studies: while group I IFN $\alpha$  was strongly induced *in vitro* and *in vivo* in many cells from various tissues upon stimulation with poly(I:C), group II IFN $\beta$  and IFN $\gamma$  were coexpressed in specific cells from lymphoid organs upon TLR7 engagement<sup>126</sup>. In contrast, opposite results were reported in zebrafish: it was observed that group I IFN $\phi$ 1 was primarily expressed by neutrophils and hepatocytes during Chikungunya virus (CHIKV) infection<sup>127</sup>, while group II IFN $\phi$ 3 was expressed by more cell types including fibroblasts, endothelial cells, hepatocytes<sup>21,99</sup>. Boudinot *et al.* (2016) also noted that, although expression patterns in cyprinids and salmonids seem to be diametrically opposed (group II specifically expressed by immune cells in salmonids vs. group I in cyprinids), no hasty conclusions can be drawn at this point due to differences in life stages and induction kinetics in the different studies<sup>99</sup>. Nonetheless, it seems that in a similar fashion to mammals, some IFNs are ubiquitously expressed in an “IFN- $\beta$ ” manner, while others are expressed in an “IFN- $\alpha$ ” manner by specific immune cells<sup>21</sup>.

In terms of promoter structure activity, it was reported that Atlantic salmon *IFNa1* and *IFNa2* genes are controlled by two distinct promoter regions called PR-I and PR-II<sup>128</sup>. In a similar fashion to mammalian *IFNB* gene, PR-I contains IRF-binding elements and NF- $\kappa$ B-binding element and is highly induced by poly(I:C) treatment, while PR-II contains binding sites for IRFs and AP-1 but is poorly induced by poly(I:C)<sup>128</sup>. In zebrafish, it was shown that the promoter of group I IFN $\phi$ 1 is controlled by IRF3, IRF7 and IRF1, and that of group II IFN $\phi$ 3 by IRF7 and IRF1 but not IRF3<sup>129</sup>, which is not in line with the *in vivo* cell-specific expression of these genes mentioned above, if we consider the mammalian model framework. These results further highlight the fact that the different subgroups of fish and mammalian type I IFNs do not function in a similar fashion and no immediate parallel can be drawn.

### At the cellular level: secreted and intracellular IFNs

At the cellular level, an important and intriguing feature of some fish type I IFNs is that they can be transcribed into two forms: a short transcript encoding a secreted protein with a signal peptide and a long transcript encoding an intracellular protein<sup>106,117,130</sup>. This phenomenon has been described in both cyprinids and salmonids in group I IFN genes only<sup>99</sup>. Interestingly, type I IFN genes harboring

or lacking a signal peptide have also been identified in catfish, suggesting that secreted and intracellular IFNs may exist in other species <sup>131</sup>.

In zebrafish, the mechanism is based on alternative splicing (exon 1' is spliced out in the secreted form while part of exon 1 is spliced out in the intracellular form) coupled with alternative start codons <sup>106</sup> (**Figure 5, left**). The intracellular IFN $\phi$ 1 form is constitutively expressed but poorly induced upon viral infection, while the secreted form is highly induced upon SVCV infection <sup>106</sup>. In rainbow trout, IFN $\alpha$  variants result from the alternative splicing of two introns leading to the alternative localization of the start codon <sup>130</sup> (**Figure 5, right**). In a similar fashion to zebrafish, intracellular splice variants are constitutively expressed while the secreted form is highly induced following poly(I:C) stimulation and viral infection <sup>130</sup>. It has also been suggested that the transcription of secreted and intracellular forms were under the control of two distinct promoter regions, as discussed above <sup>117,128</sup>. Importantly, both forms were able to induce the expression of downstream ISGs and to limit viral infections <sup>130</sup>.

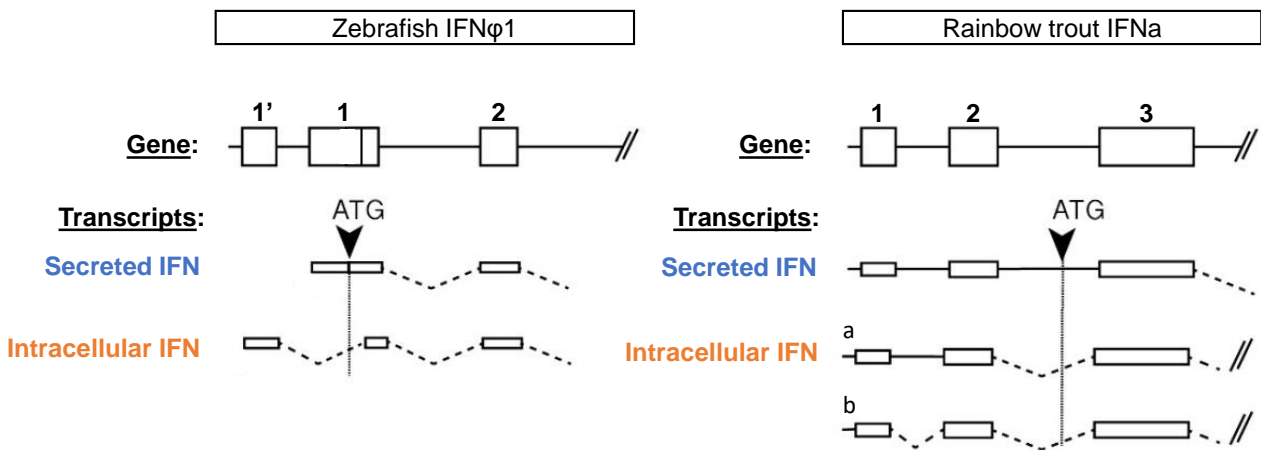


**Figure 5: Mechanisms leading to the expression of secreted and intracellular type I IFNs in zebrafish and rainbow trout**

White boxes represent exons (numbered 1-3); in transcripts, dotted lines represent spliced introns and plain lines represent unspliced introns. The black arrow corresponds to the start codon of the secreted IFN CDS. Figure modified from Boudinot *et al.* (2016) <sup>99</sup>.

### 4. 3. Type I IFN signaling pathway and other ISG induction pathways

#### 4. 3. 1. JAK-STAT pathway

*In mammals.* In mammals, binding of type I IFNs to their respective receptors in an autocrine or paracrine fashion triggers a signal transduction cascade *via* the JAK-STAT pathway, which relies on Janus kinases (JAKs) and signal transducers and activators of transcription (STATs) <sup>90</sup> (**Figure 6**). The JAK family contains 4 members, JAK1, JAK2, JAK3 and tyrosine kinase 2 (TYK2); JAK1 and TYK2 are essential in the type I IFN signaling pathway <sup>90</sup>. At the steady state, the cytoplasmic

domains of IFNAR1 and IFNAR2 are bound to TYK2 and JAK1, respectively. Upon IFN binding, the two JAK proteins are activated by transphosphorylation and promote the phosphorylation of STAT1 and STAT2. Activated STAT1 and STAT2 heterodimerize and assemble with IRF9 to form a complex called ISG factor 3 (ISGF3). ISGF3 then translocates to the nucleus where it binds to IFN-stimulated response elements (ISREs) in the promoter region of *ISGs*, thereby inducing their transcription<sup>90</sup>.

***In fish.*** As recently reviewed by Gan *et al.* (2019), homologs of genes encoding components of the JAK-STAT pathway – TYK2, JAK1, STAT1, STAT2 and IRF9 – have been identified in several fish species, although several copies may exist<sup>20</sup>. Studies in Grass carp also showed that poly(I:C) stimulation induced the phosphorylation of both TYK2 and JAK1<sup>132</sup>. Similarly, Atlantic salmon STAT1a, STAT2a and STAT2b were phosphorylated at tyrosine residues and could translocate into the nucleus following the stimulation with recombinant type I IFN<sup>133,134</sup>. Co-IP assays further demonstrated that STAT1a could interact with STAT2a, STAT2b and IRF9, suggesting that the ISGF3 complex may also occur in fish<sup>134</sup>. Similar results were recently obtained with Mandarin fish STAT1, STAT2 and IRF9<sup>135</sup>. Our team also confirmed using a *stat2*<sup>-/-</sup> and *stat1a1*<sup>-/-</sup> *stat1a2*<sup>-/-</sup> cell lines combined with RNA-Seq and RT-qPCR analysis that STAT2 was required for type I IFN signaling but not type II IFN signaling while STAT1a1 and/or STAT1a2 were required for both pathways<sup>136</sup>. Taken together, these results suggest that the JAK-STAT signaling pathway downstream of type I IFN receptors is conserved in fish and mammals.

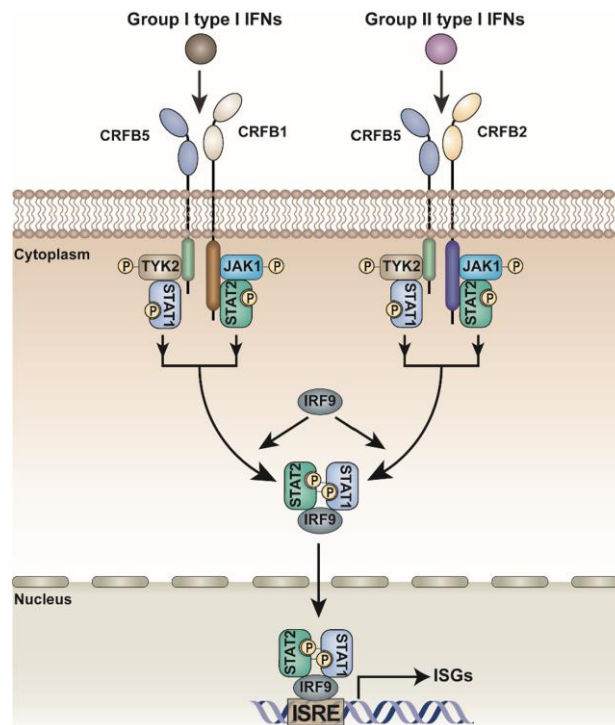


**Figure 6: Ligand-receptor and downstream signaling pathway for type I IFNs in fish**

Figure taken from Gan *et al.* (2019)<sup>20</sup>

### 4. 3. 2. IFN-independent pathway

***In mammals.*** While *ISGs* are, by definition, upregulated following type I IFN stimulation, a subset can also be directly induced *via* binding of IRF3, IRF1 and/or NF- $\kappa$ B to their promoter, in a JAK-STAT- and IFN-independent manner<sup>137–139</sup>. This subset of *ISGs* includes *Mx1*, *Mx2*, C-X-C motif ligand (*CXCL*) 10, *ISG15*, *Viperin* and *PKR* among others<sup>139</sup>. The IFN-independent transcription of *PKR* and *Viperin* and the underlying mechanisms are presented in **Chapter 2, Section 4. 2** and **Chapter 3, Section 4. 2**, respectively.

***In fish.*** Several studies have reported that some *ISGs*, including *mx1-3*, *viperin* and *rig-I*, could be induced in fish models even in presence of the protein synthesis inhibitor cycloheximide<sup>140–142</sup>. Similar results were recently obtained using CRFB1 and CRFB2 knockdown zebrafish larvae infected with CHIKV<sup>15,143</sup>. Taken together, these findings indicate that IFN-independent pathways are also present in fish.

## 4. 4. ISG diversity in fish and mammals

### 4. 4. 1. Diversity of genes and functions in mammals

The type I IFN pathway and other alternative pathways described above induce the expression of several hundreds of *ISGs* that have a wide range of activities. Overall, *ISG* products can be classified into four categories based on their functions: (1) effectors with direct antiviral function that target specific viral components; (2) modulators of host metabolic pathways exploited during specific steps of the viral life cycle; (3) positive regulators of the type I IFN response (*i.e.* enhancers of pathogen sensing and downstream signaling pathway) and (4) negative regulators of the type I IFN system<sup>138</sup>.

***Antiviral effectors.*** Examples of *ISG* products falling into category 1 and category 2 include *Mx* and Cholesterol-25-hydroxylase (*Ch25h*), respectively. *Mx* proteins are known for their direct antiviral action relying on the sequestration of viral nucleocapsids into oligomer rings, thereby inhibiting viral replication<sup>144</sup>. On the other hand, *Ch25h* produces oxysterols that modify the plasma membrane, thereby blocking the virus-cell membrane fusion of enveloped viruses<sup>145</sup>.

***Positive regulators.*** Positive regulators of the type I IFN (category 3) typically include genes encoding PRRs, adaptors, signal transducers and transcription factors. These genes are often expressed in cells at the steady state, but they are further induced following IFN stimulation to reinforce pathogen detection and IFN signaling in a positive feedback loop<sup>138,146</sup>.

***Negative regulators.*** Although the type I IFN response is effective to fight viral infection and limit viral spread, it also disrupts normal cell metabolism and has to be controlled to avoid detrimental hyperinflammation and so-called “interferonopathies”, which may result from overactivation of the

type I IFN pathway<sup>147</sup>. Control of the IFN response is mediated by negative regulators, which allow IFN-stimulated cells to recover from IFN signaling and restore cellular homeostasis. Negative regulators include ubiquitin ligases, phosphatases and direct inhibitors, among others<sup>147</sup>. For instance, E3 ubiquitin ligase ring finger protein 125 (RNF125) can target RIG-I, MDA5, and MAVS for ubiquitin-mediated proteasomal degradation<sup>148</sup>. Similarly, several TRIM proteins are involved in ubiquitination of PRRs and signaling adaptors, leading to inhibition of type I IFN induction<sup>147</sup>. In addition, IFN-stimulated suppressor of cytokine signaling proteins (SOCS) act as pseudosubstrates for JAKs, while protein inhibitors of activated STAT (PIAS) proteins bind phosphorylated STATs, thereby interrupting the JAK-STAT pathway<sup>147</sup>.

It should also be noted that the aforementioned categories (especially categories 1-3) are non-exclusive and some genes can be classified into more than one category. For instance, ISG15 can be covalently conjugated onto both viral and host proteins through a process called ISGylation leading to inhibition of viral replication *via* both direct (category 1) and indirect (category 2) mechanisms. In addition, unconjugated ISG15 operates as a cytokine with immunomodulatory activities (category 3), including induction of NK cell proliferation, dendritic cell maturation and stimulation of IFN- $\gamma$  production, among others<sup>149</sup>. Similarly, Viperin falls into the first three categories, as it inhibits viral RNA-dependent RNA polymerases<sup>150</sup>, promotes the degradation of viral proteins through the proteasome pathway, inhibits cholesterol biosynthesis (important for the budding of specific viruses) and modulates specific innate immune signaling pathways<sup>151</sup>. PKR is another “multitasking” ISG, as it inhibits host protein translation and promotes apoptosis, which are both detrimental to viral replication, but also potentiates the type I IFN and inflammatory responses<sup>75</sup>. The mechanisms of action of PKR and Viperin are described in detail in [Chapter 2](#) and [Chapter 3](#), respectively.

Taken together, these few examples highlight the diversity of direct and indirect antiviral functions by which ISGs combat viral infections. Nonetheless, despite extensive biochemical and functional studies on dozens of ISGs, the functions of many others remain unknown. In mammals, large-scale screens have started to evaluate the antiviral properties of each ISG against different types of viruses in different species<sup>146</sup>. These screens revealed that some ISGs, such as IRF1, RIG-I and MDA5, have a broad antiviral activity, while others are virus-specific<sup>146</sup>.

#### 4. 4. 2. Identification of conserved “core” ISGs in fish

Several ISGs described in mammals have also been found in fish, although several paralogs are often present due to whole genome duplication and tandem duplication events that occurred during evolution. Microarray and RNA-seq studies of poly(I:C)-stimulated, IFN-treated or virus-infected cells confirmed that many of the typical highly induced mammalian ISGs are also found in different

fish species, including zebrafish <sup>15,143</sup>, common carp (*Cyprinus carpio*) <sup>152</sup> and salmonids <sup>136,153</sup>. For instance, 337 ISGs were identified in IFN $\alpha$ 1-stimulated zebrafish larvae, of which 200 genes were orthologous to at least one human gene, including 97 genes orthologous to at least one human ISG, which could be classified 72 orthology groups <sup>15</sup>. These data imply that, although there are still gaps of knowledge concerning IFN and ISG induction pathways in fish, core ISG subsets are conserved between mammals and fish. Function-wise, this core ISG repertoire includes most of the components of the IFN system as well as many downstream antiviral effectors <sup>15</sup> (Figure 7).

This notion of a conserved core ISG group in fish was further confirmed in Atlantic salmon and rainbow trout by analyzing the transcriptomic response to poly(I:C) in both head kidney tissue (*in vivo*) and in purified head kidney leukocytes (*ex vivo*) in both species <sup>153</sup>. Similarly, most of the genes included in the core ISG group defined by Levraud *et al.* (2019) were also found in both sub-genomes of allotetraploid common carp following poly(I:C) stimulation, indicating a high degree of retained ohnologs <sup>152</sup>. Interestingly, these studies revealed that a significant proportion (~one third) of the ISG repertoire in fish have no human ortholog and vice-versa indicating the presence of a large diversity of ISGs adapted to each species, likely due to the strong pressure from pathogens <sup>15,153</sup>.

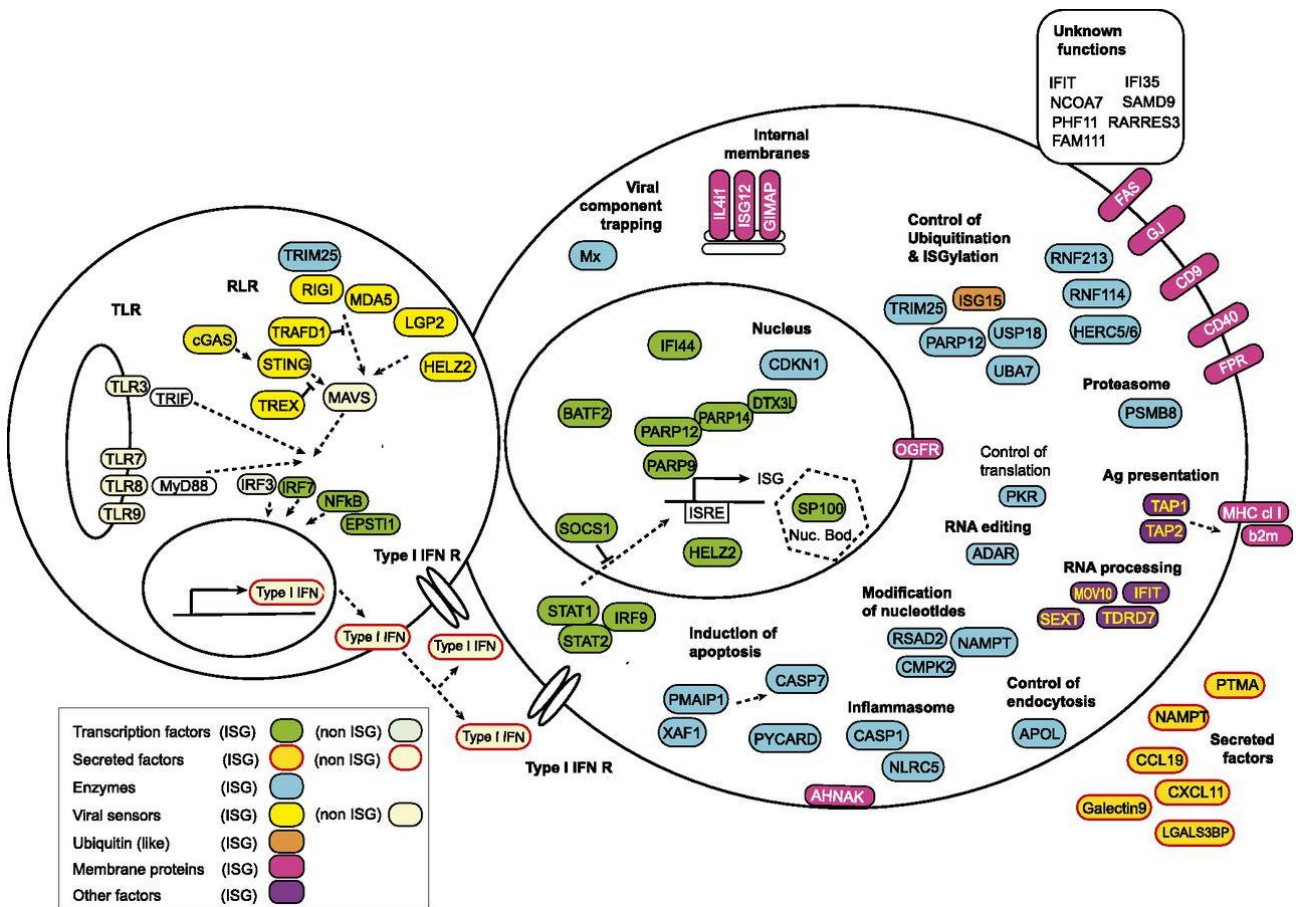


Figure 7: Schematic representation of a “core ISG repertoire” conserved between zebrafish and mammals, classified by molecular functions

Figure taken from Levraud *et al.* (2019) <sup>15</sup>.

Nonetheless, it should be kept in mind that even for fish genes with a true mammalian ortholog, whether the underlying antiviral mechanisms are similar often remains to be explored.

#### 4. 4. 3. Context-specific diversity of expression

Although hundreds of ISGs have been identified in both mammals and fish, all of them are not expressed in a given cell during viral infection. Indeed, the ISG expression profile may vary depending on the virus and its evasion strategies, the infection stage, the cell type or tissue and the host life stage. In mammals, many studies based on high-throughput approaches (*e.g.* microarrays, RNA-Seq) have explored differential ISG expression patterns between cell types and viruses<sup>154,155</sup>. In fish, similar contrasting results were obtained in zebrafish larvae infected with CHIKV and IHNV<sup>143</sup>. This study further showed that ISGs were expressed in a tissue-specific manner, mainly in liver, gut and blood vessels<sup>143</sup>.

#### 4. 5. Apoptosis: at the crossroad of type IFN cascade and TNF cascade

Apoptosis, also known as programmed cell death, is a highly regulated biological process, whereby cells undergo systematic self-destruction in response to diverse stimuli, including exposure to pathogens<sup>156</sup>. Unlike necrotic cells, apoptotic cells do not spill out their cellular contents but produce apoptotic bodies that can be phagocytosed without initiating an inflammatory response. It is commonly accepted that apoptosis is a host defense mechanism against viruses. Indeed, during a viral infection, triggering apoptosis at an early infection stage can limit viral propagation by preventing the virus from complete its life cycle in infected cells<sup>157</sup>.

Mechanistically, apoptosis can be triggered by two distinct signaling cascades: (1) the extrinsic pathway *aka.* death receptor pathway and (2) the intrinsic pathway *aka.* mitochondrial pathway (**Figure 8**).

The extrinsic pathway is activated *via* binding to extracellular ligands (*e.g.* TNF- $\alpha$ , FS-7-associated surface antigen (FAS) ligand (FASL), TNF related apoptosis inducing ligand (TRAIL)) to transmembrane death receptors (*e.g.* TNF receptor 1 (TNFR1), FAS receptor (FASR)). The ligand/receptor binding results in the recruitment of adaptor proteins, such as FAS-associated death domain protein (FADD) upon engagement of FASR and TNFR1 associated death domain protein (TRADD), FADD and RIP upon engagement of TNFR1. In both cases, FADD associates with procaspase-8 resulting in the formation of a death-inducing signaling complex (DISC) and in the auto-catalytic activation of procaspase-8<sup>158</sup>.

In contrast, the intrinsic pathway mediated by B-cell lymphoma 2 (BCL-2)-associated X protein (BAX)/BCL-2 homologous antagonist killer (BAK) insertion into mitochondrial membrane with

subsequent cytochrome *c* released which associates with apoptotic peptidase activating factor 1 (APAF1) and procaspase-9 to produce the apoptosome.

Both of these pathways converge on the activation of the caspase cascade, which constitutes the execution phase of apoptosis<sup>158</sup>. Of note, cross-talk exists between the two pathways: for instance, the release of mitochondrial cytochrome *c* can be triggered *via* cleavage of BH3 interacting-domain death agonist (BID) by Caspase 8 following activation of the FAS/FASR pathway<sup>159,160</sup>.

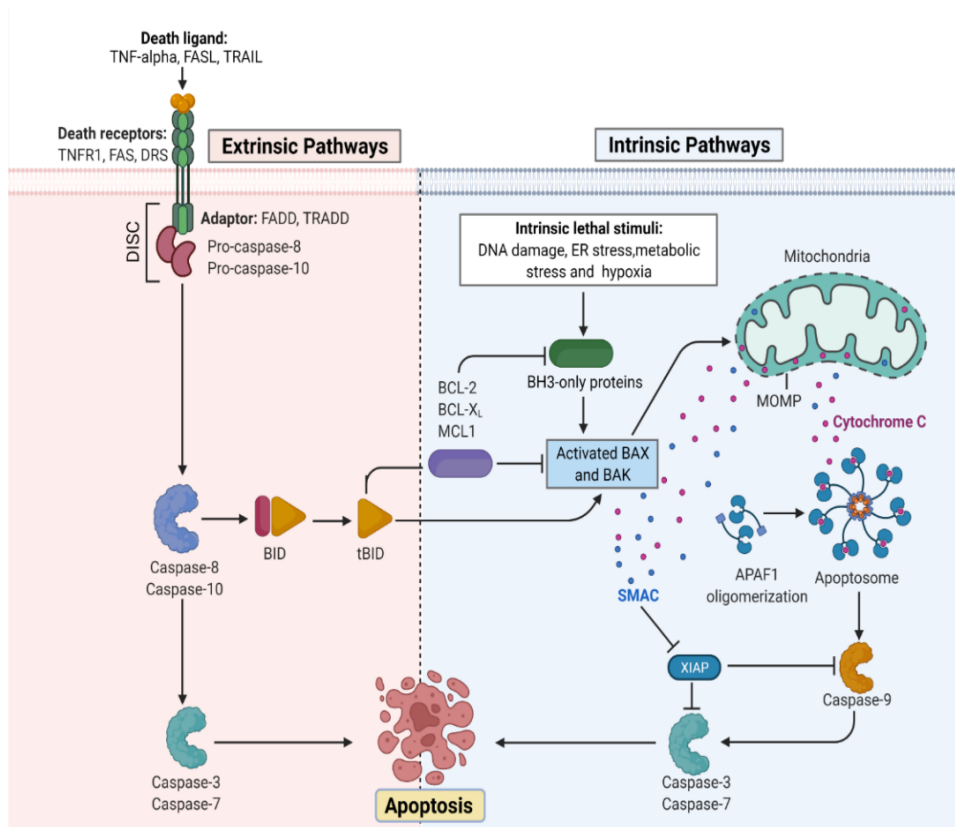


**Figure 8: Mechanism of intrinsic and extrinsic pathways leading to apoptosis**

Figure taken from Wani *et al.* (2023)<sup>161</sup>

In mammals, type I and type II IFNs were shown to induce the expression of pro-apoptotic *ISGs*, including genes coding for proteins from the aforementioned extrinsic pathway as well other pro-apoptotic genes such as *PKR*<sup>1,162</sup>. The molecular mechanisms by which PKR activates apoptosis will be discussed in **Chapter 2**. In addition, the pro-inflammatory cytokine TNF- $\alpha$ , primarily induced by NF- $\kappa$ B, plays a direct role in the activation of the extrinsic pathway, as mentioned above. Furthermore, TRADD also binds TRAF2, which activates both the NF- $\kappa$ B pathway and the MAPK pathway, *via* a positive feedback loop<sup>1</sup>.

It is important to keep in mind that apoptosis can also be advantageous for the virus at the late stage of viral replication, as it may facilitate viral release and dissemination<sup>163,164</sup>. In mammals, many viruses were found to exploit the host apoptotic pathways *via* modulation key apoptotic proteins<sup>163</sup>.

A few examples of fish viruses hijacking host apoptotic mechanisms are discussed in the following section.

## 5. Viral subversion mechanisms of the type I IFN response

Thanks to their ligand diversity and subcellular localization, PRRs form a complex surveillance network at the cellular level, allowing the host to respond rapidly to viral infection *via* activation of different transduction pathways resulting in the production of a wide array of cytokines and ISG products. The complexity of the signaling pathways and the diversity of cytokines and antiviral factors testify to the dynamic interactions between host and virus. Indeed, it is commonly accepted that the evasion strategies developed by viruses have participated in shaping the current host antiviral immune mechanisms. Similar evasion mechanisms are implemented by fish viruses, but they remain poorly described compared to viruses affecting mammals<sup>21,165</sup>. Overall, subversion strategies include inhibition of PRR activation, dampening of signaling transduction, evasion of specific ISG function and manipulation of apoptosis and autophagy<sup>165</sup>. A few examples of immune evasion strategies exploited by three important fish virus families, namely novirhabdoviruses (*e.g.* VHSV, IHNV), birnaviruses (*e.g.* Infectious pancreatic necrosis virus, IPNV) and orthomyxoviruses (*e.g.* Infectious salmon anemia virus, ISA-V) are briefly discussed hereafter.

### 5.1. VHSV and IHNV evasion strategies

Novirhabdoviruses are enveloped negative-sense single-stranded RNA viruses known for infecting various fish species. Their genome contains six genes coding for six distinct proteins, including the nucleoprotein N, the polymerase-associated protein P, the matrix protein M, the surface glycoprotein G, the RNA-dependent RNA polymerase L and the small non-structural non-virion protein NV; which are expressed in a concentration gradient manner (N > P > M > G > NV > L)<sup>166</sup>. Over the past few years, several proteins, including NV, M and N have been found to be involved in immune evasion strategies, as recently reviewed by He *et al.* (2021)<sup>167</sup>. It was initially observed that a recombinant VHSV lacking NV (rVHSV-ΔNV-EGFP) induced the expression of a reporter gene under the control of Japanese flounder *mx* promoter at a higher level than WT VHSV, suggesting that NV inhibits the type I IFN response<sup>168</sup>. The immunosuppressive function of VHSV NV was further confirmed by transcriptomic analysis in rainbow trout after intraperitoneal injection of recombinant NV from VHSV<sup>169</sup> and following infection with rVHSV-ΔNV compared to WT virus<sup>170</sup>. Mechanistically, Biacchesi *et al.* (2017) demonstrated that VHSV NV protein recruits host Mg<sup>2+</sup>/Mn<sup>2+</sup>-dependent protein phosphatase (PPM) 1Bb, which acts as a negative regulator of the IFN response through modulation of TBK1 phosphorylation<sup>171</sup>. Importantly, it seems that this

immunosuppressive effect is strain/isolate-dependent: indeed, NV from VHSV genotype IVb appear to enhance the type I IFN pathway <sup>172</sup>.

Using both rVHSV- $\Delta$ NV and overexpression approaches, it was further shown that VHSV NV could suppress TNF- $\alpha$ -mediated NF- $\kappa$ B activation <sup>173</sup>. Similarly, IHNV NV could block the degradation of the I $\kappa$ B $\alpha$  and suppress NF- $\kappa$ B nuclear translocation <sup>174</sup>. VHSV and IHNV NV were also reported to inhibit apoptosis at the early stage of viral infection <sup>175</sup>.

## 5. 2. IPNV evasion strategies

Aquabirnaviruses are non-enveloped segmented dsRNA viruses affecting fish species, IPNV being the main representative of this genus. In a similar fashion to VHSV, IPNV has been shown to suppress type I IFN signaling in a RTG-derived reporter system stimulated with poly(I:C) but not in rainbow trout head kidney macrophages <sup>176</sup>. IPNV VP4 and VP5 were further reported to inhibit IFN $\alpha$ 1-induced activation of *mx* promoter <sup>177</sup>. Similarly, IPNV preVP2, VP3 and VP4 were able to inhibit MAVS- and IRF1- and IRF3-mediated activation of *ifnal* promoter, while IPNV VP5 exerted an inhibitor effect against MAVS- and IRF1-mediated activation only <sup>178</sup>. Nonetheless, the exact mechanisms by which IPNV impairs these signaling pathways are presently not understood. Of note, it has been suggested that IPNV evasion from the type I IFN response could contribute to viral persistence and development of persistently infected carrier fish <sup>179</sup>, which is a phenomenon commonly observed in farmed Atlantic salmon <sup>180,181</sup>.

## 5. 3. ISAV evasion strategies

ISAV is an enveloped segmented negative-sense ssRNA virus belonging to the family *Orthomyxoviridae*. At least two ISAV proteins encoded by the genomic segments 7 and 8, s7ORF1 and s8ORF2 respectively, display type I IFN antagonist properties <sup>182–184</sup>. Cytoplasmic s7ORF1 was reported to inhibit induction of both *IFN* and *mx* transcription following poly(I:C) stimulation <sup>182,184</sup>. Similarly, nucleus-located s8ORF2 was shown to inhibit poly(I:C)-mediated type I IFN promoter activity <sup>182</sup>. Mechanistically, it was later demonstrated that s7ORF1 and s8ORF2 could bind IRF1, IRF3, IRF7A and IRF7B from Atlantic salmon and inhibit IFN $\alpha$ 1 promoter activity <sup>183</sup>. Recent evidence also suggests that s8ORF2 may act as an RNA silencing suppressor <sup>185</sup>.

## 6. Alternative antiviral system: RNA interference

While the type I IFN system is the first line of defense against viruses in vertebrates, the RNA interference (RNAi) system is an effective antiviral mechanism in plants, fungi and invertebrates <sup>186</sup>. Broadly speaking, RNAi refers to gene silencing at the mRNA level through small complementary

non-coding RNA species<sup>187</sup>. There are different types of small RNAs, each one of them having distinct functions in gene expression, epigenetic modifications and host-pathogen interactions<sup>187</sup>. Among them, short interfering (si)RNAs are involved in antiviral immunity. Schematically, in the antiviral RNAi pathway, virus-derived long dsRNAs are cleaved by the host ribonuclease Dicer into 20-24 bp-long siRNAs, which are incorporated into an RNA-induced silencing complex (RISC). In this complex, the double-stranded siRNA unwinds, the passenger sense strand is cleaved by an Argonaute protein and the antisense strand remains associated with RISC. This complex ultimately targets complementary viral RNAs resulting in their degradation by endonucleolytic cleavage<sup>188</sup>.

Like most eukaryotic cells, mammalian cells still possess the cellular machinery needed for RNAi, which is thought to be primarily involved in host gene expression regulation<sup>186</sup>. However, whether RNAi plays an active role in antiviral defenses in mammals remains a matter of debate<sup>188</sup>. In particular, some evidence point towards a physiologically relevant role when dsRNA concentrations are below the threshold of IFN induction<sup>189</sup>. It is still unclear whether similar mechanisms exist in fish.

## 7. Conclusion

Like most vertebrates, fish and mammals share most of the key antiviral pathways. However, due to their complex genome evolution and diversity of habitats, fish exhibit a much more diverse type I IFN and ISG repertoire than mammals. In particular, the functional role of each IFN gene in terms of spatio-temporal expression patterns, antiviral properties and downstream induced ISGs remains to be explored in detail. Similarly, the antiviral functions and molecular mechanisms of fish ISGs have not been fully elucidated yet. The following chapters aim to provide a detailed analysis of the antiviral role of PKR and Viperin in fish and mammals.

---

## CHAPTER 2

# The role of PKR in antiviral defenses in fish and mammals

---

### 1. Introduction

The following chapter focuses on dsRNA-dependent protein kinase (PKR), which is undoubtedly one of the most extensively studied antiviral proteins. PKR is recognized as a multifunctional key factor of innate immunity, as it acts both as a sensor and an effector in response to viral infections.

This introduction chapter aims to provide an analysis of the current knowledge on the implication of fish PKR and fish-specific paralog Z-DNA-dependent protein kinase (PKZ) in antiviral defenses. A systematic comparison of mammalian and fish PKR/PKZ has been made for each antiviral function. In this regard, it is divided as follows: (1) overview of the historical discovery of PKR and PKZ; (2) structure and evolution of PKR/PKZ and related eIF2 $\alpha$  kinases; (3) induction and antiviral activity of PKR/PKZ, (4) underlying molecular mechanisms, including (4a) PKR-mediated phosphorylation of eIF2 $\alpha$ , (4b) activation of apoptosis and (4c) its role of PKR in transduction of inflammatory and IFN responses of PKR and (5) its modulation during viral infections.

It should also be noted that, while the focus here is on the role of PKR in the antiviral response, this protein is also involved in other cellular pathways, including the regulation of cell growth, proliferation and differentiation<sup>75</sup>. These alternative roles will not be further discussed in this chapter but further information on this topic is available elsewhere<sup>75</sup>.

Importantly, this chapter is based on a literature review article entitled “Double-stranded RNA-dependent protein kinase (PKR) in antiviral defence in fish and mammals” and published in August 2023 in a special issue dedicated to the career of Professor Mike Belosevic in the Journal *Developmental & Comparative Immunology*<sup>190</sup>; the review paper is available as an appendix to this manuscript ([Appendix 4](#)).

### 2. Brief overview of the historical discovery of PKR

In 1976, the research group of Ian M. Kerr at the National Institute for Medical Research, London, UK, discovered that lysates from IFN-treated human and mouse cells displayed an enhanced protein kinase activity upon exposure to dsRNA<sup>191</sup>. This activity was attributed to a 68-kDa protein in human cells and a 67-kDa protein in rabbit/mouse cells, which were all shown to phosphorylate the  $\alpha$ -subunit of the eukaryotic initiation factor 2 (eIF2), leading to the inhibition of protein synthesis<sup>192–195</sup>. Cloned

in 1990 from human Daudi cells treated with IFN- $\alpha$ <sup>196</sup>, this protein, initially called p68 (human) and p67 (mouse and rabbit), was later named dsRNA-dependent protein kinase (PKR)<sup>197</sup>. In fish, the fish-specific paralog *pkz* was cloned from a Crucian carp cell line in 2004<sup>198</sup>, before the *pkz* gene was identified in fish models. At that time, the authors suggested it was possibly the fish homolog of mammalian PKR<sup>198</sup>. However, in 2008, true orthologs of *PKR* were cloned in Japanese flounder<sup>199</sup>, in zebrafish and Green-spotted pufferfish<sup>200</sup>. PKR is now also referred to as the eukaryotic translation initiation factor 2 $\alpha$  (eIF2 $\alpha$ ) kinase 2 (EIF2AK2), according to the Human genome organization (HUGO) gene nomenclature committee (HGNC)-approved nomenclature.

### 3. Structure and evolution of PKR and PKZ

#### 3. 1. eIF2 $\alpha$ kinase family

Both PKR and fish PKZ belong to the small family of eIF2 $\alpha$  kinases, which can phosphorylate eIF2 $\alpha$  at the same site (Ser51 in humans) in response to distinct intrinsic and extrinsic stress stimuli. Phosphorylation of eIF2 $\alpha$  on serine 51 results in the shutdown of the cell translation machinery, which protects the cells in two ways: it reduces the general rate of protein synthesis and it triggers the translation of specific stress-induced gene sets, which can promote two opposite cell fates, survival/recovery or apoptosis<sup>201</sup>. eIF2 $\alpha$  phosphorylation is part of a signaling pathway termed “integrated stress response” (ISR), which allows the cell to restore its homeostasis<sup>201,202</sup>.

eIF2 $\alpha$  can be phosphorylated by a family of five kinases, including: (1) PERK (PKR-like ER kinase; EIF2AK3); (2) GCN2 (general control non-derepressible 2; EIF2AK4), (3) HRI (heme-regulated inhibitor; EIF2AK1), (4) PKR (dsRNA-dependent protein kinase, EIF2AK2), (5) fish specific PKZ (Z-DNA-dependent protein kinase)<sup>198,202,203</sup>. eIF2 $\alpha$  kinases possess distinct regulatory domains allowing them to respond to specific types of stress stimuli<sup>202</sup>: PERK senses misfolded proteins in the ER and transduces this signal to attenuate protein synthesis; GCN2 is activated under amino acid starvation conditions through binding to uncharged tRNAs; HRI is activated under conditions of heme deprivation and regulates globin chain synthesis based on the amount of heme available for hemoglobin production in erythroid cells; PKR and fish PKZ are the main members of the family that are activated during viral infections upon detection of viral nucleic acids. Interestingly, although eIF2 $\alpha$  kinases primarily respond to specific stresses, a few studies suggest that they may have cooperative functions (reviewed by Pakos-Zebrucka *et al.* (2016)<sup>201</sup>). For instance, eIF2 $\alpha$  phosphorylation can be mediated by PKR but also PERK and GCN2 during viral infections<sup>204,205</sup>. Conversely, PKR was shown to play a significant role in the ER-stress signaling pathway along with PERK<sup>206</sup>. This cooperative phenomenon has also been reported with fish viruses such as VHSV<sup>172</sup>.

### 3. 2. Structure of PKR and PKZ

The mammalian PKR protein has a bipartite structure: it contains an N-terminal regulatory region comprising two dsRNA binding motifs (dsRBMs) and a C-terminal kinase domain (KD) <sup>207</sup>. This bipartite structure is well conserved in the PKR of other vertebrates, including birds, amphibians and fish (**Figure 9A**). However, while mammalian PKR consists of two (or more) dsRBMs, this number varies from one to three in fish PKR <sup>200</sup>. Fish PKZ has a similar structure, although its N-terminal regulatory region contains two  $Z\alpha$  motifs instead of dsRBMs <sup>200,203</sup>. Structural and biochemical studies have helped identify the important features of these proteins, in mammals and, to a lesser extent, in fish.

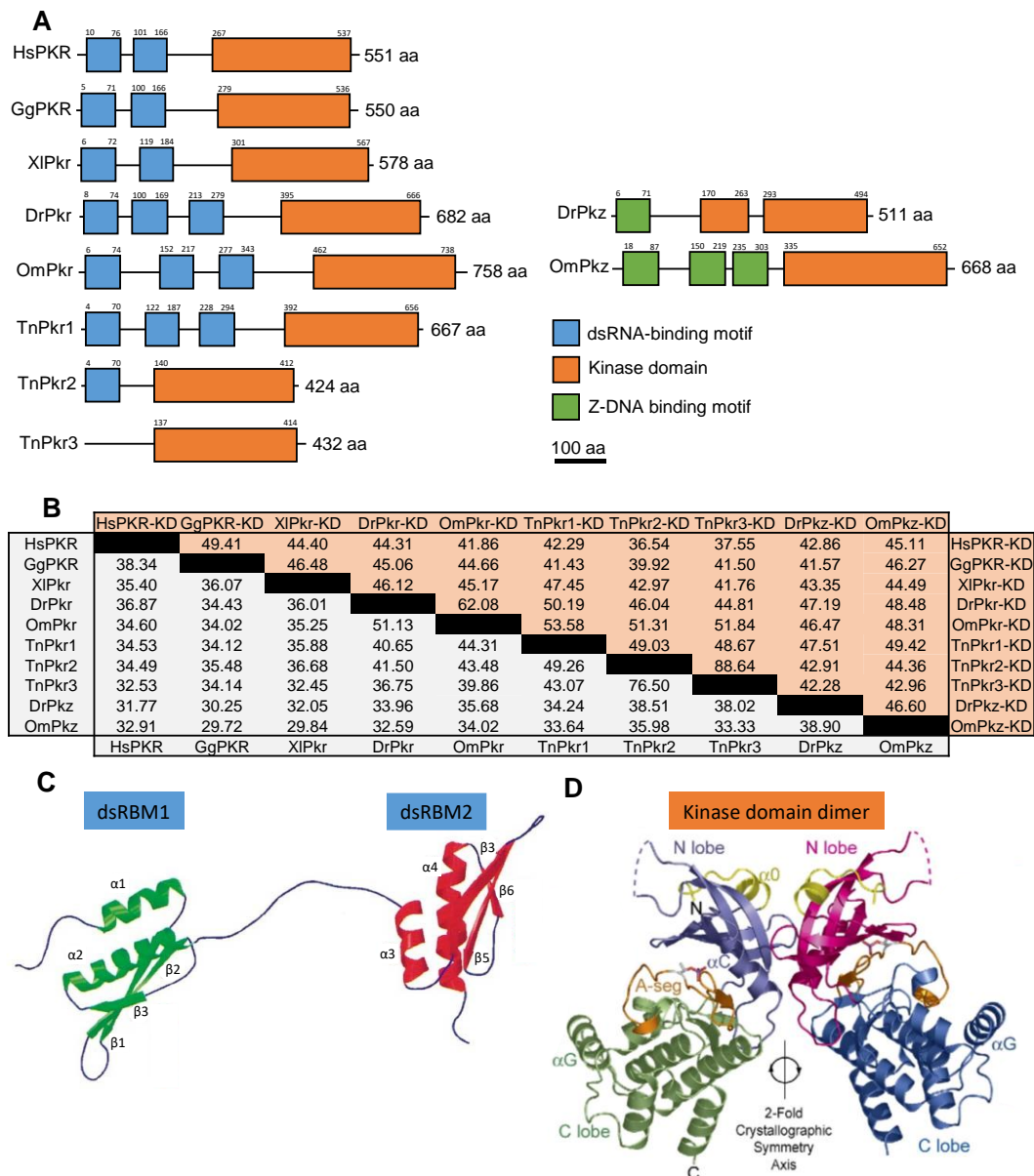


**Figure 9: Overall structure of mammalian and fish PKR and fish PKZ proteins**

(A) Schematic representation of domain organisation of PKR and PKZ proteins from *Homo sapiens* (Hs) (NP\_001129123.1/5610), *Gallus gallus* (Gg) (NP\_989818.3/395147), *Xenopus laevis* (Xl) (NP\_001091256.1/100037060), *Danio rerio* (Dr) (DrPKR: NP\_001107942.1/100001092; DrPKZ:

NP\_001035466.1/503703), *Oncorhynchus mykiss* (Om) (OmPKR: NP\_001139363.1/100271898; OmPKZ: XP\_036801832.1/110491201) and *Tetraodon nigroviridis* (Tn) (TnPKR1: CAM07147.1; TnPKR2: CAM07148.1; TnPKR3: CAM07149.1). The localization of predicted domains and motifs was obtained using SMART (Simple Modular Architecture Research Tool) <sup>208,209</sup> (B) Percent identity matrix of full length PKR and PKZ proteins (in grey) and their respective kinase domains (KD) (in orange). (C) Ribbon representation of dsRNA-binding motifs from human PKR; adapted from Nanduri *et al.* (1998) <sup>210</sup>. (D) Ribbon representation of a back-to-back dimer of the C-terminal kinase domain from human PKR. The N- and C-lobes are represented in purple and green (left) and magenta and blue (right), the activation loop (A-seg) is colored in orange, dashed lines represent disordered regions (including acidic insert). Adapted from Dar *et al.* (2005) <sup>211</sup>.

### 3. 2. 1. Double-stranded RNA binding domain

Mammalian PKR contains two 65-aa dsRBMs within its N-terminus. The two motifs are joined together by a flexible linker and adopt a dumbbell shaped structure <sup>210</sup> (Figure 9C). Each motif forming this dsRNA-binding domain shares similarities with a number of different RNA-binding proteins <sup>212</sup>. In terms of secondary structure, they both show a canonical  $\alpha$ - $\beta$ - $\beta$ - $\beta$ - $\alpha$  fold in which the two  $\alpha$ -helices are packed against a three-stranded anti-parallel  $\beta$ -sheet <sup>210</sup>. Conserved residues and/or regions that have been identified as important for the fold of the domain and/or for dsRNA binding in the dsRBMs from other proteins are present in the amino acid sequence of mammalian PKR <sup>213</sup>. Interestingly, most of these residues and regions are also found in fish PKR (Figure 10).

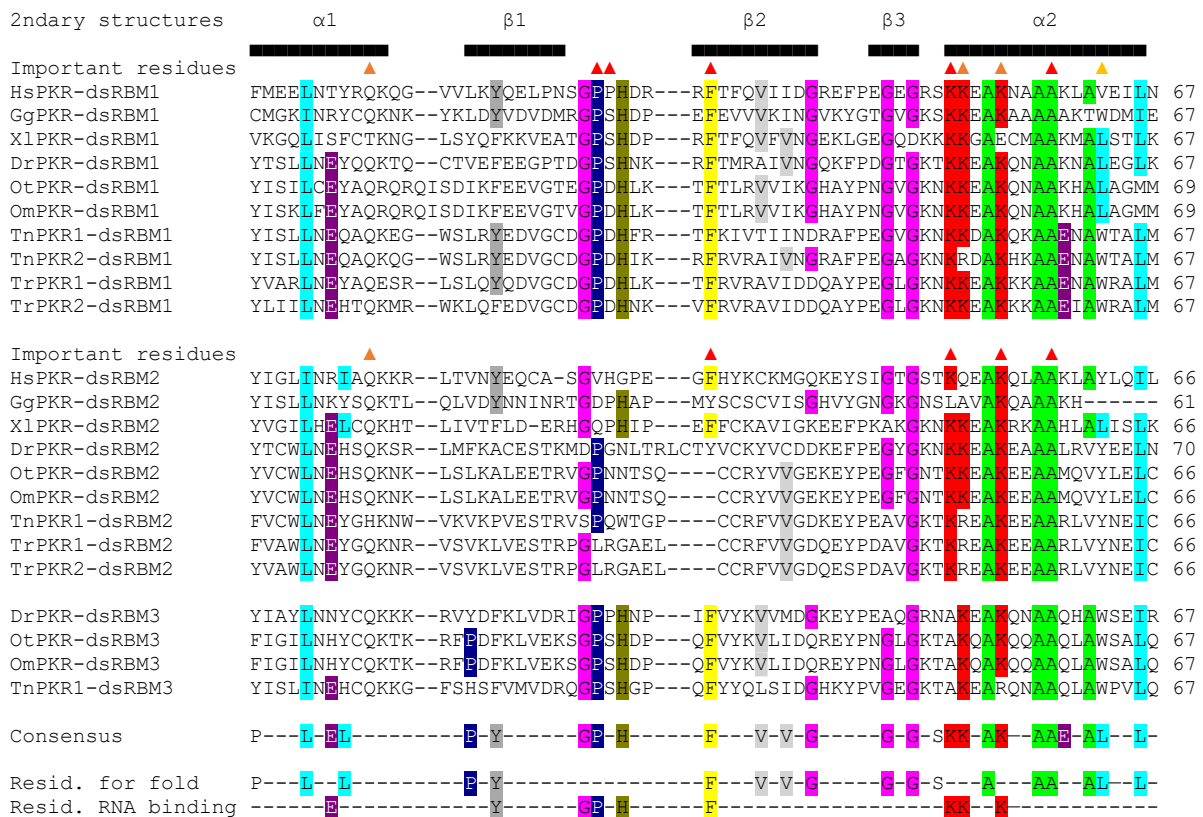


Figure 10: Sequence alignment of PKR dsRNA-binding motifs from vertebrate species

The sequences used were taken from protein sequences indicated in Figure 9. The sequence consensus identified in most dsRNA-binding motifs from other proteins and the corresponding residues conserved for the fold and/or dsRNA binding are taken from Maslah *et al.* (2013) <sup>213</sup> and drawn below the alignment. The canonical secondary structured elements are shown above the alignment <sup>210,213</sup>. The triangles above the sequences show residues that have identified as important for dsRNA binding in human PKR <sup>214,215</sup>.

In mammals, several mutational studies have shown that both motifs are essential for PKR dsRNA binding ability and for an effective kinase function: deletion of either dsRBM1 or dsRBM2 or point mutation in one copy drastically reduced the dsRNA binding capacity of mutants and negatively affected their kinase activity <sup>214–216</sup>. On the other hand, simply swapping their locations in the molecule did not result in a loss of dsRNA binding <sup>215,217</sup>, indicating that the two copies are both required for dsRNA binding but that their relative positions are less important. Interestingly, most of the key residues identified in mammals are also present in fish (**Figure 10**). The importance of dsRNA binding in PKR antiviral activity will be discussed in **Section 5.1.2**.

### 3.2.2. Z-DNA binding domain

Instead of dsRBMs, PKZ proteins contain two Z-DNA binding motifs ( $Z\alpha 1$  and  $Z\alpha 2$ ) within their N-termini.  $Z\alpha$ -binding motifs are also found in human adenosine deaminase RNA-specific binding protein 1 (ADAR1, an RNA editing enzyme) <sup>218</sup> and in a number of viral proteins from dsDNA viruses, such as poxviruses <sup>219</sup>.  $Z\alpha$  motifs are known for binding dsDNA and dsRNA in the left-handed Z conformation <sup>220</sup>. In fish PKZ, each  $Z\alpha$  motif contains 3  $\alpha$ -helices and 3 antiparallel  $\beta$ -strands arranged in a canonical  $\alpha$ - $\beta$ - $\alpha$ - $\alpha$ - $\beta$ - $\beta$  fold. In addition, key residues required for Z-DNA recognition and binding described for ADAR1  $Z\alpha$  are also present the amino acid sequence of fish PKZ <sup>221,222</sup>. In a similar fashion to what has been described for PKR, both motifs have non-redundant functions; for instance,  $Z\alpha 1$  is reported to bind more strongly to Z-DNA than  $Z\alpha 2$  <sup>223</sup>.

### 3.2.3. Kinase domain

The C-terminal kinase domain of PKR is the most conserved region of the protein when comparing different vertebrate PKRs (**Figure 9B**). In particular, the primary structures of the different kinase domains of both mammalian and fish PKR share extensive homology with other protein kinases, as they contain the 11 conserved kinase subdomains described by Hanks *et al.* (1988) <sup>224</sup> (**Figure 11**). Subdomain I contains an ATP-binding region with the canonical Gly-X-Gly-X-X-Gly motif and subdomain II comprises the invariant lysine residue (at position 296 in human PKR) that was reported to be directly involved in the transfer of the phosphate from ATP to its substrate <sup>196</sup>. Of note, mutation of this lysine to arginine or proline results in a catalytically inactive protein <sup>214,225</sup>. Subdomains VI and VII also contain putative ATP binding sites (Asp-Leu-Lys-Pro-Ser-Asn and Asp-Phe-Gln, respectively) <sup>196</sup>. Furthermore, an Ala/Ser-Pro-Glu sequence can be found in subdomain VIII and autophosphorylation sites are present within the 20 residues upstream of this consensus sequence called the activation loop. Indeed, these autophosphorylation sites (Thr451 and Thr446 in human PKR) were found to be essential for PKR activation, although only Thr446 was reported to be phosphorylated *in vivo* <sup>225</sup>.

Introduction – Chapter 2

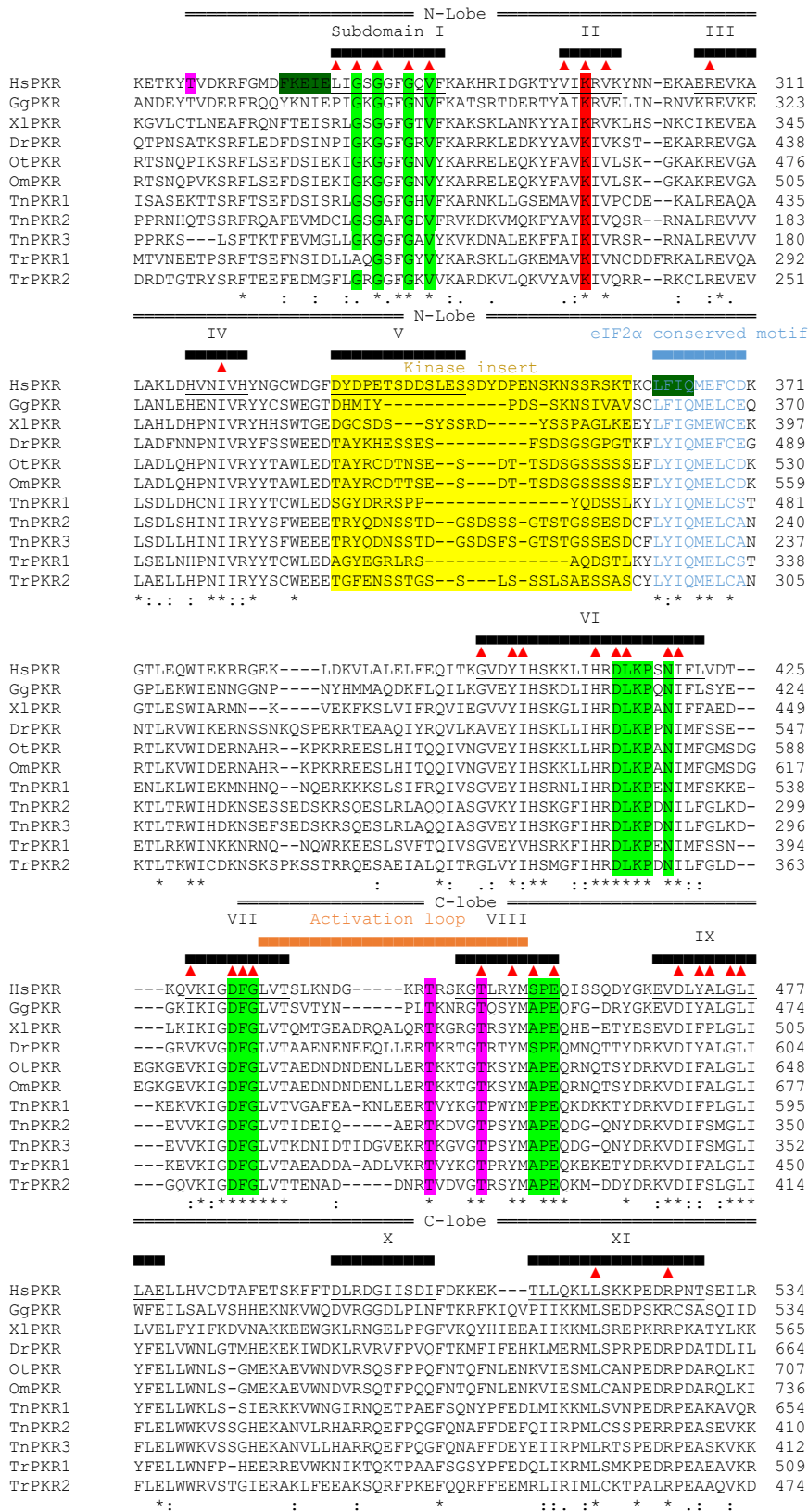


Figure 11: Sequence alignment of PKR kinase domain from vertebrate species

The sequences used were taken from protein sequences indicated in Figure 9. The different subdomains (I-XI) conserved in kinase proteins were taken from Hanks *et al.* (1988)<sup>224</sup> and Meurs *et al.* (1990)<sup>196</sup>. The red triangles show the residues conserved for in more than 63 protein kinases Hanks *et al.* (1988)<sup>224</sup>. Residues involved in ATP binding are highlighted in green, the invariant lysine residue involved in the phosphoryl transfer reaction is highlighted red, autophosphorylation sites described for PKR<sup>225</sup> are highlighted in pink and are located in the activation loop in orange. The residues highlighted in yellow correspond to the acidic kinase insert and the residues in blue form the eIF2 $\alpha$  kinase motif, which are features found in eIF2 $\alpha$ <sup>200,226</sup>. The locations shown on the N-lobe and the C-lobe were taken from Dar *et al.* (2005)<sup>211</sup>.

PKR also has an acidic kinase insert known to be critical for PKR kinase activity that spans subdomain V and continues in the inter-region between subdomains V and VI<sup>227</sup>. Notably this insert can greatly vary in size among vertebrates and from one fish species to another<sup>200</sup> (**Figure 11**). A few amino acids away from this kinase insert is located a conserved eIF2 $\alpha$  kinase motif LFIQMEFCD, that is required for autophosphorylation, phosphorylation of eIF2 $\alpha$  and contribute to its interaction with eIF2 $\alpha$ <sup>226</sup>. Of note, most of these features are also conserved in fish PKZs, although they exhibit a much longer kinase insert compared to fish PKR<sup>200,222</sup>.

The three-dimensional arrangement of PKR in space was revealed by crystallographic studies. In a similar fashion to other eukaryotic protein kinases, the catalytic kinase domain of PKR has a typical bilobal structure, consisting in a smaller N-terminal lobe and a larger C-terminal lobe (**Figure 9D**), with ATP binding sites and the activation loop being in the catalytic cleft between the two lobes<sup>211</sup>.

### 3. 3. Evolution of fish PKR and PKZ

*pkr* genes are present across jawed vertebrates from cartilaginous fish (*e.g.* in the great white shark, *Carcharodon carcharias*, LOC121278105), to bony fish and tetrapods. Only one copy is present in zebrafish and salmonids, but two or more paralogs are often present next to each other in a head-to-tail orientation in percomorph species (*e.g.*, tongue sole (*Cynoglossus semilaevis*), Japanese medaka, and Green spotted pufferfish). A detailed phylogenetic analysis revealed an accelerated evolution of the kinase domain of PKR, compared to other related kinases<sup>200,228</sup>. This domain showed a robust signature of diversifying positive selection, with variations at positively selected sites altering the sensitivity to viral inhibitors involved in immune evasion, highlighting the importance of PKR in antiviral immunity.

*pkz* genes were initially identified in Crucian carp<sup>198</sup>, zebrafish, Green spotted puffer fish, Fugu, Medaka<sup>203</sup> and Atlantic salmon<sup>229</sup>. Although it seems to be absent from many fish groups, it is not restricted to cyprinids, salmonids and percomorphs. It also found in clupeids (herrings) as well as in some osteoglossomorphs (*e.g.* *Paramorpyrops kingsleyae* and *Scleropages formosus*). *pkz* genes, in species in which they are present, are located next to *pkr* in a head-to-tail orientation<sup>222</sup>.

Phylogenetic analyses showed that fish *pkr* genes are more closely related to fish *pkz* than to their mammalian counterparts<sup>200</sup>. This suggests that *pkr* and *pkz* are paralogous genes that derive from an ancestral kinase gene, which was duplicated after the divergence from the tetrapod lineage<sup>200</sup>. The same authors further proposed that the dsRBMs of one duplicated copy were replaced by *Z $\alpha$*  domains. Because both *Z $\alpha$*  domains in PKZ are encoded by a single exon, it was speculated that they have been acquired from another cellular Z-DNA-binding protein<sup>200</sup>. Function-wise, it was suggested that the existence of PKZ in certain fish species reflects an adaptation to specific fish viruses.

## 4. Induction of PKR/PKZ and their antiviral activity

### 4. 1. Subcellular localization of PKR and PKZ

Within the cell, mammalian PKR mainly localizes in the cytoplasm but it has also been detected in the nucleus<sup>230</sup>. Similarly, cytoplasmic localization of PKR but also PKZ has been described in fish<sup>231,232</sup>.

### 4. 2. Transcriptional regulation of PKR and PKZ

#### 4. 2. 1. Induction pathways of PKR/PKZ

The *PKR* gene is constitutively expressed at low levels in mammalian cells and is then further induced by a variety of stress associated responses, including type I IFNs, viral infections and TNF- $\alpha$ <sup>196,233,234</sup>. Of note, PKR expression was also reported to be induced in response to lipopolysaccharide (LPS) as well as both Gram-positive and Gram-negative bacterial infections<sup>234,235</sup>. This distinctive feature was also found in fish PKR and PKZ *in vivo* as well as *in vitro* in fish cell lines (**Table I**).

In both mammals and fish, there is evidence that PKR can be induced through both IFN-dependent and IFN-independent pathways. For instance, it was reported that dsRNA treatment could induce the expression of PKR in mouse embryonic stem cells, which are unable to express type I IFNs in response to viral infections and poly(I:C) exposure<sup>236</sup>. In fish, expression kinetics studies using cycloheximide as a translation inhibitor, provide evidence that Grass carp CiPKR can be induced early (*ie.* 6h post-treatment) in a IFN-independent manner and later (starting from 24h) in a IFN-dependent manner in response to poly(I:C) and viral infections<sup>237,238</sup>. In contrast, Liu *et al.* (2011) reported that IFN synthesis was required for transcriptional induction of Crucian carp *CaPkr* and *CaPgz* upon a 24h treatment with poly(I:C)<sup>239</sup>. However, no early time point was examined in this study, which leaves open the possibility of an initial IFN-independent induction.

#### 4. 2. 2. Molecular basis of PKR transcription

***In mammals.*** PKR is regulated in a coordinated fashion by its transcription factor binding sites in the promoter region of the *PKR* gene, which include an ISRE, a kinase-conserved sequence (KCS) response element, as well as a p53 response element<sup>240</sup> (**Figure 12**). KCS and p53 response elements were shown to play a critical role in IFN-independent transcription of mammalian *PKR*. The KCS response element from *PKR* promoter possesses binding sites for the transcription factors Sp1 and Sp3, which cooperatively activate basal PKR expression in the absence of IFN stimulation<sup>241</sup>. In addition, Yoon *et al.* (2009) confirmed with *p53*<sup>-/-</sup> cell lines that p53 induces the expression of PKR under genotoxic stress, regardless of viral infection or IFN treatment. In the same study, luciferase reporter assay showed that p53 activates the *PKR* promoter independently from ISRE<sup>242</sup>. Early work

also provides evidence that IRF1 could induce the expression of PKR in a IFN-independent manner<sup>243,244</sup>, but molecular binding of IRF1 to PKR promoter was not demonstrated.

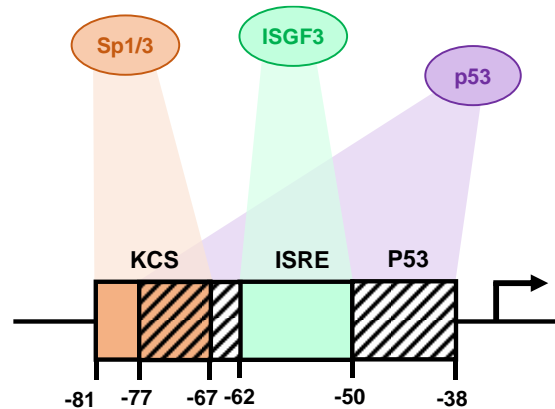


**Figure 12: Promoter region and transcriptional regulation of the human *pkr* gene**

Promoter region of the human *pkr* gene include a KCS response element (orange box), an ISRE response element (green box), and a p53 (striped boxes) response element. The arrow indicates the transcription start. Figure modified from Pindel & Sadler (2011)<sup>240</sup>.

**In fish.** The promoters of fish *pkr* and *pkz* contain ISRE elements, which can be activated by poly(I:C) and type I IFN treatment<sup>239,245</sup>, thereby highlighting the relevance of both PKR and PKZ during IFN-mediated antiviral response. It was also found that Grass carp p53 could bind to *pkr* promoter with high affinity. In addition, when p53 was knocked-down in CIK cells, the mRNA levels of *pkr* were decreased, confirming an effect on *pkr* transcription<sup>246</sup>.

### 4. 3. Antiviral activity

#### 4. 3. 1. Antiviral activity of mammalian PKR

In mammals, knockdown/knockout *in vitro* and *in vivo* studies have shown that PKR constitutes an efficient defense mechanism against a wide array of RNA viruses as well as a few dsDNA viruses. These PKR-sensitive viruses include: positive-sense ssRNA viruses, such as Picornaviruses (*e.g.* Encephalomyocarditis (ECMV), Coxsackievirus)<sup>247,248</sup>, Alphaviruses (*e.g.* Sindbis virus)<sup>249</sup>, Flaviviruses (*e.g.* WNV)<sup>250</sup>; negative-sense ssRNA viruses, such as Paramyxoviruses (*e.g.* Sendai virus)<sup>249</sup> and Rhabdoviruses (*e.g.* vesicular stomatitis virus (VSV))<sup>251</sup>; dsRNA viruses (*e.g.* reoviruses)<sup>252</sup> and dsDNA viruses (*e.g.* Vaccinia virus)<sup>253</sup>. Nonetheless, this phenomenon appears to be virus-dependent and PKR deficiency does not always translate into higher viral replication or higher viral loads, likely due to viral subversion strategies: for instance, PKR-deficient cells infected with flavivirus DENV<sup>254</sup> or paramyxovirus measles virus<sup>255</sup> showed no detectable increase in virus yield and PKR-deficient mouse embryonic fibroblasts (MEFs) infected with flavivirus HCV even displayed reduced titers<sup>256</sup>.

**Table I: Functions of PKR and PKZ described in fish**

Species	Order	Gene	Cloned?	Expression		Antiviral activity	Mechanisms described	References
				Constitutive	Induced			
<b>PKR</b>								
Japanese flounder ( <i>Paralichthys olivaceus</i> )	Pleuronectiformes	PoPKR	Yes	All tissues FEC cell line	Induction upon SMRV infection <i>in vivo</i> and <i>in vitro</i> (FEC)	Scophthalmus maximus rhabdovirus (SMRV)	- Binding to poly(I:C) <i>via</i> dRBMs - Interaction between eIF2 $\alpha$ and PKR - eIF2 $\alpha$ phosphorylation dependent on kinase activity - Inhibition of protein synthesis	199
Crucian carp ( <i>Carassius auratus</i> )	Cypriniformes	CaPKR	Yes	CAB cell line	Induction upon poly(I:C) transfection and rIFN treatment <i>in vitro</i> (CAB) Induction upon rIFN treatment <i>in vitro</i> (CAB)	Grass Carp Reovirus (GCRV)	- Homodimer formation - eIF2 $\alpha$ phosphorylation by both PKR and PKZ - Inhibition of protein synthesis - Apoptosis	239,257
Grass carp ( <i>Ctenopharyngodon idellus</i> )	Cypriniformes	CiPKR	Yes	All tissues CIK cell line	Induction upon injection with UV-inactivated GCHV (Grass carp hemorrhagic virus) <i>in vivo</i> Induction upon GCHV infection and poly(I:C) stimulation <i>in vitro</i> (CIK)		- Binding to poly(I:C) <i>via</i> dRBMs - eIF2 $\alpha$ phosphorylation - Inhibition of translation - Reduced cell viability upon transfection - Modulation of apoptosis-related genes ( <i>bax</i> , <i>bcl-2</i> ) - Interaction with p53 - Interaction with IKKB	238,246,258–262
Zebrafish ( <i>Danio rerio</i> )	Cypriniformes	DrPKR	Yes	All tissues	Induction upon poly(I:C) stimulation <i>in vivo</i> Induction upon cyprinid herpesvirus 3 infection <i>in vivo</i>		- Binding to poly(I:C) <i>via</i> dRBMs - eIF2 $\alpha$ phosphorylation	200,239,263
Rock bream ( <i>Oplegnathus fasciatus</i> )	Perciformes	OfPKR	Yes	All tissues, highest expression in spleen	Induction upon poly(I:C) injection <i>in vivo</i>			264
Nile Tilapia ( <i>Oreochromis niloticus</i> )	Perciformes	OnPKR	Yes	All tissues, but highest expression in HK and liver	Induction upon poly(I:C) and group I and group II IFN stimulation <i>in vivo</i>	Grass Carp Reovirus (GCRV)	- Inhibition of protein synthesis	265
Orange-spotted grouper ( <i>Epinephelus coioides</i> )	Perciformes	EcPKR	Yes	All tissues GS cell line	Induction upon poly(I:C) <i>in vivo</i> in spleen and <i>in vitro</i> (GS cell line)	Red-spotted grouper nervous necrosis virus (RGNNV)		231
Fugu ( <i>Takifugu rubripes</i> )	Tetraodontiformes	TrPKR1 TrPKR2	Yes	All tissues, but highest expression in skin	fPKR1: No induction upon poly(I:C) <i>in vivo</i> fPKR2: Induction upon poly(I:C) <i>in vivo</i>		- Inhibition of protein synthesis - Activation of NF- $\kappa$ B luciferase reporter	266

## Introduction – Chapter 2

Chinook salmon ( <i>Oncorhynchus tshawytscha</i> )	Salmoniformes	OtPKR	No	CHSE214	Induction upon IFN $\alpha$ stimulation <i>in vitro</i> (CHSE214)	Proviral activity for IPNV		267
<b>PKZ</b>								
Crucian carp ( <i>Carassius auratus</i> )	Cypriniformes	CaPKZ	Yes	CAB	Induction upon GCHV infection, UV-inactivated GCHV and rIFN treatment <i>in vitro</i> (CAB) Induction upon transfection with poly(dA:dT), poly(dG:dC) and calf genomic DNA	Grass Carp Reovirus (GCRV)	- Binding to Z-DNA - Homodimer formation - eIF2 $\alpha$ phosphorylation by both PKR and PKZ - Inhibition of protein synthesis	198,239
Grass carp ( <i>Ctenopharyngodon idellus</i> )	Cypriniformes	CiPKZ	Yes	All tissues CIK CO	Induction upon stimulation with poly(dA:dT) and poly(dG:dC), poly(I:C) <i>in vivo</i> and <i>in vitro</i> (CIK)		- Binding to Z-DNA <i>via</i> dRBMs - eIF2 $\alpha$ phosphorylation - Inhibition of translation - Apoptosis - Modulation of the activity of IFN promoter in CIK and CO cells - Interaction with IRF3, STING, ZDHHC1, IRF9, STAT2	232,262,268
Zebrafish ( <i>Danio rerio</i> )	Cypriniformes	DrPKZ		All tissues	Induction upon poly(I:C) stimulation <i>in vivo</i> Induction upon cyprinid herpesvirus 3 infection <i>in vivo</i>		- Binding to Z-DNA - Interaction between eIF2 $\alpha$ and PKZ - eIF2 $\alpha$ phosphorylation - Inhibition of translation	200,203,263,269
Rare minnow ( <i>Gobiocypris rarus</i> )	Cypriniformes	GrPKZ		All tissues	Induction upon infection with GCRV and <i>Aeromonas hydrophila</i>			270
Atlantic salmon ( <i>Salmo salar</i> )	Salmoniformes	SsPKZ		At least in head kidney TO	Induction upon stimulation with poly(I:C) <i>in vivo</i> (head kidney) Induction upon stimulation with IFN in TO cells		- eIF2 $\alpha$ phosphorylation - Inhibition of translation	229

### 4.3.2. Antiviral activity of fish PKR and PKZ

In fish, studies focusing on the antiviral activity of PKR and PKZ are scarce (**Table II**): Liu *et al.* (2011) showed that overexpression of either Grass carp CiPKR or CiPKZ lead to inhibition of GCRV; this antiviral activity was enhanced when both kinases were overexpressed <sup>239</sup>. Conversely, knockdown assays of either or both kinases made fish cells more permissive to virus infection, although the antiviral ability of CiPKZ seemed weaker than CiPKR, which correlated with its lower ability to phosphorylate eIF2 $\alpha$  <sup>239</sup>. Recent overexpression studies showed that overexpressed Nile tilapia OnPKR leads to reduced GCRV in FHM cells <sup>265</sup>. Similar results were obtained with Orange spotted grouper EcPKR in GS cells infected with RGNNV <sup>231</sup>. Interestingly, although chemical inhibition of rainbow trout OmPKR in RTG-2 and RTGill resulted in increased VHSV N mRNA levels, it did not have any impact on viral titers in comparison to untreated cells <sup>271</sup>. An *in vivo* study in zebrafish larvae infected with Cyprinid herpes virus 3 (CyHV-3) also showed that *pkz* KO, *pkz* KO or *pkz/pkr* double KOs had no drastic effect on viral levels <sup>263</sup>.

Curiously, treatment with pharmaceutical inhibitors of PKR resulted in reduced IPNV titers in CHSE214 <sup>267</sup>. Although IPNV infection in CHSE214 induces phosphorylation of eIF2 $\alpha$  and protein synthesis inhibition, PKR transcripts and proteins were not induced over the course of IPNV infection <sup>267,272</sup>. It was suggested that host protein translation inhibition might be part of IPNV strategy to evade the host antiviral response.

## 5. Underlying molecular mechanisms of PKR/PKZ antiviral action

The following section summarizes the main functions of PKR and PKZ in a context of viral infection and shed light on the underlying molecular mechanisms identified in mammals and in fish, including activation of PKR/PKZ, PKR/PKZ-mediated phosphorylation of eIF2 $\alpha$ , PKR/PKZ-dependent activation of apoptosis and their role(s) in transduction of inflammatory and IFN responses.

**Figure 13** provides an overview of the mechanisms of action of PKR identified in mammals during viral infections.

**Table II: Antiviral activity of fish PKR and PKZ**

Species	PKR/PKZ gene	Cells	Virus	Virus family and type	Viral titer	Hypothetical mode of action	References
<b>Overexpression</b>							
Crucian carp ( <i>Carassius auratus</i> )	CaPKR CaPKZ	CAB	Grass Carp Reovirus (GCRV)	<i>Reoviridae</i> Aquareovirus dsRNA, non-enveloped	Reduced titer	Cooperative role of CaPKR and CaPKZ to phosphorylate eIF2 $\alpha$	239
Nile Tilapia ( <i>Oreochromis niloticus</i> )	OnPKR	FHM	Grass Carp Reovirus (GCRV)	<i>Reoviridae</i> Aquareovirus dsRNA, non-enveloped	Reduced titer	Inhibition of protein synthesis	265
Orange-spotted grouper ( <i>Epinephelus coioides</i> )	EcPKR	GS	Red Grouper Nervous Necrosis Virus (RGNNV)	<i>Nodaviridae</i> Betanodavirus (+)-ssRNA, non-enveloped	Reduced titer Reduced viral transcription	PKR-mediated induction of ISG	231
Japanese flounder ( <i>Paralichthys olivaceus</i> )	PoPKR	FEC	Scophthalmus maximus rhabdovirus (SMRV)	<i>Rhabdoviridae</i> Scophrhavirus (-)-ssRNA, enveloped	Reduced titer	Phosphorylation of eIF2 $\alpha$	199
<b>Knock-down or chemical inhibition</b>							
Crucian carp ( <i>Carassius auratus</i> )	CaPKR CaPKZ	CAB	Grass Carp Reovirus (GCRV)	<i>Reoviridae</i> Aquareovirus dsRNA, non-enveloped	Increased titer	Cooperative role of CaPKR and CaPKZ to phosphorylate eIF2 $\alpha$	239
Chinook salmon ( <i>Oncorhynchus tshawytscha</i> )	OtPKR	CHSE2 14	Infectious Pancreatic Necrosis Virus (IPNV)	<i>Birnaviridae</i> Aquabirnavirus dsRNA, non-enveloped	Reduced viral titer following chemical inhibition of PKR	Reduced apoptosis	267
Rainbow trout ( <i>Oncorhynchus mykiss</i> )	OmPKR	RTG-2 RTGill	Viral Hemorrhagic Septicemia Virus (VHSV)	<i>Rhabdoviridae</i> Novirhabdovirus (-)-ssRNA, enveloped	Increased viral transcription but titre not different from control	PKR-mediated induction of IFN and ISG	271
Zebrafish ( <i>Danio rerio</i> )	DrPKR	<i>In vivo</i> (larvae)	Cyprinid Herpesvirus 3 (CyHV-3)	<i>Alloherpesviridae</i> Cypinivirus dsDNA, enveloped	PKR: No difference with WT PKZ KO: Higher viral levels at 1-4dpi but not at 5dpi	-	263

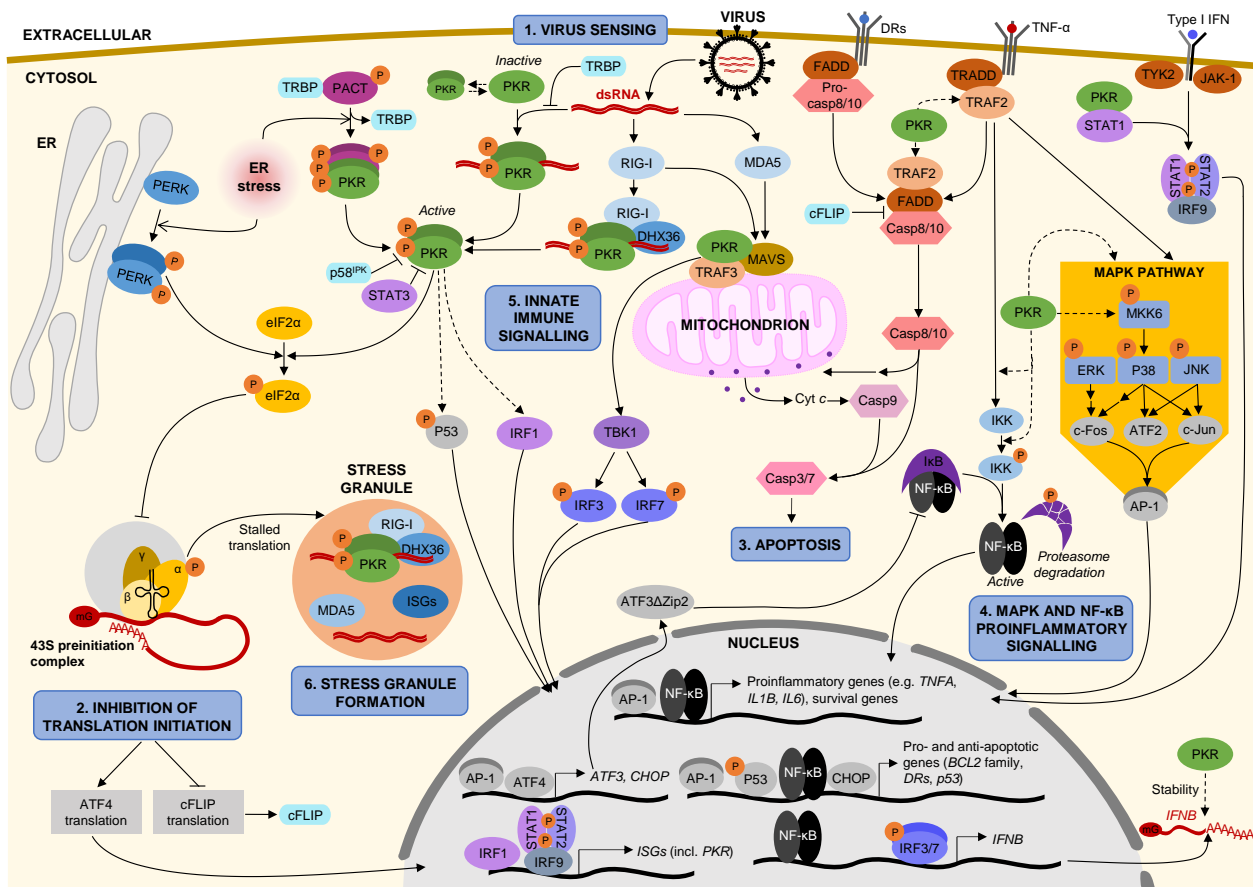


**Figure 13: Overview of mammalian PKR mechanisms of action during viral infection**

**(1) Virus sensing.** PKR can be activated either by virus-derived double-stranded RNA (dsRNA) or protein activator of PKR (PACT) in response to endoplasmic reticulum (ER) stress (misfolded proteins), which can be caused by virus infection. DEAH-box helicase 36 (DHX36)-RIG-I complex also facilitates PKR activation upon dsRNA exposure. PKR activation is modulated by cellular inhibitors p58<sup>IPK</sup> (58-kDa inhibitor of protein kinase) which inhibits PKR autophosphorylation, and transactivation response RNA-binding protein (TRBP), which sequesters dsRNA and PACT.

**(2) Inhibition of translation initiation.** Both PKR-like ER kinase (PERK) and activated PKR can phosphorylate eukaryotic translation initiation factor 2  $\alpha$  (eIF2 $\alpha$ ). This results in the inhibition of translation initiation and a global shutdown of protein synthesis.

**(3) Activation of apoptosis.** PKR also triggers apoptosis *via* several pathways: inhibition of protein synthesis leads to (1) upregulation of transcription factors such as activating transcription factor 4 (ATF4), ATF3 and C/EBP homologous protein (CHOP) and activation of p53, resulting in the induction of proapoptotic genes, including B-cell lymphoma 2 (*BCL2*) family and death receptors (*DRs*); (2) downregulation of antiapoptotic regulators, such as cellular FADD-like interleukin (IL)-1 $\beta$ -converting enzyme inhibitory protein (cFLIP). Apoptosis is triggered by a signaling cascade involving FAS-associated protein with death domain (FADD), tumor necrosis factor (TNF) receptor type 1-associated death domain (TRADD), TNF receptor-associated factor 2 (TRAF2), resulting in activation of the caspase (casp) cascade, involving upstream initiator casp8, 10 and 9 and downstream executioner casp3 and 7.

**(4) MAPK and NF- $\kappa$ B proinflammatory signaling.** PKR stimulates mitogen-activated protein kinases (MAPK) mediated proinflammatory signaling pathway involving MAPK kinase 6 (MKK6), extracellular signal-regulated kinases (ERK), c-Jun N-terminal kinases (JNK), p38 and their downstream targets such as c-Fos, c-Jun, which form together activator protein 1 (AP-1) and ATF2. PKR also activates the nuclear factor- $\kappa$ B (NF- $\kappa$ B) signaling pathway by acting upstream of inhibitor of NF- $\kappa$ B (I $\kappa$ B) kinase (IKK) and/or by recruiting signal transducers such as members of the TRAF family. Both pathways converge on the induction of proinflammatory genes, such as *TNFA*, *IL6* and *IL1B*.

**(5) Innate immune signaling.** PKR interacts with cytosolic nucleic acid sensors retinoic acid-inducible gene I (RIG-I) and melanoma differentiation-associated protein 5 (MDA5). This enhances downstream signaling pathways involving mitochondrial antiviral signaling protein (MAVS), TRAF3, TANK-binding kinase 1 (TBK1), interferon regulatory factor 1 (IRF1), IRF3, IRF7, resulting in induction of interferon (IFN). Subsequent activation of the JAK/STAT cascade occurs involving janus kinase 1 (JAK1), tyrosine kinase 2 (TYK2), signal transducer and activator of transcription 1 (STAT1), STAT2 and IRF9. This eventually leads to the induction of IFN-stimulated genes (ISGs). PKR is also involved in stabilising of *IFNB* transcripts *via* an unknown mechanism.

**(6) Formation of stress granules.** Stalled protein synthesis promotes the formation of stress granules, which function as a platform for dsRNA sensing and for potentiating proinflammatory and IFN responses. Solid arrows represent direct interactions or actions; while dashed arrows indicate speculated interactions or unknown mechanisms.

## 5. 1. Activation of PKR and PKZ

### 5. 1. 1. PKR latent state

Protein kinases have been described as molecular switches with a default latent state (“off”), which is switched to an active state (“on”) in response to a signal. Two distinct non-mutually exclusive regulatory mechanisms have been identified: (1) pseudosubstrate inhibition, in which a portion from the kinase itself or another protein hides the protein substrate-binding site; (2) inactive conformation, in which the key active site residues are shifted from their functional positions<sup>273</sup>. Transition from inactive to active state requires phosphorylation, removal of inhibitory domains or subunits, and/or association with other domains or subunits<sup>273</sup>.

In the cytoplasm, mammalian PKR is predicted to exist in a weak monomer-dimer equilibrium, the latent monomeric state being predominant<sup>207,274</sup>. It has been suggested that latent PKR is locked into an inactive state *via* an auto-inhibition mechanism<sup>275</sup>. The proposed mechanism relies on direct blockade of the activation loop in the kinase domain by dsRBM2, keeping PKR in a closed conformation, which is released upon binding to dsRNA<sup>275,276</sup>. Nuclear magnetic resonance (NMR) studies also confirmed that dsRBM2 is able to bind to the kinase domain<sup>277</sup>.

However, this autoinhibition model has been challenged over the past 20 years. Indeed, PKR can be activated at high protein concentrations in the absence of dsRNA<sup>274</sup>. Moreover, kinetic analysis of ATP binding to PKR revealed that ATP can interact with the unphosphorylated enzyme, suggesting that access to the activation loop is not blocked<sup>278</sup>. Furthermore, atomic force microscopy images of latent PKR showed that PKR spontaneously adopts different conformations, ranging from closed and compact arrangements to almost fully opened conformations<sup>278</sup>.

However, very recent studies support the initial auto-inhibition model *via* autophosphorylation mechanisms: Wang *et al.* (2017) proposed a model, in which constitutive phosphorylation of Ser33 and/or Thr42 residues in dsRBM1 of human PKR restrains conformational changes required for PKR activation<sup>279</sup>. Another study also identified Ser6 and Ser97, located 3 amino acids upstream of dsRBM1 and dsRBM2 in human PKR, as negative regulators of PKR activation: mutational analysis suggested that the phosphorylation of these residues helps maintain PKR in a closed conformation and participates in PKR regulation<sup>280</sup>. Nonetheless, these residues are poorly conserved in the PKR sequences of other organisms including fish, chicken and amphibians, which raises the question of the conservation of this regulatory mechanism between species.

Regardless of this autoinhibition model, PKR requires an activation step to be fully catalytically functional, in a similar fashion to other eIF2 $\alpha$  kinases. For PKR, activation can either be mediated by binding to dsRNA or by protein-protein interactions.

### 5. 1. 2. Double-stranded RNA-mediated activation

**Mammalian PKR.** The canonical and best-characterized substrate and activator of PKR is dsRNA, which is primarily generated during the replication cycle of RNA viruses. PKR activation is triggered *via* dsRNA binding to its N-terminal dsRBMs. Interestingly, activation by dsRNA is length-dependent and requires a minimum of 30 bp<sup>281</sup>. NMR studies further showed that dsRBM1 has a dominant role in molecular recognition of short dsRNA sequences (20 bp), whereas both motifs participate significantly in binding to longer dsRNA sequences (> 30 bp) thereby allowing PKR activation<sup>282</sup>.

RNA binding results in activation of PKR kinase activity, but the detailed mechanisms of PKR activation have not been fully elucidated yet. Several authors have proposed a model where activation requires both dimerization and autophosphorylation steps<sup>211,283</sup>. In this model, dsRNA serves as a scaffold to bind PKR monomers, thereby increasing the local concentration and facilitating dimerization<sup>283</sup>. dsRNA binding results in back-to-back homodimer formation which is mediated by the N-terminal lobe of the kinase domain<sup>211</sup> (**Figure 9D**). PKR dimerization induces conformational changes that allows PKR to catalyze *in trans* (*i.e.* intermolecularly), the phosphorylation of the activation loop at critical conserved threonine residues (Thr446 and Thr451 in human PKR) of another ‘substrate’ PKR (as a monomer or dimer) docked in a front-to-front geometry<sup>283</sup>. It was proposed that the autophosphorylation of PKR kinase domain enhances dimer stability<sup>274,284</sup> and reduces dsRNA binding affinity<sup>285</sup>. Eventually, the phosphorylated PKR dimer dissociates from dsRNA<sup>207</sup>. It is believed that PKR dimers represent the active enzyme form that phosphorylates eIF2 $\alpha$ <sup>207</sup>.

**Fish PKR.** In fish, the dsRNA binding capacity of the N-terminal dsRBMs was demonstrated for Japanese flounder PoPKR<sup>199</sup>, zebrafish DrPKR<sup>239</sup> as well as Grass carp CiPKR<sup>258</sup> *via* poly(I:C)-sepharose pull-down assays. Interestingly, each dsRBM from Japanese flounder could bind poly(I:C) separately<sup>199</sup> while dsRBMs from Grass Carp needed two or three dsRBMs to cooperate *in vitro*<sup>258</sup>. This activity was never directly demonstrated for other fish PKR but the systematic presence of double or triple dsRBMs<sup>200</sup> along with functional analysis suggest that fish PKR activation is similar to its mammalian counterparts.

**Fish PKZ.** The N-terminal regulatory domain of PKZ binds tightly and specifically to Z-DNA and Z-dsRNA, resulting in its activation through homodimerization and autophosphorylation<sup>203,221,239</sup>. Unlike dsRNA, which is produced during the replication cycle of many viruses, Z-DNA/RNA are non-canonical nucleic acids, whose biological functions are still unclear<sup>220</sup>. Left-handed Z-DNA is a higher energy conformation of the dsDNA helix. Unlike canonical right-handed B-DNA, Z-DNA

adopts a zigzag arrangement of the phosphate backbone, which can be stabilized by negative supercoiling or the binding of a conformation-specific protein<sup>286</sup>. Importantly, in contrast to the low-energy forms of right-handed duplexes of RNA and DNA, which are structurally different from each other, Z-RNA adopts a very similar conformation to Z-DNA<sup>287</sup>, which can also be recognized by Z $\alpha$  domains<sup>288</sup>. As a consequence, PKZ might bind Z-dsDNA as well as Z-dsRNA, although the natural (viral) substrate recognized by PKZ *in vivo* has not been identified yet. Nonetheless, the involvement of PKZ in detection of viral nucleic acids during infections is strongly supported by the capacity of the Z $\alpha$  protein encoded by the cyprinid herpesvirus 3 (CyHV-3) ORF112 to outcompete the binding of PKZ to Z-DNA, suggesting that ORF112 acts as an inhibitor of PKZ<sup>289</sup>.

### 5. 1. 3. Alternative activation pathways

Other studies have suggested that PKR can be activated in the absence of dsRNA binding, under specific conditions, including ER stress and artificially high concentrations of PKR.

#### 5. 1. 3. 1. Protein activator of PKR (PACT)

**Mammalian PKR.** Mammalian PKR can be activated in a seemingly dsRNA-independent manner by protein activator of PKR (PACT) in response to diverse stress stimuli including serum starvation, peroxide, arsenite or thapsigargin (ER stress) treatment<sup>206,290</sup>. Exposure to these stress stimuli leads to PACT phosphorylation and activation<sup>206,290,291</sup>. Once activated, PACT interacts with PKR through its dsRBMs, leading to PKR activation<sup>290</sup>. PACT binding to the same region as dsRNA is believed to result in similar conformational changes required for PKR activation<sup>292</sup>. Although the primary signals inducing endogenous PACT-mediated PKR activation remain unclear, it is possible that PACT potentiates PKR activation in viral infections, insofar as viral proteins induce ER stress<sup>293</sup>.

**Fish PKR.** Fish orthologs of mammalian PACT have been reported in the literature<sup>259,294</sup>. PACT-PKR interaction was also described *in vitro* in HEK293T transfected with Grass Carp CiPACT and CiPKR<sup>259</sup>. Furthermore, similarly to their mammalian counterparts, overexpression of CiPACT increased the phosphorylation of CiPKR. Taken together, these results suggest that PACT-mediated activation of PKR is likely functional in fish.

#### 5. 1. 3. 2. High protein concentrations

**Mammalian PKR.** PKR was found in a phosphorylated (*i.e.* activated) state when overexpressed in *E. coli*<sup>295</sup>. Although the presence of dsRNA or structured ssRNA of bacterial origin could not be ruled out, it was suggested that the high intracellular concentration of PKR was enough to induce dimerization and subsequent autophosphorylation. This hypothesis was later supported by *in vitro* studies<sup>274</sup>, which showed that at high protein concentrations, PKR could dimerize,

autophosphorylate, and catalyze eIF2 $\alpha$  phosphorylation<sup>207,274,295</sup>. Similarly, PKR autophosphorylation was observed when incubated with heparin<sup>296,297</sup> or other polyanions (reviewed by García *et al.* (2006)<sup>75</sup>). Although such concentrations are unlikely to happen in physiological conditions, it was suggested that PKR activation is initiated by monomers coming into close proximity in a similar manner to dimerization of PKR mediated through dsRNA binding<sup>274</sup>.

**Fish PKR.** A few observations suggest that activation of fish PKR at high concentrations might occur: firstly, Xu *et al.* (2018) have reported that only catalytically inactive mutated Crucian carp CaPKR could be detected by Western blot when the proteins were overexpressed in EPC cells<sup>257</sup>, likely because of the translational shut-off induced by active PKR; secondly, overexpression of both mammalian and fish PKR could induce apoptosis in transfected cells<sup>257,298</sup>. Altogether, these results suggest that overexpressed fish PKR are seemingly functionally active even in the absence of dsRNA substrate.

### 5. 1. 3. 3. Caspases

Mammalian PKR can also be activated during apoptosis triggered by diverse stimuli (including TNF  $\alpha$ , anti-FAS and staurosporine) *via* proteolysis at Asp251 by caspases (3, 7 and 8). This cleavage-mediated release of PKR kinase domain leads to eIF2 $\alpha$  phosphorylation resulting in translation inhibition during apoptosis<sup>299</sup>. It was suggested that inhibition of *de novo* protein synthesis during apoptosis might be of importance to prevent inadvertent synthesis of proinflammatory molecules allowing safe clearance once phagocytosed<sup>300</sup>. Whether this phenomenon exists with fish PKR/PKZ is currently not known.

## 5. 2. Phosphorylation of eIF2 $\alpha$ and inhibition of protein synthesis

### 5. 2. 1. Mammalian PKR

Like all members of the eIF2 $\alpha$  kinase family, activated PKR catalyzes the phosphorylation of eIF2 $\alpha$  (on Ser51 in human eIF2 $\alpha$ ) resulting in inhibition of protein synthesis. eIF2 $\alpha$  is the main regulatory subunit of the eIF2 complex, which consists of 3 subunits (eIF2 $\alpha$ , eIF2 $\beta$ , and eIF2 $\gamma$ ). Under normal stress-free conditions, the eIF2 complex plays a key role in the initiation of mRNA translation: eIF2 forms a ternary complex by binding the initiator tRNA (Met-tRNA<sub>i</sub>) in a GTP-dependent manner. The eIF2-tRNA complex then joins the 40S ribosome subunit, which forms the 43S pre-initiation complex with other initiation factors<sup>301,302</sup>. As initiation proceeds, GTP on eIF2 is hydrolyzed upon binding of the Met-tRNA<sub>i</sub> anticodon with the AUG start codon. This results in the dissociation of the eIF2-GDP complex from the 40S ribosome subunit. Inactive eIF2-GDP complexes are continuously

recycled for further rounds of mRNA translation initiation in a process catalyzed by the GTP exchange factor eIF2B. Eventually, this results in the return of eIF2 to its active form<sup>301,302</sup>.

Under stress conditions, Ser51-phosphorylated eIF2 $\alpha$  blocks the eIF2B-mediated exchange of GDP by sequestering eIF2B into a tight complex. This inhibition of eIF2B activity results in a deficient eIF2 recycling preventing formation of new 43S pre-initiation complex. This leads to the attenuation of protein synthesis, thereby limiting the production of virions in the infected cells<sup>75,201</sup> (**Figure 14**).

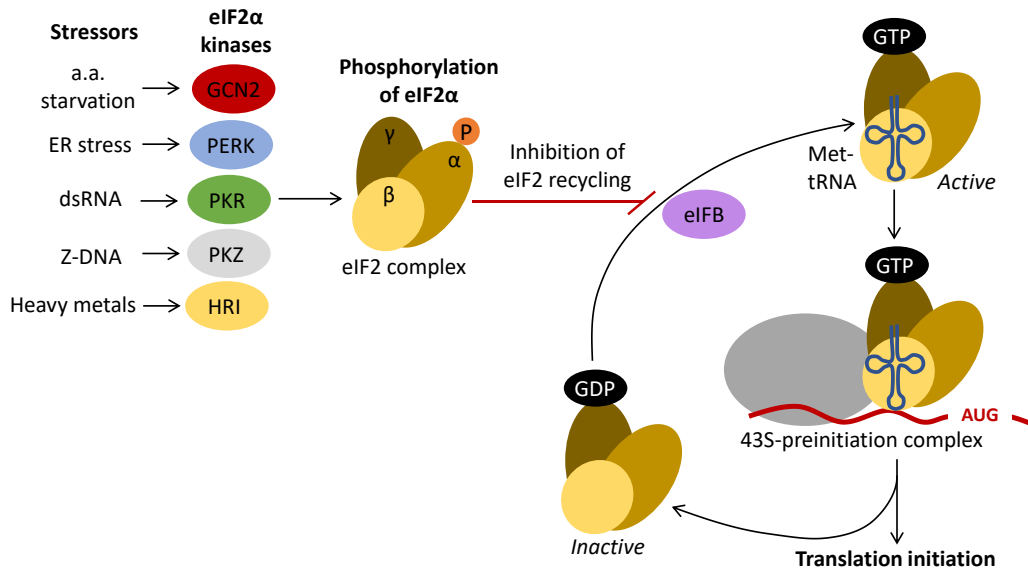


**Figure 14: Molecular mechanism of inhibition of protein translation initiation via phosphorylation of eIF2 $\alpha$  in response to environmental stresses**

### 5. 2. 2. Fish PKR

Inhibition of *de novo* protein synthesis is probably one of the best studied functions of fish PKR (**Table I**). This function has been established with *in vitro* overexpression studies combined with luciferase assays. It was reported that Japanese flounder PoPKR<sup>199</sup>, Crucian carp CaPKR<sup>239</sup>, Grass carp CiPKR<sup>238,258</sup>, Fugu TrPKR1 and TrPKR2<sup>266</sup>, and Nile tilapia OnPKR<sup>265</sup> limited the activity of a luciferase reporter gene upon transient co-transfection in mammalian and/or fish cells, and that this function was dependent on a functional kinase domain.

Mechanistically, it was further demonstrated that fish PKR could catalyze the phosphorylation of eIF2 $\alpha$ . For instance, eIF2 $\alpha$  phosphorylation was increased in FEC cells transiently transfected with wildtype PoPKR and subsequently infected with *Scophthalmus maximus* rhabdovirus (SMRV); it was not the case with the catalytically inactive mutant K421R, suggesting that eIF2 $\alpha$  phosphorylation results from the catalytic activity of PoPKR<sup>199</sup>. Likewise, overexpression of wildtype CaPKR but not catalytically inactive mutant CaPKR in EPC cells resulted in phosphorylation of eIF2 $\alpha$ <sup>257</sup>. Similar results were obtained with Grass carp CiPKR<sup>258</sup> and zebrafish DrPKR<sup>200</sup>. Additional evidence comes

from co-IP assays, which confirmed that Japanese flounder PoPKR could physically interact with eIF2 $\alpha$  in fish cells infected with SMRV, resulting in enhanced levels of phosphorylated eIF2 $\alpha$  bound to catalytically active PoPKR compared to catalytically inactive mutant<sup>199</sup>.

Knockdown studies further corroborate the hypothesis that fish PKR is able to phosphorylate eIF2 $\alpha$ : knockdown of Grass carp CiPKR leads to reduced levels of phosphorylated eIF2 $\alpha$  upon poly(I:C) stimulation in CIK cells<sup>259,261</sup>. Similarly, knockdown of Crucian carp CaPKR and Japanese flounder PoPKR also resulted in inhibition of eIF2 $\alpha$  phosphorylation upon GCRV and SMRV infections, respectively<sup>199,239</sup>, thereby confirming that eIF2 $\alpha$  phosphorylation is mediated by PKR.

### 5. 2. 3. Fish PKZ

In a similar fashion to PKR, fish PKZ has the capacity to inhibit protein synthesis and this function requires a functional kinase domain, as described for zebrafish DrPKZ<sup>203,269</sup>, Grass carp CiPKZ<sup>268</sup> and Atlantic salmon SsPKZ<sup>229</sup>. Interestingly, Liu *et al.* (2011) also showed that co-transfection of both CaPKR and CaPKZ potentiated this effect using the same reporter system<sup>239</sup>, suggesting that fish PKR and PKZ may act in a cooperative manner.

PKZ was also shown to phosphorylate eIF2 $\alpha$ : Grass carp CiPKZ phosphorylated eIF2 $\alpha$  *in vitro* when incubated with Z-DNA but not poly(I:C)<sup>268</sup>. Wu *et al.* (2016) also confirmed Grass carp CiPKZ capacity to phosphorylate eIF2 $\alpha$  *in cellulo*: CIK cells transiently transfected with CiPKZ displayed increased levels of phosphorylated eIF2 $\alpha$ , contrary to catalytically inactive mutant<sup>262</sup>. Similarly, Atlantic Salmon SsPKZ was also able to phosphorylate recombinant human eIF2 $\alpha$  and rabbit eIF2 *in vitro* but not the non-phosphorylatable mutant eIF2 $\alpha$ <sup>229</sup>. Zebrafish DrPKZ and Crucian carp CaPKZ were found to interact with endogenous eIF2 $\alpha$  when overexpressed in mammalian cell lines or in yeast leading to its phosphorylation<sup>200,239,269</sup>. Similarly, knockdown of CaPKZ also led to reduced levels of phosphorylated eIF2 $\alpha$  upon GCRV infection, although to a lesser extent than CaPKR<sup>239</sup>.

## 5. 3. PKR-mediated activation of apoptosis

PKR is known for limiting viral replication not only through inhibition of global protein synthesis (*aka.* viral “shut-off”) but also by inducing apoptosis<sup>303</sup>. The different pathways resulting in apoptosis and its role during viral infections are described in [Chapter 1, Section 4. 5.](#)

### 5. 3. 1. Activation of apoptosis

#### 5. 3. 1. 1. Apoptosis triggered by PKR expression

*In mammals.* Several studies have reported that overexpression of PKR is sufficient to induce apoptosis in transfected mammalian cells<sup>298,304–306</sup>. Furthermore, it was reported that *Pkr*<sup>-/-</sup> MEFs and

macrophages were resistant to apoptosis in response to dsRNA, TNF- $\alpha$ , or LPS<sup>307–309</sup>. The role of PKR in apoptosis is also supported by transcriptional analysis of HeLa cells overexpressing wild-type PKR but not catalytically inactive mutant: pro-apoptotic genes (*e.g.* *CASP9*) were upregulated in PKR-expressing cells while anti-apoptotic genes (*e.g.* heat-shock protein *HSP70*, that inhibits mitochondrial release of cytochrome *c* and blocks procaspase-9 recruitment), were downregulated<sup>310</sup>.

***In fish.*** Similar results were obtained in fish cell lines transfected with fish PKR: for instance, overexpression of wildtype Crucian carp CaPKR, but not catalytically inactive mutant, was sufficient to induce apoptosis in EPC cells<sup>257</sup>. A comparable response was observed for both Grass carp CiPKR and CiPKZ when overexpressed in CIK cells<sup>238,258,262</sup>. Overexpression of Grass carp CiPKR also led to upregulation of pro-apoptotic *bax* and down-regulation of anti-apoptotic *bcl-2* while its knockdown resulted in opposite effects<sup>259</sup>.

### 5. 3. 1. 2. Activation of caspase cascade

***In mammals.*** Mechanistically, a few studies showed that PKR was able to activate the FADD/caspase-8/caspase-3 pathway, independently from FAS/FASL and TNF- $\alpha$ /TNFR1 interaction<sup>308,311–313</sup>. However, to date, the precise connection between PKR and FADD is still unclear. PKR overexpression can also trigger the intrinsic pathway *via* BAX translocation into the mitochondria, subsequent release of cytochrome *c* to the cytoplasm and activation of caspase 9<sup>314</sup>. However, the same study demonstrated that caspase 9 activation occurs downstream of caspase 8 and that this pathway is dispensable to induce PKR-mediated apoptosis<sup>314</sup>. Consistently, poly(I:C) transfection resulted in reduced levels of both activated caspases 8 and 9 in *PKR*<sup>-/-</sup> HeLa cells, compared to wildtype cells<sup>249</sup>. In contrast, cleavage of caspases 3/7 and 9, but not caspase 8 was observed in macrophages stimulated with LPS, suggesting that PKR is a critical mediator of the intrinsic apoptotic pathway in these experimental conditions<sup>309</sup>. These results suggest that PKR is involved in different apoptosis pathways depending on the cell types and the stimuli.

***In fish.*** In fish, caspases 8 and 9 were also activated in EPC transfected with Crucian carp CaPKR<sup>257</sup>. Further research is needed to determine which apoptotic pathways are triggered by fish PKZ.

### 5. 3. 2. Underlying mechanism: PKR/eIF2 $\alpha$ mediated apoptosis

Several studies have demonstrated that PKR-mediated apoptosis was a process dependent on eIF2 $\alpha$  phosphorylation *via* induction of specific subsets of pro-apoptotic genes and inhibition of anti-apoptotic regulatory factors.

### 5. 3. 2. 1. PKR/ATF4/CHOP pathway

**Mammalian PKR.** Although the translation of most cell mRNAs is inhibited by PKR-mediated eIF2 $\alpha$  phosphorylation, it also induces the translation of specific host genes involved in the stress response, such as *ATF4*, *ATF3* and C/EBP homologous protein (*CHOP*)<sup>310,315</sup>. Under normal conditions, translation of *ATF4* mRNAs is limited by the presence the upstream short ORFs in their 5'-UTR, which attract ribosomes. Alternatively, under stress conditions, limited number of 43S preinitiation complexes leads to longer ribosomal scanning along the *ATF4* transcript, resulting in re-initiation of translation at the *ATF4* coding region<sup>316</sup>. The resulting elevated translation of *ATF4* mRNA promotes transcriptional upregulation of a subset of genes involved in cellular stress adaptation, including *ATF3* and *CHOP*, in a sequential manner<sup>317</sup>. *CHOP* is known for regulating the expression of many anti-apoptotic and pro-apoptotic genes, including genes encoding the BCL-2-family proteins and the death receptors DR4 and DR5, which trigger the intrinsic and extrinsic apoptotic pathways<sup>318</sup>.

Current understanding of eIF2 $\alpha$ /ATF4/CHOP signaling pathway comes largely from studies on ER stress and amino acid starvation involving the eIF2 $\alpha$  phosphorylation by PERK and GCN2, respectively. Nevertheless, it has been shown that PKR also can induce apoptosis under ER stress conditions through PACT leading to the activation of eIF2 $\alpha$ /ATF4/CHOP signaling pathway in a PERK-independent manner<sup>206</sup>. Furthermore, ATF3 was reported to be induced upon overexpression of wildtype PKR but not the catalytically inactive mutant<sup>310</sup>. Further investigation revealed that the absence of ATF3 decreased PKR-induced apoptosis when PKR was overexpressed in cell lines<sup>310</sup>. Interestingly, PKR overexpression also upregulated the expression of an alternative spliced isoform of ATF3, called ATF3 $\Delta$ Zip2, which promotes apoptosis *via* competition for the binding with the 65-kDa subunit of the NF- $\kappa$ B complex<sup>310</sup>. ATF3 $\Delta$ Zip2 was reported to suppress the NF- $\kappa$ B-dependent transcription of survival genes, referred to as cellular inhibitors of apoptosis, thereby indirectly making the cells more sensitive to apoptosis<sup>319</sup>.

Viral infections can also induce apoptosis through the eIF2 $\alpha$ /ATF4/CHOP pathway (reviewed by Liu *et al.* (2020)<sup>293</sup>), although the kinase which phosphorylates eIF2 $\alpha$  may vary from one virus to another. While many studies have reported the activation of the PERK/eIF2 $\alpha$ /ATF4/CHOP pathway in virus-infected cells, a few others mention PKR as one of the kinase activators. For instance, knockdown of both PKR and PERK inhibited *CHOP* upregulation and apoptosis in infectious bronchitis virus-infected cells<sup>320</sup>.

**Fish PKR.** The PKR/eIF2 $\alpha$ /ATF4/CHOP axis has not been directly investigated in fish. However, unique orthologs of *atf3*, *atf4* and *chop* are present in most fish genomes, suggesting that this pathway is might be functional in these organisms. Several studies have also reported the activation the

eIF2 $\alpha$ /ATF4/CHOP pathway in case of ER stress in Crucian carp<sup>321</sup>, zebrafish<sup>322,323</sup>, Spotted seabass (*Lateolabrax maculatus*)<sup>324</sup>, although in most cases, PERK was identified as the initiator kinase.

### 5. 3. 2. 2. PKR-mediated inhibition of translation promotes apoptosis

**Mammalian PKR.** A few studies suggested that PKR-mediated translational arrest indirectly promotes apoptosis by inhibiting the synthesis of anti-apoptotic regulators. Hsu *et al.* (2004) observed that transfection of bone marrow-derived macrophages (BMDMs) with poly(I:C) followed by LPS treatment inhibited accumulation of anti-apoptotic proteins, such as cellular inhibitor of apoptosis 1 (cIAP1). Consistently, *Pkr*<sup>-/-</sup> BMDMs did not show reduced levels of these proteins<sup>309</sup>. Using eIF2a(S51A) BMDMs, the authors further showed that phosphorylation of eIF2 $\alpha$  was required for maximal induction of apoptosis upon incubation of LPS<sup>309</sup>.

Recently, it was reported that PKR downregulates the expression of cFLIP (cellular FLICE (FADD-like IL-1 $\beta$ -converting enzyme)-inhibitory protein), which is a key anti-apoptotic regulator<sup>249</sup>. Mechanistically, cFLIP isoforms regulate the activation of apoptosis by binding to Caspase 8<sup>325</sup>. Zuo *et al.* (2022) observed that coumermycin A1-mediated activation of PKR led to decreased cFLIP levels, while apoptosis markers including caspases 8 and 9 were upregulated<sup>249</sup>. Conversely, in poly(I:C) transfected wildtype HeLa cells but not *PKR*<sup>-/-</sup> cells, cFLIP expression was decreased and proapoptotic markers became apparent. As cycloheximide, a potent translation inhibitor, displayed a similar response to PKR activation, the authors suggested that PKR-driven inhibition of cFLIP was mediated by translational arrest<sup>249</sup>.

**Fish PKR.** The functional role of cFLIP in PKR-mediated apoptosis has not been investigated in fish. Nevertheless, Sakamaki *et al.* (2015) showed that cFLIP proteins retain a relatively conserved structure across vertebrates<sup>326</sup>. Further investigation revealed that zebrafish cFLIP, along with other non-mammalian cFLIP proteins, had the ability to inhibit the extrinsic apoptotic pathway when overexpressed in mammalian HeLa cells<sup>326</sup>. These results provide evidence that cFLIP proteins have conserved functions from fish to mammals.

### 5. 3. 3. Underlying mechanism: eIF2 $\alpha$ -independent apoptosis

Although most studies have reported that PKR-mediated apoptosis is dependent on eIF2 $\alpha$  phosphorylation, a few others have described the existence of a PKR-mediated but eIF2 $\alpha$ -independent pathway triggering apoptosis. Von Roretz & Gallouzi (2010) have shown that PKR-mediated activation of the FADD/caspase 8/caspase 3 pathway after staurosporine treatment (ER stressor) does not require the phosphorylation of eIF2 $\alpha$ <sup>313</sup>. Similarly, Hsu *et al.* (2004) reported the existence of a residual PKR-mediated apoptotic response in eIF2a(S51A) macrophages stimulated with LPS,

suggesting the existence of an alternative PKR-dependent pro-apoptotic pathway triggered by specific conditions<sup>309</sup>. It was later shown that PKR can also induce apoptosis independently of eIF2 $\alpha$  phosphorylation *via* activation of transcription factors NF- $\kappa$ B and p53 (reviewed by García *et al.* (2006)<sup>75</sup>).

NF- $\kappa$ B controls the transcription of a large number of genes involved in immune and inflammatory responses, cell growth, cell survival<sup>327</sup>. This transcription factor is commonly known for controlling development, survival and inflammation programs, but reports have also linked NF- $\kappa$ B activation to apoptosis<sup>328,329</sup>. Indeed, under certain conditions including viral infections, NF- $\kappa$ B is known for inducing several pro-apoptotic transcription genes (*e.g.* p53, FAS, FASL)<sup>312</sup>. The molecular mechanisms by which PKR activates the NF- $\kappa$ B pathway will be discussed in **Section 5.4.2**.

The p53 tumor suppressor plays a key role in cellular homeostasis through the modulation of cell-cycle arrest, DNA repair, senescence, and apoptosis<sup>242</sup>. Studies using *Pkr*<sup>-/-</sup> MEFs also suggest that PKR might modulate p53 function<sup>330</sup>. Mechanically, *in vitro* studies showed that PKR can associate with p53 resulting in its phosphorylation, activation and stabilization as a transcription factor<sup>331,332</sup>. Since p53 transcription factor activates several effector processes, including the intrinsic apoptotic pathway<sup>333</sup>, it was suggested that PACT/PKR-mediated p53 stabilization could result in apoptosis<sup>334,335</sup>.

#### **5.4. PKR as a transducer of the inflammatory and interferon responses**

In addition to inhibiting cellular translation and promoting apoptosis, PKR is also involved in various signal transduction pathways of the inflammatory and IFN responses, which are both triggered upon viral infection. Activation of those responses leads to cytokine production and promotion of a systemic immune response, thereby preventing spreading of the viral infection. However, in most cases, the precise role of PKR in the activation of these pathways remains elusive.

##### **5.4.1. PKR role in mitogen-activated protein kinase (MAPK) signaling**

MAPKs are a family of highly conserved serine-threonine protein kinases, involved in signal transduction pathways that regulate mitosis, cell differentiation, metabolism and cell death in eukaryotes<sup>336</sup>. The MAPKs can be classified into 3 groups: (1) ERKs, responding primarily to growth factors and mitogens; (2) JNKs, activated by environmental stress stimuli, inflammatory cytokines and growth factors; and (3) p38, strongly activated in response to stress and inflammatory cytokines. During viral infections, the MAPK cascade participates in regulating the immune response and apoptosis<sup>337</sup>. Downstream targets of the MAPK pathway include transcriptional factors such as NF-

$\kappa$ B p65, c-Jun, c-Fos, ATF1/2/6, CHOP, p53, STAT1, STAT3 which modulate the expression of genes involved in proliferation, apoptosis and immune and inflammatory responses<sup>337</sup>.

PKR appears to be involved in the modulation of the MAPK pathway: *Pkr*<sup>-/-</sup> MEFs displayed limited activation of p38 and JNK MAPKs in response to proinflammatory signals including poly(I:C), LPS, IL-1 $\beta$ , and TNF- $\alpha$ <sup>234</sup>. Similarly, *PKR* deficiency in HeLa cells impaired the phosphorylation of JNK and p38 in response to dsRNA, a mutant strain of vaccinia virus or measles virus<sup>338,339</sup>. From a mechanistic point of view, it was discovered that p38 MAPK kinase 6 (MKK6) was efficiently phosphorylated by PKR *in vitro* and that activated PKR was able to directly regulate MKK6 activity *in vivo* upon poly(I:C) treatment<sup>340</sup>. Nevertheless, other studies demonstrated that although dsRNA-mediated activation of the JNK pathway was greatly reduced in cells lacking RNaseL and PKR, activation of the p38 pathway happened in a RNaseL- and PKR-independent manner, suggesting existence of alternative dsRNA-triggered signaling pathways<sup>341</sup>. Taken together, these results suggest a role of PKR in the activation of the MAPK pathway but whether PKR acts directly or indirectly remains to be clarified.

#### 5. 4. 2. PKR role in NF- $\kappa$ B signaling

Besides activating the MAPK signaling pathway, PKR is also known for regulating the inflammatory response by modulating the NF- $\kappa$ B signaling pathway.

In *Pkr*<sup>-/-</sup> MEFs dsRNA treatment was unable to activate NF- $\kappa$ B<sup>342</sup>. Furthermore, *PKR* knock-down assays combined with NF- $\kappa$ B electrophoretic-mobility shift assay and I $\kappa$ B $\alpha$  detection by western blot showed that PKR was required for maximal NF- $\kappa$ B activation upon poly(I:C) transfection as well as during measles virus infection<sup>343,344</sup>. Early studies indicated that PKR could phosphorylate I $\kappa$ B $\alpha$  and induce NF- $\kappa$ B DNA-binding *in vitro*<sup>345</sup>, although evidence for a direct phosphorylation of I $\kappa$ B $\alpha$  by PKR *in vivo* was not demonstrated. It was later discovered that PKR could interact with the IKK complex, leading to the degradation of the inhibitors I $\kappa$ B $\alpha$  and I $\kappa$ B $\beta$  and the concomitant release of NF- $\kappa$ B<sup>345,346</sup>. It is still unclear whether the PKR-driven activation of IKK involves PKR catalytic activity or not, as discrepancies can be found in the literature<sup>309,310,347–349</sup>.

Another hypothesis is that PKR provides a signaling platform *via* its kinase domain, which recruits signaling molecules such as members of the TRAF family, which are well-known signal transducers of the signaling pathway resulting in NF- $\kappa$ B activation<sup>350</sup>. Direct interactions between PKR kinase domain and C-terminal domains of TRAF2, TRAF5 and TRAF6 support this hypothesis<sup>350,351</sup>.

However, to date, the exact relationship between PKR and NF- $\kappa$ B still remains unclear. This is particularly evident in fish models, where the studies tackling this question are scarce. Nevertheless, co-IP and pull-down assays showed that Grass carp CiPKR binds to IKK $\beta$  and that IKK $\beta$  interacts

with IκBα<sup>260</sup>. Furthermore, Fugu TrPKR1 and TrPKR2 induced transcriptional activity of a mammalian NF-κB luciferase reporter upon transfection in HINAE cells<sup>266</sup>. This pathway of action of PKR is therefore likely functional in fish.

### 5. 4. 3. PKR role in type I IFN response

#### 5. 4. 3. 1. PKR potentiates the production of type I IFN

The importance of PKR in the production of type I IFNs has been strongly debated over the years<sup>352</sup> but evidence point to a role of PKR in potentiating the IFN response during viral infections.

Der & Lau (1995) initially showed that the induction of *IFNA* and *IFNB* genes was impaired in PKR-deficient cells upon exposure to several inducers including LPS and encephalomyocarditis virus (EMCV)<sup>247</sup>. In addition, PKR knock-down reduces IFN-β and/or IFN-α induction upon transfection with dsRNA<sup>344,353</sup> but also during infection with a measles virus vaccine strain<sup>343</sup>. In contrast, PKR silencing or inhibition with pharmacological inhibitors both led to increased induction levels of IFN-β upon HCV infection<sup>256</sup>.

Further studies showed that PKR can act as an enhancer for IFN-β production for some but not all viruses. In particular, PKR seems to be not required for IFN-α/β production in cells infected with RIG-I dependent viruses (*e.g.* Sendai virus, influenza virus), while it promotes IFN-α/β production to MDA5-dependent viruses (*e.g.* EMCV, rotavirus, WNV, Semliki Forest virus)<sup>354</sup>.

#### 5. 4. 3. 2. Underlying mechanisms

***In mammals.*** PKR-dependent enhancement of IFN-β induction seems to involve several pathways, including activation of NF-κB and modulation of the RIG-I/MDA5 signaling pathway. PKR may also act as a stabilizer of *IFNB* transcripts and as an activator of the IRF1 pathway.

***Activation of NF-κB.*** During measles virus infection, enhancement of IFN-β induction was shown to involve PKR-dependent NF-κB activation while IRF3 activation was a PKR-independent process<sup>343</sup>. Another study showed that LPS stimulation also led to induction of IFN-β through PKR-mediated activation of NF-κB, resulting in STAT1 phosphorylation<sup>355</sup>. Consistently, chemical inhibition of PKR activity and/or PKR knock-down resulted in inhibition of STAT1 phosphorylation and subsequent STAT-mediated transcription of inflammatory genes, as well as suppression of nuclear factors binding activity to ISRE upon LPS treatment<sup>355</sup>. Nevertheless, as mentioned above, the molecular mechanisms by which PKR activates NF-κB are still poorly understood.

***PKR as an adaptor in RIG-I/MDA5 signaling pathway.*** PKR was shown to directly interact with components of RIG-I/MDA5 signaling pathway, which stimulates IFN-β production. For example, knockdown and co-IP studies showed that upon HCV infection PKR interacts with MAVS and

TRAF3 but not RIG-I leading to a strong induction of protein ISG15 as well as other IRF3-dependent ISGs<sup>356</sup>. These associations required dsRBMs but not the kinase activity of PKR, suggesting that PKR acts as an adaptor protein in this pathway<sup>356</sup>. PKR was also reported to associate with MDA5 and to stimulate IFN- $\beta$  production in a kinase-dependent manner after vaccinia virus infection without eIF2 $\alpha$  phosphorylation requirement<sup>357</sup>. Further investigation revealed that PKR was required for IRF3 phosphorylation and nuclear translocation during vaccinia virus or EMCV infection<sup>357,358</sup>. Furthermore, activation of PKR resulted in IFN- $\beta$  upregulation even in the absence of MDA5, but required MAVS, suggesting that PKR acts as a signal transducer between these two pathway elements<sup>357</sup>. Consistent with this hypothesis, a direct interaction between PKR and MAVS has also been reported<sup>359</sup>.

Direct interaction between PKR and RIG-I during influenza or vaccinia virus infections has also been recently reported<sup>357,360</sup> but PKR activation was not required in RIG-I signaling pathway, suggesting that PKR role downstream of RIG-I might be redundant with other signal transduction proteins.

***PKR as a stabilizer of IFNB transcripts.*** Schulz *et al.* (2010) reported that EMCV infection strongly induced *IFNB* transcription in PKR-deficient cells, but little or no IFN- $\beta$  protein was produced<sup>354</sup>. Similarly, Sen *et al.* reported low IFN- $\beta$  secretion in *Pkr*<sup>-/-</sup> MEFs infected with rotavirus compared to wildtype MEFs although the transcript levels were not reduced<sup>361</sup>. Further investigation revealed that *IFNB* mRNAs produced in EMCV-infected PKR-deficient cells lacked a polyA-tail, suggesting that PKR is required for the integrity and stability of *IFNB* transcripts<sup>354</sup>. However, the regulation of this mechanism by PKR is currently not known.

***PKR as a component of the IRF1 pathway.*** IRF1 regulates the expression of *IFNA* and *IFNB* genes (among others) and is strongly induced upon viral infections<sup>362</sup>. Activation of the promoters of IRF1 and IRF1-induced genes in response to dsRNA exposure was shown to be defective in *Pkr*<sup>-/-</sup> MEFs, suggesting that PKR acts as a signal transducer for IRF1-dependent gene induction by regulating IRF1 promoter<sup>342</sup>. This hypothesis is also supported by another study showing that HCV-mediated inhibition of PKR blocks IRF1 activation and IRF1-dependent gene expression<sup>363</sup>. Nonetheless, the mechanisms by which PKR promotes IRF1 activation are poorly understood.

***In fish.*** Very few studies have focused on PKR role in type I IFN production in fish. Nevertheless, chemical inhibition of PKR (but also PERK) resulted in reduced mRNA levels of *ifn* and *mx1* in RTG2 and RTgill cells upon VHSV infection<sup>271</sup>. It was also reported that *irf1*, *irf3* and *irf7*, *isg15*, *isg56*, and *mx* were all significantly increased in cells overexpressing orange-spotted grouper EcPKR<sup>231</sup>. In the same study, reporter assays further revealed that EcPKR overexpression led to increased activity of *ifnb* and *nfkB* promoters compared to the cells transfected with the empty vector<sup>231</sup>. Similarly, overexpression of Grass carp CiPKZ leads to enhanced activity of *ifn* promoter

in CIK and CO cells, and CiPKZ knock-down results in reduced induction of type I IFN mRNA upon poly(G:C) stimulation <sup>232</sup>. Co-IP assays showed that CiPKZ can separately interact with IRF3, STING, eIF2 $\alpha$ , IRF9, and STAT2 <sup>232</sup>. Taken together, these results suggest that fish PKR and PKZ might be a modulator of the type I IFN response in fish, in a similar fashion to their mammalian counterparts.

## 6. Modulation of PKR during viral infections

Given its critical role in apoptosis and shutdown of the cellular translation machinery, PKR requires fine tuning. Indeed, excessive PKR activity can be detrimental, as is observed in Aicardi-Goutières syndrome patients where mutations in ADAR1 lead to increased levels of endogenous dsRNA, thereby triggering PKR activation and uncontrolled IFN production <sup>364</sup>.

### 6. 1. Autoregulation of PKR

#### 6. 1. 1. Translational autoregulation

Activated PKR negatively regulates its expression *via* the inhibition of protein translation initiation of its own mRNA <sup>365</sup>. Similar results were suggested in fish, as non-functional Crucian carp CaPKR but not catalytically active CaPKR can be detected by western blot in transfected EPC cells <sup>257</sup>.

#### 6. 1. 2. Splice variants

*In mammals.* Splice variants have been reported for mammalian PKR and it was suggested that they might play a role in the regulation of PKR <sup>366–368</sup>. For instance, Li & Koromilas (2001) described a human PKR splice variant (PKR $\Delta$ E7) in which exon 7 was spliced out, resulting in a frame shift and the appearance of a premature stop codon <sup>369</sup>. The truncated 174-aa protein, contained only the dsRBMs and was weakly expressed compared to full length PKR. Interestingly, it exhibits a dominant negative function, as co-expression of both isoforms resulted in inhibition of PKR autophosphorylation and eIF2 $\alpha$  phosphorylation by full length PKR <sup>369</sup>.

*In fish.* In fish, alternative splice variants have also been described in zebrafish DrPKZ <sup>203,269</sup> but the functional characterization of these variants has not been carried out.

### 6. 2. Cellular inhibitors of PKR functions

The list of PKR cellular inhibitors has been extensively reviewed by García *et al.* (2006) <sup>75</sup>. Cellular inhibitors of PKR include: 58-kDa inhibitor of PKR (P58<sup>IPK</sup>), trans-activation response RNA-binding protein (TRBP), 67-kDa-glycoprotein (p67), MDA7, HSP90 and HSP70, among others <sup>75</sup>. The

inhibitory mechanisms of these molecules are diverse and include sequestering dsRNA or PACT away from PKR (*e.g.* TRBP, HSP70), blocking PKR activation step (*e.g.* P58<sup>IPK</sup>) or inhibiting PKR-dependent eIF2 $\alpha$  phosphorylation (*e.g.* p67). However, the role of these inhibitors during viral infections is often unclear and will not be further discussed in this review. Importantly, those inhibitors have been identified in mammalian systems and it is currently not known if their fish counterparts exist and/or function in a similar fashion.

### 6. 3. PKR modulation in stress granules (SGs)

#### 6. 3. 1. SGs in mammals

PKR-mediated inhibition of the translation machinery results in the accumulation of stalled translation pre-initiation complexes, which assemble into cytoplasmic ribonucleoprotein complexes called stress granules (SGs)<sup>370,371</sup>. Importantly, SG formation is induced in response to environmental stress conditions, including heat/cold shock, oxidative and osmotic stress, UV irradiation but also viral infections<sup>372</sup>. Substantial evidence indicates that PKR plays a key role in the SG formation and that SGs potentiate PKR antiviral action. Indeed, SG formation often occurs in an eIF2 $\alpha$  phosphorylation-dependent manner upon viral infections<sup>373</sup>. Overexpression and knockout studies demonstrated that PKR is necessary for formation of SGs upon transfection with poly(I:C) and infection with influenza A virus<sup>374</sup>. The newly formed SGs provide a platform for antiviral signaling pathways by recruiting PKR as well as other RNA-binding proteins (MDA5, RIG-I, OAS) thereby potentiating eIF2 $\alpha$  phosphorylation and promoting transcription of type I IFNs and inflammatory cytokines *via* MAVS-driven activation of IRF3/7 and NF- $\kappa$ B transcription factors<sup>374,375</sup>.

#### 6. 3. 2. SGs in fish

In fish, a recent study showed that SG formation is triggered by PERK and not PKR upon VHSV infection in EPC cells but also RTG-2 and RTGill<sup>271</sup>. This is consistent with previous studies reporting that VHSV infection in EPC cells regulates translation by activating the PERK/eIF2 $\alpha$  pathway rather than by PKR<sup>172</sup>. Similar results were obtained in a GS cell lines upon RGNNV infection: chemical inhibition of PKR had little effect on the formation of SGs, whereas inhibition of PERK significantly limited their formation and decreased eIF2 $\alpha$  phosphorylation<sup>376</sup>. The possible role of fish PKZ in the formation of SG induced by fish viruses has, however, not been studied.

### 6. 4. Viral subversion of PKR and PKZ activation

*In mammals.* PKR subversion mechanisms were recently reviewed for mammalian viruses by Cesaro & Michiels (2021)<sup>377</sup>. These mechanisms are diverse and include PKR degradation through the

proteasomal pathway (*e.g.* Rift valley fever virus NSs), dsRNA sequestration or degradation (*e.g.* Vaccinia virus E3L, reovirus  $\sigma 3$ ), inhibition of PKR dimerization, autophosphorylation and/or kinase function (*e.g.* HCV NS5A), synthesis of PKR pseudosubstrates (*e.g.* Vaccinia virus K3L mimics eIF2 $\alpha$ ), enhancement of eIF2 $\alpha$  dephosphorylation through recruitment of antagonist phosphatases (*e.g.* RSV N) and hijacking of cellular inhibitors (*e.g.* Influenza NP hijacks P58<sup>IPK</sup>)<sup>75,377</sup>.

***In fish.*** No specific studies were conducted in fish. There are a few reports demonstrating the ability of some fish viral proteins to sequester dsRNA, thereby preventing optimal activation of PKR and other dsRNA receptors. For instance, betanodavirus B2 protein is capable of binding its own dsRNA<sup>378,379</sup>, thereby inhibiting dsRNA-dependent responses. The ORF2 protein encoded by the segment 8 of ISAV has been described as a type I IFN suppressor<sup>184</sup> with some dsRNA binding properties<sup>182,380</sup>. Some viruses can also subvert RNA-binding properties of cellular proteins to favor replication in infected cells. This is the case for GCRV, where Grass carp TIA1 binds viral dsRNA, thereby protecting it from degradation and potentially from activating PKR<sup>381</sup>. These are indirect observations and further specific studies would be required to evaluate the limitation of PKR activation. Finally, the vIF2 $\alpha$  protein from *Rana catesbeiana* iridovirus Z is a functional inhibitor of human PKR and zebrafish DrPKR, and probably functions as a pseudosubstrate of PKR<sup>382</sup>.

Concerning PKZ, the Z $\alpha$ -containing ORF112 protein of CyHV-3 was identified as a potent inhibitor of PKZ by competing for Z-DNA binding<sup>289</sup>. The discovery of Z-DNA binding domains in fish viruses suggests host-pathogen antagonism with PKZ, in a similar fashion to poxvirus E3L previously described in mammals as a PKR inhibitor<sup>383</sup>.

## 7. Conclusion

As presented in this review, PKR is a versatile kinase at the crossroads of virus sensing, stress response and innate immune signaling pathways: once activated, it initiates protein translation inhibition and promotes apoptosis, but it also acts as a transducer in the inflammatory and IFN responses. Its crucial role in the antiviral response is further supported by the fact that many viruses evolved subversion strategies to antagonize PKR-mediated antiviral mechanisms. Although studies focusing on fish PKR are relatively scarce, it seems that the antiviral functions attributed to mammalian PKR are also relatively conserved in these organisms. The existence of a fish specific PKR-like protein, namely PKZ, raises further questions about their respective and/or cooperative roles in fish antiviral response. This opens many interesting avenues for future investigation to provide insights into fish PKR and PKZ mode of action.

---

## CHAPTER 3

# The role of Viperin in antiviral defenses in fish and mammals

---

### 1. Introduction

The following chapter focuses on virus inhibitory protein, endoplasmic reticulum-associated, interferon-inducible (Viperin), also known as radical S-adenosyl-methionine (SAM) domain-containing protein 2 (RSAD2), which ranks among the most highly induced *ISGs* during viral infections. Extensive research over the past 25 years has cemented its place as a broad-spectrum antiviral effector. Nevertheless, some of the underlying molecular mechanisms of action of Viperin have only recently been discovered.

The aim of this introduction chapter is to summarize the current knowledge about the biological functions attributed to Viperin, with a special focus on the underlying molecular mechanisms of its antiviral action. In a similar fashion to **Chapter 2** on PKR, comparisons between mammalian and fish systems are presented, wherever possible. For this purpose, this chapter is divided as follows: (1) overview of the historical discovery of Viperin; (2) structure and evolution of Viperin; protein structure; (3) induction pathways and antiviral activity of Viperin; (4) underlying molecular mechanisms of its antiviral action, including (4a) direct antiviral mechanisms against viruses (4b) indirect antiviral mechanisms involving interactions with host proteins; (5) modulation of Viperin during viral infections and (6) its emerging regulatory role in metabolic processes under non-pathological conditions.

### 2. Brief overview of the historical discovery of Viperin

The discovery of Viperin is well worth a special mention, as it is one of the few immune genes that were first described in lower vertebrates and later characterized in mammalian models. This gene was initially found as a cDNA fragment (named *cig5* for cytomegalovirus-induced gene 5) identified by differential display analysis in primary human foreskin fibroblasts infected with human cytomegalovirus (HCMV) <sup>384</sup>. A homologous gene was later cloned and described in rainbow trout leukocytes incubated with VHSV and was then named *vig-1* for VHSV-induced gene 1 <sup>140</sup>. The mouse and rat homologs of *vig-1*, named *mvig* and *best5* (for bone-expressed sequence tag 5), were later cloned from VSV and pseudorabies virus-infected splenocytes and from osteoblasts, respectively <sup>385,386</sup>. It was not until 2001 that the full length transcript of the human homolog was cloned and further characterized from primary human macrophages treated with IFN- $\gamma$  <sup>387</sup>. On this

occasion, it was renamed Viperin, which stands for virus inhibitory protein, ER-associated, IFN-inducible. According to the HGNC-approved nomenclature, Viperin is now also referred to as radical SAM domain-containing protein 2 (RSAD2), in relation to the protein family to which it belongs.

### 3. Structure and evolution of Viperin

#### 3.1. Radical SAM enzyme superfamily

As its HGNC name (RSAD2) suggests, Viperin is part of the radical SAM enzyme superfamily due to the presence of a CX<sub>3</sub>CX<sub>2</sub>C motif located in its central domain (described in greater detail hereafter), which is characteristic of this family. Radical SAM enzymes are able to generate radical species by reductive cleavage of the cofactor SAM through a [4Fe–4S] cluster into a 5'-deoxyadenosyl radical (5'-Ado<sup>•</sup>) and methionine<sup>388</sup>. The generated radical species enables remarkably diverse biochemical reactions, such as sulfur insertion, ring formation, anaerobic oxidation and protein radical formation, among others<sup>388</sup>. Nonetheless, the vast majority of the radical SAM enzymes in this family have unknown enzymatic activities and/or biological functions. Although the size of this superfamily was initially estimated at ~600 members<sup>388</sup>, this number has dramatically expanded over the past few years and is currently estimated at ~700 000 members found across all domains of life (Bacteria, Archaea, Eukarya), making it the largest enzyme superfamily in nature<sup>389</sup>. Importantly, most radical SAM enzymes are found in prokaryotic species and only a few of them are present in animals. For instance, the human genome contains nine genes encoding radical SAM enzymes<sup>390</sup>, including: (1) molybdenum cofactor synthesis 1 (MOCS1) *aka.* MoaA, which catalyzes the first step of molybdenum cofactor synthesis required for the catalytic activity of molybdenum-dependent enzymes<sup>391</sup>; (2) lipoic acid synthase (LIAS), involved in the synthesis of lipoyl cofactor, which is involved in energy metabolism and the degradation of specific amino acids<sup>392</sup>; (3) CDK5 regulatory subunit associated protein (CDK5RAP1), (4) CDK5RAP1-like (CDKAL1), (5,6) tRNA-yW synthesizing protein (TYW1) and the closely related TYW1 homolog B (TYW1B), (7) elongator acetyltransferase complex subunit 3 (ELP3); the five latter enzymes being involved in the modification of tRNAs<sup>390</sup>; (8) radical SAM domain containing 1 (RSAD1), which is likely involved in cardiac function and/or development, although its precise function is still unknown<sup>393</sup> and (9) Viperin *aka.* RSAD2, which is involved in the innate immune response.

#### 3.2. Structure of Viperin

Structurally, mammalian Viperin is composed of 3 distinct regions: an N-terminal extension that contains an amphipathic  $\alpha$ -helix; a conserved central domain bearing the canonical CX<sub>3</sub>CX<sub>2</sub>C motif

characteristic of the radical SAM superfamily and a conserved C-terminal extension<sup>140,394,395</sup> (Figure 15). Importantly, this structure is widely conserved among vertebrates, including fish<sup>396–399</sup>.

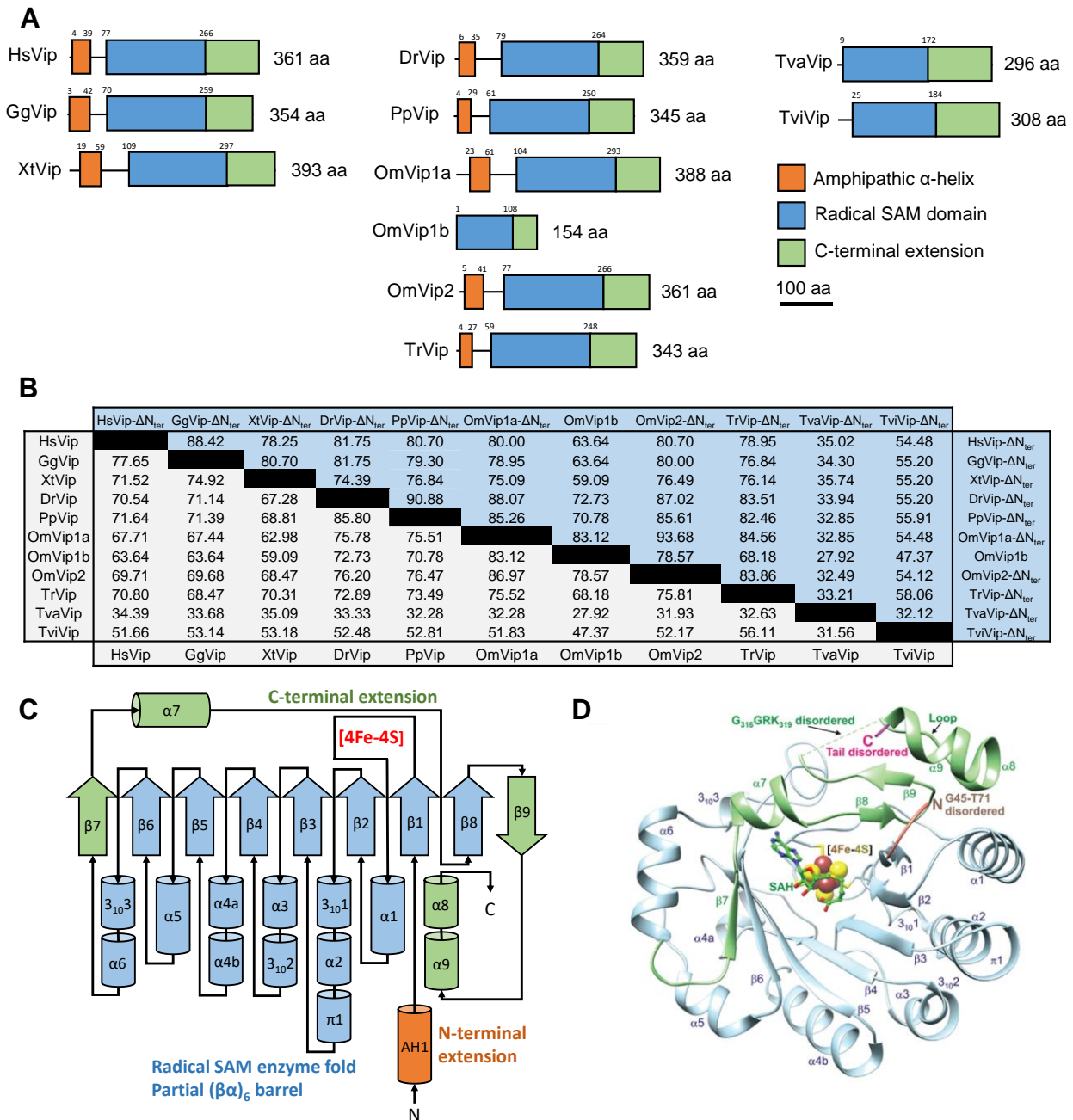


**Figure 15: Molecular structure Viperin proteins from vertebrates and lower eukaryotes**

(A) Schematic representation of domain organization of Viperin proteins from *Homo sapiens* (Hs) (NP\_542388.2), *Gallus gallus* (Gg) (NP\_001305372.2), *Xenopus tropicalis* (Xt) (XP\_002935073.2), *Danio rerio* (Dr) (NP\_001020727.1), *Pimephales promelas* (Pp) (XP\_039523815.1), *Oncorhynchus mykiss* (Om) (OmVip1a: XP\_021438647.2, OmVip1b: XP\_036818203.1, OmVip2: XP\_021430389.2) and *Tetraodon rubripes* (Tr) (XP\_003962537.1), *Trichomonas vaginalis* (Tva) (XP\_001324419.1), *Trichoderma virens* (Tvi) (XP\_013958240.1). The localization of the radical SAM domain and of the  $\alpha$ -helix were obtained using SMART and JPred4, respectively. (B) Percent identity matrix of full length Viperin proteins (in grey) and the corresponding sequence truncated from the N-terminal domain (in blue). (C) Topology diagram of mouse Viperin; the  $\beta$ -strands and helices are represented by arrows and cylinders, respectively. Figure adapted from Fenwick *et al.* (2017)<sup>394</sup>. (D) Ribbon representation of mouse Viperin- $\Delta$ 44 bound to a [4Fe-4S] cluster and SAH and crystallized by Fenwick *et al.* Note that the N-terminal amphipathic  $\alpha$ -helix is not represented as this domain was excised from the crystallized protein (for technical reasons). Figure adapted from Fenwick *et al.* (2020)<sup>400</sup>.

### 3. 2. 1. N-terminal domain

The N-terminal extension of Viperin is the most variable region in terms of sequence identity and length among vertebrate species<sup>395,401,402</sup> (**Figure 15A,B**).

***In mammals.*** In mammals, this domain contains a leucine-zipper motif within an amphipathic  $\alpha$ -helix<sup>387</sup>. Amphipathic helices are known to get inserted into one leaflet of the lipidic bilayer and to induce membrane curvature<sup>403</sup>. Consistently, the  $\alpha$ -helix of Viperin plays an important role in the subcellular localization of Viperin to the ER cytosolic face<sup>404,405</sup> and to lipid droplets<sup>404,406</sup>, likely *via* anchoring into the membrane. The crystal structure of mouse Viperin revealed that residues 45-73 of the N-terminal domain (linking the  $\alpha$ -helix to the radical SAM domain) are disordered and may act as a flexible linker that aids molecular mobility after localization to the ER membrane<sup>394</sup> (**Figure 15D**).

The N-terminal domain seems to be involved in the antiviral activity of Viperin in a virus-dependent manner. In mammals, it was reported that deletion of the first 50 or 70 aa residues did not drastically affect human Viperin's antiviral activity against HCV<sup>396</sup>, DENV<sup>407</sup> and Tick-borne encephalitis virus (TBEV)<sup>408</sup>. In contrast, deletion of the N-terminal domain resulted in loss of Viperin's ability to inhibit Porcine reproductive and respiratory syndrome virus (PRRSV)<sup>409</sup>, Zika virus (ZIKV)<sup>410</sup> or CHIKV replication<sup>411</sup>. It is noteworthy that, in the latter study, the N-terminal domain was even found to be sufficient to inhibit viral replication<sup>411</sup>. Interestingly, for TBEV, the  $\Delta$ 50-Viperin mutant reduced TBEV replication in a similar manner to WT Viperin at an early time point of infection (5h), but it was not as effective during a later time point (24h), suggesting that it is mainly involved in the long-term antiviral activity of Viperin<sup>408</sup>. The importance of N-terminus in Viperin's antiviral activity is likely due to its essential role in determining intracellular localization and may also depend on the virus replication site: for instance, TBEV and CHIKV replications both occur in proximity to the ER<sup>408,411</sup>.

***In fish.*** In fish, *in silico* analysis and computational modeling show that the N-terminal sequences from fish Viperin lack the leucine-zipper motif but display similar physico-chemical properties, suggesting the existence of an amphipathic  $\alpha$ -helix in fish too<sup>396,401,402,412</sup> (**Figure 16**). Of note, it was also shown that the N-terminal domain drives the ER-associated localization of Crucian carp CaViperin and Gibel carp (*Carassius gibelio*) CgViperins<sup>402,413</sup>.

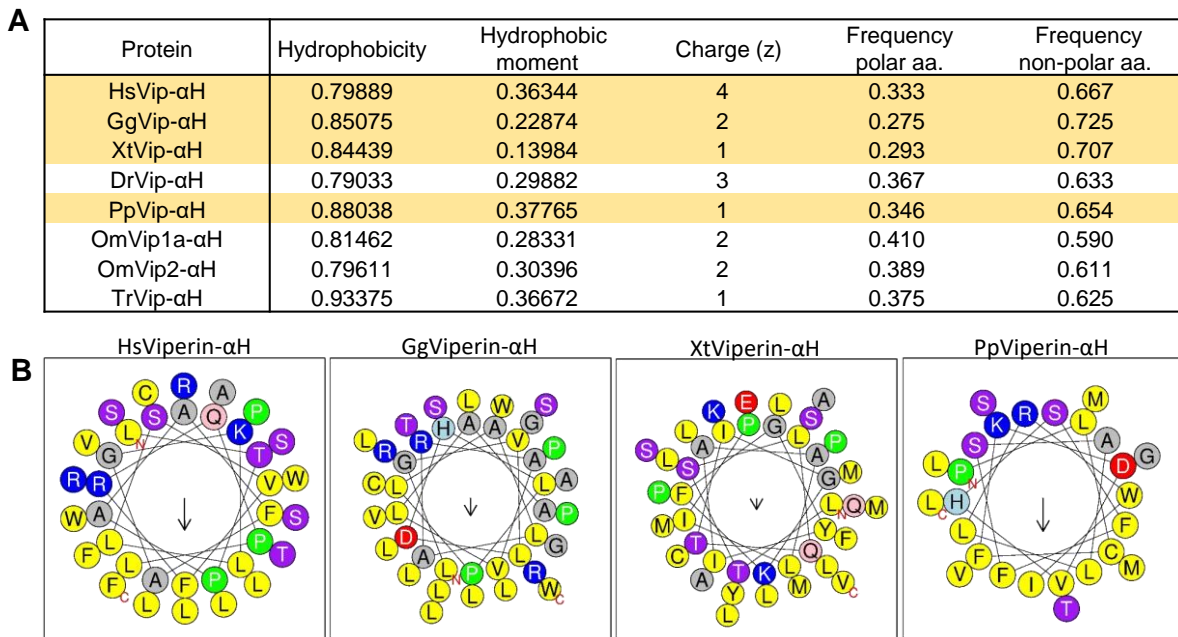


**Figure 16: Characteristics of N-terminal amphipathic  $\alpha$ -helices of Viperin proteins from vertebrates**

(A) Physico-chemical properties responsible for the amphipathic nature of the predicted  $\alpha$ -helices from Viperin proteins indicated in [Figure 15](#). (B) Corresponding helical wheel projections obtained using Heliquest.

### 3. 2. 2. Radical SAM central domain

The radical SAM central domain contains four conserved sequence motifs (motifs I to IV) associated with the radical SAM superfamily<sup>140,388</sup> ([Figure 17](#)). In particular, motif I, previously called MoaA motif, corresponds to the canonical  $CX_3CX_2C$  sequence, characteristic of the radical SAM superfamily and responsible for binding the [4Fe-4S] cluster required for its enzymatic activity<sup>388</sup>. Although this motif had been described since the first characterization of Viperin<sup>140,385</sup>, the radical SAM enzymatic activity of Viperin was only demonstrated a decade later<sup>414,415</sup> and its substrate was only recently identified<sup>150</sup> (see [Section 3. 3](#) for more details). Interestingly, this radical SAM motif is included into another motif  $N\Phi HX_4CX_3CX_2CF$  ( $\Phi$  being either W, Y or F), which has recently been identified as a marker of 3'-deoxy-3',4'-didehydro-nucleoside triphosphate (ddhNTP) synthases<sup>416</sup>. ddhNTP synthases together constitute a novel subfamily within the radical SAM superfamily<sup>416</sup>. The crystal structure of Viperin further revealed that this central domain adopts a canonical “partial  $\beta$ -barrel” ( $\beta\alpha$ )<sub>6</sub> fold, that is shared between other radical SAM enzymes<sup>394</sup> ([Figure 15C,D](#)).

The importance of this radical SAM motif in Viperin’s antiviral action has been widely demonstrated in several studies: in particular, mutations of the cysteine residues in motif I and other motifs were shown to abolish the antiviral activity of Viperin against most viruses, including HCV<sup>396</sup>, CHIKV<sup>411</sup>, TBEV<sup>408</sup>, among others. In contrast, mutational studies showed that a catalytically active radical

SAM domain was dispensable for the antiviral activity of Viperin against DENV<sup>407</sup> and ZIKV<sup>410</sup>. Similarly, the truncation of the radical SAM domain from Japanese seabass (*Lateolabrax japonicus*) LjViperin did not affect its ability to inhibit VHSV<sup>417</sup>.

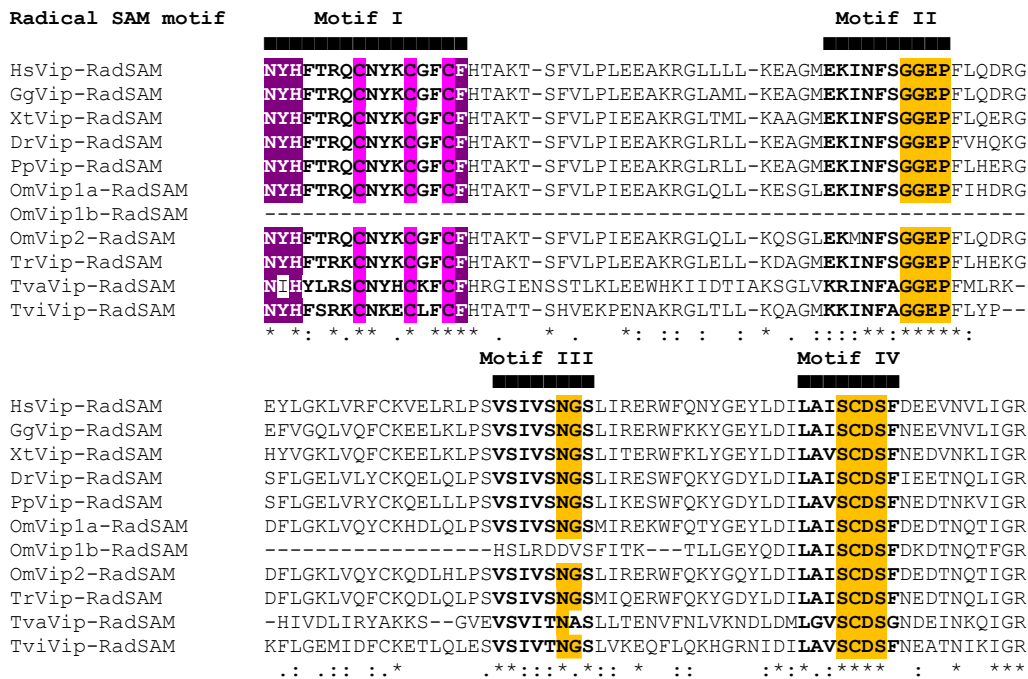


**Figure 17: Sequence alignment of a portion of the radical SAM domains of Viperin proteins from vertebrates and lower eukaryotes**

The sequences used were taken from protein sequences indicated in Figure 15. Radical SAM motifs I-IV were taken from Boudinot *et al.* (1999) and Jiang *et al.* (2008)<sup>140,396</sup>. The three cysteines (motif I) binding the redox-active [4Fe-4S] cluster are highlighted in pink; the ddhNTP synthase motif is indicated in purple. Conserved residues identified by Boudinot *et al.* (1999) are highlighted in yellow.

### 3. 2. 3. Conserved C-terminal domain

The C-terminal domain of Viperin is highly conserved among vertebrate and non-vertebrate species<sup>395,401,402</sup> but its precise function has not been completely elucidated yet.

**In mammals.** It was initially speculated that this domain was involved in protein-protein interactions and/or substrate recognition<sup>418</sup>. This hypothesis was later proven correct by crystallographic studies: it was observed that in the absence of a substrate, the C-terminal tail (extreme 25 residues) of Viperin was disordered (Figure 15D); in contrast, binding to CTP leads to ordering of the C-terminal tail that forms a cap over the top of the catalytic site. The ordered C-terminal tail bound to CTP is composed of two short  $\alpha$ -helices framing an 8 aa P-loop, that participate in binding the triphosphate moiety of CTP<sup>394,400</sup>.

The importance of the C-terminal domain in the antiviral action of mammalian Viperin has also been established by several studies: indeed, sequential deletions of this resulted in loss of Viperin's antiviral action against HCV<sup>396,404</sup>, DENV<sup>407</sup>, TBEV<sup>408</sup> and ZIKV<sup>410</sup>, among others. Interestingly,

the mutation of the extreme C-terminal tryptophane residue, which is conserved in all vertebrate Viperins, was enough to abolish Viperin's antiviral activity<sup>396,408</sup>. It was later shown that this residue is involved in binding the cellular proteins Cytosolic iron-sulfur assembly component (CIAO) 1 and CIAO2B, which are cytosolic Fe-S protein assembly factors required for the insertion of the [4Fe-4S] cluster into Viperin<sup>408,419</sup>.

***In fish.*** In fish, a recent study showed that the C-terminal domain of Japanese seabass LjViperin (but not the N-terminal or radical SAM domains) was required for Viperin to exert its antiviral action against VHSV<sup>417</sup>. Similarly, C-terminal domain of gibel carp CgViperin-A and -B was indispensable for the colocalization with ORF46R of Crucian carp herpes virus (CaHV), suggesting that the C-terminus of fish Viperin is also required for protein-protein interactions<sup>413</sup>.

### 3. 2. 4. Dimerization

Human Viperin was also found to form dimers *in vitro* and upon overexpression HEK293T cells. Interestingly, dimerization was more pronounced *in cellulo*, suggesting that Viperin's anchoring to the ER enhances this phenomenon<sup>405</sup>. In fish, it was demonstrated *via* co-IP assays that Crucian carp CaViperin proteins were able to self-associate<sup>402</sup>. Nonetheless, a clear role for Viperin's dimerization has not been identified yet.

### 3. 2. 5. Limits of mutational studies

As mentioned above, several studies have sought to understand the function of each Viperin domain by generating truncated or mutated variants of Viperin. This approach was mainly based on the assumption that the domains function independently from one another. However, a growing body of evidence suggests that this is not the case: for instance, both radical SAM and C-terminal domains seem to be involved in CTP binding<sup>400</sup>. In addition, mutations of the CX<sub>3</sub>CX<sub>2</sub>C motif into AX<sub>3</sub>AX<sub>2</sub>A were predicted to destabilize the whole protein structure due to the lack of the central [4Fe-4S] cluster, thereby introducing elements of bias<sup>420</sup>. Therefore, the functions mentioned for each domain/extension in the previous paragraphs must be seen in this light.

## 3. 3. Radical SAM activity of Viperin: substrates and products

### 3. 3. 1. Radical SAM activity

As mentioned above, the assumption that Viperin was a radical SAM enzyme was initially based on the presence of specific motifs commonly observed in other radical SAM enzymes in its primary sequence<sup>140,387</sup>.

The mechanism known for all radical SAM enzymes is based on one-electron reduction of SAM by the [4Fe-4S] cluster, leading to homolytic cleavage of the C-5'-S bond to form a highly reactive 5'-Ado<sup>•</sup> radical and methionine (Figure 18). The 5'-Ado<sup>•</sup> radical subtracts a hydrogen atom from a substrate, thereby forming 5'-deoxyadenosine (5'-dA) and a substrate radical, which undergoes further chemical reaction, ultimately leading to product formation<sup>421</sup>. The generation of 5'-dA is considered to be one of the hallmarks of radical SAM enzymes.

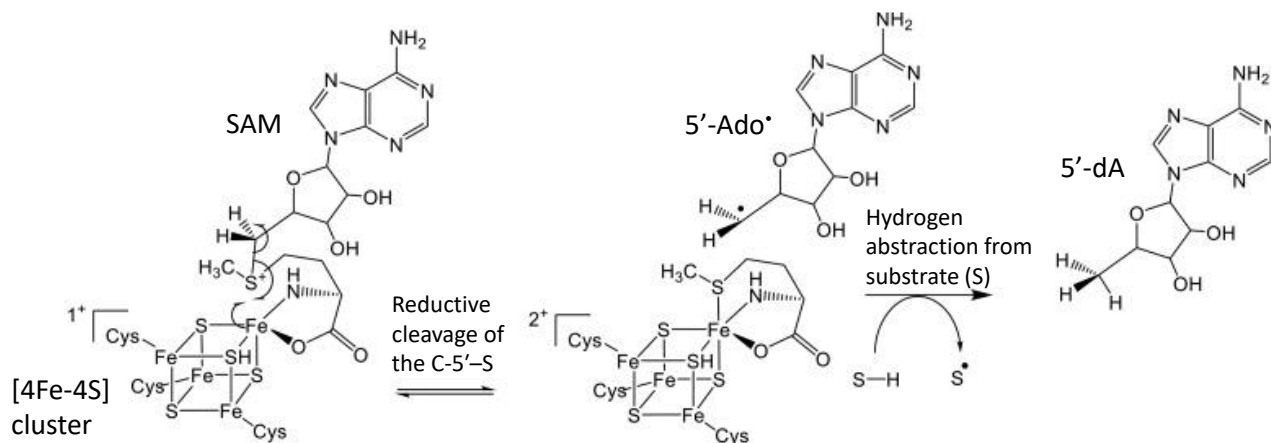


**Figure 18: Reaction mechanism of radical SAM enzymes**

Reductive cleavage of SAM by the [4Fe-4S] cluster results in the generation of a 5'-deoxyadenosyl radical (5'-Ado<sup>•</sup>), which abstracts a hydrogen atom from the substrate (S-H) to form 5'-deoxyadenosine (5'-dA) and a substrate radical (S<sup>•</sup>). Adapted from Makins *et al.* (2016)<sup>422</sup>.

However, identification of radical SAM properties in Viperin has proved technically difficult for several reasons. Firstly, expressing recombinant full-length Viperin in a bacterial expression system such as *E. coli* has failed in the hands of several research teams<sup>405,414,415</sup>. It was suggested the N-terminal domain required the presence of an ER membrane structure and/or specific chaperones to fold properly and in their absence, full-length Viperin was prone to misfolding and degradation<sup>423</sup>. As a consequence, structural studies have been conducted on N-terminally deleted mutants (Viperin- $\Delta N_{\text{ter}}$ ). Secondly, the [4Fe-4S] clusters of radical SAM enzymes are air sensitive and require anaerobic conditions for all processes, from purification to downstream *in vitro* tests<sup>421</sup>.

The first biochemical evidence that Viperin was indeed a radical SAM enzyme came in 2010 by two different groups. Shaveta *et al.* provided the first evidence of the presence of a [4Fe-4S] cluster bound by Viperin- $\Delta N_{\text{ter}}$  under anaerobic conditions<sup>415</sup>. Duschene & Broderick further demonstrated that Viperin- $\Delta N_{\text{ter}}$  was able to bind a [4Fe-4S] cluster *in vitro* and showed by High performance liquid chromatography (HPLC) analysis that it catalyzes the reductive cleavage of SAM resulting in the production of 5'-dA<sup>414</sup>. Very recently, Patel *et al.* (2022) confirmed that full-length human Viperin, purified from transfected HEK293T cells using nanodiscs, was also catalytically active by measuring 5'-dA production following incubation of Viperin with SAM, CTP and dithionite (reducing agent)<sup>423</sup>.

### 3.3.2. Identification of Viperin's substrates

Although Viperin was confirmed to be a radical SAM enzyme in 2010, the substrate involved in Viperin's catalytic antiviral activity was only identified in 2018 by Gizzi *et al.*<sup>150</sup>. Two main observations guided this identification: (1) Firstly, the *viperin* gene is found adjacent to the cytidine monophosphate kinase 2 (*CMPK2*) gene in the genomes of all vertebrate species<sup>150,424</sup>. It was shown that *CMPK2* encodes a mitochondria-located nucleoside kinase phosphorylating CDP/UDP into CTP/UTP<sup>150</sup>. In mammals, both genes are induced during IFN stimulation, while in lower organisms, such as bacterium *Lacinutrix mariniflava*, these two genes are sometimes fused, suggesting a functional link<sup>150</sup>. (2) Secondly, the crystal structure of mouse Viperin revealed that its catalytic site shares high structural similarity with the binding site of MOCS1<sup>394</sup>, which is known for catalyzing the conversion of GTP into a cyclic nucleotide intermediate involved in molybdenum cofactor biosynthesis<sup>425</sup>. Based on these observations, it was hypothesized that Viperin might use a nucleotide or a derivative as substrate<sup>150,394</sup>.

By testing the radical SAM activity of rat (*Rattus norvegicus*) Viperin against a diverse set of nucleotides and deoxynucleotides *in vitro*, CTP was identified as a substrate of Viperin. NMR and LC-MS analysis confirmed that rat Viperin was able to catalyze the conversion of CTP to 3',4'-dideoxy-cytidine triphosphate (ddhCTP)<sup>150</sup>. The proposed reaction is as follows: the 5'-Ado<sup>•</sup> radical generated from reductive cleavage of SAM abstracts a hydrogen atom from the 4'-carbon of CTP forming a substrate radical, which rearranges to ddhCTP. Isotope labeling further confirmed that the hydrogen atom from the 4'-carbon of CTP was transferred to 5'-dA during the enzymatic reaction<sup>150</sup> (**Figure 19**). Lacking the 3'-hydroxyl, ddhCTP was shown to act as a chain terminator for viral RNA-dependent RNA polymerases from several flaviviruses, including HCV, DENV, WNV and ZIKV<sup>150</sup>. For more details see **Section 5.1.1**.

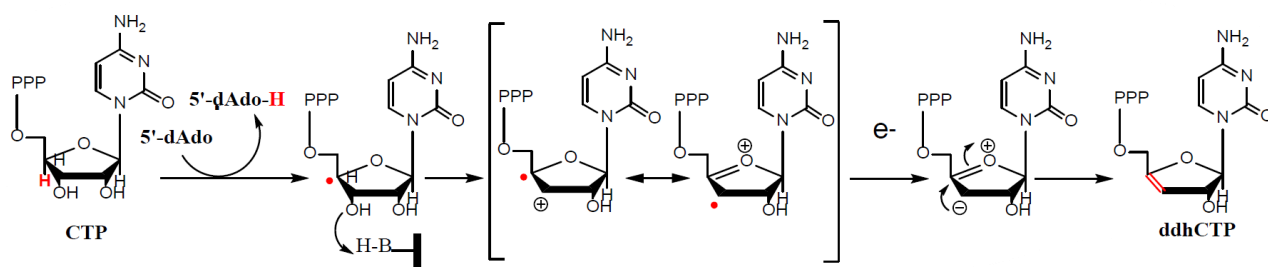


**Figure 19: Proposed mechanism for the generation of ddhCTP catalyzed by Viperin**

5'-deoxyadenosyl radical (5'-Ado) abstracts a hydrogen atom (in red) from the 4'-C on the ribose sugar of CTP, followed by the loss of the 3'-OH group (assisted by a protein side chain playing the role of a general acid) and resulting in resonance-stabilized radical-cation intermediate that is reduced by one electron to yield the ddhCTP product. Adapted from Grunkemeyer *et al.* (2021)<sup>426</sup>.

Of note, it has been reported that mammalian Viperin can also produce ddhUTP from UTP, although at a much lower efficiency than the reaction with CTP due to structural specificities at the binding site<sup>400</sup>. *In cellulo* experiments confirmed that Viperin had a ~1000-fold preference for CTP over UTP as the substrate<sup>416</sup>.

### 3. 4. Evolution of Viperin

#### 3. 4. 1. Fish Viperin

As mentioned above, Viperin is a highly conserved protein among with orthologs found throughout vertebrate species, including mammals, fish, birds, reptiles, and amphibians<sup>396–399</sup>. In fish, a single copy is typically present in the genome of jawless fish (*e.g.* Sea lamprey, *Petromyzon marinus*, LOC116945135) cartilaginous fish (*e.g.* Great white shark, LOC121278311) as well as in teleost fish that have undergone a unique WGD event (teleost-specific 3R), such as diploid cyprinids (*e.g.* Crucian carp<sup>427</sup>; zebrafish<sup>399</sup>) and percomorph species (*e.g.* Mandarin fish<sup>428</sup>, Nile tilapia<sup>429</sup>; Orange spotted grouper<sup>430</sup>). In salmonids, whose common ancestor have undergone an additional whole-genome duplication event (salmonid-specific 4R), two or more *viperin* copies are located on distinct loci on different chromosomes. For instance, three paralogs are found in species belonging the genus *Oncorhynchus*, including rainbow trout, chinook salmon (*O. tshawytscha*), coho salmon (*O. kisutch*), sockeye salmon (*O. nerka*). Two of the three paralogs are tandemly arranged in head-to-tail orientation on the same chromosome, suggesting that they resulted from an independent tandem duplication event specific to the genus *Oncorhynchus*. A similar but not systematic pattern can be found in species belonging to the genus *Salmo*: three paralogs are present in the genome of Atlantic salmon, three of which are triplicated on Chr25; in contrast, the genome of brown trout (*S. trutta*) only comprises 2 *viperin* paralogs on distinct chromosomes (**Figure 20**).

Interestingly, although Gizzi *et al.* (2018) claimed that the *viperin* gene is found adjacent to the *cmpk2* gene in the genomes of all vertebrate species<sup>150</sup>, a few specificities can be found in salmonids concerning this aspect. While Gizzi's statement is true for most fish *viperin* paralogs, the *cmpk2* gene was only retained in one of the two paralogous regions duplicated in salmonids, which suggest that different sub-functionalizations might have occurred.

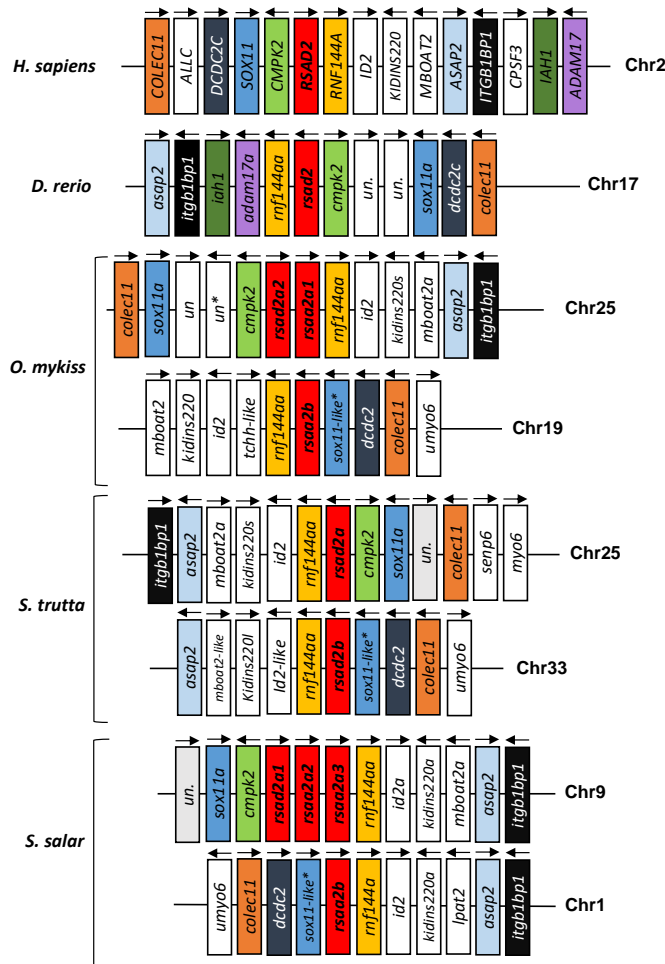


**Figure 20: Synteny of fish viperin genes**

Synteny analysis of viperin loci in human (*Homo sapiens*, LOC91543), zebrafish (*Danio rerio*, LOC570456), rainbow trout (*Oncorhynchus mykiss*, LOC100135876, LOC110504183, LOC110498119), brown trout (*Salmo trutta*, LOC115172835, LOC115162541) and Atlantic salmon (*Salmo salar*, LOC100195910, LOC123744592, LOC123744591, LOC106566099). The synteny was predicted using information extracted from recently released NCBI reference genomes. The viperin genes are colored in red.

### 3. 4. 2. Viperin-like genes in all domains of life

Interestingly, Viperin genes are not only found in the genome of vertebrate species: homologs have been identified in non-vertebrate animals, including Cephalochordata (e.g. Amphioxius, *Branchiostoma japonicus*<sup>431</sup>) Cnidaria (e.g. sea anemone, *Nematostella vectensis*<sup>432</sup>) and Mollusca (e.g. oyster, *Crassostrea gigas*<sup>433</sup>).

Besides the kingdom Animalia, bioinformatic analyses revealed that viperin-like genes are present across all the other kingdoms of life, including Fungi (e.g. *Trichoderma virens*, *Thielavia terrestris*), Protozoa (e.g. *Trichomonas vaginalis*), Plantae (e.g. green algae *Chlamydomonas reinhardtii*), Bacteria (e.g. *Lacinutrix mariniflava*, *Shewanella baltica*), and Archaea (e.g. *Methanofollis liminatans*)<sup>394,416,434</sup>. These Viperin-like enzymes from lower eukaryotes and prokaryotes also comprise the central catalytic domain and the C-terminal extension but lack the vertebrate-specific

ER-associated domain and the final 15 C-terminal residues, which are conserved in vertebrates<sup>394,434</sup> (**Figure 15A**).

Recent studies have demonstrated that Viperin-like enzymes from Cnidaria, Fungi, Bacteria, and Archaea all operate through the same mechanism as mammalian Viperin, thereby classifying them as ddhNTP synthases<sup>416,434,435</sup>. However distinct substrate preferences were reported for each Viperin: while sea anemone NvViperin preferentially utilized CTP as a substrate (like mammalian Viperin), fungal TviViperin and TtViperin and bacterial SbViperin preferentially converted UTP into ddhUTP, and bacterial LmViperin converted GTP into ddhGTP<sup>416,436</sup>. Generally speaking, most prokaryotic Viperins were found to produce a single ddhNTP (either ddhCTP, ddhGTP or ddhUTP) but a few of them could generate multiple ddhNTPs<sup>435</sup>. Similarly to mammalian Viperin, it seems that non-vertebrate Viperins are highly selective for their respective NTP substrates *in vitro*, even in presence of high concentrations of competing nucleotides<sup>416</sup>. Nonetheless, the structural determinants responsible for the selective substrate recognition involve specific residues in the variable  $\beta$ -8 loop located in the C-terminal domain (309-321 aa in human Viperin) but cannot be easily predicted based on the primary sequence<sup>416</sup>. Of note, a few studies have also reported that Viperin-like enzymes can utilize non-nucleotide substrates, including UDP-glucose<sup>437</sup> and isopentyl pyrophosphate<sup>434</sup>, although these alternative substrates seem to be unable to outcompete nucleotides as substrates<sup>416</sup>.

Importantly, it was reported that prokaryotic Viperin-like proteins provided protection against T7 phage infection upon expression in *E. coli* strains<sup>435</sup>. In a similar fashion to their mammalian counterparts, they were capable of blocking T7 RNA polymerase-dependent transcription of a GFP reporter gene, likely because Viperin-generated ddhNTPs act as RNA chain terminators<sup>435,438</sup>. It was proposed that Viperins were likely part of an ancient antiviral defense mechanism<sup>151,435</sup>.

## 4. Induction pathways and antiviral activity of Viperin

### 4.1. Constitutive expression and inducers

***In mammals.*** Mammalian Viperin is expressed at very low basal levels in most cell types but constitutive expression levels can be relatively high in some tissues, such as adipose tissue<sup>439</sup>. Viperin's expression is induced by a large variety of stressors, including stimulation with type I ( $\alpha$  and  $\beta$ ), II ( $\gamma$ ) and III ( $\lambda$ ) IFNs, dsDNA, poly I:C and infection with multiple viruses<sup>387,418,440</sup>. Interestingly, Viperin expression can also be induced following LPS treatment<sup>385,440</sup> or bacterial infections, such as Gram-negative *Salmonella typhimurium* and intracellular Gram-positive *Listeria monocytogenes*, *Shigella flexneri* and *Mycobacterium tuberculosis*<sup>440-442</sup>. Of note, it was reported that some cell lines, such as HeLa cells, failed to express Viperin regardless of the treatment<sup>387,443,444</sup>.

Table III: Functions of Viperin described in fish

Species	Order	Gene	Cloned ?	Expression		Antiviral/ bactericidal activity	Mechanisms described	References
				Constitutive	Induced			
Crucian carp ( <i>Carassius auratus</i> )	Cypriniformes	CaVip	Yes		Induction upon UV-inactivated GCHV stimulation <sup>427</sup> , GCRV infection and poly(I:C) transfection <sup>445</sup>	Against GCRV	Promoter activation upon poly(I:C), type I and II IFN, and overexpression of RLR and JAK-STAT signaling molecules <sup>445</sup>  Cytoplasmic expression associated with ER, required Nter domain <sup>402</sup>	402,427,445
Gibel carp ( <i>Carassius gibelio</i> )	Cypriniformes	CgVip-A CgVip-B	Yes	Constitutive expression in most tissues CgVip-A: high expression in spleen and liver CgVip-B: high expression in gills		Against CaHV (interactions only, no evidence of reduced titers)	Interaction with ORF46R protein from CaHV leading to the proteasomal and/or autophagosomal degradation of ORF46R  Cytoplasmic expression associated with ER, required Nter domain	413
Zebrafish ( <i>Danio rerio</i> )	Cypriniformes	DrVip	No	Constitutive expression on most tissues in adults and in larvae	No verification that <i>viperin</i> is induced upon VHSV infection in zebrafish larvae	Against VHSV	Higher expression of immune genes ( <i>ifn<math>\phi</math>1</i> , <i>ifn<math>\phi</math>3</i> , <i>cmpk2</i> , <i>mpx</i> ) in the <i>viperin</i> <sup>-/-</sup> compared to WT at 48h post-infection with VHSV (due to higher replication?)  Higher ROS production upon <i>viperin</i> overexpression  Higher cholesterol production in VHSV-infected <i>viperin</i> <sup>-/-</sup> larvae compared to WT	399,446
Fathead minnow ( <i>Pimephales promelas</i> )	Cypriniformes	PpVip PpVip-sv1 (lacking exon 5)	Yes		Induction of <i>PpVip</i> upon poly(I:C) and SVCV infection Induction of <i>PpVip-sv1</i> only by SVCV and by the P protein	Against SVCV (stronger antiviral activity of PpVip-sv1)	Upregulation of immune genes following overexpression of PpVip-sv1 only (incl. IFN-1, MxA, PKR, RIG-I, IRF3, IRF7) <sup>447</sup>  Viperin-RIG-I interactions; Viperin-mediated enhancement of RIG-I stability at the protein level by increasing its half-life <sup>448</sup>	447,448
Mandarin fish ( <i>Siniperca chuatsi</i> )	Perciformes	ScVip	Yes	Low expression in spleen and HK	Induction in all organs upon poly(I:C) and UV-inactivated ISKNV in vivo		IFN-inducible <i>via in silico</i> promoter study	428

## Introduction – Chapter 3

Red drum ( <i>Sciaenops ocellatus</i> )	Perciformes	SoVip	Yes	Low expression in most tissues	Induction in HK and liver upon poly(I:C) and <i>Edwardsiella tarda</i> but inhibition upon <i>Listonella anguillarum</i> , <i>Streptococcus iniae</i> infections <i>in vivo</i> and <i>ex vivo</i> in primary hepatocytes			449
Nile tilapia ( <i>Oreochromis niloticus</i> )	Perciformes	OnVip	Yes		Induction mostly in kidney, liver, spleen upon poly(I:C) or LPS stimulation and <i>Staphylococcus agalactide in vivo</i>	Against <i>Vibrio vulnificus</i>	Modulation of immune genes following overexpression+ <i>Vibrio vulnificus</i> infection: (not convincing): ↓ TLR9, TLR4; ↑ TNF $\alpha$	429
Rock bream ( <i>Oplegnathus fasciatus</i> )	Perciformes	OfVip	Yes	Low expression in most tissues	Induction in kidney, liver, spleen upon megalocytivirus infection	Against RBIV	Subcellular redistribution upon RBIV infection Upregulation of immune genes in kidney following overexpression (incl. IL-8, IFN1, IFN2, ISG15, NKEF, lysozyme C, TRAF2)	450
Yellow croaker ( <i>Larimichthys crocea</i> )	Perciformes	LcrVip	Yes	Low expression in most tissues	Induction in blood, kidney, liver, spleen upon poly(I:C) stimulation		IFN-inducible <i>via in silico</i> promoter study	451
Barramundi / Asian seabass ( <i>Lates calcarifer</i> )	Perciformes	LcaVip	Yes	Ubiquitous expression in most tissues	Induction in HK upon poly(I:C) stimulation and RGNNV infection			452
Golden pompano ( <i>Trachinotus ovatus</i> )	Perciformes	ToVip	Yes	Ubiquitous expression in most tissues	Induction upon poly(I:C) stimulation, NNV and SIGV infections in TOPF cells and <i>ex vivo</i> in HK leukocytes	Against SIGV (+) and NNV (++)	Cytoplasmic localization  Upregulation of immune genes in TOPF cells following overexpression (incl. IFN $\gamma$ , IRF3 and ISG15 IL-6)	453
Orange-spotted grouper ( <i>Epinephelus coioides</i> )	Perciformes	EcVip	Yes	Low expression in most tissues	Induction in GS cells upon Singaporean grouper iridovirus (SGIV)		Cytoplasmic expression and colocalization with the ER Modulation of immune genes following overexpression (↑IRF3, IRF7, ISG15, Mx, TNF- $\alpha$ and IL-6; ↓IL-1 $\beta$ ) Increased activity of interferon and NF- $\kappa$ B promoters following overexpression	430

Introduction – Chapter 3

Japanese seabass ( <i>Lateolabrax japonicus</i> )	Perciformes	LjVip	Yes		Induction in LfJ cells upon type I (IFN $\alpha$ , IFN $\beta$ ) and type II (IFN $\gamma$ ) IFN upon VHSV infection Induction in spleen upon VHSV infection	Against VHSV	IFN-dependent (via MAVS) and IFN-independent (via IRF1) induction pathway C-ter domain needed to exert antiviral activity Viperin binds N and P proteins <i>via</i> RS domain and C-ter domain and interferes with dimerization (N-N and N-P) Promotes degradation of N and P through autophagy pathway	417
Redlip mullet ( <i>Liza haematocheila</i> )	Mugiliformes	LhVip	Yes	Low expression in most tissues	Induction in blood, HK, and spleen upon poly(I:C) stimulation	Against VHSV	Cytoplasmic expression and colocalization with the ER	454
Atlantic cod ( <i>Gadus morhua</i> )	Gadiformes	GmVip	No	Low expression in most tissues	Induction in isolated HK macrophages upon poly(I:C) stimulation			401
Rockfish ( <i>Sebastes schlegelii</i> )	Scorpaeniformes	SscVip	Yes	Low expression in all tissues	Induction in blood and spleen upon poly(I:C), <i>Streptococcus iniae</i> , LPS	Against VHSV	Cytoplasmic expression and colocalization with the ER	455
Big-belly seahorse ( <i>Hippocampus abdominalis</i> )	Syngnathiformes	HaVip	Yes	Low expression in all tissues	Induction in blood, kidney, intestine upon stimulation with poly(I:C), LPS, <i>Streptococcus iniae</i>	Against VHSV	Cytoplasmic expression and colocalization with the ER	412
Rainbow trout ( <i>Oncorhynchus mykiss</i> )	Salmoniformes	OmVip	Yes	Weak expression HK and spleen but not muscle  No constitutive expression in RTS11 and RTG-2 cells	Induction in HK, muscle upon VHSV infection, VHSV G plasmid infection <i>in vivo</i>  Induction in HK leukocytes infected <i>ex vivo</i> with VHSV, BPL-inactivated VHSV, IPNV, medium with IFN-like activity  Induction upon poly(I:C) stimulation and chum salmon reovirus (CSV) infection in RTS11 and RTG-2, and with IFN-containing medium in RTS11 only <sup>141</sup>		Cytoplasmic expression (indirect evidence)  IFN-dependent and IFN-independent induction pathway	140,141

***In fish.*** Similarly in fish, several studies have reported that Viperin was constitutively expressed at low basal levels, both *in vivo* in most organs and *in vitro* in various fish cell lines, although the basal expression levels can greatly vary from organ/cell line to another (**Table III**). Most inducers described for mammals can also trigger Viperin expression in fish models, including type I and type II IFNs, poly(I:C), LPS as well as fish-specific viral and bacterial pathogens (**Table III**).

## 4. 2. Transcriptional regulation of Viperin

### 4. 2. 1. IFN-dependent and IFN-independent induction pathway

In both mammals and fish, early experimental work using anti-IFN antibodies and/or cycloheximide (inhibitor of *de novo* protein synthesis blocking IFNs translation and signaling) treatment identified that induction of Viperin could occur through two main pathways upon stimulation: an IFN-dependent pathway and an IFN-independent pathway<sup>140,141,385</sup>. The activation of both pathways appeared to be inducer-dependent: for instance, in mammals, it was reported that VSV and JEV could directly trigger the expression of Viperin in a IFN-independent manner, contrary to pseudorabies virus, Sindbis virus, Sendai virus, which required a functional IFN pathway to induce Viperin<sup>385,456,457</sup>. In mammals, LPS and poly(I:C) also induced Viperin through an IFN-mediated pathway in BMDMs<sup>457</sup>. In fish models, VHSV infection and to a lesser extent poly(I:C) led to direct induction of Viperin without the need for protein intermediates<sup>140,141</sup>. To add another layer of complexity, this response also seems to be cell type-dependent: indeed, while Viperin could be induced by Chum salmon virus (CSV) in an IFN/replication-independent manner in RTS11, it was not the case in RTG-2<sup>141</sup>.

### 4. 2. 2. Molecular basis of Viperin transcriptional regulation

Mechanistically, these two induction pathways are closely linked to the promoter of the *Viperin* gene.

***In mammals.*** The transcription of the *Viperin* gene is regulated *via* transcription factor binding sites in the promoter region, which include two ISRE sites immediately upstream of the transcription start site, three IRF-binding elements (IRF-E) and an AP-1 binding site in humans<sup>395,456,458</sup> (**Figure 21**). It was later shown that IFN-mediated induction of Viperin occurred through ISRE sites *via* binding of the canonical ISGF3 complex<sup>456,457</sup>. In contrast, JEV-mediated induction of Viperin was reported to be directly regulated by the transcription factors IRF3 and AP-1<sup>456</sup>. In case of IFN- $\gamma$  stimulation and VSV infection, it was shown that induction of *Viperin* mainly relies on IRF1, which binds to the two proximal IRF-E of the murine *Viperin* promoter<sup>459</sup>.

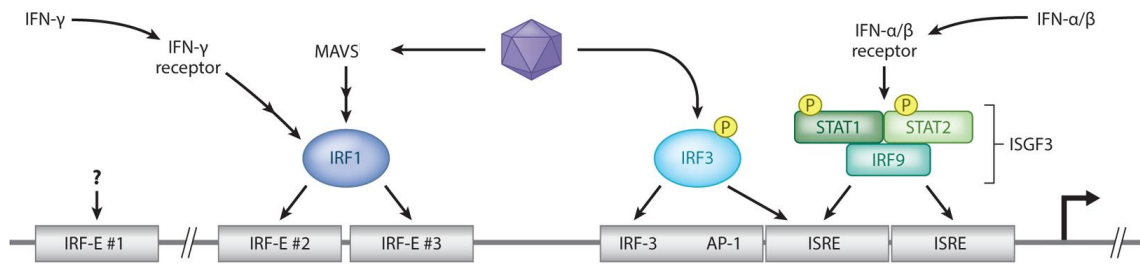


**Figure 21: Promoter region and transcriptional regulation of the human *Viperin* gene**

Figure adapted from Rivera-Serrano *et al.* (2020) <sup>395</sup>.

**In fish.** In fish, *in silico* studies of the promoters of the *viperin* gene from Mandarin fish, Crucian carp, Yellow croaker and zebrafish also revealed the presence of several putative ISRE and IRF-E <sup>428,445,451</sup>. Using *CaViperin* promoter-driven reporter gene, it was shown that the promoter of *CaViperin* was activated following overexpression of RLR signaling molecules as well as components of the JAK-STAT signaling pathways (IRF9, STAT2). Consistently, blockade of IRF3 and IRF7 inhibited induction of *viperin* upon poly(I:C) treatment, confirming that induction of fish *Viperin* can occur through the canonical type I IFN signaling cascade <sup>445</sup>. Recently, it was also demonstrated using ChIP assay that IRF9 and IRF1 could directly bind to Japanese seabass *LjViperin* promoter, suggesting that IFN-dependent and IFN-independent induction pathways are conserved between fish and mammals <sup>417</sup>.

### 4. 3. Subcellular localization of *Viperin*

**In mammals.** Mammalian *Viperin* resides in cytoplasm and is localized to the cytoplasmic face of the ER under physiological conditions <sup>387,444</sup>. It was demonstrated that mammalian *Viperin* is anchored into the ER membrane *via* its N-terminal amphipathic  $\alpha$ -helix and that deletion of this N-terminal domain resulted in the accumulation of *Viperin* in the cytosol <sup>404,405</sup>. *Viperin* was also found to localize to mitochondria-associated ER membranes (MAM) <sup>460</sup> and to the surface of lipid droplets *via* its N-terminal amphipathic  $\alpha$ -helix <sup>404,406</sup>. The localization of *Viperin* to lipid droplets has been associated with its ability to bind to viral proteins during infection and to recruit innate immune signaling components, as discussed in **Section 5. 2. 1** <sup>404,406,440</sup>. Interestingly, the localization of mammalian *Viperin* can shift upon viral infection: for instance, it was observed that HCMV infection caused redistribution of *Viperin* protein from cytosolic face to the Golgi apparatus and to cytoplasmic vacuoles <sup>387</sup>. Similarly, it was shown the viral mitochondrial inhibitor of apoptosis (vMIA) from HCMV interacts with *Viperin*, resulting in its relocation to the mitochondria <sup>461</sup>. Implications of this subcellular redistribution as a viral subversion strategy to favor HCMV infection will be discussed in **Section 6. 2. 3**.

**In fish.** In fish, Boudinot *et al.* (1999) provided the first indirect evidence that rainbow trout OmViperin had a cytoplasmic localization<sup>140</sup>. Using GFP fusion proteins, it was later confirmed that crucian carp CaViperin, bigbelly seahorse (*Hippocampus abdominalis*) HaViperin, grouper EcViperin, rock fish (*Sebastes schlegelii*) SscViperin, redlip mullet (*Liza haematocheila*) LhViperin were cytoplasmic proteins and colocalized with ER<sup>402,412,430,454,455</sup>. Furthermore, construction of mutants CaViperins and CgViperins demonstrated that N-terminal amphipathic alpha-helix (1-74) was responsible of ER-localization of Crucian carp and Gibel carp Viperins<sup>402,413</sup>. Zhang *et al.* (2014) also provided preliminary evidence that viral infections can alter the subcellular localization of fish Viperin; in particular, they observed that megalocytivirus infection induced dissociation of rock bream (*Oplegnathus fasciatus*) OfViperin from the ER<sup>450</sup>.

#### 4. 4. Viperin’s antiviral activity

##### 4. 4. 1. In mammals

In mammals, numerous studies using both overexpression of knockdown/knockout approaches have reported that Viperin was able to inhibit a broad spectrum of DNA and RNA viruses, as recently summarized by two excellent reviews<sup>151,395</sup>. Viperin-sensitive viruses include positive sense ssRNA viruses, including flaviviruses (HCV, WNV, ZIKV, DENV) and alphaviruses (Sindbis, CHIKV); negative sense ssRNA viruses, such as orthomyxoviruses (influenza A), rhabdoviruses (rabies, VSV), paramyxoviruses (measles, Sendai); and DNA viruses, including herpesviruses (HCMV, Herpes simplex 1) and retroviruses (HIV-1)<sup>151</sup>. Nonetheless, Viperin’s capacity to inhibit viral replication can drastically differ from one virus to another: for instance, Viperin had no antiviral effects against flaviviruses JEV<sup>456</sup> and Yellow fever virus<sup>462</sup>, as well as paramyxovirus Shaan Virus<sup>463</sup>. The potential underlying mechanisms will be discussed in [Section 5](#).

##### 4. 4. 2. In fish

In fish, studies focusing on the antiviral activity of Viperin are relatively recent and have been published over the past 10 years only ([Table IV](#)). The vast majority of these studies are based on overexpression approaches in diverse fish cell lines. Fish Viperins were reported to inhibit the replication and/or viral titers of positive-strand sRNA viruses, such as nodaviruses (NNV<sup>453</sup>); negative-strand RNA viruses, such as rhabdoviruses (*e.g.* VHSV<sup>412,417,454,455</sup>, SVCV<sup>447,448</sup>), dsRNA viruses, such as GCRV<sup>402</sup>, as well as DNA viruses including iridoviruses (Rock bream iridovirus C1<sup>450</sup>, SGIV<sup>430,453</sup>).

Table IV: Antiviral activity of fish Viperin

Species	Gene	Cells	Virus	Virus family, genus and type	Method used	Antiviral effect	Hypothetical mode of action	References
Overexpression								
Rock bream ( <i>Oplegnathus fasciatus</i> )	OfVip	GF Whole organism: rock bream muscle	Rock bream iridovirus (RBIV-C1)	<i>Iridoviridae</i> Megalocytivirus dsDNA, non-enveloped	Overexpression in GF cells following by infection Overexpression <i>in vivo</i> followed by infection	Lower viral copies in GF cells (~0.5-log) and in kidney (~0.5-log)	Upregulation of immune genes in kidney following overexpression (incl. IFN1, IFN2, ISG15, NKEF)	450
Orange-spotted grouper ( <i>Epinephelus coioides</i> )	EcVip	GS	Singaporean grouper iridovirus (SGIV)	<i>Iridoviridae</i> Ranavirus dsDNA, non-enveloped	Overexpression in GS cells followed by infection	Reduced CPE Reduced expression of viral transcripts	- Modulation of immune genes following overexpression (↑IRF3, IRF7, ISG15, Mx, TNF- $\alpha$ and IL-6; ↓IL-1 $\beta$ ) - Increased activity of interferon and NF- $\kappa$ B promoters following overexpression	430
Golden pompano ( <i>Trachinotus ovatus</i> )	ToVip	TOPF	Singaporean grouper iridovirus (SGIV)	<i>Iridoviridae</i> Ranavirus dsDNA, non-enveloped	Overexpression in MKD cells followed by infection	Reduced CPE Reduced viral titers (~1-log)	Upregulation of immune genes following overexpression (incl. IFNc, IRF3 and ISG15 IL-6)	453
			Nervous Necrosis Virus (NNV)	<i>Nodaviridae</i> Betanodavirus (+)-ssRNA, non-enveloped				
Crucian carp ( <i>Carassius auratus</i> )	CaVip	CAB	Grass Carp Reovirus (GCRV)	<i>Reoviridae</i> Aquareovirus dsRNA, non-enveloped	Overexpression in CAB cells followed by infection	Reduced CPE Reduced viral titer (1-log)		445
Big-belly seahorse ( <i>Hippocampus abdominalis</i> )	HaVip	FHM	Viral Hemorrhagic Septicemia Virus (VHSV)	<i>Rhabdoviridae</i> Novirhabdovirus (-)-ssRNA, enveloped	Overexpression in FHM cells followed by infection	Reduced expression of N transcripts		412
Rockfish ( <i>Sebastes schlegelii</i> )	SsVip	FHM	VHSV	<i>Rhabdoviridae</i> Novirhabdovirus (-)-ssRNA, enveloped	Overexpression in FHM cells followed by infection	Reduced viral titer (~1-log) Reduced amount of N, P, G, RdPp transcripts		455
Redlip mullet ( <i>Liza haematocheila</i> )	LhVip	MKD	VHSV	<i>Rhabdoviridae</i> Novirhabdovirus (-)-ssRNA, enveloped	Overexpression in MKD cells followed by infection	Reduced viral titer (<1-log) Reduced expression of viral transcripts		454
Japanese seabass ( <i>Lateolabrax japonicus</i> )	LjVip	LJF	VHSV	<i>Rhabdoviridae</i> Novirhabdovirus (-)-ssRNA, enveloped	Overexpression in LJF cells followed by infection	Reduced CPE Reduced expression of N, P, M, G, NV and L transcripts	- C-ter domain needed to exert antiviral activity - Viperin binds N and P proteins via RS domain and C-ter domain	417

						Reduced expression of G protein	and interferes with dimerization (N-N and N-P) - Promotes degradation of N and P through autophagy pathway - N limits expression of Viperin by promoting proteasomal degradation of IRF1 and IRF9	
Fathead minnow ( <i>Pimephales promelas</i> )	PpVip	FHM	Spring Viremia of Carp Virus (SVCV)	<i>Rhabdoviridae</i> Vesiculovirus (-)-ssRNA, enveloped	Overexpression of PpVip and PpVip-sv1 (lacking exon 5) in FHM cells followed by infection	Reduced expression of G transcripts, M and G proteins (but more potent inhibitory effect of PpVip-sv1)  Lower viral titers (for PpVip-sv1)	- Upregulation of immune genes following overexpression of PpVip-sv1 only (incl. IFN-1, MxA, PKR, RIG-I, IRF3, IRF7) - Viperin-RIG-I interactions; Viperin-mediated enhancement of RIG-I stability at the protein level by increasing its half-life <sup>448</sup> - N promotes the degradation of Viperin-sv1 via proteasomal pathway	447,448,464
Nile tilapia ( <i>Oreochromis niloticus</i> )	OnVip	Whole organism: zebrafish muscle	<i>Vibrio vulnificus</i>	Gram-negative	Electroporation of <i>viperin</i> plasmid into zebrafish muscle followed by infection	Reduced bacterial loads (CFU/g muscle) of <i>V. vulnificus</i>	No differences between vector and viperin only; modulation of immune genes following infection (no convincing): ↓ TLR9, TLR4; ↑ TNFα	429
Knockdown / Knockout								
Zebrafish ( <i>Danio rerio</i> )	DrVip	Whole organism	Viral Hemorrhagic Septicemia Virus (VHSV)	<i>Rhabdoviridae</i> Novirhabdovirus (-)-ssRNA, enveloped	Injection of VHSV into the yolk of WT or <i>viperin</i> <sup>-/-</sup> larvae Caudal fin injury followed by VHSV infection by bath	- Higher fluorescence in the yolk (injection exp) and in the caudal fin (bath exp) of <i>viperin</i> <sup>-/-</sup> larvae at 2-3dpi - Higher expression of NP transcripts at 2-9dpi - Higher VHSV copy number at 3-5dpi but no differences at 7-9dpi - Higher titers (1-log) at 48hpi - Lower survival of <i>viperin</i> <sup>-/-</sup> larvae	- Higher expression of immune genes ( <i>ifn<math>\alpha</math>1</i> , <i>ifn<math>\alpha</math>3</i> , <i>cmpk2</i> , <i>mpx</i> ) in the <i>viperin</i> <sup>-/-</sup> compared to WT at 48hpi (due to higher replication?) - Higher ROS production upon <i>viperin</i> overexpression - Higher cholesterol production in VHSV-infected <i>viperin</i> <sup>-/-</sup> larvae compared to WT	399,446

Interestingly, Wang *et al.* (2019) have recently reported that FHM cells expressed two splice variants of Viperin upon SVCV infection: a full-length variant and a splicing variant (named Viperin\_sv1) lacking exon 5 and resulting in a 11-aa deletion in the C-terminal region. Overexpression of both variants in FHM cells subsequently infected with SVCV showed that PpViperin\_sv1 had a stronger inhibitory effect on the transcription of viral genes and on virus titers in the supernatant compared to full-length Viperin<sup>447</sup>, suggesting that different variants may have distinct antiviral effects.

Only one study used a knockout approach to investigate the antiviral activity of fish Viperin: it was reported that *viperin*<sup>-/-</sup> zebrafish larvae infected with rVHSV-ΔNV-EGFP displayed a higher GFP signal and a 10-fold increase in VHSV titer compared to WT larvae (1.6 x 10<sup>7</sup> vs 2.8 x 10<sup>6</sup> TCID<sub>50</sub>/mL)<sup>399,446</sup>.

#### 4. 4. 3. Viperin's antibacterial activity?

A few studies in both mammalian and fish models provide evidence that Viperin can restrict bacterial infections: for instance, overexpression of WT Viperin but not catalytically inactive mutants limited intracellular bacterial loads in HEK293T and HeLa cells infected with intracellular bacteria *Shigella flexneri* and *Listeria monocytogenes*, while *S. flexneri* infection was enhanced in *Viperin*<sup>-/-</sup> MEFs and upon knockdown in Huh7 cells<sup>441</sup>. Similarly, one study also provides evidence that Nile tilapia OnViperin is able to limit *Vibrio vulnificus* infection in fish<sup>429</sup>.

## 5. Underlying molecular mechanisms of Viperin's antiviral action

The wide array of viruses against which Viperin has an antiviral action has made it difficult to identify the underlying molecular mechanisms explaining its antiviral properties. Broadly speaking, Viperin's antiviral mechanisms of action can be classified into two categories: (1) a direct antiviral action by targeting the viral components and (2) an indirect antiviral action relying on interactions with the host proteins to modulate specific pathways required during viral replication cycles (**Figure 22**).

### 5. 1. Direct antiviral mechanisms

#### 5. 1. 1. Enzymatic activity

##### 5. 1. 1. 1. Chain terminator ddhCTP

**In mammals.** Although it was shown early on that Viperin had to be catalytically active to exert its antiviral action<sup>396,408,461</sup>, it was only recently discovered that Viperin was able to catalyze the conversion of CTP into ddhCTP *via* a SAM-dependent radical mechanism<sup>150</sup> (for more details on the generation of ddhCTP, refer to **Section 3. 3. 2**). Biochemical studies further showed that ddhCTP

could be used as a substrate by viral RNA-dependent RNA polymerases (RdRp) from flaviviruses DENV, WNV, HCV and ZIKV and picornavirus human rhinovirus type C (HRV-C) and inhibited further RNA synthesis<sup>150</sup>. Molecularly, the absence of 3'-hydroxyl group (**Figure 19**) precludes further nucleotide incorporation into the nascent strand of viral RNA, thereby acting as a chain terminator. It was reported that ddhCTP blocked viral RNA synthesis even in presence of competing CTP for several RdRp from flaviviruses, including DENV and WNV. Curiously, the RNA-dependent RNA polymerases from picornavirus HRV-C and poliovirus RdRp were poorly inhibited by ddhCTP in presence of competing NTPs<sup>150</sup>, suggesting the existence of circumvention strategies implemented by these viruses.

*In cellulo*, HEK293T overexpressing recombinant Viperin and IFN- $\alpha$  stimulated macrophages expressing high levels of endogenous Viperin could produce intracellular ddhCTP. Furthermore, pretreatment of Vero cells with pro-drug ddhC nucleoside, which can be converted into ddhCTP by host kinases, resulted in a dose-dependent reduction in ZIKV virus titers<sup>150</sup>.

*In fish*. In fish, no studies have investigated the generation of ddhCTP by Viperin, presumably because of the technical difficulties associated with this type of enzymology-based experiments (*e.g.* anaerobic conditions for *in vitro* experiments with recombinant Viperin).

#### 5. 1. 1. 2. Cooperation of Viperin with CMPK2

Gizzi *et al.* (2018) have demonstrated that Viperin cooperates with CMPK2 to produce higher levels of ddhCTP<sup>150</sup>. Indeed, CMPK2 was reported to be cotranscribed with Viperin upon type I IFN stimulation<sup>424</sup>. Furthermore, cotransfections of Viperin- and CMPK2-encoding plasmids resulted in a ~4-fold increase in the amount of ddhCTP in HEK293 cells<sup>150</sup>. Because CMPK2 converts CDP and UDP into CTP and UTP, respectively, it was suggested that CMPK2 increases the local concentration of CTP that is subsequently converted into ddhCTP by Viperin, thereby enhancing its antiviral action<sup>150</sup>.

#### 5. 1. 1. 3. Does ddhCTP affect the host transcription arsenal?

One question that arises is whether ddhCTP is toxic to host cells. It was initially reported that, although mammalian Viperin-generated ddhCTP was capable of inhibiting viral polymerase-dependent transcription, it had no detectable negative effect on the growth rate or viability of HEK293T or Vero cells<sup>150</sup>. Importantly, it was also demonstrated that human Viperin inhibited the transcription of a reporter gene by bacteriophage T7 polymerase expressed in mammalian cells but did not inhibit host RNA polymerase II-dependent transcription of a reporter gene under a cytomegalovirus promoter, highlighting the specificity of Viperin for some polymerases<sup>438</sup>. More recently, it was further confirmed that Viperin overexpression in 293T cells had no significant effect

on global cellular transcription<sup>465</sup>. Similarly, Bernheim *et al.* (2021) reported that ddhNTPs generated by prokaryotic Viperins were capable of restricting phage replication, but had no effect on the viability of the bacteria<sup>435</sup>. Based on these observations, it was suggested that Viperin-expressing organisms were unaffected by the action of the Viperin-generated ddhNTPs in two different ways: (1) the host nucleic acid polymerases are not sensitive to ddhNTPs, or (2) they possess other protective mechanisms to inhibit incorporation of ddhNTPs or excise them during RNA synthesis<sup>150,416</sup>. Nonetheless, it was recently discussed that the mitochondrial RNA polymerase was structurally most closely related to bacteriophage T7 polymerase, lacked proofreading function<sup>466</sup> and could therefore be more susceptible to ddhCTP misincorporation compared to their nuclear counterparts<sup>467</sup>. The authors raised the question whether ddhCTP might act as a regulator of mitochondrial RNA transcription. More studies are needed to understand why host cells do not seem to be affected by Viperin-generated ddhCTP and to identify whether it regulates mitochondrial RNA transcription<sup>467</sup>.

#### 5. 1. 1. 4. *Controversy: is ddhCTP really a chain terminator?*

There is currently some controversy as to whether ddhCTP is indeed a chain terminator for RdRps. Indeed, Ebrahimi *et al.* (2020) recently argued that ddhCTP does not exert its antiviral action by acting as a viral replication chain terminator. This statement is based on the re-evaluation of published datasets from Gizzi *et al.* (2018)<sup>150</sup> and on calculating IC<sub>50</sub> of ddhCTP competing with CTP, which appears to be at least 400-fold larger than those reported for antiviral nucleotide analogs. The authors concluded that ddhCTP may not act as an effective chain terminator under physiologically relevant conditions but provide evidence that it may affect mitochondrial metabolism<sup>468</sup> (for more details, see [Section 7. 2](#)). However, this proposition was also met with skepticism: it was argued that even low misincorporation of ddhCTP into viral RNA would effectively inhibit viral replication, as viral genomes contain thousands of cytidine nucleotides<sup>151</sup>. Furthermore, how modulation of mitochondrial metabolism is involved in Viperin's antiviral activity is still unclear.

#### 5. 1. 1. 5. *An alternative role of ddhCTP: inhibition of protein translation?*

An alternative role of ddhCTP has recently been proposed by Hsu *et al.* (2022)<sup>465</sup>. This proposition stems from the observation that Viperin overexpression resulted in inhibition of host translation *via* a mechanism requiring its catalytic activity<sup>465</sup>. Mechanistically, it was demonstrated that Viperin-generated ddhCTP triggers ribosome collisions, leading to the activation of the GCN2 arm of the integrated stress response, ultimately resulting in inhibition of protein translation. In a context of viral infection, it was further shown that GCN2-mediated translational shutoff initiated by prodrug ddhC (which crosses the plasma membrane and is metabolized into ddhCTP in the cytosol) restricted WNV

infection by limiting viral protein synthesis<sup>465</sup>. However, the mechanisms by which ddhCTP initiates ribosome collisions are still elusive and would require further study.

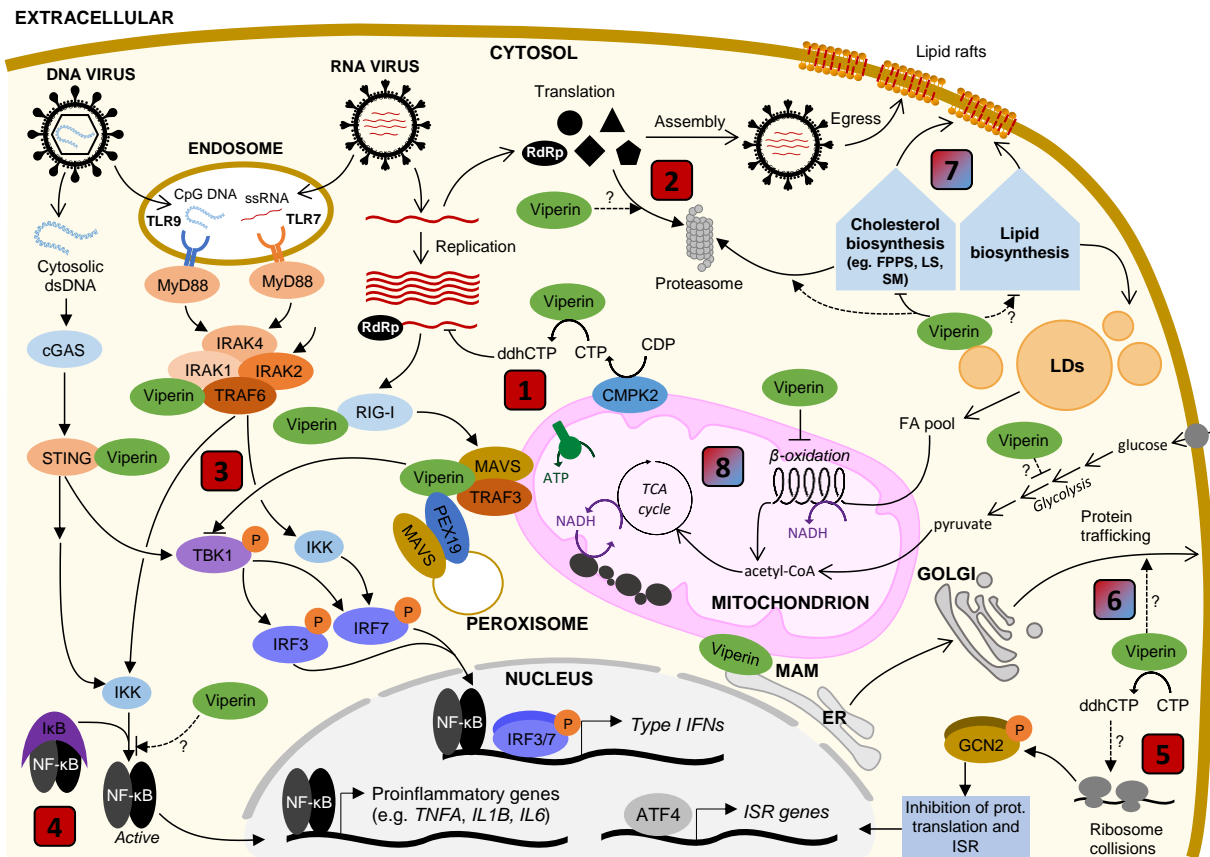


**Figure 22: Overview of mammalian Viperin's mechanisms of action during viral infection and under non-pathological conditions**

Viperin localizes on the cytosolic face of the endoplasmic reticulum (ER), to lipid droplets (LDs) and to mitochondria-associated ER membranes (MAM). It exerts its biological functions *via* different mechanisms numbered from 1 to 8; numbers in a red box represent antiviral mechanisms, while numbers in a blue-red box represent mechanisms described for Viperin in a context of infection and/or under *in vitro* conditions and/or in a non-pathological context. **(1) Enzymatic activity.** Viperin catalyzes the conversion of CMPK2-generated CTP to ddhCTP (*via* a radical SAM mechanism), which acts as a chain terminator for some specific viral RdRps. **(2) Direct interactions with viral proteins.** Viperin is able to bind viral proteins and to promote their degradation through the ubiquitin-dependent proteasomal pathway. **(3) Interactions with adaptor proteins from innate immune signaling pathways.** Viperin interacts with protein kinase IRAK1 and E3 ubiquitin ligase TRAF6 downstream ssRNA-sensing TLR7 and CpG DNA-sensing TLR9 in plasmacytoid dendritic cells, as well as with adaptor protein STING downstream cytosolic dsDNA-sensing cGAS pathway. Viperin also stabilizes dsRNA-sensing RIG-I, associates with its downstream adaptor protein MAVS and with peroxisomal PEX19 protein. This enhances downstream signaling pathways involving TBK1, IRF3, IRF7, resulting in induction of type I IFN, although the response may be cell-type dependent. **(4) Modulation of the inflammatory response.** Viperin modulates the inflammatory response in a cell-type dependent manner *via* unknown mechanisms. **(5) Inhibition of translation initiation.** Viperin-generated ddhCTP triggers ribosome collisions, leading to the activation of GCN2, ultimately resulting in inhibition of protein translation and induction of specific integrated stress response (ISR) genes. **(6) Modulation of protein secretion.** Viperin interferes with trafficking of soluble proteins *via* unknown mechanisms. **(7) Inhibition of cholesterol biosynthesis.** Viperin limits the activity of a pool of enzymes involved in cholesterol biosynthesis, including FPPS, squalene monooxygenase (SM) and lanosterol synthase (LS) by promoting their proteasome-mediated degradation (FPPS, SM) or directly inhibiting their catalytic activity (LS). Downregulation of cholesterol production limits the formation of lipid rafts, which are important for the budding of some enveloped viruses. Viperin also associates with other enzymes involved in lipid biosynthesis but their interactions have not been characterized yet. **(8) Modulation of mitochondrial metabolism.** Mitochondria-located Viperin alters mitochondrial metabolism by inhibiting the activity of HADHB, the  $\beta$ -subunit of the trifunctional protein (TFP) complex involved in fatty acid  $\beta$ -oxidation, resulting in reduced ATP levels, enhanced lipogenesis, accumulation of lipid droplets and reduced thermogenesis. Viperin may also inhibit the catalytic activity of  $\text{NAD}^+$ -dependent enzymes, involved in glycolysis and the TCA cycle.

### 5. 1. 2. Direct interactions with viral proteins

*In mammals.* Although the production of ddhCTP provides a convincing explanation for some antiviral effects of Viperin, its antiviral activity cannot be entirely explained by it. For instance, it was reported for some viruses that Viperin mutants harboring a catalytically inactive radical SAM domain were still able to inhibit viral replication<sup>407,410</sup>. In addition, ddhCTP is not an effective chain terminator for all RdRps (*e.g.* picornaviruses)<sup>150</sup>.

Several studies in mammalian models have reported that Viperin was able to bind viral proteins and to promote their degradation through the proteasomal pathway. For example, Panayiotou *et al.* (2018) showed that Viperin was capable of binding the NS3 protein from TBEV and ZIKV and to facilitate their degradation in a proteasome-dependent manner<sup>462</sup>. Similarly, Viperin was found to interact with NS5A protein from HCV resulting in the proteasomal degradation of the viral protein in an independent manner from Viperin's radical SAM activity<sup>404,469,470</sup>.

*In fish.* In fish, co-IP assays revealed that Viperin from different fish species was also able to interact with viral proteins. Gibel carp CgViperin-A and CgViperin-B were both found to interact with ORF46R of herpesvirus CaHV at the ER *via* their C-terminal domain and their overexpression led to the reduction of CaHV ORF46R protein independently from their catalytic activity<sup>413</sup>. Using proteasome-, lysosome- and autophagosome-specific inhibitors, the authors showed that CgViperin-A and CgViperin-B mediated ORF46R proteasomal degradation by suppressing K63-linked ubiquitination. In addition, CgViperin-B but not CgViperin-A also promoted the autophagic degradation of ORF46R<sup>413</sup>. Another study showed that Asian seabass LjViperin could interact with the N and P proteins of VHSV and promote their degradation through the autophagic pathway<sup>417</sup>.

## 5. 2. Indirect antiviral mechanisms

Besides a direct antiviral action by targeting viral replication and/or maturation, many studies have also shown that Viperin alleviates viral infection by enhancing innate immune signaling and by modulating metabolic pathways exploited during the viral life cycle.

### 5. 2. 1. Interaction with cellular proteins involved in innate immune signaling

#### 5. 2. 1. 1. Viperin as a modulator of the type I IFN response

*In mammals.* Several works on mammalian models have shown that Viperin may play a role in the regulation of the type I IFN response in a cell-type and inducer-dependent manner.

It was initially described that mammalian Viperin was required for the production of type I IFN upon stimulation with heat-treated Newcastle disease virus (TLR7 agonist) and CpG DNA (TLR9 agonist)

in plasmacytoid dendritic cells<sup>440</sup> as well as upon stimulation with poly(dA:dT) (agonist of dsDNA sensors) in MEFs<sup>471</sup>. However, it was not involved in the production of type I IFN upon transfection or stimulation with poly(I:C) in MEFs<sup>440</sup> or BMDMs<sup>472</sup>. In contrast, a recent study has reported a positive regulatory role of Viperin in the induction of IFN- $\beta$  upon poly(I:C) stimulation and Sendai virus infection in MEFs<sup>473</sup>. Opposite results were obtained in BMDMs, in which Viperin was found to act as a negative regulator of IFN- $\beta$  induction upon poly(I:C) and 5'ppp-dsRNA transfection or treatment with type I IFN<sup>460</sup>. It was suggested that these discrepancies could be explained by the differences in cell types, inducers and/or assays used<sup>395</sup>. In line with this hypothesis, a recent study showed that Viperin differentially modulated the induction of ISGs in a cell type- and inducer-dependent manner: Viperin upregulated the expression of ISGs in BMDMs treated with type I and II IFNs, but opposite results were observed in MEFs. In contrast, Viperin potentiated the expression of ISGs in both BMDMs and MEFs stimulated with poly(I:C), CpG DNA, or cytomegalovirus<sup>474</sup>.

#### 5. 2. 1. 2. *Underlying mechanisms identified in mammals*

**Interactions with IRAK1 and TRAF6.** In plasmacytoid dendritic cells, Viperin is involved in the signaling pathways downstream ssRNA-sensing TLR7 and CpG DNA-sensing TLR9. It was found to recruit IRAK1 and E3 ubiquitin ligase TRAF6 to ER-derived LDs<sup>440</sup>. Co-IP assays showed that IRAK1 binds both Viperin and TRAF6, which do not associate independently otherwise<sup>475</sup>. Mechanistically, Viperin facilitates K63-linked polyubiquitination of IRAK1 by TRAF6, leading to IRF7 phosphorylation and subsequent induction of type I IFNs<sup>440,475</sup>. Interestingly, the radical SAM activity of Viperin was not required in this process but the Fe-S cluster binding appeared to be necessary to stabilize Viperin. Altogether, it was proposed that Viperin primarily acts as a scaffold in this pathway, although binding to IRAK1 and TRAF6 curiously increased the catalytic activity of Viperin<sup>475</sup>.

**Interactions with STING.** Similar interactions have also been identified between Viperin and components of the cytosolic dsDNA-sensing cGAS-STING pathway<sup>471</sup>. Indeed, it was recently reported that Viperin could bind STING upon stimulation with poly(dA:dT) resulting in enhanced activation of its target protein TBK1 by stimulating its K63-linked polyubiquitination *via* a yet unidentified E3 ubiquitin ligase in human cell lines and in MEFs<sup>471</sup>. Subsequently, TBK1 phosphorylates transcription factor IRF3, thereby inducing the expression of type I IFN genes. Similar to what has been observed for IRAK1 and TRAF6, co-expression of Viperin with STING and TBK1 increased the catalytic activity of Viperin by 10-fold<sup>471</sup>.

**Viperin-mediated stability of RIG-I.** Another study demonstrated *via* co-IP assays that Viperin interacts with several helicases, including the cytosolic dsRNA sensor RIG-I, in MEFs and that Viperin increases RIG-I protein levels but not mRNA expression levels in a radical SAM-dependent manner, suggesting that it might play a role in protein stabilization rather than gene induction<sup>476</sup>. Mass spectroscopy analysis and mutational studies provide evidence that Viperin-mediated stabilization involved the oxidization of specific methionine residues on RIG-I resulting in enhanced IFN- $\beta$  expression<sup>476</sup>. However, no mechanism was proposed to explain how Viperin leads to methionine oxidization and this novel function of Viperin has been met with skepticism<sup>151</sup>.

**Interactions with PEX19 and MAVS.** Recently, peroxisomal biogenesis factor 19 (PEX19) was identified as a Viperin binding partner in mammalian cell lines<sup>473</sup>. PEX19 is essential for early genesis of peroxisomes and acts as a chaperone to stabilize and shuttle newly synthesized peroxisomal membrane proteins from the ER to the peroxisome. It was further shown that PEX19-Viperin interaction drives the peroxisome to associate to lipid droplets, to localize in close proximity to mitochondria and to potentiate the expression of IFN- $\beta$ <sup>473</sup>. Furthermore, close association between Viperin and MAVS at the surface of LDs and mitochondria was identified by immunofluorescence microscopy. It was suggested that Viperin (in association with PEX19) acts as a chaperone and repositions the peroxisome to facilitate mitochondrial and peroxisomal MAVS-dependent activation by RLRs upon poly(I:C) stimulation and to enhance the type I IFN response<sup>473</sup>.

In macrophages, where Viperin may act as a negative regulator of type I IFN, MAM-located Viperin colocalizes and interacts with MAVS under physiological conditions<sup>460</sup>. It was also observed that IRF3 phosphorylation, which ultimately results in type I IFN transcription, was enhanced in *Viperin*<sup>-/-</sup> BMDMs upon poly(I:C) transfection, suggesting that Viperin suppresses MAVS-dependent signaling. However, mutational studies revealed that Viperin mutants that bind less effectively to MAVS, were better inhibitors of IFN- $\beta$  promoter compared to WT Viperin. The authors hypothesized that Viperin-MAVS interactions affect IFN- $\beta$  transcription *via* an indirect mechanism, possibly by sequestering Viperin and preventing it from performing its inhibitory function through other pathways<sup>460</sup>.

Overall, there is no consensus on the regulatory role of Viperin in the IFN response, which appears to be positive, negative or absent depending on the study, suggesting that complex underlying mechanisms are at play.

### 5. 2. 1. 3. Role of Viperin in modulating the type I IFN response in fish

**In fish.** In fish, several studies have reported that Viperin overexpression promoted the expression of specific ISGs<sup>399,412,447,450,453</sup> (Table III). Interestingly, Fathead minnow splicing variant

PpViperin\_sv1 but not full-length PpViperin upregulated the transcription of ISGs, suggesting that the Viperin-mediated modulation of the type I IFN may be isoform-dependent<sup>447</sup>. In any case, the underlying mechanisms are still poorly understood and only one study explored this question: in line with what has been found in mammalian models Gao *et al.* (2021) provide evidence that PpViperin\_sv1 interacts with RIG-I and enhances its stability by increasing its half-life *via* a mechanism requiring its radical SAM domain<sup>448</sup>. Whether this mechanism also exists for full length PpViperin is still unknown.

## 5. 2. 2. Modulation of the inflammatory response by Viperin

### 5. 2. 2. 1. Viperin as a modulator of the inflammatory response?

***In mammals.*** In a similar fashion to what has been described for Viperin's role in the type I IFN response, there is no consensual view concerning the contribution of Viperin to the inflammatory response. Some studies have reported that Viperin acts as a positive regulator of the NF- $\kappa$ B and AP-1 signaling pathway in T cells<sup>477</sup> and promotes the expression of pro-inflammatory cytokines in LPS-stimulated microglia<sup>478</sup>. In contrast, Saitoh *et al.* (2011) have shown that Viperin deficiency had no impact on the production of proinflammatory cytokines (CXCL10, TNF- $\alpha$ , IL-6, IL-1 $\beta$ ) in dendritic cells and/or macrophages upon engagement of TLR2, TLR4, TLR7 and TLR9<sup>440</sup>. In contrast, it was reported that the levels of secreted cytokines and macrophage markers were significantly higher in *Viperin*<sup>-/-</sup> polarized M1 and M2 macrophages compared to their WT counterparts, suggesting that Viperin acts as a negative regulator of the inflammatory response in macrophages<sup>479</sup>. In line with these observations, another study recently shown that *Viperin*<sup>-/-</sup> dendritic cells produced higher amounts of NO and proinflammatory cytokines and chemokines, including IL-12, IL-6, TNF $\alpha$ , IL-1 $\beta$ , CXCL1, CXCL2 and CXCL10 upon *M. tuberculosis* infection<sup>442</sup>. Taken together, these findings suggest that Viperin's contribution to the inflammatory response may also be cell type- and/or treatment-dependent.

### 5. 2. 2. 2. Underlying mechanisms?

The mechanisms by which Viperin may modulate the pro-inflammatory response remain largely unknown. In mammals, it was shown that Viperin promotes the activation of the TLR2/MyD88/NF- $\kappa$ B signaling pathway upon LPS stimulation in microglia<sup>478</sup>. In dendritic cells, Viperin suppressed the production of pro-inflammatory cytokines and chemokines during *M. tuberculosis* infection by inhibiting NF- $\kappa$ B p65 activation, although the exact mechanisms are still unknown<sup>442</sup>.

An potential mechanism involving balance between the catalytic activity of Viperin of CMPK2 has recently been suggested by Rivera-Serrano *et al.* (2020)<sup>395</sup>. This proposition is based on the

observation that the catalytic activity of nucleoside kinase CMPK2 (*i.e.* the generation of CTP) is essential for NLRP3 inflammasome activation<sup>480</sup>. Because CTP is the preferential substrate for Viperin, it was hypothesized that CMPK2 and Viperin act as positive and negative regulators of the inflammatory response by increasing CTP production or consumption, respectively<sup>395</sup>. However, this proposition is only speculative and would need further experimental investigation to be confirmed.

### 5. 2. 2. 3. Role of Viperin in modulating the inflammatory response in fish

**In fish.** Studies focusing on the role of Viperin in the regulation of the inflammatory response in a fish model are scarce. A few studies have reported the expression modulation of genes encoding pro-inflammatory cytokines (including TNF- $\alpha$ , IL-6, IL-8, IL-1 $\beta$ ) following overexpression of Viperin in fish cell lines or tissues<sup>429,430,450,453</sup>. Similarly, overexpression of grouper EcViperin zebrafish DrViperin resulted in a higher activity of the NF- $\kappa$ B promoter<sup>430</sup> and increased higher ROS generation<sup>446</sup>, respectively. However, as for mammals, the underlying mechanisms linking fish Viperin to the inflammatory response are yet to be elucidated.

## 5. 2. 3. Cellular metabolic pathways exploited during the viral life cycle

### 5. 2. 3. 1. Lipid and cholesterol biosynthesis

**In mammals.** Early work showed that overexpression of Viperin was able to disrupt lipid rafts on the plasma membrane of HeLa cells, resulting in decreased membrane fluidity and limited budding of influenza A viral particles<sup>444</sup>. Similar observations were made with other viruses, which utilize cholesterol-rich lipid rafts to bud from the host cell membrane, such as rabies virus in RAW264.7 macrophages<sup>481</sup> and human immunodeficiency (HIV-1) in monocyte-derived macrophages<sup>482</sup>. In addition, it was observed that overexpression of Viperin resulted in reduced cholesterol levels in several cell lines<sup>426,441,481</sup>.

Mechanistically, it was initially reported that Viperin reduced cholesterol production by binding to farnesyl-pyrophosphate synthase (FPPS), an enzyme involved in cholesterol synthesis, leading to reduced catalytic activity of the endogenous FPPS pool<sup>444</sup>. It was later shown that Viperin does not affect the catalytic activity of FPPS *per se* but reduces the cellular levels of the enzyme *via* a C-terminal domain-dependent but radical SAM activity-independent mechanism<sup>422</sup>. Because *FPPS* mRNA levels were unaffected by Viperin expression, it was suggested that Viperin promoted FPPS degradation, likely *via* the proteasome pathway<sup>422</sup>. More recently, an interactome study coupled with co-IP assays revealed that Viperin interacts with cholesterol biosynthetic enzymes distinct from FPPS (which was not found in the interactome), including squalene monooxygenase (SM) and lanosterol synthase (LS) by forming a ternary complex *in cellulo*<sup>426</sup>. Further experiments showed that Viperin

inhibited the enzymatic activity of LS but not SM; however, it reduced the cellular levels of SM by ~30%, likely by increasing its rate of proteasomal degradation<sup>426</sup>. However, whether the generation of ddhCTP by Viperin is needed to have an impact on the activity or the concentration of these enzymes remains to be elucidated. Of note, in addition to cholesterol biosynthetic enzymes, the interactome from Grunkemeyer *et al.* (2021) revealed other cellular proteins interacting with Viperin, including enzymes involved in membrane lipid metabolism, suggesting that Viperin may have an impact on lipid metabolism as a whole that may expand beyond its antiviral activity<sup>426</sup>. The role of Viperin in lipid metabolism will be further discussed in **Section 7.1**.

***In fish.*** In fish, only one recent study investigated the role of Viperin in cholesterol and lipid metabolism: Shanaka *et al.* (2023) provide preliminary evidence that *viperin*<sup>-/-</sup> zebrafish larvae display higher cholesterol amounts during VHSV infection than their WT counterparts<sup>446</sup>.

#### 5.2.3.2. Modulation of protein secretion

***In mammals.*** Besides cholesterol biosynthesis, a few studies point to a role of Viperin in the modulation of protein secretion<sup>405,483</sup>. It was reported early on that Viperin overexpression slowed down the transport rate of soluble proteins but not membrane-associated proteins *via* a mechanism requiring its N-terminal  $\alpha$ -helix domain<sup>405</sup>. It was speculated that this function may contribute to Viperin's antiviral effect by inhibiting the trafficking of soluble viral proteins and/or cellular proteins necessary for viral replication, although no experimental evidence was provided to support this hypothesis. Opposite results were recently reported in another study, in which the secretion of a reporter protein was reduced following Viperin knockdown and increased upon Viperin overexpression in ATDC5 cells<sup>484</sup>. In addition, Viperin was shown to sequester cellular protein Golgi brefeldin A-resistant guanine nucleotide exchange factor 1 (GBF1) involved in vesicle trafficking in the secretory pathway<sup>483</sup>. Viperin-GBF1 interactions affected TBEV virion assembly and enhanced the release of malfunctioning non-infectious viral particles.

***In fish.*** Whether similar mechanisms are present in fish is currently unknown.

#### 5.2.4. Towards a common mechanism: interactions with ubiquitin ligases?

One emerging function of Viperin is that it seems to promote the ubiquitin-dependent proteasomal degradation of specific proteins. Ubiquitin is a small evolutionarily conserved protein containing 7 lysine residues that can form polymeric chains<sup>485</sup>. It can be conjugated to substrates by an enzymatic cascade involving E1 (ubiquitin activating enzyme), E2 (ubiquitin conjugating enzyme), and E3 (ubiquitin ligase). Cellular proteins can be mono-, multi-, or polyubiquitinated; the latter can trigger diverse functions depending on the linkage type of the ubiquitin chain: for instance, polyubiquitin

chains linked *via* Lys48 are the canonical signal for proteasome-mediated protein degradation, while chains linked *via* Lys63 play nondegradative roles in diverse signaling and trafficking pathways<sup>485,486</sup>. The fact that Viperin seems to stimulate the proteasomal degradation of both viral<sup>413,417,469</sup> and host proteins<sup>467,475</sup> suggests that it can associate with specific E3 ubiquitin ligases<sup>151</sup>. Nonetheless, how Viperin recognizes its target proteins and which E3 ubiquitin ligase it is able to recruit still remains to be determined.

## 6. Regulation of Viperin at the steady state and during viral infections

### 6. 1. Negative regulation of Viperin

#### 6. 1. 1. Negative regulation at the transcription level

In mammals, ISGF3 binding to the *Viperin* promoter is negatively regulated through competition by positive regulatory domain I binding factor 1 (PRDI-BF1) for the ISRE sites, thereby mediating its transcriptional repression<sup>457</sup>. Interestingly, it was further reported that PRDI-BF1 was highly induced during the early phase (1-2hr) of Sendai virus infection and LPS stimulation and effectively blocked the expression of *Viperin* transcripts during early infection but not after<sup>457</sup>. The authors suggested that the resulting negative regulation may prevent potential detrimental effects of excessive Viperin.

Using a knockdown approach, a recent study also provides evidence that IFN-inducible *lncRNA-CMPK2* negatively regulates the expression of *Viperin* (among other *ISGs*) both at the steady state and following IFN- $\alpha$  treatment, likely *via* interactions with transcription factors or chromatin remodeling complexes<sup>424</sup>.

#### 6. 1. 2. Proteasomal degradation of Viperin protein

*In mammals.* Recently, Yuan *et al.* (2020) have observed that *viperin* mRNAs are induced in response to both type I IFNs and viral infections (VSV, Sendai virus, herpes simplex virus 1) in primary epithelial lung cells and in lung cell lines (A549, H358), but the Viperin protein was barely detected following immunoblotting<sup>487</sup>. It was shown that Viperin proteins were degraded through the ubiquitin-proteasome pathway. Mechanistically, both IFNs and viral infections induced the expression of histone acetyltransferase (HAT) 1, resulting in the acetylation of Viperin, which in turn recruited ubiquitin ligase UBE4A, ultimately resulting in the proteasomal degradation of Viperin<sup>487</sup>. Interestingly, UBE4A was highly expressed in epithelial cells but not in macrophages and fibroblasts. It was suggested that UBE4A acted as a negative regulator of Viperin but the benefits of this tight control were not further discussed by the authors.

*In fish.* Whether epithelial cells from fish present a similar UBE4A-dependent mechanism is currently unknown.

## 6.2. Viral subversion of Viperin activation

Viruses have evolved subversion strategies to counteract the antiviral effects of ISG products and Viperin is no exception. Viral subversion strategies against Viperin can be classified into three categories, including blocking its induction, promoting its degradation and hijacking it.

### 6.2.1. Inhibition of Viperin induction

In both mammals and fish, some viruses were reported to inhibit the induction of *viperin* transcripts, either by inhibiting the type I IFN cascade or by specifically targeting *viperin* mRNAs. In mammals, it was shown that the endoribonuclease UL41 protein from herpes simplex virus 1 could counteract the induction of the endogenous *Viperin* gene in HEK293T likely *via* its RNase activity<sup>488</sup>. In fish, Lu *et al.* (2024) recently showed that the N protein of VHSV could attenuate Japanese seabass *LjViperin* promoter activity by blocking IRF1 and IRF9 function *via* ubiquitination of IRF1 and IRF9 leading to their proteasomal degradation<sup>417</sup>.

### 6.2.2. Promotion of Viperin degradation

*In mammals.* Virus-mediated inhibition of Viperin can also take place at the protein level by promoting its degradation. For instance, in mammals, although *Viperin* transcripts are highly induced upon JEV infection, the virus negatively regulates Viperin at the protein level by promoting its degradation *via* the proteasomal pathway<sup>456</sup>. The precise mechanisms were not identified, it could be speculated that they involve UBE4A (described above), as the experiments were performed in A549 epithelial cells.

*In fish.* In fish, Wang *et al.* (2019) have shown that SVCV inhibited the expression of exogenous Viperin<sub>sv1</sub> but not PpViperin and that SVCV-mediated Viperin<sub>sv1</sub> downregulation could be rescued after treatment with proteasome inhibitor<sup>447</sup>. It was later demonstrated the N protein of SVCV can stimulate the ubiquitination of Viperin<sub>sv1</sub> at Lys201 (in the SAM domain), thereby promoting its degradation through the ubiquitin-proteasome pathway<sup>464</sup>.

### 6.2.3. Hijacking of Viperin's functions

In mammals, another example of viral subversion is illustrated with HCMV, which appeared to have hijacked Viperin's cellular functions to favor the infectious process<sup>461</sup>. It was shown that the viral protein vMIA could interact with Viperin and induce its relocalization to the mitochondrion, where it binds the  $\beta$ -subunit (HADHB) of the mitochondrial trifunctional protein (TFP), a multienzyme

complex that catalyzes the last three steps of the fatty acid (FA)  $\beta$ -oxidation pathway. Binding to HADHB reduces TFP activity *via* a mechanism requiring a catalytically active radical SAM domain<sup>461,467</sup>. It was later identified that mitochondrially targeted Viperin reduced HADHB levels by promoting its degradation *via* the proteasome pathway, likely by increasing the rate of HADHB retrotranslocation to the mitochondrial outer membrane<sup>467</sup>. The reduction in TFP activity results in lower ATP levels leading to a disruption of the actin cytoskeleton<sup>461,467</sup>. In addition, reduced ATP levels activate AMP-activated protein kinase (AMPK), resulting in the induction of glucose transporter GLUT4 and increased glucose uptake. Increasing glucose concentrations trigger translocation into the nucleus of the glucose-regulated transcription factor ChREBP, which activates the expression of lipogenic genes, resulting in enhanced lipogenesis and accumulation of lipid droplets<sup>489</sup>. In a context of viral infection, it was hypothesized that disruption of the actin cytoskeleton facilitates release of virions from the cells<sup>461</sup>, while increased lipogenesis aided the formation of HCMV viral envelope<sup>489</sup>. Importantly, Viperin mutant in which the N-terminal domain was replaced with by a mitochondrial localization sequence (MLS) but not a similar catalytically inactive mutant, WT Viperin or a MLS-GFP construct was reported to induce disruption of the cytoskeleton and to enhance lipogenesis, suggesting that Viperin can act independently of vMIA but requires both mitochondrial localization and Fe-S cluster binding<sup>461,489</sup>.

## **7. Emerging role of Viperin in regulating metabolic processes under non-pathological conditions**

A growing but still flimsy body of evidence suggests that mammalian Viperin might play a role, beyond its antiviral function, in regulating metabolic processes under non-infectious conditions.

### **7. 1. Viperin-mediated regulation of lipid metabolism and thermogenesis**

*In mammals.* When it was discovered that mitochondrially-targeted Viperin upon HCMV infection could have an effect on cellular metabolism and more specifically on FA  $\beta$ -oxidation pathway and lipogenesis *via* reduction of TFP activity, the authors suggested that this process was certainly an intrinsic function of Viperin that the virus hijacked to its benefit<sup>418,489</sup>.

Recent studies further investigated the role of Viperin in FA  $\beta$ -oxidation at the organism and tissue level. In particular, endogenous Viperin was found to be highly expressed in brown adipose tissue of mice (involved in thermogenesis) and to localize to the mitochondria in this specific tissue<sup>439</sup>. Using *Viperin*<sup>-/-</sup> mice, it was reported that Viperin deficiency reduced fat mass and increased heat production. At the tissue and cellular level, Viperin deficiency resulted in reduced size of adipocytes and hepatic lipid droplets<sup>439</sup>. In addition, the expression levels of canonical thermogenesis- and FA

$\beta$ -oxidation-related genes were increased in adipose tissues and more specifically in both mature brown and white adipocytes of *Viperin*<sup>-/-</sup> mice but treatment with fatty acid  $\beta$ -oxidation inhibitor could bring the expression of thermogenic genes down to a wildtype level<sup>439</sup>. Taken together, these findings suggest that Viperin acts as a negative regulator of thermogenesis in adipose tissues by inhibiting fatty acid  $\beta$ -oxidation in adipocytes resulting in the accumulation of lipid droplets<sup>439</sup>, likely *via* similar molecular mechanisms described in [Section 6. 2. 3](#) involving reduction in TFP activity *via* binding to HADHB. In line with these findings, it was also recently reported that Viperin played a role in metabolic reprogramming in cancer cells, by increasing lipogenesis *via* inhibition of fatty acid  $\beta$ -oxidation<sup>490,491</sup>.

***In fish.*** In mammals, the research investigating the role of Viperin in lipid metabolism is still in its infancy. Unsurprisingly, whether Viperin-mediated regulation of lipid metabolism exists in cold-blooded animals like fish has not been really explored yet. Nonetheless, Shanaka *et al.* (2023) have recently reported that genes encoding enzymes involved in lipid metabolism, such as fatty acid synthase (*fasna*) and acetyl-CoA carboxylase (*acc*), were upregulated in non-infected *viperin*<sup>-/-</sup> zebrafish larvae compared to WT<sup>446</sup>. Furthermore, Oil Red O staining revealed lower intracellular amounts of lipid droplets following Viperin overexpression in ZF4 cells<sup>446</sup>. These findings, albeit partial, suggest that fish Viperin may also play a role in lipid metabolism.

## 7. 2. Regulation of mitochondrial metabolism

A related subject to the regulation of lipid metabolism is the study of Viperin's role in mitochondrial metabolism. Ebrahimi *et al.* (2020) recently showed that the enzymatic activity of Viperin reduces cellular concentrations of UTP and CTP over time following overexpression in HEK293 cells<sup>468</sup>. Because Viperin-mediated generation of ddhCTP is coupled with the enzymatic activity of mitochondrial enzyme CMPK2 generating CTP, it was suggested that ddhCTP synthesis specifically leads to depletion of UTP and CTP in mitochondria, which may affect the cell metabolism. Evidence was provided that the radical SAM activity of Viperin negatively affects mitochondrial metabolism by reducing mitochondrial respiration rate and amino acid consumption rate<sup>468</sup>. In a later study, the same authors showed that Viperin-produced ddhCTP was able to inhibit NAD<sup>+</sup>-dependent enzymes, including glyceraldehyde 3-phosphate, lactate and malate dehydrogenases (GAPDH, LDH, MDH). Molecular docking simulations predicted that ddhCTP-mediated inhibition involved ddhCTP binding to the NAD<sup>+</sup>-binding pocket of these enzymes<sup>492</sup>. These results have recently been challenged by another research team, which showed that NAD<sup>+</sup>-dependent enzyme inhibition properties of ddhCTP claimed by Ebrahimi *et al.* were probably an artifact arising from the presence of residual dithionite (reducing agent) in the ddhCTP used, which likely reduced NAD<sup>+</sup> into NADH<sup>493</sup>.

### 7. 3. Bone metabolism

The rat ortholog of human *Viperin*, initially called *Best5*, was found to be expressed *in vitro* in differentiating primary rat osteoblasts as well as in human osteosarcoma MG63 cell line upon IFN- $\alpha$  and IFN- $\gamma$  stimulation<sup>386</sup>. It was also detected *in vivo* by immunostaining in osteoblast progenitors as well as in mature osteoblasts in sections of neonatal rat tibiae and in sections of mechanically loaded bones<sup>386</sup>. At that time of discovery, little was known on Viperin and it was suggested to be an intermediate in the response of osteoblasts to stimuli modulating proliferation/differentiation<sup>386</sup>. The role of Viperin in osteoblast differentiation was not further investigated for many years but a few research teams have begun to take a renewed interest in it. A few papers have reported that Viperin was highly expressed in middle zone articular cartilage chondrocytes compared to superficial zone chondrocytes<sup>494</sup>. More recently, the *Viperin* gene was identified in one of the QTLs explaining the size variation of Meishan pigs, suggesting that it might play a role in skeletal development<sup>495</sup>. Furthermore, Viperin knockdown in bone marrow mononuclear cells led to inhibition of osteoclast differentiation, which are cells that initiate bone resorption and remodeling<sup>496</sup>. In the same vein, Viperin was found to be expressed during chondrogenic differentiation *in vivo* in the developing embryonal growth plate of mouse embryos as well as *in vitro* in chondrogenic ATDC5 cell line and in primary human bone marrow stem cells at a late differentiation stage<sup>484</sup>. Interestingly, downregulation of endoribonuclease MRP/RNase P, which was shown to degrade *Viperin* mRNA, and concomitant upregulation of Viperin expression were also linked to bone growth disorders<sup>443</sup>.

Taken together, these results suggest that Viperin is likely involved in bone and cartilage metabolism and more specifically in cell differentiation although the precise regulatory mechanisms are still elusive.

## 8. Conclusion

The past 25 years of research on Viperin have greatly contributed to our understanding of how Viperin exerts its antiviral function. The identification of Viperin's substrate and catalytic product has provided major advances in elucidating Viperin's biological functions. Nonetheless, several lines of evidence point to additional mechanisms of action that are seemingly unrelated to the production of ddhCTP and that involve a complex network of protein-protein interactions. Furthermore, an emerging function of Viperin is that it may have a regulatory role in diverse cellular processes, even under non-pathological conditions, as exemplified by its implication in lipid metabolism and bone metabolism. However, how a single protein can be involved in so many seemingly unrelated processes and whether the underlying mechanisms involve its radical SAM activity remain unclear. These questions should be addressed in future research studies.

# CHAPTER 4

## Development of *in vitro* fish models for the aquaculture sector

### 1. Introduction

The term “aquaculture” broadly refers to the cultivation of aquatic organisms under controlled conditions, including fish, shellfish and algae, as opposed to “fisheries” which consists in the harvesting of wild aquatic animals. Contrary to fisheries, which have experienced stagnating production since the 1990s, aquaculture has emerged as a fast-growing sector, steadily increasing its share of total fisheries and aquaculture production. Of the 178 million tons of aquatic animals (fish and shellfish) produced in 2020, 51% (90 million tons) was from capture fisheries and 49% (88 million tons) from aquaculture (Figure 23). This is a major change from the 1950s, where aquaculture represented merely 4% of the total share. Since then, aquaculture has continued to expand rapidly, reaching 20% in the 1990s and 44% in the 2010s. This exponential growth aligns with the rising consumer demand observed over the past 60 years, with mean global consumption of aquatic products per capita increasing from 9.9 kg/year in the 1960s to 20.2 kg/year in 2020<sup>497</sup>.

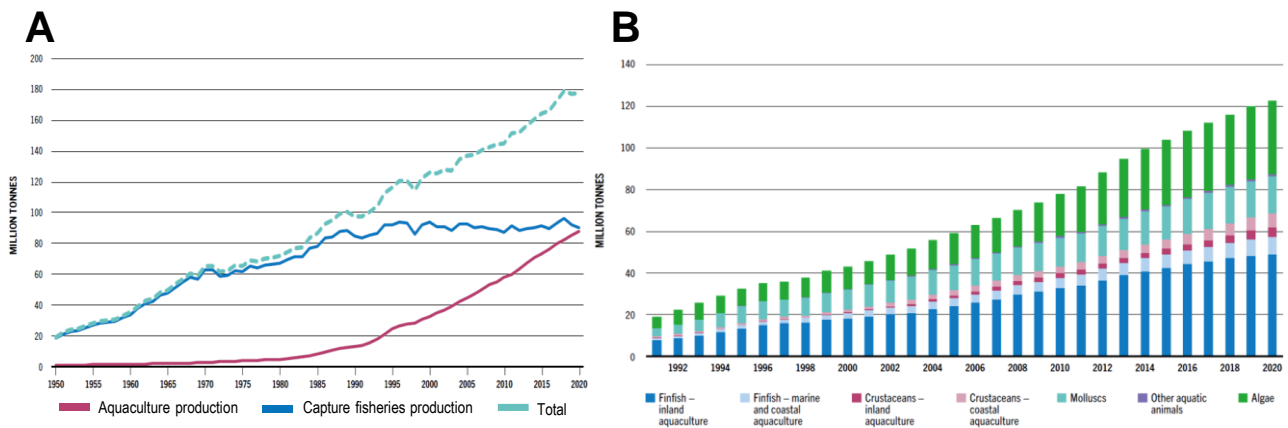


**Figure 23: World capture fisheries and aquaculture production**

(A) World capture fisheries and aquaculture production (excluding algae) from 1950 to 2020. (B) World aquaculture production by production types from 1991 to 2020. Graphs modified from FAO (2022)<sup>497</sup>.

In this manuscript, the primary focus is on fish farming, which represents two thirds of farmed aquatic animal production<sup>497</sup>. In this chapter, the importance of fish health for the aquaculture sector and the challenges faced by fish immunology and disease research are discussed in the first section. The second section provides an overview of *in vitro* fish cell-based approaches for fish health research with particular attention given to knockout techniques developed in fish cell lines.

## 2. The importance of fish health in aquaculture

### 2. 1. Fish farming: a fast-growing sector

In 2020, global aquaculture production (including fish and shellfish but excluding algae) reached a record 87.5 million tons of farmed aquatic animals (USD 264.8 billion) and is expected to increase to 106 million tons in 2030, which would represent a 53% share in global production of aquatic animals. Among aquatic animal farming, finfish farming accounts for the largest share of world aquaculture. In 2020, farmed finfish production was estimated at 57.5 million tons (USD 146.1 billion), including 49.1 million tons (USD 109.8 billion) from inland aquaculture and 8.3 million tons (USD 36.2 billion) from marine and coastal aquaculture <sup>497</sup>.

The aquaculture production, including fish farming, is dominated by a small number of major producers, including China, India, Indonesia for warm water species and Norway and Chile for cold water species. Despite the great diversity of farmed fish species, only a few of them are predominantly produced; carp and tilapia are the main warm water species, whereas Atlantic salmon is by far the most important cold water species, accounting for one third of marine and coastal aquaculture <sup>497</sup>.

### 2. 2. Challenges of fish disease management

#### 2. 2. 1. Fish infectious diseases

Most pathologies affecting farmed fish are caused by infectious agents (viruses, bacteria, fungi, parasites), environmental factors like fluctuations in water quality or nutritional deficiencies <sup>498</sup>. Aquatic systems pose a heightened risk of infectious diseases, as animals are continually exposed to both endemic or introduced pathogens. Furthermore, the intensification and expansion of aquaculture alongside the globalization of trade in aquatic products have favored the spread and emergence of infectious diseases <sup>499</sup>. To date, infectious disease outbreaks are still considered one of the main causes of economic losses in the aquaculture industry <sup>500</sup> and are estimated to cost the global aquaculture industry about USD 6 billion a year <sup>499</sup>. Of note, infectious diseases were still the leading cause of mortality in farmed Atlantic salmon in 2023 in Norway, which is renowned for having the most technologically advanced fish farming industry <sup>501</sup>. Among infectious diseases, viral diseases are responsible for serious, epidemic episodes in fish farms. A telling example is infectious salmon anemia (ISA), which caused massive production losses in marine-farmed Atlantic salmon <sup>502</sup>. The causative agent, a negative sense ssRNA virus belonging to the family of *Orthomyxoviridae*, was responsible for an unprecedented economic crisis in Chile between 2007 and 2010 <sup>503</sup>. During this period, Chilean production of Atlantic salmon plummeted from 376,000 tons in 2006 to 123,000 tons

in 2010 (Figure 24), representing a drastic 67% decline and resulting in huge economic losses (USD 2 billion) along with major social repercussions including the loss of 20,000 to 25,000 jobs<sup>504</sup>.

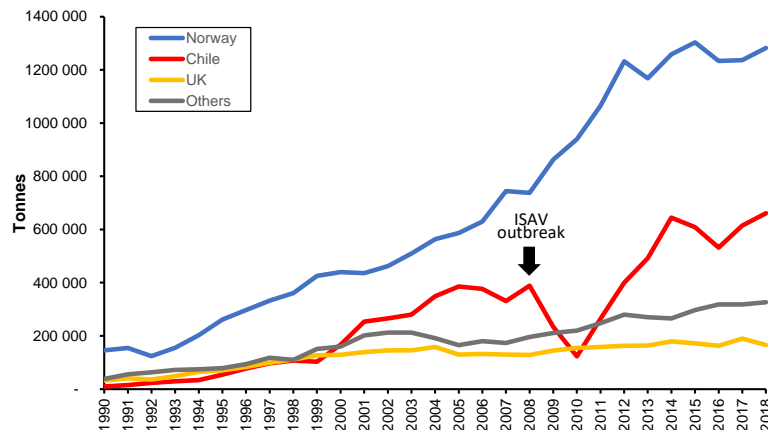


**Figure 24: Atlantic salmon production from 1990 to 2018**

Data were taken from FAO (2020), FishStatJ database

Other deadly viruses affecting important aquaculture species (including salmonids and cyprinids) and notifiable to the World Organization for Animal Health (WOAH, previously known as Office International des Epizooties, OIE) are presented in Table V. In addition to these long-known viral diseases, emerging viruses are becoming a growing concern to the aquaculture sector. These include Piscine orthoreovirus (PRV) responsible for heart and skeletal muscles inflammation (HSMI) syndrome and totivirus Piscine myocarditis virus (PMCV) causing cardiomyopathy syndrome in Atlantic salmon, as well as Tilapia lake virus (TiLV), which has become notifiable to WOAH in 2023, betanodavirus Nervous Necrosis Virus (NNV), responsible for viral encephalopathy and retinopathy in various marine species such as Asian and European seabass, gilthead sea bream and Japanese flounder, and *Lates calcarifer* Birnavirus (LCBV), which cause high mortality outbreaks in farmed Asian seabass<sup>505–509</sup>.

### 2. 2. 2. Disease control methods

Infectious diseases represent a significant constraint on aquaculture productivity and disease control strategies have been implemented to limit outbreaks. These measures include curative treatments by using antibiotics, disinfectants and other chemicals against bacterial, fungal and parasitic diseases and a preventive approach *via* implementation of biosecurity measures at all scales (international, national, farm scales), good management practices, vaccination, selective breeding of disease-resistant fish, functional feeds to promote fish health and disease surveillance<sup>498,510</sup>. Examples of improved fish health status and system productivity following the implementation of these methods are abundant. For instance, breeding of IPN-resistant salmon, has led to a sharp decline of IPNV

outbreaks in Norwegian aquaculture after 2009<sup>511–513</sup>, although recent outbreaks caused by emerging IPNV variants in genetically resistant fish have been reported in Chile and Norway<sup>514,515</sup>. Preventive vaccination against bacterial diseases (including vibriosis, cold-water vibriosis and furunculosis) in Norway has also greatly contributed to the development of Norwegian salmon farming in the late 20<sup>th</sup> century while reducing the use of antibiotics to virtually zero<sup>516</sup>. In aquaculture, most licensed fish vaccines are based on inactivated pathogens but novel vaccine technologies based on live, subunit, recombinant and nucleic acid vaccines are also promising for the development of new aquaculture vaccines<sup>517,518</sup>.

**Table V: Viral diseases notifiable to WOA in 2023**

	Virus name	Virus family and genus	Susceptible fish species	Location	Reference
Cold water viruses (<15°C)	Infectious Hematopoietic Necrosis Virus (IHNV)	<i>Rhabdoviridae</i> <i>Novirhabdovirus</i> .	Arctic charr, <b>Atlantic salmon</b> , brook trout, brown trout, chinook salmon, chum salmon, coho salmon, <b>rainbow trout</b> , sockeye salmon, pike	Worldwide	509,519
	Viral Hemorrhagic Septicemia Virus (VHSV)	<i>Rhabdoviridae</i> <i>Novirhabdovirus</i> .	Atlantic and Pacific herring, European anchovy, Northern pike, Atlantic cod, wrass, olive flounder, <b>Atlantic salmon</b> , brook trout, brown trout, chinook salmon, chum salmon, coho salmon, <b>rainbow trout</b> , sockeye salmon, among others	Worldwide	509,520
	Salmonid Alphavirus (SAV)	<i>Togaviridae</i> . <i>Alphavirus</i>	Arctic charr, <b>Atlantic salmon</b> , common dab, <b>rainbow trout</b>	Europe	509,521
	Infectious Salmon Anemia Virus (ISAV)	<i>Orthomyxoviridae</i> <i>Isavirus</i>	<b>Atlantic salmon</b> , brown trout; <b>rainbow trout</b>	Mainly Norway and Chile, but also Europe and North America	509,522
Intermediate temperature (15-20°C)	Spring Viremia Carp Virus (SVCV)	<i>Rhabdoviridae</i> <i>Sprivivirus</i> .	Bream, goldfish, <b>grass carp</b> , <b>common carp</b> , zebrafish, among others	Worldwide	509,523
	Epizootic Hematopoietic Necrosis Virus (EHNV)	<i>Iridoviridae</i> <i>Ranavirus</i>	Northern pike, European perch, pike-perch, silver perch, <b>rainbow trout</b> , among others	Australia, Europe	509,524
Warm water viruses (>25°C)	Koi Herpesvirus (KHV)	<i>Alloherpesviridae</i> <i>Cyprinivirus</i>	<b>Common carp</b> and hybrids	Worldwide	509,525
	Red Sea bream Iridovirus (RSIV)	<i>Iridoviridae</i> <i>Megalocytivirus</i>	Red sea bream, yellowtail, amberjack, <b>sea bass</b> , mandarin fish, red drum, mullet, groupers	East and South-East Asia	509,526
	Infectious Spleen and Kidney Necrosis Virus (ISKNV)				
	Tilapia Lake Virus (TiLV)	<i>Amnoonviridae</i> <i>Tilapinevirus</i>	Tilapia species	South-East Asia, Israel and Africa	509,527

## 2. 3. Challenges of fish health research

As presented above, fish health is one of the most important aspects for a successful aquaculture system. In their report on the state of fisheries and aquaculture, the FAO advocated a 10-point biosecurity best practice, the first three of which were “(1) know your species, (2) know your system, (3) know your pathogens”<sup>497</sup>. Interestingly, not only does this sentence insist on the knowledge – both empiric and scientific – on the specific farmed fish, it also highlights the importance of the three components host-pathogen-environment triad and their interactions<sup>498</sup>. In this regard, basic research in fish immunology and microbiology is important to decipher host-pathogen interactions and ultimately nourish applied research to improve disease control solutions.

However, the current knowledge on fish pathogens and fish immune responses is still fragmented. As mentioned in **Chapter 1**, fish immunology is a relatively recent discipline fraught with pitfalls, including the remarkably huge number of fish species from very diverse habitats (hence, the first point from the FAO) as well as genome duplication events, which make functional studies of specific immune gene families even more complex. Concerning the third point from the FAO, research focusing host-pathogen interactions often necessitates the ability to cultivate the pathogen of interest. Cell culture-based approaches are primarily used to propagate viruses. However, for emerging fish viruses, this prerequisite is not always met. This shortcoming is exemplified by PRV, the causative agent of HSMI in farmed Atlantic salmon, which has not been cultivable so far: for instance, it was recently reported that none of the 31 fish cell lines tested were able to support PRV amplification<sup>528</sup>. Therefore, the development of robust cell line models capable of supporting the replication and study of emerging fish diseases is crucial for advancing the understanding of diseases affecting aquaculture<sup>517</sup>.

## 3. *In vitro* fish cell lines for fish health research

### 3. 1. Uses

Fish primary cells and immortalized cell lines are *in vitro* tools commonly used in both basic and applied research for toxicological, pathological, and immunological studies<sup>529</sup>. As mentioned above, fish cell culture-based propagation of virus has greatly facilitated research on specific viral pathogens. Fish cell lines are also widely used to decipher cellular functions involved in the fish innate immune response and study host/pathogen interactions, thereby providing valuable insights into the molecular mechanisms behind fish innate immunity. In applied science, cell lines are also essential for cell culture-based diagnostic tools, which are still considered the gold standard for viral diagnostics<sup>530</sup>,

and for the development of inactivated viral vaccines, which still represent the majority of viral vaccines available on the market for the aquaculture sector.

### 3. 2. From conventional to engineered cell lines

In the past few decades, considerable efforts have been made to establish and characterize new fish cell lines representative of diverse fish species and tissue types <sup>529</sup>. At the time of writing this manuscript, the online cell line database Cellosaurus included more than 900 fish cell lines isolated from more than 200 fish species. While some fish cell lines like Bluegill fry (BF-2), Chinook salmon embryo (CHSE-214), Epithelioma papulosum cyprini (EPC), Fathead minnow (FHM), rainbow trout gonad (RTG-2) are permissive to a wide range of viruses (including VHSV, IHNV, IPNV, SVCV, among others) <sup>531</sup>, other cell lines are specifically used to amplify viruses known to be difficult to propagate such as ISKNV and SKIV <sup>532</sup>.

Despite the growing number of fish cell lines, Collet *et al.* (2018) noted that little effort has been made towards their functional characterization and towards the development of cell culture-based genetic engineering tools <sup>533</sup>. In *in vitro* fish models, gene function studies are mainly based on gain-of-function approaches based on the transfection of cells with a plasmid encoding the gene of interest using either constitutive or inducible expression systems <sup>533</sup>. Although relatively easy to implement, overexpression approaches are intrinsically biased as they are based on unnaturally high levels of the protein of interest.

Alternatively, gene function can be studied using loss-of-function approaches. In *in vitro* fish models, these methodologies are less common as they are more difficult to implement and they are mainly based on transient knockdown techniques using morpholino oligonucleotides, short interfering RNAs, or chemical inhibition (examples are given in **Chapter 2**). In addition, knockdown approaches also suffer from other flaws: they provide only temporary inhibition of gene function and are often incomplete with remanent levels of the protein of interest, which can mask some gene functions <sup>534</sup>.

In that respect, knockout approaches are more robust, as there is – in theory – no residual levels of the protein of interest. However, the development of knockout fish cell lines has not become as widespread as with mammalian lines and it is still in its infancy, as described hereafter <sup>533</sup>.

### 3. 3. Development of knockout fish cell lines

#### 3. 3. 1. Overview of knockout gene editing methods

##### 3. 3. 1. 1. Principle of knockout mechanism

Development of knockout cell lines typically relies on nuclease-based gene editing platforms, including zinc finger nucleases (ZFNs), transcription-activator like effector nucleases (TALENs) and clustered regularly interspaced short palindromic repeats/CRISPR associated nuclease (CRISPR/Cas) systems (**Table VI**). Regardless of their nature, these systems are composed of a sequence-specific DNA-binding module (targeting a specific sequence) linked to a non-specific DNA cleavage module<sup>534</sup>. Mechanistically, these nucleases generate site-specific double-strand breaks (DSBs) at the specific target sequence. DSBs are then repaired *via* either non-homologous end-joining (NHEJ) or homologous recombination through homology directed repair (HDR), resulting in targeted sequence modifications<sup>534</sup>. While NHEJ directly ligates break ends without any template, HDR uses a homologous sequence as a template for regenerating DNA sequences at the DSB<sup>535</sup>. Both repair techniques can be exploited in genome editing: NHEJ-mediated repair is often error-prone and can lead to small insertions or deletions at the cut site, which generate frameshifts into the coding sequence; in addition, simultaneous generation of two DSBs can lead to deletions, inversions and translocations of the intermediate DNA sequence<sup>534</sup>. Alternatively, HDR-based repair relies on introduction of a modified repair template (*e.g.* DNA construct with extended homology arms identical to the flanking sequences of the targeted DSB) leading to the introduction of modified gene sequence<sup>534,536</sup>.

##### 3. 3. 1. 2. Genome editing technologies

As mentioned above, three main nuclease-based technologies have been developed for genome editing:

**Zinc-finger nucleases (ZFNs).** ZFNs are chimeric proteins, consisting of an array of 3-4 site-specific DNA-binding zinc-finger domains (each recognizing a 3-bp sequence) linked together and attached to the endonuclease domain of the bacterial FokI restriction enzyme<sup>536,537</sup>. ZFNs are designed as a pair that recognizes two sequences flanking the target site (one on the forward strand, the one on the reverse strand); upon binding, the FokI domains dimerize and generate a DSB between the binding sites.

**Transcription-activator like effector nucleases (TALENs).** TALENs function in a similar fashion to ZFNs, but their DNA-binding domain is composed of an array of 10 to 30 repeat domains, each recognizing a single base pair *via* 2 hypervariable residues (repeat-variable di-residues)<sup>538</sup>. Contrary

to ZFNs where each zinc-finger domain recognizes a nucleotide triplet, the one-to-one correspondence for each repeat/nucleotide pair in TALENs provides greater flexibility<sup>534</sup>.

**CRISPR/Cas9.** The CRISPR/Cas system consists of a Cas endonuclease (usually *Streptococcus pyogenes* Cas9) that binds a guide RNA, composed of a variable CRISPR (cr)RNA, comprising a 20 nt variable protospacer sequence in 5', complementary of a target sequence, and a 3' constant sequence that hybridizes with a transactivating (tra)crRNA<sup>539</sup>. In current CRISPR/Cas9-based methods, crRNA and tracrRNA are fused to form a single guide RNA (**Figure 25A**). The sgRNA (or crRNA-tracrRNA hybrids) guides Cas9 to cleave complementary target DNA sequences, that are adjacent to specific sequences known as protospacer adjacent motifs (PAMs), downstream of the crRNA-binding sequence. The PAM sequence has the canonical form 5'-NGG in the CRISPR/Cas9 system. Upon hybridization of the protospacer with its complementary sequence on the DNA strand, Cas9 generates a DSB in the DNA sequence at a position 3 bp upstream of the PAM<sup>540</sup> (**Figure 25B**). Of note, alternative CRISPR/Cas systems from other bacterial species can also be used for genome editing<sup>541</sup> but it is much less common than Cas9 and will not be further discussed in this manuscript.

**Table VI: Comparison of genome editing tools ZFNs, TALENs and CRISPR/Cas9.**

Adapted from Janik *et al.* (2020)<sup>542</sup>.

	<b>ZFNs</b>	<b>TALENs</b>	<b>CRISPR/Cas9</b>
<b>Species of origin</b>	Eukaryotes	Genus <i>Xanthomonas</i>	Prokaryotes
<b>Construction</b>	Protein engineering for every single target	Protein engineering for every single target	20-Nucleotide sequence of single-guide RNA (sgRNA)
<b>Target sequence recognition</b>	Zinc fingers protein, protein-DNA interactions	Repeat variable di-residues (RVDs) repeats, protein-DNA interactions	sgRNA, RNA-DNA interactions
<b>DNA-binding domains</b>	3-4 Zinc fingers domains 1 domain = 30 aa	10-30 RVD repeats 1 domain = 33-35 aa	sgRNA synthesis or cloning
<b>Specificity</b>	Recognition of a nucleotide triplet by each ZF domain	For each domain, two residues recognize a single bp	20 first nucleotides of crRNA or sgRNA + Presence of PAM downstream of the target sequence
<b>DNA sequence recognition size</b>	(9 or 12 bp) x 2	(10–30 bp) x 2	17–20 bp + NGG x 1
<b>Endonuclease</b>	FokI	FokI	Cas9 and its different variants
<b>Mechanism</b>	Tandem operation: two ZFNs around the target sequence; dimerization of FokI domains and cleavage of the spacer sequence	Tandem operation: two TALENs around the target sequence; dimerization of FokI domains and cleavage of the spacer sequence	sgRNA complementary to the target sequence and cleavage of target sequence by Cas9 3 pb upstream of the PAM
<b>Targeting efficiency</b>	Low	Moderate	High
<b>Affordability</b>	Resource intensive and time consuming	Affordable but time consuming	Highly affordable and rapid

Although ZFNs and TALENs had their glory days in the early years of genome editing, these techniques were completely supplanted by the arrival of the CRISPR/Cas9-based genome engineering tools. Indeed, contrary to ZFNs and TALENs, which require the design of specific proteins for each new target site and are time- and labor-consuming, CRISPR/Cas9 technology is more flexible and can be adapted to any genomic sequence (provided that there is a PAM downstream of it) only by changing the 20 nt-protospacer of the sgRNA <sup>536</sup>. The CRISPR/Cas9 technology can also be used for multiplexing approaches, by using a cocktail of multiple sgRNAs targeting different genes <sup>543</sup>.

In 2012, it was demonstrated that the CRISPR/Cas9 system could be adapted to cut specific DNA sites *in vitro* <sup>544</sup>, paving the way for genome editing applications. A series of articles published the following year showed that this technology could be used to disrupt genes in various cells and organisms, including bacteria <sup>545</sup>, yeast <sup>546</sup>, human cell lines <sup>547,548</sup>, zebrafish <sup>549</sup>, mouse <sup>543</sup> and plants <sup>550</sup>, among others.

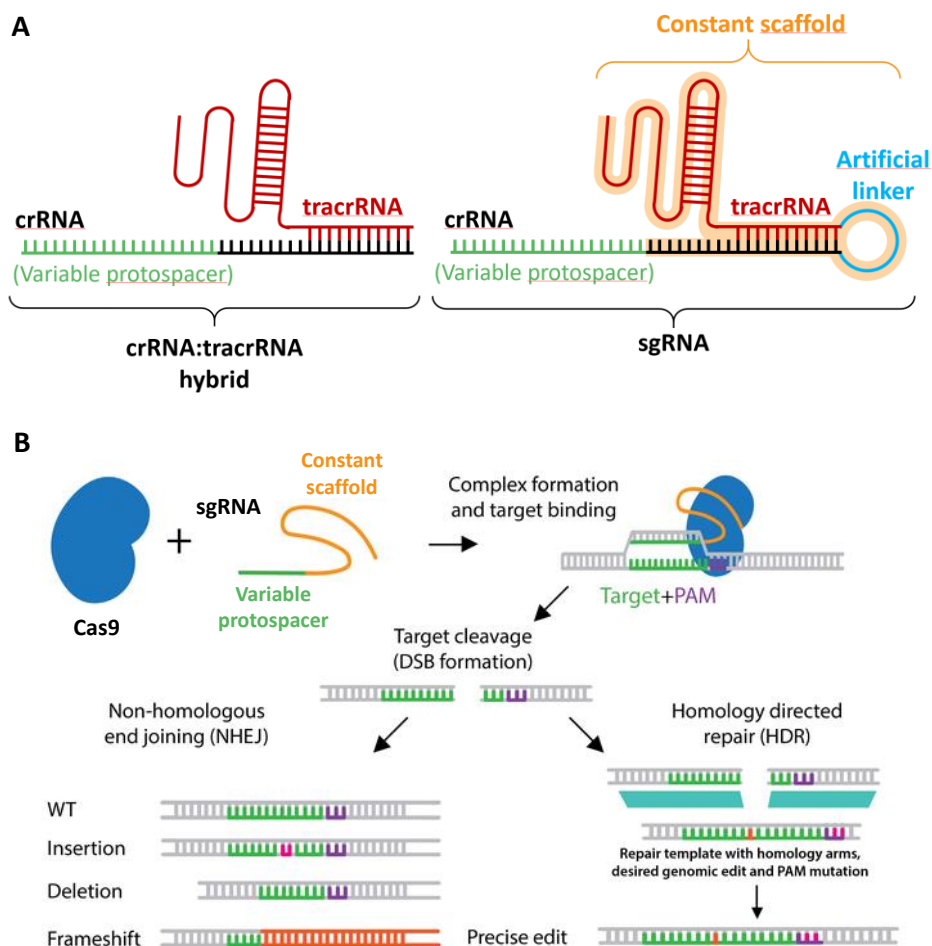


**Figure 25: Overview of CRISPR/Cas9-based genome editing**

(A) Structure of the CRISPR RNA (crRNA)-transactivating crRNA (tracrRNA) hybrid (left) and artificial single guide RNA (sgRNA) (right). Adapted from Nidhi *et al.* (2021) <sup>551</sup>. (B) Schematic representation of CRISPR/Cas9-based gene knockout process *via* the NHEJ or HDR DNA repair processes. Adapted from Addgene (2024) <sup>552</sup>.

### 3.3.2. Knockout fish cell lines

Besides zebrafish <sup>549</sup>, CRISPR/Cas9-based technology was also successfully used in Atlantic salmon <sup>553</sup> and in rohu (*Labeo rohita*) <sup>554</sup> by injecting into eggs, *in vitro* transcribed sgRNA and Cas9-encoding mRNA or Cas9 and sgRNA encoding plasmids, respectively.

In fish cell lines, the first proof-of-concept was only published in 2016 by Dehler *et al.* <sup>555</sup> using a salmonid cell line (CHSE-EC) genetically engineered overexpress a monomeric, cytosolic form of EGFP (mEGFP) and the nuclear nCas9n. It was demonstrated that the *mEGFP* gene could be knocked out following transfection of a specific sgRNA targeting the transgene. This cell line was later used to disrupt endogenous genes, including *stat2* and the two paralogs *stat1a1* and *stat1a2* using the same methodology <sup>136</sup>, opening the way for functional studies based on knockout cell lines in *in vitro* fish models. In the years following these first publications, other research groups successfully generated knockout cell lines from various species using different Cas9 and sgRNA delivery techniques, such as plasmids <sup>556</sup>, sgRNA-Cas9 ribonucleoprotein <sup>557</sup> and lentiviruses <sup>558</sup>. Published examples of fish cell lines knocked out for endogenous genes are presented in **Table VII**.

**Table VII: non-exhaustive list of published fish knockout cell lines**

Cell line	Species	Target gene	Delivery system	Clonal ?	Reference
CHSE-EC	Chinook salmon	<i>mEGFP</i>	Transfection of sgRNA	Yes	<sup>555</sup>
CHSE-EC	Chinook salmon	<i>mEGFP+</i> <i>stat2</i> or <i>stat1a1-2</i>	Transfection of sgRNA	Yes	<sup>136</sup>
CHSE-EC	Chinook salmon	<i>mEGFP+</i> <i>rig1</i>	Lentivirus	No	<sup>558</sup>
CHSE-214	Chinook salmon	<i>mavs</i> , <i>irf3</i> , <i>irf7-1</i> , double KO <i>irf3+irf7-1</i>	RNPs	Yes	<sup>559</sup>
ASK-1 SHK-1	Atlantic salmon	<i>cr2</i> <i>mmp9</i>	RNPs Plasmid	Yes	<sup>560</sup>
EPC	Fathead minnow	<i>hif1a</i>	Plasmid	Yes	<sup>556</sup>
EPC	Fathead minnow	<i>irf9</i>	Plasmid	Yes	<sup>561</sup>
HX1	Medaka	<i>ntrk3b</i>	RNP	Yes	<sup>557</sup>
Cas9-OmB	Tilapia	<i>impal.1</i> , <i>nanos3</i> , <i>nfat5</i>	Plasmids	No	<sup>562</sup>
Cas9-OmB	Tilapia	<i>impal.1</i> , <i>mips</i>	sgRNA-encoding plasmids	Yes	<sup>563</sup>
CIK	Grass carp	<i>jam-a</i>	Plasmids	Yes	<sup>564</sup>

The development of knockout fish cell lines is still in its infancy but the widespread of the CRISPR/Cas technology applied to *in vitro* fish models is likely to help deepen our understanding of the underlying molecular mechanisms of the innate immune response in fish.

---

# OBJECTIVES

---

In mammals, the main components of type I IFN response have been identified over the past 50 years. Overall, most of the key antiviral pathways are conserved in fish, but they display a more diverse repertoire of type I IFNs and ISGs compared to mammals, due to their complex evolutionary history and physiological specificities. In particular, the antiviral functions of most fish ISGs, their underlying molecular mechanisms and interactions remain to be explored in detail.

Until recently, functional studies aiming to characterize specific ISGs in fish models were mainly based on cloning, overexpression and, to a much lesser extent, knockdown and chemical inhibition approaches. Although informative, these approaches suffer from intrinsic flaws, including unnaturally high levels or remanent levels of the protein of interest and debatable specificity of chemical inhibitors, respectively. However, the expansion of genome editing technologies associated with the massive sequencing of the genomes of many fish species is currently revolutionizing the field of fish immunology, making knockout approaches in fish models more accessible.

In this context, the overarching aim of my PhD project was to develop and characterize fish cell lines, in which selected *ISGs* have been knocked-out using the CRISPR/Cas9 system in order to understand their respective contribution to the antiviral immune response. This work is an integral part of a larger research project initiated in our laboratory, which is focusing on the development of *in vitro* knock-out fish cell lines to elucidate the function of specific components of the type I IFN pathway in teleosts<sup>136,555</sup>. In my PhD project, two key *ISGs*, namely *pkr* and *viperin*, were chosen as candidate targets. In this regard, the objectives of my project were three-fold:

- (1) to develop and validate ***pkr*<sup>-/-</sup> and *viperin*<sup>-/-</sup> fish cells**, using the salmonid CHSE-EC cell line and cyprinid EPC-EC cell line as parental cell lines, respectively;
- (2) to **functionally characterize** the *pkr*<sup>-/-</sup> and *viperin*<sup>-/-</sup> cell lines, in order to decipher their respective **mechanisms of action** and their potential **role in regulating the type I IFN response** through feedback loops;
- (3) to assess their **permissivity to viral infections** and evaluate their potential for **viral particle production at higher yields** than their wildtype counterparts.

Objective 3 is of industrial interest and stems from a collaboration with Virbac, a pharmaceutical company specializing in animal health that is co-funding this PhD project along with ANRT. Indeed, inactivated vaccines are still the main antiviral vaccines currently available on the market for the aquaculture sector. However, the development and industrial production of such vaccines is still hampered by the low yields of conventional viral particle production systems, relying on *in vitro* virus replication in permissive cell lines. In this project, we hypothesized that the type I IFN response limits the yield of viral particle production in available cell culture systems.

To achieve Objective 1, the process of gene knockout in fish cell lines implemented in this project is presented below for greater clarity.

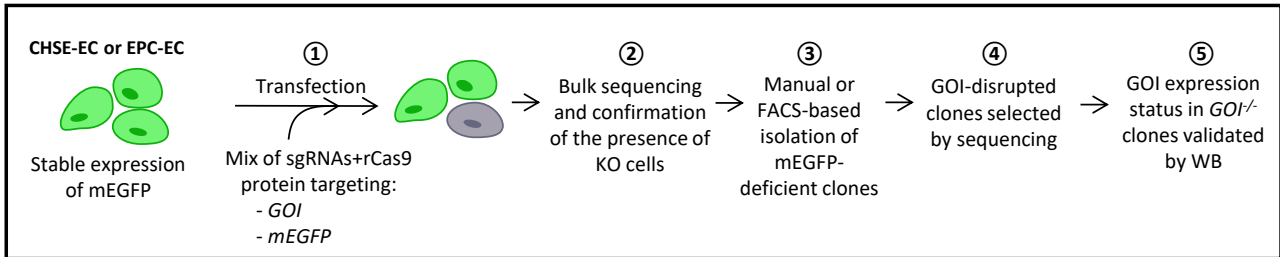


**Figure 26: Workflow implemented in this project to develop fish knockout cell lines**

The workflow was adapted from Dehler *et al.*<sup>136,555</sup>. CHSE-EC or EPC-EC – two clonal cell lines stably expressing mEGFP – were used as parental cell lines to develop KO cell lines by CRISPR/Cas9 genome editing. (1) Cells are transfected with recombinant Cas9 and a cocktail of sgRNAs targeting the gene of interest (GOI) and the mEGFP transgene (for screening purposes); (2) the bulk of transfected cells is sequenced to validate the presence of cells knocked-out for the *GOI* and for the *mEGFP* gene; (3) clonally derived mEGFP-deficient cells are subcultured following manual isolation or fluorescence-activated cell sorting (FACS); (4) after a few weeks of propagation, isolated clones are sequenced to validate the disruption of the gene of interest at the genomic level; (5) the GOI expression status is validated in the selected clones at the protein level by western blot (WB).

---

# RESULTS

---

---

# RESULTS 1

## Characterization of the molecular functions of salmonid PKR using overexpression and knockout approaches

---

### 1. Introduction

The first axis of this thesis was to functionally characterize salmonid PKR using both overexpression and knockout approaches. PKR is one of the most studied proteins encoded by an ISG in mammalian models and is commonly considered a key factor of innate immunity against viruses. PKR is known for being involved in central cellular processes in response to stress signals including inhibition of protein translation *via* phosphorylating eukaryotic initiation factor 2 $\alpha$  (eIF2 $\alpha$ ), regulation of apoptosis through activation of the caspase cascade and enhancement of the type I IFN and inflammatory responses. In fish, orthologs of mammalian *PKR* have been cloned from species of various taxonomic orders, including Tetraodontiformes (*e.g.* fugu <sup>266</sup>), Perciformes (*e.g.* rock bream <sup>264</sup>, Nile tilapia <sup>265</sup>, orange-spotted grouper <sup>231</sup>), Pleuronectiformes (Japanese flounder <sup>199</sup>), Cypriniformes (crucian carp <sup>239</sup>, grass carp <sup>238</sup>, zebrafish <sup>200</sup>). These studies have not investigated the antiviral function of fish PKR as extensively as mammalian studies; nonetheless, they provide evidence, through overexpression and knockdown approaches, that some molecular functions are conserved between fish and mammalian PKR. Curiously, studies focusing on salmonid PKR are scarce; to the best of my knowledge, only one article on salmonid PKR was published in 2016 by Gamil *et al.* <sup>267</sup>. Using a chemical inhibitor-based approach, the authors showed that endogenous Chinook salmon PKR seems to favor IPNV replication <sup>267</sup>.

In our study, we went a step further by characterizing the molecular functions of Chinook salmon PKR using complementary overexpression and knockout approaches. We addressed the following questions: **(1) does Chinook salmon PKR activate apoptosis? (2) does it inhibit host protein translation? (3) Is it involved in the inhibition of viral replication?**

### 2. Article

Chaumont, L., Peruzzi, M., Huetz, F., Raffy, C., Le Hir, J., Minke, J., Boudinot, P., & Collet, B. (2024). Salmonid Double-stranded RNA-Dependent Protein Kinase Activates Apoptosis and Inhibits Protein Synthesis. *Journal of immunology (Baltimore, Md. : 1950)*, 213(5), 700–717. <https://doi.org/10.4049/jimmunol.2400076>

# **Salmonid double-stranded RNA-dependent protein kinase (PKR) activates apoptosis and inhibits protein synthesis**

Lise Chaumont<sup>\*</sup>, Mathilde Peruzzi<sup>\*</sup>, François Huetz<sup>†</sup>, Claudine Raffy<sup>‡</sup>, Jérôme Le Hir<sup>‡</sup>, Jules Minke<sup>‡</sup>, Pierre Boudinot<sup>\*</sup>, Bertrand Collet<sup>\*</sup>

<sup>\*</sup> Université Paris-Saclay, INRAE, UVSQ, VIM, 78350 Jouy-en-Josas, France

<sup>†</sup> Unit of Antibodies in Therapy and Pathology, UMR 1222 INSERM, Institut Pasteur, 75015 Paris, France

<sup>‡</sup> VIRBAC S.A., 06510 Carros, France

Corresponding author:

[bertrand.collet@inrae.fr](mailto:bertrand.collet@inrae.fr)

This project was funded in part by the European Union through AQUAEXCEL3.0 (Grant Agreement 871108) and AQUAFAANG (Grant Agreement 817923) and by the Research Council of Norway through the project PMCV (Project 301083). LC was a recipient of PhD funded by Virbac and the French Association for Research and Technology (ANRT) [Convention CIFRE #2020/0646] in collaboration with the Fish Infection and Immunity laboratory (INRAE, VIM, Jouy-en-Josas, France).

## Abstract

The dsRNA-dependent protein kinase (PKR) is a key factor of innate immunity. It is involved in translation inhibition, apoptosis and enhancement of the proinflammatory and interferon responses. However, how these antiviral functions are conserved during evolution remains largely unknown. Overexpression and knockout studies in a Chinook salmon (*Oncorhynchus tshawytscha*) cell line were conducted to assess the role of salmonid PKR in the antiviral response. Three distinct mRNA isoforms from a unique *pkr* gene, named *pkr-fl* (full length), *pkr-ml* (medium length) and *pkr-sl* (short length), were cloned and a *pkr*<sup>-/-</sup> clonal fish cell line was developed using CRISPR/Cas9 genome editing. PKR-FL includes an N-terminal dsRNA-binding domain and a C-terminal kinase domain, while PKR-ML and PKR-SL display a truncated or absent kinase domain, respectively. PKR-FL is induced during IFNA2 stimulation but not during viral hemorrhagic septicemia virus (VHSV) infection. Overexpression experiments showed that only PKR-FL possesses antiviral functions including activation of apoptosis and inhibition of *de novo* protein synthesis. Knockout experiments confirmed that PKR is involved in apoptosis activation during late stage of VHSV infection. Endogenous PKR also plays a critical role in translation inhibition upon poly(I:C) transfection after IFNA2 treatment. It is, however, not involved in translational arrest during VHSV infection. Extra- and intracellular titrations showed that endogenous PKR does not directly inhibit viral replication but apparently favors virion release into the supernatant, likely by triggering late apoptosis. Altogether, our data confirm that salmonid PKR has conserved molecular functions, that VHSV appears to bypass with subversion strategies.

## Key points

- Three isoforms of Chinook salmon PKR are present in CHSE-EC cells
- Full-length PKR triggers apoptosis and inhibits *de novo* protein synthesis
- Endogenous PKR is not involved in translational arrest during VHSV infection
- Endogenous PKR favors virion release into the supernatant at a late infection stage

**Keywords:** PKR, EIF2AK2, Chinook salmon, *Oncorhynchus tshawytscha*, interferon response, apoptosis, translational arrest, antiviral activity

## Introduction

The host innate immunity is the first line of defense against viral infections. Rapid and efficient detection of viruses is critical to mount an immune response capable of limiting virus replication and propagation to neighboring cells. It is well established that pathogen-associated molecular patterns (PAMPs) are recognized by sensors called pattern recognition receptors (PRRs). Activation of PRRs triggers signaling cascades, which subsequently leads to the production of host defense molecules, including type I interferons (IFNs), proinflammatory cytokines and chemokines. Type I IFNs induce the transcription of hundreds of IFN-stimulated genes (*ISGs*), including effector genes, which can have direct antiviral actions or modulate cell physiology to inhibit viral infection, replication and propagation <sup>1</sup>.

Eukaryotic translation initiation factor 2 alpha kinase 2 (EIF2AK2), better known as dsRNA-dependent protein kinase (PKR), is one of the most studied proteins encoded by an *ISG*. It is recognized as a multifunctional key factor of innate immunity, as it acts both as a sensor and an effector in response to viral infections. Mammalian PKR is constitutively and ubiquitously expressed at low levels in all tissues and as all *ISG* products, its expression is induced by a variety of stress associated responses, including type I IFNs, LPS stimulation and viral infections <sup>2,3</sup>. Structurally, PKR contains an N-terminal regulatory region with two dsRNA-binding motifs (dsRBMs) and a C-terminal kinase domain <sup>2,4</sup>. PKR requires an activation step to be fully catalytically functional <sup>5,6</sup>. This activation is primarily mediated by binding to dsRNA, which is produced during the replication cycle of RNA viruses <sup>6</sup>. Interactions with dsRNA occur through its dsRBMs, leading to homodimer formation mediated by the N-terminal lobe of the kinase domain <sup>4,7</sup>. PKR dimerization induces conformational changes that allow the *trans* autophosphorylation of the activation loop at critical conserved threonine residues <sup>7</sup>. Once activated, PKR phosphorylates the  $\alpha$ -subunit of the eIF2 complex, which is required for the initiation of mRNA translation. Phosphorylation of eIF2 $\alpha$  blocks the recycling of inactive eIF2-GDP complex by the GTP exchange factor eIF2B, resulting in the inhibition of the cell translation machinery <sup>8</sup>.

Although PKR is best described for its effect on protein translation, it is also involved in many other antiviral mechanisms. Overexpression of mammalian PKR is known for promoting apoptosis in transfected cells via both the intrinsic mitochondrial and extrinsic death receptor pathways <sup>9-12</sup> while *Pkr*<sup>-/-</sup> mouse embryonic fibroblasts (MEFs) or *PKR*<sup>-/-</sup> HeLa cells displayed resistance to apoptosis in response to dsRNA, TNF- $\alpha$ , or LPS <sup>13,14</sup>. The molecular mechanisms underlying PKR-mediated apoptosis involve eIF2 $\alpha$  phosphorylation-dependent induction of specific stress response genes <sup>14-18</sup> and activation of transcription factors NF- $\kappa$ B and p53 <sup>19-21</sup>. PKR was also reported to modulate the

inflammatory and the type I IFN responses, by activating mitogen-activated protein kinases (MAPKs)-dependent<sup>22–24</sup> and NF- $\kappa$ B signaling pathways<sup>20,25</sup> and enhancing type I IFN production upon infection with some but not all viruses<sup>21,26–29</sup>. In most cases, the precise role of PKR in the activation of these different pathways remains elusive and whether PKR acts directly or indirectly has not been fully clarified. The importance of PKR role in the antiviral response is further emphasized by the numerous subversion strategies developed by viruses to antagonize PKR-mediated antiviral mechanisms, as recently reviewed by Cesaro and Michiels<sup>30</sup>.

Orthologs of mammalian *PKR* have been found in fish genomes, in cartilaginous fish as well as bony fish<sup>31</sup>. Some teleost fish families, including cyprinids, salmonids and clupeids, also possess a fish-specific paralog of *pkr*, called *pkz*, which encodes a Z-DNA-dependent protein kinase<sup>32</sup>. *pkz* genes in fish were isolated before fish *pkr* genes, in Crucian carp<sup>33</sup>, zebrafish<sup>34</sup> and Atlantic salmon<sup>35</sup>, among other species. Although most studies on fish PKR did not dissect the structure-function relationship as extensively as in mammals, they indicate that most antiviral functions attributed to mammalian PKR are overall conserved in these organisms. Briefly, a few studies have reported that fish PKR (and PKZ) are able to phosphorylate eIF2 $\alpha$  and inhibit *de novo* protein synthesis<sup>36–40</sup>, trigger apoptosis<sup>38,41,42</sup>, modulate the NF- $\kappa$ B signaling pathway<sup>36,43</sup> and the production of type I IFN<sup>44,45</sup>, although the molecular mechanisms have not been investigated. Of note, in fish, most studies were performed using overexpression approaches, which generally lead to unnaturally high levels of the protein of interest. A few other studies have also used knock-down approaches based on morpholino oligonucleotides<sup>46</sup>, short interfering RNAs<sup>40</sup> or chemical inhibition<sup>44,47</sup> but to the best of our knowledge, no knockout *in cellulo* fish models have been developed so far.

In this study, we identified and cloned three different isoforms of *pkr* in a salmonid cell line from Chinook salmon (*Oncorhynchus tshawytscha*). To investigate their respective antiviral functions, we used both overexpression and knockout approaches. For this purpose, we developed the first *pkr* knockout clonal fish cell line using CRISPR/Cas9 genome editing. We showed that PKR is involved in apoptosis activation and plays a major role in translational arrest upon poly(I:C) stimulation but not during VHSV infection. Our data further suggest that PKR favors the release of VHSV virions into the supernatant at a late infectious stage, likely by triggering apoptosis. Taken together, our results indicate that salmonid PKR exhibits conserved molecular functions but the endogenous protein does not have a major antiviral effect against VHSV, likely due to evasion strategies evolved by the virus.

## Material and methods

### 1. Cell lines, culture conditions and viruses

The *Epithelioma papulosum cyprinid* (EPC) cell line was grown in Leibovitz's L-15 medium (Gibco) supplemented with 10% fetal bovine serum (FBS, Eurobio) and penicillin (100 U/mL)-streptomycin (100 µg/mL) (P/S) (BioValley). The Chinook salmon (*Oncorhynchus tshawytscha*) embryo (CHSE-214) cell line was maintained in Glasgow's modified Eagle's medium (GMEM) containing 25 mM HEPES (Biosera) supplemented with 10% FBS, 2 mM L-glutamine (Eurobio), and penicillin (100 U/mL)-streptomycin (100 µg/mL). The CHSE-EC cell line, that was previously genetically modified to stably express a monomeric enhanced green fluorescence protein (mEGFP)<sup>48</sup>, as well as its derivatives were grown in L-15 medium supplemented with 10% FBS, penicillin (100 U/mL)-streptomycin (100 µg/mL), 500 µg/mL G418 (Invivogen), 30 µg/mL hygromycin B Gold (Invivogen). All cell lines were maintained at 20°C without CO<sub>2</sub>.

Recombinant viral hemorrhagic septicemia virus expressing tomato red fluorescent protein (rVHSV-Tomato) was a kind gift from Dr. Stéphane Biacchesi (Université Paris-Saclay, INRAE, UVSQ, VIM, Jouy-en-Josas, France)<sup>49</sup>. rVHSV-Tomato was propagated in EPC cells (multiplicity of infection (MOI) of 1): briefly, the virus was adsorbed onto the cells for 1h at 14°C with regular gentle shaking; L-15+2% heat-inactivated FBS was added afterwards and the supernatants were collected at 5 days post-infection, 0.2 µm-filtered, aliquoted and stored at -80°C. Golden shiner virus (GSV) was propagated in CHSE-214 (MOI 1.5) at 22°C in GMEM+2% FBS, as described above for rVHSV-Tomato. At 10 days post-infection, the remaining cells were scraped and the cell suspension was bath-sonicated (4 x 1 min at ~40 kHz) (EMAG AG), clarified at 400 g for 5 min, 0.2 µm-filtered, aliquoted and stored at -80°C. rVHSV-Tomato and GSV titers were determined by plaque assay (as described in section 11).

### 2. Development and validation of a *pkr*<sup>-/-</sup> cell line

The previously established CHSE-EC cell line (hereafter referred to as EC) was used to develop a *pkr*<sup>-/-</sup> cell line. Four single guide RNAs (sgRNAs) were designed within the first and second coding exons of the *pkr* gene (LOC112253229, LG24), using CRISPOR v5.01 web tool ([Table I](#))<sup>50</sup>. To ensure the specificity of the sgRNAs, care was taken that no off-target genes with more than 3 mismatches in the first 12 bp adjacent to the PAM (most likely off-targets) were identified in the Chinook salmon genome (Otsh\_v2.0, NCBI RefSeq assembly GCF\_018296145.1). A sgRNA targeting the *mEGFP* gene was also used as previously designed<sup>48</sup>.

The sgRNAs were synthesized using the T7 RiboMAX™ Express Large Scale RNA Production System kit (Promega) using 0.5 µg of each primer, incubated with 1µL of RQ1 DNase (Promega) for

1h at 37°C and purified using TRIzol™ reagent (Invitrogen), according the manufacturers' instructions. The sgRNAs were resuspended in RNase- and DNase-free water and quantified using a Nanodrop spectrophotometer. The purity of the sgRNAs was checked on a 2% agarose-EtBr gel before or after a 30 min treatment with RNase A (Qiagen) at room temperature. Each sgRNA was mixed with recombinant TrueCut™ Cas9 Protein v2 (Invitrogen) at a 1:1 molar ratio (0.2 µg sgRNA and 1 µg rCas9 *i.e.* 6.1 pmol each in 2 µL) and incubated at room temperature for 20 min. The sgRNA-mEGFP/Cas9 complex was mixed with each sgRNA-PKR/Cas9 complex at 1:1 volume ratio in resuspension buffer R (Neon™ Transfection System kit, Invitrogen) (1 µL of each complex in a final volume of 5 µL). The mix was transfected into EC cells using the Neon™ Transfection System (Invitrogen): EC cells were prepared as described in section 4 and 5 µL of cell suspension at  $2 \times 10^7$  cells/mL was mixed with 5 µL of sgRNA/Cas9 complex (*i.e.*  $1 \times 10^5$  cells, 6.1 pmol of Cas9 and 6.1 pmol of sgRNA per 10 µL of transfection reaction). The cells were transfected using the same conditions established for plasmids, as described in section 4. All transfected cells ( $\sim 5 \times 10^5$  cells) were mixed in 5 mL L-15+10%FBS+P/S in a 25 cm<sup>2</sup> flask (Sarstedt) and incubated at 20°C for 3-4 weeks.

Once the cell population reached confluency, the transfected cells were passaged (surface ratio 1:4), and  $\sim 2 \times 10^6$  cells were used for genomic DNA extraction using NucleoSpin Tissue Mini kit (Macherey-Nagel), according to the manufacturer's instructions. Genomic DNA segments containing the targeted sites were amplified by PCR using GoTaq® G2 Flexi DNA Polymerase (Promega) using the following genotyping primers: PKR-gen1-F/PKR-gen1-R and PKR-gen2-F/PKR-gen2-R for *pkc* coding exon 1 and exon 2, respectively (**Table I**). The PCR cycling program was performed in a thermal cycler (Eppendorf) and was as follows: 94°C for 3 min then 35 cycles of 94°C for 15 s, 58°C for 15 sec, 72°C for 40 sec, and a final extension of 72°C for 5 min. The PCR products were purified using NucleoSpin Gel and PCR Clean-up Mini kit (Macherey-Nagel) and directly sequenced using the same amplification primers (Sanger sequencing service, Eurofins) (**Table I**). Sequences were analyzed using Synthego ICE analysis tool v3 (Synthego)<sup>51</sup> to assess the percentage of mutated cells in the transfected cell populations (bulks). sgRNA-PKR2-4 failed to show any genome editing at the targeted sites so only the bulks transfected with sgRNA-PKR1 were further used for clonal isolation.

Cells from two independent cell populations transfected with sgRNA-PKR1 were either manually isolated or sorted by FACS, respectively. For manual isolation,  $\sim 1 \times 10^5$  cells were seeded in a 6-well plate and serially diluted (6-fold dilutions) in duplicates. Three to four weeks post-seeding, clonal cell patches were marked, analyzed under a fluorescent Axio Observer Z1 microscope (Zeiss, Oberkochen, Germany) and  $\sim 50$  mEGFP-deficient clones were selected, detached mechanically by scraping with a pipette tip and sub-cultured into 48-well plates. After 3-4 weeks, 22 clones were sub-

cultured and propagated in 25 cm<sup>2</sup> flasks and their genotype was characterized as described above. For FACS-sorted clones, cells were detached by trypsin-EDTA action and mEGFP-deficient single cells at a density of  $\sim 4 \times 10^6$  cells/mL were individualized by a BD FACSAria™ Fusion Flow Cytometer (Institut Pasteur, Paris, France) using a 100  $\mu$ m nozzle into a 96-well plate (Sarstedt) in L-15 supplemented with 10% FBS, penicillin (200 U/mL)-streptomycin (200  $\mu$ g/mL), 500  $\mu$ g/mL G418 and 30  $\mu$ g/mL hygromycin B Gold. Seven weeks later, 5 clones were sub-cultured and propagated in 25 cm<sup>2</sup> flasks and their genotype was characterized as described above.

Two manually isolated clones, EC-PKR-C19 and EC-PKR-C28, presenting a 1-nt insertion (29\_30insT resulting in V11fsX22, KO) and a 6-nt deletion (30\_35delGTGCGA, resulting in C11\_E12del, WT-like) at the sgRNA targeted site respectively, and two FACS-sorted clones, EC-PKR-C3 and EC-PKR-C5, presenting the same 1-nt insertion (29\_30insT resulting in V11fsX22, KO) at the targeted site, were kept for knock-out validation by western blot. For this purpose, these clones and the WT EC cell line were seeded into 6-well plates at a density of  $1.2 \times 10^6$  cells/well in L-15+2%FBS+P/S. The next day, cells were stimulated in triplicates with *Salmo salar* IFNA2 supernatant (produced as described in section 5) diluted to 1:10 in L-15+2%FBS+P/S or left untreated and incubated at 20°C. At 72h post-stimulation, medium was removed, cells were washed once with ice-cold DPBS, scraped in 1 mL ice-cold DPBS supplemented with 2.5 mM EDTA and centrifuged at 1500 g at 4°C for 5 min. The cell pellets were drained, resuspended in 100  $\mu$ L NP-40 lysis buffer (50 mM Tris-HCl pH 7.4, 150 mM NaCl, 2 mM EDTA, 0.5% NP40, 1 mM DTT, 10% glycerol, cOmplete™ protease inhibitor (Merck), PhosSTOP™ phosphatase inhibitor (Merck)) and lysed for 45 min at 4°C under gentle shaking. The cell lysates were clarified by centrifugation at 5000 g at 4°C for 5 min and stored at -80°C until use for western blot analysis as described in section 7.

### 3. Plasmid constructions

Chinook salmon *pkc* open reading frame (ORF) sequences were identified *in silico* using NCBI Reference Otsh\_v2.0 Primary Assembly and predicted transcripts XM\_042305680.1 and XM\_042305681.1. Total RNA from  $1.5 \times 10^6$  EC cells infected with rVHSV-Tomato (MOI 1) at 48 and 72hpi in triplicates was extracted using the QiaShredder and RNeasy mini kits (Qiagen) according to the manufacturer's instructions. RNA (1  $\mu$ g) was used as template for reverse transcription and generation of cDNA using the QuantiTect Reverse Transcription kit (Qiagen) with random primers.

The cDNA was diluted two-fold with RNase-free water and used as template to amplify the *pkc* ORF sequence. Nested PCR amplifications were performed using Q5 2X High-Fidelity mastermix (New England Biolabs) and 2 sets of specific primers according to the manufacturer's instructions: OtPKR-R0-F/ OtPKR-R0-R and OtPKR-R0bis-F/OtPKR-R0bis-R were used for the first PCR round while OtPKR-P2A-F and OtPKR-HindIII-R were used for the second PCR round (**Table I**). The PCR

cycling programs were performed in a thermal cycler (Eppendorf) and were as follows: 98°C for 30 sec followed by 35 cycles of 98°C for 15 s, 66°C (1<sup>st</sup> round) or 60°C (2<sup>nd</sup> round) for 15 sec, 72°C for 90 sec, and a final extension of 72°C for 2 min. PCR products were purified with the NucleoSpin Gel and PCR Clean-up Mini kit (Macherey-Nagel) and sent to sequencing. Purified PCR products were digested with HindIII enzymes (ThermoFisher), cloned into HindIII/EcoRV-digested pcDNA3.1-Zeo-BFP vector using T4 DNA ligase (New England Biolabs) according to the manufacturer's instructions and fully sequenced. The pcDNA3.1-Zeo-BFP vector was initially obtained by subcloning the BFP gene amplified from pCite-P-BFP<sup>52</sup> into a pcDNA3.1(-)-Zeo backbone (Invitrogen) using BFP-F/BFP-R primers (**Table I**) followed by XhoI/HindIII digestion. The pCite-PBFP plasmid was a kind gift from Dr. Hortense Decool (Université Paris-Saclay, INRAE, UVSQ, VIM, France). All plasmids were produced in Stellar<sup>TM</sup> Competent Cells (Takara) and were purified using NucleoBond Xtra Maxi EF (Macherey-Nagel) according to the manufacturer's instructions.

#### 4. Transfections

Transfections were performed by electroporation using the Neon<sup>TM</sup> Transfection System (Invitrogen) as described previously<sup>48</sup>. Briefly, the cells were washed in DPBS (Sigma-Aldrich), detached by trypsin-EDTA action, resuspended in L-15+10%FBS+P/S and centrifuged at 400 g for 5 min. The cell pellet was drained, resuspended in L-15 without Phenol Red (Gibco), centrifuged at 13 000g for 30 sec, and resuspended again in L-15 without Phenol Red. The cell concentration was adjusted to  $2 \times 10^7$  cells/mL. Depending on the experiment, the cell suspension was mixed with various plasmid constructs (**Table II**) to reach a final concentration of  $0.5 \mu\text{g}/1 \times 10^5$  cells in 10  $\mu\text{L}$  of transfection reaction. A fluorescent vector (mEGFP or RFP-KDEL) was added to verify and/or normalize transfection efficiency between each condition.

The cells were then transfected using the same conditions established for plasmids for CHSE-214 cells or EPC cells<sup>53</sup>. Briefly, transfections were carried out in an electroporator MPK5000 (Neon<sup>TM</sup> Transfection System, Invitrogen) using either a 10  $\mu\text{L}$  or a 100  $\mu\text{L}$  transfection kit (Neon<sup>TM</sup> Transfection System, Invitrogen) set to two pulses for 20 ms at 1300 V (CHSE-214 and derivatives) or 1400 V (EPC). All transfected cells were mixed in L-15+10%FBS+P/S, split into flasks or plates (depending on the experiment) and incubated at 20°C for a time determined for each experiment.

#### 5. Production of *Salmo salar* IFNA2 supernatant

In order to produce IFNA2-containing supernatant,  $44 \times 10^6$  EPC cells were transfected with pcDNA3.1-Zeo-ssIFNA2<sup>54</sup> or pcDNA3.1-Zeo-mEGFP (control) using the conditions described in section 3. The transfected cells were pooled in 24 mL of L15+10%FBS+P/S, split into two 75 cm<sup>2</sup> flasks and incubated at 20°C. At 48h post-transfection, supernatants were collected and clarified by centrifugation 400 g, 5 min, 0.2  $\mu\text{m}$  filtered, aliquoted and stored at -80°C until use. The RTG-P1 cell

line (ATCC CRL-2829), which constitutively expresses the firefly luciferase gene under the promoter of the IFN-induced *mx1* gene<sup>55</sup>, was used to determine the IFN activity of the IFNA2 supernatants produced. Briefly, 1:4 serial dilutions in L-15 of the harvested supernatants were applied onto  $4.5 \times 10^4$  RTG-P1 cells in 96-well plates in quadruplicates and cells were incubated at 20°C. At 30h post-stimulation, medium was removed and 75 µL of Steady-Glo® Luciferase Assay System (Promega) was added in each well and the cell lysates were processed as described in section 8.

## 6. Real-time quantitative PCR

EC (WT) cells were seeded in 6-well plates to a final density of  $1.5 \times 10^6$  cells/well in L-15+2%FBS+P/S. The next day, cells in triplicates or quadruplicates were infected with rVHSV-Tomato (MOI 1) at 14°C for 8 or 24h, stimulated with recombinant *Salmo salar* IFNA2 supernatant (produced as described in section 5) diluted to 1:10 in L-15+2%FBS+P/S for 72h or left untreated.

Total RNA was extracted from cells in individual P6 wells in triplicates or quadruplicates using QiaShredder and RNeasy mini kits (Qiagen) in accordance with the manufacturer's instructions. Quality control of the samples was determined using a Nanodrop spectrophotometer. The cDNA was generated from 1.5 µg of total RNA using the iScript™ Advanced cDNA Synthesis Kit for RT-qPCR (BioRad) and the synthesis was performed in a thermal cycler (Eppendorf) as recommended by the manufacturer. cDNA was diluted to 1:3 in DNase- and RNase-free water and stored at -20°C until use. “No RT” control reactions were made by omitting the reverse transcriptase. The cDNA was mixed with TB Green qPCR Premix Ex Taq (Tli RNaseH Plus) (Takara) along with forward and reverse primers (Table III) at a final concentration of 210 nM each in Twin.tec® real-time PCR plates (Eppendorf). Amplification was performed using a CFX Connect cycler (BioRad) using the following cycling program: initial denaturation at 95°C for 30 sec followed by 40 cycles of 10 sec at 95°C and 30 sec at 60°C. For each biological replicate, mean Cq values of target genes were calculated based on technical duplicate reactions and then normalized using the geometric mean of Cq values of 3 housekeeping genes (*otelf1a*, *otrps29*, *otgapdh3*). The relative expression of each target gene (*otpr-fl*, *otpr-ml*, *otpr-fl* and *otmx123*) was expressed as  $2^{-\Delta Cq}$ , which was then used to calculate their respective fold change in comparison to non-stimulated cells.

For each set of primers, the efficiency was calculated by linear regression obtained by using ten-fold serial dilutions of plasmid containing the target sequence (target genes) or of a pool of cDNA (housekeeping genes) and the qPCR products were validated by gel migration and sequencing. For the primers targeting each PKR isoform, the specificity of each primer set was validated by checking their cross-reactivity using plasmid constructs developed in this study.

## 7. Immunoblotting

Aliquots of 60  $\mu$ L of cell lysates (obtained as described in sections 2 and 8) were mixed with 30  $\mu$ L Laemmli buffer (45 mM Tris, 345 mM glycine, 38% glycerol, 4.8% SDS, 20%  $\beta$ -mercaptoethanol, 0.04% bromophenol blue) and incubated at 100°C for 5 min.

A volume of 8  $\mu$ L of cell lysates was loaded on 10% or 12% polyacrylamide gels and protein samples were separated by electrophoresis in Tris-glycine buffer (25 mM Tris, 192 mM glycine, pH 8,3). Proteins were then transferred onto a nitrocellulose membrane (BioRad) using the mixed molecular weight program from the Trans-Blot® Turbo™ Transfer System (BioRad). The blots were blocked either with 5% non-fat milk or 5% BSA in TBST (10 mM Tris pH 7.4, 150 mM NaCl, 0.1% Tween 20) for 1h at room temperature and then incubated with primary antibodies overnight at 4°C. The following primary antibodies were used with the dilution factors and buffers indicated in **Table VI**: rabbit anti-PKR antiserum, mouse monoclonal anti-GFP, rabbit polyclonal anti-eIF2 $\alpha$ -P, mouse monoclonal anti-puromycin, mouse monoclonal anti-VHSV N, rabbit anti-GSV antiserum, rabbit anti-Mx123 antiserum. The custom-made anti-PKR antibody, initially raised against *Salmo salar* PKR<sup>47</sup>, was a generous gift from Pr. Øystein Evensen (NMBU, Oslo, Norway). The anti-VHSV N antibody was a kind gift from Dr. Stéphane Biacchesi (Université Paris-Saclay, INRAE, UVSQ, VIM, Jouy-en-Josas, France). The anti-Mx123 antibody, raised against rainbow trout Mx3<sup>56</sup>, was a generous gift from Dr. Marta Alonso-Hearn (Department of Animal Health, NEIKER-Basque Institute for Agricultural Research and Development, Basque Research and Technology Alliance, Derio, Spain) and Pr. Jorunn Jorgensen (UiT The Arctic University of Norway, Tromsø, Norway). The blots were washed 5 times in TBST, incubated with horseradish peroxidase (HRP)-conjugated anti-mouse or anti-rabbit (1:4000) secondary antibodies (SeraCare), washed 4 times in TBST and once in PBS. Western blots were developed using Clarity™ Western ECL substrate (BioRad) and detected using ChemiDoc Touch Imaging System (BioRad). After the first detection, the membrane was washed twice with TBST, stripped for 15 min at 37°C using Restore™ Plus buffer (Thermo Scientific), washed twice in TBST, saturated with TBST-5% non-fat milk for 1h and re-probed with a new primary antibody for 2.5h-3h and developed as described above. The following primary antibodies were used for the second round of detection: mouse monoclonal anti- $\alpha$ -tubulin antibody, rabbit polyclonal anti-actin, mouse monoclonal anti-eIF2 $\alpha$  (**Table IV**). Densitometric analysis of the blots was performed using Image Lab software (v 6.1.0, Biorad).

## 8. Assays for assessing translation inhibition activity of Chinook salmon PKR

The translation inhibition activity of Chinook salmon PKR was assessed by luciferase assay and immunoblotting. Luciferase assay is a method commonly used for detecting protein synthesis inhibition activity of PKR in mammalian models and other vertebrates<sup>36–38,40,46,57,58</sup> and was adapted

to quantify the translation inhibition activity of PKR isoforms. For this purpose, EC-PKR-C19 cells were co-transfected with pcDNA3.1-Hyg-RFP-KDEL (0.2 µg/10 µL), pcDNA3-Neo-Luc (0.25 µg/10 µL) and either pcDNA3.1-Zeo-BFP or pcDNA3.1-Zeo-BFP-P2A-PKR-FL/ML/SL (0.25 µg/10 µL) or mock transfected, split into 96-well plates (~1 x 10<sup>4</sup> cells/well in 16 wells per condition) and incubated at 20°C. At 24h post-transfection, medium was removed, 100 µL DPBS was added into each well and RFP fluorescence was measured using a fluorometer (Tecan Infinite M200PRO) with excitation and emission wavelengths of 544 and 603 nm, respectively. Then, DPBS was removed, 75 µL of Steady-Glo® Luciferase Assay System (Promega) was added in each well and the cell lysates were incubated in the dark at room temperature for 5 min. Cell lysates were transferred into a flat-bottom white-walled plate (Greiner Bio-One) and luminescence was measured using a Tecan Infinite M200 Pro luminometer over an integration period of 1000 ms (Tecan, Männedorf, Switzerland). The luminescence value from each well was corrected by subtracting the mean values obtained from the wells containing medium (blank), normalized to the corrected fluorescence value from each well and graphed as fold change relative to the BFP transfected cells.

In a similar fashion, the protein synthesis inhibition activity of PKR isoforms was assessed by western blot using mEGFP as a reporter system and puromycin as a marker of de novo protein synthesis. For this purpose, EC-PKR-C19 cells were co-transfected with pcDNA3-Hyg-mEGFP (0.2 µg/10 µL) and either pcDNA3.1-Zeo-BFP or pcDNA3.1-Zeo-BFP-P2A-PKR-FL/ML/SL (0.5 µg/10 µL) or mock transfected, split into 6-well plates (~1.5 x 10<sup>6</sup> cells/well in quadruplicates) and incubated at 20°C for 30h. In parallel, cells were either treated with cycloheximide (CHX, 50 µg/mL, Thermofisher) for 24h or treated with thapsigargin (Tg, 2 µM, Merck) for 30 min. Both drugs are well-established translation inhibitors were used as positive controls for translational inhibition<sup>59,60</sup>. At 30h post-transfection, cells were pulsed with 5 µg/mL puromycin (Gibco) diluted in growth medium for 15 min at 20°C. The cells were then processed as described in section 2, with a lysis step performed in 75 µL NP-40 lysis buffer, and cell lysates were stored at -80°C until use for western blot analysis as described in section 7.

For knockout experiments, poly(I:C) treatment and virus infections were carried out. Poly(I:C) transfections and not simple incubation were performed, as CHSE-214 are known for not responding to extracellular poly(I:C)<sup>61</sup>. Non-stimulated or IFN-pretreated EC, EC-PKR-C28 and EC-PKR-C19 were transfected with high molecular weight poly(I:C)-rhodamine (Invivogen) at a final concentration of 0.15 µg per 1 x 10<sup>5</sup> cells per 10 µL of transfection reaction. Transfected cells were split into 12-well plates (~3.3 x 10<sup>5</sup> cells/well in triplicates), incubated at 20°C for 24h. For virus infections, EC, EC-PKR-C28 and EC-PKR-C19 were seeded in 6-well plates to a final density of 1.5x10<sup>6</sup> cells/well in L-15+2%FBS+P/S. The next day, cells were infected in triplicates with rVHSV-

Tomato or GSV at MOI 1 or left uninfected and incubated at 14°C or 22°C, respectively. At 24h post-transfection or 16, 24 and 40h post-infection, cells were pulsed with puromycin and processed as described above until use for western blot analysis.

### 9. Apoptosis assay

Apoptosis was assessed by genomic DNA (gDNA) fragmentation and by measuring enzymatic activity of caspase 3/7, caspase 8 and caspase 9.

For the gDNA fragmentation assay, EC-PKR-C19 cells were co-transfected with pcDNA3.1-Hyg-RFP-KDEL (2 µg/100 µL) and either pcDNA3.1-Zeo-BFP or pcDNA3.1-Zeo-BFP-P2A-PKR-FL/ML/SL (5 µg/100 µL). Around  $4 \times 10^6$  transfected cells were seeded in 25 cm<sup>2</sup> flasks incubated at 20°C. At 6hpt, growth medium was removed, cells were washed three times in PBS to eliminate dead cells and new growth medium was added into each flask. At 72 hpt, growth medium was collected, pooled with trypsinized cells and centrifuged at 400 g for 5 min. The cell pellets were drained and used for genomic DNA extraction using NucleoSpin Tissue Mini kit (Macherey-Nagel), according to the manufacturer's instructions. For each condition, 3 µg of gDNA was loaded onto a 1.5% agarose-EtBr gel for each condition.

The enzymatic activity of caspase 3/7, caspase 8 and caspase 9 was measured by using the Caspase-Glo<sup>®</sup> 3/7 assay kit (Promega), in accordance with the manufacturer's instructions. For overexpression experiments, EC-PKR-C19 cells were co-transfected with pcDNA3.1-Hyg-RFP-KDEL (0.2 µg/10 µL) and either pcDNA3.1-Zeo-BFP or pcDNA3.1-Zeo-BFP-P2A-PKR-FL/ML/SL (0.5 µg/10 µL) or mock transfected with water instead of plasmid. A volume of 75 µL of transfected cells was seeded in 96-well plates (Sarstedt) to a final density of  $1 \times 10^5$  cells/well and incubated at 20°C. In parallel, EC-PKR-C19 cells were stimulated with staurosporine (STS, 1µM, Santa Cruz) or infected with GSV (MOI 1) and incubated at 22°C for 24h. At 72h post-transfection or 24h post-treatment (STS or GSV), 75 µL of either Caspase-Glo<sup>®</sup> 3/7, Caspase-Glo<sup>®</sup> 8 or Caspase-Glo<sup>®</sup> 9 reagent was added to each well (8 and 4 technical replicates per condition for transfection and treatment conditions, respectively). The plates were gently shaken on a plate shaker for 30 sec and incubated in the dark at room temperature for 30 min. The luminescence levels in the cell lysates were measured as described above in section 8. For knockout experiments, EC, EC-PKR-C28, EC-PKR-C19, EC-PKR-C3 and EC-PKR-C5 cells were seeded in 96-well plates to a final density of  $5 \times 10^4$  cells/well in L-15+2%FBS+P/S. The next day, the growth medium was removed and the cells were infected in quadruplicates with 75 µL of rVHSV-Tomato suspension at MOI 10, MOI 1 or MOI 0.1 or left uninfected and incubated at 14°C. At 24, 48 and 72 hpi, cells were lysed with 50 µL of Caspase Glo<sup>®</sup> 3/7 reagent and the same protocol described above was applied for luminescence measurement.

### 10. rVHSV-Tomato fluorescence monitoring

The replication of rVHSV-Tomato in cells expressing PKR isoforms or in knockout cell lines was monitored by sequential fluorescence measurement. For overexpression experiments, EC-PKR-C19 cells were co-transfected with pcDNA3.1-Pur-mEGFP (0.2 µg/10 µL) and either pcDNA3.1-Zeo-BFP or pcDNA3.1-Zeo-BFP-P2A-PKR-FL/ML/SL (0.5 µg/10 µL) or mock transfected and split in quadruplicates in 96-well plates and incubated at 20°C for 24h. For knockout experiments, EC, EC-PKR-C28, EC-PKR-C19, EC-PKR-C3 and EC-PKR-C5 cells were seeded in 96-well plates to a final density of  $5 \times 10^4$  cells/well in L-15+2%FBS+P/S. The next day, the medium was removed and cells were infected in quadruplicates (overexpression experiment) or octuplicates (KO experiment) with rVHSV-Tomato at MOI 0.1, 1 or 10 in L-15 without Phenol Red (Gibco)+2%FBS+P/S or left uninfected. At 24, 32, 48, 56, 72, 80 and 96h post-infection, the tomato red fluorescence was measured using a fluorometer (Tecan Infinite M200PRO) with excitation and emission wavelengths of 548 and 593 nm, respectively. The fluorescence values were corrected by subtracting the mean values obtained from the non-infected wells.

### 11. Virus titration in extracellular supernatants and intracellular sonicates

EC, EC-PKR-C28, EC-PKR-C19 cells were seeded in 25 cm<sup>2</sup> flasks to a final density of  $4 \times 10^6$  cells/flask in L-15+2%FBS+P/S. The next day, cells were infected in quadruplicates with rVHSV-Tomato at MOI 1 incubated at 14°C. At 96 h post-infection, the supernatants (4 mL) were collected and kept on ice. The remaining cells were washed 3 times in cold DPBS, scrapped in 2 mL of new growth medium and bath-sonicated (4 x 1 min~40 kHz) (EMAG AG). Supernatants and sonicates were clarified by centrifugation at 400 g for 5 min and virus titers were determined by plaque assay on EPC cells under a carboxymethylcellulose overlay (0.75% in MEM (Eurobio) supplemented with 25 mM HEPES, 2 mM L-glutamine, 350 mg/L NaHCO<sub>3</sub>, 2.5% FBS and P/S. At 3 to 4 dpi, cell monolayers were fixed with 3.7% formol for 1h at room temperature, stained with 0.5% crystal violet and plaque forming units (PFU) were counted.

### 12. Statistical analysis

Results shown in each figure were derived from at least two independent experiments; the data presented are means ± standard deviation (SD). Statistical tests used are indicated in the legend of each. All statistical analyses were performed using GraphPad Prism software version 9.5.1.

## Results

### *Diversity of pkr mRNA isoforms in salmonid EC cells*

In addition to the two rounds of whole genome duplication (WGD) events that occurred during the early evolution of chordates and vertebrates, the genomes of salmonid fish have undergone two supplementary WGD rounds, including a teleost-specific third WGD that dates back to 225-333 million years ago and a salmonid-specific WGD ~80-100 million years ago<sup>62-64</sup>. As a consequence, for each single-copy gene in tetrapods, up to four copies can be found in distinct loci in salmonids, if all have been retained. In reality, following WGD events, duplicated genes can either be lost, pseudogenized, sub- or neo-functionalized, with frequent additional tandem duplication events<sup>65</sup>. In mammals and birds, the *pkr* gene is typically unique<sup>31,32</sup>. In contrast, two or three *pkr* paralogs have been reported in amphibians (*e.g. Xenopus laevis* and *X. tropicalis*)<sup>32</sup>. Similarly, several fish genomes also comprise two or more *pkr* paralogs and several ancient paralogs including *pkz* (Ensembl release 110). In salmonids, tBlastn analysis revealed a unique *pkr* gene in species belonging to genus *Salmo* and *Oncorhynchus*. In the genome of Chinook salmon (*Oncorhynchus tshawytscha*), the *pkr* gene was found at the locus LOC112253229 on LG24. The sequences of predicted isoforms XP\_042161614.1 and XP\_042161615.1, which result from alternative splicing, contain 729 and 728 amino acids, and share 34.5%, 33.6% and 35.2% identity with human PKR (NP\_001129123.1), chicken PKR (NP\_989818.3) and amphibian PKR (NP\_001091256.1), respectively.

We first analyzed the diversity of *pkr* mRNAs in CHSE-EC cells (hereafter referred to as EC)<sup>48</sup>. Amplification of the full-length CDS using cDNA of rVHSV-Tomato-infected EC cells resulted in 3 distinct products of 2187 bp, 1122 bp and 464 bp, respectively (**Figure 1A**, **Table V**). In the following paragraphs, these three products will be referred to as *pkr-fl* (full length), *pkr-ml* (medium length) and *pkr-sl* (short length). The *pkr-fl* product matched the predicted *pkr* transcript (XM\_042305681.1) with 99.95% identity. It spans 19 exons, which corresponds to NCBI's predicted model, and encodes a 728 aa polypeptide matching the predicted PKR protein (XP\_042161615.1) with 99.86% identity. In contrast, the two shorter 1122 pb (*pkr-ml*) and 464 pb (*pkr-sl*) products covered 51% and 21% of the sequence, respectively, and comprise 9 exons and 6 exons only. Of note, missing exons from *pkr-ml* were also absent in *pkr-sl* and were all located in the middle part of the ORF. *pkr-ml* and *pkr-sl* are likely products of alternative splicing and encode polypeptides of 373 aa and 107 aa, respectively.

Using SMART (Simple Modular Architecture Research Tool)<sup>66,67</sup> and InterProScan database, three double-stranded RNA binding motifs (dsRBM1-3) and a kinase domain were identified in the N-terminal and C-terminal domains of PKR-FL, respectively (**Figure 1C**). This organization of functional domains is generally shared by PKR of other vertebrates. Indeed, although only two

dsRBMs are found in mammalian and amphibian PKR, the numbers of dsRBMs present in fish PKR actually varies from one to three <sup>32</sup>. Importantly, PKR-ML only contains one complete dsRBM and the N-terminal portion of a second dsRBM fused to a truncated kinase domain, while PKR-SL only comprises one dsRBM and no kinase domain.

Several important structural features known in mammalian PKR are conserved in Chinook salmon PKR. The dsRBM(s) of all PKR isoforms are highly conserved, as shown by the alignment with human PKR dsRBMs and consensus motif reported by Masliah *et al.* <sup>68</sup>. In particular, the three motifs of PKR-FL contain most of the residues involved in the canonical  $\alpha_1$ - $\beta_1$ - $\beta_2$ - $\beta_3$ - $\alpha_2$  fold and/or dsRNA binding (**Figure 1D**). In addition, dsRBM1 matches dsRBM consensus more closely than dsRBM2 and dsRBM3, as also observed for dsRBM1 and dsRBM2 in human PKR <sup>69</sup>.

The primary structure of PKR-FL kinase domain contains the 11 conserved kinase subdomains described by Hanks *et al.* <sup>70</sup>, as mammalian PKR and other protein kinases (**Figure 1E**). In particular, ATP binding motifs can be found, including the canonical Gly-X-Gly-X-X-Gly in subdomain I, Asp-Leu-Lys-Pro-Ser-Asn in subdomain VI and Asp-Phe-Gln in subdomain VII, which are predicted to interact with ATP through Mg<sup>2+</sup> salt bridges <sup>2</sup>. Subdomain II contains at position 461 the invariant lysine residue that is directly involved in the transfer of the phosphate from ATP to its substrate <sup>2</sup>. Equivalents of the two threonine residues Thr446 and Thr451 in human PKR <sup>71</sup>, which are key autophosphorylation sites involved in PKR activation, are also present in the so-called activation loop of PKR-FL (Thr616 and Thr621). Finally, PKR-FL also contains features specific to eIF2 $\alpha$  kinases, including an acidic kinase insert, that spans subdomain V and continues in the inter-region between subdomains V and VI, and a conserved eIF2 $\alpha$  kinase motif located a few amino acids away from the kinase insert, that is required for PKR kinase activity <sup>32,57</sup>. On the other hand, PKR-ML is missing the first 78 amino acids of a full-length kinase domain, which comprise domains I to V. The invariant lysine residue of subdomain II is also absent from PKR-ML kinase domain. This residue is required for mammalian PKR kinase activity <sup>71,72</sup>. Therefore, the catalytic activity of PKR-ML is expected to be limited or absent. PKR-SL lacks the entire kinase catalytic domain and is expected to be catalytically inactive.

#### *PKR-FL is induced following IFN stimulation but not during VHSV or GSV infections*

The expression profiles of PKR isoforms in response to different stimuli were characterized by western blot and RT-qPCR in EC cells stimulated with recombinant *Salmo salar* IFNA2 or infected with two different viruses: viral hemorrhagic septicemia virus (VHSV), an enveloped negative-sense single-stranded RNA virus belonging to the genus *novirhabdovirus*, and golden shiner virus (GSV), a naked, double-stranded RNA virus belonging to the genus *aquareovirus*. A recombinant VHSV

encoding the fluorescent protein tdTomato, rVHSV-Tomato, was used to facilitate the monitoring of the infection before each sampling timepoint<sup>49</sup>. For both viruses, CPE appearance was also visually checked and the progression of the infection was verified by western blot using specific antibodies (data not shown).

At the protein level, PKR-FL was constitutively expressed at low levels in non-treated EC cells and its expression was significantly induced in IFNA2-stimulated cells at the protein level from 48h post-stimulation (~1.7-fold increase) to 72h post-stimulation (~2.4-fold increase) (**Figure 2A,B**). However, no induction of PKR-FL was detected during viral infections with either rVHSV-Tomato or GSV at any of the time points examined (16-40h post-infection). These results correlate with *pkr-fl* expression at the transcript level: a strong induction of *pkr-fl* mRNA expression was observed after at 72h post-stimulation compared to non-stimulated cells (~31-fold increase) (**Figure 2D**) but no significant induction was detected in rVHSV-Tomato-infected cells at 8 or 24hpi. Remarkably, a similar response was observed with transcripts of *mx1/2/3*, which are well-known IFN stimulated genes both in mammals and fish<sup>73,74</sup>. A ~5 log-fold increase in relative expression was observed upon IFNA2 stimulation, while no induction was detected in rVHSV-Tomato infected cells.

Although recombinant PKR-ML was detected by western blot using the same polyclonal anti-PKR serum used to detect PKR-FL, endogenous PKR-ML could not be detected at the protein level in EC cells in response to IFNA2 stimulation or virus infection (**Figure 2A**). However, *pkr-ml* mRNA was amplified by RT-qPCR. Although its expression was lower than *pkr-fl* at the steady state (**Figure 2C**), it displayed a modest but significant induction at 24h post-infection with rVHSV-Tomato and upon IFNA2 stimulation (5-fold and 3.8-fold increase, respectively) (**Figure 2D**).

Endogenous PKR-SL expression could not be assessed by western blot, as recombinant PKR-SL was not detected by our polyclonal anti-PKR antibody. RT-qPCR data revealed a very low expression of *pkr-sl* compared to *pkr-ml* or *pkr-fl* (**Figure 2C**) and no induction was observed upon rVHSV-Tomato infection or IFNA2 treatment.

Overall, our observations show that PKR-FL expression is predominant at both transcript and protein levels and is strongly induced by type I IFN but not viral infection in EC cells. On the other hand, *pkr-ml* mRNA expression is slightly induced by both type I IFN and viral infection, contrary to *pkr-sl*, which is not induced in all contexts.

### *CRISPR/Cas9-based edition of the *pkr* gene leads to null mutation and abolishes PKR expression in EC cells*

To further characterize Chinook salmon PKR function in the antiviral response, we disrupted the unique *pkr* gene in EC cells, using CRISPR/Cas9 technology. In the following study, four isolated clones were further characterized. Three of them, namely EC-PKR-C19; EC-PKR-C3 and EC-PKR-C5 presented a 1-nt insertion at the targeted cut site leading to a frameshift resulting in the introduction of a premature codon at position 22 (29\_30insT resulting in V11fsX22) (Figure 3A). A fourth clone, EC-PKR-C28, exhibited a 6-nt deletion leading to the deletion of two amino acids, Cys11 and Glu12 (30\_35delGTGCGA, resulting in C11\_E12del). This clone was considered “WT-like” and it was used as an additional positive control for further experiments. As previous experiments showed that IFNA2 was a fast and potent inducer of PKR-FL in EC cells, the PKR expression status in each clone was validated by western blot using IFNA2 stimulated cells. Our results confirm that PKR-FL was strongly expressed in WT EC cells and WT-like EC-PKR-C28 cells stimulated with IFNA2 for 72h, while no induction of PKR-FL was observed in *pkr*<sup>-/-</sup> EC-PKR-C19 and -C3 and -C5 clones (Figure 3B,C).

### *Chinook salmon PKR triggers apoptosis during viral infection*

The functional role of mammalian PKR in apoptosis has been widely described in the literature<sup>9,11,13</sup> and has also been reported in fish<sup>38,39,41</sup>. However, the contribution of PKR to apoptotic reaction during viral infection remains poorly defined especially in non-mammalian models. We therefore characterized the activation of the caspase cascade in EC cells by gain and loss-of-function experiments after viral infection. For this purpose, we performed a genomic DNA laddering test, which is a hallmark of apoptosis, and used a luminescence-based enzymatic assay to quantify the catalytic activity of specific caspases, including Caspase 3/7, Caspase 8 and Caspase 9. Caspase3/7 is an executioner caspase that is activated downstream of the caspase cascade upon apoptosis signaling. It can either be activated by (1) the extrinsic pathway via extracellular signals or (2) the intrinsic pathway *aka.* mitochondrial pathway upon intracellular signals and stresses. Caspase 8 is known for being activated by the extrinsic pathway while caspase 9 is mainly activated by the intrinsic pathway<sup>75</sup>.

**Overexpression of PKR-FL induces apoptosis.** To avoid inadvertent activation of endogenous PKR in transfected cells, the ability of PKR isoforms to trigger apoptosis was assessed in *pkr*<sup>-/-</sup> EC-PKR-C19 cells transfected with the corresponding expression plasmids. Cells stimulated with staurosporine (STS), a well-known activator of apoptosis<sup>76,77</sup> or infected with GSV, a lytic virus known for inducing apoptosis (unpublished data), were included as positive controls. Electrophoresis results

show gDNA laddering in GSV-infected cells and, to a lesser extent, in STS-stimulated cells, suggesting that apoptosis was triggered by both treatments (**Figure 4A**, right panel). These qualitative results were confirmed by measuring caspase enzymatic activity: indeed, caspase3/7 was activated upon stimulation with STS or GSV (3.6-fold and 6.5-fold increase, respectively), thereby validating the assay (**Figure 4B**). For cells transfected with PKR-FL but not with PKR-ML and PKR-SL, a faint gDNA fragmentation was visible, suggesting the presence of apoptotic cells following overexpression of PKR-FL (**Figure 4A**, left panel). Similarly, transfection of PKR-FL but not PKR-ML or PKR-SL triggered the activation of caspase3/7 in *pkrr*<sup>-/-</sup> EC-PKR-C19 cells, with a 2.6-fold increase of activity compared to BFP transfected cells (**Figure 4B**).

To decipher if both extrinsic and intrinsic pathways are involved in PKR-FL-mediated Caspase3/7 activation, the activation of Caspase 8 and Caspase 9 was assessed after overexpression of PKR isoforms (**Figure 4C,D**). Our data show that both caspase 8 and caspase 9 were activated upon overexpression of PKR-FL but not with PKR-ML or PKR-SL, although caspase 8 activation was less pronounced (1.2-fold increase for caspase 8 compared to 1.6 fold-increase for caspase 9). Of note, caspase 9 but not caspase 8 was activated in EC cells treated with STS, which is known to primarily trigger apoptosis *via* the intrinsic pathway<sup>78,79</sup>.

**Loss of function experiment in *pkrr*<sup>-/-</sup> cells show that endogenous PKR triggers apoptosis during VHSV infection.** Although PKR-FL was not induced during rVHSV-Tomato infection (**Figure 2A,B**), constitutively expressed endogenous PKR could play a role in apoptosis activation during viral infection. To test this hypothesis, WT EC cells, WT-like EC-PKR-C28 cells and *pkrr*<sup>-/-</sup> EC-PKR-C19, -C3 and -C5 clones were infected with rVHSV-Tomato at two different MOI (MOI 1 or MOI 0.1) and caspase3/7 activity was measured at 24h, 48h and 72h post-infection.

Our results show that the caspase 3/7 activity observed in WT EC and WT-like EC-PKR-C28 was almost fully abolished in all *pkrr*<sup>-/-</sup> clones starting from 48h post-infection at MOI 1 (**Figure 5A**). A similar but delayed response was observed at MOI 0.1, with a significantly higher caspase3/7 signal in WT EC and WT-like EC-PKR-C28 cells compared to *pkrr*<sup>-/-</sup> clones that occurred at 72h post-infection (**Figure 5B**). Interestingly, caspase 3/7 signal was significantly lower in WT-like EC-PKR-C28 compared to WT EC cells at 48h post-infection at MOI 1 (**Figure 5A**) and this difference was even more marked at MOI 10 (data not shown). Two hypotheses can explain this discrepancy: (1) the 6-nt deletion resulting in a 2-aa deletion (Cys11 and Glu12) might alter PKR ability to induce apoptosis; (2) as shown in **Figure 3C**, PKR-FL is slightly but significantly less induced in WT-like EC-PKR-C28 upon IFNA2, suggesting that endogenous PKR-FL expression level is somewhat lower in this clone for a reason independent from the 2-aa deletion (clonal effect) and as a consequence, apoptosis might be slightly less activated. The fact that PKR-FL-C11\_E12del isolated from EC-PKR-

C28 exhibits a similar translation inhibition activity that WT PKR-FL supports the second hypothesis (**Figure S2**).

Our data illustrate that PKR-FL induces apoptosis *via* the caspase 8 and caspase 9 pathways and that it plays a key role in the activation of apoptosis during rVHSV-Tomato infection.

#### *Chinook salmon PKR is involved in host translational arrest*

PKR is also known for its role in host translation inhibition in virus infected cells *via* phosphorylation of eIF2 $\alpha$ . The role of PKR in protein synthesis inhibition in EC cells was investigated by western blot using two different approaches: overexpression of PKR isoforms and activation of endogenous PKR with poly(I:C).

**Overexpression of PKR-FL induces a cellular shutoff of host protein translation.** To examine the role of Chinook salmon PKR isoforms on host protein translation, *pk<sup>r</sup>-/-* EC-PKR-C19 cells were co-transfected with expression vectors encoding PKR isoforms and with a plasmid featuring a reporter gene encoding either mEGFP or firefly luciferase. Protein synthesis was assessed by quantification of mEGFP expression by western blot or by luciferase luminescence assay, respectively. Importantly, in contrast to WT EC cells, *pk<sup>r</sup>-/-* EC-PKR-C19 cells do not constitutively express mEGFP, as the disruption of the transgene is our screening criterion for successful gene editing (see Material and Methods, data not shown). Therefore, the GFP signal only corresponds to the mEGFP encoded by the transiently transfected plasmid. Co-transfections with plasmids encoding PKR-FL but not PKR-ML or PKR-SL resulted in a drastic reduction of GFP signal intensity (**Figure 6A,B**). Similar results were obtained with luciferase as a reporter gene (**Figure 6D**). A similar assay was performed to compare luciferase activity upon transfection with WT PKR-FL and mutated PKR-FL-C11\_E12del isolated from WT-like EC-PKR-C28 (**Figure S2**). Our results showed that co-transfection with PKR-FL-C11\_E12del expression plasmid resulted in a severe decrease in luciferase activity, as WT PKR-FL overexpression, indicating that they exhibit similar translation inhibition. These observations further suggest that the loss of Cys11 and Glu12 in WT-like EC-PKR-C28 does not affect drastically the protein functions.

Since these assays only assess the expression of exogenous reporter genes and not on endogenous cellular proteins, we also evaluated the impact of each PKR isoform on the translation of endogenous proteins. For this purpose, transfected cells were pulsed with puromycin, an aminonucleoside which is incorporated into nascent peptides, leading to premature chain termination and spontaneous dissociation from the ribosome<sup>80,81</sup>. Puromycylated nascent chains can be detected by western blot using anti-puromycin antibodies. Puromycin can therefore replace radioactive tracers such as S<sup>35</sup> methionine and be used as a metabolic probe to measure *de novo* protein synthesis<sup>80</sup>. Cycloheximide

and thapsigargin were used are positive controls, since these drugs are well-established translation inhibitors<sup>59,60</sup>. Consistent with reporter gene experiments, western blot analysis showed that the levels of puromycin incorporated into newly synthesized proteins decreased significantly with PKR-FL but not with PKR-ML or PKR-SL overexpression (**Figure 6A,C**). These results suggest that PKR-FL overexpression is able to inhibit host protein translation in the absence of any PKR activator.

**Translation shutoff induced by type I IFN and poly(I:C) is abolished in *pkr*<sup>-/-</sup> cells.** In order to confirm the role of endogenous PKR in host translation inhibition, we compared the response of WT and WT-like cells (EC and EC-PKR-C28, respectively) and *pkr*<sup>-/-</sup> EC-PKR-C19 cells upon transfection with poly(I:C), a synthetic analog of dsRNA. Poly(I:C) was used as a viral dsRNA mimic to activate PKR, while simultaneously avoiding the potential viral subversion mechanisms that can occur during viral infections. Before transfection, all cells were either pretreated with IFNA2 for 48h in order to induce PKR expression or left untreated. Western blot analysis showed no differences in puromycin signal intensity after poly(I:C) transfection between non-pretreated cell lines (**Figure 7A,B**, left panel). In contrast, when cells were pretreated with IFNA2, the levels of puromycin incorporated into newly synthesized proteins significantly decreased upon poly(I:C) transfection in WT EC and WT-like EC-PKR-C28 cells (37% and 48% reduction, respectively) but not in *pkr*<sup>-/-</sup> EC-PKR-C19 cells (**Figure 7A,B**, right panel). Taken together, these results show that endogenous PKR expression is required for the inhibition of host translation induced by poly(I:C).

*Endogenous PKR is not the main driver of protein synthesis shutoff induced by rVHSV-Tomato infection*

To assess the role of endogenous PKR in translation inhibition in a context of viral infection, which is intrinsically more complex than poly(I:C) stimulation, we compared the response of WT EC and WT-like EC-PKR-C28 cells with that of *pkr*<sup>-/-</sup> EC-PKR-C19 cells during rVHSV-Tomato infection. In all cell lines, the puromycin signal intensity decreased as early as 24h post-infection and drastically dropped at 40h post-infection (**Figure 8A,D**). These data negatively correlate with eIF2 $\alpha$  phosphorylation, which increased at 24h and peaked at 40h post-infection (**Figure 8A,C**). Interestingly, VHSV N was expressed as early as 16h post-infection and expression levels increased over time (24-40h post-infection), despite the decrease in host *de novo* protein synthesis (**Figure 8A,B**). However, no significant differences between WT, WT-like and *pkr*<sup>-/-</sup> cell lines were detected at all infection time points examined. These results indicate that VHSV-induced phosphorylation of eIF2 $\alpha$  closely correlates with a decrease in host translation, while viral protein synthesis continued to increase during the shutoff of host protein synthesis. The absence of differences between cell lines shows this phenomenon involves a PKR-independent mechanism.

To further verify those results, all cell lines were pretreated with IFNA2 before rVHSV-Tomato infection. However, there were, once again, no differences between cell lines despite high levels of PKR expression (**Figure S3**). These findings further confirm the hypothesis that phosphorylation of eIF2 $\alpha$  and host translation inhibition is not mediated by PKR during rVHSV-Tomato infection. Similar results were obtained with GSV, a dsRNA virus. Indeed, although GSV infection led to decreased levels of puromycin incorporated into proteins and increased phosphorylation of eIF2 $\alpha$  at 24h post-infection, no differences between cell lines could be observed (**Figure S3**).

#### *Chinook salmon PKR can play antagonistic roles in virus replication*

Immunoblots showing a similar expression of VHSV N protein in WT, WT-like and *pkr*<sup>-/-</sup> cell lines were indicative that PKR had little to no effect on VHSV replication at an early stage of infection. To investigate further PKR role in virus replication and production, we used rVHSV-Tomato, in which the expression cassette encoding tdTomato was inserted in the N-P intergenic region of VHSV genome and is therefore expressed only during its viral replication cycle<sup>49</sup>. The use of this virus enabled us to monitor viral replication using fluorescence as a non-invasive proxy for viral replication.

**Overexpression of PKR-FL inhibits rVHSV-Tomato replication.** To assess whether Chinook salmon PKR is involved in the inhibition of viral replication, *pkr*<sup>-/-</sup> EC-PKR-C19 cells were transfected with plasmids encoding different PKR isoforms and subsequently infected with rVHSV-Tomato. The fluorescence of rVHSV-Tomato was monitored from 24h to 96h post-infection. A modest but constant reduction in measured fluorescence was observed in PKR-FL transfected cells from 48h post-transfection to 96h post-transfection (**Figure 9A**). Once normalized to the mean fluorescence measured in BFP-transfected cells at each time point, this represents a decrease of around 30% (**Figure 9B**). Similarly, overexpression of PKR-FL but not PKR-ML or PKR-SL resulted in a limited but significant decrease in viral titer in the supernatants at 96h post-infection (**Figure 9C**). Consistent with previous fluorescence results, this constitutes a drop of ~25% (calculated on the basis of non-log transformed titers) compared to BFP-transfected cells. Taken together, these results suggest that overexpression of PKR-FL but not other isoforms inhibits rVHSV-Tomato replication.

**Endogenous PKR favors the release of virus into the supernatants.** The role of endogenous PKR during rVHSV-Tomato infection was investigated by comparing the evolution of the red fluorescence in WT EC, WT-like EC-PKR-C28 and *pkr*<sup>-/-</sup> EC-PKR-C19 cell lines from 24h to 96h post-infection. The fluorescence signal was significantly higher in *pkr*<sup>-/-</sup> EC-PKR-C19 compared to the WT and WT-like cell lines and this difference was more pronounced at a high MOI: significant differences between *pkr*<sup>-/-</sup> and WT cell lines started to appear as early as 48h, 72h and 96h post-infection at MOI 10, MOI

1 and MOI 0.1, respectively (**Figure 10A-C**). Importantly, a similar trend was observed in other *pkrr*<sup>-/-</sup> clones (EC-PKR-C3 and EC-PKR-C5), excluding the hypothesis of a clone-specific effect (**Figure S4**). Because tdTomato is not present in newly formed virions, supernatants of infected cells were titrated by plaque assay. Surprisingly, viral titers in the supernatants were slightly but significantly lower in *pkrr*<sup>-/-</sup> EC-PKR-C19 cells compared to WT EC and WT-like EC-PKR-C28 cells (**Figure 10D**), which was inconsistent with our fluorescence data, indicative of the intracellular level of tdTomato. Because our previous results showed that PKR was involved in apoptosis at a late stage of viral infection, we hypothesized that absence of PKR could inhibit virion release. If this were true, virions would accumulate in the infected cells and a higher intracellular viral titer could be expected. To clarify this point, after supernatant collection, remaining infected cells were washed three times, sonicated and the sonicates were titrated by plaque assay. Our results show that intracellular viral titers were weakly but significantly higher in *pkrr*<sup>-/-</sup> EC-PKR-C19 cells compared to WT EC cells (**Figure 10E**). However, there was no difference between *pkrr*<sup>-/-</sup> EC-PKR-C19 and WT-like EC-PKR-C28 cells. As mentioned earlier, this discrepancy may be explained by the fact that PKR is less expressed in WT-like EC-PKR-C28 compared to WT EC.

Whilst there are differences in extracellular and intracellular titers between cell lines, the “total titer”, *i.e.* the total amount of extracellular and intracellular infectious virions produced by each cell line, was not significantly modified by *pkrr* disruption. These results suggest that endogenous PKR does not affect viral replication *per se*, but rather favors the release of viral particles into the supernatant.

## Discussion

In this study, we have identified and cloned three isoforms of a unique Chinook salmon *pkR* gene, named *pkR-fl*, *pkR-ml* and *pkR-sl*, the last two lacking important catalytic regions. Using complementary *in cellulo* approaches based on overexpression and knockout studies, we showed that salmonid PKR is involved in apoptosis activation and plays a major role in translational arrest upon poly(I:C) stimulation but not during VHSV infection. Our data further indicate that PKR favors the release of VHSV virions into the supernatant at a late infectious stage, likely by triggering apoptosis. Taken together, our results demonstrate that salmonid PKR has conserved molecular functions compared to their mammalian counterparts. However, the endogenous protein did not have a major antiviral effect against VHSV, likely due to subversion strategies evolved by the virus.

In line with previous studies on mammalian and fish cell lines<sup>2,47</sup> both RT-qPCR and western blot analysis revealed a constitutive but modest expression of PKR-FL in EC cells, which was strongly induced after IFNA2 treatment. In contrast, neither *pkR-fl* nor *mx1/2/3* expression was induced during infection with either rVHSV-Tomato or GSV, both at transcript and protein levels. Comparable results were previously obtained in the rainbow trout RTG-P1 cell line, which expresses the firefly luciferase gene under the control of the *mx1* gene promoter<sup>55</sup>. These observations suggest that the IFN response was limited in the epithelial-like salmonid EC cells during rVHSV-Tomato infection, due to virus-mediated IFN suppression mechanisms, possibly *via* its NV protein<sup>82–85</sup>.

Although endogenous PKR was not induced in EC cells during rVHSV-Tomato infection, we still investigated the potential antiviral activity of PKR *via* overexpression and loss-of-function approaches. In line with other overexpression studies in fish models<sup>37,45,46</sup>, we observed that overexpression of PKR-FL but not PKR-ML or PKR-SL resulted in a limited but significant decrease in rVHSV-Tomato titers in the supernatant. Using a knockout approach, we further showed that VHSV extracellular titers were slightly but significantly lower, while intracellular titers were higher in the *pkR*<sup>-/-</sup> cell line, compared to the WT cell line. Our results therefore suggest that endogenous PKR does not affect viral replication and virion assembly *per se*, but favors the release of viral particles into the supernatant. In contrast, it was recently reported that chemical inhibition of PKR in rainbow trout RTG2 and RTGill cells lines did not have any impact on extracellular VHSV titers in comparison to untreated cells<sup>44</sup>. Differences between our results and this study may arise from remanent PKR activity following chemical inhibition, which may downplay the full effect observed in our study.

Enzymatic assays also showed that PKR plays a preponderant role in the activation of apoptosis and triggers it at a relatively late stage of VHSV infection. Based on previous titration results, we propose

that *pkr* knockout could reduce virion release by limiting apoptosis activation at a late infection stage. In contrast, PKR-FL antiviral activity upon overexpression would mainly occur through early activation of apoptosis, when it is detrimental to efficient virus replication. Interestingly, the kinetics of caspase 3 activation correlated with apoptotic kinetics described in the literature for novirhabdoviruses<sup>86</sup>. This relatively late activation of apoptosis has been attributed to VHSV NV protein, which inhibits apoptosis at the early stage of viral infection and prevents infected cells from undergoing cell death before mature viral particles are produced<sup>86</sup>. On the other hand, apoptosis can be advantageous at the late stage of viral replication to facilitate viral release and dissemination<sup>87,88</sup>. Precisely, while VHSV NV protein has an “early” anti-apoptotic function, the matrix (M) protein of novirhabdoviruses is known for its pro-apoptotic properties<sup>89</sup>. At a late stage of infection, it has been suggested that abundant proapoptotic M protein takes over and triggers a late apoptosis activation, which facilitates viral release and spread<sup>86</sup>. It is therefore tempting to speculate that VHSV has evolved a NV-driven strategy which takes advantage of PKR-mediated apoptosis.

Besides apoptosis, a key antiviral mechanism of PKR is the inhibition of the translation machinery *via* phosphorylation of eIF2 $\alpha$ . By using reporter genes and quantifying puromycin incorporation into newly synthesized proteins, we further demonstrated that both overexpressed PKR-FL and endogenous poly(I:C)-activated PKR were able to inhibit host *de novo* protein synthesis. These results are in line with several studies on mammalian and fish PKR, as recently reviewed by Chaumont *et al.*<sup>31</sup>. In a context of viral infection, we showed that VHSV-induced phosphorylation of eIF2 $\alpha$  closely correlates with a decrease in host protein translation. However, no differences were observed between WT and *pkr*<sup>-/-</sup> cell lines, revealing that this phenomenon is PKR-independent. Importantly, PKR is not the only kinase that can trigger host translational arrest; eIF2 $\alpha$  can be phosphorylated by four other kinases: PERK (PKR-like ER kinase), GCN2 (general control non-derepressible 2), HRI (heme-regulated inhibitor) and PKZ (Z-DNA-dependent protein kinase)<sup>34,90</sup>. Although each eIF2 $\alpha$  kinase primarily responds to specific stresses, several studies provide evidence that they may have cooperative functions. For instance, eIF2 $\alpha$  phosphorylation can be mediated by PKR but also PERK and GCN2 during viral infections<sup>91,92</sup>. A recent study using chemical inhibitors showed that eIF2 $\alpha$  phosphorylation and shutoff of host translation was mediated by PERK and not PKR during VHSV infection<sup>44,93</sup>. Using *pkr*<sup>-/-</sup> cell lines instead of chemical inhibitors, our results confirm that PKR is not to be the main driver of host translational arrest during VHSV infection. These results suggest that VHSV is able to bypass PKR-mediated translation inhibition but not an alternative host signaling pathway activated by another eIF2 $\alpha$  kinase.

Besides PKR-FL, we have also identified and cloned two other isoforms expressed in EC cells during VHSV infection, namely PKR-ML and PKR-SL, which are splice variants of PKR-FL. We

demonstrated that PKR-ML and PKR-SL do not mediate apoptosis and inhibition of translation, most likely because that they both lack important catalytic regions and are defective in kinase activity. The fact that these two isoforms exist but do not retain any of the typical antiviral functions established for PKR-FL raises the question of their physiological role(s) in the cell. Interestingly, weakly expressed splice variants have been reported for mammalian PKR<sup>94-96</sup> as well as for zebrafish PKZ<sup>34,97</sup>. Li and Koromilas reported a splice variant (PKR $\Delta$ E7), in which exon 7 was spliced out, resulting in a truncated 174-aa protein containing only dsRNA binding domains. Interestingly, PKR $\Delta$ E7 exhibited a dominant negative function, as co-expression of both isoforms relieved PKR-mediated translation inhibition<sup>95</sup>. Because PKR-SL also contains dsRBM1 and a truncated dsRBM2, it might have a similar dominant negative activity as human PKR $\Delta$ E7. Abraham *et al.* also reported that murine lymphocytic leukemia cells expressed a *Pkr* transcript presenting an in-frame deletion of 579 bp. The resulting truncated protein is strikingly similar to PKR-ML: in both cases, the in-frame deletion occurred within dsRBM2 and in the C-terminal portion of the acidic kinase insert of the kinase domain. Abraham *et al.* showed that this truncated protein was able to form dimers with endogenous PKR and to bind dsRNA<sup>96</sup>. Whether PKR-ML possesses similar characteristics remains to be determined.

In conclusion, our results establish that salmonid PKR has conserved molecular functions, including apoptosis activation and inhibition of protein synthesis. However, endogenous PKR does not play a major antiviral role during VHSV infection. It seems that VHSV has evolved a strategy to subvert PKR antiviral action, by limiting early PKR induction and evading PKR-mediated translational arrest. VHSV also appeared to take advantage of PKR-mediated apoptosis to favor viral spread at a late stage of infection.

## Acknowledgements

We thank Pr. Øystein Evensen and Dr. Amr Gamil (NMBU, Oslo, Norway) for their kind gift of anti-PKR Ab. We thank Marta Alonso-Hearn (Department of Animal Health, NEIKER-Basque Institute for Agricultural Research and Development, Basque Research and Technology Alliance, Derio, Spain) and Pr. Jorunn Jorgensen (UiT The Arctic University of Norway, Tromsø, Norway) for their generous gift of anti-Mx Ab. We are grateful to Dr. Stéphane Biacchesi and Emilie Mérour (INRAE, Jouy-en-Josas, France) for providing rVHSV-Tomato and anti-VHSV N Ab as well as for helpful discussions. We thank Dr. Hortense Decool (INRAE, Jouy-en-Josas, France) for providing pCite-P-BFP plasmid. We thank Dr. Dean Porter (INRAE, Jouy-en-Josas, France) for careful reading of the manuscript and Dr. Irene Salinas (CETI, Department of Biology, University of New Mexico, Albuquerque, USA) for insightful exchanges on apoptosis.

## References

- (1) Flajnik, M. *Paul's Fundamental Immunology*; Lippincott Williams & Wilkins, 2022.
- (2) Meurs, E.; Chong, K.; Galabru, J.; Thomas, N. S.; Kerr, I. M.; Williams, B. R.; Hovanessian, A. G. Molecular Cloning and Characterization of the Human Double-Stranded RNA-Activated Protein Kinase Induced by Interferon. *Cell* **1990**, *62* (2), 379–390. [https://doi.org/10.1016/0092-8674\(90\)90374-n](https://doi.org/10.1016/0092-8674(90)90374-n).
- (3) Thomis, D. C.; Doohan, J. P.; Samuel, C. E. Mechanism of Interferon Action: cDNA Structure, Expression, and Regulation of the Interferon-Induced, RNA-Dependent P1/eIF-2 Alpha Protein Kinase from Human Cells. *Virology* **1992**, *188* (1), 33–46. [https://doi.org/10.1016/0042-6822\(92\)90732-5](https://doi.org/10.1016/0042-6822(92)90732-5).
- (4) Dar, A. C.; Dever, T. E.; Sicheri, F. Higher-Order Substrate Recognition of eIF2 $\alpha$  by the RNA-Dependent Protein Kinase PKR. *Cell* **2005**, *122* (6), 887–900. <https://doi.org/10.1016/j.cell.2005.06.044>.
- (5) Lemaire, P. A.; Lary, J.; Cole, J. L. Mechanism of PKR Activation: Dimerization and Kinase Activation in the Absence of Double-Stranded RNA. *J Mol Biol* **2005**, *345* (1), 81–90. <https://doi.org/10.1016/j.jmb.2004.10.031>.
- (6) Lemaire, P. A.; Anderson, E.; Lary, J.; Cole, J. L. Mechanism of PKR Activation by dsRNA. *J Mol Biol* **2008**, *381* (2), 351–360. <https://doi.org/10.1016/j.jmb.2008.05.056>.
- (7) Mayo, C. B.; Erlandsen, H.; Mouser, D. J.; Feinstein, A. G.; Robinson, V. L.; May, E. R.; Cole, J. L. Structural Basis of Protein Kinase R Autophosphorylation. *Biochemistry* **2019**, *58* (27), 2967–2977. <https://doi.org/10.1021/acs.biochem.9b00161>.
- (8) García, M. A.; Gil, J.; Ventoso, I.; Guerra, S.; Domingo, E.; Rivas, C.; Esteban, M. Impact of Protein Kinase PKR in Cell Biology: From Antiviral to Antiproliferative Action. *Microbiol Mol Biol Rev* **2006**, *70* (4), 1032–1060. <https://doi.org/10.1128/MMBR.00027-06>.
- (9) Gil, J.; Esteban, M. The Interferon-Induced Protein Kinase (PKR), Triggers Apoptosis through FADD-Mediated Activation of Caspase 8 in a Manner Independent of Fas and TNF- $\alpha$  Receptors. *Oncogene* **2000**, *19* (32), 3665–3674. <https://doi.org/10.1038/sj.onc.1203710>.
- (10) Lee, S. B.; Esteban, M. The Interferon-Induced Double-Stranded RNA-Activated Protein Kinase Induces Apoptosis. *Virology* **1994**, *199* (2), 491–496. <https://doi.org/10.1006/viro.1994.1151>.
- (11) Srivastava, S. P.; Kumar, K. U.; Kaufman, R. J. Phosphorylation of Eukaryotic Translation Initiation Factor 2 Mediates Apoptosis in Response to Activation of the Double-Stranded RNA-Dependent Protein Kinase \*. *Journal of Biological Chemistry* **1998**, *273* (4), 2416–2423. <https://doi.org/10.1074/jbc.273.4.2416>.
- (12) Yeung, M. C.; Liu, J.; Lau, A. S. An Essential Role for the Interferon-Inducible, Double-Stranded RNA-Activated Protein Kinase PKR in the Tumor Necrosis Factor-Induced Apoptosis in U937 Cells. *Proc Natl Acad Sci U S A* **1996**, *93* (22), 12451–12455.
- (13) Der, S. D.; Yang, Y.-L.; Weissmann, C.; Williams, B. R. G. A Double-Stranded RNA-Activated Protein Kinase-Dependent Pathway Mediating Stress-Induced Apoptosis. *Proc Natl Acad Sci U S A* **1997**, *94* (7), 3279–3283.
- (14) Zuo, W.; Wakimoto, M.; Kozaiwa, N.; Shirasaka, Y.; Oh, S.-W.; Fujiwara, S.; Miyachi, H.; Kogure, A.; Kato, H.; Fujita, T. PKR and TLR3 Trigger Distinct Signals That Coordinate the Induction of Antiviral Apoptosis. *Cell Death Dis* **2022**, *13* (8), 1–15. <https://doi.org/10.1038/s41419-022-05101-3>.
- (15) Guerra, S.; López-Fernández, L. A.; García, M. A.; Zaballos, A.; Esteban, M. Human Gene Profiling in Response to the Active Protein Kinase, Interferon-Induced Serine/Threonine Protein Kinase (PKR), in Infected Cells. *Journal of Biological Chemistry* **2006**, *281* (27), 18734–18745. <https://doi.org/10.1074/jbc.M511983200>.
- (16) Hsu, L.-C.; Park, J. M.; Zhang, K.; Luo, J.-L.; Maeda, S.; Kaufman, R. J.; Eckmann, L.; Guiney, D. G.; Karin, M. The Protein Kinase PKR Is Required for Macrophage Apoptosis after Activation of Toll-like Receptor 4. *Nature* **2004**, *428* (6980), 341–345. <https://doi.org/10.1038/nature02405>.
- (17) Lee, E.-S.; Yoon, C.-H.; Kim, Y.-S.; Bae, Y.-S. The Double-Strand RNA-Dependent Protein Kinase PKR Plays a Significant Role in a Sustained ER Stress-Induced Apoptosis. *FEBS Letters* **2007**, *581* (22), 4325–4332. <https://doi.org/10.1016/j.febslet.2007.08.001>.
- (18) Liao, Y.; Fung, T. S.; Huang, M.; Fang, S. G.; Zhong, Y.; Liu, D. X. Upregulation of CHOP/GADD153 during Coronavirus Infectious Bronchitis Virus Infection Modulates Apoptosis by Restricting Activation of the Extracellular Signal-Regulated Kinase Pathway. *J Virol* **2013**, *87* (14), 8124–8134. <https://doi.org/10.1128/JVI.00626-13>.
- (19) Cuddihy, A. R.; Li, S.; Tam, N. W. N.; Wong, A. H.-T.; Taya, Y.; Abraham, N.; Bell, J. C.; Koromilas, A. E. Double-Stranded-RNA-Activated Protein Kinase PKR Enhances Transcriptional Activation by Tumor Suppressor P53. *Mol Cell Biol* **1999**, *19* (4), 2475–2484.
- (20) Kumar, A.; Yang, Y. L.; Flati, V.; Der, S.; Kadereit, S.; Deb, A.; Haque, J.; Reis, L.; Weissmann, C.; Williams, B. R. Deficient Cytokine Signaling in Mouse Embryo Fibroblasts with a Targeted Deletion in the PKR Gene: Role of IRF-1 and NF-kappaB. *EMBO J* **1997**, *16* (2), 406–416. <https://doi.org/10.1093/emboj/16.2.406>.
- (21) McAllister, C. S.; Toth, A. M.; Zhang, P.; Devaux, P.; Cattaneo, R.; Samuel, C. E. Mechanisms of Protein Kinase PKR-Mediated Amplification of Beta Interferon Induction by C Protein-Deficient Measles Virus. *J Virol* **2010**, *84* (1), 380–386. <https://doi.org/10.1128/JVI.02630-08>.
- (22) Silva, A. M.; Whitmore, M.; Xu, Z.; Jiang, Z.; Li, X.; Williams, B. R. G. Protein Kinase R (PKR) Interacts with and Activates Mitogen-Activated Protein Kinase Kinase 6 (MKK6) in Response to Double-Stranded RNA Stimulation. *J Biol Chem* **2004**, *279* (36), 37670–37676. <https://doi.org/10.1074/jbc.M406554200>.

- (23) Taghavi, N.; Samuel, C. E. Protein Kinase PKR Catalytic Activity Is Required for the PKR-Dependent Activation of Mitogen-Activated Protein Kinases and Amplification of Interferon Beta Induction Following Virus Infection. *Virology* **2012**, *427* (2), 208–216. <https://doi.org/10.1016/j.virol.2012.01.029>.
- (24) Zhang, P.; Langland, J. O.; Jacobs, B. L.; Samuel, C. E. Protein Kinase PKR-Dependent Activation of Mitogen-Activated Protein Kinases Occurs through Mitochondrial Adapter IPS-1 and Is Antagonized by Vaccinia Virus E3L. *J Virol* **2009**, *83* (11), 5718–5725. <https://doi.org/10.1128/JVI.00224-09>.
- (25) Zamanian-Daryoush, M.; Mogensen, T. H.; DiDonato, J. A.; Williams, B. R. G. NF- $\kappa$ B Activation by Double-Stranded-RNA-Activated Protein Kinase (PKR) Is Mediated through NF- $\kappa$ B-Inducing Kinase and I $\kappa$ B Kinase. *Mol Cell Biol* **2000**, *20* (4), 1278–1290.
- (26) Arnaud, N.; Dabo, S.; Maillard, P.; Budkowska, A.; Kalliampakou, K. I.; Mavromara, P.; Garcin, D.; Hugon, J.; Gatignol, A.; Akazawa, D.; Wakita, T.; Meurs, E. F. Hepatitis C Virus Controls Interferon Production through PKR Activation. *PLoS One* **2010**, *5* (5), e10575. <https://doi.org/10.1371/journal.pone.0010575>.
- (27) McAllister, C. S.; Samuel, C. E. The RNA-Activated Protein Kinase Enhances the Induction of Interferon- $\beta$  and Apoptosis Mediated by Cytoplasmic RNA Sensors. *J Biol Chem* **2009**, *284* (3), 1644–1651. <https://doi.org/10.1074/jbc.M807888200>.
- (28) Pham, A. M.; Santa Maria, F. G.; Lahiri, T.; Friedman, E.; Marié, I. J.; Levy, D. E. PKR Transduces MDA5-Dependent Signals for Type I IFN Induction. *PLoS Pathog* **2016**, *12* (3), e1005489. <https://doi.org/10.1371/journal.ppat.1005489>.
- (29) Schulz, O.; Pichlmair, A.; Rehwinkel, J.; Rogers, N. C.; Scheuner, D.; Kato, H.; Takeuchi, O.; Akira, S.; Kaufman, R. J.; Reis e Sousa, C. Protein Kinase R Contributes to Immunity against Specific Viruses by Regulating Interferon mRNA Integrity. *Cell Host Microbe* **2010**, *7* (5), 354–361. <https://doi.org/10.1016/j.chom.2010.04.007>.
- (30) Cesaro, T.; Michiels, T. Inhibition of PKR by Viruses. *Front Microbiol* **2021**, *12*, 757238. <https://doi.org/10.3389/fmicb.2021.757238>.
- (31) Chaumont, L.; Collet, B.; Boudinot, P. Double-Stranded RNA-Dependent Protein Kinase (PKR) in Antiviral Defence in Fish and Mammals. *Developmental & Comparative Immunology* **2023**, *145*, 104732. <https://doi.org/10.1016/j.dci.2023.104732>.
- (32) Rothenburg, S.; Deigendesch, N.; Dey, M.; Dever, T. E.; Tazi, L. Double-Stranded RNA-Activated Protein Kinase PKR of Fishes and Amphibians: Varying the Number of Double-Stranded RNA Binding Domains and Lineage-Specific Duplications. *BMC Biol* **2008**, *6* (1), 12. <https://doi.org/10.1186/1741-7007-6-12>.
- (33) Hu, C.-Y.; Zhang, Y.-B.; Huang, G.-P.; Zhang, Q.-Y.; Gui, J.-F. Molecular Cloning and Characterisation of a Fish PKR-like Gene from Cultured CAB Cells Induced by UV-Inactivated Virus. *Fish & Shellfish Immunology* **2004**, *17* (4), 353–366. <https://doi.org/10.1016/j.fsi.2004.04.009>.
- (34) Rothenburg, S.; Deigendesch, N.; Dittmar, K.; Koch-Nolte, F.; Haag, F.; Lowenhaupt, K.; Rich, A. A PKR-like Eukaryotic Initiation Factor 2 Kinase from Zebrafish Contains Z-DNA Binding Domains Instead of dsRNA Binding Domains. *Proceedings of the National Academy of Sciences* **2005**, *102* (5), 1602–1607. <https://doi.org/10.1073/pnas.0408714102>.
- (35) Bergan, V.; Jagus, R.; Lauksund, S.; Kileng, Ø.; Robertsen, B. The Atlantic Salmon Z-DNA Binding Protein Kinase Phosphorylates Translation Initiation Factor 2 Alpha and Constitutes a Unique Orthologue to the Mammalian dsRNA-Activated Protein Kinase R. *The FEBS Journal* **2008**, *275* (1), 184–197. <https://doi.org/10.1111/j.1742-4658.2007.06188.x>.
- (36) del Castillo, C. S.; Hikima, J.; Ohtani, M.; Jung, T.-S.; Aoki, T. Characterization and Functional Analysis of Two PKR Genes in Fugu (Takifugu Rubripes). *Fish & Shellfish Immunology* **2012**, *32* (1), 79–88. <https://doi.org/10.1016/j.fsi.2011.10.022>.
- (37) Gan, Z.; Cheng, J.; Hou, J.; Chen, S.; Xia, H.; Xia, L.; Kwok, K. W. H.; Lu, Y.; Nie, P. Tilapia dsRNA-Activated Protein Kinase R (PKR): An Interferon-Induced Antiviral Effector with Translation Inhibition Activity. *Fish Shellfish Immunol* **2021**, *112*, 74–80. <https://doi.org/10.1016/j.fsi.2021.02.016>.
- (38) Hu, Y.-S.; Li, W.; Li, D.-M.; Liu, Y.; Fan, L.-H.; Rao, Z.-C.; Lin, G.; Hu, C.-Y. Cloning, Expression and Functional Analysis of PKR from Grass Carp (Ctenopharyngodon Idellus). *Fish & Shellfish Immunology* **2013**, *35* (6), 1874–1881. <https://doi.org/10.1016/j.fsi.2013.09.024>.
- (39) Xu, C.; Gamil, A. A. A.; Munang'andu, H. M.; Evensen, Ø. Apoptosis Induction by dsRNA-Dependent Protein Kinase R (PKR) in EPC Cells via Caspase 8 and 9 Pathways. *Viruses* **2018**, *10* (10), 526. <https://doi.org/10.3390/v10100526>.
- (40) Zhu, R.; Zhang, Y.-B.; Zhang, Q.-Y.; Gui, J.-F. Functional Domains and the Antiviral Effect of the Double-Stranded RNA-Dependent Protein Kinase PKR from *Paralichthys Olivaceus*. *J Virol* **2008**, *82* (14), 6889–6901. <https://doi.org/10.1128/JVI.02385-07>.
- (41) Hu, Y.; Fan, L.; Wu, C.; Wang, B.; Sun, Z.; Hu, C. Identification and Function Analysis of the Three dsRBMs in the N Terminal dsRBD of Grass Carp (Ctenopharyngodon Idella) PKR. *Fish Shellfish Immunol* **2016**, *50*, 91–100. <https://doi.org/10.1016/j.fsi.2016.01.011>.
- (42) Wu, C.; Hu, Y.; Fan, L.; Wang, H.; Sun, Z.; Deng, S.; Liu, Y.; Hu, C. Ctenopharyngodon Idella PKZ Facilitates Cell Apoptosis through Phosphorylating eIF2 $\alpha$ . *Molecular Immunology* **2016**, *69*, 13–23. <https://doi.org/10.1016/j.molimm.2015.11.006>.

- (43) Wang, H.; Xu, Q.; Xu, X.; Hu, Y.; Hou, Q.; Zhu, Y.; Hu, C. Ctenopharyngodon Idella IKK $\beta$  Interacts with PKR and I $\kappa$ B $\alpha$ . *Acta Biochim Biophys Sin (Shanghai)* **2017**, *49* (8), 729–736. <https://doi.org/10.1093/abbs/gmx065>.
- (44) Ramnani, B.; Powell, S.; Shetty, A. G.; Manivannan, P.; Hibbard, B. R.; Leaman, D. W.; Malathi, K. Viral Hemorrhagic Septicemia Virus Activates Integrated Stress Response Pathway and Induces Stress Granules to Regulate Virus Replication. *Viruses* **2023**, *15* (2), 466. <https://doi.org/10.3390/v15020466>.
- (45) Wei, J.; Zang, S.; Li, C.; Zhang, X.; Gao, P.; Qin, Q. Grouper PKR Activation Inhibits Red-Spotted Grouper Nervous Necrosis Virus (RGNNV) Replication in Infected Cells. *Developmental & Comparative Immunology* **2020**, *111*, 103744. <https://doi.org/10.1016/j.dci.2020.103744>.
- (46) Liu, T.-K.; Zhang, Y.-B.; Liu, Y.; Sun, F.; Gui, J.-F. Cooperative Roles of Fish Protein Kinase Containing Z-DNA Binding Domains and Double-Stranded RNA-Dependent Protein Kinase in Interferon-Mediated Antiviral Response  $\nu$ . *J Virol* **2011**, *85* (23), 12769–12780. <https://doi.org/10.1128/JVI.05849-11>.
- (47) Gamil, A. A. A.; Xu, C.; Mutoloki, S.; Evensen, Ø. PKR Activation Favors Infectious Pancreatic Necrosis Virus Replication in Infected Cells. *Viruses* **2016**, *8* (6). <https://doi.org/10.3390/v8060173>.
- (48) Dehler, C. E.; Boudinot, P.; Martin, S. A. M.; Collet, B. Development of an Efficient Genome Editing Method by CRISPR/Cas9 in a Fish Cell Line. *Mar Biotechnol (NY)* **2016**, *18* (4), 449–452. <https://doi.org/10.1007/s10126-016-9708-6>.
- (49) Biacchesi, S.; Lamoureux, A.; Méroux, E.; Bernard, J.; Brémont, M. Limited Interference at the Early Stage of Infection between Two Recombinant Novirhabdoviruses: Viral Hemorrhagic Septicemia Virus and Infectious Hematopoietic Necrosis Virus. *J Virol* **2010**, *84* (19), 10038–10050. <https://doi.org/10.1128/JVI.00343-10>.
- (50) Concordet, J.-P.; Haeussler, M. CRISPOR: Intuitive Guide Selection for CRISPR/Cas9 Genome Editing Experiments and Screens. *Nucleic Acids Research* **2018**, *46* (W1), W242–W245. <https://doi.org/10.1093/nar/gky354>.
- (51) Conant, D.; Hsiao, T.; Rossi, N.; Oki, J.; Maures, T.; Waite, K.; Yang, J.; Joshi, S.; Kelso, R.; Holden, K.; Enzmann, B. L.; Stoner, R. Inference of CRISPR Edits from Sanger Trace Data. *CRISPR J* **2022**, *5* (1), 123–130. <https://doi.org/10.1089/crispr.2021.0113>.
- (52) Diot, C.; Richard, C.-A.; Risso-Ballester, J.; Martin, D.; Fix, J.; Eléouët, J.-F.; Sizun, C.; Rameix-Welti, M.-A.; Galloux, M. Hardening of Respiratory Syncytial Virus Inclusion Bodies by Cyclopamine Proceeds through Perturbation of the Interactions of the M2-1 Protein with RNA and the P Protein. *Int J Mol Sci* **2023**, *24* (18), 13862. <https://doi.org/10.3390/ijms241813862>.
- (53) Collet, B.; Collins, C.; Cheyne, V.; Lester, K. Plasmid-Driven RNA Interference in Fish Cell Lines. *In Vitro Cell Dev Biol Anim* **2022**, *58* (3), 189–193. <https://doi.org/10.1007/s11626-022-00645-2>.
- (54) Collins, C.; Ganne, G.; Collet, B. Isolation and Activity of the Promoters for STAT1 and 2 in Atlantic Salmon Salmo Salar. *Fish Shellfish Immunol* **2014**, *40* (2), 644–647. <https://doi.org/10.1016/j.fsi.2014.07.025>.
- (55) Collet, B.; Boudinot, P.; Benmansour, A.; Secombes, C. J. An Mx1 Promoter-Reporter System to Study Interferon Pathways in Rainbow Trout. *Dev Comp Immunol* **2004**, *28* (7–8), 793–801. <https://doi.org/10.1016/j.dci.2003.12.005>.
- (56) Trobridge, G. D.; Chiou, P. P.; Leong, J. A. Cloning of the Rainbow Trout (*Oncorhynchus Mykiss*) Mx2 and Mx3 cDNAs and Characterization of Trout Mx Protein Expression in Salmon Cells. *J Virol* **1997**, *71* (7), 5304–5311.
- (57) Cai, R.; Williams, B. R. G. Mutations in the Double-Stranded RNA-Activated Protein Kinase Insert Region That Uncouple Catalysis from eIF2 $\alpha$  Binding \*. *Journal of Biological Chemistry* **1998**, *273* (18), 11274–11280. <https://doi.org/10.1074/jbc.273.18.11274>.
- (58) Park, S.-H.; Choi, J.; Kang, J.-I.; Choi, S.-Y.; Hwang, S.-B.; Kim, J. P.; Ahn, B.-Y. Attenuated Expression of Interferon-Induced Protein Kinase PKR in a Simian Cell Devoid of Type I Interferons. *Mol Cells* **2006**, *21* (1), 21–28.
- (59) Schneider-Poetsch, T.; Ju, J.; Eyler, D. E.; Dang, Y.; Bhat, S.; Merrick, W. C.; Green, R.; Shen, B.; Liu, J. O. Inhibition of Eukaryotic Translation Elongation by Cycloheximide and Lactimidomycin. *Nat Chem Biol* **2010**, *6* (3), 209–217. <https://doi.org/10.1038/nchembio.304>.
- (60) Wong, W. L.; Brostrom, M. A.; Kuznetsov, G.; Gmitter-Yellen, D.; Brostrom, C. O. Inhibition of Protein Synthesis and Early Protein Processing by Thapsigargin in Cultured Cells. *Biochem J* **1993**, *289* (Pt 1), 71–79.
- (61) Jensen, I.; Larsen, R.; Robertsen, B. An Antiviral State Induced in Chinook Salmon Embryo Cells (CHSE-214) by Transfection with the Double-Stranded RNA Poly I:C. *Fish & Shellfish Immunology* **2002**, *13* (5), 367–378. <https://doi.org/10.1006/fsim.2002.0412>.
- (62) Berthelot, C.; Brunet, F.; Chalopin, D.; Juanchich, A.; Bernard, M.; Noël, B.; Bento, P.; Da Silva, C.; Labadie, K.; Alberti, A.; Aury, J.-M.; Louis, A.; Dehais, P.; Bardou, P.; Montfort, J.; Klopp, C.; Cabau, C.; Gaspin, C.; Thorgaard, G. H.; Boussaha, M.; Quillet, E.; Guyomard, R.; Galiana, D.; Bobe, J.; Volff, J.-N.; Genêt, C.; Wincker, P.; Jaillon, O.; Crollius, H. R.; Guiguen, Y. The Rainbow Trout Genome Provides Novel Insights into Evolution after Whole-Genome Duplication in Vertebrates. *Nat Commun* **2014**, *5* (1), 3657. <https://doi.org/10.1038/ncomms4657>.
- (63) Lien, S.; Koop, B. F.; Sandve, S. R.; Miller, J. R.; Kent, M. P.; Nome, T.; Hvidsten, T. R.; Leong, J. S.; Minkley, D. R.; Zimin, A.; Grammes, F.; Grove, H.; Gjuvsland, A.; Walenz, B.; Hermansen, R. A.; von Schalburg, K.; Rondeau, E. B.; Di Genova, A.; Samy, J. K. A.; Olav Vik, J.; Vigeland, M. D.; Caler, L.; Grimholt, U.; Jentoft, S.; Inge Våge, D.; de Jong, P.; Moen, T.; Baranski, M.; Palti, Y.; Smith, D. R.; Yorke, J. A.; Nederbragt, A. J.;

- Tooming-Klunderud, A.; Jakobsen, K. S.; Jiang, X.; Fan, D.; Hu, Y.; Liberles, D. A.; Vidal, R.; Iturra, P.; Jones, S. J. M.; Jonassen, I.; Maass, A.; Omholt, S. W.; Davidson, W. S. The Atlantic Salmon Genome Provides Insights into Rediploidization. *Nature* **2016**, *533* (7602), 200–205. <https://doi.org/10.1038/nature17164>.
- (64) Macqueen, D. J.; Johnston, I. A. A Well-Constrained Estimate for the Timing of the Salmonid Whole Genome Duplication Reveals Major Decoupling from Species Diversification. *Proceedings of the Royal Society B: Biological Sciences* **2014**, *281* (1778), 20132881. <https://doi.org/10.1098/rspb.2013.2881>.
- (65) Pasquier, J.; Cabau, C.; Nguyen, T.; Jouanno, E.; Severac, D.; Braasch, I.; Journot, L.; Pontarotti, P.; Klopp, C.; Postlethwait, J. H.; Guiguen, Y.; Bobe, J. Gene Evolution and Gene Expression after Whole Genome Duplication in Fish: The PhyloFish Database. *BMC Genomics* **2016**, *17* (1), 368. <https://doi.org/10.1186/s12864-016-2709-z>.
- (66) Letunic, I.; Khedkar, S.; Bork, P. SMART: Recent Updates, New Developments and Status in 2020. *Nucleic Acids Research* **2021**, *49* (D1), D458–D460. <https://doi.org/10.1093/nar/gkaa937>.
- (67) Letunic, I.; Bork, P. 20 Years of the SMART Protein Domain Annotation Resource. *Nucleic Acids Res* **2018**, *46* (Database issue), D493–D496. <https://doi.org/10.1093/nar/gkx922>.
- (68) Masliah, G.; Barraud, P.; Allain, F. H.-T. RNA Recognition by Double-Stranded RNA Binding Domains: A Matter of Shape and Sequence. *Cell Mol Life Sci* **2013**, *70* (11), 1875–1895. <https://doi.org/10.1007/s00018-012-1119-x>.
- (69) Nanduri, S.; Carpick, B. W.; Yang, Y.; Williams, B. R.; Qin, J. Structure of the Double-Stranded RNA-Binding Domain of the Protein Kinase PKR Reveals the Molecular Basis of Its dsRNA-Mediated Activation. *EMBO J* **1998**, *17* (18), 5458–5465. <https://doi.org/10.1093/emboj/17.18.5458>.
- (70) Hanks, S. K.; Quinn, A. M.; Hunter, T. The Protein Kinase Family: Conserved Features and Deduced Phylogeny of the Catalytic Domains. *Science* **1988**, *241* (4861), 42–52. <https://doi.org/10.1126/science.3291115>.
- (71) Romano, P. R.; Garcia-Barrio, M. T.; Zhang, X.; Wang, Q.; Taylor, D. R.; Zhang, F.; Herring, C.; Mathews, M. B.; Qin, J.; Hinnebusch, A. G. Autophosphorylation in the Activation Loop Is Required for Full Kinase Activity in Vivo of Human and Yeast Eukaryotic Initiation Factor 2alpha Kinases PKR and GCN2. *Mol Cell Biol* **1998**, *18* (4), 2282–2297. <https://doi.org/10.1128/MCB.18.4.2282>.
- (72) Patel, R. C.; Stanton, P.; Sen, G. C. Specific Mutations near the Amino Terminus of Double-Stranded RNA-Dependent Protein Kinase (PKR) Differentially Affect Its Double-Stranded RNA Binding and Dimerization Properties. *J Biol Chem* **1996**, *271* (41), 25657–25663. <https://doi.org/10.1074/jbc.271.41.25657>.
- (73) Pavlovic, J.; Haller, O.; Staeheli, P. Human and Mouse Mx Proteins Inhibit Different Steps of the Influenza Virus Multiplication Cycle. *J Virol* **1992**, *66* (4), 2564–2569. <https://doi.org/10.1128/JVI.66.4.2564-2569.1992>.
- (74) Trobridge, G. D.; Leong, J. A. Characterization of a Rainbow Trout Mx Gene. *J Interferon Cytokine Res* **1995**, *15* (8), 691–702. <https://doi.org/10.1089/jir.1995.15.691>.
- (75) Elmore, S. Apoptosis: A Review of Programmed Cell Death. *Toxicol Pathol* **2007**, *35* (4), 495–516. <https://doi.org/10.1080/01926230701320337>.
- (76) Belmokhtar, C. A.; Hillion, J.; Ségal-Bendirdjian, E. Staurosporine Induces Apoptosis through Both Caspase-Dependent and Caspase-Independent Mechanisms. *Oncogene* **2001**, *20* (26), 3354–3362. <https://doi.org/10.1038/sj.onc.1204436>.
- (77) Bertrand, R.; Solary, E.; O'Connor, P.; Kohn, K. W.; Pommier, Y. Induction of a Common Pathway of Apoptosis by Staurosporine. *Experimental Cell Research* **1994**, *211* (2), 314–321. <https://doi.org/10.1006/excr.1994.1093>.
- (78) Inoue, S.; Browne, G.; Melino, G.; Cohen, G. M. Ordering of Caspases in Cells Undergoing Apoptosis by the Intrinsic Pathway. *Cell Death Differ* **2009**, *16* (7), 1053–1061. <https://doi.org/10.1038/cdd.2009.29>.
- (79) Manns, J.; Daubrawa, M.; Driessen, S.; Paasch, F.; Hoffmann, N.; Löffler, A.; Lauber, K.; Dieterle, A.; Alers, S.; Iftner, T.; Schulze-Osthoff, K.; Stork, B.; Wesselborg, S. Triggering of a Novel Intrinsic Apoptosis Pathway by the Kinase Inhibitor Staurosporine: Activation of Caspase-9 in the Absence of Apaf-1. *FASEB J* **2011**, *25* (9), 3250–3261. <https://doi.org/10.1096/fj.10-177527>.
- (80) Enam, S. U.; Zinshteyn, B.; Goldman, D. H.; Cassani, M.; Livingston, N. M.; Seydoux, G.; Green, R. Puromycin Reactivity Does Not Accurately Localize Translation at the Subcellular Level. *eLife* **2020**, *9*, e60303. <https://doi.org/10.7554/eLife.60303>.
- (81) Nathans, D. Puromycin Inhibition of Protein Synthesis: Incorporation of Puromycin into Peptide Chains. *Proc Natl Acad Sci U S A* **1964**, *51* (4), 585–592.
- (82) Biacchesi, S.; Mérour, E.; Chevret, D.; Lamoureux, A.; Bernard, J.; Brémont, M. NV Proteins of Fish Novirhabdovirus Recruit Cellular PPM1Bb Protein Phosphatase and Antagonize RIG-I-Mediated IFN Induction. *Sci Rep* **2017**, *7*, 44025. <https://doi.org/10.1038/srep44025>.
- (83) Chinchilla, B.; Encinas, P.; Estepa, A.; Coll, J. M.; Gomez-Casado, E. Transcriptome Analysis of Rainbow Trout in Response to Non-Virion (NV) Protein of Viral Haemorrhagic Septicaemia Virus (VHSV). *Appl Microbiol Biotechnol* **2015**, *99* (4), 1827–1843. <https://doi.org/10.1007/s00253-014-6366-3>.
- (84) Chinchilla, B.; Encinas, P.; Coll, J. M.; Gomez-Casado, E. Differential Immune Transcriptome and Modulated Signalling Pathways in Rainbow Trout Infected with Viral Haemorrhagic Septicaemia Virus (VHSV) and Its Derivative Non-Virion (NV) Gene Deleted. *Vaccines (Basel)* **2020**, *8* (1), 58. <https://doi.org/10.3390/vaccines8010058>.
- (85) Kim, M. S.; Kim, K. H. Effects of NV Gene Knock-out Recombinant Viral Hemorrhagic Septicemia Virus (VHSV) on Mx Gene Expression in Epithelioma Papulosum Cyprini (EPC) Cells and Olive Flounder

- (Paralichthys Olivaceus). *Fish Shellfish Immunol* **2012**, *32* (3), 459–463. <https://doi.org/10.1016/j.fsi.2011.12.014>.
- (86) Ammayappan, A.; Vakharia, V. N. Nonvirion Protein of Novirhabdovirus Suppresses Apoptosis at the Early Stage of Virus Infection. *J Virol* **2011**, *85* (16), 8393–8402. <https://doi.org/10.1128/JVI.00597-11>.
- (87) Hay, S.; Kannourakis, G. A Time to Kill: Viral Manipulation of the Cell Death Program. *J Gen Virol* **2002**, *83* (Pt 7), 1547–1564. <https://doi.org/10.1099/0022-1317-83-7-1547>.
- (88) Mi, J.; Li, Z. Y.; Ni, S.; Steinwaerder, D.; Lieber, A. Induced Apoptosis Supports Spread of Adenovirus Vectors in Tumors. *Hum Gene Ther* **2001**, *12* (10), 1343–1352. <https://doi.org/10.1089/104303401750270995>.
- (89) Chiou, P. P.; Kim, C. H.; Ormonde, P.; Leong, J.-A. C. Infectious Hematopoietic Necrosis Virus Matrix Protein Inhibits Host-Directed Gene Expression and Induces Morphological Changes of Apoptosis in Cell Cultures. *J Virol* **2000**, *74* (16), 7619–7627.
- (90) Donnelly, N.; Gorman, A. M.; Gupta, S.; Samali, A. The eIF2 $\alpha$  Kinases: Their Structures and Functions. *Cell. Mol. Life Sci.* **2013**, *70* (19), 3493–3511. <https://doi.org/10.1007/s00018-012-1252-6>.
- (91) Berlanga, J. J.; Ventoso, I.; Harding, H. P.; Deng, J.; Ron, D.; Sonenberg, N.; Carrasco, L.; de Haro, C. Antiviral Effect of the Mammalian Translation Initiation Factor 2 $\alpha$  Kinase GCN2 against RNA Viruses. *EMBO J* **2006**, *25* (8), 1730–1740. <https://doi.org/10.1038/sj.emboj.7601073>.
- (92) Cheng, G.; Feng, Z.; He, B. Herpes Simplex Virus 1 Infection Activates the Endoplasmic Reticulum Resident Kinase PERK and Mediates eIF-2 $\alpha$  Dephosphorylation by the  $\Gamma$ 134.5 Protein. *J Virol* **2005**, *79* (3), 1379–1388. <https://doi.org/10.1128/JVI.79.3.1379-1388.2005>.
- (93) Kesterson, S. P.; Ringiesn, J.; Vakharia, V. N.; Shepherd, B. S.; Leaman, D. W.; Malathi, K. Effect of the Viral Hemorrhagic Septicemia Virus Nonvirion Protein on Translation via PERK-eIF2 $\alpha$  Pathway. *Viruses* **2020**, *12* (5), 499. <https://doi.org/10.3390/v12050499>.
- (94) Baltzis, D.; Li, S.; Koromilas, A. E. Functional Characterization of Pkr Gene Products Expressed in Cells from Mice with a Targeted Deletion of the N Terminus or C Terminus Domain of PKR \*. *Journal of Biological Chemistry* **2002**, *277* (41), 38364–38372. <https://doi.org/10.1074/jbc.M203564200>.
- (95) Li, S.; Koromilas, A. E. Dominant Negative Function by an Alternatively Spliced Form of the Interferon-Inducible Protein Kinase PKR\*. *Journal of Biological Chemistry* **2001**, *276* (17), 13881–13890. <https://doi.org/10.1074/jbc.M008140200>.
- (96) Abraham, N.; Jaramillo, M. L.; Duncan, P. I.; Méthot, N.; Icely, P. L.; Stojdl, D. F.; Barber, G. N.; Bell, J. C. The Murine PKR Tumor Suppressor Gene Is Rearranged in a Lymphocytic Leukemia. *Exp Cell Res* **1998**, *244* (2), 394–404. <https://doi.org/10.1006/excr.1998.4201>.
- (97) Liu, Z.-Y.; Jia, K.-T.; Li, C.; Weng, S.-P.; Guo, C.-J.; He, J.-G. A Truncated Danio Rerio PKZ Isoform Functionally Interacts with eIF2 $\alpha$  and Inhibits Protein Synthesis. *Gene* **2013**, *527* (1), 292–300. <https://doi.org/10.1016/j.gene.2013.05.043>.
- (98) Teige, L. H.; Aksnes, I.; Røsæg, M. V.; Jensen, I.; Jørgensen, J.; Sindre, H.; Collins, C.; Collet, B.; Rimstad, E.; Dahle, M. K.; Boysen, P. Detection of Specific Atlantic Salmon Antibodies against Salmonid Alphavirus Using a Bead-Based Immunoassay. *Fish & Shellfish Immunology* **2020**, *106*, 374–383. <https://doi.org/10.1016/j.fsi.2020.07.055>.
- (99) Dehler, C. E.; Lester, K.; Pelle, G. D.; Houel, A.; Collins, C.; Dovgan, T.; Machat, R.; Zou, J.; Boudinot, P.; Collet, B. Viral Resistance and IFN Signaling in STAT2 Knockout Fish Cells. **2019**, *12*. <https://doi.org/doi:10.4049/jimmunol.1801376>.
- (100) Macqueen, D. J.; Kristjánsson, B. K.; Johnston, I. A. Salmonid Genomes Have a Remarkably Expanded Akirin Family, Coexpressed with Genes from Conserved Pathways Governing Skeletal Muscle Growth and Catabolism. *Physiol Genomics* **2010**, *42* (1), 134–148. <https://doi.org/10.1152/physiolgenomics.00045.2010>.
- (101) Jami, R.; Mérour, E.; Bernard, J.; Lamoureux, A.; Millet, J. K.; Biacchesi, S. The C-Terminal Domain of Salmonid Alphavirus Nonstructural Protein 2 (nsP2) Is Essential and Sufficient To Block RIG-I Pathway Induction and Interferon-Mediated Antiviral Response. *Journal of Virology* **2021**, *95* (23). <https://doi.org/10.1128/JVI.01155-21>.

Figures

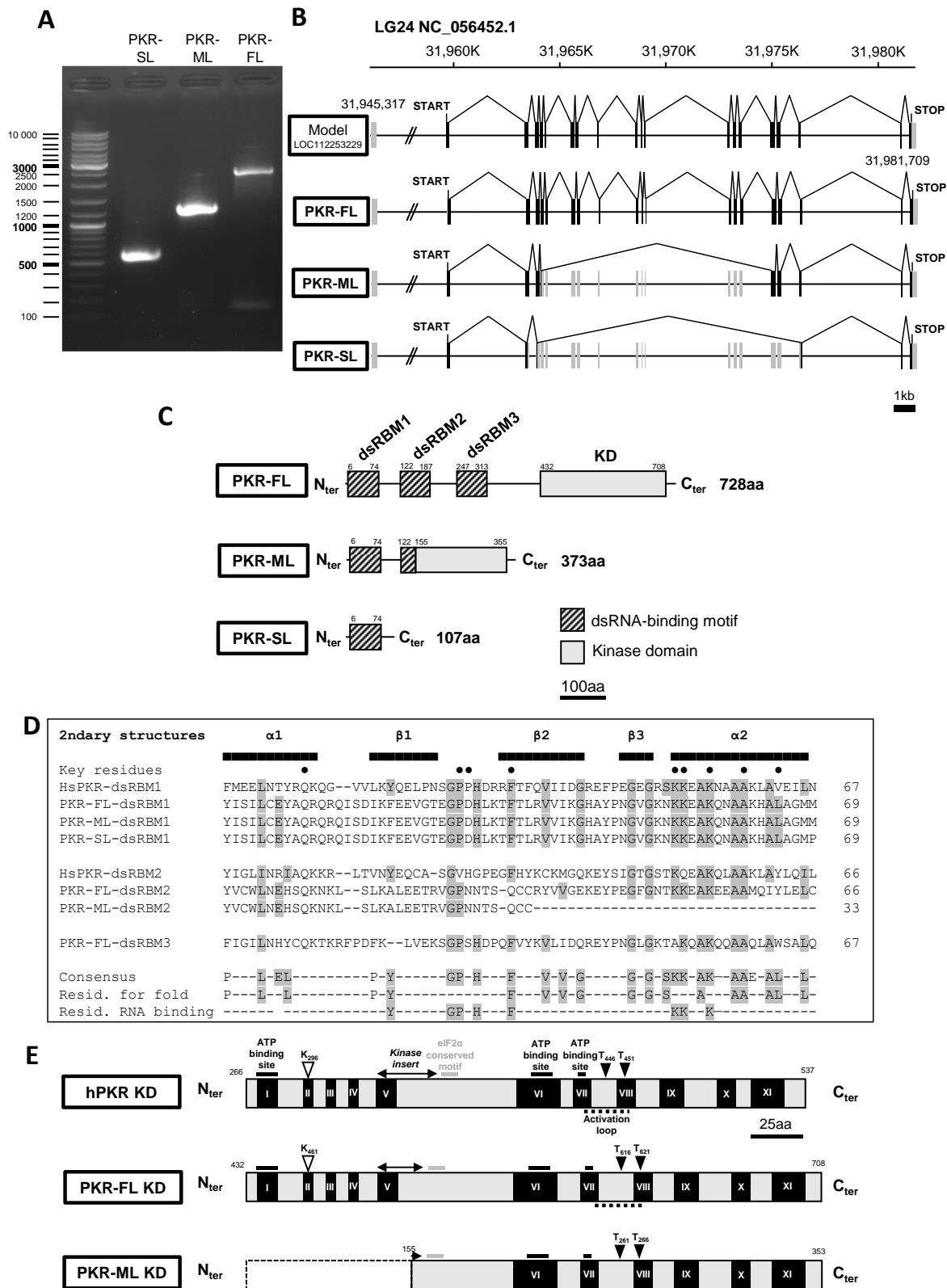
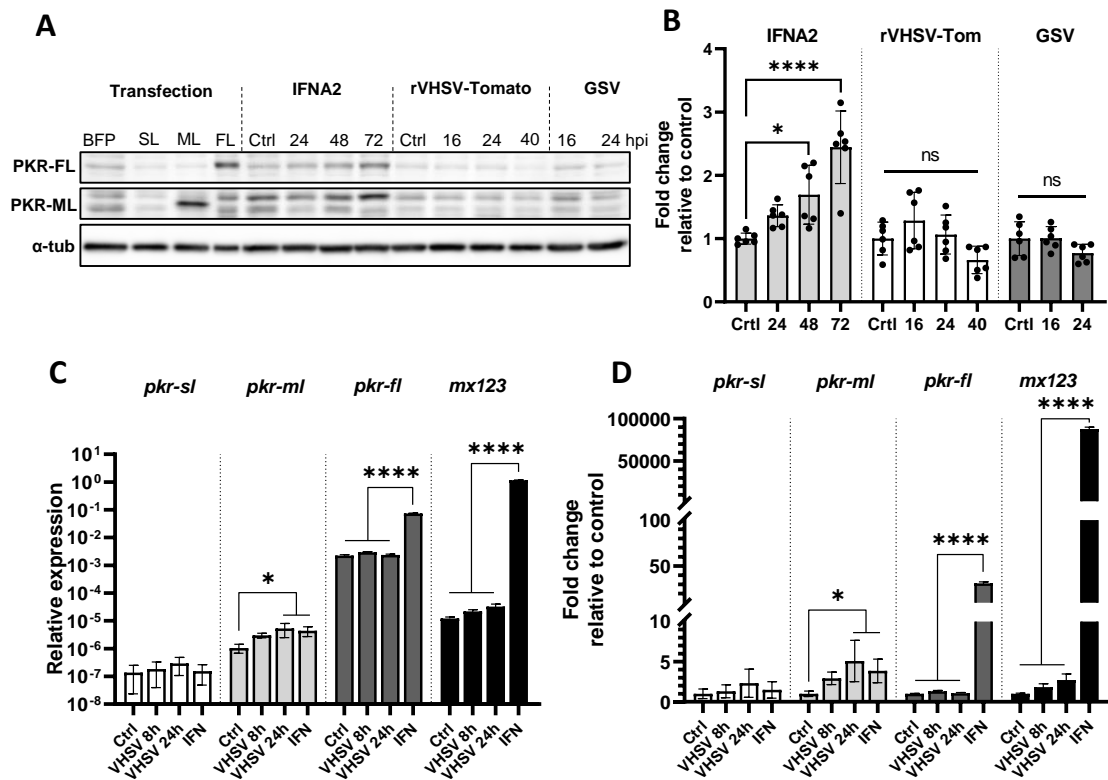


Figure 1: Isolation of three Chinook salmon PKR isoforms expressed during rVHSV-Tomato infection in EC cells.

(A) Electrophoresis on 1.5% agar gel (100 V, 60 min) of PKR isoforms (FL = full length, ML = medium length, SL = short length) amplified from cDNA of EC cells infected with rVHSV-Tomato (MOI 1). (B) Chromosomal localisation of Chinook salmon PKR (LOC112253229) and schematic representation of the 3 isolated PKR isoforms at the transcript level. Boxes represent exons and straight lines represent introns. The transcripts of PKR-FL, PKR-ML and PKR-SL are

represented in black and untranscribed regions are in grey. (C) Schematic representation of the 3 isolated PKR isoforms at the protein level. dsRBM = dsRNA binding motif, KD = kinase domain. The location of each predicted domain or motif was obtained using SMART (Simple Modular Architecture Research Tool). (D) Sequence alignment of dsRNA binding motifs from Chinook salmon PKR isoforms and human PKR. The sequence consensus identified in most dsRNA-binding motifs from other proteins and the corresponding residues conserved for the fold and/or dsRNA binding are taken from Masliah *et al.* and drawn below the alignment. The canonical secondary structured elements are shown above the alignment 68,69. The circles above the sequences show residues that have identified as important for dsRNA binding in human PKR 71,72. (E) Schematic representation of human PKR (hPKR) and Chinook salmon PKR-FL and PKR-ML kinase domains. The different subdomains (I-XI) conserved in kinase proteins were taken from Hanks *et al.* 70 and Meurs *et al.* 2. Motifs involved in ATP binding are represented by a black line, the invariant lysine residue involved in the phosphoryl transfer reaction is represented by an inverted white triangle, autophosphorylation sites described for hPKR 71 are represented by inverted black triangles and are located in the activation loop (black dotted line). The acidic kinase insert is indicated by a black double arrow and the eIF2 $\alpha$  kinase conserved motif is represented by a grey line; both features are conserved in eIF2 $\alpha$  kinases.



**Figure 2: Expression profile of the three PKR isoforms in EC cells during IFNA2 stimulation or virus infection determined by western blot (A;B) and by RT-qPCR (C;D).**

(A) EC cells were stimulated with *S. salar* IFNA2 supernatant for (24-72h), infected with rVHSV-Tomato (16-40 hpi), GSV (16-24hpi) or left untreated (Ctrl). Negative and positive controls are EC cells transfected with pcDNA3.1-Zeo-BFP or plasmids encoding PKR isoforms (PKR-SL [ $\sim$ 12 kDa], PKR-ML [ $\sim$ 42 kDa], PKR-FL [ $\sim$ 82 kDa]), respectively. Cell lysates were separated by SDS-PAGE and immunoblotted with antibodies against *S. salar* PKR and  $\alpha$ -tubulin ( $\alpha$ -tub). PKR-SL was not detected by the anti-PKR antibody and was therefore not represented. Endogenous PKR-ML was not detected following IFNA2 stimulation and viral infections; the double bands present on the blot are believed to be non-specific bands. (B) Densitometric quantification of (A). PKR-FL signal intensity normalized to  $\alpha$ -tubulin signal intensity and graphed as fold change relative to non-stimulated or non-infected cells. Bars show means  $\pm$  SD from 2 pooled independent experiments ( $n=3$  for each experiment); ns, non-significant ( $p > 0.05$ ), \*,  $p < 0.05$ , \*\*\*\*,  $p < 0.0001$ , Kruskal-Wallis test with Dunn's post-hoc multiple comparison tests. (C;D) EC cells were stimulated with *S. salar* IFNA2 supernatant for 72h, infected with rVHSV-Tomato (8-24 hpi) or left untreated (Ctrl). (C) Relative expression levels of *pkr* isoforms and *mx123* genes. (D) Expression fold change relative to non-stimulated and non-infected controls. Bars show means  $\pm$  SD from 2 pooled independent experiments ( $n=3$  or  $n=4$  for each experiment); \*,  $p < 0.05$ , \*\*\*\*,  $p < 0.0001$ , ordinary one-way ANOVA with Tukey's post-hoc multiple comparison tests.

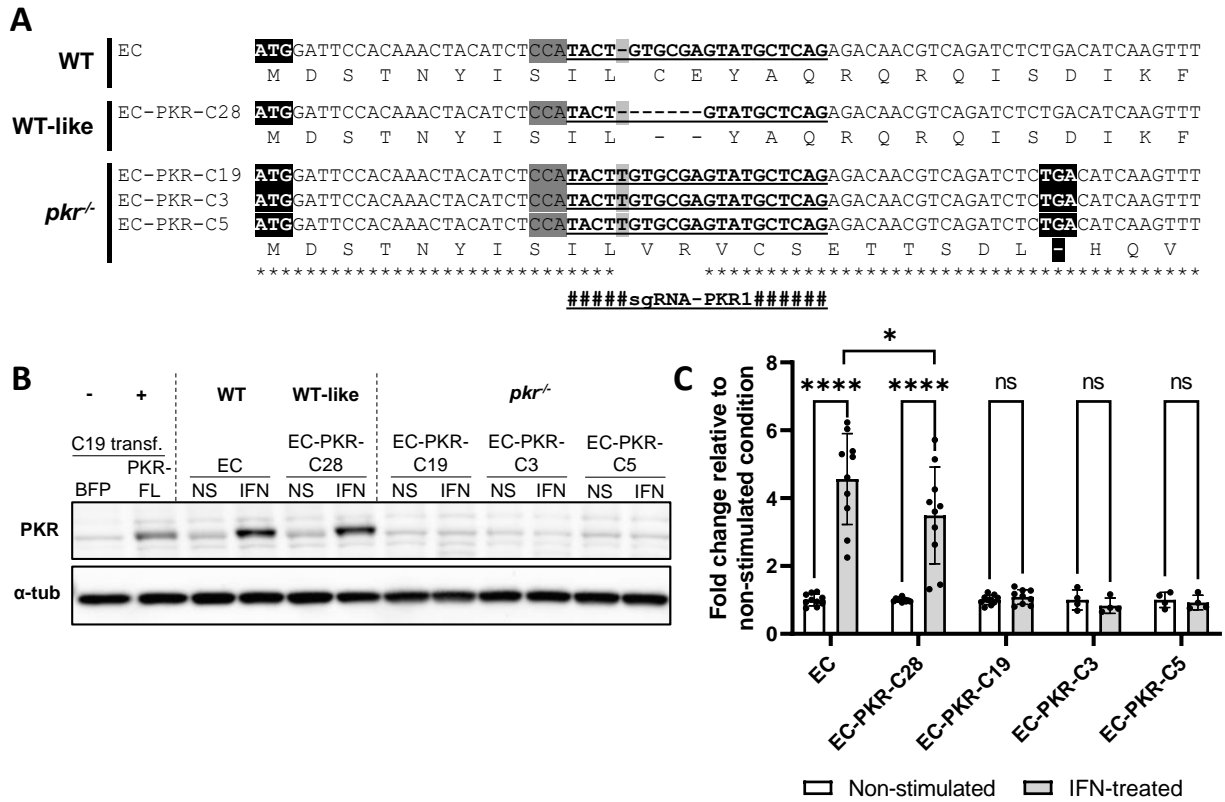


**Figure 3: Development and validation of a *pkr<sup>-/-</sup>* cell line.**

(A) Genotype of EC cells (WT), EC-PKR-C28 (6-nt deletion, 30\_35delGTGCGA, resulting in C11\_E12del, WT-like) and EC-PKR-C19, EC-PKR-C3 and EC-PKR-C5 (1-nt insertion, 29\_30insT resulting in V11fsX22, *pkr<sup>-/-</sup>*) obtained from sequencing of purified PCR products amplified from genomic DNA from each cell line. The location of the sgRNA is underlined, the protospacer adjacent motif is in dark grey, the start codon and the premature stop codon are highlighted in black, the 1-nt insertion in EC-PKR-C19, -C3 and -C5 is in light grey. The corresponding chromatograms are available in Figure S1. (B) EC and EC-PKR clones were stimulated with *S. salar* IFNA2 supernatant for 72h; positive and negative controls are EC-PKR-C19 cells transfected with pcDNA3.1-Zeo-BFP or pcDNA3.1-Zeo-BFP-P2A-PKR-FL, respectively. Cell lysates were separated by SDS-PAGE and immunoblotted with antibodies against PKR and  $\alpha$ -tubulin ( $\alpha$ -tub). (C) Densitometric quantification of (B). PKR signal intensity normalized to  $\alpha$ -tubulin signal intensity and graphed as fold change relative to non-stimulated cells. Bars show means  $\pm$  SD from 3 pooled independent experiments (n=3 or n=4 for each experiment); \*,  $p < 0.05$ , \*\*\*\*,  $p < 0.0001$ , ordinary two-way ANOVA with Bonferroni's post-hoc multiple comparison tests.



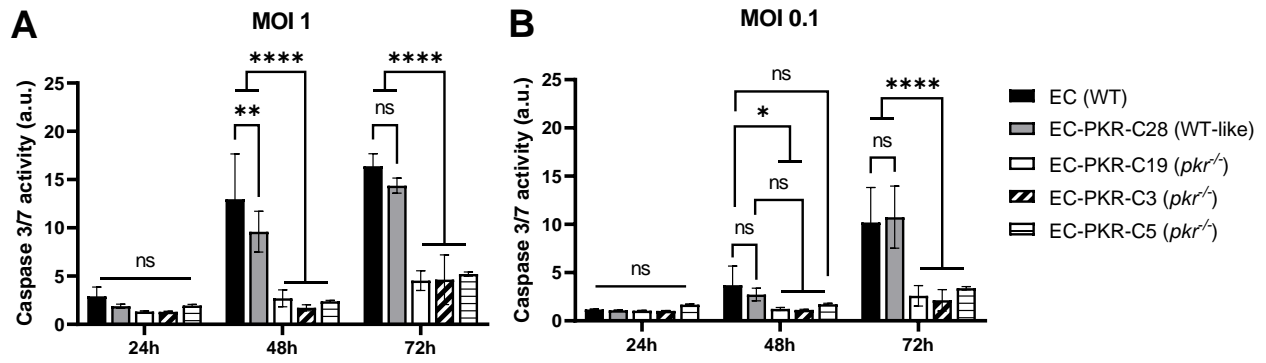


**Figure 5: Endogenous Chinook salmon PKR triggers apoptosis during rVHSV-Tomato infection.**

EC (WT), EC-PKR-C28 (WT-like) and EC-PKR-C19, -C3 and -C5 (*pkrr*<sup>-/-</sup>) were infected with rVHSV-Tomato at (A) MOI 1 or (B) MOI 0.1 and caspase 3/7 activity was measured at 24, 48 and 72 h post-infection. Bars show means  $\pm$  SD from two pooled independent experiments ( $n=4$  for each experiment); ns, non-significant ( $p > 0.05$ ), \*,  $p < 0.05$ , \*\*,  $p < 0.01$ , \*\*\*\*,  $p < 0.0001$ , ordinary two-way ANOVA with Tukey's post-hoc multiple comparison tests.

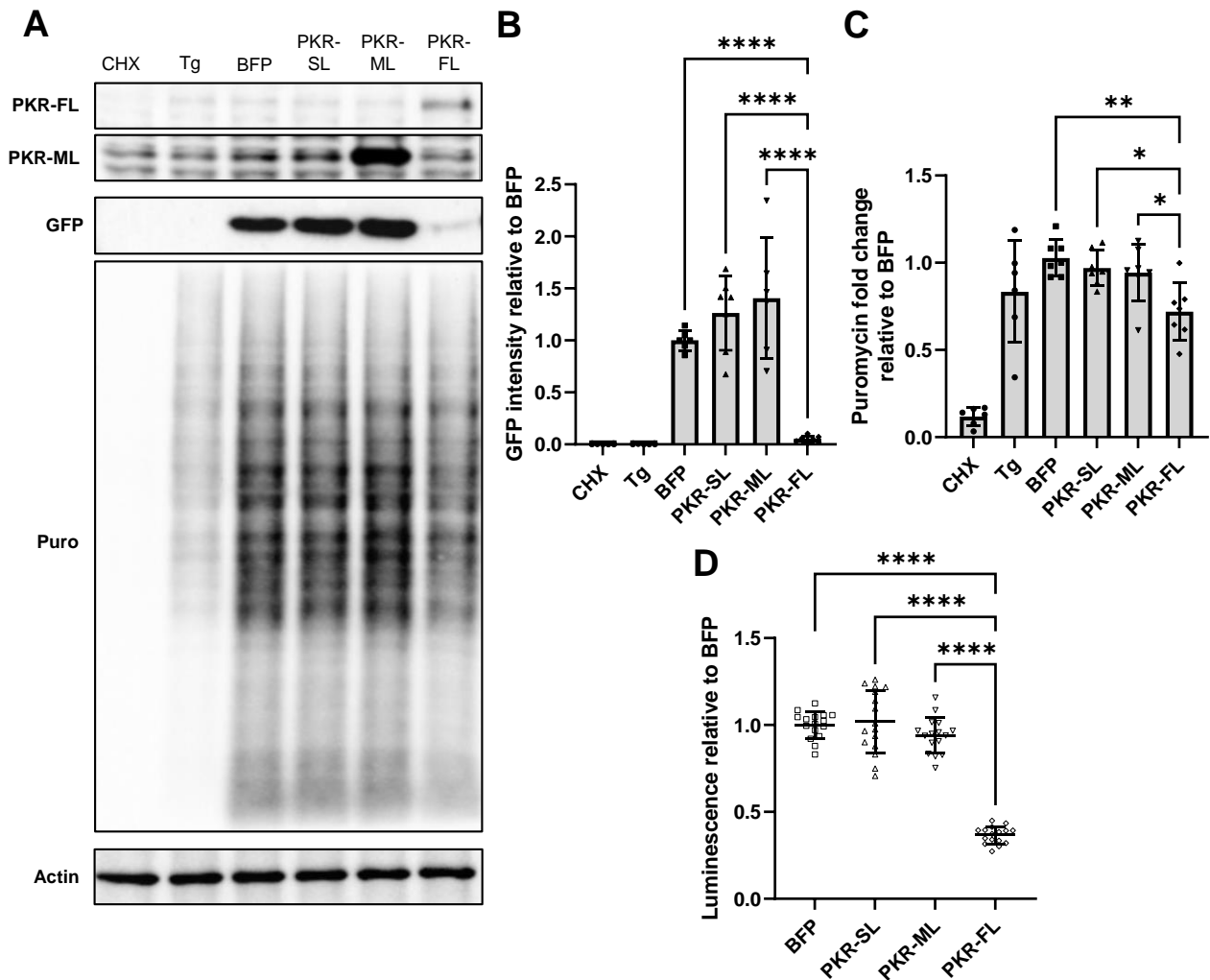


**Figure 6: Overexpression of PKR-FL inhibits host translation.**

(A) *pk<sup>r</sup>-/-* EC-PKR-C19 cells were cotransfected with pcDNA3.1-Hyg-mEGFP and plasmids encoding BFP or different PKR isoforms (PKR-SL, -ML, -FL). At 8 hpt, mock transfected cells were treated with cycloheximide (CHX, 50  $\mu$ g/mL, 24h) or thapsigargin (Tg, 2  $\mu$ M, 45 min). At 30 hpt, cells were pulsed with puromycin (5  $\mu$ g/mL) for 15 min and cell lysates were separated by SDS-PAGE and immunoblotted with antibodies against PKR, GFP, puromycin (puro) or actin. The bands corresponding to PKR-FL and -ML are located at ~82 kDa and ~42 kDa, respectively. PKR-SL was not detected by the anti-PKR antibody and was therefore not represented. (A,B) Densitometric quantification of (A). (B) GFP signal intensity normalized to actin signal intensity and graphed as fold change relative to BFP transfected cells. Bars show means  $\pm$  SD from two pooled independent experiments (n=3 or n=4 for each experiment), \*,  $p < 0.05$ ; \*\*,  $p < 0.01$ , \*\*\*\*,  $p < 0.0001$ , ordinary one-way ANOVA with Tukey's post-hoc multiple comparison tests. (C) Puromycin signal intensity normalized to actin signal intensity and graphed as fold change relative to BFP transfected cells. (D) *pk<sup>r</sup>-/-* EC-PKR-C19 cells were cotransfected with pcDNA3-G418-Luc and plasmids encoding BFP or different PKR isoforms (PKR-SL, -ML, -FL). At 24 hpt, luciferase activity was measured. Luminescence signal intensity graphed as fold change relative to BFP transfected cells. Data shown are means  $\pm$  SD (n=16) and are representative of 2 independent experiments; \*\*\*\*,  $p < 0.0001$ , ordinary one-way ANOVA with Tukey's post-hoc multiple comparison tests.

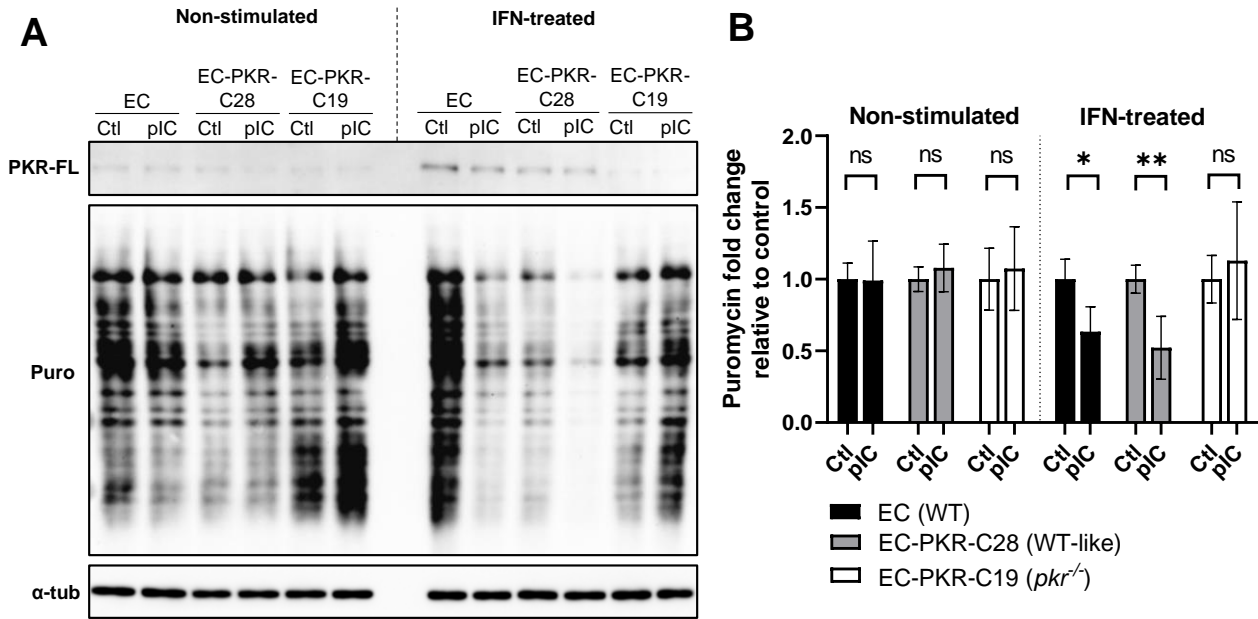


**Figure 7: Endogenous Chinook salmon PKR inhibits host translation upon transfection with poly(I:C).**

(A) Non-stimulated or ssIFNA2-pretreated EC (WT), EC-PKR-C28 (WT-like) and EC-PKR-C19 (*pkr*<sup>-/-</sup>) cells were transfected with rhodamine-labeled poly(I:C)-HMW (pIC) or mock transfected (Ctl). At 24 hpt, cells were pulsed with puromycin (5  $\mu$ g/mL) for 15 min and cell lysates were separated by SDS-PAGE and immunoblotted with antibodies against PKR, puromycin and  $\alpha$ -tubulin. (B) Densitometric quantification of (A). Puromycin signal intensity normalised to  $\alpha$ -tubulin signal intensity and graphed as fold change relative to mock transfected cells. Bars show means  $\pm$  SD from two pooled independent experiments ( $n=3$  for each experiment), ns, non-significant ( $p > 0.05$ ); \*,  $p < 0.05$ ; \*\*,  $p < 0.01$ , two-way ANOVA with Bonferroni's post-hoc multiple comparison tests.

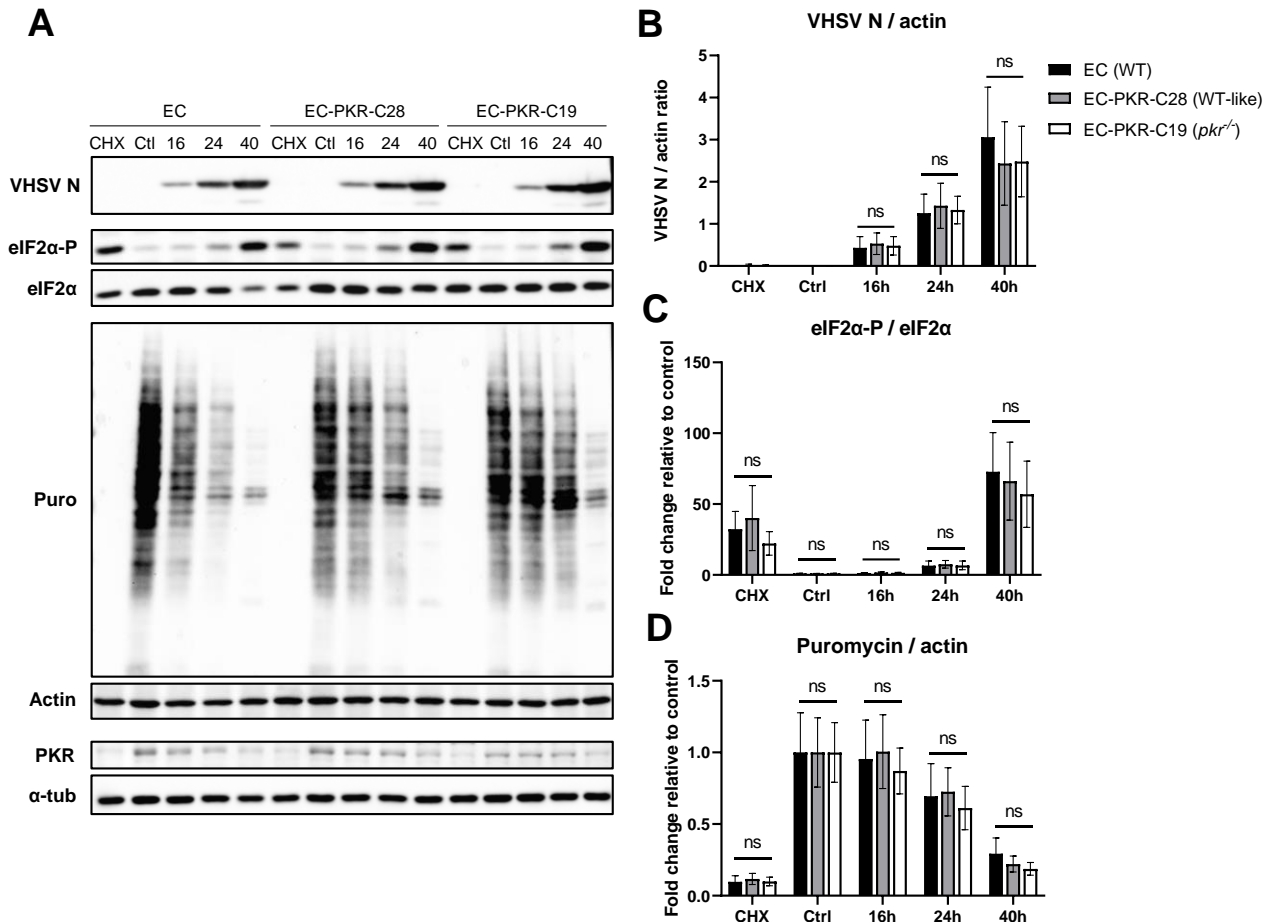


**Figure 8: Endogenous Chinook salmon PKR is not the main driver of protein synthesis inhibition during rVHSV-Tomato infection.**

(A) EC (WT), EC-PKR-C28 (WT-like) and EC-PKR-C19 (*pkrr*<sup>-/-</sup>) cells were either infected with rVHSV-Tomato at MOI 1, left uninfected (Ctrl) or stimulated with cycloheximide (CHX, 50  $\mu$ g/mL) for 24h. At 16, 24 or 40 hpi, cells were pulsed with puromycin (5  $\mu$ g/mL) for 15 min and cell lysates were separated by SDS-PAGE and immunoblotted with antibodies against VHSV N, eIF2 $\alpha$ -P, eIF2 $\alpha$ , puromycin (puro), actin, PKR and  $\alpha$ -tubulin ( $\alpha$ -tub). (B,C,D) Densitometric quantification of (A). (B) VHSV N signal intensity normalized to actin signal intensity. (C) eIF2 $\alpha$ -P signal intensity normalised to eIF2 $\alpha$  signal intensity and graphed as fold change relative to control cells. (D) Puromycin signal intensity normalized to actin signal intensity and graphed as fold change relative to control cells. Bars show means  $\pm$  SD from two pooled independent experiments ( $n=3$  for each experiment); ns, non-significant ( $p > 0.05$ ), ordinary two-way ANOVA with Tukey's post-hoc multiple comparison tests.

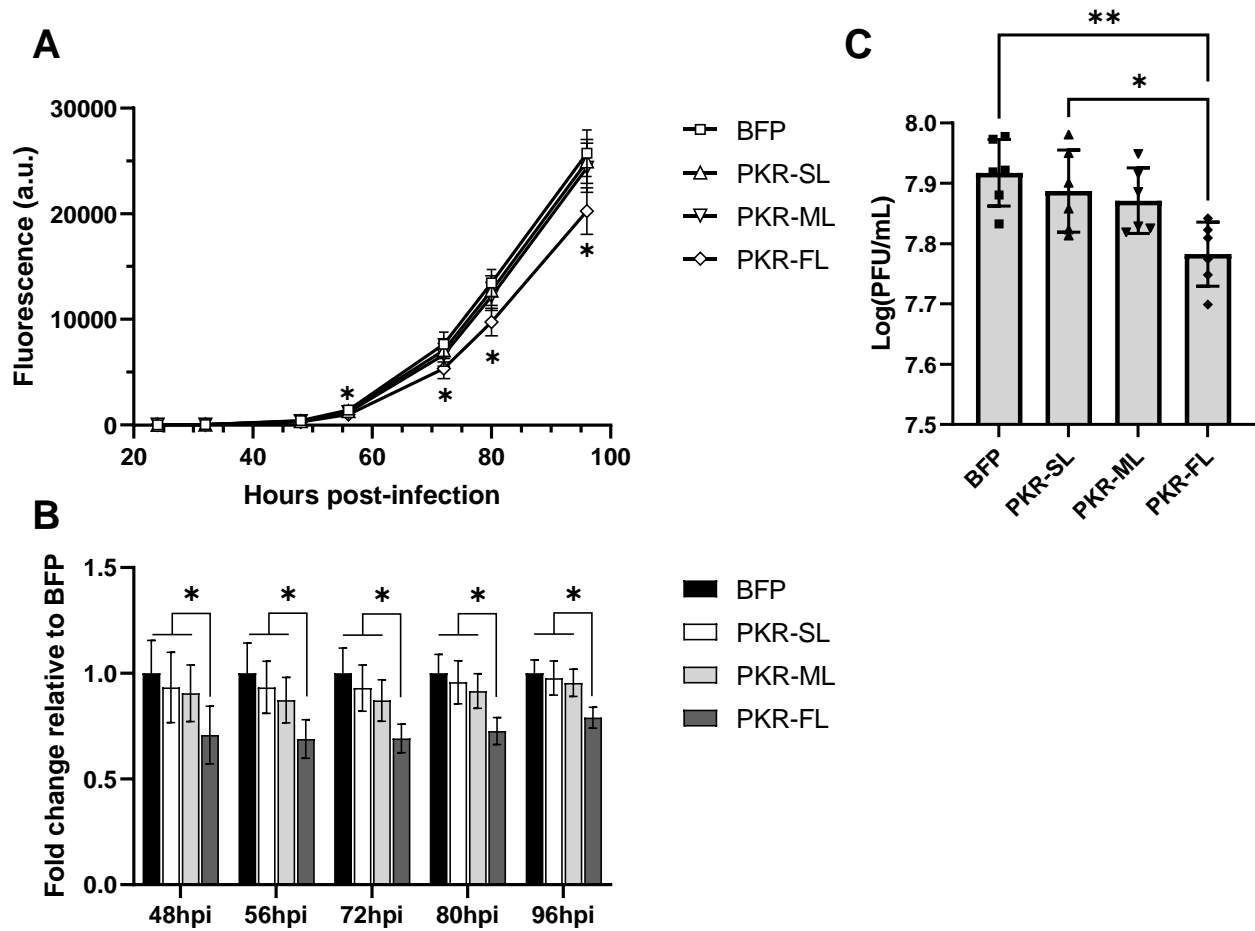


**Figure 9: Overexpression of PKR-FL inhibits rVHSV-Tomato replication.**

*pkrr*<sup>-/-</sup> EC-PKR-C19 cells were transfected with pcDNA3.1-Zeo-BFP or plasmids encoding PKR isoforms. At 24hpt, cells were infected with rVHSV-Tomato (MOI 1) and fluorescence was measured at different time points post-infection. **(A)** Fluorescence signal intensity measured over time; data shown are means  $\pm$  SD from 6 independent experiments (n=4 for each experiment); two-way ANOVA with Tukey's post-hoc multiple comparison tests were performed on log-transformed data: \*,  $p < 0.05$ ; \*\*,  $p < 0.01$ , comparison to BFP. **(B)** Fluorescence signal intensity graphed as fold change relative to BFP transfected cells; \*,  $p < 0.05$ , two-way RM ANOVA with Tukey's post-hoc multiple comparison tests. **(C)** Supernatant was collected at 96hpi, pooled (4 wells per condition) and titrated by plaque assay. Data shown are means  $\pm$  SD from 6 independent experiments (n=1 for each experiment, 4 pooled wells); \*,  $p < 0.05$ ; \*\*,  $p < 0.01$ , ordinary one-way ANOVA with Tukey's post-hoc multiple comparison tests.

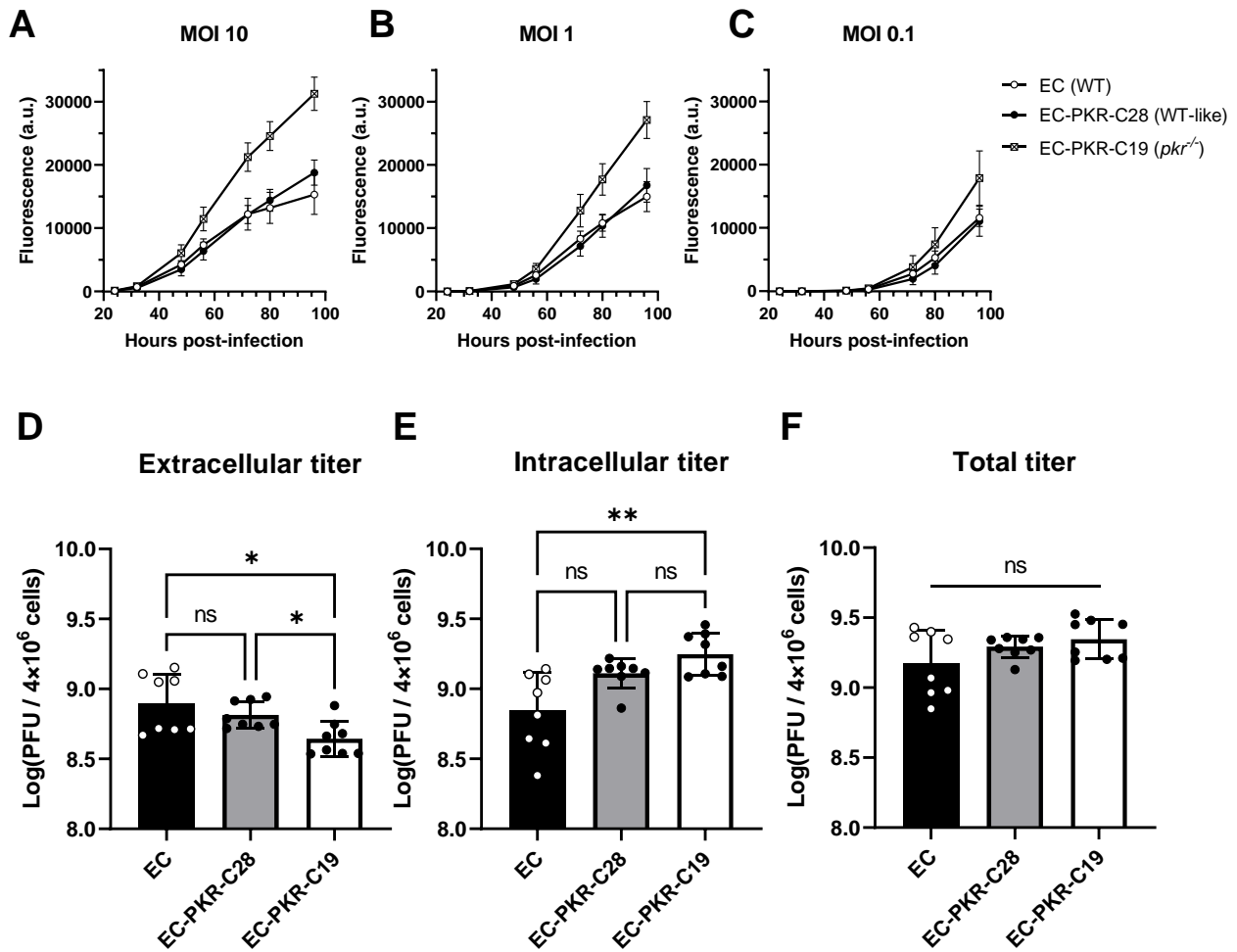


**Figure 10: Endogenous Chinook salmon PKR favors the release of rVHSV-Tomato particles into the supernatant.**

(A;B;C) EC (WT), EC-PKR-C28 (WT-like) and EC-PKR-C19 (*pkrr*<sup>-/-</sup>) cells were infected with rVHSV-Tomato at (A) MOI 10, (B) MOI 1 or (C) MOI 0.1 and fluorescence was measured at different time points post-infection. Graphs show means  $\pm$  SD from 4 independent experiments (n=8 for each experiment). two-way RM ANOVA with Tukey's post-hoc multiple comparison tests were performed on each log-transformed data set: (A) \*,  $p < 0.05$  starting from 48 hpi ; (B) \*,  $p < 0.05$  starting from 72 hpi ; (C) \*,  $p < 0.05$  at 96 hpi. (D;E;F) EC (WT), EC-PKR-C28 (WT-like) and EC-PKR-C19 (*pkrr*<sup>-/-</sup>) cells were infected with rVHSV-Tomato at MOI 1; supernatants were collected at 96 hpi and the remaining cells were scraped and sonicated; both supernatants and sonicates were titrated by plaque assay. Log-transformed plaque forming unit (PFU) counts from (D) supernatants, (E) sonicated cells and (F) total sum of both values of EC, EC-PKR-C28, EC-PKR-C19 cells ( $4 \times 10^6$  cells) infected with rVHSV-Tomato for 96 hpi. Bars show means  $\pm$  SD from two pooled independent experiments (n=4 for each experiment), \*,  $p < 0.05$ ; \*\*,  $p < 0.01$ , Kruskal-Wallis test with Dunn's post-hoc multiple comparison tests on log-transformed data.

## Tables

Table I: Primers used in this study

Primer name	Sequence (5'→3')	Source or reference	Specificities
<b>Plasmid constructs:</b>			
<b>BFP-F</b>	CTGCTGCT <b>GGCTAGC</b> TCTAGACT <b>CTCGAGATGAGCGAGCTGATT</b> AAGGAGA	pCite-P-BFP	<i>NheI</i> <i>XbaI</i> <b>XhoI</b>
<b>BFP-R</b>	CAGCAGCAG <b>AAGCTT</b> GGTACCC <b>TGCAGGGATCCGATATC</b> GTG CCCCAGTTTGCTAGG	pCite-P-BFP	<b>HindIII</b> <i>KpnI</i> <b>PstI</b> <i>BamHI</i> <b>EcoRV</b>
<b>OtPKR-R0-F</b>	GCGATGACTGGACACTGACA	XM_042305681.1	
<b>OtPKR-R0-R</b>	ATTTCGGCGCATGTGACAAAT	XM_042305681.1	
<b>OtPKR-R0bis-F</b>	AAGCCATGGATTCCACAAACTAC	XM_042305681.1	
<b>OtPKR-R0bis-R</b>	CCACTGACTGTCTTTAGACTGTTC	XM_042305681.1	
<b>OtPKR-P2A-F</b>	GGAAGCGGAGCTACTA <b>ACTT</b> CAGCCTGCTGAAGCAGGCTGGA GACGTGGAGGAGA <b>ACCCTGGACCTATGGATTCCACAACTAC</b> ATCTCC	XM_042305681.1	<i>P2A</i>
<b>OtPKR-HindIII-R</b>	CTGCTGCTG <b>AAGCTT</b> TTAGACTGTCTGTTGTCTTGATGG	XM_042305681.1	<b>HindIII</b>
<b>sgRNA:</b>			
<b>sgRNA-mEGFP-S</b>	<b>TCCTAATACGACTCACTATA</b> GGCGAGGGCGATGCCACCTAG TTTTAGAGCTAGAAATAGCAAGTTAAAAATAAGGCTAGTCCG TTATCAACTTGAAAAAGTGGCACCAGTCCGGTGCTTTT	48	<b>T7 promoter</b> sgRNA target <i>Scaffold</i>
<b>sgRNA-mEGFP-AS</b>	AAAAGCACCGACTCGGTGCCACTTTTTCAAGTTGATAACGG ACTAGCCTTATTTTAACTTGCTATTTCTAGCTCTAAACTA GGTGGCATCGCCCTCGCCT <b>TATAGTGAGTCGTATTAGGA</b>	48	<b>T7 promoter</b> sgRNA target <i>Scaffold</i>
<b>sgRNA-PKR1-S</b>	<b>TCCTAATACGACTCACTATA</b> CTGAGCATACTCGCACAGTAGT TTTAGAGCTAGAAATAGCAAGTTAAAAATAAGGCTAGTCCGTT ATCAACTTGAAAAAGTGGCACCAGTCCGGTGCTTTT	XM_042305681.1 Coding exon 1	<b>T7 promoter</b> sgRNA target <i>Scaffold</i>
<b>sgRNA-PKR1-AS</b>	AAAAGCACCGACTCGGTGCCACTTTTTCAAGTTGATAACGG CTAGCCTTATTTTAACTTGCTATTTCTAGCTCTAAACTACT GTGCGAGTATGCTCAG <b>TATAGTGAGTCGTATTAGGA</b>	XM_042305681.1 Coding exon 1	<b>T7 promoter</b> sgRNA target <i>Scaffold</i>
<b>sgRNA-PKR2-S</b>	<b>TCCTAATACGACTCACTATA</b> CATGCCATCCTAACGGGGTGT TTTAGAGCTAGAAATAGCAAGTTAAAAATAAGGCTAGTCCGTT ATCAACTTGAAAAAGTGGCACCAGTCCGGTGCTTTT	XM_042305681.1 Coding exon 2	<b>T7 promoter</b> sgRNA target <i>Scaffold</i>
<b>sgRNA-PKR2-AS</b>	AAAAGCACCGACTCGGTGCCACTTTTTCAAGTTGATAACGG CTAGCCTTATTTTAACTTGCTATTTCTAGCTCTAAAC <b>ACCCTC</b> CGTTAGGATAGGCAT <b>GTATAGTGAGTCGTATTAGGA</b>	XM_042305681.1 Coding exon 2	<b>T7 promoter</b> sgRNA target <i>Scaffold</i>
<b>sgRNA-PKR3-S</b>	<b>TCCTAATACGACTCACTATA</b> CTGACATCAAGTTTGAGGGT TTTAGAGCTAGAAATAGCAAGTTAAAAATAAGGCTAGTCCGTT ATCAACTTGAAAAAGTGGCACCAGTCCGGTGCTTTT	XM_042305681.1 Coding exon 1	<b>T7 promoter</b> sgRNA target <i>Scaffold</i>
<b>sgRNA-PKR3-AS</b>	AAAAGCACCGACTCGGTGCCACTTTTTCAAGTTGATAACGG CTAGCCTTATTTTAACTTGCTATTTCTAGCTCTAAAC <b>CCCTC</b> AAACTTGATGTCAGAG <b>TATAGTGAGTCGTATTAGGA</b>	XM_042305681.1 Coding exon 1	<b>T7 promoter</b> sgRNA target <i>Scaffold</i>
<b>sgRNA-PKR4-S</b>	<b>TCCTAATACGACTCACTATA</b> TTTGAGGAGGTTGGAACAGAGT TTTAGAGCTAGAAATAGCAAGTTAAAAATAAGGCTAGTCCGTT ATCAACTTGAAAAAGTGGCACCAGTCCGGTGCTTTT	XM_042305681.1 Coding exon 1	<b>T7 promoter</b> sgRNA target <i>Scaffold</i>
<b>sgRNA-PKR4-AS</b>	AAAAGCACCGACTCGGTGCCACTTTTTCAAGTTGATAACGG CTAGCCTTATTTTAACTTGCTATTTCTAGCTCTAAACT <b>CTCTG</b> TTCCAACCTCCTCAA <b>TATAGTGAGTCGTATTAGGA</b>	XM_042305681.1 Coding exon 1	<b>T7 promoter</b> sgRNA target <i>Scaffold</i>
<b>Genotyping:</b>			
<b>PKR-gen1-F</b>	CAGCCATGGTCGCTTTCACC	LOC112253229	
<b>PKR-gen1-R</b>	CTGAAGGCAATGCAGCTCTGC	LOC112253229	
<b>PKR-gen2-F</b>	AAGTATTGCCTTAAACATTCCCC	LOC112253229	
<b>PKR-gen2-R</b>	ACGGTCAAATGTCACCAGGG	LOC112253229	

Table II: Plasmids used in this study

Plasmid	Use	Addgene ID	Reference
pcDNA3.1(-)-Zeo	Plasmid backbone	NA	V86520, Invitrogen
pCite-P-BFP	Amplification of BFP gene		52
pcDNA3.1-Zeo-mEGFP	mEGFP expression vector	#214145	This study
pcDNA3.1-Zeo-BFP	BFP expression vector	#214367	This study
pcDNA3.1-Zeo-BFP-P2A-PKR-FL	Chinook salmon PKR-FL expression vector	#214364	This study
pcDNA3.1-Zeo-BFP-P2A-PKR-ML	Chinook salmon PKR-ML expression vector	#214365	This study
pcDNA3.1-Zeo-BFP-P2A-PKR-SL	Chinook salmon PKR-ML expression vector	#214366	This study
pcDNA3.1-Zeo-ssIFNA2	Atlantic salmon IFNA2 expression vector	#183469	54
pcDNA3.1-Hyg-mEGFP	mEGFP expression vector	#191847	98
pcDNA3.1-Hyg-RFP-KDEL	ER-located RFP expression vector	#138660	99
pcDNA3-Neo-Luc	Firefly luciferase expression vector	#214368	This study

Table III: qPCR primers used in this study

Name	Sequence 5'-3'	Target name	Target accession number	Size	Reference
otelf1a-ex-F	CACTGCTCAAGTAATCATCCTG	Elongation factor 1-alpha, oocyte form	XM_024441752.2	259 pb	This study
otelf1a-ex-R	CACAGCAAAACGACCAAGAG				
otgapdh3-ex-F	CCAGTGTATGAAGCCCCATGAG	glyceraldehyde-3-phosphate dehydrogenase	XM_024414049.1	187 pb	This study
otgapdh3-ex-R	CTTGTCCCTCGTTGACTCCCATG				
otrps29-ex-F	GGGTCATCAGCAGCTCTATTGG	40S ribosomal protein S29	XM_024422712.2	164 pb	Adapted from <sup>100</sup>
otrps29-ex-R	CCAGCTTAACAAAGCCGATGTGC				
otmx123-ex-F	CAACTTGGTGGTTGTGCCATG	Interferon-induced GTP-binding protein Mx	XM_024415949.2 XM_042295559.1 XM_042295553.1 XM_024415946.2	111 pb	This study
otmx123-ex-R	GGCTTGGTCAGGATGCCTAAT				
otprk-fl-ex-F	CTGAGTAAAGGAAAGCTAAGCGG				
otprk-fl-ex-R	GCCTGAATCTGAAGTGGTGTGCG	Protein kinase R, full length isoform	XM_042305681.1	147 pb	This study
otprk-ml-ex-F	CGAGCAGTTATCTCCAGCC				
otprk-ml-ex-R	GAACTGCTGCCTGAACTACAGC	Protein kinase R, medium length isoform		140 pb	This study
otprk-sl-ex-F	CACCTGAAAACCTTCACTCTGAGG	Protein kinase R, short length isoform		132 pb	This study
otprk-sl-ex-R	TGCTCGGACAGGAGGCAT				

**Table IV: List of primary antibodies used for Western blots in this study**

Name	Target	Ab type	Species	Expected size (kDa)	Working dilution	Commercial reference	Reference
<b>Anti-Actin</b>	Actin	Polyclonal	Rabbit	42 kDa	1:4000 <sup>a</sup>	#A5060, Sigma Aldrich	<sup>47</sup>
<b>Anti-<math>\alpha</math>-Tubulin</b>	$\alpha$ -Tubulin	Monoclonal	Mouse	55 kDa	1:3000 <sup>a</sup>	T9026, Sigma Aldrich	<sup>101</sup>
<b>Anti-GFP</b>	mEGFP	Monoclonal	Mouse	27 kDa	1:2000 <sup>a</sup>	G6539, Merck	
<b>Anti-GSV</b>	GSV proteins	Polyclonal	Rabbit	NA	1:1000 <sup>a</sup>	NA	
<b>Anti-eIF2<math>\alpha</math></b>	eIF2 $\alpha$	Monoclonal	Mouse	36 kDa	1:1000 <sup>a</sup>	AHO0802, Invitrogen	<sup>47</sup>
<b>Anti-eIF2<math>\alpha</math>-P</b>	eIF2 $\alpha$ -P	Polyclonal	Rabbit	36 kDa	1:1000 <sup>b</sup>	#9721, Cell signaling	<sup>47</sup>
<b>Anti-Mx123</b>	Mx1, Mx2, Mx3	Polyclonal	Rabbit	70 kDa	1:2000 <sup>a</sup>	NA	<sup>56</sup>
<b>Anti-PKR</b>	PKR	Polyclonal	Rabbit	84 kDa	1:1000 <sup>b</sup>	NA	<sup>47</sup>
<b>Anti-Puromycin</b>	Puromycin incorporated into newly synthesized proteins	Monoclonal	Mouse	NA	1:1000 <sup>a</sup>	MABE343, Sigma-Aldrich	<sup>93</sup>
<b>Anti-VHSV N</b>	VHSV N	Monoclonal	Mouse	44 kDa	1:2000 <sup>a</sup>	NA	<sup>49</sup>

<sup>a</sup> Dilution in TBST supplemented with 5% milk<sup>b</sup> Dilution in TBST supplemented with 5% BSA**Table V: Molecular characteristics of Chinook salmon PKR isoforms isolated in this study**

PKR isoforms	NCBI accession number	ORF length (bp)	aa length	Theoretical molecular weight (kDa)
<b>PKR-FL</b>	LOC112253229 XM_042305681.1 XP_042161615.1	2 187	728	81.6
<b>PKR-ML</b>	NA	1 122	373	42.3
<b>PKR-SL</b>	NA	464	107	11.9

Supplementary figures

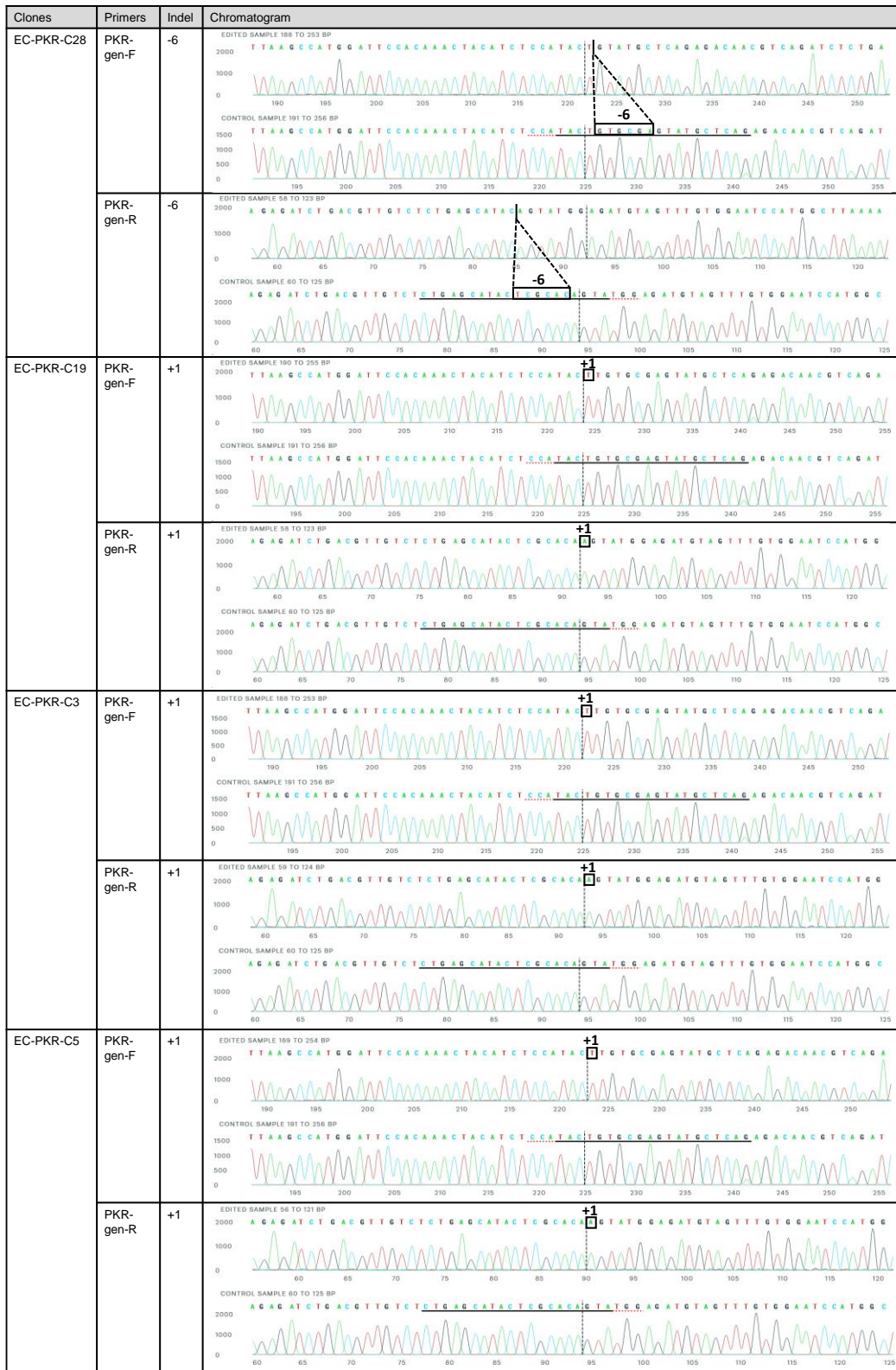
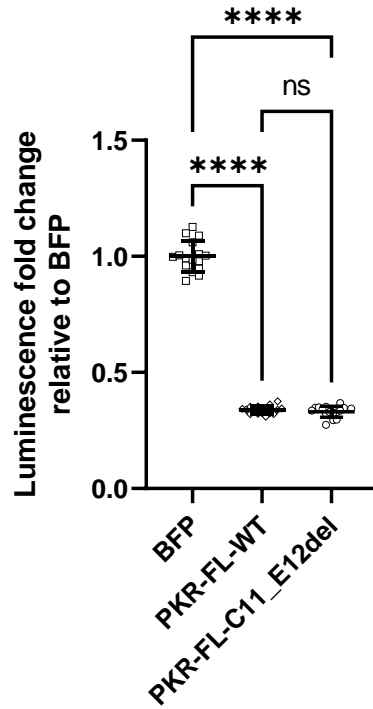


Figure S1: Alignment of chromatograms from EC-PKR clones with EC (WT) cell line.

Chromatograms showing edited and wild-type (control) sequences in the region around the sequence targeted by sgRNA-PKR1 from EC-PKR-C28 (WT-like), EC-PKR-C19, EC-PKR-C3 and EC-PKR-C5 (*pkrr*<sup>-/-</sup>) clones. The horizontal black line represents the guide sequence; the horizontal red dotted line corresponds to the PAM site; the vertical black dotted line represents the actual cut site. The black boxes show the inserted or deleted nucleotides in each edited clone. Alignments were obtained using Synthego ICE Analysis tool (v3).



**Figure S2: WT PKR-FL and PKR-FL-C11\_E12del isolated from EC-PKR-C28 exhibit similar protein translation inhibition activity.**

*pk<sup>r-/-</sup>* EC-PKR-C19 cells were cotransfected with pcDNA3-Neo-Luc and plasmids encoding BFP, PKR-FL isolated from WT EC cells (PKR-FL-WT) and PKR-FL isolated from EC-PKR-C28 (PKR-FL-C11\_E12del), which exhibits a 6-nt deletion at the sgRNA cut site (Figure 3 and figure S1). At 24 hpt, luciferase activity was measured. Luminescence signal graphed as fold change relative to BFP transfected cells. Data shown are means ± SD (n=16) and are representative of 2 independent experiments; ns, non-significant ( $p > 0.05$ ), \*\*\*\*,  $p < 0.0001$ , ordinary one-way ANOVA with Tukey's post-hoc multiple comparison tests.

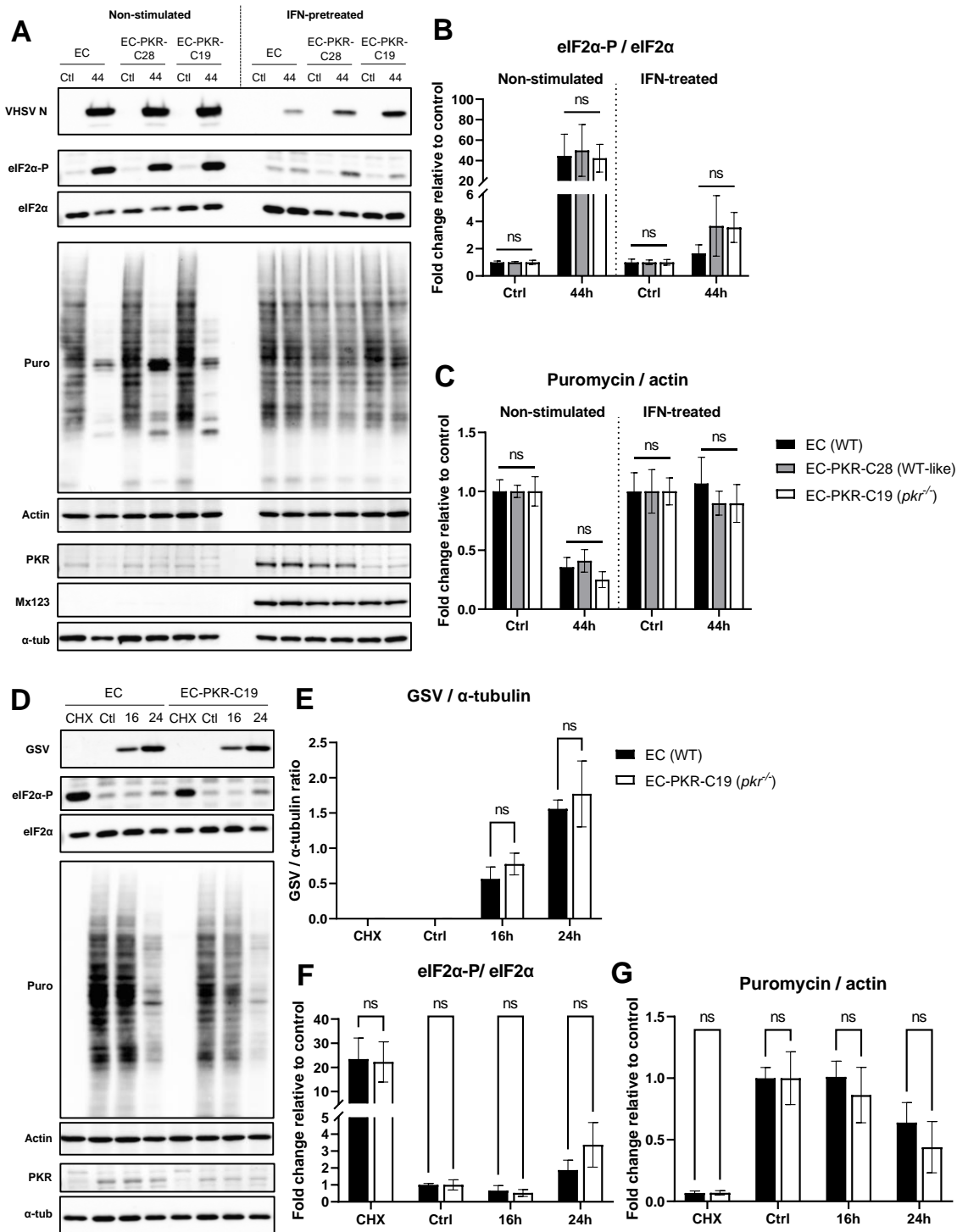


**Figure S3: Endogenous Chinook salmon PKR is neither the driver of protein synthesis inhibition during rVHSV-Tomato infection even after IFN pretreatment nor during GSV infection.**

(A) Non-stimulated or ssIFNA2-pretreated EC (WT), EC-PKR-C28 (WT-like) and EC-PKR-C19 (*pkr*<sup>-/-</sup>) cells were either infected with rVHSV-Tomato at MOI 1 or left uninfected (Ctl). At 44hpi, cells were pulsed with puromycin (5 μg/mL) for 15 min and cell lysates were separated by SDS-PAGE and immunoblotted with antibodies against VHSV N, eIF2α-P, eIF2α, puromycin (puro), actin, PKR, Mx123 and α-tubulin (α-tub). (B,C) Densitometric quantification of (A). (B) eIF2α-P signal intensity normalized to eIF2α signal intensity and graphed as fold change relative to control cells. (C) Puromycin signal intensity normalized to actin signal intensity and graphed as fold change relative to control cells. Bars show means ± SD from two pooled independent experiments (n=3 for each experiment), ns, non-significant ( $p > 0.05$ ), two-way ANOVA with Tukey's post-hoc multiple comparison tests. (D) EC (WT) and EC-PKR-C19 (*pkr*<sup>-/-</sup>) cells were either infected with GSV at MOI 1, left uninfected (Ctl) or stimulated with cycloheximide (CHX, 50 μg/mL) for 24h. At 16 or 24 hpi, cells were pulsed with puromycin (5 μg/mL) for 15 min and cell lysates were separated by SDS-PAGE and immunoblotted with antibodies against GSV, eIF2α-P, eIF2α, puromycin (puro), actin, PKR and α-tubulin (α-tub).

tub). (E;F;G) Densitometric quantification of (A). (B) GSV signal intensity normalized to  $\alpha$ -tubulin signal intensity. (C) eIF2 $\alpha$ -P signal intensity normalized to eIF2 $\alpha$  signal intensity and graphed as fold change relative to control cells. (D) Puromycin signal intensity normalized to actin signal intensity and graphed as fold change relative to control cells. Bars show means  $\pm$  SD from two pooled independent experiments (n=3 for each experiment); ns, non-significant ( $p > 0.05$ ), ordinary two-way ANOVA with Bonferroni's post-hoc multiple comparison tests.

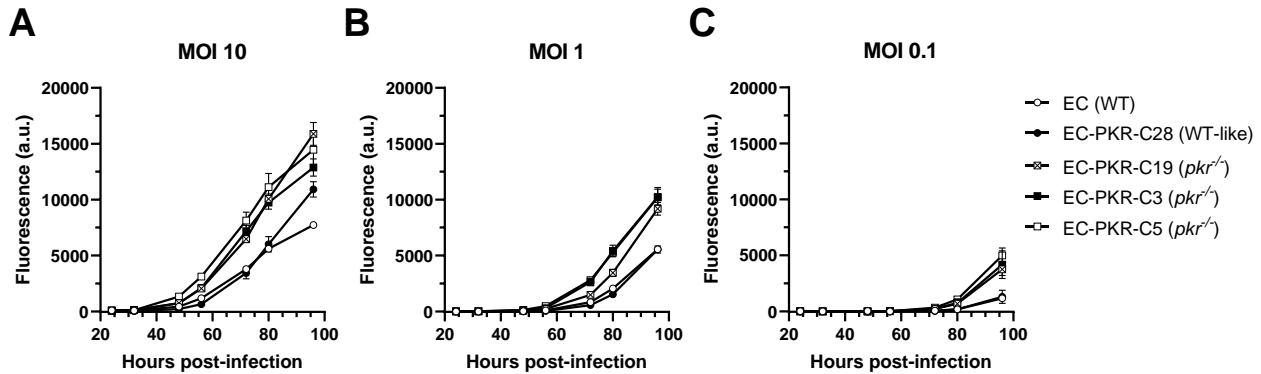


**Figure S4:  $pkr^{-/-}$  clones share a similar phenotype confirming that invalidation of  $pkr$  favors rVHSV-Tomato replication.**

(A;B;C) EC (WT), EC-PKR-C28 (WT-like) and EC-PKR-C19, -C3 and -C5 ( $pkr^{-/-}$ ) cells were infected with rVHSV-Tomato at (A) MOI 10, (B) MOI 1 or (C) MOI 0.1 and fluorescence was measured at different time points post-infection. Graphs show means  $\pm$  SD and is representative of two independent experiments (n=8 for each experiment).

### 3. Supplementary data

#### Testing the dominant negative effect of PKR-SL and PKR-ML

To assess whether PKR-SL and/or PKR-ML exert a dominant negative effect on PKR-FL, a variation of the luciferase assay described in Material and Methods - section 8 was performed. The aim of this experiment was to evaluate whether the inhibitory effect on luciferase expression mediated by PKR-FL was modulated upon co-expression with PKR-SL or PKR-ML. For this purpose, EC-PKR-C19 cells were co-transfected with pcDNA3.1-Hyg-RFP-KDEL (0.2  $\mu\text{g}/10 \mu\text{L}$ ), pcDNA3-Neo-Luc (0.15  $\mu\text{g}/10 \mu\text{L}$ ) and several combinations of different plasmids encoding PKR isoforms or BFP (0.6  $\mu\text{g}/10 \mu\text{L}$  in total), as described in [Figure 27](#). Cells were then processed as described in Material and Methods - [Section 8](#).

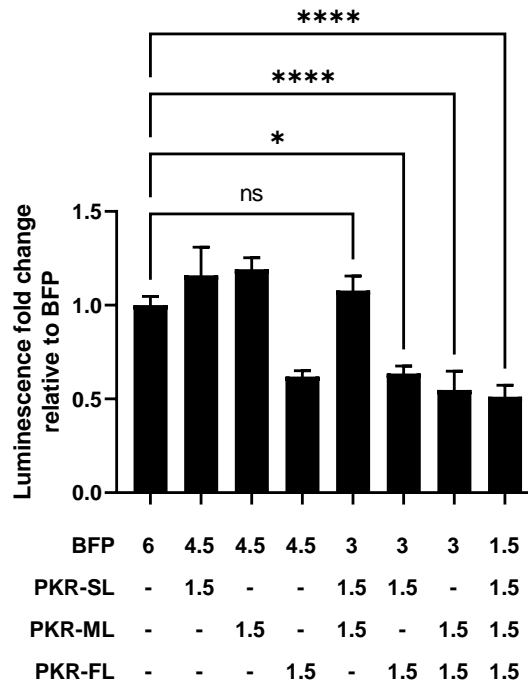


**Figure 27: PKR-ML and PKR-SL do not have a dominant negative effect**

*pkr*<sup>-/-</sup> EC-PKR-C19 cells were co-transfected with pcDNA3-Neo-Luc and plasmids encoding BFP and/or different PKR isoforms (PKR-SL, -ML, -FL) as described in the table. Numbers in the table correspond to the amount of plasmids (in  $\mu\text{g}$ ) per 100  $\mu\text{L}$  of transfection reaction. At 24 hpt, luciferase activity was measured. Luminescence signal intensity graphed as fold change relative to BFP transfected cells. Data shown are means  $\pm$  SD from 2 pooled independent experiments ( $n=8$  for each experiment); ns, non-significant, \*,  $p < 0.05$ , \*\*\*\*,  $p < 0.0001$ , Kruskal-Wallis test with Dunn's post-hoc multiple comparison tests.

As previously observed in the article presented above, transfections with plasmids encoding PKR-FL but not PKR-ML or PKR-SL (lanes 4, 3 and 2, respectively) resulted in a drastic reduction of luminescence signal intensity. However, co-transfections of PKR-FL with PKR-ML and/or PKR-SL (lanes 6-8), did not restore the luminescence level, indicating that PKR-ML and PKR-SL do not have a dominant negative effect on PKR-FL.

## 4. Summary and conclusion

In our study, we showed that endogenous Chinook salmon PKR was highly induced upon type I IFN stimulation but not during VHSV or GSV infections. Mechanistically, endogenous PKR was involved in apoptosis activation and played a major role in translational arrest following poly(I:C) stimulation, indicating that salmonid and mammalian PKR have conserved molecular functions. During VHSV infection, however, endogenous PKR was not the main driver of host protein translation inhibition. Our data further suggest that PKR favors the release of VHSV virions into the supernatant at a late stage of infection. Taken together, our results imply that VHSV has evolved a strategy to subvert PKR antiviral action, by limiting early PKR induction and evading PKR-mediated translational arrest. VHSV also appeared to take advantage of PKR-mediated apoptosis to favor viral spread at a late stage of infection (Figure 28). It adds to the numerous subversion strategies developed by viruses to antagonize or hijack PKR-mediated antiviral mechanisms that have been described in mammals <sup>377</sup>.

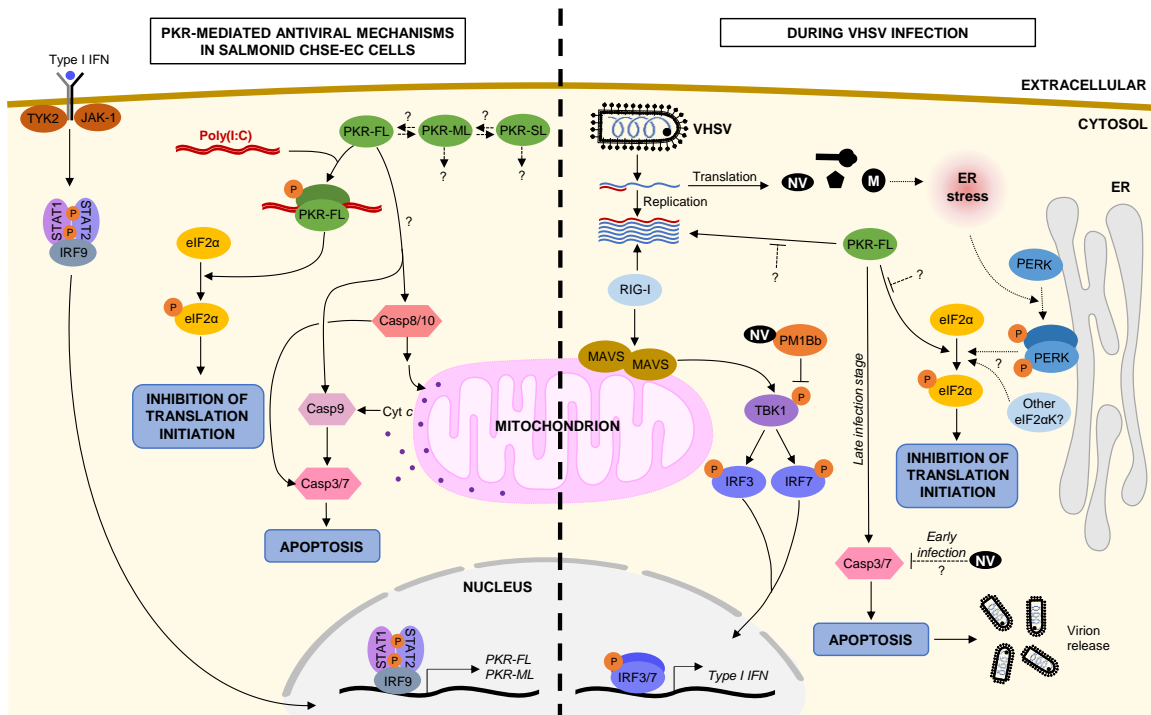


**Figure 28: Model of PKR-mediated molecular functions in Chinook salmon CHSE-EC cells and PKR-dependent mechanisms activated during VHSV.**

**Left:** Chinook salmon CHSE-EC cells express 3 different isoforms of PKR: PKR-FL (full-length), PKR-ML (medium-length) and PKR-SL (short-length), which are likely products of alternative splicing. PKR-ML and PKR-FL are induced following type I IFN stimulation. PKR-FL exhibits similar molecular functions to its mammalian counterparts, including inhibition of translation initiation (likely *via* phosphorylation of eIF2 $\alpha$ ) and activation of apoptosis *via* both the intrinsic and extrinsic pathways. The functions of PKR-ML and PKR-SL are currently not understood but they do not have a dominant negative effect on translational arrest activity of PKR-FL. **Right:** Endogenous PKR-FL as well as 3 Mx paralogs are not induced during VHSV infection. This may be linked to VHSV ability to dampen the RIG-I-mediated type I IFN response *via* NV-dependent recruitment of host PPM1Bb protein phosphatase <sup>171</sup>. VHSV is also able to bypass PKR-mediated translation inhibition *via* unknown mechanisms (either by evading dsRNA binding and/or blocking its enzymatic activity). However, VHSV infection triggers the activation another eIF2 $\alpha$  kinase, presumably PERK <sup>172</sup>, leading to host translational arrest. VHSV is known for inhibiting apoptosis at an early infection stage *via* an NV-dependent mechanism <sup>175</sup> but likely takes advantage of PKR-mediated activation of apoptosis at a late infection stage, to favor virion dissemination.

---

## RESULTS 2

# Characterization of cyprinid Viperin by transcriptomic study in *viperin*<sup>-/-</sup> cell lines

---

### 1. Introduction

The second axis of this thesis was to investigate the functional role of fish Viperin. Viperin is one of the most highly induced *ISGs* during infections with various viruses and/or type I IFN treatment, as shown by many transcriptomic studies in both in both mammalian<sup>424,565</sup> and fish models<sup>15,143,153</sup>. In mammals, Viperin is known for its broad antiviral action against both DNA and RNA viruses<sup>151</sup>. However, the precise molecular functions of Viperin remained elusive for a long time. It was only recently discovered that Viperin was able to generate an antiviral ribonucleotide, which could inhibit specific viral RNA-dependent RNA polymerases<sup>150</sup>. Viperin also exerts its antiviral action by interacting viral components as well as host proteins involved in innate immune signaling and in metabolic pathways exploited during viral life cycle<sup>151</sup>. Overall, *viperin* genes are widely conserved among both invertebrates and vertebrates, including fish species. In a similar fashion to their mammalian counterparts, several overexpression studies showed that fish Viperins inhibit a wide range of viruses, including DNA, dsRNA and ssRNA viruses (**Chapter 3, Table IV**), although the underlying mechanisms of action remain unclear. In both mammalian and fish models, very few studies have investigated the role of Viperin on the regulation of gene expression at the transcriptome level. This question is particularly relevant as a growing body of evidence suggests that Viperin may have a regulatory role in diverse metabolic processes that seems to be unrelated to its antiviral action. Indeed, several studies revealed that Viperin is likely involved in bone and cartilage formation<sup>386,484</sup>, fatty acid  $\beta$ -oxidation<sup>439,467</sup> and mitochondrial metabolism<sup>492</sup>.

In our study, we tried to decipher the contribution of endogenous fish Viperin to the antiviral response at the transcript level and its potential regulatory role beyond the scope of the innate immune response. We addressed the following questions: **(1) Does fish Viperin contribute to the regulation of the type I IFN response? (2) Is fish Viperin involved in the transcriptional regulation of other metabolic/functional pathways?**

For this purpose, we aimed to develop a *viperin*<sup>-/-</sup> fish cell line using CRISPR/Cas9 genome editing. It was initially planned to use the Chinook salmon CHSE-EC cell line; however, preliminary RT-qPCR experiments performed at the beginning of this project failed to induce expression of any of the *viperin* genes (LOC112256495, LOC112255730, LOC112262031, Otsh\_v2.0 NCBI RefSeq assembly GCF\_018296145.1) in this cell line, for an unknown reason. We then switched to another

clonal epithelial-like cyprinid EPC-EC cell line, previously developed in our laboratory and deriving from the fathead minnow (*Pimephales promelas*) epithelioma papulosum cyprini (EPC) cell line, which is widely used in diagnostics. The EPC-EC cell line was used as parental cell line to develop and validate *viperin*<sup>-/-</sup> clones, which were further used for functional studies. To have a global overview of the impact of Viperin on the cellular transcriptome, we conducted a comparative RNA-seq analysis of the *viperin*<sup>-/-</sup> and wild-type cell lines with or without stimulation with recombinant fathead minnow type I IFN.

## 2. Article

Chaumont, L., Jouneau, L., Huetz, F., van Muilekom, D. R., Peruzzi, M., Raffy, C., Le Hir, J., Minke, J., Boudinot, P., & Collet, B. (2024). Unexpected regulatory functions of cyprinid Viperin on inflammation and metabolism. *BMC genomics*, 25(1), 650. <https://doi.org/10.1186/s12864-024-10566-x>

## **Unexpected regulatory functions of cyprinid Viperin on inflammation and metabolism**

Lise Chaumont<sup>1</sup>, Luc Jouneau<sup>1</sup>, François Huetz<sup>2</sup>, Doret R. van Muilekom<sup>1</sup>, Mathilde Peruzzi<sup>1</sup>, Claudine Raffy<sup>3</sup>, Jérôme Le Hir<sup>3</sup>, Jules Minke<sup>3</sup>, Pierre Boudinot<sup>1</sup>, Bertrand Collet<sup>1</sup>

<sup>1</sup> Université Paris-Saclay, INRAE, UVSQ, VIM, 78350 Jouy-en-Josas, France

<sup>2</sup> Unit of Antibodies in Therapy and Pathology, UMR 1222 INSERM, Institut Pasteur, 75015 Paris, France

<sup>3</sup> VIRBAC S.A., 06510 Carros, France

Corresponding author:

[bertrand.collet@inrae.fr](mailto:bertrand.collet@inrae.fr)

## Abstract

**Background:** Viperin, also known as radical S-adenosyl-methionine domain containing protein 2 (RSAD2), is an interferon-inducible protein that is involved in the innate immune response against a wide array of viruses. In mammals, Viperin exerts its antiviral function through enzymatic conversion of cytidine triphosphate (CTP) into its antiviral analog ddhCTP as well as through interactions with host proteins involved in innate immune signaling and in metabolic pathways exploited by viruses during their life cycle. However, how Viperin modulates the antiviral response in fish remains largely unknown.

**Results:** For this purpose, we developed a fathead minnow (*Pimephales promelas*) clonal cell line in which the unique *viperin* gene has been knocked out by CRISPR/Cas9 genome-editing. In order to decipher the contribution of fish Viperin to the antiviral response and its regulatory role beyond the scope of the innate immune response, we performed a comparative RNA-seq analysis of *viperin*<sup>-/-</sup> and wildtype cell lines upon stimulation with recombinant fathead minnow type I interferon.

**Conclusions:** Our results revealed that Viperin does not exert positive feedback on the canonical type I IFN but acts as a negative regulator of the inflammatory response by downregulating specific pro-inflammatory genes and upregulating repressors of the NF- $\kappa$ B pathway. It also appeared to play a role in regulating metabolic processes, including one carbon metabolism, bone formation, extracellular matrix organization and cell adhesion.

**Keywords:** Viperin, RSAD2, fathead minnow, *Pimephales promelas*, RNA-Seq, interferon response, inflammatory response, one carbon metabolism, extracellular matrix, cell adhesion

## Background

The host innate immune system is the first line of defense against viral infections. Innate antiviral defenses are primarily based on type I interferons (IFNs), which are cytokines secreted upon the recognition of viruses. Type I IFNs bind to cell surface class II cytokine receptors and elicit the expression of hundreds of IFN-stimulated genes (*ISGs*) through the JAK-STAT signaling cascade (1). *ISGs* are engaged in diverse functions within the cell, and include virus sensors, receptors, transcription factors, signaling adaptors involved in upstream molecular signaling cascades as well as other cytokines, which enhance the IFN response. Other *ISGs* encode antiviral effectors, which directly target specific viral components or modulate pathways and/or functions required during the virus life cycle. Altogether, *ISG* products participate in mounting an antiviral state refractory to viral infection, replication and propagation (2).

The radical S-adenosyl-methionine (SAM) domain-containing protein 2 (RSAD2), also known as virus inhibitory protein endoplasmic reticulum-associated, interferon-inducible (Viperin), ranks among the most highly induced *ISGs* upon stimulation with IFNs, dsRNA, viral infections; it is also induced upon lipopolysaccharide stimulation and bacterial infections (3–5). The *viperin* transcript was initially identified by differential display analysis in primary human fibroblasts infected with human cytomegalovirus (HCMV) (6), later described in rainbow trout (*Oncorhynchus mykiss*) leukocytes infected with viral hemorrhagic septicemia virus (VHSV) (7) and further characterized from primary human macrophages treated with IFN- $\gamma$  (8). Structurally, VIPERIN is composed of three distinct domains: an N-terminal domain that greatly varies in length among vertebrates (5,9) and contains an amphipathic alpha helix mediating its localization to the cytosolic face of the endoplasmic reticulum and lipid droplets (10,11); a conserved central domain bearing the canonical CX<sub>3</sub>CX<sub>2</sub>C motif, which is characteristic of the radical SAM superfamily and coordinates the binding to a [Fe<sub>4</sub>S<sub>4</sub>] cluster required for its enzymatic activity, and a conserved C-terminal domain of unknown function (7,12). Importantly, *viperin* genes are widely conserved among both vertebrates and invertebrates (4,13). *viperin*-like genes have also recently been identified across all kingdoms of life, including fungi, bacteria, and archaea, hinting at an ancient defense mechanism possibly connected to antiviral defense (12,14,15).

In mammals, Viperin inhibits a broad spectrum of DNA and RNA viruses, (16), although its capacity to limit viral replication may drastically differ from one virus to another (17,18). Viperin exerts its antiviral action through different mechanisms, involving its enzymatic activity and/or protein-protein interactions (16). It was reported early on that Viperin often had to be catalytically active to exert its antiviral action (4,19), but its substrate remained elusive for many years (20). Recent biochemical studies have demonstrated that it converts cytidine triphosphate (CTP) to its analogue 3'-deoxy-3',4'-

didehydro-cytidine triphosphate (ddhCTP) through a SAM-dependent radical mechanism (21). ddhCTP was shown to inhibit the replication of some RNA viruses by acting as a natural chain terminator for RNA-dependent RNA polymerases, although this mechanism has recently been challenged (22). Besides its radical SAM enzymatic activity, Viperin also interacts with a wide range of viral and cellular proteins. It was reported to bind viral proteins and to promote their degradation through the proteasomal pathway (18,23). Furthermore, Viperin interacts with cellular mediators involved in innate immune signaling, including ssRNA-sensing TLR7 pathway, unmethylated CpG DNA-sensing TLR9 pathways (24,25) and cytosolic dsDNA cGAS-STING pathway (26), thereby enhancing the IFN response. It was also reported that Viperin is involved in the oxidation of methionine residues in DNA and RNA helicases, including the cytosolic viral RNA sensor RIG-I, which increases its stability leading to enhanced expression of IFN- $\beta$  in Mouse Embryonic Fibroblasts (MEFs) (27). Furthermore, a growing body of evidence suggests Viperin also modulates metabolic pathways exploited during the viral life cycle, including cholesterol biosynthesis (28,29) and secretion of soluble proteins (10,30). Additionally, a few studies point to a role of Viperin in the regulation of metabolic processes under non-infectious conditions, including bone and cartilage formation (31,32), reduction of fatty acid  $\beta$ -oxidation (33,34) and regulation of the mitochondrial metabolism (35). Nonetheless, how Viperin can have such broad cellular functions is currently still unclear.

In fish, orthologs of mammalian *viperin* have been identified in many species (7,9,36–38). Recently, Wang *et al.* have cloned the *viperin* gene from fathead minnow (*Pimephales promelas*) FHM cells (39). Intriguingly, they have also identified a splicing variant lacking exon 5, that is expressed upon Spring viremia of carp virus (SVCV) infection but not poly(I:C) stimulation. Several studies have reported that fish Viperins, including Viperin from fathead minnow, retain antiviral properties (9,37–39). Furthermore, although studies on fish Viperin have not investigated the underlying molecular mechanisms as thoroughly as in mammals, they still provide evidence that fish Viperin is able to modulate the expression of genes involved in IFN and inflammatory response following overexpression in fish cell lines (9,38–40), stabilize RIG-I by increasing its half-life (40), interact with viral proteins to promote their degradation *via* the proteasomal and/or autophagosome pathways (36) and modulate cholesterol metabolism (41). Importantly, most studies were performed using overexpression approaches and to the best of our knowledge, no knockout *in vitro* models have been developed so far using fish cell lines.

In order to better understand the contribution of fish Viperin to the antiviral response and its regulatory role beyond the scope of the innate immune response, we developed a clonal epithelial-like cyprinid cell line in which the *viperin* gene has been knocked out by CRISPR/Cas9 genome-

editing. This cell line derives from the fathead minnow (*Pimephales promelas*) epithelioma papulosum cyprini (EPC) cell line, which is widely used in diagnostic and research. To achieve a global overview of the transcriptional response between the knockout and the wildtype cell lines, we performed a comparative RNA-seq analysis of the whole transcriptome of the two cell lines with or without a 24h-long stimulation with recombinant fathead minnow type I IFN. Our transcriptomic analysis indicates that Viperin is not involved in the regulation of the canonical type I IFN in this model but acts as a negative regulator of specific inflammatory pathways. In addition, our study sheds light on other metabolic functions in which Viperin may play a role even under non-pathological conditions, including extracellular matrix organization, cell adhesion, bone formation and one carbon metabolism.

## Methods

### Cell lines, culture conditions and viruses

The *Epithelioma papulosum cyprini* (EPC) cell line (ATCC CRL-2872, *Pimephales promelas*), was grown in Leibovitz's L-15 medium (Gibco) supplemented with 10% fetal bovine serum (FBS, Eurobio) and penicillin (100 U/mL)-streptomycin (100 µg/mL) (BioValley). The EPC-EC cell line (described below) and its derivatives were grown in L-15 medium supplemented with 10% FBS, penicillin (100 U/mL)-streptomycin (100 µg/mL), 500 µg/mL G418 (Invivogen), 30 µg/mL hygromycin B Gold (Invivogen). The Chinook salmon (*Oncorhynchus tshawytscha*) embryo (CHSE-214) cell line was maintained in Glasgow's modified Eagle's medium (GMEM) containing 25 mM HEPES (Biosera) supplemented with 10% FBS, 2 mM L-glutamine (Eurobio), and penicillin (100 U/mL)-streptomycin (100 µg/mL). All cell lines were maintained at 20°C without CO<sub>2</sub>.

Recombinant viral hemorrhagic septicemia virus expressing the tdTomato red fluorescent protein (rVHSV-Tomato) was a kind gift from Dr. Stéphane Biacchesi (Université Paris-Saclay, INRAE, UVSQ, VIM, Jouy-en-Josas, France) (42). rVHSV-Tomato was propagated in EPC cells (multiplicity of infection (MOI) of 1); briefly, the virus was adsorbed onto the cells for 1h at 14°C with regular gentle shaking; L-15 supplemented with 2% heat-inactivated FBS was added afterwards and the supernatants were collected at 5 days post-infection, 0.2 µm-filtered, aliquoted and stored at -80°C. Infectious pancreatic necrosis virus (IPNV), isolate 31.75 (43), was propagated in CHSE-214 (MOI 0.001) at 14°C in GMEM supplemented with 2% FBS, as described above for rVHSV-Tomato. The supernatants were collected at 3-4 days post-infection, 0.2 µm-filtered, diluted 1:5 (v/v) in TEN buffer (10 mM Tris, 1 mM EDTA, 150 mM NaCl, pH 7.1) and mixed again 1:1 (v/v) in glycerol 100%, aliquoted and stored at -20°C. rVHSV-Tomato and IPNV31.75 titers were determined by plaque assay.

### Development and validation of a *viperin*<sup>-/-</sup> cell line

The EPC cell line was genetically engineered to overexpress a monomeric, cytosolic form of EGFP (mEGFP) and the nuclear nCas9n using the same method used to develop the CHSE-EC cell line (44). Briefly, the EPC cell line was engineered using the plasmid pcDNA3.1-Hyg-nCas9n (Addgene #217487); single cells were individualized by flow cytometry sorting (BD FACSAria™ II Cell Sorter, INEM, Paris, France) and after propagation, clones expressing high levels of *nCas9n* transcripts were selected by RT-qPCR, as previously described (44). The resulting cell line was engineered a second time using the plasmid pmEGFP-N1 (Addgene #217486); single mEGFP-positive cells were isolated by FACS (BD FACSAria™ III Cell Sorter, INRAE, Jouy-en-Josas, France) to generate a clonal cell line, named EPC-EC.

The EPC-EC cell line was used to develop a *viperin*<sup>-/-</sup> cell line. Two single guide RNAs (sgRNAs) were designed within the first exon of the *viperin* gene (LOC120476724), using CRISPOR v5.01 web tool (Table 1) (45). To ensure the specificity of the sgRNAs, care was taken that no off-target genes with more than 3 mismatches in the first 12 bp adjacent to the PAM (most likely off-targets) were identified in the fathead minnow genome (EPA\_FHM\_2.0, NCBI RefSeq assembly GCF\_016745375.1). A sgRNA targeting the *mEGFP* gene was also used as previously designed (44).

The sgRNAs were synthesized using the T7 RiboMAX™ Express Large Scale RNA Production System kit (Promega) according to the manufacturers' instructions using 0.5 µg of each primer that spontaneously annealed as the dsDNA template. The RNA synthesis mix was then incubated with 1 µL of RQ1 DNase (Promega) for 1h at 37°C and purified using TRIzol™ reagent (Invitrogen), according the manufacturers' instructions. The sgRNAs were resuspended in RNase- and DNase-free water and quantified using a Nanodrop spectrophotometer. The purity of the sgRNAs was checked on a 2% agarose-EtBr gel before or after a 30 min treatment with RNase A (Qiagen) at room temperature. The ability of each sgRNA to cut the target sequence was confirmed by *in vitro* efficiency assay. Briefly, genomic DNA was extracted from  $\sim 3 \times 10^6$  EPC-EC cells using NucleoSpin Tissue Mini kit (Macherey-Nagel), according to the manufacturer's instructions. Genomic DNA segments containing the targeted sites were amplified by PCR using GoTaq® G2 Flexi DNA Polymerase (Promega) with the primers mEGFP-gen-F/mEGFP-gen-R and PpViperin-gen-F/PpViperin-gen-R (Table 1). The PCR cycling program was performed in a thermal cycler (Eppendorf) and was as follows: 94°C for 3 min then 35 cycles of 94°C for 15 s, 59°C for 15 sec, 72°C for 40 sec, and a final extension of 72°C for 5 min. The PCR products were purified using NucleoSpin Gel and PCR Clean-up Mini kit (Macherey-Nagel). Each sgRNA was mixed with recombinant TrueCut™ Cas9 Protein v2 (Invitrogen) at a 1:1 molar ratio (0.2 µg sgRNA and 1 µg rCas9 *i.e.* 6.1 pmol each in 12 µL of resuspension buffer R (Neon™ Transfection System kit,

Invitrogen)) and incubated at room temperature for 15 min. Each sgRNA/Cas9 complex was mixed with the purified PCR product at a 5:1 molar ratio (*i.e.* 6.1 pmol sgRNA/Cas9 and 1.22 pmol PCR product) and incubated at room temperature overnight. The Cas9 enzyme was heat-inactivated at 80°C for 20 min and double-strand break of the PCR products was confirmed on a 1.5% agarose-EtBr gel.

To generate *viperin*<sup>-/-</sup> cells, each sgRNA (sgRNA-mEGFP, sgRNA-Vip1, sgRNA-Vip2) was mixed with recombinant TrueCut™ Cas9 Protein v2 at a 1:1 molar ratio (0.2 µg sgRNA and 1 µg rCas9 *i.e.* 6.1 pmol each in 2 µL) and incubated at room temperature for 20 min. The sgRNA-mEGFP/Cas9 complex was mixed with pooled sgRNA-Vip1/Cas9+ sgRNA-Vip2/Cas9 complexes at a 2:1 volume ratio in resuspension buffer R (Neon™ Transfection System kit, Invitrogen) (*i.e.* 1µL of sgRNA-mEGFP/Cas9 and 0.5 µL of each sgRNA-Vip/Cas9 complex in a final volume of 5 µL). The mix was transfected into EPC-EC cells using the Neon™ Transfection System (Invitrogen). EPC-EC cells were prepared as described in the “transfections” section and 5 µL of cell suspension at  $2 \times 10^7$  cells/mL was mixed with 5 µL of sgRNA/Cas9 complex (*i.e.*  $1 \times 10^5$  cells, 6.1 pmol of Cas9 and 6.1 pmol of sgRNA per 10 µL of transfection reaction). The cells were transfected using the same conditions established for plasmids, as described in the “transfections” section. All transfected cells ( $\sim 5 \times 10^5$  cells) were mixed in 5 mL L-15 supplemented with 10% FBS and penicillin (100U/mL)-streptomycin (100 µg/mL) in a 25 cm<sup>2</sup> flask (Sarstedt) and incubated at 20°C. The next day, cells were washed with PBS, fresh medium (L-15 medium supplemented with 10% FBS, penicillin (100 U/mL)-streptomycin (100 µg/mL), 500 µg/mL G418, 30 µg/mL hygromycin B Gold) was added into each flask and cells were incubated at 20°C for 4 weeks.

Once the cell population reached confluency, the transfected cells were passaged (surface ratio 1:4), and  $\sim 3 \times 10^6$  cells were used for genomic DNA extraction using NucleoSpin Tissue Mini kit (Macherey-Nagel), according to the manufacturer’s instructions. Genomic DNA regions containing the sgRNA-targeted sequences were amplified by PCR using genotyping primers mEGFP-gen-F/mEGFP-gen-R and PpViperin-gen-F/PpViperin-gen-R, as described above. The PCR products were purified using NucleoSpin Gel and PCR Clean-up Mini kit (Macherey-Nagel) and directly sequenced using the same amplification primers. Sequences were analyzed using Synthego ICE analysis tool v3 (Synthego) (46) to assess the percentage of mutated cells in the transfected cell population (bulk). ICE analysis confirmed efficient genome editing for *mEGFP* and *viperin* in the bulk transfected with sgRNA-mEGFP and sgRNA-Vip1+2. This bulk was further used for isolation of *viperin*<sup>-/-</sup> clones by FACS. For this purpose, cells were detached by trypsin-EDTA action and mEGFP-deficient single cells at a density of  $\sim 4 \times 10^6$  cells/mL were individualized by FACS (BD FACS Aria™ Fusion Flow Cytometer, Institut Pasteur, Paris, France) using a 100 µm nozzle at the

lowest pressure (1 out of a scale of 11) into a 96-well plate (Sarstedt) in L-15 supplemented with 10% FBS, penicillin (200 U/mL)-streptomycin (200 µg/mL), 500 µg/mL G418 and 30 µg/mL hygromycin B Gold. Three months later, 16 clones were sub-cultured and propagated in 25 cm<sup>2</sup> flasks and their genotype was characterized as described above. Two clones, EPC-EC-Vip-C7 and EPC-EC-Vip-C11, were kept for further knockout validation. Because both clones presented heterozygous mutations at the cutsites targeted by the two sgRNA used, the previously obtained genotyping PCR products were cloned into the pCR4-TOPO TA vector using TOPO™ TA Cloning™ kit (Invitrogen), according to the manufacturer's instructions, and sent to sequencing. The sequencing results showed that both clones presented heterozygous mutations at both sgRNA targeted sites: a 1-nt deletion (152delC) or 2-nt deletion (152\_153delAC) at sgRNA-Vip2 target site and a partial 1-nt insertion (230\_231insT) at sgRNA-Vip1 target site, resulting in frameshifts and the appearance of a premature stop codons (D51fsX53 or G52fsX96).

The disruption of *viperin* was also validated by western blot. For this purpose, EPC-EC-Vip-C7 and EPC-EC-Vip-C11 clones and the WT EPC-EC cell line were seeded into 25 cm<sup>2</sup> flasks at a density of  $6.5 \times 10^6$  cells/well in L-15 supplemented with 2% FBS and penicillin (100 U/mL)-streptomycin (100 µg/mL) and incubated at 20°C overnight. The next day, the cells were stimulated with poly(I:C) (Sigma-Aldrich) diluted in L-15 supplemented with 10% FBS and penicillin (100 U/mL)-streptomycin (100 µg/mL) at a final concentration of 500 µg/mL or left untreated and incubated at 20°C. At 24, 48 and 72h post-stimulation, medium was removed, cells were washed once with ice-cold DPBS, scraped in 1 mL ice-cold DPBS supplemented with 2.5 mM EDTA and centrifuged at 1500 g at 4°C for 5 min. The cell pellets were drained, resuspended in 100 µL NP-40 lysis buffer (50 mM Tris-HCl pH 7.4, 150 mM NaCl, 2 mM EDTA, 0.5% NP40, 1 mM DTT, 10% glycerol, cOmplete™ protease inhibitor (Merck)) and lysed for 45 min at 4°C under gentle shaking. The cell lysates were clarified by centrifugation at 5000 g at 4°C for 5 min and stored at -80°C until use.

Aliquots of 60 µL of cell lysates were mixed with 30 µL Laemmli buffer 3X (45 mM Tris, 345 mM glycine, 38% glycerol, 4.8% SDS, 20% β-mercaptoethanol, 0.04% bromophenol blue) and incubated at 100°C for 5 min. A volume of 8 µL of cell lysates was loaded onto 12% polyacrylamide gels and protein samples were separated by electrophoresis in Tris-glycine buffer (25 mM Tris, 192 mM glycine, pH 8,3). Proteins were then transferred onto a nitrocellulose membrane (BioRad) using the mixed molecular weight program from the Trans-Blot® Turbo™ Transfer System (BioRad). The blots were blocked with 5% non-fat milk in TBST (10 mM Tris pH 7.4, 150 mM NaCl, 0,1% Tween 20) for 1h at room temperature and then incubated with rabbit polyclonal anti-Viperin antibody (PA5-42231, Invitrogen) (1:500, TBST+5% non-fat milk) overnight at 4°C. Care was taken to use an antibody raised against an immunogenic polypeptide (Tyr301-Tyr350, human RSAD2) that shares

92% identity with the corresponding sequence on fathead minnow Viperin (XP\_039523815.1). The blots were washed 5 times in TBST, incubated with horseradish peroxidase (HRP)-conjugated anti-mouse or anti-rabbit (1:4000) secondary antibodies (SeraCare), washed 4 times in TBST and once in PBS. Western blots were developed using Clarity™ Western ECL substrate (BioRad) and detected using ChemiDoc Touch Imaging System (BioRad). After the first detection, the membrane was washed twice with TBST, saturated with TBST-5% non-fat milk for 1h and re-probed with mouse monoclonal anti- $\alpha$ -tubulin antibody (T9026, Sigma Aldrich) (1:3000, TBST+5% non-fat milk) for 2.5h-3h and developed as described above. Densitometric analysis of the blots was performed using Image Lab software (v 6.1.0, BioRad).

### Plasmid constructions

Fathead minnow *viperin* open reading frame (ORF) sequence was identified *in silico* using NCBI Reference EPA\_FHM\_2.0 Primary Assembly and predicted transcript XM\_039667881.1.

Total RNA from  $4 \times 10^6$  EPC-EC cells infected with IPNV31.75 (MOI 0.001) at 72 h post-infection in quadruplicates was extracted using the QiaShredder and RNeasy mini kits (Qiagen) according to the manufacturer's instructions. RNA (4  $\mu$ g) was used as template for reverse transcription and generation of cDNA using the iScript™ Advanced cDNA Synthesis Kit for RT-qPCR (BioRad) and the synthesis was performed in a thermal cycler (Eppendorf) as recommended by the manufacturer. cDNA was diluted to 1:20 in DNase- and RNase-free water. Diluted cDNA from rVHSV-Tomato infected cells (n=4) were pooled and used as template to amplify the *viperin* ORF sequence. Nested PCR amplifications were performed using Q5 2X High-Fidelity mastermix (New England Biolabs) and 2 sets of specific primers according to the manufacturer's instructions: PpViperin-R0-F/PpViperin-R0-R were used for the first PCR round while PpViperin-P2A-F and PpViperin-HindIII-R were used for the second PCR round (Table 1). The PCR cycling programs were performed in a thermal cycler (Eppendorf) and were as follows: 98°C for 30 sec followed by 35 cycles of 98°C for 10 s, 65°C for 10 sec, 72°C for 90 sec (1<sup>st</sup> round) or 60 sec (2<sup>nd</sup> round), and a final extension of 72°C for 2 min. PCR products were purified with the NucleoSpin Gel and PCR Clean-up Mini kit (Macherey-Nagel), quantified using a Nanodrop spectrophotometer, digested with HindIII enzymes (ThermoFisher), cloned into HindIII/EcoRV-digested pcDNA3.1-Hyg-BFP vector (Addgene #214363) using T4 DNA ligase (New England Biolabs) according to the manufacturer's instructions and fully sequenced. The pcDNA3.1-Hyg-BFP vector was initially obtained by amplifying the BFP gene from pCite-P-BFP (47) using BFP-F/BFP-R primers (Table 1) and subcloning it into the plasmid backbone of pcDNA3.1-Hyg-mEGFP (Addgene #191847) by XhoI/HindIII digestion. The pCite-PBFP plasmid was a kind gift from Dr. Hortense Decool (Université Paris-Saclay, INRAE, UVSQ, VIM, France). The resulting plasmid was named pcDNA3.1-Hyg-BFP-P2A-PpViperin (Addgene

#217481). All plasmids were produced in Stellar™ Competent Cells (Takara) and were purified using NucleoBond Xtra Maxi EF (Macherey-Nagel) according to the manufacturer's instructions.

### Transfections

Transfections were performed by electroporation using the Neon™ Transfection System (Invitrogen) as described previously (44). Briefly, EPC cells were washed in DPBS (Sigma-Aldrich), detached by trypsin-EDTA action, resuspended in L-15 supplemented with 10% FBS and penicillin (100 U/mL)-streptomycin (100 µg/mL) and centrifuged at 400 g for 5 min. The cell pellet was drained, resuspended in L-15 without Phenol Red (Gibco), centrifuged at 13 000g for 30 sec, and resuspended again in L-15 without Phenol Red. The cell concentration was adjusted to  $2 \times 10^7$  cells/mL. The cell suspension was mixed either with pcDNA3.1-Hyg-BFP or pcDNA3.1-Hyg-BFP-P2A-PpViperin at a final concentration of 5 µg per  $1 \times 10^6$  cells per 100 µL of transfection reaction. The fluorescent vector pcDNA3.1-Hyg-RFP-KDEL (Addgene #138660; 2 µg/ $1 \times 10^6$  cells/100 µL of transfection reaction) was added to check transfection efficiency between each condition. Transfections were carried out in an electroporator MPK5000 (Neon™ Transfection System, Invitrogen) using a 100 µL transfection kit (Neon™ Transfection System, Invitrogen) set to two pulses for 20 ms at 1400 V, as previously established for EPC cells (48). All transfected cells ( $\sim 3 \times 10^6$  cells) were mixed in L-15 supplemented with 10% FBS and penicillin (100 U/mL)-streptomycin (100 µg/mL), incubated at 20°C. At 24h post-transfection, medium was removed, cells were washed once with ice-cold DPBS and directly lysed in Laemmli buffer (45 mM Tris, 345 mM glycine, 38% glycerol, 4.8% SDS, 20% β-mercaptoethanol, 0.04% bromophenol blue) for 45 min at 4°C. Cell lysates were collected, incubated at 100°C for 5 min and stored at -80°C until use for western blot analysis.

### Real-time quantitative PCR

EPC-EC cells were seeded in 6-well plates to a final density of  $2.5 \times 10^6$  cells/well in L-15 supplemented with 2% heat-inactivated FBS and penicillin (100 U/mL)-streptomycin (100 µg/mL) and incubated overnight at 20°C. The next day, cells were either infected with rVHSV-Tomato (MOI 0.05) or IPNV31.75 (MOI 0.001) at 14°C for 24, 48 or 72hpi (n=4 for each time point), stimulated with recombinant *Pimephales promelas* type I IFN supernatant diluted to 1:10 in L-15 supplemented with 2% FBS and penicillin (100 U/mL)-streptomycin (100 µg/mL) for 24h or left untreated (n=3 for each condition). Recombinant *Pimephales promelas* type I IFN $\phi$ 1 supernatant was a kind gift from Dr. Stéphane Biacchesi (Université Paris-Saclay, INRAE, UVSQ, VIM, Jouy-en-Josas, France) and was produced as previously described (49).

Total RNA was extracted from cells in individual P6 wells in triplicates or quadruplicates using QiaShredder and RNeasy mini kits (Qiagen) in accordance with the manufacturer's instructions.

Quality control of the samples was determined using a Nanodrop spectrophotometer. The cDNA was generated from 4 µg (VHSV experiment) or 3 µg (IFN experiment) of total RNA using the iScript™ Advanced cDNA Synthesis Kit for RT-qPCR (BioRad) and the synthesis was performed in a thermal cycler (Eppendorf) as recommended by the manufacturer. cDNA was diluted in DNase- and RNase-free water to reach a final concentration of 10 ng/µL and stored at -20°C until use. “No RT” control reactions were made by omitting the reverse transcriptase.

The cDNA was mixed with iTaq™ Universal SYBR® Green SupermixTB (Biorad) along with forward and reverse primers (Table 2) at a final concentration of 300 nM each in Twin.tec® real-time PCR plates (Eppendorf). Amplification was performed using a Realplex<sup>2</sup> Mastercycler (Eppendorf) using the following cycling program: initial denaturation at 95°C for 3 min followed by 40 cycles of 10 sec at 95°C and 30 sec at 60°C. For each biological replicate, mean Cq values of target genes were calculated based on technical duplicate reactions and then normalized using Cq values of a housekeeping gene (*Ppactin*). The relative expression of each target gene (*Ppviperin* and *Ppmsx1*) was expressed as  $2^{-\Delta C_t}$ , which was then used to calculate their respective fold change in comparison to non-stimulated cells. For each set of primers, the efficiency was calculated by linear regression obtained by using five-fold serial dilutions of a pool of cDNA and the qPCR products were validated by sequencing.

## RNA-Seq analysis

### *Cell stimulation and RNA extraction*

WT EPC-EC cells and *viperin*<sup>-/-</sup> EPC-EC-Vip-C7 cells were seeded, stimulated with recombinant *Pimephales promelas* type I IFN $\phi$ 1 supernatant or left untreated, and total RNA was extracted and quantified, as described in the “RT-qPCR” section. To remove any contaminating DNA, 3 µg of total RNA from each sample were DNase-treated, using Turbo DNA-free™ kit (Invitrogen), according to the manufacturer’s instructions.

### *Illumina sequencing and mapping of reads*

Sequencing of RNA samples was performed at I2BC sequencing platform (Gif-sur-Yvette, France), using a NextSeq 500/550 High Output v2 kit (Illumina). Raw data were processed using bcl2fastq2-2.18.12 (demultiplex), Cutadapt 3.2 (adapter trimming), FastQC v0.11.5 (quality control), resulting in 58-90M reads (72M reads in average per sample post-adapter trimming). In total, 87.5% of the sequences could be aligned with STAR (v2.7.10b; options: --sjdbGTFtagExonParentTranscript Parent) on the *Pimephales promelas* genome/transcriptome (GCA\_016745375.1 with NCBI annotation release 100 for the genes definition). 76.4% of these alignments were assigned to genes

using featureCounts (subreads v1.5.2; options: -p -C -t gene). All raw sequences have been deposited in the Sequence Read Archive repository under accession number PRJNA1076136.

#### *Identification of human and zebrafish orthologs*

All putative proteins corresponding to retrieved fathead minnow genes were subjected to tBlastn analysis against the NCBI peptide sequences of zebrafish (Ensembl version 104, genome reference GRCz11) and human (Ensembl version 104, genome reference GRCh38p13) to generate for each fathead minnow gene a corresponding zebrafish best Blast hit and human genome nomenclature committee identifiers (HGNC IDs) (*aka.* official gene symbols). For genes with several isoforms, the one encoding for the longest protein was chosen and used as bait for Blast analysis.

#### *Identification of differentially expressed genes*

Pre-processing checks and identification of any potential outliers was performed through graphical analysis, including hierarchical clustering and PCA plots. Differentially expressed genes between IFN-treated WT EPC-EC cells or *viperin*<sup>-/-</sup> EPC-EC-Vip-C7 cells and their respective non-treated controls (*i.e.* IFN vs Ctrl for each cell line) and between *viperin*<sup>-/-</sup> EPC-EC-Vip-C7 compared to WT EPC-EC cells at the steady state or following IFN treatment (*i.e.* KO vs WT for each treatment condition), were identified. Differentially expressed genes were identified using DESeq2 R package (50). *p*-values were adjusted for multiple testing using Benjamini-Hochberg procedure. Genes were considered differentially expressed if they met the following criteria: adjusted *p* value < 0.05; log2fold change >1 (upregulated genes) or <-1 (downregulated genes).

#### *Gene set enrichment analysis*

For functional gene set enrichment, Gene Ontology (GO) analysis and Kyoto Encyclopedia of Genes and Genomes (KEGG) pathway analysis were performed on DEGs using the web interface DAVID (51). The predicted GO terms and KEGG pathways were based on the lists of official gene symbols corresponding to fathead minnow DEGs without using expression or fold change values. In order to identify effects on the pathways, up- and downregulated DEGs were inputted into DAVID separately. The same lists of official gene symbols were also analyzed with Ingenuity Pathway Analysis (IPA, Qiagen).

#### **rVHSV-Tomato fluorescence monitoring**

The replication of rVHSV-Tomato in infected cell lines was monitored by sequential fluorescence measurement. WT EPC-EC, *viperin*<sup>-/-</sup> EPC-EC-Vip-C7 and EPC-EC-Vip-C11 cells were seeded in 96-well plates to a final density of  $1 \times 10^5$  cells/well in L-15 medium supplemented with 2% heat-inactivated FBS and penicillin (100 U/mL)-streptomycin (100 µg/mL) and incubated overnight at

20°C. The next day, the medium was removed and the cells were infected in octuplicates with 100 µL of rVHSV-Tomato diluted in L-15 without Phenol Red (Gibco) supplemented with 2% heat-inactivated FBS and penicillin (100 U/mL)-streptomycin (100 µg/mL) to reach MOI 0.1, 1 or 10 or left uninfected. At 24, 32, 48, 56, 72, 80 and 96h post-infection, the tomato red fluorescence was measured using a fluorometer (Tecan Infinite M200PRO) with excitation and emission wavelengths of 548 and 593 nm, respectively. The fluorescence values were corrected by subtracting the mean values obtained from the non-infected wells.

### Statistical analysis

Apart from RNA-seq analysis, results shown in each figure were derived from at least two independent experiments; the data presented are means ± standard deviation (SD). Statistical tests used are indicated in the legend of each figure. All statistical analyses were performed using GraphPad Prism software version 9.5.1. For RNA-seq data, the statistical tests used in this study are included in the “RNA-seq analysis” section.

## Results

### Comparative analysis indicates that the genome of fathead minnow likely contains a unique *viperin* gene

Although a single *viperin* gene has been found in mammals and birds, reported numbers of *viperin* paralogs can vary from one to three in bony fish. For instance, tBlastn analysis revealed the presence of a unique *viperin* gene in fugu (*Takifugu rubripes*, LOC101074024), Japanese medaka (*Oryzias latipes*, LOC101175536), and zebrafish (*Danio rerio*, LOC570456). In contrast, in salmonid species - whose common ancestor has undergone a whole genome duplication event (52), two *viperin* paralogs are located on distinct loci in species belonging to the genus *Salmo*, including Atlantic salmon (*S. salar*, LOC100195910, LOC106566099) and brown trout (*S. trutta*, LOC115162541, LOC115172835) and three paralogs in species belonging the genus *Oncorhynchus*, including rainbow trout (*O. mykiss*, LOC100135876, LOC110504183, LOC110498119) (**Figure 1A**), chinook salmon (*O. tshawytscha*, LOC112256495, LOC112255730, LOC112262031), sockeye salmon (*O. nerka*, LOC115138320, LOC115138321, LOC115146395) and coho salmon (*O. kisutch*, LOC109903880, LOC109903881, LOC109894649). Two of the three paralogs are tandemly arranged in head-to-tail orientation on the same chromosome, suggesting that they resulted from an independent tandem duplication event specific to the genus *Oncorhynchus*.

A unique *viperin* sequence (LOC120476724) is present in the current genome assembly EPA\_FHM\_2.0 (NCBI RefSeq assembly GCF\_016745375.1) of the fathead minnow (*Pimephales*

*promelas*), located on the unplaced scaffold NW\_024121099.1. A 874-bp EST sequence (GH713605.1) covering 76% of the CDS from the predicted transcript (XM\_039667881.1) with 100% identity supports the assembly and shows that the gene is expressed. The existence of a single *viperin* gene in fathead minnow is further supported by the presence of a unique ortholog in closely related cyprinid species, including zebrafish (*Danio rerio*; LOC570456), amur ide (*Leuciscus waleckii*; FLSR01004878:5743602-5746539), and grass carp (*Ctenopharyngodon idella*; LOC127498383); importantly these genes are located in a well-conserved synteny group (Figure 1A). The sequence of the predicted protein XP\_039523815.1 contains 345 amino acids and shares 70.9%, 70.8% and 68.6% identity with human VIPERIN (*Homo sapiens*, NP\_542388.2), chicken Viperin (*Gallus gallus*, NP\_001305372.2) and frog Viperin (*Xenopus tropicalis*, XP\_002935073.2), respectively. These results confirm that this protein is highly conserved in teleosts as well as among vertebrates (7,12).

To determine whether the *viperin* gene was present in the EPC-EC genome and expressed by these cells, nested PCR primers specific to the 5' and 3' untranslated regions (UTR) and to the 5' and 3' ends of the CDS (Figure 1B) were used with cDNA from IPNV-infected EPC-EC cells and resulted in the amplification of a fragment of 1038 bp. This product matched the coding sequence of the *viperin* transcript (XM\_039667881.1) predicted from the NCBI model with 100% identity (Figure 1B). Structural domain analysis of the Viperin 345-aa polypeptide using SMART (Simple Modular Architecture Research Tool) (53) revealed the presence of a N-terminal transmembrane helix region (Phe13-Ile35) and a central radical SAM domain (Tyr61-Leu247), which comprises the canonical motif CX<sub>3</sub>CX<sub>2</sub>C (67-74) characteristic of the radical SAM superfamily (Figure 1B). More specifically, the conserved motif NΦHX<sub>4</sub>CX<sub>3</sub>CX<sub>2</sub>CF (Φ being W, Y or F), recently described for all ddhNTP synthases (15) is also present in the sequence of fathead minnow Viperin (residues 60-75). Of note, the C-terminal tryptophane residue (W345), which is required for Viperin antiviral activity by playing a role in substrate recognition and/or interaction with partner proteins or cofactors such as cytosolic Fe/S protein assembly factor CIAO1 (4,54), is also conserved in fathead minnow Viperin. This organization of functional domains is shared with the Viperin of other vertebrates (7,12).

### ***viperin* is induced following type I IFN stimulation and during viral infections in EPC-EC cells**

The expression profile of *viperin* transcripts in EPC-EC cells in response to recombinant type I IFN and to viral infection was determined by RT-qPCR. For this purpose, two different viruses were used: viral hemorrhagic septicemia virus (VHSV), an enveloped negative-sense single-stranded RNA virus belonging to the genus *novirhabdovirus*, and infectious pancreatic necrosis virus (IPNV), a naked, double-stranded RNA virus belonging to the genus *aquabirnavirus*. To track the progression of the viral infection, we used a recombinant VHSV encoding the fluorescent protein tdTomato (rVHSV-

Tomato) (42). In addition to *viperin*, the expression pattern of *mx1*, another conserved type I IFN stimulated gene, was also examined for comparative purposes.

A strong induction of both *viperin* and *mx1* mRNA expression was observed at 24h post-stimulation with recombinant fathead minnow type I IFN $\phi$ 1 (3.2- and 2.5-logfold increase, respectively) compared to non-stimulated cells (**Figure 2**). Similarly, both genes were significantly induced at 72h post-infection with rVHSV-Tomato (2.6- and 1.5-logfold increase, respectively) (**Figure 2**). In contrast, while *viperin* was also highly induced at 72h post-infection with IPNV31.75 (3.1-logfold increase), *mx1* only displayed a weak but still significant induction at the same timepoint with this virus (0.5-logfold increase) (**Figure 2**). Comparable results were previously obtained in the rainbow trout RTG-P1 cell line, where it was reported that IPNV suppressed the early activation of *mx* expression (55).

Altogether, our results show that *viperin* transcripts are strongly induced by both type I IFN and viral infections in EPC-EC cells. Furthermore, these observations support the use of EPC-EC as a parental cell line for the development of a *viperin*<sup>-/-</sup> cell line to investigate the effects of its gene on responses to viral infection.

### **CRISPR/Cas9-based edition of the *viperin* gene leads to null mutation and abolishes Viperin expression in EPC-EC cells**

To better understand the functions of fathead minnow Viperin, we disrupted the *viperin* gene in the EPC-EC cell line, using CRISPR/Cas9 technology. Two clonal cell lines deriving from FACS-sorted single cells, named EPC-EC-Vip-C7 and EPC-EC-Vip-C11, were further characterized. Both clones presented heterozygous mutations at the cutsites targeted by the two sgRNA used: a 1-nt deletion and 2-nt deletion at sgRNA-Vip2 target site and a partial 1-nt insertion at sgRNA-Vip1 target site, most likely affecting one haplotype only (**Additional file 1**). In order to fully genotype these clones, the PCR products comprising the sgRNA target sites were cloned into TOPO TA vectors and individual clones were sequenced. Surprisingly, the results revealed the presence of 3 distinct haplotypes from each clone (**Figure 3A,B**), hereafter referred to as sequence A, sequence B and sequence C. Sequence A displayed a 1-nt deletion (152delC) at sgRNA-Vip2 cut site and no indel at sgRNA-Vip1 cut site (noted as -1/0); sequence B featured the same 1-nt deletion at sgRNA-Vip2 and a 1-nt insertion (230\_231insT) at sgRNA-Vip1 cut site (noted as -1/+1) and sequence C had a 2-nt deletion (152\_153delAC) at sgRNA-Vip2 cut site and a 1-nt insertion (230\_231insT) at sgRNA-Vip1 cut site (noted as -2/+1). All indels resulted in frameshifts and in the appearance of premature stop codons at position 53 (D51fsX53 for sequences A and B) or at position 96 (G52fsX96 for sequence C) (**Figure 3B**). Importantly, in sequence B, the frameshift at sgRNA-Vip2 generated a premature stop

codon upstream the sgRNA-Vip1 ensuring an overall null mutation ([Additional file 2](#)). The existence of three and not just two different sequences can be explained in three ways: (1) each “clone” does not derive from a single cell; (2) there are at least two *viperin* paralog genes in the genome of fathead minnow; (3) the EPC-EC cell line and/or EPC-EC-Vip clones have undergone a local duplication event or (partial) chromosome gain during their respective development processes, resulting in more than two copies of the *viperin* gene.

As we could not exclude that these observations were due the presence of two highly similar *viperin* genes in the genome of EPC-EC cells, it was important to assess the expression of Viperin at the protein level. Preliminary western blot experiments showed that the expression of Viperin was induced in EPC-EC cells upon stimulation with poly(I:C), a synthetic dsRNA (data not shown). Therefore, we investigated the abolition of the Viperin expression in both EPC-EC-Vip-C7 and -C11 clones by western blot using poly(I:C) as an inducer. Our results showed that Viperin was induced in WT EPC-EC cells following exposure with poly(I:C) and its expression peaked as early as 24h post-stimulation. In contrast, no Viperin signal was detected at any of the time points examined (24-72hpi) in *viperin*<sup>-/-</sup> EPC-EC-Vip-C7 and -C11 clones ([Figure 3C,D, Additional file 3](#)). Similar results were obtained using type I IFN supernatant as an inducer of Viperin expression ([Additional file 4](#)). These results confirmed that the expression of Viperin was effectively disrupted in both clones.

### ***viperin* knockout has a significant impact on the cellular transcriptome regardless of its induction status**

To explore the functions of Viperin, we used a whole transcriptome sequencing approach to compare gene expression in WT EPC-EC cells and *viperin*<sup>-/-</sup> EPC-EC-Vip-C7 cells, at the steady state and following a 24h treatment with type I IFN. To visualize the transcriptome response of WT EPC-EC and *viperin*<sup>-/-</sup> EPC-EC-Vip-C7 to type I IFN, a principal component analysis (PCA) and hierarchical clustering were performed on gene expression datasets and revealed the clustering of individual samples into groups reflecting Viperin status (presence/absence) and stimulation status (non-stimulated/IFN-treated) ([Figure 4A, Additional file 5](#)). In particular, the *viperin* knockout explains 38.6% of the variance (horizontal axis, dimension 1) while IFN treatment explains 22.2% of the variance (vertical axis, dimension 2). A total of 19,871 expressed genes were subjected to differential expression analysis, of which 18,955 were protein-coding genes ([Additional file 6](#)). The accuracy of the RNA sequencing and the resulting differential expression analysis were verified by assessing the expression of a few ISGs by RT-qPCR. The results showed the same expression pattern for all the genes examined, thereby validating the RNA-Seq data ([Additional file 7](#)).

In the following paragraphs, four different sets of DEGs were analyzed, depending on the type of comparison intended: [set 1] genes differentially expressed upon type I IFN treatment compared to non-stimulated condition (control) in the WT cell line; [set 2] genes differentially expressed upon type I IFN treatment compared to control condition in the *viperin*<sup>-/-</sup> cell line; [set 3] genes differentially expressed in the *viperin*<sup>-/-</sup> cell line compared to the WT cell line at the steady state (control condition); [set 4] genes differentially expressed in the *viperin*<sup>-/-</sup> cell line compared to the WT cell line upon type I IFN treatment. In other words, sets 1 and 2 focus on the transcriptomic response to type I IFN in each cell line, respectively, while sets 3 and 4 highlight the impact of Viperin (presence/absence) on the cellular transcriptome at the steady state (*i.e.* without Viperin expression being induced) and following type I IFN stimulation (*i.e.* under Viperin induction condition).

Concerning sets 1 and 2, a large number of protein-coding genes were upregulated upon type I IFN treatment compared to the control condition in both cell lines (487 DEGs in the WT cell line and 661 DEGs in the *viperin*<sup>-/-</sup> cell line) whilst fewer genes were downregulated (124 DEGs in the WT cell line and 189 DEGs in the *viperin*<sup>-/-</sup> cell line) (**Figure 4B,D; Additional file 8**). Of note, a large majority of genes upregulated upon IFN treatment (> 60%) are shared in both cell lines. In contrast, when comparing DEGs in the *viperin*<sup>-/-</sup> cell line compared to the WT cell line (sets 3 and 4), more protein-coding genes were significantly differentially expressed both at the steady state and upon type I IFN treatment: 722 and 875 genes were more expressed in the *viperin*<sup>-/-</sup> cell line compared to the WT cell line at the steady state and upon type I IFN treatment, respectively, while 943 and 1087 were less expressed in these same conditions, respectively (**Figure 4C,E; Additional file 8**). Strikingly, more than 60% of the genes which are less expressed in *viperin*<sup>-/-</sup> cells compared to WT are shared at the steady state and following IFN treatment and more than 55% of the genes which are more expressed in *viperin*<sup>-/-</sup> cells than in WT are also common to both conditions, indicating that Viperin has a significant impact on the whole transcriptome, regardless of its induction status.

### **Viperin does not modulate the canonical type I IFN response but likely plays a role in the modulation of the inflammatory response**

To analyze the transcriptomic changes in both cell lines and identify the different pathways in which Viperin might be involved, we performed gene set enrichment for GO terms and KEGG pathways, based on official names (HGNC) of human orthologs of the differentially expressed fathead minnow genes, using the web interface DAVID (51).

***Viperin does not modulate the canonical type I IFN response.*** Most GO terms were commonly enriched in the set of genes upregulated upon type I IFN treatment in the WT cell line (set 1) and in the *viperin*<sup>-/-</sup> cell line (set 2) (**Additional file 9**). The 26 Biological Processes significantly enriched

in the WT cell line were included in the 46 terms obtained from the *viperin*<sup>-/-</sup> cell line. Many of these terms include generic GO terms associated with immune or inflammatory responses. In particular, the most significantly enriched terms (*i.e.* with the lowest of *p* value) were “GO:0051607~defense response to virus” and “GO:0045087~innate immune response” in both cell lines. More specific terms related to IFN response ranked among the terms with the highest fold enrichment, including “GO:0002753~cytoplasmic pattern recognition receptor signaling pathway” (26-fold enrichment in WT, 18-fold enrichment in *viperin*<sup>-/-</sup> cell line), “GO:0060333~interferon-gamma-mediated signaling pathway” (18-fold enrichment in WT, 14-fold enrichment in *viperin*<sup>-/-</sup> cell line), “GO:0032727~positive regulation of interferon-alpha production” (19-fold enrichment in WT, 13-fold enrichment in *viperin*<sup>-/-</sup> cell line) and “GO:0032727~positive regulation of interferon-alpha production” (13-fold enrichment in WT, 10-fold enrichment in *viperin*<sup>-/-</sup> cell line). Consistent results were obtained from the KEGG pathway analysis, where “hsa04623:Cytosolic DNA-sensing pathway”, “hsa04622:RIG-I-like receptor signaling pathway” as well as virus-specific pathways (e.g “hsa05160:Hepatitis C”, “hsa05164:Influenza A”) were among the most enriched pathways (**Additional file 10**). These results confirm that the type I IFN treatment was effective and further suggest that the IFN response was similar in both cell lines.

However, DAVID analysis is only based on the lists of official gene symbols without using expression or fold change values. Therefore, it does not take into account a potential differential amplitude in gene expression between the two cell lines. In addition, differences of expression between multiple fish paralogs sharing a unique human ortholog cannot be analyzed in this way. To investigate whether the response magnitude to IFN treatment was different between the two cell lines, a linear regression was performed on the fold changes obtained for the 417 upregulated genes in both cell lines (**Figure 4D**) revealing a regression coefficient of 1.0693 ( $R^2 = 0.9625$ ). This observation shows that the intensity of the *ISG* response is remarkably similar between/in the two cell lines, suggesting that Viperin does not have a significant global impact on the modulation of this response. Consistent with this observation, no GO terms associated with the innate immune response were enriched in the lists of genes differentially expressed in the *viperin*<sup>-/-</sup> cell line compared to WT following type I IFN (**Figure 5**, right panel). For further confirmation, we compared the lists of genes differentially expressed in the *viperin*<sup>-/-</sup> cell line versus WT following type I IFN with a list of genes modulated by IFN $\phi$ 1 in zebrafish larvae (56) (**Additional file 11**). Once again, very few genes were shared with the latter, further supporting that Viperin does not modulate the type I IFN response. It is therefore likely that *viperin* is essentially an effector gene in this pathway in EPC-EC cells.

***Viperin acts as a regulator of the inflammatory response.*** Although both cell lines share a majority of DEGs following IFN treatment, a fair share of genes are exclusively modulated in one of them. In

particular, 70 and 244 genes were exclusively upregulated in the WT and the *viperin*<sup>-/-</sup> cell line, respectively, while 81 and 147 genes were downregulated in the WT or the *viperin*<sup>-/-</sup> cell line only (**Figure 4B,D**). GO analysis of these sublists did not result in significantly enriched pathways except for the list of genes that are exclusively upregulated in the *viperin*<sup>-/-</sup> cell line upon IFN stimulation. Furthermore, for the other sublists, visual curation and IPA analysis did not lead to the identification of genes or pathways of interest. For the genes exclusively upregulated in the *viperin*<sup>-/-</sup> cell line upon type I IFN, two GO terms were significantly enriched: “GO:0032088~negative regulation of NF-kappaB transcription factor activity” (9.1-fold enrichment) and “GO:0006954~inflammatory response” (4.4-fold enrichment) (**Figure 6A**). To further analyze the role of Viperin in the inflammatory response, the specific genes identified as being enriched in this pathway were extracted and their expression levels were represented in a heatmap ((**Figure 6B**)). Interestingly, this subset of genes includes members of the NOD-like receptors (NLR) family, involved in the formation of signaling platforms (including inflammasomes and nodosomes) of the inflammatory response (57); genes involved in both canonical and non-canonical NF-κB pathways; as well as other genes playing a role in the inflammatory response.

These genes can be classified into three categories depending on their expression pattern in the *viperin*<sup>-/-</sup> compared to the WT cell line: “pattern 1” includes genes (*e.g.* *NOD1*, *NFKBIA*, *NFKB2*, *IL1R1*) displaying no expression difference at the steady state but a higher induction in the *viperin*<sup>-/-</sup> cells compared to WT upon IFN treatment; “pattern 2” corresponds to genes (*e.g.* *CYLD*, *CD40*, *ADM*) that are significantly less expressed in *viperin*<sup>-/-</sup> cells versus WT at the steady state and upon IFN treatment, but that display a higher fold change (Ctrl vs. IFN) in the *viperin*<sup>-/-</sup> cells; “pattern 3” corresponds to the genes (*e.g.* most *NLRC3* genes, *UMOD*, *IL34*) that show no significant expression difference between both cell lines at the steady state and upon type I IFN stimulation but still display a significant upregulation (Ctrl vs. IFN) in the *viperin*<sup>-/-</sup> cells. Pattern 1 highlights genes that are downregulated by Viperin upon IFN treatment only, pattern 2 reveals genes that are upregulated by Viperin at the steady state while their induction is mitigated by Viperin upon type I IFN treatment; pattern 3 shows genes of which expression can be modulated by Viperin, but not in all conditions. This suggests that Viperin modulates the expression of inflammatory genes in distinct and complex ways.

NLRs proteins encoded by genes whose expression is modulated by Viperin have diverse structural domain compositions, which have been described in fish (58) (**Figure 6C**). Indeed, mammalian NLRs are typically composed of an N-terminal effector domain, a central nucleotide-binding domain (NACHT) and a C-terminal ligand-binding region that comprises several leucine-rich repeats (LRRs) (57). Members of the NLR family have been classified based on their N-terminal effector domain:

for instance, NOD1-2 exhibit a N-terminal CARD domain; NLRP1-14 present a pyrin domain, NLRC3-5 feature an untypical CARD or unknown effector domain (57). Although only a few of these NLRs-encoding genes, including NOD1-2 and NLRC3, present a direct ortholog in fish genomes, fish NLRs have also expanded into very large families of hundreds of proteins (58). Several of them are characterized by the presence of a C-terminal B30.2 domain, which is typically present in some tripartite motif containing (TRIM) and Pyrin proteins (58). Interestingly, in EPC-EC cells, Viperin-modulated NLRs present diverse domain combinations (CARD, LRR, B30.2), which excludes the modulation of a single type of NLRs by Viperin. The genes annotated as NLRC4 and NLRP12 only present a partial structure (CARD and PYD, respectively), hence are not classified within the canonical NLR family. Finally, the gene wrongly annotated *mefv* (*aka. pyrin*, another inflammasome) presents a typical TRIM structure (**Figure 6C**).

It is noteworthy that most of the *NLRs* genes modulated by Viperin are homologous to mammalian NLRC3, which is a non-inflammasome-forming NLR member that negatively regulates inflammation by inhibiting NF- $\kappa$ B activation (59,60). NLRC3-like genes mainly follow expression patterns 2 and 3, suggesting that Viperin promotes their expression at the steady state but may limit their induction upon type I IFN. In contrast, *NOD1*, which promotes the inflammatory response by triggering the NF- $\kappa$ B and/or the MAPK pathways (61), follows expression pattern 1, indicating that Viperin downregulates its expression upon IFN treatment only.

In addition to NLRs, Viperin downregulates the expression of proinflammatory genes, including *IL1R1*, encoding the IL1 $\beta$  receptor. Of note, the fathead minnow gene annotated as *IL1R1* is homologous to the zebrafish CABZ01054965.1 gene, which was reported to be a functional ortholog for human *IL1RL2* (62). IL1RL2 was shown to mediate IL-36-driven activation of NF- $\kappa$ B and to promote the secretion of proinflammatory chemokines and cytokines in epithelial tissues, likely in a similar fashion as IL-1 $\alpha/\beta$  and IL-1R1 (63). Furthermore, genes involved in both canonical and non-canonical NF- $\kappa$ B pathways (*TRAF3*, *TRAF3IP2*, *NFKB2*), which promote inflammation, were also more expressed in the *viperin*<sup>-/-</sup> cell line compared to WT upon type I IFN treatment (pattern 1). Other genes involved in the inflammatory response and following expression pattern 1 include genes with dual inflammatory functions, such as *ADORA2a* (64), as well as a few anti-inflammatory genes, such as *TNIP1* (*aka. TNFAIP3* interacting protein 1), which is an inflammation repressor that regulates NF- $\kappa$ B signaling (65) and *NFKBIA*, which inhibits the activity of dimeric NF- $\kappa$ B/Rel complex (66). In addition, *CYLD*, which encodes a deubiquitinase that down-regulates NF- $\kappa$ B activation and limits inflammation (67), and *ADM*, which encodes an anti-inflammatory peptide (68), both follow expression pattern 2, suggesting that Viperin promotes their expression at the steady state but limit their induction upon type I IFN.

Taken together, these results suggest that Viperin downregulates the expression of pro-inflammatory genes, including *NOD1*, *IL1R1* as well as intermediate molecules and regulators of the NF- $\kappa$ B pathways, upon type I IFN treatment. Viperin also seems to modulate the expression of negative regulators of NF- $\kappa$ B activation (including *NLRC3*, *CYLD*) depending of its induction status: it may promote their expression at the steady state but limit their induction upon type I IFN.

### **rVHSV-Tomato does not replicate better in *viperin*<sup>-/-</sup> cell lines**

Although Viperin does not seem to have a global impact on the IFN response in EPC-EC cells, we still assessed its antiviral role upon VHSV infection, as rVHSV-Tomato infection leads to a strong induction of *viperin* in this cell line (**Figure 2**). To investigate the effect of Viperin on virus replication, we used rVHSV-Tomato, in which an expression cassette encoding tdTomato was inserted in the N-P intergenic region of VHSV genome (42). As a consequence, tdTomato protein is only expressed during the replication cycle of the virus and fluorescence measurement can be used as a non-invasive indicator of viral replication. The evolution of the red fluorescence was sequentially monitored in WT EPC-EC and *viperin*<sup>-/-</sup> EPC-EC-Vip-C7 and -C11 cell lines from 24h to 96h post-infection. Remarkably, the fluorescence signal was not significantly different in both *viperin*<sup>-/-</sup> clones compared to the WT cell line at any of the time points and MOI examined, suggesting that the knockout of *viperin* does not favor the replication of VHSV in this cell line (**Figure 7**).

In addition, complementary experiments performed at lower MOIs (starting from MOI = 0.05) revealed that there was no difference in the appearance of CPE between WT EPC-EC cells and *viperin*<sup>-/-</sup> EPC-EC-Vip-C7 and -C11 clones infected with 10-fold serial dilutions of VHSV (data not shown). These results further indicate that the *viperin* knockout does not have a drastic effect on VHSV replication.

### **Gene set enrichment analysis shows that Viperin may be involved in multiple pathways in addition to the type I IFN response**

To further explore the functional role of Viperin, we analyzed the results of gene set enrichment on DEGs in the *viperin*<sup>-/-</sup> cell line compared to the WT cell line, by combining analyses of set 3 (steady state) and set 4 (upon IFN treatment) (**Figure 5**). These two datasets highlight DEGs specifically modulated by the presence/absence of Viperin, under physiological conditions *i.e.* when *viperin* transcripts are weakly expressed (steady state, set 3); and under pathological conditions *i.e.* when *viperin* transcripts are highly expressed (IFN treatment, set 4), respectively. In other words, analysis of both sets helps identify a potential regulatory role of Viperin in either treatment condition (*i.e.* role dependent on the induction status of Viperin), or in both (*i.e.* constitutive role, regardless of induction status).

**Viperin modulates ECM organization and cell adhesion.** Several GO terms were commonly enriched in both data sets regardless of the treatment. For downregulated DEGs, these shared GO terms fall into the large category of cellular adhesion and extracellular matrix (ECM) (**Figure 5**), such as “GO:0030199~collagen fibril organization” (8.7-fold enrichment in *viperin*<sup>-/-</sup> cell line compared to the WT cell line at the steady state; 7.2-fold enrichment upon IFN treatment) and “GO:0030198~extracellular matrix organization” (4.1-fold enrichment at the steady state; 3.9-fold enrichment upon IFN treatment). A few GO terms associated to this category were also specifically found in either treatment condition, such as “GO:0007160~cell-matrix adhesion” (3.6-fold enrichment) and “GO:0007157~heterophilic cell-cell adhesion via plasma membrane cell adhesion molecules” (5.0-fold enrichment), which were specifically enriched in downregulated DEGs at the steady state.

The ECM is a non-cellular network of macromolecules that are essential for many fundamental cellular functions, including structural support, cell adhesion, cell-to-cell communication and differentiation (69). It is mainly composed of proteoglycans, fibrous proteins (including collagens and fibronectin, which are primarily produced by fibroblasts and laminins, which are mainly specific to epithelial, endothelial, and mesenchymal cells) and other secreted globular proteins such as growth factors, cytokines and ECM-specific enzymes (metalloproteases, matrix crosslinking enzymes and their respective regulators) (70). In our study, several genes encoding fibrillar collagen  $\alpha$ -chains (*e.g.* *COL1A1*, *COL2A1*, *COL4A1*, *COL5A1*, *COL5A2*, *COL11A1*, *COL13A1*, *COL16A1*, *COL18A1*) and non-collagenous proteins, such as laminins (*LAMA1*, *LAMA2*, *LAMA4*) and fibronectins (*FNI*) were found in the aforementioned enriched ECM-related GO terms (**Figure 8, Additional file 12**). Other genes enriching either pathway include metalloproteases (including *ADAMTS7*, *ADAMTS2*, *ADAMTS14*, *MMP2*, *MMP14*, *TLL1*, *BMP1*), involved in the remodeling of the ECM (71), members of the lysyl oxidase (LOX) family (*e.g.* *LOX*, *LOXL2*, *LOXL3*, *LOXL4*) as well as regulators of matrix proteases (*e.g.* *RECK*, *SPINT1*), that are important for the assembly, structural organization, maintenance and homeostasis of the ECM (72).

As mentioned above, adhesion is one of the major biological functions of the ECM. ECM-cell adhesion is mediated by ECM transmembrane receptors, such as integrins, which bind to several ECM components, such as laminins, collagens, and fibronectin via their extracellular domain, thereby forming hemidesmosomes or focal adhesions (73). Furthermore, cell adhesion also involves cell-cell junctions, which are mainly mediated by the cadherins for adherens junctions and desmosomes, or by claudins and occludins for tight junctions (74). In our study, the GO term “GO:0007155~cell adhesion” obtained from the list of downregulated genes in the *viperin*<sup>-/-</sup> cell line compared to the WT cell line in both treatment conditions ranked among the most significantly enriched terms (*i.e.* with

the lowest of *p* value) (Figure 5). Besides collagen-encoding genes, modulated genes include most of the adhesion proteins mentioned above, including integrins (*ITGs*) (e.g. *ITGA2*, *ITGA6*, *ITGA8*, *ITGA9*, *ITGA10*, *ITGA11*, *ITGB3*), proteins belonging to the cadherin superfamily, such as cadherin 2 (*CDH2*) and protocadherins (e.g. *PCDH1*, *PCDHA2*, *PCDHAC2*, *PCDH10*, *PCDH17*, *PCDH18*), cadherin related proteins (*CDHR1*, *CDHR5*) as well as genes from the claudin (*CLDN*) family (*CLDN6*, *CLDN11*, *CLDN19*) (Additional file 12). Furthermore, genes coding adapter proteins, such as talins (*TLN2*),  $\alpha$ -actinins (*ACTN2*), and catenins (*CTNND2*) which make the connection between the intracellular domains of *ITG* and *CDH*, respectively, and the cytoskeleton (75,76) are also included in the lists of DEGs between WT and *viperin*<sup>-/-</sup> cell lines. Finally, thrombospondins (*THBS1-4*), which are glycoproteins that play an essential role in regulating cell-cell and cell-matrix interactions (77), are also downregulated in the *viperin*<sup>-/-</sup> cell line compared to the WT. Of note, KEGG pathway analysis revealed similar pathways enriched in the downregulated gene sets, including “hsa04512:ECM-receptor interaction” and “hsa04510:Focal adhesion” (Additional file 13). Visualization of DEGs imposed on top of the ECM-receptor interaction pathway (Additional file 14) illustrates the extent to which this pathway is modulated in the *viperin*<sup>-/-</sup> cell line compared to the WT.

Altogether, these results suggest that Viperin promotes ECM organization and cell adhesion, mainly independently from its induction status.

***Viperin is a positive regulator of bone and cartilage metabolism.*** Several GO terms related to bone and cartilage formation are also strikingly enriched in the lists of genes downregulated in the *viperin*<sup>-/-</sup> cell line compared to the WT cell line, including “GO:0035988~chondrocyte proliferation” (10.7-fold enrichment) and “GO:0001503~ossification” (4.7-fold enrichment) in the control condition, “GO:0060346~bone trabecula formation” (13.2-fold enrichment) and “GO:0001501~skeletal system development” (3.3-fold enrichment) in the IFN stimulated condition and “GO:0001649~osteoblast differentiation” shared in both conditions (3.3- and 3.5-fold enrichment, respectively) (Figure 5). The ECM is known for playing a critical role in bone formation (78), a significant number of genes involved in ECM organization and cell adhesion are also found in bone-related GO terms, including collagens (in particular type I collagen encoded *COL1A1*) as well as genes encoding non-collagenous proteins, such as *MMPs* (e.g. *MMP2*, *MMP14*, *MMP16*) and *THBSs* (e.g. *THBS3*). Furthermore, several genes encoding bone morphogenetic proteins (BMPs), including *BMP3* and *BMP5*, were also among these downregulated genes. BMPs are secreted cytokines, members of the TGF- $\beta$  superfamily, and integral components of the bone ECM involved in developmental processes and bone formation. They trigger activation cascades through receptor binding leading to the transcription modulation of target genes involved in developmental processes and bone formation (79). Interestingly, several

genes involved in the BMP signaling pathways were also downregulated in the *viperin*<sup>-/-</sup> cell line compared to the WT cell line, including a few receptors of BMPs (*BMPRI1B*), BMP antagonists such as Noggin (*NOG*) and Follistatins (*FST*, *FSTL1*, *FSTL4*), which inhibit BMP activity by direct binding to BMPs and/or to their respective cell surface receptors (80,81), molecules involved in their signaling pathways such as mitogen activated protein kinases (MAPKs) (*e.g.* *MAPK11*, *MAP2K6*), as well as their downstream targets such as MSX transcription factors (*MSX2*) (79,82). Altogether, our results suggest that Viperin is involved in the modulation of a genes sets involved in bone metabolism, regardless of its induction status.

***Viperin downregulates one-carbon metabolism.*** The GO term “GO:0006730~one-carbon metabolic process’ is enriched in the list of genes upregulated in the *viperin*<sup>-/-</sup> cell line compared to the WT cell line in the control condition (**Figure 5**). This term is of particular interest as one carbon metabolism results in the generation of SAM, which is a cofactor used by Viperin for the generation of ddhCTP. One carbon metabolism is a network of biochemical reactions that deliver one-carbon units (*i.e.* methyl groups) to various biosynthetic pathways supporting biosynthesis of nucleotides (purines and thymidines), homeostasis of amino acids (glycine, serine, and methionine), epigenetic maintenance via histone methylation, and maintenance of redox balance (**Figure 9B**) (83). It comprises two interconnected metabolic pathways: the folate cycle and the methionine cycle. In the latter, methionine is converted into SAM by the methionine adenosyltransferase (MAT), encoded by *MAT2A/B*, in an ATP-dependent manner (84). SAM is considered the main methyl donor in various biochemical reactions, including radical-mediated biochemical transformations; S-adenosylhomocysteine (SAH), the product of enzymatic extraction of the methyl group from SAM is converted to homocysteine, which can be “recycled” to methionine for the cycle to continue. This process requires vitamin B12 as a cofactor and uses a one-carbon unit that can be sourced from the folate cycle (methyl-THF) (84). In the *viperin*<sup>-/-</sup> cell line, upregulated genes comprise *MAT2A*, which is directly involved in the generation of SAM, as well as enzymes from the folate cycle, including aldehyde dehydrogenases (*ALDHs*), serine hydroxymethyl transferases (*SHMTs*) and methylenetetrahydrofolate dehydrogenases (*MTHFDs*) (**Figure 9**). Of note, the KEGG pathway “hsa00270:Cysteine and methionine metabolism”, which is directly connected to one-carbon metabolism, is also enriched in the *viperin*<sup>-/-</sup> cell line compared to the WT (4.2-fold enrichment), and specific genes involved in glutathione synthesis (*e.g.* cystathionine gamma-lyase (*CTH*), glutathione synthetase (*GSS*)) are upregulated (**Additional file 13**). These results suggest that in non-induced conditions but not after type I IFN stimulation, Viperin may act a negative regulator of the one-carbon metabolism, likely leading to reduced SAM generation *via* a negative feedback loop.

**Viperin downregulates exocytosis.** The GO term “GO:0006887~exocytosis” is enriched in the list of genes upregulated in the *viperin*<sup>-/-</sup> cell line compared to the WT cell line upon stimulation with type I IFN (**Figure 5**). Exocytosis is a type of active bulk transport resulting in the fusion of a vesicle with the plasma membrane and the release of molecules into the extracellular space (85). It involves vesicle trafficking along cytoskeleton filaments, vesicle tethering, vesicle docking and vesicle fusion with the plasma membrane. In the *viperin*<sup>-/-</sup> cell line, upregulated genes are mainly involved in the regulation of vesicle exocytosis (*e.g.* *CADPS2*, *RIMS1*, *RIMS2*) or in vesicle tethering (*e.g.* *EXOC3L4*). These results indicate that Viperin might be involved in the regulation of exocytosis.

## Discussion

In this study, we have developed a fathead minnow epithelial-like cell line, in which the unique *viperin* gene has been knocked-out by CRISPR/Cas9 genome editing. Using a transcriptomic approach, we showed that in our model Viperin does not modulate the type I IFN response as many other ISG products do (86), suggesting that Viperin is only an effector gene of the type I IFN response *stricto sensu*. Our data indicate that it negatively regulates a number of genes involved in the inflammatory response, especially at steady state. In addition, Viperin appears to regulate the expression of key genes involved in multiple cellular processes, including one carbon metabolism, bone formation, extracellular matrix (ECM) organization and cell adhesion, even under non-pathological conditions.

### Are EPC-EC and/or EPC-EC-Vip cell lines aneuploid?

During the sequencing step in the development of the *viperin*<sup>-/-</sup> clonal cell line, we identified three distinct genotyping sequences amplified by PCR from the gDNA of two isolated clones. The existence of three and not just two different sequences, corresponding in theory to each haplotype, can be explained in three ways: (1) each cell line does not derive from a single cell and is therefore not clonal and homogeneous; (2) there are at least two *viperin* paralog genes in the genome of fathead minnow; (3) the EPC-EC cell line and/or EPC-EC-Vip clones have undergone a local duplication event (tandem duplication), full chromosome gain (trisomy) or partial chromosome gain (*e.g.* partial trisomy following unbalanced translocation event, for instance) of the portion carrying the *viperin* gene during their respective development processes, resulting in more than two copies of the *viperin* gene. The first hypothesis is unlikely insofar as the clones were FACS-sorted and the sequencing of manually obtained subclones resulted in similar results (**Additional file 15**). Although the second hypothesis cannot be completely ruled out, *in silico* analysis of the most recent genome assembly strongly suggests that the fathead minnow genome only comprises a unique *viperin* gene, like the

closely related species. The third hypothesis provides a fitting explanation for the three different sequences obtained from both EPC-EC-Vip-C7 and EPC-EC-Vip-C11 clones. Indeed, aneuploidy is a phenomenon relatively common in cultured mammalian cell lines (87,88) and several lines of evidence support the hypothesis that EPC-EC cells and/or its derivatives have undergone (partial) chromosome gain or local duplication during their respective development processes. Firstly, the three sequences obtained from the sequencing of both *viperin*<sup>-/-</sup> clones can reflect the three haplotypes arising from a (partial) trisomy or from a duplication event affecting one copy of the *viperin* gene. Secondly, it has been shown that chromosome gain is often associated with impaired proliferation (89). The EPC-EC cell line and all its derived clones have a much slower growth rate than the parental cell line EPC (data not shown), which is a phenomenon not observed in CHSE-EC cell line, deriving from CHSE-214 (44). Assuming that this aneuploidy hypothesis is true, the question arises as to whether both EPC-EC cells and EPC-EC-Vip-C7 and -C11 or only the *viperin*<sup>-/-</sup> clones are aneuploid, as it may have consequences on the transcriptomic data. We speculate that the event resulting in aneuploidy occurred during the development of the EPC-EC cell line and equally affects EPC-EC cells and their derivatives. Indeed, EPC-EC-Vip clones grow as slowly as EPC-EC cells. Furthermore, both *viperin*<sup>-/-</sup> EPC-EC-Vip-C7 and -C11 clones present a “triple” genotype; because independent identical aneuploidy-resulting events (or local duplication events) are unlikely, this suggests that this phenomenon predates the cloning step. Finally, it has been previously shown in MEFs containing a single extra copy of a chromosome that the expression of genes located on the additional chromosome was proportional to the gene copy number (~1.5-fold increase in trisomic cells for the duplicated genes) (89). In our case, the current fathead minnow genome (GCF\_016745375.1, EPA\_FHM\_2.0) does not include chromosomes or linkage groups, which makes the analysis of additional (partial) chromosome(s) difficult. However, we assume that if (partial) chromosome gain happened during the development of the EPC-EC-Vip clones, it would be reflected in the expression of the genes located on the NW\_024121099.1 containing the *viperin* gene. The analysis of the 925 genes located on NW\_024121099.1 revealed that there were no significant and consistent fold change differences between EPC-EC-Vip-C7 and EPC-EC cells for both treatment conditions ([Additional file 16](#)). These results further support the hypothesis that if an event resulting in aneuploidy has affected the cells, it has most likely occurred during development of the parental line, EPC-EC.

Altogether, we propose that both the EPC-EC cell line and its derivatives (EPC-EC-Vip-C7 and -C11) have more than one copy of *viperin*, resulting in the genotyping sequences observed.

### **Role of Viperin in the IFN response and in the antiviral response**

We have shown that Viperin does not globally modulate the amplitude of the canonical type I IFN response, suggesting that it mainly acts as an effector gene in the canonical type I IFN response in

our epithelial fish cell line model. These results are not in line with previous published work, which reported that fish Viperin modulates the expression of some genes involved in IFN and inflammatory response (9,38,39). However, these studies were based on overexpression approaches, which lead to unnaturally high levels of the protein of interest that may distort the effects of the endogenous protein. Alternatively, the use of type I IFN as an inducer of Viperin might also explain this discrepancy: indeed, Wang *et al.* found that overexpression of the splicing variant (lacking exon 5) but not the full-length isoform of fathead minnow Viperin could induce the expression of RIG-I, IRF3 IRF7, type I IFN, MxA and PKR in FHM cells and this variant was only expressed upon infection with SVCV and not upon poly(I:C) stimulation (39). Whether this variant can be expressed in our fathead minnow EPC-EC cell line is currently not known but the putative corresponding protein was not detected by Western blot upon stimulation with type I IFN supernatant (**Additional file 4**). Several studies on mammalian models did not provide unified results either concerning the role of Viperin on the regulation of the IFN response (25,90,91). It was initially described that mammalian Viperin could promote the activation of key signaling mediators involved in the TLR7 and TLR9 pathways in plasmacytoid dendritic cells, thereby facilitating the production of type I IFN, but it was not involved in the production of type I IFN upon transfection with intracellular nucleic acids in MEFs (25). In contrast, Viperin was found to act as a negative regulator of IFN- $\beta$  induction in bone-marrow derived macrophages (BMDMs) upon poly(I:C) or 5'ppp-dsRNA transfection or type I IFN treatment (90). These discrepancies may arise from the differences in cell types, inducers and/or assays used (92). As a matter of fact, a recent study has reported that Viperin differentially modulated the induction of *ISGs* in a cell type- and inducer-dependent manner (91). Altogether, our results show that, in epithelial cells, fathead minnow Viperin does not seem to have a major regulatory role on the expression of *ISGs* upon treatment with type I IFNs. Nonetheless, this observation does not exclude a role of fathead minnow Viperin in regulating the canonical IFN response in other cell types (dendritic cells, macrophages) and/or with another inducer (dsRNA, virus infection).

We observed no differences in fluorescence between *viperin*<sup>-/-</sup> and WT cell lines infected with rVHSV-Tomato, suggesting that the *viperin* knockout did not result in higher replication of VHSV. In contrast, a recent study in *viperin*<sup>-/-</sup> zebrafish larvae infected with rVHSV- $\Delta$ NV-EGFP reported a higher GFP signal and a 10-fold increase in VHSV titer in *viperin*<sup>-/-</sup> larvae compared to WT larvae ( $1.6 \times 10^7$  vs  $2.8 \times 10^6$  TCID<sub>50</sub>/mL) (13,41). Taken together, these observations are consistent with the cell-type dependent role of Viperin in the antiviral response, leading to more complex effects in a whole organism.

## Role of Viperin in the inflammatory response

Although Viperin does not seem to be involved in the regulation of the IFN response, the functional analysis of our transcriptomic data revealed that a specific subset of proinflammatory genes were exclusively induced in the *viperin*<sup>-/-</sup> cell line upon IFN stimulation, suggesting that Viperin might be a negative regulator of the inflammatory response. More specifically, our data revealed that Viperin modulates the expression of inflammatory genes in a complex manner: Viperin seems to downregulate the expression of specific pro-inflammatory genes upon type I IFN treatment and may also promote the expression of negative regulators of NF- $\kappa$ B activation at the steady state while limiting their induction upon type I IFN treatment.

In the literature, some studies have shown that Viperin enhanced the proinflammatory response (93,94), while others have reported that it either did not modulate (25) or decreased the expression of proinflammatory genes (95). Similarly to what is known about the role of Viperin in the IFN response, these studies suggest its contribution to the proinflammatory response may also be cell type- and treatment-dependent. In addition, the mechanisms by which it may modulate the pro-inflammatory response remain largely unknown. It was recently shown that the catalytic activity of nucleoside kinase CMPK2 is essential for NLRP3 inflammasome activation (96). This nucleoside kinase functionally cooperates with Viperin, as it phosphorylates CDP into CTP, which is Viperin's substrate (21). It was suggested that CMPK2 proinflammatory function was linked to its capacity to enhance mitochondrial DNA synthesis *via* a mechanism that involves CTP synthesis (92,96). Because CTP is the preferential substrate for Viperin and it was proposed that CMPK2 and Viperin modulate the inflammatory response by increasing CTP production or consumption, respectively (92). This hypothesis is supported by the observation that Viperin-mediated conversion of CTP into ddhCTP leads to the depletion of the mitochondrial pool of CTP (22).

Our transcriptomic data also point to some potential mechanisms leading the downregulation of the NF- $\kappa$ B pathways and other pro-inflammatory genes upon type I IFN treatment. In addition, Viperin seems to promote the expression of negative regulators of the NF- $\kappa$ B pathways, including several NLRC3-like genes, at the steady state. Of note, although mammalian NLRC3 has been shown to inhibit NF- $\kappa$ B activation via interactions with TRAF6, IRAK1 and/or TRAF3 (59,60), the functional role of NLRC3-like genes in fish is still unclear and their large expansion makes their characterization even more challenging (58,97).

Overall, this study highlights a role for Viperin in the inflammatory response that would be interesting to characterize in more detail in a future study. In particular, investigating the role of Viperin during bacterial infections could be an area for future research.

## Role of Viperin in other pathways

### *Role of Viperin in one-carbon metabolism*

The gene set enrichment analysis of *viperin*<sup>-/-</sup> cell line compared to WT revealed that at the steady state, Viperin may downregulate one carbon metabolism. One carbon metabolism encompasses both folate and methionine cycles and participates in the generation of SAM, a cofactor required for the enzymatic activity of Viperin (20). We propose that Viperin might act as a negative regulator of one carbon metabolism under non-induced conditions, as a way to self-regulate the generation of ddhCTP. Indeed, although ddhCTP has been identified as a natural chain terminator of RNA-dependent RNA polymerase, endogenous ddhNTPs are small molecules with undefined functions (98). Recent studies have explored the role of ddhCTP in cellular metabolism: Hsu *et al.* have shown that ddhCTP generated by Viperin can lead to the activation of the integrated stress response and inhibition of protein translation by enhancing ribosome collisions upon overexpression and during infection with West Nile virus (99); Ebrahimi *et al.* have also provided evidence (albeit controversial) that ddhCTP was capable of inhibiting the enzymatic activity of NAD<sup>+</sup>-dependent enzymes (35). Although the underlying mechanisms are still not well understood, it therefore appears that ddhCTP is not harmless to the cells and may affect their metabolism. It is tempting to speculate that, at least in non-infectious conditions, Viperin downregulates the generation of its cofactor, in order to limit the generation of ddhCTP when not needed. Nonetheless, because SAM is involved in a variety of metabolic processes, including DNA methylation, amino acid metabolism and transsulfuration (83), it may have major consequences on the cellular metabolism. First and foremost, confirmation of this hypothesis would require quantification of the cellular concentration of SAM in the *viperin*<sup>-/-</sup> cells compared to the WT.

### *Role of Viperin in cell adhesion and ECM*

Intriguingly, our study suggests that Viperin positively modulates the expression of genes involved in cellular adhesion and ECM, including genes coding for structural proteins (collagens, fibronectin, laminin), ECM-specific enzymes and adhesion proteins (*e.g.* integrins, cadherins) among others. Interestingly, similar results were obtained in a very recent RNA-Seq study performed on 12Z endometriotic epithelial cells (100): genes upregulated following Viperin overexpression were enriched for GO terms “ECM organization”, “cell-substrate adhesion”, “cell-matrix adhesion” and “collagen fibril organization” and opposite results were obtained upon *viperin* knockdown (100). The identification of those enriched terms was not further discussed in this paper but it supports our findings and further suggests that our observations are not caused by a possible clonal effect. Altogether, these results shed light on a previously undiscovered function of Viperin. However, how Viperin modulates the expression of these genes remains to be determined.

### *Role of Viperin in bone metabolism*

In our study, downregulated genes in the *viperin*<sup>-/-</sup> cell line compared to the WT were also unexpectedly enriched for GO terms related to bone and cartilage formation. Although Viperin is not commonly associated with bone metabolism in the literature, a few studies have reported that Viperin is expressed in bone tissues and/or in bone or cartilage cells (31,101). In particular, the rat ortholog of *viperin* was highly expressed in differentiating primary osteoblasts *in vitro* as well in osteoblast progenitors and mature osteoblasts in sections of rat tibiae and in mechanically loaded bones (31). More recently, *viperin* was identified in one of the QTLs explaining the size variation of Meishan pigs, suggesting that it might play a role in bone and skeletal development (102). Viperin was also found to be involved in osteoclast differentiation (101) and chondrogenic differentiation (32). Taken together, these results suggest that Viperin might be active as a regulator of cellular differentiation during cartilage and bone formation. However, the mechanisms by which Viperin modulates these metabolic processes are not well understood. Steinbusch *et al.* have shown that Viperin promotes the secretion of CXCL10, which in turn inhibits TGF- $\beta$ /SMAD2/3 activity involved in chondrogenic differentiation (32). Our study may provide another potential line of action, as many DEGs included genes involved in ECM organization and cell adhesion. The ECM is known for playing a key role in bone formation (78); therefore, we propose that Viperin is involved in bone metabolism *via* modulating the expression genes involved in ECM and cellular adhesion. Consistent with the fact that EPC-ECs are epithelial cells, genes specifically expressed by bone-specific cells were not identified in our transcriptomic datasets. As a consequence, a regulatory role of Viperin on the expression of this specific gene subset could not be explored in this study.

### **Conclusions**

In conclusion, our transcriptomic analysis revealed that Viperin does not modulate the type I IFN response but may downregulate specific subsets of pro-inflammatory genes while upregulating negative regulators of the NF- $\kappa$ B pathways. It also appeared to play a role in regulating metabolic processes, including one carbon metabolism, bone formation, ECM organization and cell adhesion.

## **Declarations**

### **Ethics approval and consent to participate**

Not applicable

### **Consent for publication**

Not applicable

### **Availability of data and materials**

The RNA-seq datasets generated and analyzed during the current study are available in the Sequence Read Archive repository, under accession number PRJNA1076136.

### **Competing interests**

LC, JM, JLH and CR are employees of Virbac S.A. LC received funding from Virbac S.A. under an industrial research training agreement [Convention CIFRE #2020/0646]. JM, JLH, CR had the following involvement in the study: conceptualization, supervision, and review of the manuscript. The remaining authors declare that the research was conducted in the absence of any commercial or financial relationships that could be construed as a potential conflict of interest.

### **Funding**

This project was funded in part by the European Union through AQUAEXCEL3.0 (Grant Agreement 871108) and AQUAFAANG (Grant Agreement 817923) and by the Research Council of Norway through the project PMCV (Project 301083). LC was a recipient of PhD funded by Virbac and the French Association for Research and Technology (ANRT) [Convention CIFRE #2020/0646] in collaboration with the Fish Infection and Immunity laboratory (INRAE, VIM, Jouy-en-Josas, France).

### **Authors' contributions**

**LC:** Conceptualization, Methodology, Investigation, Formal analysis, Data curation, Visualization, Writing – original draft, Writing – review & editing. **LJ:** Methodology, Software, Formal analysis, Data curation, Visualization, Writing – review & editing. **FH:** Methodology, Investigation, Formal analysis, Writing – review & editing. **DVM:** Investigation, Formal analysis, Writing – review & editing. **MP:** Investigation, Writing – review & editing. **CR:** Conceptualization, Supervision, Writing – review & editing. **JLH:** Conceptualization, Supervision, Writing – review & editing. **JM:** Conceptualization, Supervision, Funding acquisition, Writing – review & editing. **PB:** Conceptualization, Methodology, Formal analysis, Supervision, Funding acquisition, Writing –

review & editing. **BC**: Conceptualization, Methodology, Formal analysis, Supervision, Funding acquisition, Writing – review & editing. All authors read and approved the final manuscript.

## Acknowledgements

We thank Dr. Stéphane Biacchesi and Emilie Mérour (INRAE, Jouy-en-Josas, France) for their generous gifts of rVHSV-Tomato and recombinant type I IFN supernatant as well as for helpful discussions. We thank Dr. Hortense Decool (INRAE, Jouy-en-Josas, France) for providing pCite-P-BFP plasmid. We thank Dr. Yan Jaszczyszyn (I2BC sequencing platform, Gif-sur-Yvette, France) for his help with RNA-Seq. We are grateful to the genotoul bioinformatics platform Toulouse Occitanie (Bioinfo Genotoul, <https://doi.org/10.15454/1.5572369328961167E12>) for providing computing and storage resources. We thank Dr. Dean Porter (INRAE, Jouy-en-Josas, France) for careful reading of the manuscript and for insightful discussions on gene set enrichment analysis.

## References

1. Stark GR, Kerr IM, Williams BR, Silverman RH, Schreiber RD. How cells respond to interferons. *Annu Rev Biochem.* 1998;67:227–64.
2. Ertl HCJ. Chapter 44: Response to Viruses. In: Paul's Fundamental Immunology. Eighth edition. Lippincott Williams & Wilkins; 2022.
3. Boudinot P, Riffault S, Salhi S, Carrat C, Sedlik C, Mahmoudi N, *et al.* Vesicular stomatitis virus and pseudorabies virus induce a *vig1/cig5* homologue in mouse dendritic cells via different pathways. *J Gen Virol.* 2000 Nov;81(Pt 11):2675–82.
4. Jiang D, Guo H, Xu C, Chang J, Gu B, Wang L, *et al.* Identification of three interferon-inducible cellular enzymes that inhibit the replication of hepatitis C virus. *J Virol.* 2008 Feb;82(4):1665–78.
5. Seo JY, Yaneva R, Cresswell P. Viperin: a multifunctional, interferon-inducible protein that regulates virus replication. *Cell Host Microbe.* 2011 Dec 15;10(6):534–9.
6. Zhu H, Cong JP, Shenk T. Use of differential display analysis to assess the effect of human cytomegalovirus infection on the accumulation of cellular RNAs: Induction of interferon-responsive RNAs. *Proc Natl Acad Sci U S A.* 1997 Dec 9;94(25):13985–90.
7. Boudinot P, Massin P, Blanco M, Riffault S, Benmansour A. *vig-1*, a New Fish Gene Induced by the Rhabdovirus Glycoprotein, Has a Virus-Induced Homologue in Humans and Shares Conserved Motifs with the MoeA Family. *J Virol.* 1999 Mar;73(3):1846–52.
8. Chin KC, Cresswell P. Viperin (*cig5*), an IFN-inducible antiviral protein directly induced by human cytomegalovirus. *Proc Natl Acad Sci U S A.* 2001 Dec 18;98(26):15125–30.
9. Zhang B, Zhang J, Xiao Z, Sun L. Rock bream (*Oplegnathus fasciatus*) viperin is a virus-responsive protein that modulates innate immunity and promotes resistance against megalocytivirus infection. *Developmental & Comparative Immunology.* 2014 Jul;45(1):35–42.
10. Hinson ER, Cresswell P. The N-terminal Amphipathic  $\alpha$ -Helix of Viperin Mediates Localization to the Cytosolic Face of the Endoplasmic Reticulum and Inhibits Protein Secretion. *Journal of Biological Chemistry.* 2009 Feb;284(7):4705–12.
11. Hinson ER, Cresswell P. The antiviral protein, viperin, localizes to lipid droplets via its N-terminal amphipathic alpha-helix. *Proc Natl Acad Sci U S A.* 2009 Dec 1;106(48):20452–7.
12. Fenwick MK, Li Y, Cresswell P, Modis Y, Ealick SE. Structural studies of viperin, an antiviral radical SAM enzyme. *Proc Natl Acad Sci U S A.* 2017 Jun 27;114(26):6806–11.
13. Shanaka K, SN, Jung S, Madushani KP, Wijerathna HMSM, Neranjan Tharuka MD, Kim MJ, *et al.* Generation of viperin-knockout zebrafish by CRISPR/Cas9-mediated genome engineering and the effect of this mutation under VHSV infection. *Fish Shellfish Immunol.* 2022 Dec;131:672–81.
14. Bernheim A, Millman A, Ofir G, Meitav G, Avraham C, Shomar H, *et al.* Prokaryotic viperins produce diverse antiviral molecules. *Nature.* 2021 Jan 1;589(7840):120–4.
15. Lachowicz JC, Gizzi AS, Almo SC, Grove TL. Structural Insight into the Substrate Scope of Viperin and Viperin-like Enzymes from Three Domains of Life. *Biochemistry.* 2021 Jul 6;60(26):2116–29.
16. Ghosh S, Marsh ENG. Viperin: An ancient radical SAM enzyme finds its place in modern cellular metabolism and innate immunity. *J Biol Chem.* 2020 Aug 14;295(33):11513–28.
17. Chan YL, Chang TH, Liao CL, Lin YL. The Cellular Antiviral Protein Viperin Is Attenuated by Proteasome-Mediated Protein Degradation in Japanese Encephalitis Virus-Infected Cells. *J Virol.* 2008 Nov;82(21):10455–64.
18. Panayiotou C, Lindqvist R, Kurhade C, Vonderstein K, Pasto J, Edlund K, *et al.* Viperin Restricts Zika Virus and Tick-Borne Encephalitis Virus Replication by Targeting NS3 for Proteasomal Degradation. *J Virol.* 2018 Mar 14;92(7):e02054-17.
19. Seo JY, Yaneva R, Hinson ER, Cresswell P. Human cytomegalovirus directly induces the antiviral protein viperin to enhance infectivity. *Science.* 2011 May 27;332(6033):1093–7.

20. Duschene KS, Broderick JB. The antiviral protein viperin is a radical SAM enzyme. *FEBS Lett.* 2010 Mar 19;584(6):1263–7.
21. Gizzi AS, Grove TL, Arnold JJ, Jose J, Jangra RK, Garforth SJ, *et al.* A naturally occurring antiviral ribonucleotide encoded by the human genome. *Nature.* 2018 Jun;558(7711):610–4.
22. Ebrahimi KH, Howie D, Rowbotham JS, McCullagh J, Armstrong FA, James WS. Viperin, through its radical-SAM activity, depletes cellular nucleotide pools and interferes with mitochondrial metabolism to inhibit viral replication. *FEBS Letters.* 2020;594(10):1624–30.
23. Ghosh S, Patel AM, Grunkemeyer TJ, Dumbrepatil AB, Zegalia K, Kennedy RT, *et al.* Interactions between Viperin, Vesicle-Associated Membrane Protein A, and Hepatitis C Virus Protein NS5A Modulate Viperin Activity and NS5A Degradation. *Biochemistry.* 2020 Feb 18;59(6):780–9.
24. Dumbrepatil AB, Ghosh S, Zegalia KA, Malec PA, Hoff JD, Kennedy RT, *et al.* Viperin interacts with the kinase IRAK1 and the E3 ubiquitin ligase TRAF6, coupling innate immune signaling to antiviral ribonucleotide synthesis. *J Biol Chem.* 2019 Apr 26;294(17):6888–98.
25. Saitoh T, Satoh T, Yamamoto N, Uematsu S, Takeuchi O, Kawai T, *et al.* Antiviral Protein Viperin Promotes Toll-like Receptor 7- and Toll-like Receptor 9-Mediated Type I Interferon Production in Plasmacytoid Dendritic Cells. *Immunity.* 2011 Mar 25;34(3):352–63.
26. Crosse KM, Monson EA, Dumbrepatil AB, Smith M, Tseng YY, Van der Hoek KH, *et al.* Viperin binds STING and enhances the type-I interferon response following dsDNA detection. *Immunology & Cell Biology.* 2021;99(4):373–91.
27. Bai L, Dong J, Liu Z, Rao Y, Feng P, Lan K. Viperin catalyzes methionine oxidation to promote protein expression and function of helicases. *Sci Adv.* 2019 Aug 28;5(8):eaax1031.
28. Grunkemeyer TJ, Ghosh S, Patel AM, Sajja K, Windak J, Basrur V, *et al.* The antiviral enzyme viperin inhibits cholesterol biosynthesis. *Journal of Biological Chemistry [Internet].* 2021 Jul 1 [cited 2023 Aug 8];297(1). Available from: [https://www.jbc.org/article/S0021-9258\(21\)00622-0/abstract](https://www.jbc.org/article/S0021-9258(21)00622-0/abstract)
29. Wang X, Hinson ER, Cresswell P. The Interferon-Inducible Protein Viperin Inhibits Influenza Virus Release by Perturbing Lipid Rafts. *Cell Host & Microbe.* 2007 Aug;2(2):96–105.
30. Vonderstein K, Nilsson E, Hubel P, Nygård Skalmán L, Upadhyay A, Pasto J, *et al.* Viperin Targets Flavivirus Virulence by Inducing Assembly of Noninfectious Capsid Particles. *J Virol.* 2017 Dec 14;92(1):e01751-17.
31. Grewal TS, Genever PG, Brabbs AC, Birch M, Skerry TM. *Best5*: a novel interferon-inducible gene expressed during bone formation. *FASEB j.* 2000 Mar;14(3):523–31.
32. Steinbusch MMF, Caron MMJ, Surtel DAM, van den Akker GGH, van Dijk PJ, Friedrich F, *et al.* The antiviral protein viperin regulates chondrogenic differentiation via CXCL10 protein secretion. *J Biol Chem.* 2019 Mar 29;294(13):5121–36.
33. Dumbrepatil AB, Zegalia KA, Sajja K, Kennedy RT, Marsh ENG. Targeting viperin to the mitochondrion inhibits the thiolase activity of the trifunctional enzyme complex. *Journal of Biological Chemistry.* 2020 Feb 28;295(9):2839–49.
34. Eom J, Kim JJ, Yoon SG, Jeong H, Son S, Lee JB, *et al.* Intrinsic expression of viperin regulates thermogenesis in adipose tissues. *Proc Natl Acad Sci U S A.* 2019 Aug 27;116(35):17419–28.
35. Honarmand Ebrahimi K, Vowles J, Browne C, McCullagh J, James WS. ddhCTP produced by the radical-SAM activity of RSAD2 (viperin) inhibits the NAD<sup>+</sup>-dependent activity of enzymes to modulate metabolism. *FEBS Lett.* 2020 May;594(10):1631–44.
36. Mou CY, Li S, Lu LF, Wang Y, Yu P, Li Z, *et al.* Divergent Antiviral Mechanisms of Two Viperin Homeologs in a Recurrent Polyploid Fish. *Front Immunol.* 2021 Aug 31;12:702971.
37. Shanaka KASN, Tharuka MDN, Priyathilaka TT, Lee J. Molecular characterization and expression analysis of rockfish (*Sebastes schlegelii*) viperin, and its ability to enervate RNA virus transcription and replication in vitro. *Fish & Shellfish Immunology.* 2019 Sep;92:655–66.
38. Zhang Y, Lv S, Zheng J, Huang X, Huang Y, Qin Q. Grouper viperin acts as a crucial antiviral molecule against iridovirus. *Fish Shellfish Immunol.* 2019 Mar;86:1026–34.
39. Wang F, Jiao H, Liu W, Chen B, Wang Y, Chen B, *et al.* The antiviral mechanism of viperin and its splice variant in spring viremia of carp virus infected fathead minnow cells. *Fish & Shellfish Immunology.* 2019 Mar;86:805–13.
40. Gao Y, Li C, Shi L, Wang F, Ye J, Lu YA, *et al.* Viperin<sub>sv1</sub> promotes RIG-I expression and suppresses SVCV replication through its radical SAM domain. *Developmental & Comparative Immunology.* 2021 Oct 1;123:104166.
41. Shanaka K a. SN, Jung S, Madushani KP, Kim MJ, Lee J. Viperin mutation is linked to immunity, immune cell dynamics, and metabolic alteration during VHSV infection in zebrafish. *Front Immunol.* 2023;14:1327749.
42. Biacchesi S, Lamoureux A, Mérour E, Bernard J, Brémont M. Limited Interference at the Early Stage of Infection between Two Recombinant Novirhabdoviruses: Viral Hemorrhagic Septicemia Virus and Infectious Hematopoietic Necrosis Virus. *J Virol.* 2010 Oct;84(19):10038–50.
43. Dorson M, Torhy C, Billard R, Saudrais C, Maise G, Haffray P, *et al.* Nécrose pancréatique infectieuse des salmonidés : évaluation de méthodes destinées à couper la transmission par l'oeuf. *Bull Fr Pêche Piscic.* 1996;(340):1–14.
44. Dehler CE, Boudinot P, Martin SAM, Collet B. Development of an Efficient Genome Editing Method by CRISPR/Cas9 in a Fish Cell Line. *Mar Biotechnol (NY).* 2016;18(4):449–52.
45. Concordet JP, Haeussler M. CRISPOR: intuitive guide selection for CRISPR/Cas9 genome editing experiments and screens. *Nucleic Acids Research.* 2018 Jul 2;46(W1):W242–5.
46. Conant D, Hsiao T, Rossi N, Oki J, Maures T, Waite K, *et al.* Inference of CRISPR Edits from Sanger Trace Data. *CRISPR J.* 2022 Feb;5(1):123–30.
47. Diot C, Richard CA, Risso-Ballester J, Martin D, Fix J, Eléouët JF, *et al.* Hardening of Respiratory Syncytial Virus Inclusion Bodies by Cyclopamine Proceeds through Perturbation of the Interactions of the M2-1 Protein with RNA and the P Protein. *Int J Mol Sci.* 2023 Sep 8;24(18):13862.
48. Collet B, Collins C, Cheyne V, Lester K. Plasmid-driven RNA interference in fish cell lines. *In Vitro Cell Dev Biol Anim.* 2022 Mar;58(3):189–93.
49. Jami R, Mérour E, Bernard J, Lamoureux A, Millet JK, Biacchesi S. The C-Terminal Domain of Salmonid Alphavirus Nonstructural Protein 2 (nsP2) Is Essential and Sufficient To Block RIG-I Pathway Induction and Interferon-Mediated Antiviral

- Response. *Journal of Virology* [Internet]. 2021 Dec [cited 2024 Jan 17];95(23). Available from: <https://www.ncbi.nlm.nih.gov/pmc/articles/PMC8577375/>
50. Love MI, Huber W, Anders S. Moderated estimation of fold change and dispersion for RNA-seq data with DESeq2. *Genome Biology*. 2014 Dec 5;15(12):550.
  51. Sherman BT, Hao M, Qiu J, Jiao X, Baseler MW, Lane HC, *et al*. DAVID: a web server for functional enrichment analysis and functional annotation of gene lists (2021 update). *Nucleic Acids Res*. 2022 Mar 23;50(W1):W216–21.
  52. Macqueen DJ, Johnston IA. A well-constrained estimate for the timing of the salmonid whole genome duplication reveals major decoupling from species diversification. *Proceedings of the Royal Society B: Biological Sciences*. 2014 Mar 7;281(1778):20132881.
  53. Letunic I, Khedkar S, Bork P. SMART: recent updates, new developments and status in 2020. *Nucleic Acids Research*. 2021 Jan 8;49(D1):D458–60.
  54. Upadhyay AS, Vonderstein K, Pichlmair A, Stehling O, Bennett KL, Dobler G, *et al*. Viperin is an iron-sulfur protein that inhibits genome synthesis of tick-borne encephalitis virus via radical SAM domain activity. *Cell Microbiol*. 2014 Jun;16(6):834–48.
  55. Collet B, Munro E, Gahlawat S, Acosta F, Garcia J, Roemelt C, *et al*. Infectious pancreatic necrosis virus suppresses type I interferon signalling in rainbow trout gonad cell line but not in Atlantic salmon macrophages. *Fish & Shellfish Immunology*. 2007 Jan;22(1–2):44–56.
  56. Levraud JP, Jouneau L, Briolat V, Laghi V, Boudinot P. IFN-Stimulated Genes in Zebrafish and Humans Define an Ancient Arsenal of Antiviral Immunity. *J Immunol*. 2019 Dec 15;203(12):3361–73.
  57. Proell M, Riedl SJ, Fritz JH, Rojas AM, Schwarzenbacher R. The Nod-Like Receptor (NLR) Family: A Tale of Similarities and Differences. *PLOS ONE*. 2008 Apr 30;3(4):e2119.
  58. Howe K, Schiffer PH, Zielinski J, Wiehe T, Laird GK, Marioni JC, *et al*. Structure and evolutionary history of a large family of NLR proteins in the zebrafish. *Open Biology*. 2016 Apr;6(4):160009.
  59. Allen IC. Non-Inflammasome Forming NLRs in Inflammation and Tumorigenesis. *Frontiers in Immunology* [Internet]. 2014 [cited 2024 Mar 5];5. Available from: <https://www.ncbi.nlm.nih.gov/pmc/articles/PMC4001041/>
  60. Schneider M, Zimmermann AG, Roberts RA, Zhang L, Swanson KV, Wen H, *et al*. The innate immune sensor NLRC3 attenuates Toll-like receptor signaling via modification of the signaling adaptor TRAF6 and transcription factor NF- $\kappa$ B. *Nat Immunol*. 2012 Sep;13(9):823–31.
  61. Tattoli I, Travassos LH, Carneiro LA, Magalhaes JG, Girardin SE. The Nodosome: Nod1 and Nod2 control bacterial infections and inflammation. *Semin Immunopathol*. 2007 Sep 1;29(3):289–301.
  62. Sebo DJ, Fetsko AR, Phipps KK, Taylor MR. Functional identification of the zebrafish Interleukin-1 receptor in an embryonic model of IL-1 $\beta$ -induced systemic inflammation. *Frontiers in Immunology* [Internet]. 2022 [cited 2024 Mar 4];13. Available from: <https://www.ncbi.nlm.nih.gov/pmc/articles/PMC9643328/>
  63. Debets R, Timans JC, Homey B, Zurawski S, Sana TR, Lo S, *et al*. Two Novel IL-1 Family Members, IL-1 $\delta$  and IL-1 $\epsilon$ , Function as an Antagonist and Agonist of NF- $\kappa$ B Activation Through the Orphan IL-1 Receptor-Related Protein 21. *The Journal of Immunology*. 2001 Aug 1;167(3):1440–6.
  64. Ingwersen J, Wingerath B, Graf J, Lepka K, Hofrichter M, Schröter F, *et al*. Dual roles of the adenosine A2a receptor in autoimmune neuroinflammation. *J Neuroinflammation*. 2016 Feb 26;13:48.
  65. El Bakkouri K, Wullaert A, Haegman M, Heynincx K, Beyaert R. Adenoviral gene transfer of the NF-kappa B inhibitory protein ABIN-1 decreases allergic airway inflammation in a murine asthma model. *J Biol Chem*. 2005 May 6;280(18):17938–44.
  66. Ganchi PA, Sun SC, Greene WC, Ballard DW. I kappa B/MAD-3 masks the nuclear localization signal of NF-kappa B p65 and requires the transactivation domain to inhibit NF-kappa B p65 DNA binding. *Mol Biol Cell*. 1992 Dec;3(12):1339–52.
  67. Mukherjee S, Kumar R, Tsakem Lenou E, Basrur V, Kontoyiannis DL, Ioakeimidis F, *et al*. Deubiquitination of NLRP6 inflammasome by Cyld critically regulates intestinal inflammation. *Nat Immunol*. 2020 Jun;21(6):626–35.
  68. Ashizuka S, Kita T, Inatsu H, Kitamura K. Adrenomedullin: A Novel Therapeutic for the Treatment of Inflammatory Bowel Disease. *Biomedicines*. 2021 Aug 23;9(8):1068.
  69. Frantz C, Stewart KM, Weaver VM. The extracellular matrix at a glance. *J Cell Sci*. 2010 Dec 15;123(24):4195–200.
  70. Vigier S, Fülöp T, Vigier S, Fülöp T. Exploring the Extracellular Matrix to Create Biomaterials. In: *Composition and Function of the Extracellular Matrix in the Human Body* [Internet]. IntechOpen; 2016 [cited 2024 Feb 15]. Available from: <https://www.intechopen.com/chapters/50447>
  71. Cabral-Pacheco GA, Garza-Veloz I, Castruita-De la Rosa C, Ramirez-Acuña JM, Perez-Romero BA, Guerrero-Rodriguez JF, *et al*. The Roles of Matrix Metalloproteinases and Their Inhibitors in Human Diseases. *International Journal of Molecular Sciences*. 2020 Jan;21(24):9739.
  72. Xiao Q, Ge G. Lysyl Oxidase, Extracellular Matrix Remodeling and Cancer Metastasis. *Cancer Microenviron*. 2012 Apr 13;5(3):261–73.
  73. Danen EHJ. Integrins: An Overview of Structural and Functional Aspects. In: *Madame Curie Bioscience Database* [Internet] [Internet]. Landes Bioscience; 2013 [cited 2024 Feb 12]. Available from: <https://www.ncbi.nlm.nih.gov/books/NBK6259/>
  74. Alberts B, Johnson A, Lewis J, Raff M, Roberts K, Walter P. Cell-Cell Adhesion. In: *Molecular Biology of the Cell* 4th edition [Internet]. Garland Science; 2002 [cited 2024 Feb 15]. Available from: <https://www.ncbi.nlm.nih.gov/books/NBK26937/>
  75. Calderwood DA, Shattil SJ, Ginsberg MH. Integrins and Actin Filaments: Reciprocal Regulation of Cell Adhesion and Signaling\*. *Journal of Biological Chemistry*. 2000 Jul 28;275(30):22607–10.
  76. Kourtidis A, Ngok SP, Anastasiadis PZ. p120 catenin: an essential regulator of cadherin stability, adhesion-induced signaling, and cancer progression. *Prog Mol Biol Transl Sci*. 2013;116:409–32.
  77. Adams JC, Lawler J. The Thrombospondins. *Cold Spring Harb Perspect Biol*. 2011 Oct;3(10):a009712.
  78. Lin X, Patil S, Gao YG, Qian A. The Bone Extracellular Matrix in Bone Formation and Regeneration. *Front Pharmacol*. 2020 May 26;11:757.
  79. Bragdon B, Moseychuk O, Saldanha S, King D, Julian J, Nohe A. Bone Morphogenetic Proteins: A critical review. *Cellular Signalling*. 2011 Apr 1;23(4):609–20.

80. Iemura S ichiro, Yamamoto TS, Takagi C, Uchiyama H, Natsume T, Shimasaki S, *et al.* Direct binding of follistatin to a complex of bone-morphogenetic protein and its receptor inhibits ventral and epidermal cell fates in early *Xenopus* embryo. *Proc Natl Acad Sci U S A*. 1998 Aug 4;95(16):9337–42.
81. Zimmerman LB, De Jesús-Escobar JM, Harland RM. The Spemann organizer signal noggin binds and inactivates bone morphogenetic protein 4. *Cell*. 1996 Aug 23;86(4):599–606.
82. Tucker AS, Al Khamis A, Sharpe PT. Interactions between Bmp-4 and Msx-1 act to restrict gene expression to odontogenic mesenchyme. *Dev Dyn*. 1998 Aug;212(4):533–9.
83. Ducker GS, Rabinowitz JD. One-Carbon Metabolism in Health and Disease. *Cell Metab*. 2017 Jan 10;25(1):27–42.
84. Lu SC. S-Adenosylmethionine. *The International Journal of Biochemistry & Cell Biology*. 2000 Apr 1;32(4):391–5.
85. Wu LG, Hamid E, Shin W, Chiang HC. Exocytosis and Endocytosis: Modes, Functions, and Coupling Mechanisms. *Annu Rev Physiol*. 2014;76:301–31.
86. Langevin C, van der Aa LM, Houel A, Torhy C, Briolat V, Lunazzi A, *et al.* Zebrafish ISG15 Exerts a Strong Antiviral Activity against RNA and DNA Viruses and Regulates the Interferon Response. *J Virol*. 2013 Sep;87(18):10025–36.
87. Leibiger C, Kosyakova N, Mkrtchyan H, Gleib M, Trifonov V, Liehr T. First Molecular Cytogenetic High Resolution Characterization of the NIH 3T3 Cell Line by Murine Multicolor Banding. *J Histochem Cytochem*. 2013 Apr;61(4):306–12.
88. Stepanenko AA, Dmitrenko VV. HEK293 in cell biology and cancer research: phenotype, karyotype, tumorigenicity, and stress-induced genome-phenotype evolution. *Gene*. 2015 Sep 15;569(2):182–90.
89. Williams BR, Prabhu VR, Hunter KE, Glazier CM, Whittaker CA, Housman DE, *et al.* Aneuploidy affects proliferation and spontaneous immortalization in mammalian cells. *Science*. 2008 Oct 31;322(5902):703–9.
90. Hee JS, Cresswell P. Viperin interaction with mitochondrial antiviral signaling protein (MAVS) limits viperin-mediated inhibition of the interferon response in macrophages. Li K, editor. *PLoS ONE*. 2017 Feb 16;12(2):e0172236.
91. Kim JJ, Kim KS, Eom J, Lee JB, Seo JY. Viperin Differentially Induces Interferon-Stimulated Genes in Distinct Cell Types. *Immune Netw*. 2019 Oct 4;19(5):e33.
92. Rivera-Serrano EE, Gizzi AS, Arnold JJ, Grove TL, Almo SC, Cameron CE. Viperin Reveals Its True Function. *Annu Rev Virol*. 2020 Sep 29;7(1):421–46.
93. Gao X, Gao LF, Zhang YN, Kong XQ, Jia S, Meng CY. Huc-MSCs-derived exosomes attenuate neuropathic pain by inhibiting activation of the TLR2/MyD88/NF- $\kappa$ B signaling pathway in the spinal microglia by targeting Rsad2. *Int Immunopharmacol*. 2023 Jan;114:109505.
94. Qiu LQ, Cresswell P, Chin KC. Viperin is required for optimal Th2 responses and T-cell receptor-mediated activation of NF- $\kappa$ B and AP-1. *Blood*. 2009 Apr 9;113(15):3520–9.
95. Eom J, Yoo J, Kim JJ, Lee JB, Choi W, Park CG, *et al.* Viperin Deficiency Promotes Polarization of Macrophages and Secretion of M1 and M2 Cytokines. *Immune Netw*. 2018 Aug 23;18(4):e32.
96. Zhong Z, Liang S, Sanchez-Lopez E, He F, Shalpour S, Lin X jia, *et al.* New mitochondrial DNA synthesis enables NLRP3 inflammasome activation. *Nature*. 2018 Aug;560(7717):198–203.
97. Chang MX, Xiong F, Wu XM, Hu YW. The expanding and function of NLRC3 or NLRC3-like in teleost fish: Recent advances and novel insights. *Developmental & Comparative Immunology*. 2021 Jan 1;114:103859.
98. Lee JH, Wood JM, Almo SC, Evans GB, Harris LD, Grove TL. Chemoenzymatic Synthesis of 3'-Deoxy-3',4'-didehydrocytidine triphosphate (ddhCTP). *ACS Bio Med Chem Au*. 2023 Jul 25;3(4):322–6.
99. Hsu JCC, Laurent-Rolle M, Pawlak JB, Xia H, Kunte A, Hee JS, *et al.* Viperin triggers ribosome collision-dependent translation inhibition to restrict viral replication. *Mol Cell*. 2022 May 5;82(9):1631-1642.e6.
100. Wilson MR, Harkins S, Reske JJ, Siwicki RA, Adams M, Bae-Jump VL, *et al.* PIK3CA mutation in endometriotic epithelial cells promotes viperin-dependent inflammatory response to insulin. *Reprod Biol Endocrinol*. 2023 May 11;21:43.
101. Dong Y, Song C, Wang Y, Lei Z, Xu F, Guan H, *et al.* Inhibition of PRMT5 suppresses osteoclast differentiation and partially protects against ovariectomy-induced bone loss through downregulation of CXCL10 and RSAD2. *Cell Signal*. 2017 Jun;34:55–65.
102. Liu C, Hou L, Zhao Q, Zhou W, Liu K, Liu Q, *et al.* The selected genes NR6A1, RSAD2-CMPK2, and COL3A1 contribute to body size variation in Meishan pigs through different patterns. *J Anim Sci*. 2023 Jan 3;101:skad304.

## Tables

Table 1: Primers used in this study

Primer name	Sequence (5'→3')	Source or reference	Specificities
<b>Plasmid constructs:</b>			
BFP-F	CTGCTGCT <b>GGCTAGCT</b> CTAGACTCGAGATGAGCGAGCTGATTAAGG AGA	pCite-P-BFP	<i>NheI</i>
			<i>XbaI</i> <i>XhoI</i>
BFP-R	CAGCAGCAG <b>AAGCTT</b> TGGTACCCTGCAGGGATCC <b>GATATC</b> GTGCCCC AGTTTGCTAGG	pCite-P-BFP	<i>HindIII</i>
			<i>KpnI</i> <i>PstI</i> <i>BamHI</i> <b><i>EcoRV</i></b>
PpViperin-R0-F	ccaagttggttttgcaagaATGT	JNCE01171228 XM_039667881.1	
PpViperin-R0-R	attgagaaaggTCACCACTCC	JNCE01171228 XM_039667881.1	
PpViperin-P2A-F	GGAAGCGAGCTACTAACTTCAGCCTGCTGAAGCAGGCTGGAGACG TGGAGGAGAACCCTGGACCTATGTTGATGCCATTGTGTTCAAGG	JNCE01171228 XM_039667881.1	<i>P2A</i>
PpViperin-HindIII-R	CTGCTGCTG <b>AAGCTT</b> TCACCACTCCAGTTTCATATCTTCC	JNCE01171228 XM_039667881.1	<b><i>HindIII</i></b>
<b>sgRNA:</b>			
sgRNA-mEGFP-S	<b>TCCTAATACGACTCACTATA</b> GGCGAGGGCGATGCCACCTAGTTTT AGAGCTAGAAATAGCAAGTTAAAATAAGGCTAGTCCGTTATCAAC TTGAAAAAGTGGCACCCGAGTCGGTGCTTTT	(44)	<b>T7 promoter</b> sgRNA target Scaffold
sgRNA-mEGFP-AS	AAAAGCACCGACTCGGTGCCACTTTTTCAAGTTGATAACGGACTA GCCTTATTTTAACTTGCTATTTCTAGCTCTAAAACCTAGGTGGCAT CGCCCTCGCCTATAGTGAGTCGTATTAGGA	(44)	<b>T7 promoter</b> sgRNA target Scaffold
sgRNA-Vip1-S	<b>TCCTAATACGACTCACTATA</b> CGAACGAGGTCTTCGCAGTGGTTTTA GAGCTAGAAATAGCAAGTTAAAATAAGGCTAGTCCGTTATCAACTT GAAAAAGTGGCACCCGAGTCGGTGCTTTT	XM_039667881.1 Coding exon 1	<b>T7 promoter</b> sgRNA target Scaffold
sgRNA-Vip1-AS	AAAAGCACCGACTCGGTGCCACTTTTTCAAGTTGATAACGGACTAG CCTTATTTTAACTTGCTATTTCTAGCTCTAAAACCTGCGAAGAC CTCGTTCGTATAGTGAGTCGTATTAGGA	XM_039667881.1 Coding exon 1	<b>T7 promoter</b> sgRNA target Scaffold
sgRNA-Vip2-S	<b>TCCTAATACGACTCACTATA</b> TGGAGTGGTCACCTGTGCGCGTTTTA GAGCTAGAAATAGCAAGTTAAAATAAGGCTAGTCCGTTATCAACTT GAAAAAGTGGCACCCGAGTCGGTGCTTTT	XM_039667881.1 Coding exon 1	<b>T7 promoter</b> sgRNA target Scaffold
sgRNA-Vip2-AS	AAAAGCACCGACTCGGTGCCACTTTTTCAAGTTGATAACGGACTAG CCTTATTTTAACTTGCTATTTCTAGCTCTAAAACGCGCACAGGTGA CCACTCCA <b>TATAGTGAGTCGTATTAGGA</b>	XM_039667881.1 Coding exon 1	<b>T7 promoter</b> sgRNA target Scaffold
<b>Genotyping:</b>			
mEGFP-gen-F	GGCACC AAAATCAACGGGAC	pmEGFP-N1	
mEGFP-gen-R	GCCGTCGTCCTTGAAGAAGA	pmEGFP-N1	
PpViperin-gen-F	CACACTTCACCACATCAAACCA	LOC120476724	
PpViperin-gen-R	GGTGACATGTTAGATTACCTGCTTC	LOC120476724	

**Table 2: qPCR primers used in this study**

<b>Name</b>	<b>Sequence 5'-3'</b>	<b>Target name</b>	<b>Target accession number</b>	<b>Size</b>	<b>Reference</b>
<b>PpActin-ex-F</b>	TGACGCAGATCATGTTTCGAGA	Beta actin	XM_039687266.1	255 bp	This study
<b>PpActin-ex-R</b>	CCGTGGTGGTGAAGCTGTAA		XM_039652364.1		
<b>PpViperin-ex-F</b>	AGAGGCAAAGCGAGGGTTAC	Radical SAM domain containing 2	XM_039667881.1	214 bp	This study
<b>PpViperin-ex-R</b>	GTCCAAGTAGTCACCGTATTTCTG				
<b>PpMx1-ex-F</b>	CCAGGGGTAGTGGAATTGTTACA	Interferon-induced GTP-binding protein Mx	XM_039657463.1	161 bp	This study
<b>PpMx1-ex-R</b>	CTCATCCTGGGCTTCACGAA				
<b>PpPKR-ex-F</b>	ACAGAGACCTGAAGCCTCCAA	Eukaryotic translation initiation factor 2-alpha kinase 2	XM_039649056.1	173 bp	This study
<b>PpPKR-ex-R</b>	GGATGTTTGAGTCGCTTGCTC				
<b>PpStat2-ex-F</b>	TCAAAGTAGAGGTGATGGAGCA	Signal transducer and activator of transcription 2	XM_039689152.1	206 bp	This study
<b>PpStat2-ex-R</b>	AGCACCATCCAACATAGCCG				

## Figures

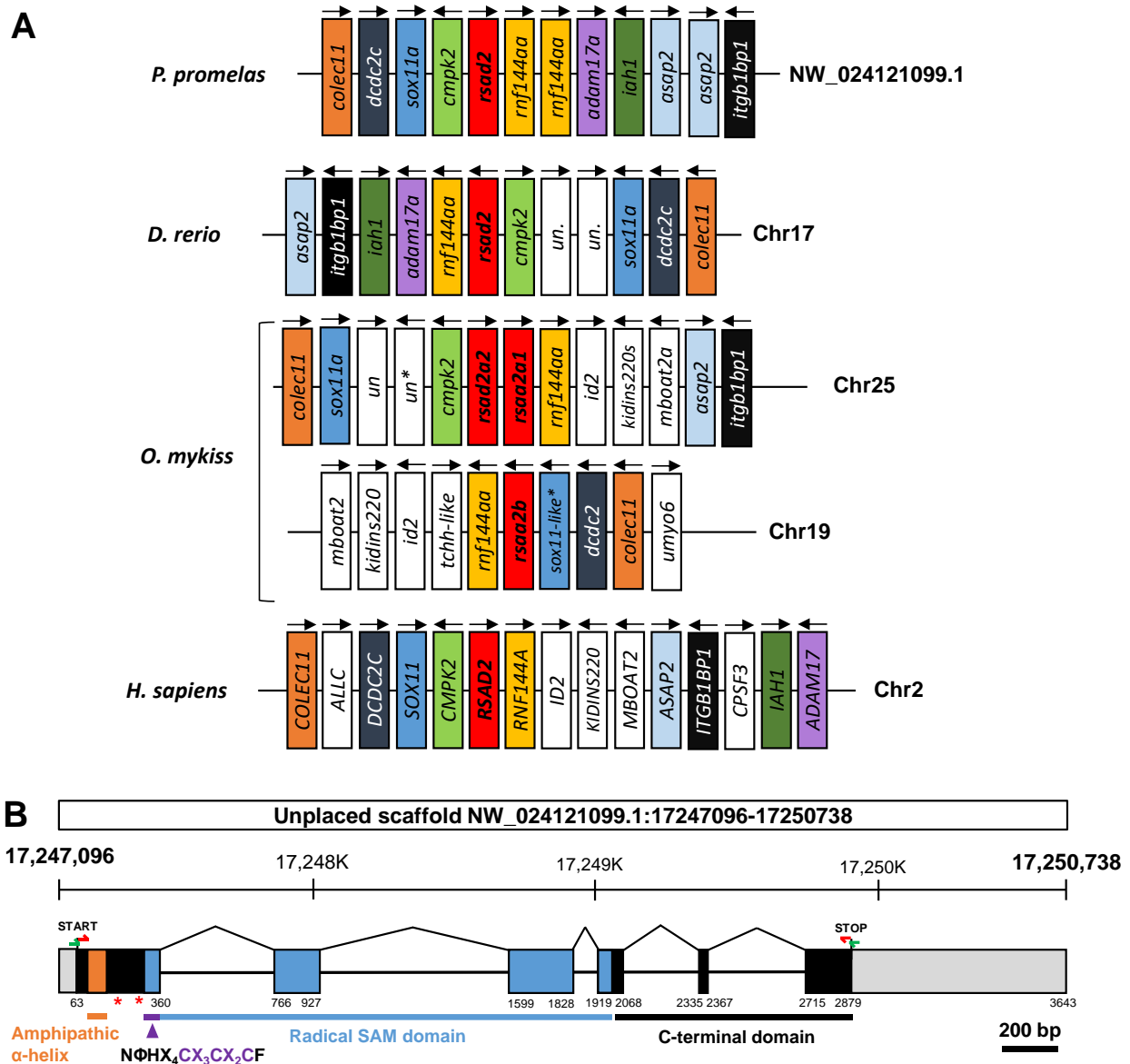


**Figure 1: Synteny and genomic location of the likely unique *viperin* gene in the fathead minnow genome.**

(A) Synteny analysis of *viperin* loci in fathead minnow (*Pimephales promelas*, LOC120476724, unplaced scaffold NW\_024121099.1, EPA\_FHM\_2.0), zebrafish (*Danio rerio*, LOC570456, GRCz11), rainbow trout (*Oncorhynchus mykiss*, LOC100135876, LOC110504183, LOC110498119, USDA\_OmykA\_1.1) and human (*Homo sapiens*, LOC91543, GRCh38.p13). The synteny was predicted using information extracted from recently released NCBI reference genomes. (B) Exon/intron structure of *P. promelas viperin* gene. Boxes represent exons and straight lines represent introns; grey boxes denote untranslated regions while colored and black boxes denote translated regions. Exonic parts encoding the N-terminal amphipathic  $\alpha$ -helix domain (orange), the central radical SAM domain (blue) and the invariant motif responsible for binding Fe-S cluster (purple), which is included in a longer motif conserved among all ddhNTP synthases are represented. The location of each predicted domain or motif was obtained using SMART (Simple Modular Architecture Research Tool). The location of sgRNA-Vip1 and sgRNA-Vip2 is indicated by a red star. Nested PCR primers, used to amplify the *viperin* CDS are indicated by green and red arrows.

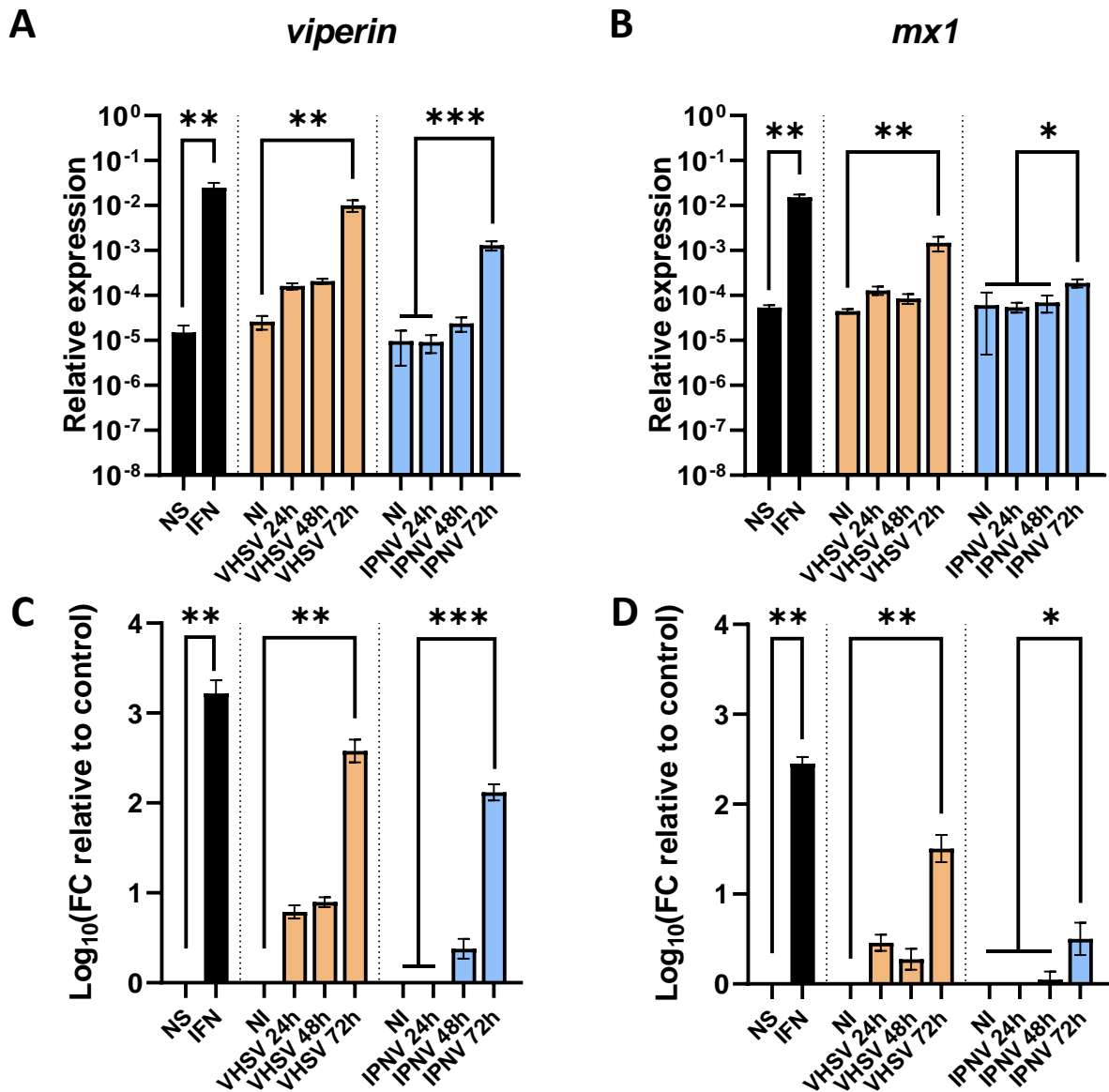


**Figure 2: viperin and mx1 expression in EPC-EC cells during type I IFN stimulation and viral infection.**

EPC-EC cells were stimulated with recombinant type I IFN (24h), infected with rVHSV-Tomato (MOI 0.05) or IPNV31.75 (MOI 0.001) for 24 to 72h post-infection, or left untreated (NI, non-infected; NS, non-stimulated). (**A,B**) Relative expression levels of *viperin* and *mx1* genes. (**C,D**) Fold change relative to non-stimulated or non-infected controls. Black bars show means  $\pm$  SD from 2 pooled independent experiments (n=3 for each experiment), orange bars show means  $\pm$  SD (n=4) and blue bars show means  $\pm$  SD from 2 pooled independent experiments (n=4 for each experiment), \*, p < 0.05, \*\*, p < 0.01, \*\*\*, p < 0.001, Kruskal-Wallis test with Dunn's post-hoc multiple comparison tests.

Results 2 – Viperin

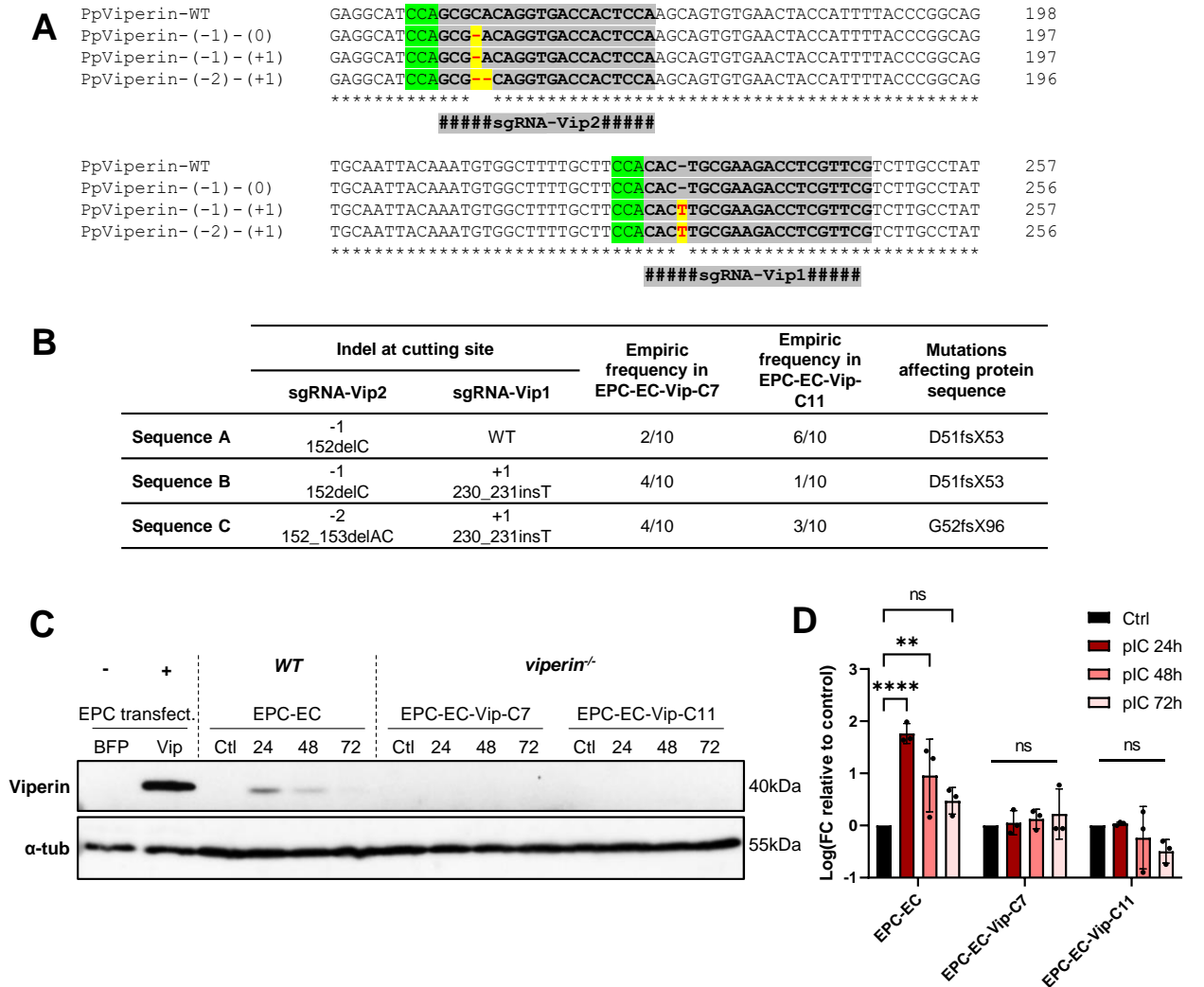


**Figure 3: Development and validation of a *viperin*<sup>-/-</sup> cell line.**

(A) Genotype of EPC-EC cells (WT) and EPC-EC-Viperin-C7 and -C11 clones obtained from sequencing of purified PCR products amplified from genomic DNA from each cell line and subcloned by TOPO TA cloning. The locations of the sgRNA-Vip1, sgRNA-Vip2 are highlighted in grey; the protospacer adjacent motif is in green and the indels in mutated sequences are in red highlighted in yellow. The corresponding amino acid sequences are available in [Additional file 2](#). (B) Table summarizing the molecular characteristics of EPC-EC-Viperin-C7 and -C11 clones. (C) Validation of the viperin knockout by western blot. EPC-EC and EPC-EC-Viperin clones were stimulated with poly(I:C) (500 µg/mL) for 24-72h; positive and negative controls are EPC cells transfected with pcDNA3.1-Hyg-BFP or pcDNA3.1-Hyg-BFP-P2A-Viperin, respectively. Cell lysates were separated by SDS-PAGE and immunoblotted with antibodies against Viperin and  $\alpha$ -tubulin ( $\alpha$ -tub). Full length blots are available in [Additional file 3](#). (D) Densitometric quantification of (B). Viperin signal intensity normalized to  $\alpha$ -tubulin signal intensity and graphed as fold change relative to non-stimulated cells. Bars show means  $\pm$  SD from 3 pooled independent experiments; ns, non-significant, \*\*,  $p < 0.01$ , \*\*\*\*,  $p < 0.0001$ , ordinary two-way ANOVA with Tukey's post-hoc multiple comparison tests.

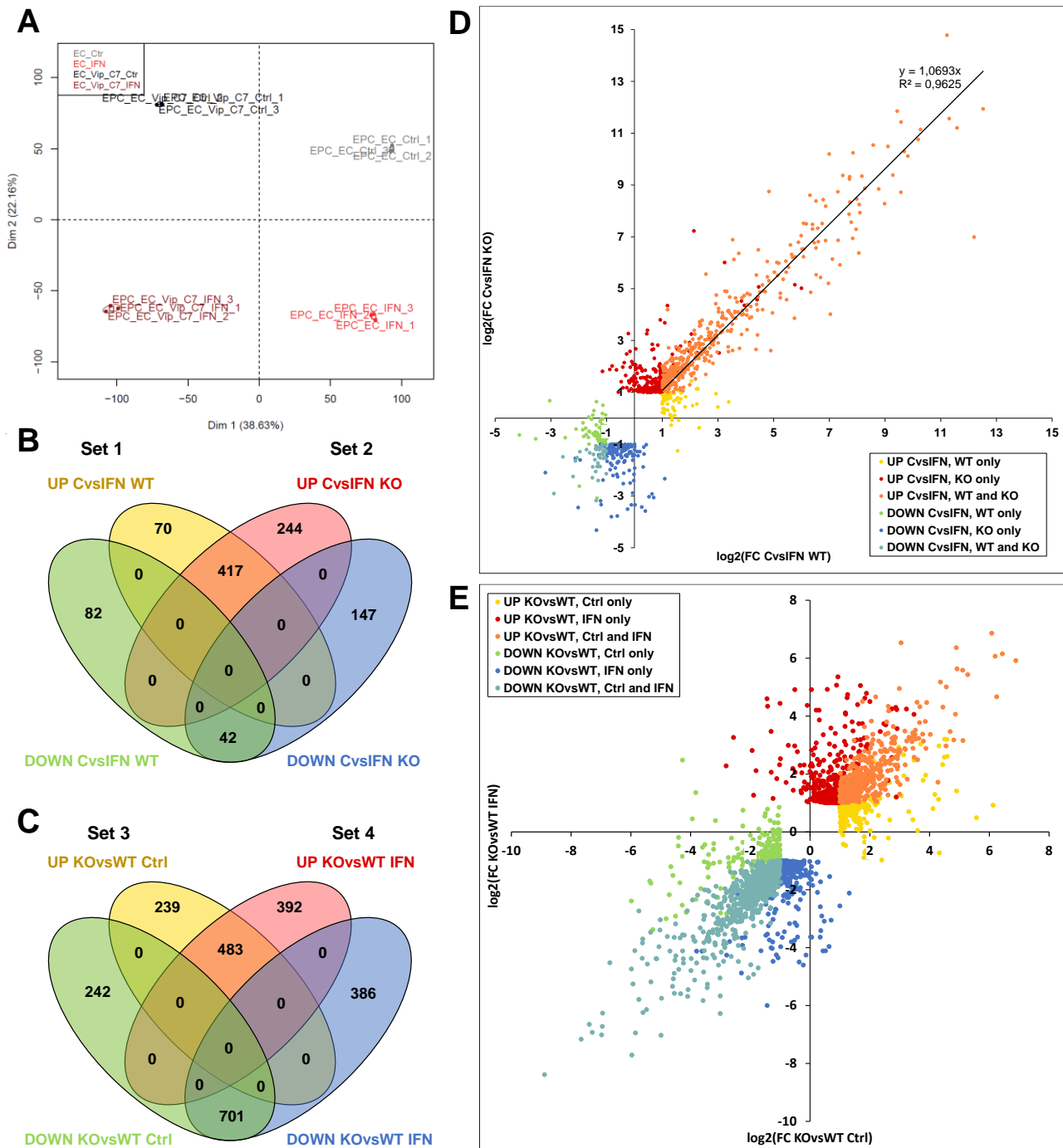


**Figure 4: Comparison of DEGs in *viperin*<sup>-/-</sup> and WT cell lines (steady state vs. IFN simulation).**

(A) Principal component analysis plot showing the distribution of all samples ( $n=3$  for each condition). Projection on the two first axes is shown (dimension 1: horizontal axis; dimension 2: vertical axis). (B) Venn diagram showing DEGs after IFN stimulation compared to non-stimulated condition (Ctrl) in the WT cell line (set 1) and in the *viperin*<sup>-/-</sup> cell line (set 2). (C) Venn diagram showing DEGs in the *viperin*<sup>-/-</sup> cell line compared to the WT cell line at the steady state (set 3) or following IFN simulation (set 4). Genes were considered DEGs if they met the following criteria:  $\log_2(\text{foldchange (FC)}) > 1$  or  $< -1$  and adjusted  $p$  value  $< 0.05$ . (D) Dotplot showing the fold change distribution of DEGs in the *viperin*<sup>-/-</sup> cell line compared to the WT cell line at the steady state (x-axis) and following IFN treatment (y-axis). (E) Dotplot showing the fold change distribution of DEGs upon IFN treatment compared to non-stimulated condition in the WT cell line (x-axis) and in the *viperin*<sup>-/-</sup> cell line (y-axis).

Results 2 – Viperin

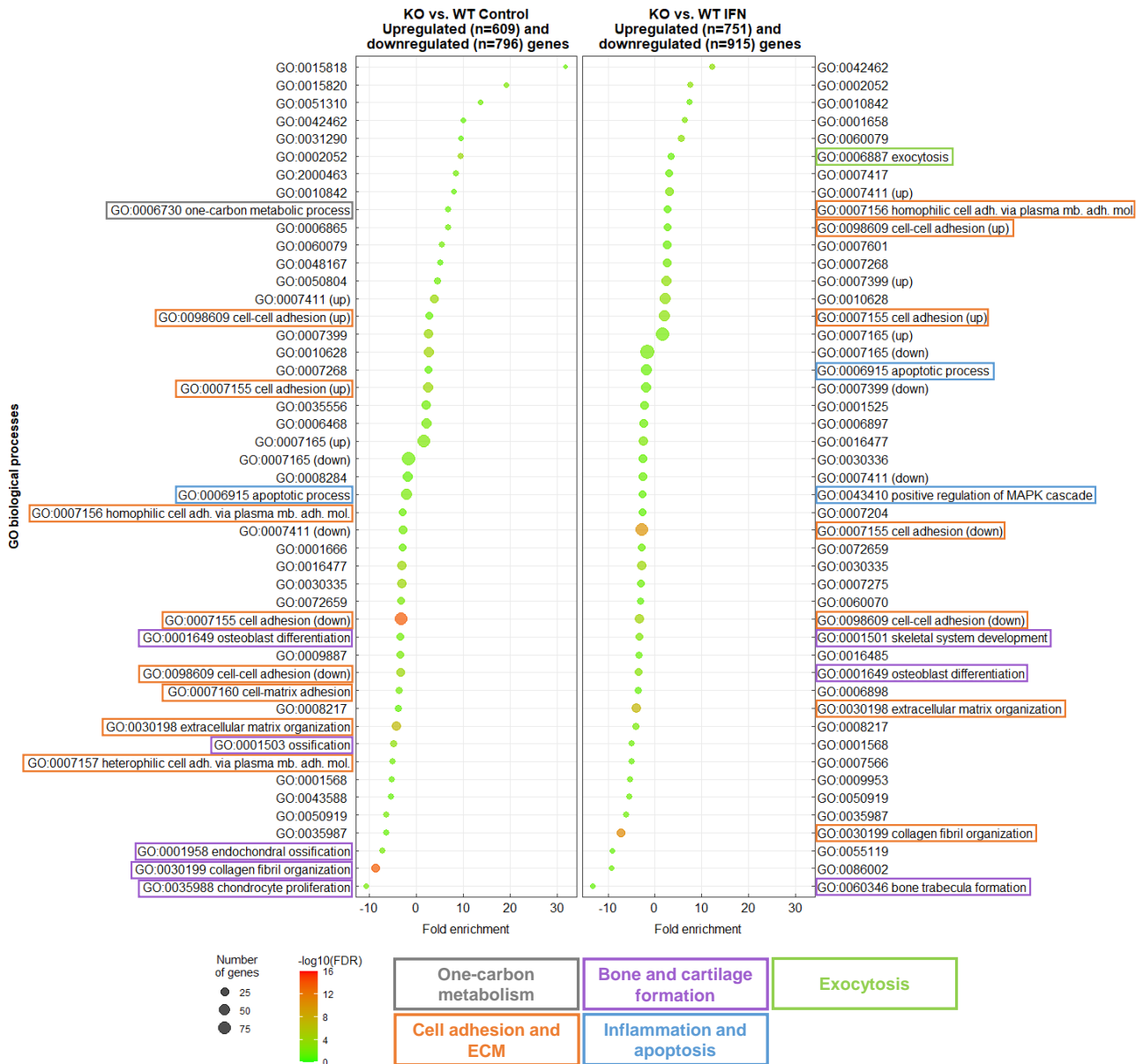


**Figure 5: Gene enrichment suggests Viperin is involved in distinct biological processes in non-induced and induced conditions.**

Gene ontology analysis from the lists of genes differentially expressed the *viperin*<sup>-/-</sup> cell line compared to the WT at the steady state (left panel) and upon type I IFN stimulation (right panel). GO terms have been filtered to show results with a Benjamini statistical score <0.05. The size of the dot represents the number of genes involved within each biological process; colors indicate  $-\log_{10}$  (False Discovery Rate) and colored boxes represent biological functions.

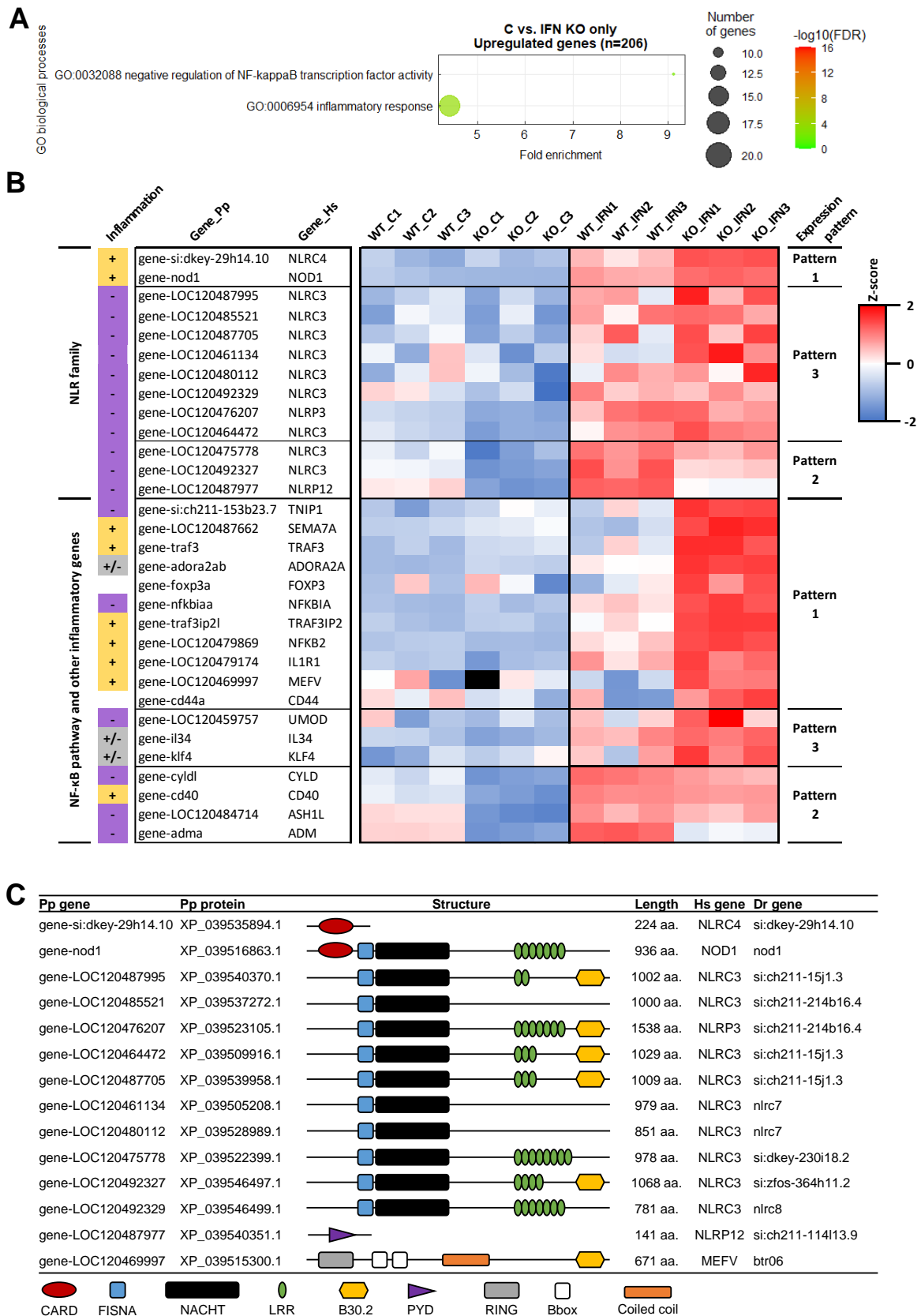


**Figure 6: Viperin modulates the inflammatory response by downregulating pro-inflammatory genes and upregulating NF-κB pathway regulators.**

(A) Gene ontology analysis obtained from the list of genes exclusively upregulated in the *viperin*<sup>-/-</sup> cell line following type I IFN treatment. GO terms have been filtered to show results with a Benjamini statistical score <0.05. The size of the dot represents the number of genes involved within each biological process; colors indicate  $-\log_{10}(\text{False Discovery}$

Rate) and colored boxes represent biological functions. **(B)** Heatmap of genes associated to the selected GO terms in (A). Colors from blue to red represent the Z-score, which was calculated on a gene-by-gene basis by subtracting the overall mean of the log-transformed counts across all samples from the log-transformed count value of each gene, and then dividing that result by the overall standard deviation. Z-scores were calculated to ensure that the expression patterns were not overwhelmed by the expression values. Pattern 1 corresponds to genes showing no expression difference between both cell lines at the steady state but a higher induction in the *viperin*<sup>-/-</sup> cell line compared to the WT upon IFN treatment; pattern 2 corresponds to genes that are less expressed in the *viperin*<sup>-/-</sup> cell line versus WT at the steady state and upon type I IFN treatment but show higher fold change (Ctrl vs. IFN) in the *viperin*<sup>-/-</sup> cell line; pattern 3 corresponds to the genes that show no significant expression difference between both cell lines at the steady state and upon type I IFN stimulation but still display a higher fold change (Ctrl vs. IFN) in the *viperin*<sup>-/-</sup> cell line. Purple and yellow boxes indicate the anti- and pro-inflammatory functions known for the mammalian genes. Full-length heatmaps are available in [Additional file 12](#). **(C)** Schematic representation of the structural domains of the NLRs listed in (B). CARD = Caspase recruitment domain, FISNA = Fish-specific NACHT associated domain, LRR = leucine-rich repeat (LRR), PYD = Pyrin domain, RING = RING-type zinc finger domain, Bbox = B-Box-type zinc finger domain, B30.2 = PRY-SPRY domain.

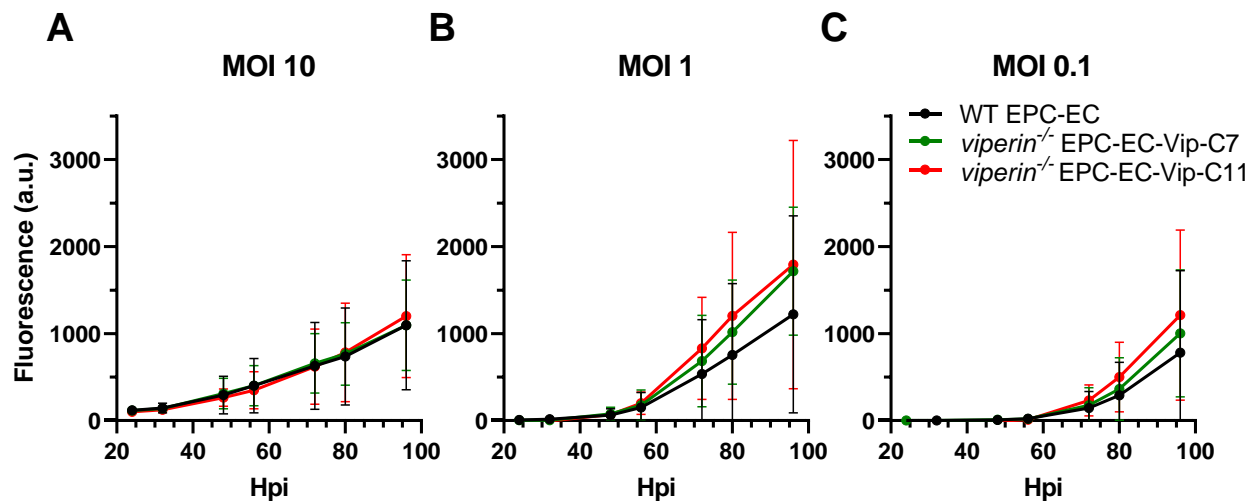


**Figure 7: The *viperin* knockout has no significant impact on rVHSV-Tomato replication.**

EPC-EC (WT), EPC-EC-Vip-C7 and EPC-EC-Vip-C11 (*viperin*<sup>-/-</sup>) cells were infected with rVHSV-Tomato at **(A)** MOI 10, **(B)** MOI 1 or **(C)** MOI 0.1 and fluorescence was measured at different time points post-infection. Graphs show means  $\pm$  SD from 6 independent experiments (n=8 for each experiment).

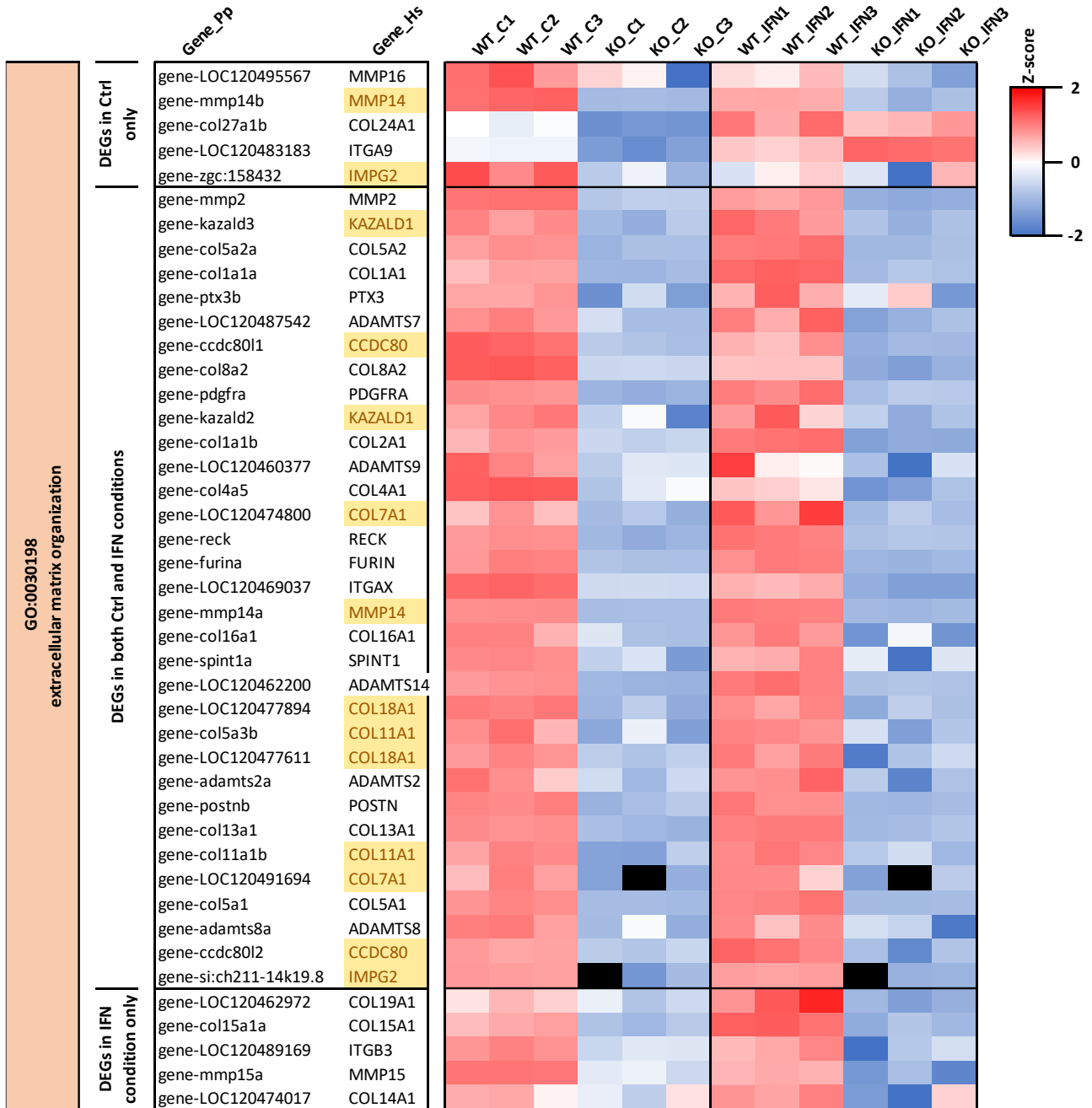


**Figure 8: Viperin modulates the extracellular matrix organization regardless of its induction status.**

Heatmap of genes associated to GO:0030198 extracellular matrix organization and differentially expressed in the *viperin*<sup>-/-</sup> cell line compared to the WT cell line at the steady state and upon IFN treatment. Colors from blue to red represent the Z-score (defined in Figure 6); human genes highlighted in yellow indicate duplicates. Full-length heatmaps are available in Additional file 12.

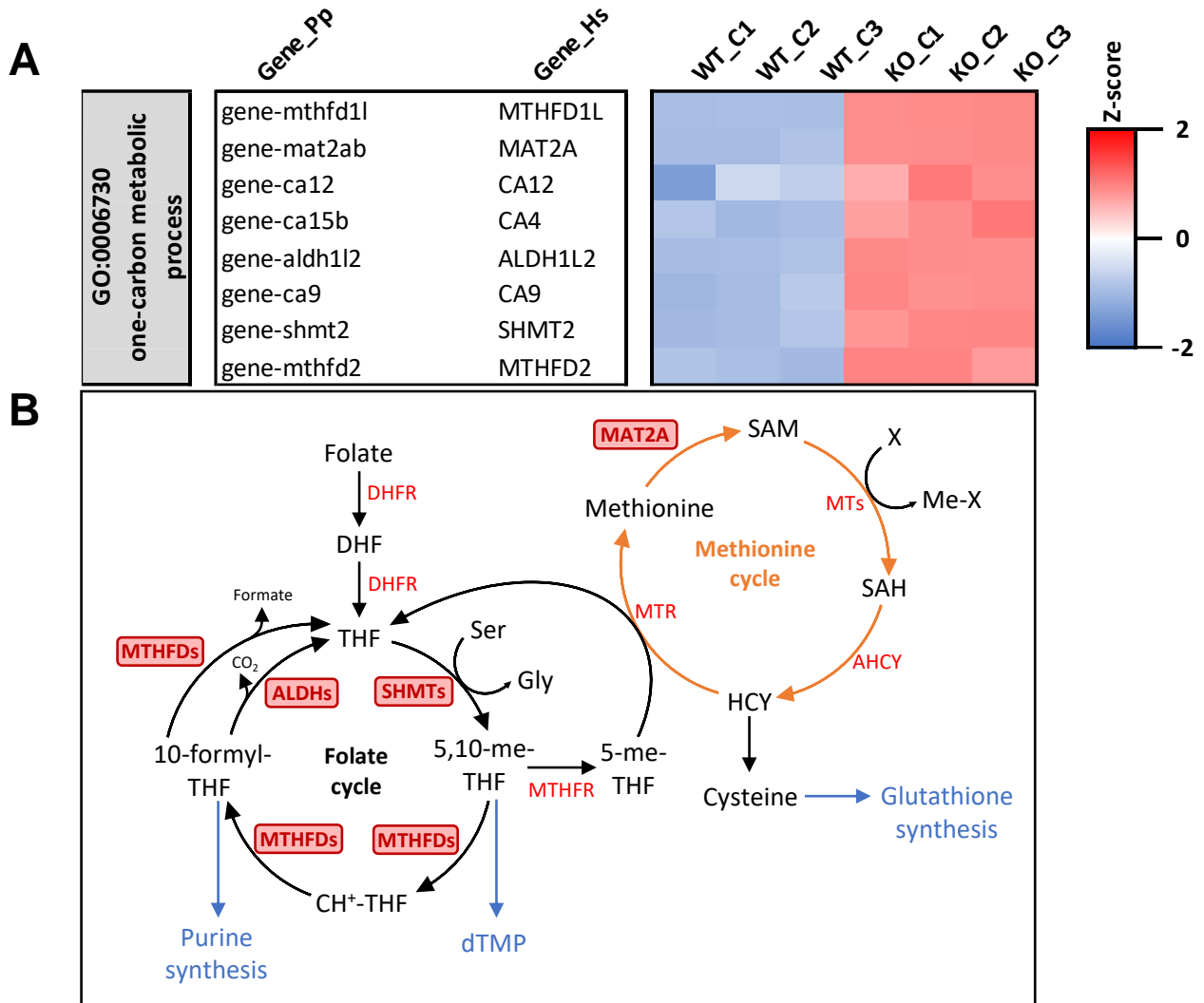


**Figure 9: Viperin downregulates one-carbon metabolism.**

(A) Heatmap of genes associated to selected GO terms and differentially expressed in the *viperin*<sup>-/-</sup> cell line compared to the WT cell line at the steady state. Colors from blue to red represent the Z-score (defined in [Figure 6](#)). Full-length heatmaps are available in [Additional file 12](#). (B) Schematic representation of one-carbon metabolism. 1C metabolism includes the methionine and folate cycles, which are central to multiple cellular functions. Metabolic intermediates are in black, enzymes are in red and red boxes indicate enzymes upregulated in the *viperin*<sup>-/-</sup> cell line. DHF, dihydrofolate; THF, tetrahydrofolate; 5,10-me-THF (*aka.* 5,10-CH<sub>2</sub>-THF), 5,10-methylene-THF; CH<sup>+</sup>-THF, methenyl-THF; 10-formyl-THF (*aka.* 10-CHO-THF); SAM, S-adenosylmethionine; SAH, S-adenosylhomocysteine; HCY, homocysteine; dTMP, deoxythymidine monophosphate; DHFR, dihydrofolate reductase; SHMT, serine hydroxymethyl transferase; MTHFD, methylenetetrahydrofolate dehydrogenase; ALDH, aldehyde dehydrogenase; MTHFR, methylenetetrahydrofolate reductase; MTR, methionine synthase; MAT2A, methionine adenosyltransferase 2A; MT, methyl transferase; AHCY, adenosylhomocysteinase.

Additional files

```
>PpViperin-LOC120476724-exon1
ATGTTGATGCCATTGTGTTTCAAGGACGTCCACAGCTTATTTTCAGCCCTGTTGAGATGGATTTTGATGATGGTATCAGGCACACTGGTGTCTCTGGGATGATCA
GTCGTCCAAAGATTTCGCACCAGAGCAGAAAGAGGGATCCAGCGCACAGGTGACCACCTCCAAGCAGTGTGAAC TACCATTTTACCCGGCAGTGC AAT
#####sgRNA-Vip2#####
TACAAATGTGGCTTTTGCTTCCACACTGCGAAGACCTCGTTCCGTTTTCGCTATTGAAGAGGCAAAGCGAGGGTTACGACTTCTGAAAGAAGCAG
#####sgRNA-Vip1#####
```

Clones	sgRNA	Primers	ICE deconvoluted sequences
EPC-EC-Vip-C7	sgRNA-Vip2	Vip-gen-F	
	sgRNA-Vip1	Vip-gen-R	
EPC-EC-Vip-C11	sgRNA-Vip2	Vip-gen-F	
	sgRNA-Vip1	Vip-gen-R	

Additional file 1: Alignment of chromatograms from *viperin*<sup>-/-</sup> EPC-EC-Viperin clones with EPC-EC (WT) cell line.

Chromatograms showing edited and wild-type (control) sequences in the region around the sequences targeted by sgRNA-Vip1 and sgRNA-Vip2 from EPC-EC-Viperin-C7 and EPC-EC-Viperin-C11 (*viperin*<sup>-/-</sup>) clones. The horizontal black line represents the guide sequence; the horizontal red dotted line corresponds to the PAM site; the vertical black dotted line represents the actual cut site. The red and purple boxes show the inserted or deleted nucleotides in each edited clone. Alignments were obtained using Synthego ICE Analysis tool (v3). Note that for the reverse sequence from EPC-EC-Viperin-C11, ICE results could not be used due to the fact that the cut site was too close from sequence start; the alignment was done manually instead.

Results 2 – Viperin

>PpViperin-WT

MLMPLCFKDVHSFFSALLRWILMMVSGTLVSLGMISRPKIRTREQKEASSAQQVTPSSVNYHFTRQCNYKCGFCFHTAKTSFVLPPIEEAKRGLRLLKEAG  
 MEKINFSGGEPFLHERGSFLGELVRYCKQELLLPSVSVSNGSLIKESWFQKYGDYLDILAVSCDSFNEDTNKVI GRGQGGKSHLDNLHKVCSWCRDYKV  
 AFKINSVINTYNVDEDMTEQITALNPVRWKVFQCLLDIGENAGENS LREA EK FVISEQQFQDFLDRHKSVKCLVPESNQKMRDS **YLILDEYMRFLDCREG**  
**RKDPKSVLDVGVVEEAIKFSGFDEKMFLIRGGKY**VWSKEDMKLEW

>PpViperin-(-1)-(0)

MLMPLCFKDVHSFFSALLRWILMMVSGTLVSLGMISRPKIRTREQKEASSDR\***PLQAV\*TTILPGSAITNVAFASTLRRPRSSCLLKRQSEGYDF\*KKQE**  
**WKKSTFQVESPFMREALFWESWSDTANRSCCFRASA SLVMAV\*SKNPGFRNTVTTWTF LQYLAIVLTKTPIKSLAEVRARRAI\*TICIKFVPGAGTTRW**  
**LSKSTF\*STPTMWTKI\*QSRSLL\*TQCAGRSSVC\*LMVKTLGRTASARQKNLSLVSSNSKTSWTAIRASSVWFQSLIKR\*ETLT\*FLMNICASWIAERGG**  
**KIRQSPFWMLVWKRPSVSVLMRRCSS\*EGGNMCGARKI\*NWSG**

>PpViperin-(-1)-( +1)

MLMPLCFKDVHSFFSALLRWILMMVSGTLVSLGMISRPKIRTREQKEASSDR\***PLQAV\*TTILPGSAITNVAFASTLAKT**SFVLPPIEEAKRGLRLLKEAG  
 MEKINFSGGEPFLHERGSFLGELVRYCKQELLLPSVSVSNGSLIKESWFQKYGDYLDILAVSCDSFNEDTNKVI GRGQGGKSHLDNLHKVCSWCRDYKV  
 AFKINSVINTYNVDEDMTEQITALNPVRWKVFQCLLDIGENAGENS LREA EK FVISEQQFQDFLDRHKSVKCLVPESNQKMRDS **YLILDEYMRFLDCREG**  
**RKDPKSVLDVGVVEEAIKFSGFDEKMFLIRGGKY**VWSKEDMKLEW

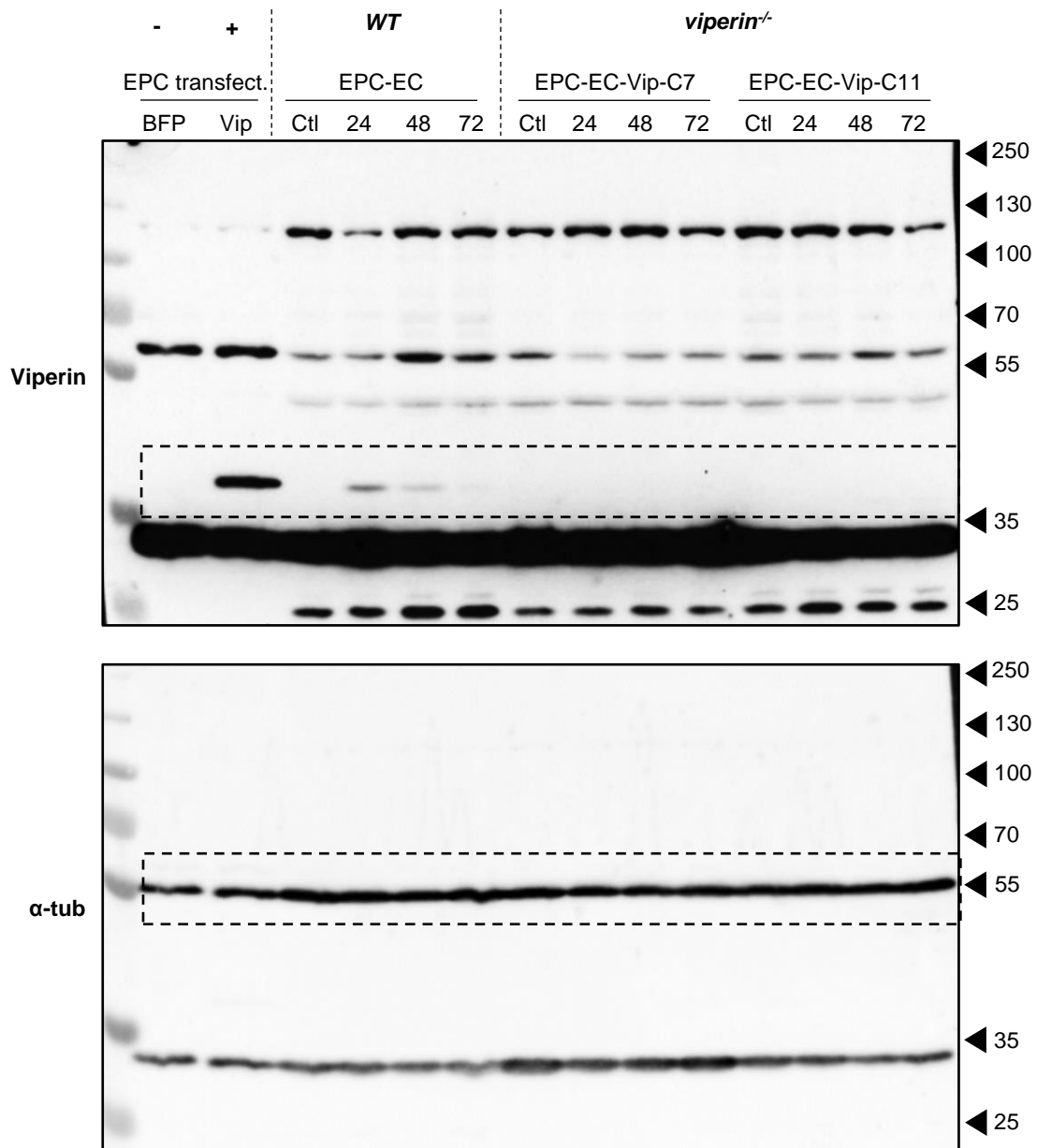
>PpViperin-(-2)-( +1)

MLMPLCFKDVHSFFSALLRWILMMVSGTLVSLGMISRPKIRTREQKEASSA**DDHSKQCELPFYPAVQLQMWLLPHLRRPRSSCLLKRQSEGYDF\*KKQE**  
**WKKSTFQVESPFMREALFWESWSDTANRSCCFRASA SLVMAV\*SKNPGFRNTVTTWTF LQYLAIVLTKTPIKSLAEVRARRAI\*TICIKFVPGAGTTRW**  
**LSKSTF\*STPTMWTKI\*QSRSLL\*TQCAGRSSVC\*LMVKTLGRTASARQKNLSLVSSNSKTSWTAIRASSVWFQSLIKR\*ETLT\*FLMNICASWIAERGG**  
**KIRQSPFWMLVWKRPSVSVLMRRCSS\*EGGNMCGARKI\*NWSG**

**Additional file 2: Amino acid sequences corresponding to the mutated viperin sequences amplified from genomic DNA from WT EPC-EC and *viperin*<sup>-/-</sup> EPC-EC-Viperin-C7 and -C11 and subcloned by TOPO TA cloning.**

The first amino acids affected by a frameshift are in red, the frameshifts are in green and the premature end of the polypeptides are represented by a red star. The immunogen peptide recognized by the anti-viperin antibody (PA5-42231, Invitrogen) is outlined in black.

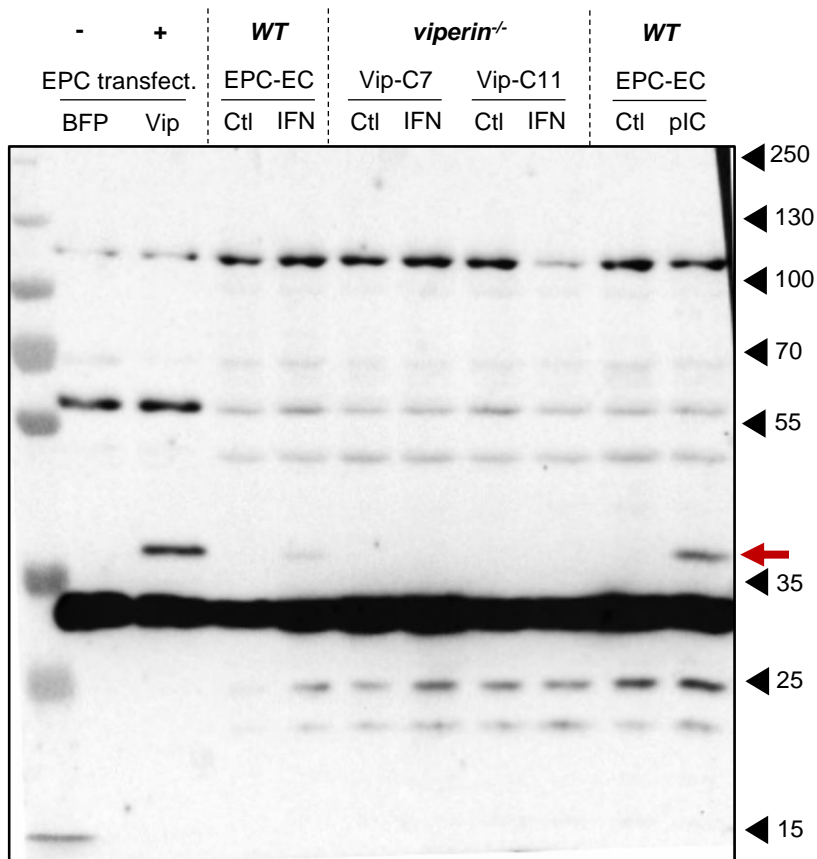
Results 2 – Viperin



**Additional file 3: Original full-length blots used in figure 3 to validate the *viperin<sup>-/-</sup>* cell lines.**

Regions corresponding to the cropped images are surrounded by a dotted line.

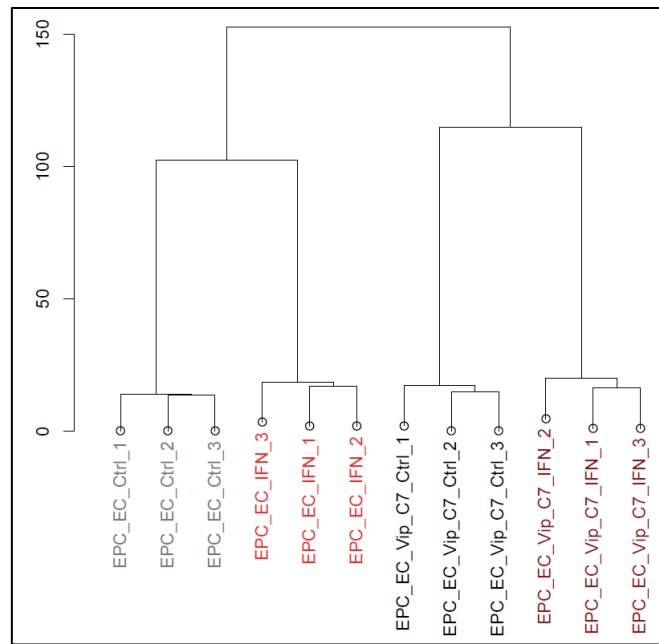
Results 2 – Viperin



**Additional file 4: Validation of the *viperin* knockout by western blot using type I IFN supernatant as an inducer.**

EPC-EC and EPC-EC-Viperin clones were stimulated with recombinant type I IFN supernatant (1:10) for 24h; positive and negative controls are EPC cells transfected with pcDNA3.1-Hyg-BFP or pcDNA3.1-Hyg-BFP-P2A-Viperin, respectively. EPC-EC cells stimulated with poly(I:C) (500 µg/mL, 24h) were also included for comparison purposes. Cell lysates were separated by SDS-PAGE and immunoblotted with antibodies against Viperin. The red arrow indicates the Viperin protein.

## Results 2 – Viperin

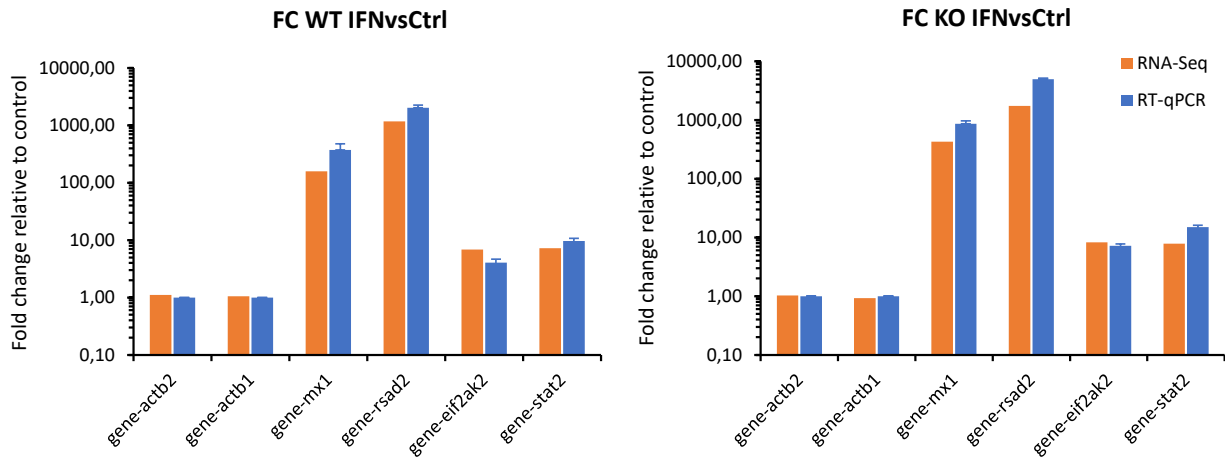


**Additional file 5: Descriptive analysis of RNAseq results from WT EPC-EC and *viperin*<sup>-/-</sup> EPC-EC-Vip-C7 (KO) stimulated with type I IFN or left untreated (Ctrl).**

Euclidian clustering showing the distribution of all samples (n=3 for each condition).

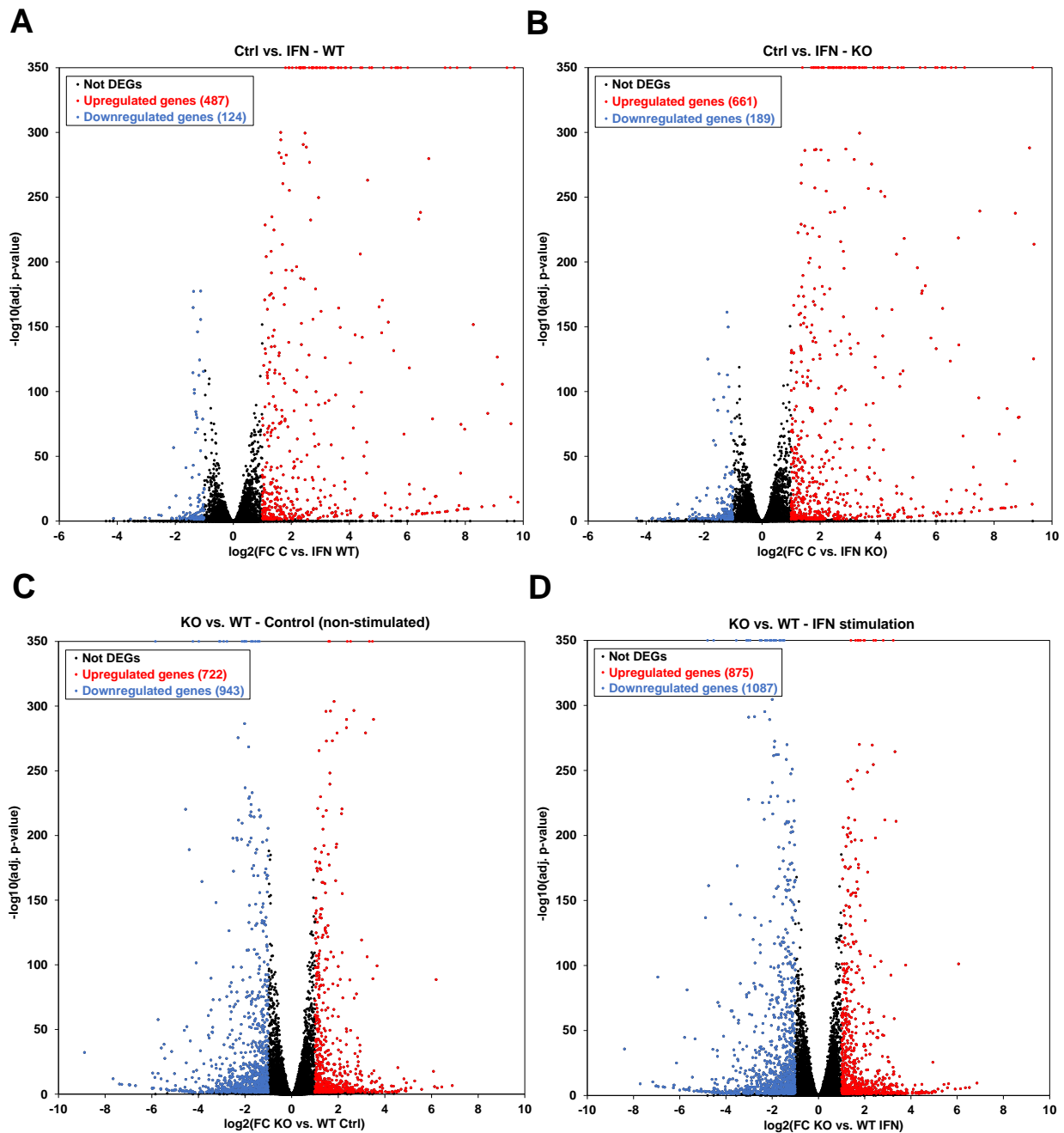
**Additional file 6: Tables showing differentially expressed transcripts in WT EPC-EC and *viperin*<sup>-/-</sup> cell lines at the steady state and following type I IFN stimulation.**

[Additional\_file\_6.xls – not included in this manuscript]



#### Additional file 7: Validation of RNA-Seq data by RT-qPCR analysis on a selected number of ISGs.

The expression levels of the following genes were analyzed by RT-qPCR and compared to RNA-Seq data: *beta-actin* (gene-actb2, LOC120489986 and gene-actb1, LOC120463340), *mx1* (gene-mx1, LOC120468849), *viperin* (gene-rsad2, LOC120476724), *pkp* (gene-eif2ak2, LOC120460990) and *stat2* (gene-stat2, LOC120491376). Orange and blue bars represent RNA-Seq data and RT-qPCR results, respectively.

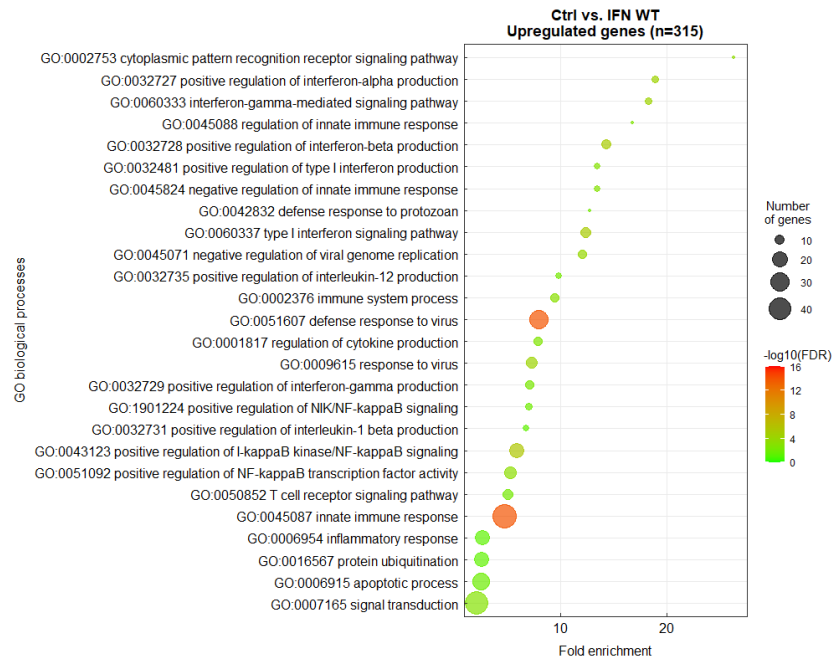


**Additional file 8: Volcano plots showing differentially expressed genes in WT EPC-EC and *viperin*<sup>-/-</sup> EPC-EC-Vip-C7 (KO) stimulated with type I IFN or left untreated (Ctrl).**

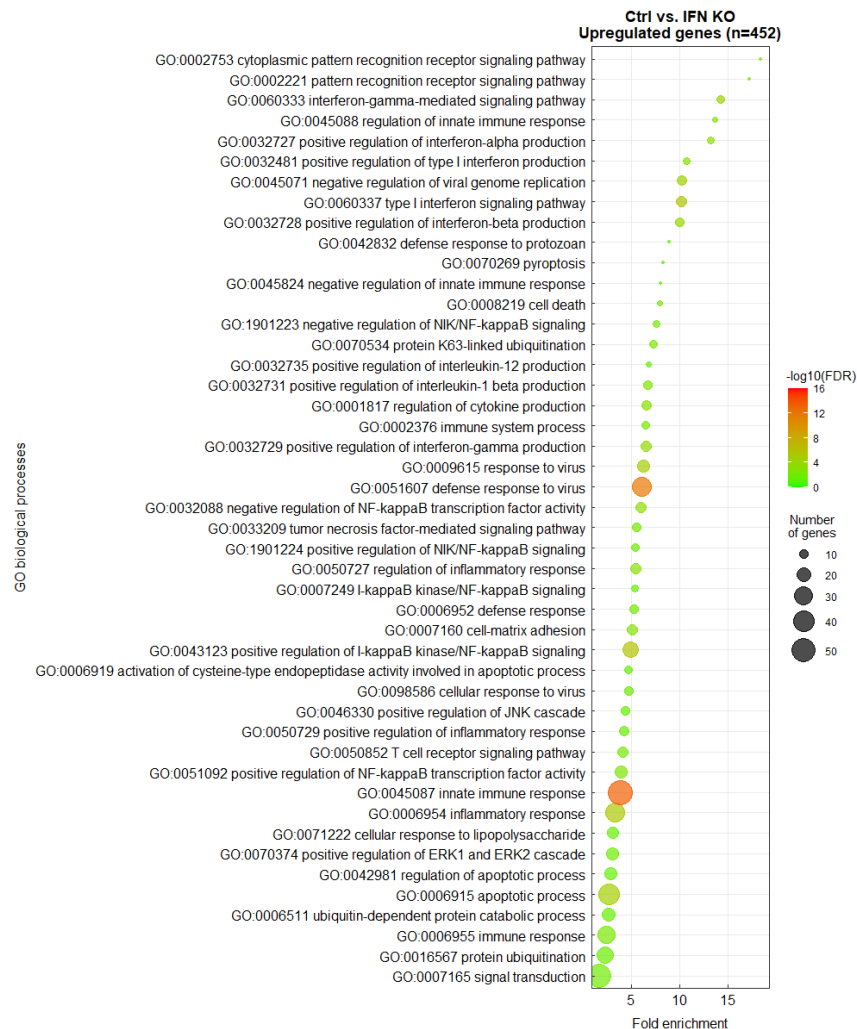
(A,B) Volcano plots showing DEGs after IFN stimulation compared to non-stimulated condition (Ctrl) in the WT cell line (A) and in the *viperin*<sup>-/-</sup> cell line (B). (C,D) Volcano plots showing DEGs ( $\log_2(\text{foldchange (FC)}) > 1$  or  $< -1$ , adjusted p.value  $< 0.05$ ), in the *viperin*<sup>-/-</sup> cell line compared to the WT cell line at the steady state (C) or following IFN stimulation (D). Red dots represent upregulated genes while blue dots represent downregulated genes.

## Results 2 – Viperin

**A**



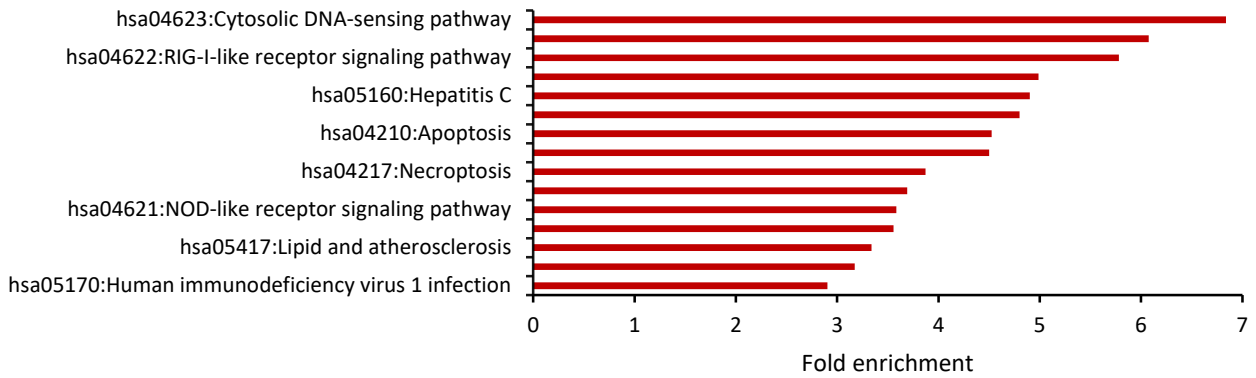
**B**



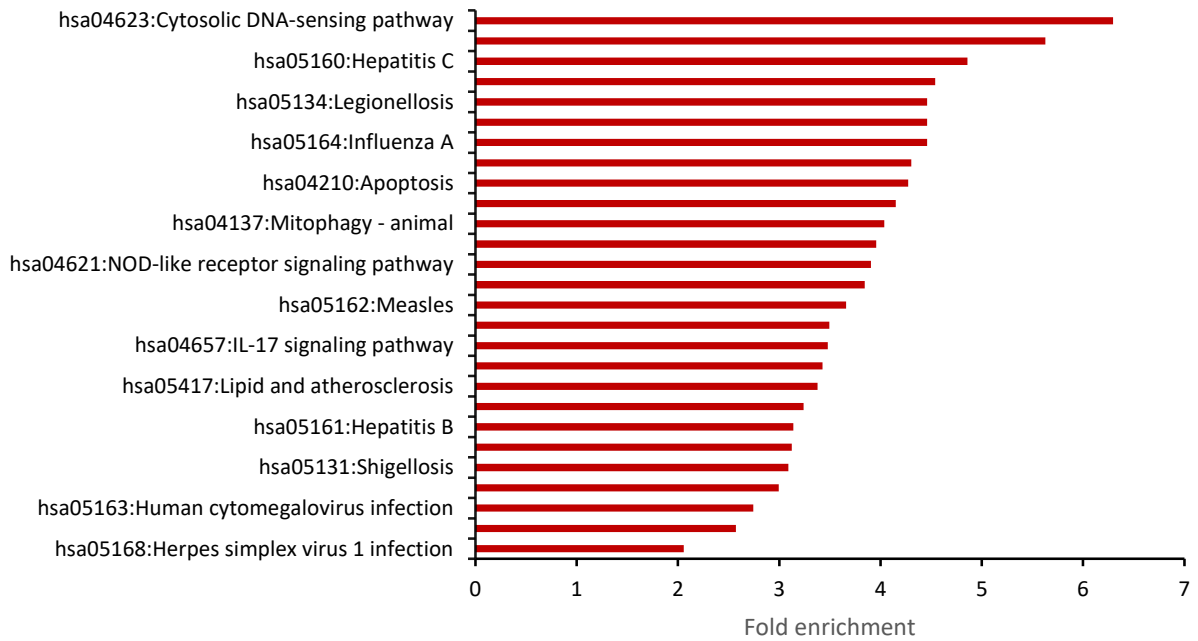
**Additional file 9: Gene ontology analysis of DEGs upon IFN treatment compared to non-stimulated condition in the WT cell line (A) and in the *viperin*<sup>-/-</sup> cell line (B).**

GO terms have been filtered to show results with a Benjamini statistical score <0.05. The size of the dot represents the number of genes involved within each biological process and colors represent  $-\log_{10}(\text{False Discovery Rate})$ .

**Ctrl vs. IFN WT  
Upregulated genes (n = 165)**

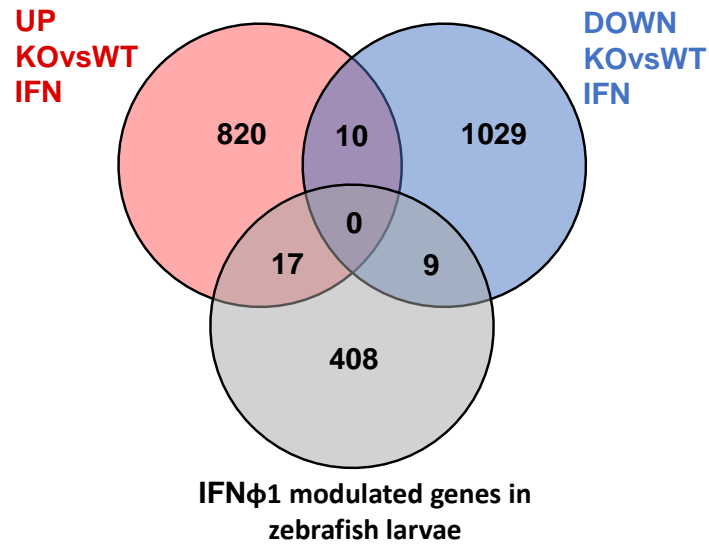


**Ctrl vs. IFN KO  
Upregulated genes (n = 233)**



**Additional file 10: KEGG pathway analysis of the DEGs upon IFN treatment compared to the control in the WT and in the *viperin*<sup>-/-</sup> cell lines.**

KEGG pathway terms have been filtered to show results with a Benjamini statistical score <0.05.



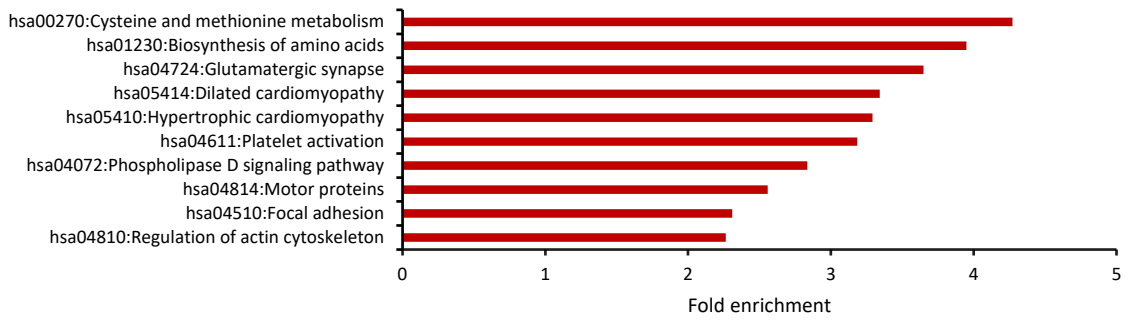
**Additional file 11: Venn diagram showing DEGs in the *viperin*<sup>-/-</sup> cell line compared to the WT cell line following type I IFN treatment and previously identified IFNφ1 modulated genes in zebrafish larvae.**

The list of IFNφ1 modulated genes comes from Levraud et al., 2019<sup>15</sup>. For comparison purposes, the the zebrafish best Blast hit corresponding to each DEG in the list (considered as the zebrafish ortholog) was used, explaining why some genes are found in both UP and DOWN categories.

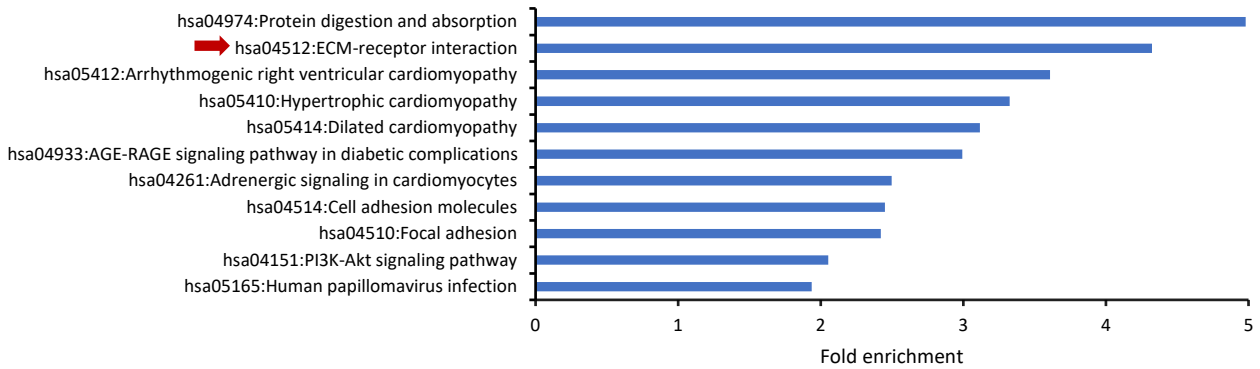
**Additional file 12: Full-length heatmaps of genes associated to selected GO terms.**

**[Additional\_file\_12.xls – not included in this manuscript]**

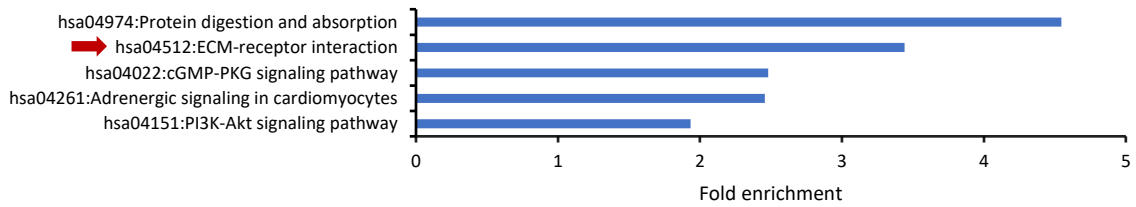
**KO vs. WT Ctrl**  
**Upregulated genes (n = 343)**



**KO vs. WT Ctrl**  
**Downregulated genes (n = 396)**



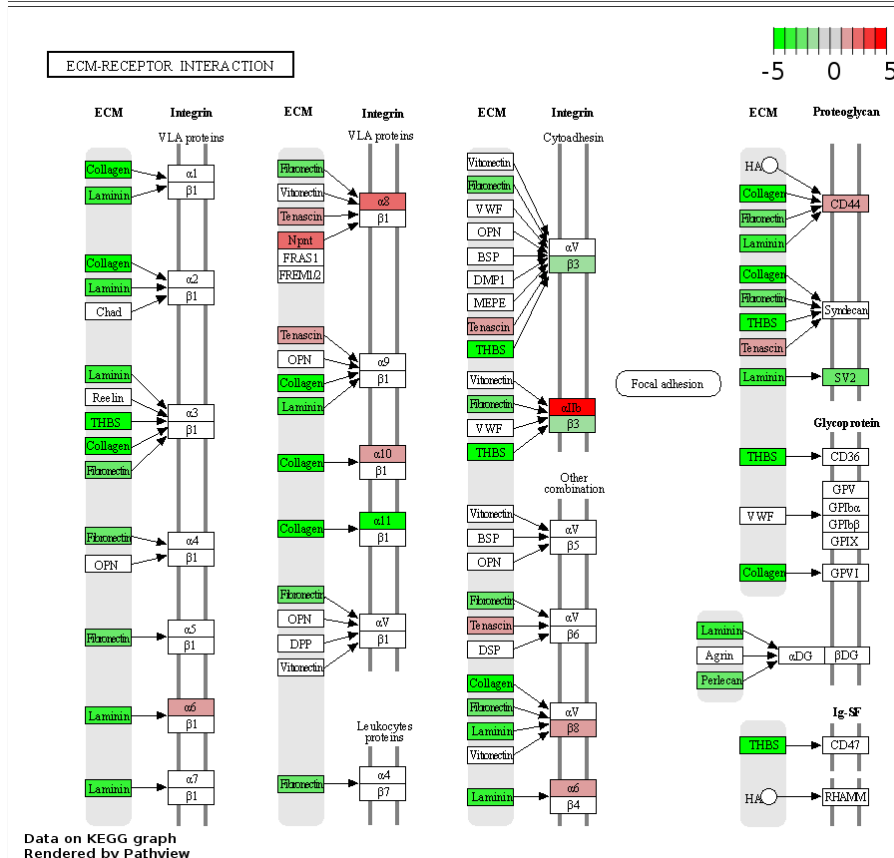
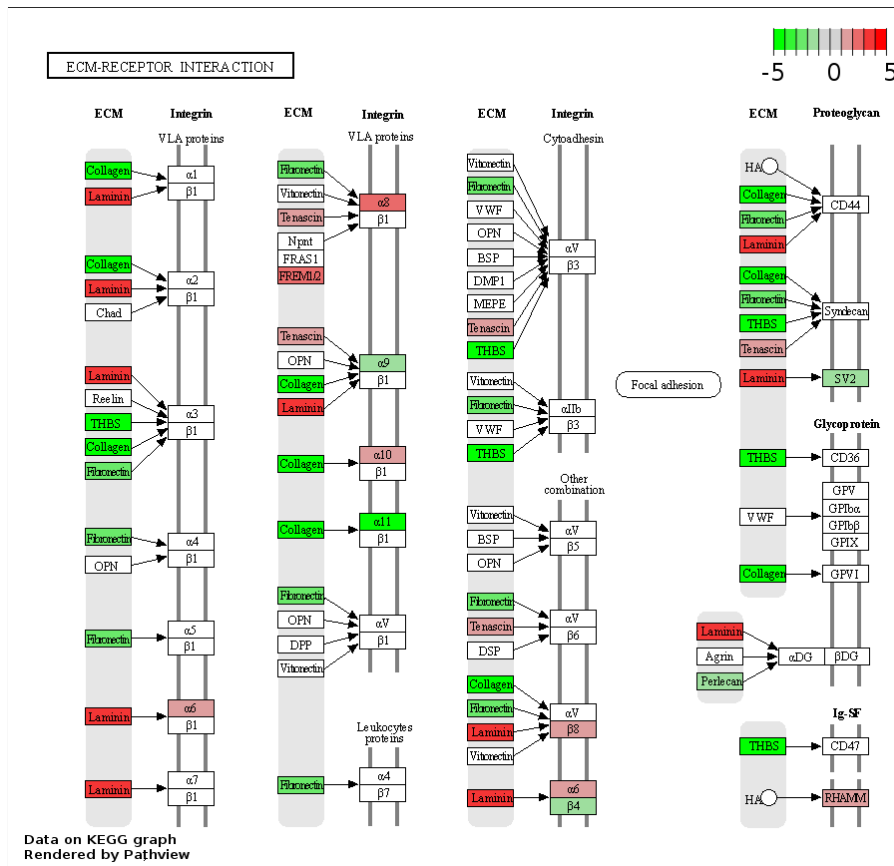
**KO vs. WT IFN**  
**Downregulated genes (n = 470)**



**Additional file 13: KEGG pathway analysis of the DEGs in the *viperin*<sup>-/-</sup> cell line compared to the WT cell line at the steady state.**

KEGG pathway terms have been filtered to show results with a Benjamini statistical score <0.05. Red arrows indicate pathways detailed in [Additional file 14](#).

Results 2 – Viperin



**Additional file 14: Modulation of ECM-receptor interactions in the *viperin*<sup>-/-</sup> cell line compared to the WT cell line at the steady state (upper panel) and upon IFN stimulation (lower panel).**

DEG datasets were mapped onto the pathway using Pathview. Green and red colors show down- and upregulation, respectively.

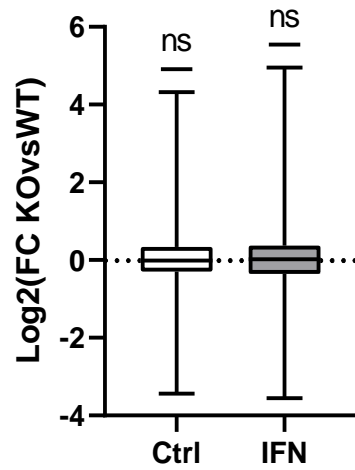
## Additional file 15: Genotyping results from EPC-EC-Vip-C7 and EPC-EC-Vip-C11 subclones.

Parental cell line	Subclones		sgRNA-Vip2 TGGAGTGGTCACTGTGCGC					sgRNA-Vip1 CGAACGAGGTCTTCGAGTG		
			Sequence	Analysis type	KO-Score	R <sup>2</sup>	Indel	Sequence	Analysis type	Indel <sup>a</sup>
EPC-EC-Vip-C7	1	EPC-EC-Vip-C7-sub2	Vip-gen-F	ICE	100	0.98	{-1: 71% ; -2: 29%}	Vip-gen-R	Manual	+1/WT
	2	EPC-EC-Vip-C7-sub3	Vip-gen-F	ICE	100	0.98	{-1: 70% ; -2: 30%}	Vip-gen-R	Manual	+1/WT
	3	EPC-EC-Vip-C7-sub4	Vip-gen-F	ICE	99	0.98	{-1: 69% ; -2: 28%}	Vip-gen-R	Manual	+1/WT
	4	EPC-EC-Vip-C7-sub5	Vip-gen-F	ICE	100	0.98	{-1: 71% ; -2: 29%}	Vip-gen-R	Manual	+1/WT
	5	EPC-EC-Vip-C7-sub6	Vip-gen-F	ICE	100	0.97	{-1: 67% ; -2: 21%}	Vip-gen-R	Manual	+1/WT
	6	EPC-EC-Vip-C7-sub8	Vip-gen-F	ICE	100	0.98	{-1: 71% ; -2: 29%}	Vip-gen-R	Manual	+1/WT
	7	EPC-EC-Vip-C7-sub9	Vip-gen-F	ICE	100	0.98	{-1: 70% ; -2: 29%}	Vip-gen-R	Manual	+1/WT
	8	EPC-EC-Vip-C7-sub10	Vip-gen-F	ICE	100	0.98	{-1: 51% ; -2: 48%}	Vip-gen-R	Manual	ND
	9	EPC-EC-Vip-C7-sub11	Vip-gen-F	ICE	99	0.98	{-1: 69% ; -2: 30%}	Vip-gen-R	Manual	+1/WT
	10	EPC-EC-Vip-C7-sub12	Vip-gen-F	ICE	100	0.98	{-1: 70% ; -2: 28%}	Vip-gen-R	Manual	+1/WT
EPC-EC-Vip-C11	1	EPC-EC-Vip-C11-sub1	Vip-gen-F	ICE	100	0.98	{-1: 71% ; -2: 28%}	Vip-gen-R	Manual	WT/+1
	2	EPC-EC-Vip-C11-sub2	Vip-gen-F	ICE	100	0.98	{-1: 72% ; -2: 26%}	Vip-gen-R	Manual	WT/+1
	3	EPC-EC-Vip-C11-sub4	Vip-gen-F	ICE	100	0.98	{-1: 70% ; -2: 30%}	Vip-gen-R	Manual	WT/+1
	4	EPC-EC-Vip-C11-sub5	Vip-gen-F	ICE	100	0.98	{-1: 71% ; -2: 29%}	Vip-gen-R	Manual	WT/+1
	5	EPC-EC-Vip-C11-sub7	Vip-gen-F	ICE	100	0.98	{-1: 73% ; -2: 27%}	Vip-gen-R	Manual	WT/+1
	6	EPC-EC-Vip-C11-sub9	Vip-gen-F	ICE	100	0.98	{-1: 71% ; -2: 29%}	Vip-gen-R	Manual	WT/+1
	7	EPC-EC-Vip-C11-sub10	Vip-gen-F	ICE	100	0.98	{-1: 69% ; -2: 28%}	Vip-gen-R	Manual	WT/+1

Indels at sgRNA-Vip2 cut site were analyzed using forward sequences with Synthego ICE analysis tool v3. Indels at sgRNA-Vip1 cutsite were manually analyzed using reverse sequences, as ICE was unable to perform the analysis due to the too short reading window around this cutsite. ICE KO-score indicates the proportion of indels leading to a frameshift; R<sup>2</sup> indicates how well the proposed distribution fits the sequence of the edited sample.

<sup>a</sup> Percentage values could not be inferred but the order indicates which sequence is predominant in the chromatograms (*e.g.* in EPC-EC-Vip-C7-sub2, the sequence presenting a 1-nt insertion is predominant over the WT sequence).

**NW\_024121099.1**



**Additional file 16: Comparison of expression pattern of genes (n=925) located on the scaffold NW\_024121099.1 in EPC-EC-Vip-C7 cells compared to EPC-EC cells at the steady state (Ctrl) and following IFN treatment (IFN).**

No increase in “gene expression” was detected. ns, non-significant, one sample t-test.

### 3. Summary and conclusion

Our comparative study of the whole transcriptomes of WT and *viperin*<sup>-/-</sup> cells shows that Viperin is not involved in positive feedback loops of the canonical type I IFN response, suggesting that, in this cell line, Viperin is only an effector of the type I IFN response *stricto sensu*. Our data further indicate that it modulates the expression of a subset of genes involved in the inflammatory response by downregulating specific pro-inflammatory genes and upregulating repressors of the NF-κB pathway. In addition, Viperin also appears to be involved in the regulation of metabolic pathways, including one carbon metabolism, bone formation, extracellular matrix organization and cell adhesion, even under non-induced conditions (Figure 29). These findings support the emerging notion that Viperin may play a role in metabolic processes beyond the scope of the antiviral response. They also open up new avenues of research to elucidate how Viperin can be involved in the regulation of so many diverse and seemingly unrelated processes.

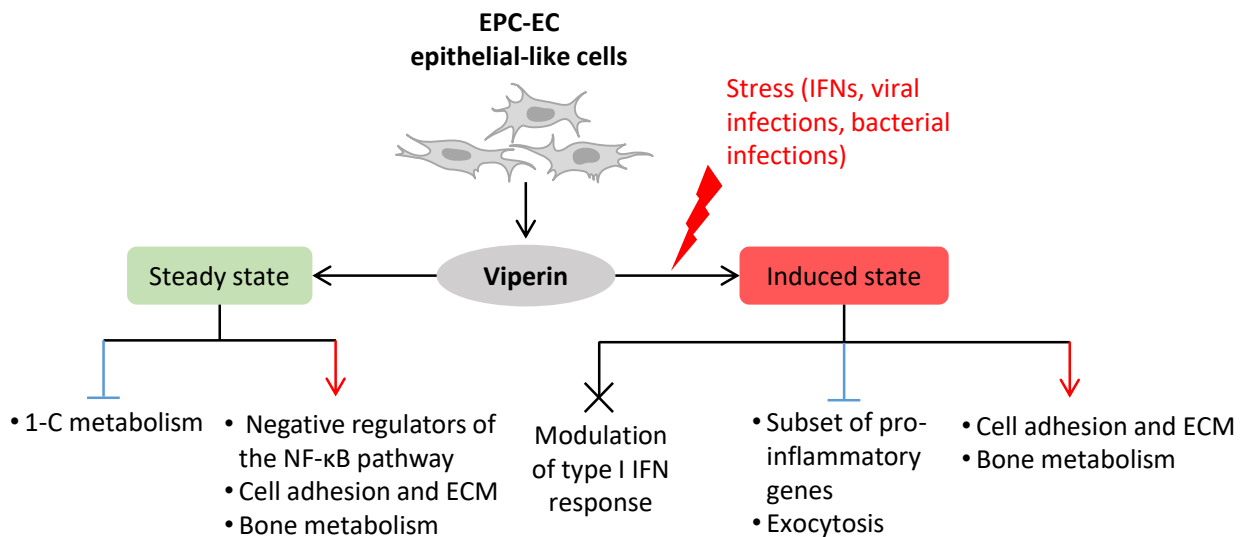


**Figure 29: Diagram of the different pathways regulated by Viperin in epithelial-like EPC-EC cells**

---

## RESULTS 3

### Characterization of cell lines persistently infected with IPNV

---

#### 1. Preamble

This chapter is not part of my thesis objectives *per se*; however, this impromptu study was a big part of my thesis journey, and as such, is included in this manuscript. Indeed, during the first year of my PhD, I developed an initial *pkr*<sup>-/-</sup> cell line and as I was testing its permissivity to viral infections, I realized the supernatants from the ‘non-infected’ control cells were contaminated by a virus which induced no CPE on these cells but appeared to be lytic once transferred onto CHSE-214. Further RT-qPCR studies confirmed that these cells were persistently infected with an IPNV strain, likely IPNV 31.75<sup>566</sup>, as this was the strain primarily used for infections at that time (winter 2021). To date, when and how this persistent infection occurred remains a mystery. Nonetheless, we speculate it initially came from a contaminated pipette. At that time, the COVID crisis was in full swing and we were experiencing many supply shortages, particularly of filter tips. It is possible that the persistent infection stemmed from an initial contamination of the flasks with a minute dose of viral particles that were in a pipette previously used with an unfiltered tip. In any case, we decided to characterize these persistently infected cells over several passages to determine whether this persistence was retained over time. The following chapter describes the experiments performed to characterize these persistently IPNV-infected cell lines.

#### 2. Introduction

Infectious pancreatic necrosis (IPN) is an acute and highly infectious viral disease causing substantial mortality in salmonid juveniles and in smolts when they have just been transferred to sea water<sup>567</sup>. IPN is historically regarded as one of the most economically damaging diseases to the aquaculture industry but the selection of IPN-resistant salmon has largely contributed to limiting high-mortality IPN outbreaks since the 2010s<sup>511–513</sup>. Nonetheless, recent outbreaks in genetically resistant fish in Chile and Norway highlight the fact that IPN still represents a latent threat to the salmon industry<sup>514,515</sup>.

The etiological agent of IPN is a non-enveloped dsRNA virus (IPNV) belonging to the genus *Aquabirnavirus* within the family *Birnaviridae*. The genome of IPNV is composed of two segments, segment A (~3.1 kb) and segment B (~2.8 kb)<sup>567,568</sup>. Segment A contains 2 overlapping ORFs: the long ORF encodes a polyprotein, pVP2-VP4-VP3 and the short ORF encodes a non-structural protein

VP5, which was suggested to have anti-apoptotic properties <sup>569</sup>. The polyprotein pVP2-VP4-VP3 is co-translationally cleaved by the VP4 protease at specific cleavage sites to generate the immature precursor of the major capsid pVP2 protein, the minor capsid protein VP3, which associates with the genome segments, and VP4 <sup>567,570</sup>. pVP2 is further processed into mature VP2 and small peptides which remain associated to the virion <sup>571</sup>. Segment B encodes the RNA-dependent RNA polymerase VP1, which is covalently linked to the 5' end of each dsRNA segment <sup>567</sup>.

Knowledge on the different steps of IPNV replication cycle is limited. Several lines of evidence suggest that attachment to host cells occurs through VP2 resulting in virion endocytosis *via* the macropinocytosis pathway <sup>567,572</sup>. A pVP2-derived peptide then induces endosome permeabilization by creating pores in the endosomal membrane <sup>573,574</sup>. The detailed mechanisms involved in the replication of birnaviruses following cell entry are currently unclear. Recent studies based on avian birnaviruses have shown that replication takes place within cytoplasmic “virus factories” displaying features of liquid-liquid phase separation <sup>575,576</sup>. Transcription is primed by VP1 and proceeds according to a semi-conservative strand-displacement mechanism <sup>568</sup>. Virion assembly occurs as soon as genome replication has been initiated, resulting in immature pro-virions containing viral precursor proteins which are further processed into mature infectious virions following precursor cleavage <sup>577</sup>. Virus release is believed to occur upon cell lysis caused by apoptosis and necrosis <sup>272,567</sup>.

Although IPNV is a lytic virus during acute infection, it is known for its capacity to establish a persistent infection both *in vivo* and *in vitro* <sup>567</sup>. In fact, a high proportion of fish surviving an IPNV outbreak become long-term asymptomatic carriers, thereby constituting an important reservoir for horizontal and vertical transmission of the virus <sup>180,578</sup>. In carrier fish, persistent IPNV was found in head kidney leukocytes and macrophages <sup>181,579</sup>. IPNV was also reported to induce persistent infections *in vitro* in various cell lines, including Chinook salmon CHSE-214 <sup>580-583</sup>, rainbow trout STE-137 <sup>580,581</sup>, RTG-2 <sup>179,581</sup> and the reporter cell line RTG-P1 <sup>179</sup> as well as fathead minnow EPC <sup>584,585</sup>. Most of these persistently IPNV-infected fish cell lines presented all the canonical characteristics of persistently infected cells <sup>586</sup>, including no morphological difference from normal virus-free cells, continuous production of infectious virions over passages, detection of viral antigens in cells, resistance to superinfection with IPNV and susceptibility to heterologous viruses <sup>179,580-583,585,587</sup>.

The underlying molecular and immunological mechanisms involved in the establishment and maintenance of IPNV persistence both *in vivo* and *in vitro* remain largely unknown. It is likely that persistence results from a tight balance between viral replication and host defense mechanisms. So far, several non-exclusive mechanisms resulting in the establishment of viral persistence have been

proposed including evasion and/or modulation of the host's immune response, generation of defective interfering particles and modulation of other host pathways<sup>583,586</sup>.

In this study, we characterized two persistently IPNV-infected Chinook salmon cell lines, a WT cell line and a *pkr*<sup>-/-</sup> cell line, both deriving from a parental CHSE-EC cell line. We observed that the extracellular titers of persistent IPNV periodically oscillated over the course of passages in both cell lines and that they correlated – at least partially – with variations in intracellular viral replication. Our results further indicate that the host innate immune response is dampened during persistent infection and that *pkr* expression does not play a key role during IPNV persistence. Taken together, these findings suggest that persistent IPNV has evolved strategies to evade the host innate immune response by inhibiting the expression of innate immune genes, while maintaining a low replication level.

### 3. Material and methods

#### 3.1. Cell lines, culture conditions and viruses

The Chinook salmon (*Oncorhynchus tshawytscha*) embryo (CHSE-214) cell line was maintained in Glasgow's modified Eagle's medium (GMEM) containing 25 mM HEPES (Biosera) supplemented with 10% FBS, 2 mM L-glutamine (Eurobio), and penicillin (100 U/mL)-streptomycin (100 µg/mL) (BioValley). The CHSE-EC cell line (hereafter referred to as 'EC') as well as its derivatives were grown in L-15 medium (Gibco) supplemented with 10% FBS, penicillin (100 U/mL)-streptomycin (100 µg/mL), 500 µg/mL G418 (Invivogen), 30 µg/mL hygromycin B Gold (Invivogen). All cell lines were maintained at 20°C without CO<sub>2</sub>.

Infectious pancreatic necrosis virus (IPNV), isolate 31.75<sup>566</sup>, was propagated in CHSE-214 (MOI 0.001); briefly, the virus was adsorbed onto the cells for 1h at 14°C with regular, gentle shaking; GMEM supplemented with 2% heat-inactivated FBS was added afterwards. The supernatants were collected at 3-4 days post-infection, 0.2 µm-filtered, diluted 1:5 (v/v) in TEN buffer (10 mM Tris, 1 mM EDTA, 150 mM NaCl, pH 7.1) and mixed again 1:1 (v/v) in glycerol 100%, aliquoted and stored at -20°C. IPNV titers were determined by plaque assay on CHSE-214, as described in [Section 3.4](#).

#### 3.2. Development of a *pkr*<sup>-/-</sup> cell line

Four manually isolated clones were initially obtained and genotypically characterized following the same procedure described in [Results 1](#). Only one of them, called EC-PKR-C4<sup>initial</sup>, presented a mutated genotype at the targeted cut site, located in the first coding exon of the unique *pkr* gene (LOC112253229, LG24). After propagation of the theoretically clonal cells, it was observed that two populations of cells were present: a majority of GFP-negative cells and a few contaminating GFP-

positive cells. The two cell populations were sorted in bulk with a BD FACSAria™ Fusion Flow Cytometer (Institut Pasteur, Paris, France) using a 100 µm nozzle into two distinct 15 mL-tubes. After sorting, cells were centrifuged at 400 g for 5 min and the cell pellets were resuspended in L-15 supplemented with 10% FBS, penicillin (200 U/mL)-streptomycin (200 µg/mL), 500 µg/mL G418 and 30 µg/mL hygromycin B Gold, transferred to 75 cm<sup>2</sup> flasks and incubated at 20°C.

The genotype of the two cell populations, called EC-PKR-C4-GFP(-) and EC-PKR-C4-GFP(+), was characterized as described in [Results 1](#). EC-PKR-C4-GFP(-) presented a 1-nt insertion (29\_30insT resulting in V11fsX22, KO) at the sgRNA-targeted site in the *pkr* gene, while EC-PKR-C4-GFP(+) had a WT genotype. The *pkr*<sup>-/-</sup> or WT status of both cell lines was confirmed by western blot using *Salmo salar* IFNA2 supernatant as inducer of *pkr*, as described in [Results 1](#).

### 3. 3. Weekly cell passages, supernatant collection and cell sampling

During the characterization process of these two cell lines, it was fortuitously discovered that the two cell lines WT EC-PKR-C4-GFP(+) and *pkr*<sup>-/-</sup> EC-PKR-C4-GFP(-) were persistently infected with IPNV. For clarity purposes, EC-PKR-C4-GFP(+) and EC-PKR-C4-GFP(-) will be referred to as EC<sup>IPNV</sup> and EC-PKR-C4<sup>IPNV</sup> in the following paragraphs.

To study the evolution of IPNV persistence over time, EC<sup>IPNV</sup> and EC-PKR-C4<sup>IPNV</sup> were maintained in culture for 40 weeks and weekly passaged, as described in [Figure 30](#). Initially, EC<sup>IPNV</sup> and EC-PKR-C4<sup>IPNV</sup> were seeded into 25 cm<sup>2</sup> flasks in triplicates to a final density of 2 x 10<sup>6</sup> cells/flask in 4 mL L15+10%FBS+P/S. For each cell line, the three flasks were then processed independently throughout the rest of the experiment. Each week (*i.e.* 7 days post-seeding), 1.2 mL of supernatant was harvested from each flask and clarified at 400 g for 5 min. 1 mL of clarified supernatant was mixed 1:1 (v/v) in sterile glycerol 100%, and stored at -20°C until use for virus titration. In parallel, cells were washed once in DPBS (Sigma-Aldrich) and trypsinized in 1 mL ATV. Once detached, cells were resuspended in 3 mL L15+10%FBS+P/S, centrifuged at 400 g for 5 min. The cell pellet was resuspended in 3 mL L15+10%FBS+P/S and cells were counted using a cell counter (Countess 3, Invitrogen) and 2 x 10<sup>6</sup> cells (~40% of the total number of detached cells per flask) were seeded into a new 25 cm<sup>2</sup> flask. For the last 17 passages (P24-P40), 1 mL of the remaining cell suspension was centrifuged at 13 000 g for 45 sec; the cell pellets were drained, resuspended in 350 µL RLT buffer (Qiagen) supplemented with 1% β-mercaptoethanol and stored at -80°C until use for RNA extraction.

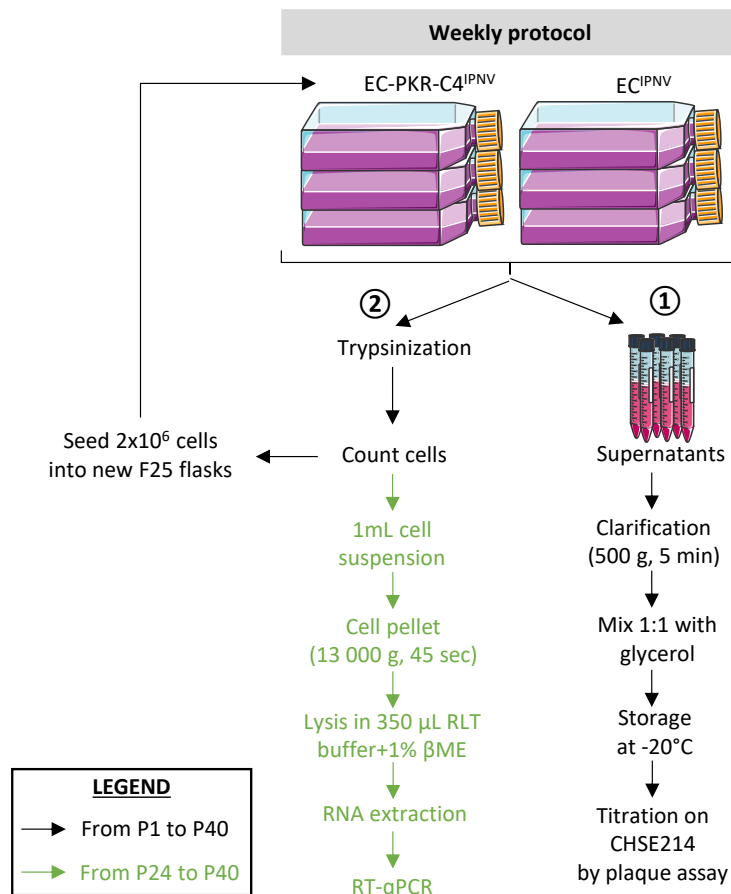


**Figure 30: Diagram illustrating the weekly protocol carried out on EC-PKR-C4<sup>IPNV</sup> and EC<sup>IPNV</sup>.**

After initial seeding, each flask was treated independently. β-ME: β-mercaptoethanol.

### 3. 4. Virus titration by plaque assay

IPNV titers were determined by plaque assay on CHSE-214 cells. CHSE-214 cells were seeded into 12-well plates at a final density of  $7 \times 10^5$  cells/well in GMEM+2%FBS+P/S. The next day, the harvested supernatants (previously stored at  $-20^{\circ}\text{C}$ ) were 10-fold serially diluted in L-15+2% decompemented FBS+P/S and 100 µL of each dilution were applied onto the cells in technical duplicates. After a 1h-long adsorption phase, a carboxymethylcellulose overlay (0.75% in MEM (Eurobio) supplemented with 25 mM HEPES, 2 mM L-glutamine, 350 mg/L NaHCO<sub>3</sub>, 2.5% FBS and P/S) was added onto the cells. At 7 days post-infection, the cells were fixed with 3.7% formaldehyde for 1h at room temperature, stained with 0.5% crystal violet and plaque forming units (PFU) were counted.

### 3. 5. Real-time quantitative PCR

Total RNA was extracted from cells in RLT buffer using QiaShredder and RNeasy mini kits (Qiagen) in accordance with the manufacturer's instructions. In addition to the persistently infected cell samples, positive and negative controls were also included. For this purpose, EC (WT) cells were

seeded into 6-well plates to a final density of  $1.5 \times 10^6$  cells/well in L-15+2%FBS+P/S. The next day, cells were infected with IPNV31.75 (MOI 1) or left untreated, in triplicates, and incubated at 14°C for 8hpi or 24hpi; in parallel, cells were stimulated with recombinant *Salmo salar* IFNA2 supernatant (produced as described in **Results 1**) diluted to 1:10 in L-15+2%FBS+P/S for 72h or left untreated. Cells were collected at indicated time points and total RNA was extracted as described above. For all samples, quality control of the extracted RNA was determined using a Nanodrop spectrophotometer. The cDNA was generated from 2.25 µg of total RNA using the iScript™ Advanced cDNA Synthesis Kit for RT-qPCR (BioRad) and the synthesis was performed in a thermal cycler (Eppendorf) as recommended by the manufacturer. cDNA was diluted to 1:4.5 in DNase- and RNase-free water and stored at -20°C until use. “No RT” control reactions were made for a few representative samples by omitting the reverse transcriptase. The cDNA was mixed with TB Green qPCR Premix Ex Taq (Tli RNaseH Plus) (Takara) along with forward and reverse primers (**Table VIII**) at a final concentration of 210 nM each in Twin.tec® real-time PCR plates (Eppendorf). As all samples did not fit on a single 96-well qPCR plate, an internal calibrator consisting of a pool of all samples was added onto each plate. Amplification was performed using a CFX Connect cycler (BioRad) using the following cycling program: initial denaturation at 95°C for 30 sec followed by 40 cycles of 10 sec at 95°C and 30 sec at 60°C. For each biological replicate, mean Cq values of target genes were calculated based on technical duplicate reactions and then normalized using the geometric mean of Cq values of 3 housekeeping genes (*otelf1a*, *otrps29*, *otgapdh3*). The relative expression of each target gene (*ipnv*, *otirf1*, *otirf3*, *otmx123*, *otpkR*) was expressed as  $2^{-\Delta Cq}$ .

**Table VIII: qPCR primers used in this study**

Name	Sequence 5'-3'	Target name	Target accession number	Size	Reference
<b>otelf1a-ex-F</b>	CACTGCTCAAGTAATCATCCTG	Elongation factor 1-alpha, oocyte form	XM_024441752.2	259 pb	This study
<b>otelf1a-ex-R</b>	CACAGCAAAACGACCAAGAG				
<b>otgapdh3-ex-F</b>	CCAGTGTATGAAGCCCCATGAG	glyceraldehyde-3-phosphate dehydrogenase	XM_024414049.1	187 pb	This study
<b>otgapdh3-ex-R</b>	CTTGTCCTCGTTGACTCCCATG				
<b>otrps29-ex-F</b>	GGGTCATCAGCAGCTCTATTGG	40S ribosomal protein S29	XM_024422712.2	164 pb	Adapted from <sup>588</sup>
<b>otrps29-ex-R</b>	CCAGCTTAACAAAGCCGATGTCG				
<b>ipnv-ex-F</b>	CCTTGACAATGACGTCCCAGTG	IPNV segment A pVP2-VP4-VP3 gene	AJ622822.1	93 pb	Adapted from <sup>589</sup>
<b>ipnv-ex-R</b>	GACTGGGTCACTTTGGCTGAG				
<b>otirf1-ex-F</b>	CCACCCACAGACTATGAAGAC	Interferon regulatory factor 1-like	XM_024432221	191 pb	This study
<b>otirf1-ex-R</b>	GCTCTATTTCCGCCCTGAG				
<b>otirf3-ex-F</b>	CAAGGCGTGGGCTGAGG	Interferon regulatory factor 3	XM_024404012.2	188 pb	This study
<b>otirf3-ex-R</b>	CTGGGTGCTGAGATCCTCCTG		XM_024404011.2		
<b>otmx123-ex-F</b>	CAACTTGGTGGTTGTGCCATG	Interferon-induced GTP-binding protein Mx	XM_024415949.2	111 pb	This study
<b>otmx123-ex-R</b>	GGCTTGGTCAGGATGCCTAAT		XM_042295559.1		
			XM_042295553.1		
			XM_024415946.2		
<b>otpkR-fl-ex-F</b>	CTGAGTAAAGGGAAAGCTAAGCGG	Protein kinase R, full length isoform	XM_042305681.1	147 pb	This study
<b>otpkR-fl-ex-R</b>	GCCTGAATCTGAAGTGGTGTTCG				

For each set of primers, the efficiency was calculated by linear regression obtained by using ten-fold serial dilutions of plasmid containing the target sequence (*otmx123*, *otpkf1*) or of a pool of cDNA (housekeeping genes, *ipnv*, *otirf3*, *otirf1*) and the qPCR products were validated by gel migration and sequencing.

### 3. 6. Viral permissivity test

WT EC, *pkr*<sup>-/-</sup> EC-PKR-C19 (described in [Results 1](#)), WT EC<sup>IPNV</sup>, *pkr*<sup>-/-</sup> EC-PKR-C4<sup>IPNV</sup> cell lines were seeded in 96-well plates at a density of  $7 \times 10^4$  cells/well in L-15+2%FPS+P/S and incubated overnight at 20°C. The next day, the cells were infected with 10-fold serial dilutions of either IPNV (isolate 31.75, stock at  $2.2 \times 10^8$  PFU/mL<sup>566</sup>) or infectious hematopoietic necrosis virus (IHNV, isolate 25.70, stock at  $1.1 \times 10^6$  PFU/mL<sup>142</sup>). The first wells were infected at different initial MOI depending on the virus (IPNV: MOI 0.005; IHNV: MOI 0.3). At 7 days post-infection, cells were fixed with 3.7% formaldehyde for 1h and stained with 0.5% crystal violet.

### 3. 7. Statistical analysis

The data presented are means  $\pm$  standard deviation (SD). Statistical tests used are indicated in the legend of each figure. All statistical analyses were performed using GraphPad Prism software version 8.0.1.

## 4. Results

### 4.1. Development of an initial *pkr*<sup>-/-</sup> cell line and identification of a persistent IPNV infection

To characterize the functions of Chinook salmon PKR, the unique *pkr* gene (LOC112253229, LG24) was disrupted in EC cells, using CRISPR/Cas9 genome editing technology and one *pkr*<sup>-/-</sup> clone, named EC-PKR-C4<sup>initial</sup>, was manually isolated and kept for amplification and further characterization. However, after propagation, observations under the fluorescence microscope revealed the presence of a few contaminating GFP-positive fluorescent cells. The GFP-positive and GFP-negative populations were FACS-sorted in bulk, and the resulting cell lines were called EC-PKR-C4-GFP(+) and EC-PKR-C4-GFP(-), respectively (**Figure 31A**). Genotyping results showed that EC-PKR-C4-GFP(+) cells had a WT genotype, while EC-PKR-C4-GFP(-) presented the same mutation as EC-PKR-C4<sup>initial</sup> *i.e.* a 1-nt insertion at the targeted cut site leading to a frameshift resulting in the introduction of a premature codon at position 22 (29\_30insT resulting in V11fsX22) (**Figure 31B,C**). The PKR expression status in both cell lines was assessed at the protein level by Western blot, using recombinant IFNA2 supernatant as an inducer of *pkr* expression. Our results showed that PKR was induced in WT EC and WT EC-PKR-C4-GFP(+) cells following IFNA2 treatment. In contrast, no PKR signal was detected in *pkr*<sup>-/-</sup> EC-PKR-C4-GFP(-) cells, thereby confirming that the expression of PKR was effectively disrupted in these cells (**Figure 31D**). EC-PKR-C4-GFP(+) was kept as an additional positive control for further experiments.

During the characterization process of *pkr*<sup>-/-</sup> EC-PKR-C4-GFP(-) along with WT EC-PKR-C4-GFP(+), it was observed that supernatants from control healthy cells showing no visible signs of CPE were able to induce cell lysis, once transferred onto CHSE-214 cells (**Figure 31E**). Further RT-qPCR experiments revealed that both cell lines expressed IPNV RNA (**Figure 31F**). In addition, preliminary titration results showed that infectious virion particles were present in the supernatants of both cell lines ( $10^3$ - $10^4$  PFU/mL). These findings indicated that both cell lines were persistently infected with IPNV. On this occasion, WT EC-PKR-C4-GFP(+) and *pkr*<sup>-/-</sup> EC-PKR-C4-GFP(-) were renamed EC<sup>IPNV</sup> and EC-PKR-C4<sup>IPNV</sup> and this denomination will be used throughout the rest of the manuscript. It should be noted that EC-PKR-C4<sup>initial</sup> was also found to be persistently infected with IPNV (data not shown), suggesting that the event leading to the establishment of IPNV persistence occurred prior to FACS sorting.

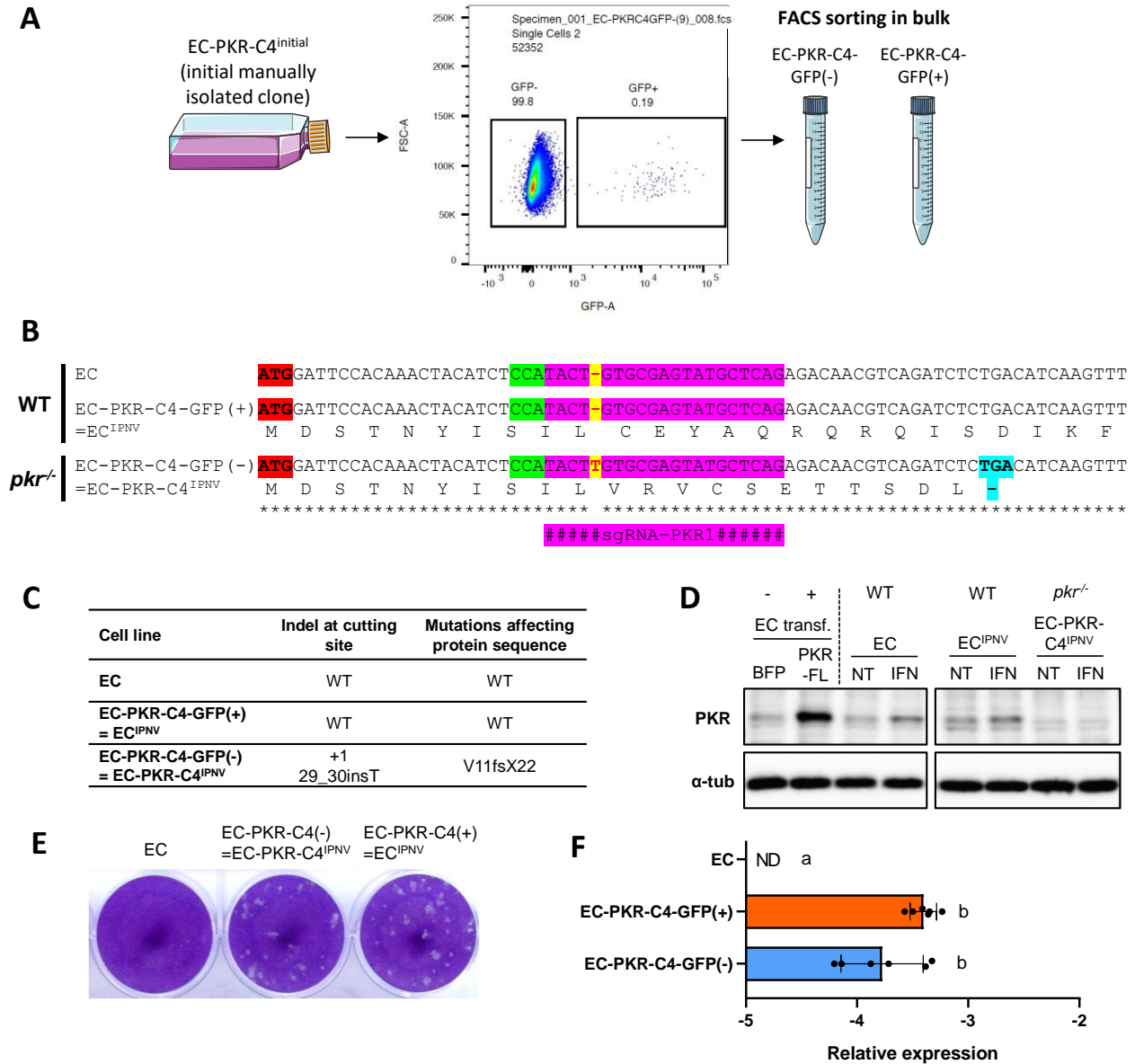


**Figure 31: Validation of the PKR expression status in EC-PKR-C4-GFP(-) and EC-PKR-C4-GFP(+) and identification of a persistent IPNV infection in both cell lines**

(A) Diagram illustrating the FACS-based isolation process of EC-PKR-C4-GFP(-) and EC-PKR-C4-GFP(+) from an initial manually isolated clone called EC-PKR-C4<sup>initial</sup> presenting a discrete population of GFP-positive cells. (B) Genotype of EC cells (WT), latently IPNV-infected EC-PKR-C4-GFP(+) (WT, *aka.* EC<sup>IPNV</sup>) and EC-PKR-C4-GFP(-) (1-nt insertion, 29\_30insT resulting in V11fsX22, *pk<sup>r</sup>-*, *aka.* EC-PKR-C4<sup>IPNV</sup>) obtained from sequencing of purified PCR products amplified from genomic DNA from each cell line. The location of the sgRNA is highlighted in pink, the protospacer adjacent motif is in green, the start codon is in red, the 1-nt insertion in EC-PKR-C4-GFP(-) is in yellow and the premature stop codon is in blue. The corresponding chromatograms are available in [Section 7, Figure 37](#). (C) Table summarizing the molecular characteristics of EC, EC<sup>IPNV</sup> and EC-PKR-C4<sup>IPNV</sup> cell lines. (D) EC, EC<sup>IPNV</sup> and EC-PKR-C4<sup>IPNV</sup> cells were stimulated with *S. salar* IFNA2 supernatant for 72h; positive and negative controls are EC cells transfected with pcDNA3.1-Hyg-BFP or pcDNA3.1-Zeo-Hyg-P2A-PKR-FL, respectively. Cell lysates were separated by SDS-PAGE and immunoblotted with antibodies against *S. salar* PKR and  $\alpha$ -tubulin ( $\alpha$ -tub). Full length blots are available in [Section 7, Figure 38](#). Blots are representative of two independent experiments. (E) CHSE-214 were incubated with supernatants from EC, EC-PKR-C4(+) and EC-PKR-C4(-) under a carboxymethylcellulose overlay at 14°C for 7 days, fixed with formaldehyde and stained with crystal violet. (F) Relative expression levels of IPNV transcripts in non-infected EC cells, EC-PKR-C4(+) and EC-PKR-C4(-). Graph shows means  $\pm$  SD from 2 independent experiments (n=6); letters indicate significant differences between cell lines ( $p < 0.05$ ), ordinary one-way Anova with Tukey's post-hoc multiple comparison test.

## 4. 2. Characterization of the persistent IPNV infection over the course of passages

We decided to characterize the IPNV persistence in both cell lines over the course of passages. The aim was to study whether IPNV persistence levels were changing over time and to investigate whether PKR was modulating this phenomenon. To this end, EC<sup>IPNV</sup> and EC-PKR-C4<sup>IPNV</sup> were maintained in culture for 40 weeks. At each weekly passage (P1-P40), supernatants from three independent flasks for each cell line were collected and IPNV titers were determined by plaque assay. For the last 17 passages, cell samples from the same flasks were also collected for RT-qPCR analysis (**Figure 30**).

### 4. 2. 1. The extracellular titers of persistent IPNV oscillate over the course of passages in both *pkr*<sup>-/-</sup> and WT cell lines

Titration of supernatants from EC<sup>IPNV</sup> and EC-PKR-C4<sup>IPNV</sup> weekly collected over 40 passages show regular oscillations in extracellular titers in each individual flask for both cell lines (**Figure 32**). In both cases, extracellular titers ranged from 10<sup>2</sup> to 10<sup>8</sup> PFU/mL. By comparison, extracellular titers obtained with an acute and lytic IPNV infection typically range from 10<sup>8</sup> to 10<sup>9</sup> PFU/mL in CHSE-214<sup>590</sup> and EC cells (unpublished data). Remarkably, the extracellular titers oscillate with a mean period of T=3.85 passages for EC<sup>IPNV</sup> and T=4.62 passages for EC-PKR-C4<sup>IPNV</sup> ( $p < 0.01$ , unpaired t-test), although there were some offsets between the flasks. These results suggest that IPNV infectious virions are released in waves, and that the absence of PKR may slow down the process.

To confirm that these fluctuations were not due to a storage issue of the supernatants before titration, a few samples were randomly selected and titrated a second time, yielding similar titers as the ones previously obtained (data not shown). In addition, extracellular titers do not correlate with the number of cells in each flask at each sampling time, indicating that extracellular titers were not determined by fluctuations in cell growth over time (**Section 7, Figure 39**).

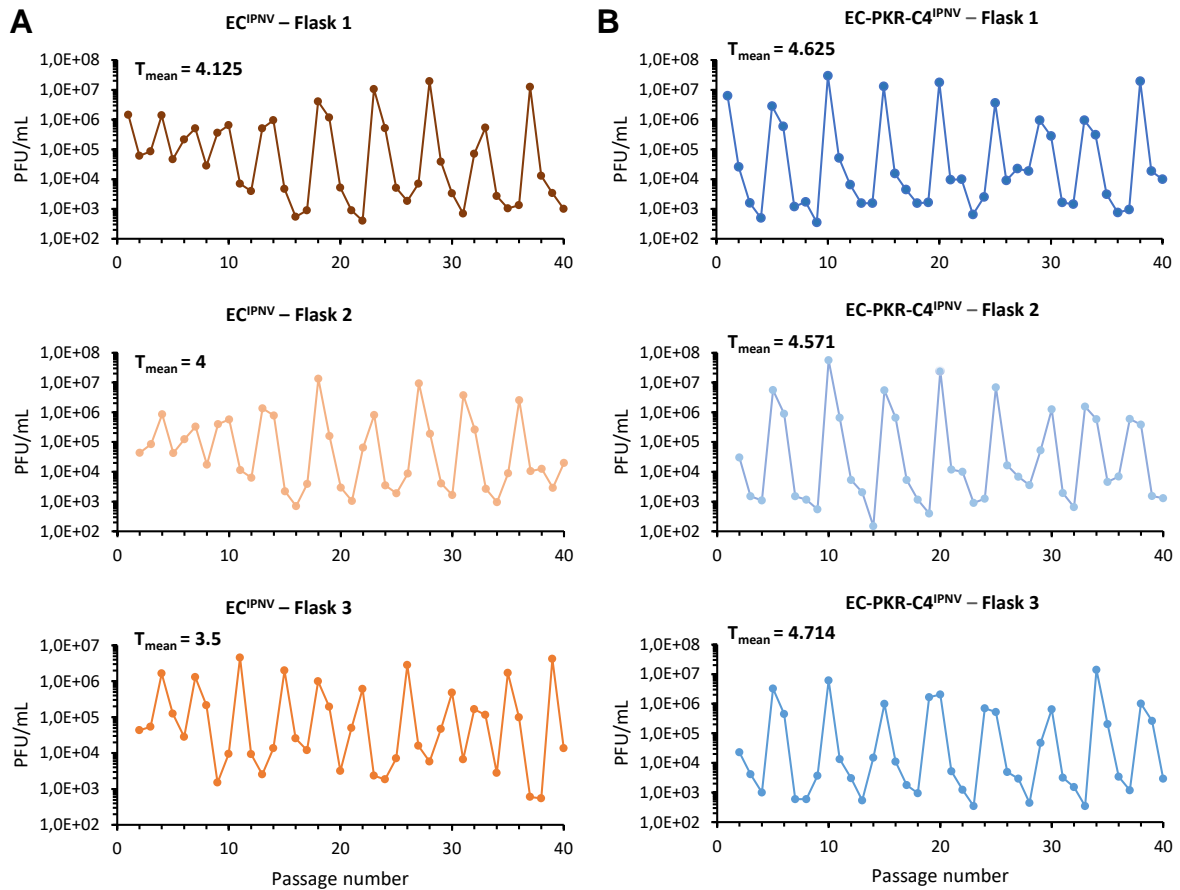


**Figure 32: Extracellular viral titers from supernatants of EC<sup>IPNV</sup> and EC-PKR-C4<sup>IPNV</sup> cells persistently infected IPNV.**

For (A) EC<sup>IPNV</sup> and (B) EC-PKR-C4<sup>IPNV</sup>, supernatants from 3 independent flasks were collected prior to weekly subcultures and titers were determined by standard plaque assay. Each colored line represents an individual flask. PFU: plaque forming unit.

#### 4.2.2. Oscillations in extracellular titers are explained by fluctuations in intracellular replication

To identify whether the fluctuations in extracellular titers were due to variations in virus replication, EC<sup>IPNV</sup> and EC-PKR-C4<sup>IPNV</sup> cell samples were collected from P24 to P40 during passaging process and extracted RNA was analyzed by RT-qPCR using primers targeting the viral *pVP2-VP4-VP3* gene. EC cells infected with IPNV 31.75 or left uninfected were used as positive and negative controls respectively. Our results revealed that both WT EC<sup>IPNV</sup> and *pkr*<sup>-/-</sup> EC-PKR-C4<sup>IPNV</sup> continuously contained IPNV RNA over passages but it was at a much lower level than acutely IPNV-infected EC cells (3-log difference at 8hpi and almost 5-log difference in relative expression at 24hpi compared to IPNV-infected EC cells) (Figure 33A).

Interestingly, IPNV RNA expression in both cell lines was positively correlated with the corresponding extracellular viral titers assessed by plaque assays with robust coefficients of

determination ( $R^2=0.62$  for EC<sup>IPNV</sup> and  $R^2=0.71$  for EC-PKR-C4<sup>IPNV</sup>) (Figure 33B). Consistently, expression fluctuations in individual flasks for both cell lines over passages, show regular oscillations with peaks in viral RNA occurring at the same time as peaks in extracellular titers (Figure 33C,D). However, it seems that the viral RNA peak levels did not systematically match extracellular titer levels, suggesting that other factors involved in modulation of replication, viral RNA degradation and/or virion release might be at play. These findings suggest that oscillations in extracellular titers in both cell lines can be (at least partially) explained by fluctuations in intracellular viral replication.

#### 4. 3. The innate immune response is dampened in persistently IPNV-infected cell lines

In order to investigate whether IPNV persistent infection modulates the expression of innate immune genes, the expression profiles of selected *ISGs* (*irf1*, *irf3*, *mx123*, *pkr*) were examined in WT EC<sup>IPNV</sup> and *pkr*<sup>-/-</sup> EC-PKR-C4<sup>IPNV</sup> over the course of passages. EC cells simulated with recombinant type I IFNA2 supernatant or left untreated were used as positive and negative controls, respectively. EC cells acutely infected with IPNV 31.75 for 8 or 24 hpi were also included for comparison purposes. For all four genes, a strong and significant induction in transcript expression was observed following type I IFN treatment compared to non-stimulated cells (660-fold-, 123-fold-, 60800-fold-, 27-fold-inductions for *irf1*, *irf3*, *mx123*, *pkr*, respectively) (Figure 34, black bars), thereby validating the assay according to the *ISG* status of the selected genes. In contrast, while *irf1* expression was induced at 24h post-infection with IPNV in EC cells (30-fold induction compared to control cells), *mx1* only displayed a weak induction (2.4-fold induction) at the same timepoint and *irf3* and *pkr-fl* transcripts were not significantly induced upon IPNV infection at any of the timepoint examined (Figure 34, black bars). These results suggest that acute infection with IPNV suppresses the early activation of specific immune genes (in comparison to IFN-treated cells). Interestingly, similar results were previously reported in rainbow trout RTG-P1 cells, which showed inhibition in *mx* expression following IPNV infection<sup>176</sup>.

In EC<sup>IPNV</sup> and EC-PKR-C4<sup>IPNV</sup>, the mean expression of *irf1* ( $1.83\pm 1.08$  fold induction in EC<sup>IPNV</sup> and  $1.57\pm 0.86$  in EC-PKR-C4<sup>IPNV</sup>) and *pkr-fl* ( $1.28\pm 0.30$  in EC<sup>IPNV</sup> and  $1.51\pm 0.42$  in EC-PKR-C4<sup>IPNV</sup>) was not significantly different compared to non-infected EC cells. Interestingly, *irf3* and *mx123* were overall weakly but significantly more expressed in EC-PKR-C4<sup>IPNV</sup> compared to non-infected cells ( $2.30\pm 0.69$  and  $4.22\pm 4.20$  fold inductions for *irf3* and *mx123*, respectively) but not in EC<sup>IPNV</sup> ( $1.64\pm 0.45$  and  $1.92\pm 1.25$ , respectively) (Figure 34, colored bars). Taken together, these results indicate that, in persistently infected cells, the expression levels of innate immune genes are overall similar to those in non-infected cells, suggesting that the host innate immune response is also dampened during persistent infection.

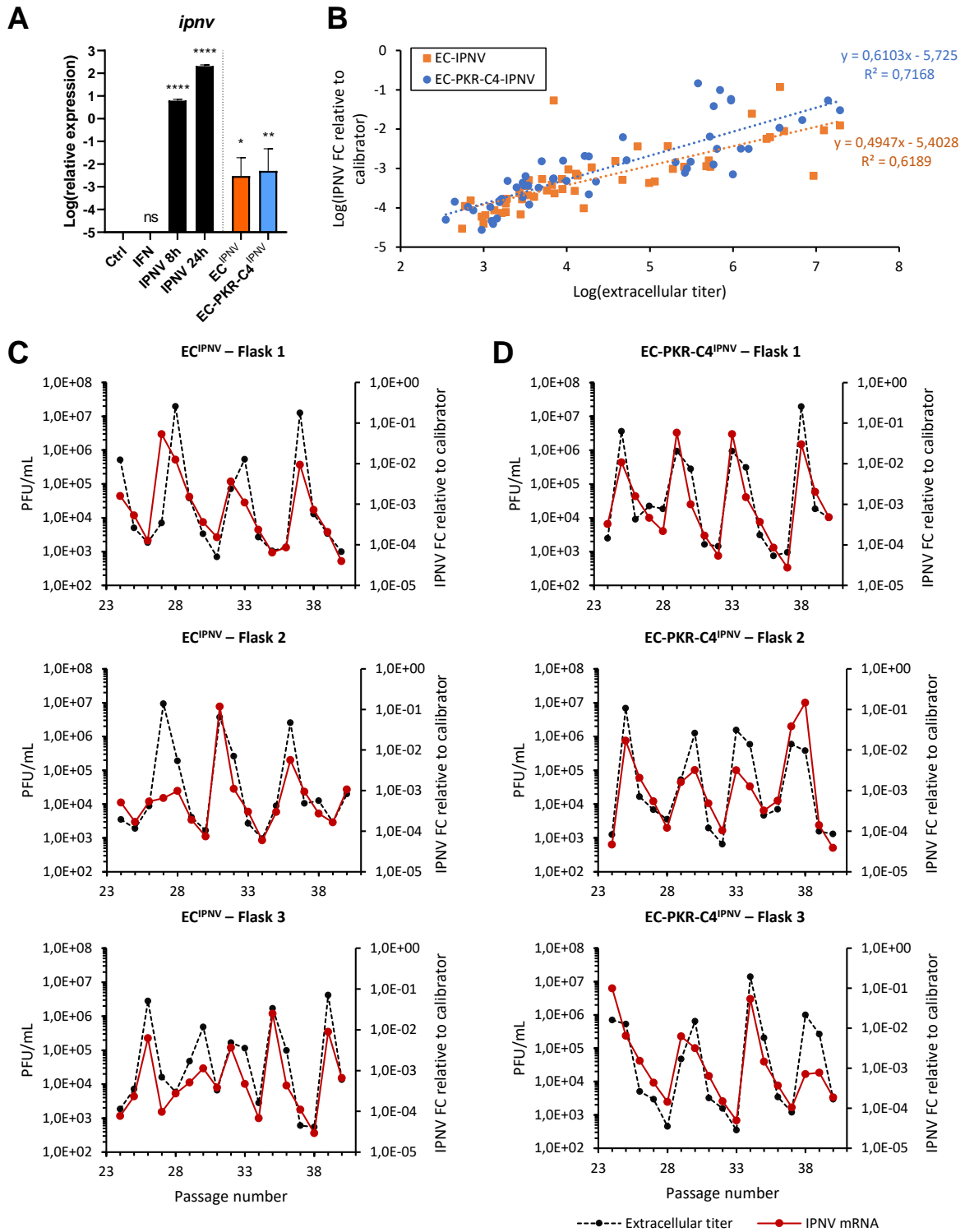


**Figure 33: Intracellular IPNV replication correlates with extracellular titers.**

(A) Black bars show means  $\pm$  SD of relative expression levels of IPNV transcripts in EC cells infected with IPNV 31.75 (MOI 1) for 8h and 24h post-infection, stimulated with recombinant type I IFN (72h) or left untreated (n=3 for each condition); ns, non-significant, \*\*\*\*,  $p < 0.0001$ , ordinary one-way Anova with Tukey's post-hoc multiple comparison test. Colored bars show means  $\pm$  SD of relative expression levels of *ipnv* mRNA in persistently IPNV-infected WT EC<sup>IPNV</sup> and *pkrr*<sup>-/-</sup> EC-PKR-C4<sup>IPNV</sup> (for each cell line, n=3x17, corresponding to all the samples collected from P24 to P40). \*,  $p < 0.05$ , \*\*,  $p < 0.01$ , Kruskal-Wallis test with Dunn's post-hoc multiple comparison test. (B) Dotplot showing log-transformed *ipnv* mRNA levels (represented as fold change relative to calibrator) as a function of log-transformed extracellular titers in persistently IPNV-infected EC<sup>IPNV</sup> and EC-PKR-C4<sup>IPNV</sup> cells. Distinct linear regressions were performed on EC<sup>IPNV</sup> and EC-PKR-C4<sup>IPNV</sup> datasets. (C,D) Graphs showing extracellular titers and *ipnv* mRNA levels over the course of passages in each individual flasks of EC<sup>IPNV</sup> (C) and EC-PKR-C4<sup>IPNV</sup> (D).

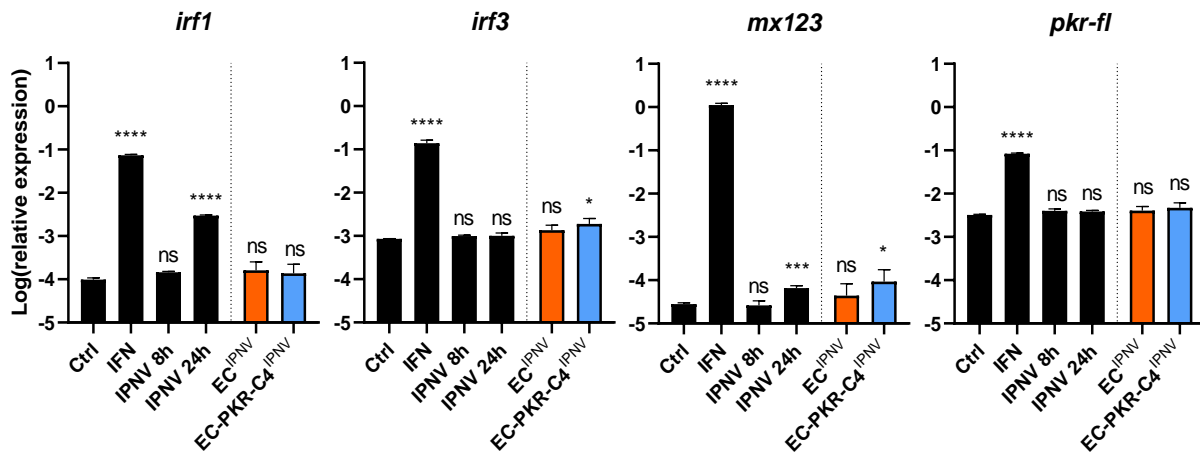


**Figure 34: Persistent and acute IPNV infections dampen the innate immune response in infected cells.**

Black bars show means  $\pm$  SD of relative expression levels of target genes (*irf1*, *irf3*, *mx123*, *pkr-fl*) in EC cells infected with IPNV 31.75 (MOI 1) for 8h and 24h post-infection, stimulated with recombinant type I IFN (72h) or left untreated (n=3 for each condition); ns, non-significant, \*\*\* p < 0.001, \*\*\*\*, p < 0.0001, ordinary one-way Anova with Tukey's post-hoc multiple comparison test. Colored bars show means  $\pm$  SD of relative expression levels in persistently IPNV-infected WT EC<sup>IPNV</sup> and *pkr*<sup>-/-</sup> EC-PKR-C4<sup>IPNV</sup> (for each cell line, n=3x17, corresponding to all the samples collected from P24 to P40). \*, p < 0.05, Kruskal-Wallis test with Dunn's post-hoc multiple comparison test.

Although these results are indicative of what happens in persistently infected cells as a whole, they do not show whether variations in expression occur over the course of passages. For both cell lines, the expression profiles of each ISG were examined in individual flasks over passages in comparison with intracellular IPNV RNA levels. For *irf3*, *mx123* and *pkr*, variations in expression over time did not correlate with the corresponding viral RNA level and no other expression pattern could be identified (Section 7, Figure 40 to Figure 42). Furthermore, the range of variation remained low for all these genes: for *irf3* and *pkr*, maximal induction was less than 2-fold in both cell lines compared to the mean expression levels in persistently-infected cells, for *mx123*, the expression amplitude was higher than 2-fold but basal expression levels were also lower (Cq values  $\sim$ 30) resulting in higher background noise. In contrast, *irf1* transcript levels were weakly correlated with viral RNA levels (Figure 35). In particular, expression variations in individual flasks for both cell lines show peaks in *irf1* expression occurring at the same time as peaks in viral transcripts in approximately half the cases (Figure 35B,C). Consistently, sample subsets expressing high levels of viral RNA display a positive correlation between *irf1* expression and viral gene expression (Figure 35A). These results suggest that *irf1* expression may be triggered when viral RNA levels are over a specific threshold, hence a correlation only visible in samples expressing high levels of viral RNA. These findings are also reminiscent of the results obtained in the case of acute infection, which induced the expression of *irf1* expression but not that of other innate immune genes (Figure 34). However, it should be noted that the fold changes in *irf1* expression in these cell lines were much lower than during acute infection: indeed, while a mean 30-fold induction in *irf1* expression was measured at 24 hpi in acutely infected

cells, *irf1* expression peaks barely reached a 2.7-fold induction on average in both cell lines compared to the basal expression levels in persistently-infected cells.

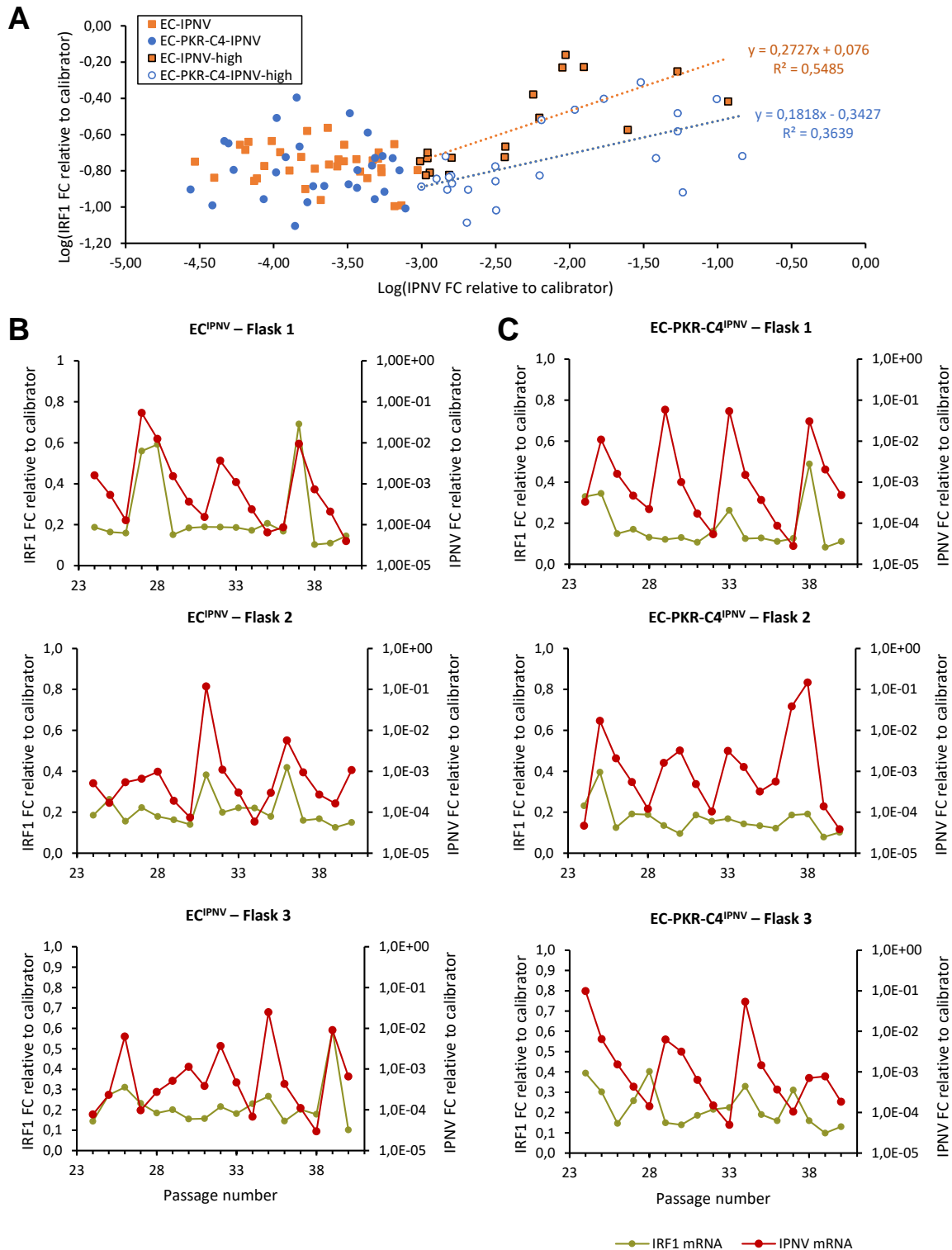


**Figure 35: IRF1 is induced in both in both acutely and persistently infected cells.**

(A) Dotplot showing log-transformed *ipnv* mRNA levels (represented as fold change relative to calibrator) as a function of log-transformed *irf1* mRNA levels in persistently IPNV-infected EC<sup>IPNV</sup> and EC-PKR-C4<sup>IPNV</sup> cells. Linear regressions were performed on EC<sup>IPNV</sup> and EC-PKR-C4<sup>IPNV</sup> subsets expressing high levels of *ipnv* mRNA (threshold log(IPNV FC relative to calibrator) > -3). (B,C) Graphs showing *ipnv* and *irf1* mRNA levels over the course of passages in each individual flask of EC<sup>IPNV</sup> (B) and EC-PKR-C4<sup>IPNV</sup> (C).

Altogether, these results suggest that persistent IPNV has evolved strategies to evade the host innate immune response and even inhibits the expression of genes that are usually induced following acute infection, such as *irf1*. However, it appears that variations in viral RNA levels may cause inhibition to “leak” when these levels are above a specific threshold, resulting in a few weak *irf1* expression peaks. In addition, the fact that some viral RNA expression peaks are not associated with higher *irf1* expression may be due to other viral evasion mechanisms.

#### 4. 4. Persistently IPNV-infected cells are refractory to acute IPNV infection but permissive to other viruses

We investigated the permissivity of EC<sup>IPNV</sup> and EC-PKR-C4<sup>IPNV</sup> to viral infections, including multiple IPNV strains as well as heterologous viruses. Persistently infected EC<sup>IPNV</sup> and EC-PKR-C4<sup>IPNV</sup> cell lines were refractory to acute infection with IPNV 31.75 and displayed no signs of CPE contrary to their IPNV-free counterparts (**Figure 36A**). Comparable results were obtained with infection at higher MOIs (up to MOI = 50) as well as with other IPNV strains, including IPNV TA and IPNV PT (data not shown). In contrast, EC<sup>IPNV</sup> and EC-PKR-C4<sup>IPNV</sup> showed no difference in permissivity following infection with IHNV 25.70 compared to non-persistently infected cells (**Figure 36B**). Similar observations were made following infection with other heterologous viruses, including VHSV and EHNV (data not shown).

Taken together, these results suggest that persistently IPNV-infected cells are refractory to acute IPNV infection, regardless of the strain/isolate. However, the IPNV persistence does not seem to alter their permissivity to infections with heterologous viruses.

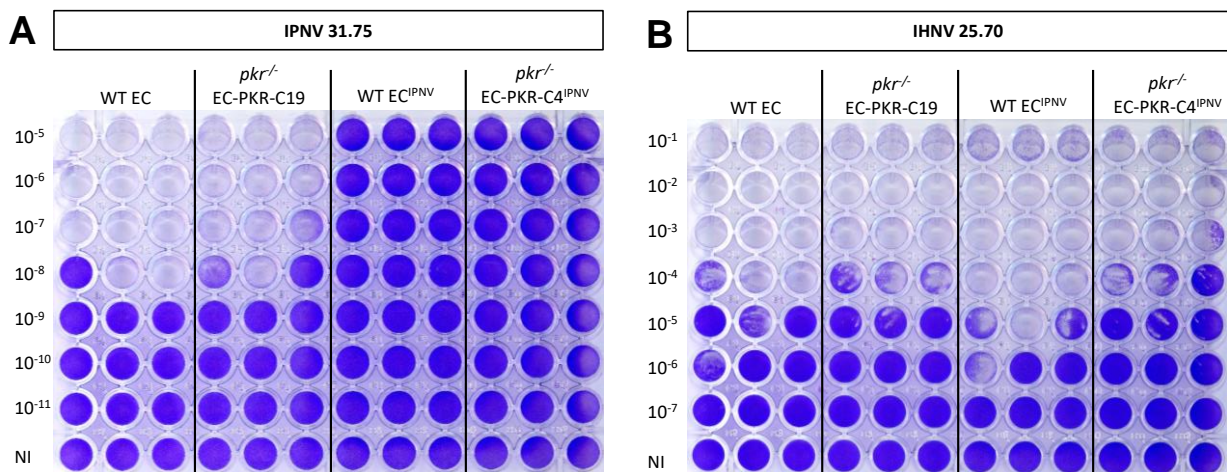


**Figure 36: Comparison of permissivity to IPNV31.75 and IHNV25.70 of IPNV-free cell lines and persistently IPNV-infected cells.**

WT EC, *pkr*<sup>-/-</sup> EC-PKR-C19, WT EC<sup>IPNV</sup>, *pkr*<sup>-/-</sup> EC-PKR-C4<sup>IPNV</sup> were infected with 10-fold serial dilutions of (A) IPNV 31.75 (starting MOI = 0.005) or (B) IHNV 25.70 (starting MOI = 0.3) and incubated for 7 dpi at 14°C and 22°C, respectively.

## 5. Discussion

In this study, we characterized two Chinook salmon cell lines deriving from the parental EC cell line, a WT cell line and a *pkr*<sup>-/-</sup> cell line, which were found to be persistently infected with IPNV, rendering them refractory to acute IPNV infection. We observed that the extracellular titers of persistent IPNV oscillate over the course of passages in both cell lines and that they correlate – at least partially – with variations in intracellular viral replication. Our results further indicate that the basal expression of key *ISGs* transcripts is dampened during persistent infection, in a similar fashion to what occurs during acute IPNV infection, and that PKR is not primarily involved in the regulation of this persistence phenomenon. Taken together, these results suggest that persistent IPNV has evolved strategies to evade the host innate immune response by inhibiting the expression of innate immune genes, while maintaining a relatively low replication level.

### **EC<sup>IPNV</sup> and EC-PKR-C4<sup>IPNV</sup> present the canonical characteristics of persistently IPNV-infected cells**

Our persistently infected cell lines present most of the characteristics typically described for viral persistence in mammalian cells, including continued growth of infected cells that are morphologically indistinguishable from virus-free cells, continued production of infectious virions over passages; resistance to superinfection by homologous virus strains and susceptibility to heterologous viruses<sup>586</sup>. One last criterion mentioned by Rima & Martin (1976) is the presence of viral antigen in a majority of cells, which was not examined in the present study. These results are fully consistent with other studies on fish cell lines persistently infected with IPNV<sup>179,580–583,585,587</sup>.

Contrary to our study, no specific patterns in extracellular titers were identified by Hedrick *et al.* (1978, 1981) in persistently IPNV infected CHSE-214 and STE-137 cells, although considerable variations were measured over weekly passages<sup>580,581</sup>. In contrast, Saint-Jean *et al.* (2010) noticed that in persistently IPNV-infected RTG-2 cells, extracellular titers fluctuated during 20 passages with a periodicity of 6 passages, following the same pattern as cells expressing viral antigens<sup>179</sup>. Our study was performed on a longer period of time and confirmed that this periodic pattern is, indeed, present in IPNV-infected EC cells. Importantly, similar oscillations in titers from persistently infected cells have been reported in both *in vitro* and *in vivo* mammalian models during persistent infections with VSV or rabies<sup>591–593</sup>.

### **What are the mechanisms underlying oscillations in IPNV extracellular titers?**

#### *Modulation of the innate immune response?*

This curious phenomenon prompted us to investigate the underlying mechanisms. For this purpose, we studied what was happening intracellularly in terms of viral replication and host innate immune

response. Our results show that, overall, intracellular viral RNA levels follow the same pattern as extracellular infectious titers. However, it appeared that the innate immune response was not triggered by the persistent infection, irrespective of the intracellular IPNV replication levels. These results are in line with early *in vitro* studies, which showed that that persistently IPNV-infected CHSE-214 and STE-137 cell lines displayed no IFN-like activity<sup>580,582</sup>. Consistently, no differentially expressed ISGs were found by suppression subtractive hybridization (SSH) in persistently IPNV-infected CHSE-214 cells compared with non-infected cells<sup>583</sup>. Similar observations were also made *in vivo* in IPNV-carrier Atlantic salmon, which displayed low viral RNA levels and no induction of *mx* in head kidney<sup>594</sup>. These results may be linked to the ability of IPNV to evade the innate immune response even during an acute infection: for instance, IPNV infection was reported to suppress poly(I:C)-induced activation of *mx* promoter in the RTG-P1 reporter cell line<sup>176</sup>. Similarly, IPNV was found to limit *mx* expression in CHSE-214 cells pre-infected with IPNV and stimulated with recombinant IFN $\alpha$ 1<sup>177</sup>. Mechanistically, it seems that IPNV-mediated inhibition of the type I IFN signaling pathway involved VP4 and VP5 but the exact underlying mechanisms are currently unknown<sup>177,178</sup>. In any case, it is possible that persistent IPNV has implemented similar mechanisms of action to block the induction of ISGs and/or IFN genes, enabling it to replicate without killing the host cells.

In addition to directly inhibiting the IFN signaling pathway, other authors have proposed that the *in vivo* persistence status may also be favored by the virus reducing its replication levels so as not to trigger host defenses<sup>594</sup>. Our results on *irf1* expression levels, which seem to be slightly induced in persistently infected cells presenting higher levels of viral RNA (although to a much lower level compared to acute infection), support this hypothesis.

#### *Presence of defective interfering particles?*

In mammalian models, oscillations in extracellular viral titers in cells persistently infected with various RNA viruses were linked to the production of viral defective interfering particles (DIPs)<sup>592,593,595</sup>. DIPs are viral particles containing “normal” structural proteins but a defective viral genome due to mutations, deletions or gene rearrangements<sup>595,596</sup>. Most of them are able to enter permissive cells but are not replicative *per se* due to their truncated genome. However, they can replicate in case of co-infection with a “helper” standard infectious virus to complement the lost functions and give rise to similar progeny DIPs<sup>595,596</sup>. By doing so, they may also interfere with the replication of non-defective WT viruses by competing for viral factors: due to their shortened length, they can replicate more efficiently than WT virus resulting in their accumulation in co-infected cells<sup>595,596</sup>. In cells persistently infected with VSV or rabies, it was observed that an increase in DIP production was occurring right after the production peak of infectious standard virus<sup>592,593</sup>. A similar periodic pattern was observed *in vivo* in mice co-infected with standard VSV and DIPs with a

periodicity of ~5 days<sup>591</sup>. Cave *et al.* (1985) proposed that this cyclic production dynamics was similar to a predator-prey relationship<sup>591</sup>, suggesting that specific subpopulations may determine the composition of the virus pool in the supernatants<sup>595</sup>. This cycling pattern was later mathematically modelled using input-output models incorporating interactions between standard virions, DIPs and cells to predict yields of infectious virus and DIPs<sup>597,598</sup>.

In our study, we did not examine the production of DIPs in persistently IPNV-infected CHSE-EC cells. Nonetheless, a few early studies provide evidence of the presence of DIPs in cells infected with both lytic IPNV and persistent IPNV<sup>580,599</sup>. More specifically, electron microscopy studies revealed the presence of incomplete virions different from the electron-dense ones observed during acute infection<sup>580</sup>. Analysis of persistent virions from infected STE-137 cells by centrifugation in cesium chloride gradients confirmed that two types of virions were produced: high-density infectious virions and low-density defective virions; the latter were able to delay CPE following infection with stock IPNV, suggesting that defective virions were DIPs<sup>580</sup>. In line with these results, CPE-suppressing activity against IPNV but not heterologous viruses (*e.g.* IHNV, VHSV) was also reported in the supernatants from persistently IPNV-infected RTG-2, suggesting the presence of DIPs<sup>179</sup>. However, whether DIPs oscillate asynchronously with infectious IPNV particles is still unclear.

The current experiments performed do not allow to conclude about the production of DIPs in our persistently IPNV-infected cells. However, due to the similarity between our results and the ones described by Kawai *et al.* (1975)<sup>592</sup> and Palma & Huang (1974)<sup>593</sup>, it is tempting to speculate that a similar phenomenon occurred in our cell lines. The presence of a few asynchronous peaks in viral RNA transcripts and in extracellular titers (**Figure 30**) may support this hypothesis, as the primers used may amplify viral RNA from both DIPs and standard viruses (although a deletion of the region amplified by the set of primers used cannot be ruled out). To go further in our analysis, it would be interesting to develop an assay to quantify DIPs in our collected supernatants, either by using centrifugation in cesium chloride gradients<sup>580,592</sup>, by measuring the CPE-suppressing activity of these supernatants against homologous and heterologous viruses<sup>179,592</sup> and/or by sequencing of the viral genome from the different particle types present in the supernatant. The presence of soluble anti-viral factors could also be assessed by testing the antiviral activity of the supernatants using size-exclusion techniques to remove virions.

## 6. Conclusion and perspectives

To conclude, our study indicates that WT EC<sup>IPNV</sup> and *pkr*<sup>-/-</sup> EC-PKR-C4<sup>IPNV</sup> cells present most of the canonical characteristics of persistently infected cells. A striking feature of these cell lines is the oscillatory pattern of extracellular titers and of intracellular viral RNA levels in both cell lines over

the course of passages. Our results further suggest that the host’s type I IFN response is not triggered during persistent infection and that PKR does not play a major role in the regulation of this persistence phenomenon. Taken together, these results suggest that persistent IPNV has evolved strategies to evade the host innate immune response, while maintaining a relatively low replication level.

To go further, it would be interesting to confirm these findings by studying the impact of IPNV persistent infection on the cellular transcriptome over time using a whole transcriptome sequencing approach. An RNA-Seq study would also provide novel insights into alternative host’s pathways that are modulated during persistent infections, thereby helping identify additional mechanisms underlying IPNV persistence. Another future research axis will be to investigate the presence of DIPs in the supernatants to ultimately study whether our system follows a predator-prey dynamic.

### 7. Supplementary data

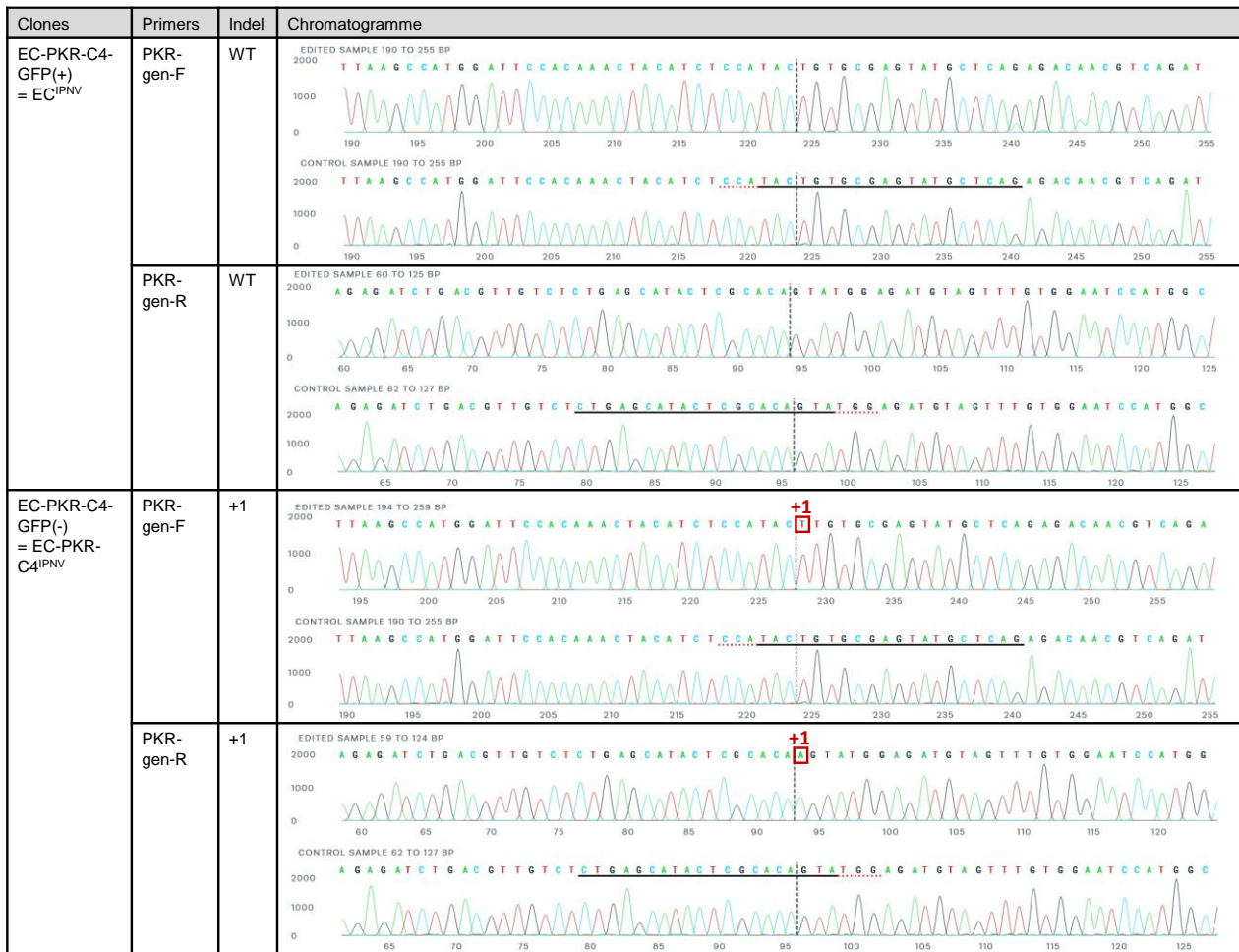


**Figure 37: Alignment of chromatograms from EC<sup>IPNV</sup> and EC-PKR-C4<sup>IPNV</sup> with EC (WT) cell line.**

Chromatograms showing edited and wild-type (control) sequences in the region around the sequence targeted by sgRNA-PKR1 from EC<sup>IPNV</sup> (*aka.* EC-PKR-C4-GFP(+)) and EC-PKR-C4<sup>IPNV</sup> (*aka.* EC-PKR-C4-GFP(-)). The horizontal black line represents the guide sequence; the horizontal red dotted line corresponds to the PAM site; the vertical black dotted line represents the actual cut site. The red boxes show inserted nucleotides. Alignments were obtained using Synthego ICE Analysis tool <sup>600</sup>.

Results 3 – Persistently IPNV-infected cell lines

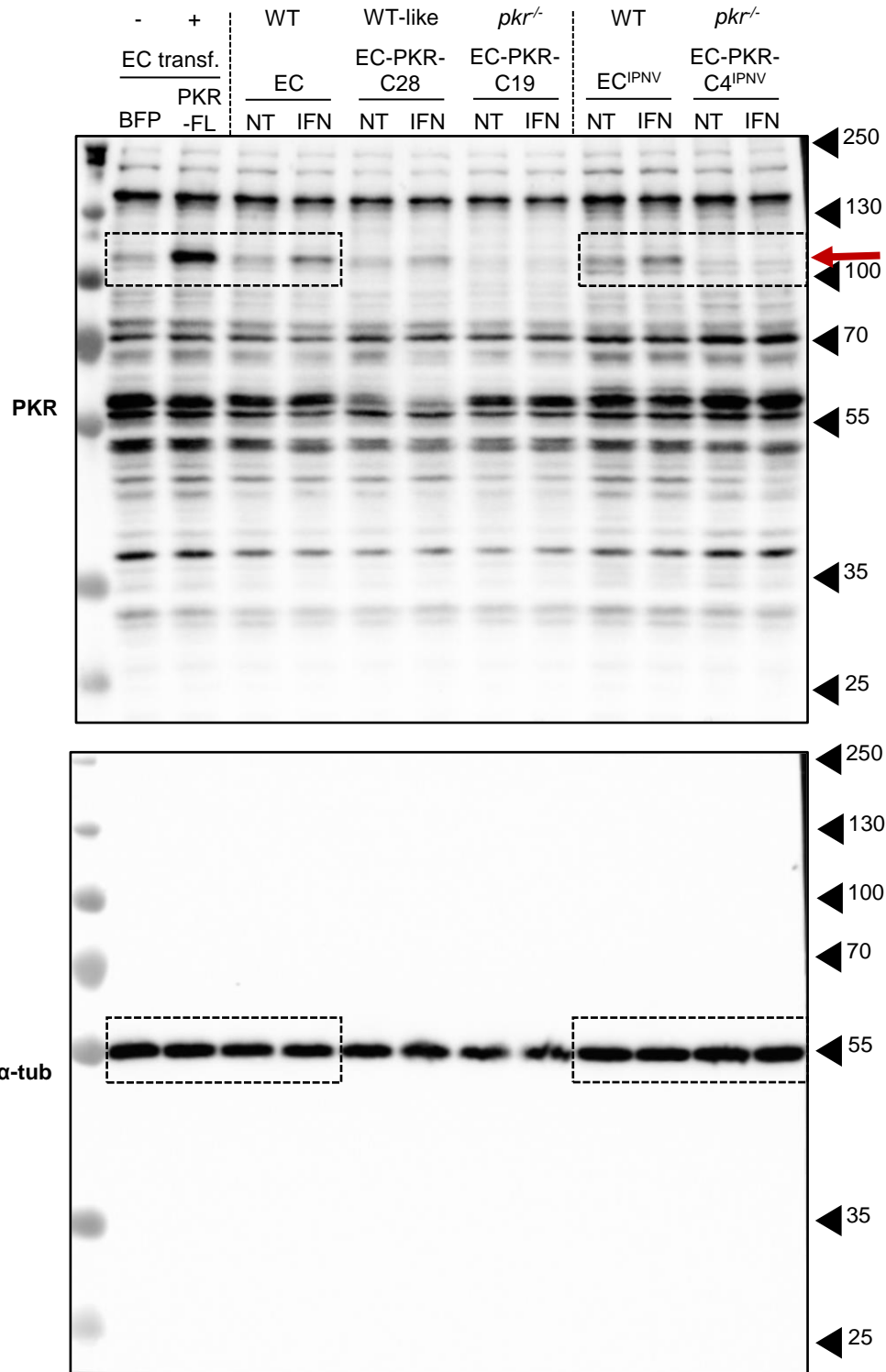


**Figure 38: Original full-length blots used in Figure 31**

Regions corresponding to the cropped images are surrounded by a dotted line. The red arrow shows the band corresponding to PKR-FL.

Results 3 – Persistently IPNV-infected cell lines

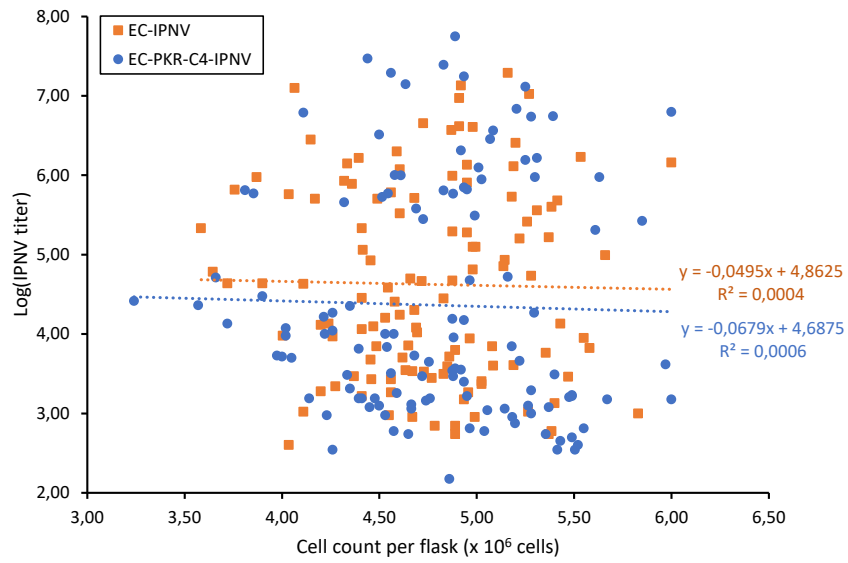


**Figure 39: Correlation between the number of cells per flask and the extracellular viral titers in the supernatants at each weekly sampling time point in EC<sup>IPNV</sup> and EC-PKR-C4<sup>IPNV</sup>**

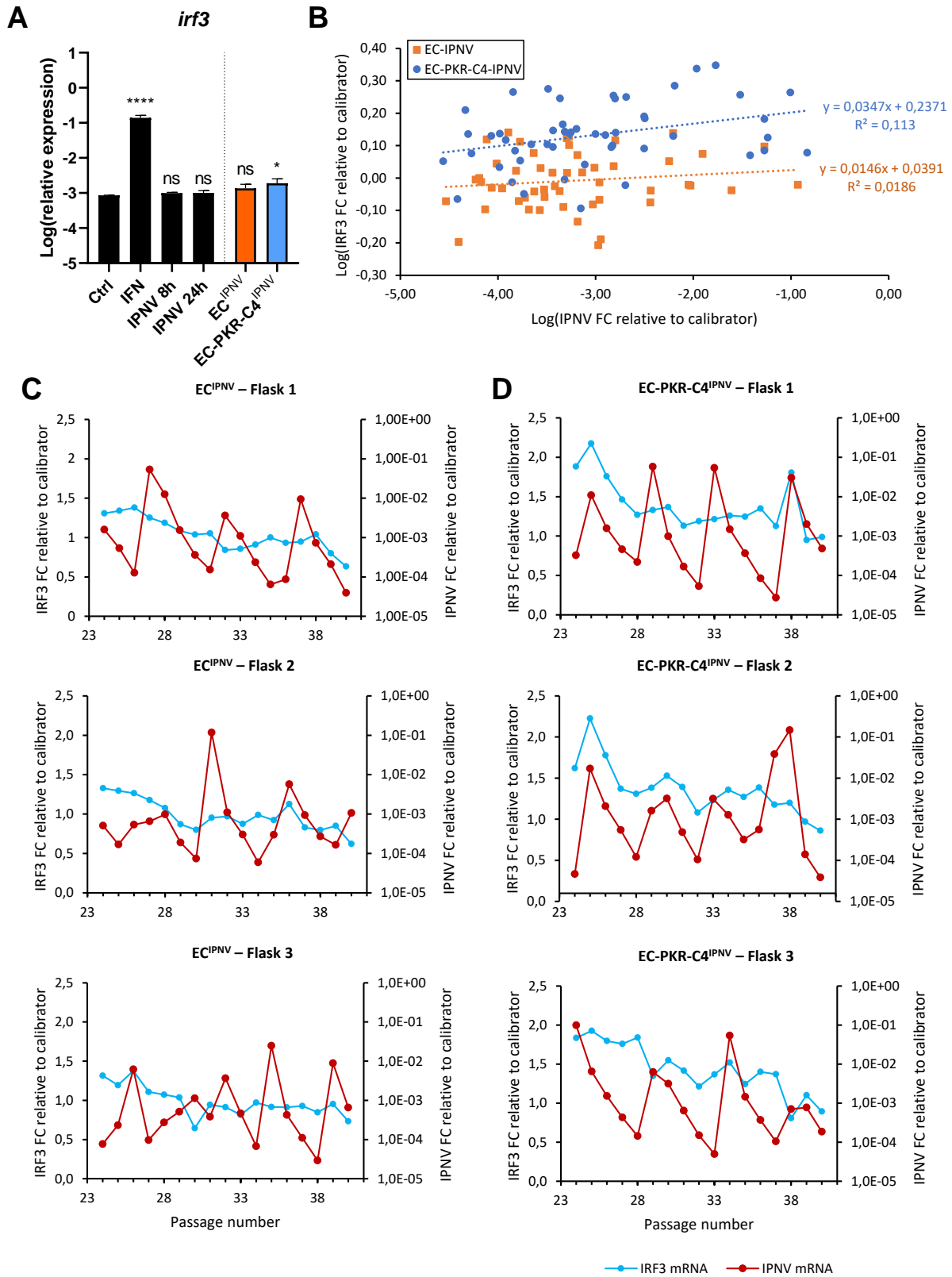


**Figure 40: IRF3 expression levels in persistently IPNV-infected cells.**

(A) Dotplot showing log-transformed *ipnv* mRNA levels (represented as fold change relative to calibrator) as a function of log-transformed *irf3* mRNA levels in persistently IPNV-infected  $EC^{IPNV}$  and  $EC-PKR-C4^{IPNV}$  cells. Distinct linear regressions were performed on  $EC^{IPNV}$  and  $EC-PKR-C4^{IPNV}$  datasets. (B,C) Graphs showing *ipnv* and *irf3* mRNA levels over the course of passages in each individual flasks of  $EC^{IPNV}$  (B) and  $EC-PKR-C4^{IPNV}$  (C).

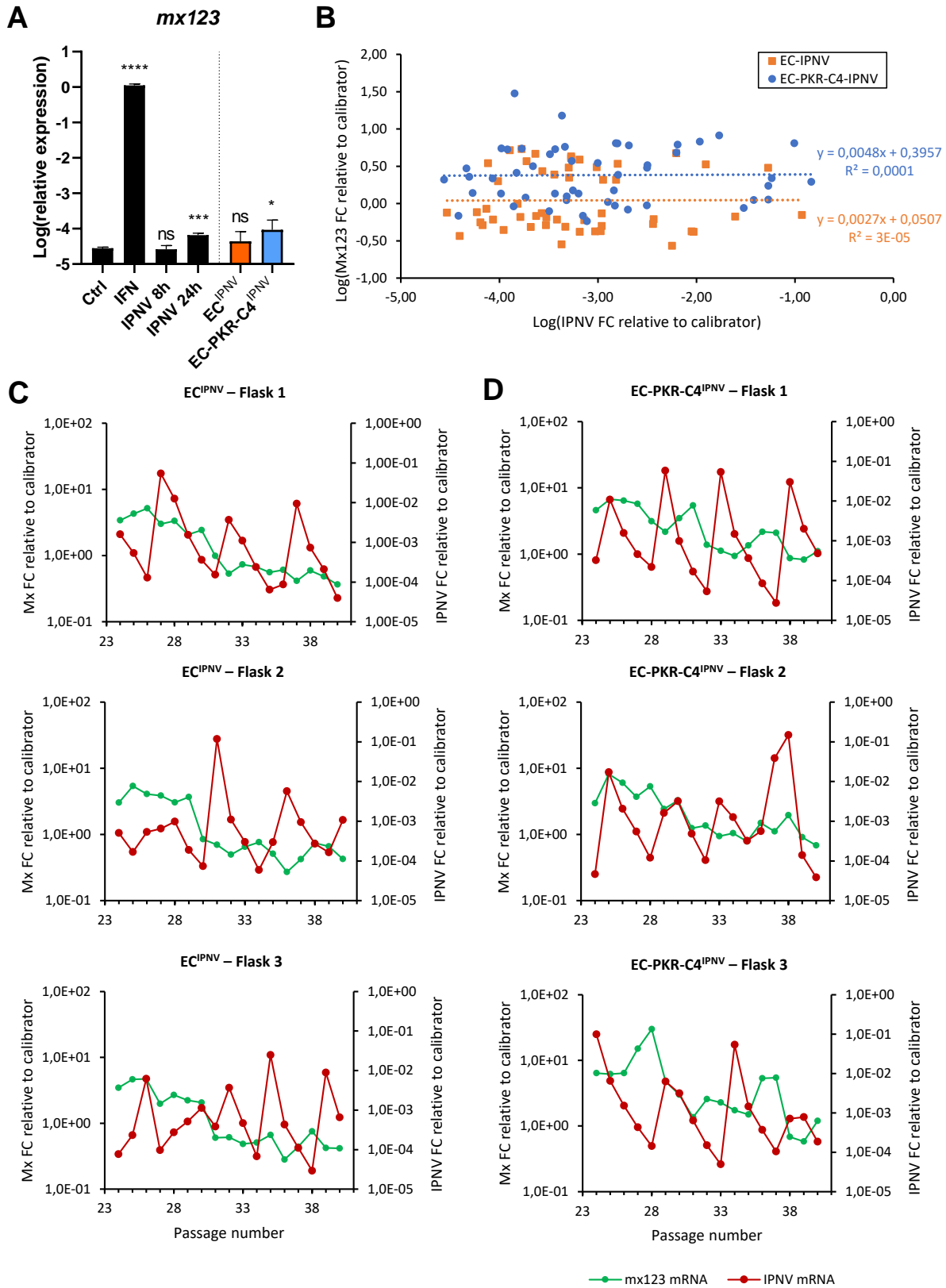


**Figure 41: Mx123 expression levels in persistently IPNV-infected cells.**

(A) Dotplot showing log-transformed *ipnv* mRNA levels (represented as fold change relative to calibrator) as a function of log-transformed *mx123* mRNA levels in persistently IPNV-infected EC<sup>IPNV</sup> and EC-PKR-C4<sup>IPNV</sup> cells. Distinct linear regressions were performed on EC<sup>IPNV</sup> and EC-PKR-C4<sup>IPNV</sup> datasets. (B,C) Graphs showing *ipnv* and *mx123* mRNA levels over the course of passages in each individual flasks of EC<sup>IPNV</sup> (B) and EC-PKR-C4<sup>IPNV</sup> (C).

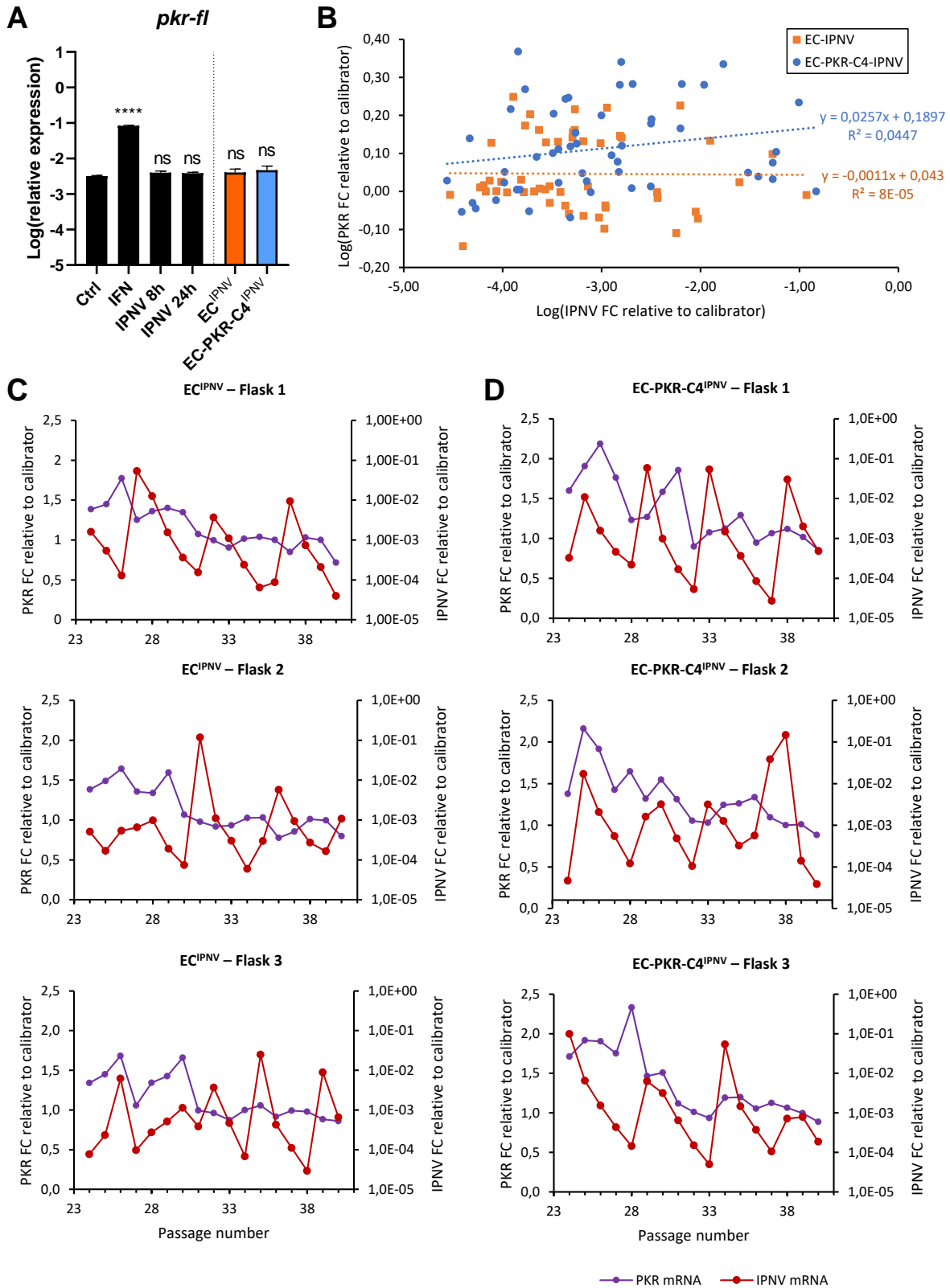


**Figure 42: PKR expression levels in persistently IPNV-infected cells.**

(A) Dotplot showing log-transformed *ipnv* mRNA levels (represented as fold change relative to calibrator) as a function of log-transformed *pkf-fl* mRNA levels in persistently IPNV-infected EC<sup>IPNV</sup> and EC-PKR-C4<sup>IPNV</sup> cells. Distinct linear regressions were performed on EC<sup>IPNV</sup> and EC-PKR-C4<sup>IPNV</sup> datasets. (B,C) Graphs showing *ipnv* and *pkf-fl* mRNA levels over the course of passages in each individual flasks of EC<sup>IPNV</sup> (B) and EC-PKR-C4<sup>IPNV</sup> (C).

---

# **GENERAL DISCUSSION**

---

Compared to mammals, the *ISGs* repertoire is more diverse in fish species, largely due to whole genome duplication events that have occurred over their evolutionary history. Apart from a few exceptions, most mammalian *ISGs* have one or more orthologs in fish species. However, in most cases, it remains unclear whether fish genes are true functional homologs, as evidence that their mechanisms of action and interactions within the type I IFN pathway are conserved is still lacking.

The aim of my PhD project was to investigate the function(s) and the contribution to the antiviral immune response of two key *ISGs* in fish, *pkc* and *viperin*, by using a CRISPR/Cas9-based knockout approach in fish cell lines. In this regard, my thesis objectives were articulated along three axes, that were (1) to develop and validate *pkc*<sup>-/-</sup> and *viperin*<sup>-/-</sup> fish cells, using the salmonid CHSE-EC cell line and cyprinid EPC-EC cell line as parental cell lines, respectively; (2) to functionally characterize these cell lines, in order to decipher the mechanisms of action of salmonid PKR and cyprinid Viperin and their potential role in regulating the type I IFN response through feedback loops; (3) to assess their permissivity to viral infections and evaluate their potential for viral particle production at higher yields than their wildtype counterparts.

In this section, I will first discuss our key scientific findings in relation to **objective 2**: the functions identified for salmonid PKR and the regulatory role of cyprinid Viperin will be examined in light of the literature. In both cases, limitations of our study and future research work that could be carried out to expand on our functional analysis will be addressed. Secondly, our results regarding **objective 3** will be summarized and the potential use of knockout fish cell lines for virus production as well as the associated challenges will be discussed. Finally, I will situate my PhD project in the context of the broader research project initiated in our laboratory and focusing on the development of knockout fish cell lines to investigate the function(s) of specific components of the type I IFN pathway in teleosts. In this regard, challenges relative to the characterization of knockout cell lines, future technical development avenues and research prospects will be outlined.

## 1. Salmonid PKR

### Salmonid PKR has conserved molecular functions that can be bypassed by fish viruses

In **Results 1**, my work builds on previous studies focusing on PKR of fish species from various taxonomic orders, including Tetraodontiformes, Perciformes, Pleuronectiformes and Cypriniformes<sup>199,200,231,238,239,265,266</sup>. Our study provides more insight into the molecular functions of salmonid PKR, which is curiously missing from these functional studies except one<sup>267</sup>. Unlike most of these studies, we used complementary approaches based on both overexpression and knockout experiments to confirm that Chinook salmon PKR has conserved molecular functions, including

apoptosis activation and inhibition of host protein synthesis. However, it appears that endogenous PKR does not play a major antiviral role during VHSV or GSV infections in CHSE-EC cells. In fact, our results suggest that VHSV has evolved a strategy to subvert PKR antiviral action, by limiting early induction of *pkr* expression and evading PKR-mediated translational arrest. In addition, VHSV seems to take advantage of PKR-mediated apoptosis to favor viral spread at a late stage of infection. This study provides a new example of the strategies developed by viruses to counter or hijack the molecular “antiviral” functions of PKR described in mammals<sup>377</sup> and in fish<sup>172,267</sup>.

### **Which other eIF2 $\alpha$ kinases are involved in the antiviral response against VHSV?**

Our findings indicate that, during VHSV (and GSV) infection, eIF2 $\alpha$  phosphorylation and host translational arrest is a PKR-independent process, which raises the question of which other kinase is mediating this particular response. Indeed, besides PKR, eIF2 $\alpha$  can be phosphorylated by four other kinases, including PERK, GCN2, HRI and PKZ<sup>200,202</sup>. Although each eIF2 $\alpha$  kinase primarily responds to specific stress (PKR and PKZ during viral infections, PERK during ER stress, GCN2 under amino acid starvation conditions, HRI during heme deprivation), several studies suggest they may have cooperative functions<sup>201,204,205</sup>. Recent chemical inhibitor-based studies provide evidence that eIF2 $\alpha$  phosphorylation is likely mediated by PERK during VHSV infection<sup>172,271</sup>. Building on these studies, our study could be followed up with additional work that examines the role of PERK (LOC112236837, LG08) during viral infections by developing a *perk*<sup>-/-</sup> CHSE-EC cell line.

Apart from PERK, the role of Chinook salmon PKZ, the fish-specific paralog of *pkr*, remains largely unexplored. PKZ is an eIF2 $\alpha$  kinase, in which the dual dsRNA-binding domain is replaced by two or more Z $\alpha$  motifs, which bind dsDNA and dsRNA in the left-handed Z conformation<sup>203</sup>. Like *pkr*, the *pkz* gene classifies as an *ISG*<sup>198,203,229,239</sup>. Interestingly, Liu *et al.* (2011) demonstrated that Crucian carp PKR and PKZ displayed a cooperative antiviral effect against GCRV by triggering inhibition of host protein synthesis<sup>239</sup>. In contrast, a recent *in vivo* study with *pkr*<sup>-/-</sup> and *pkz*<sup>-/-</sup> zebrafish larvae infected with a cyprinid herpesvirus (CyHV-3) showed that both KOs had no drastic effect on viral loads<sup>263</sup>. A *pkz* gene (LOC112251961) is present in the genome of Chinook salmon and is located downstream of *pkr* (LOC112253229). Whether this gene is expressed in CHSE-EC cells during IFNA2 stimulation and/or viral infection and whether there is a cooperative role of PKR and PKZ upon viral infections in our cell line model remains to be elucidated. These questions should be addressed in future work, with the generation of double or triple knockout mutants, to clarify the functional and synergic relationship of PKZ with PKR and/or PERK during virus infection.

## **Perspectives: what is the regulatory role of salmonid PKR in the inflammatory and IFN response?**

In addition to exploring the antiviral effects of PKR in relation to PKZ and other kinases, future research avenues could take advantage of the tools and cell lines developed in this study to investigate the role of salmonid PKR (and maybe PKZ) in the regulation of the innate immune response. Indeed, several studies in mammalian models provide evidence that PKR potentiates the type I IFN response *via* different mechanisms, including activation of NF- $\kappa$ B<sup>347,348,355</sup>, interaction with RIG-I and MDA5<sup>356,357</sup> and formation of stress granules which function as dsRNA sensing platforms<sup>374,375</sup>. In fish, it was recently reported that chemical inhibition of PKR in EPC cells resulted in a significant decrease in innate immune genes during VHSV infection<sup>271</sup>. Similarly, overexpression of Orange-spotted grouper PKR induced the expression of specific *ISGs* and increased the activity of NF- $\kappa$ B promoter<sup>231</sup>. Comparable work on Grass carp PKZ suggests that fish PKZ might also enhance the type I IFN response<sup>232</sup>. Exploring the role of salmonid PKR/PKZ in these pathways by transcriptomic analysis would provide of more comprehensive picture of the role of fish PKR in regulating inflammatory and IFN responses and may help discover non-canonical functions of fish PKR.

Another research axis would be to study the impact of a null mutation of fish *pkR* and/or *pkZ* using an *in vivo* model. Indeed, although our study and others showed that PKR and/or PKZ did not play a major antiviral role against fish viruses, including VHSV and CyHV-3<sup>172,263</sup>, the role of PKR may vary from one cell type to another and from one virus to another (as described in [Chapter 2, Section 4.3](#)). The presence of potent inhibitors of PKR in the genome of poxviruses, such as vaccinia E3L and K3L which antagonize PKR by sequestering dsRNA or acting as a pseudosubstrate, respectively<sup>383,601,602</sup>, as well as putative inhibitor of PKZ in the genome of herpesviruses, such as CyHV-3 ORF112<sup>289,603</sup>, strongly suggests that these genes have an important antiviral activity during infections with specific viruses, which remain to be identified.

## **2. Cyprinid Viperin**

### **Cyprinid Viperin plays a regulatory role in inflammation and metabolism**

In [Results 2](#), we investigated the role of fish Viperin in the regulation of the innate immune response and in other pathways by conducting a comparative analysis of the cellular transcriptome of cyprinid *viperin*<sup>-/-</sup> and wildtype cell lines with or without stimulation with type I IFN. Our analysis revealed that Viperin is not involved in positive feedback loops of the canonical type I IFN response in this cell line but modulates the expression of a subset of genes involved in the inflammatory response by downregulating specific pro-inflammatory genes and upregulating repressors of the NF- $\kappa$ B pathway.

In addition, our data further indicate that Viperin is involved in the regulation of metabolic pathways (*e.g.* one carbon metabolism, bone formation, extracellular matrix organization and cell adhesion), thereby providing further evidence to support the emerging idea that Viperin plays a role in cellular metabolism, even in a non-infectious context.

### **Limitations from our transcriptomic study and resulting research prospects**

A first limitation from our transcriptomic study to be aware of is that it was performed on an epithelial-like cell line, which is only representative of one specific cell type. However, a growing body of evidence suggest that Viperin's role greatly varies depending on the cell type and/or inducer used, even resulting in opposite outcomes<sup>474,477,479</sup> (for more details, refer to **Chapter 3, Sections 5.2.1 and 5.2.2**). Therefore, our transcriptomic results must be seen in this light. For instance, our data indicate that Viperin does not potentiate the type I IFN response following stimulation with recombinant IFN supernatant; however, it would be hazardous to extrapolate these results to a general function (or absence thereof) of cyprinid Viperin. Indeed, many antiviral ‘effector’ ISGs, including PKR (presented in introduction), ISG15<sup>142,604</sup> and others in both mammals and fish, are known for modulating the IFN pathway in addition to their “direct” antiviral functions. Consistently, mammalian Viperin was found to be required for the production of type I IFN following engagement of TLR7 and TLR9 in plasmacytoid dendritic cells<sup>440</sup>. Therefore, it is not unlikely that cyprinid Viperin enhances the type I IFN response *via* positive feedback loops in other cell types and/or upon stimulation with a different inducer. Further research in other cell types and/or in *in vivo* models needs to be carried out to explore this hypothesis.

Furthermore, although our RNA-Seq analysis highlighted specific pathways that echoed findings from other studies, such as bone metabolism<sup>386</sup> and extracellular matrix and cell adhesion<sup>605</sup>, other metabolic pathways described as being modulated by Viperin in the literature were absent from our analysis. For instance, several studies provide evidence pointing to a role of Viperin in the modulation of lipid metabolism by inhibiting cholesterol biosynthesis<sup>422,426,444,481</sup> and limiting fatty acid  $\beta$ -oxidation *via* interaction with mitochondrial trifunctional protein<sup>439,467</sup>. However, our transcriptomic datasets did not reveal major expression changes in genes involved in these pathways. One reason that may explain this discrepancy is that Viperin may not affect the transcription of the genes coding for these enzymes but only limits their enzymatic activity *via* post-translational mechanisms, including promotion of protein degradation<sup>422,426</sup>. In fact, it seems that Viperin exerts some of its functions *via* protein-protein interactions<sup>151</sup>. As a consequence, potential changes at the protein level induced by Viperin are likely to go unnoticed in a transcriptomic study. Proteomics studies should be carried out to explore those functional aspects of Viperin.

Although our transcriptomic analysis highlighted new or non-canonical pathways of interest that Viperin might be involved in, we should also proceed with caution before drawing conclusions and further studies are needed to confirm the predictions provided in this study. It should be noted that some of our analysis is based on the comparison of transcriptomes between WT and *viperin*<sup>-/-</sup> cell lines at the steady state, for which *viperin* expression is very low (normalized counts ~8 in the control WT cell line) and the biological relevance of the analysis must be seen in this light. In addition, in our transcriptomic study, we are unable to distinguish between the effect of the *viperin* knockout and the clonal effect that may arise from genetic drift during single-cell clonal expansion of our mutant cell line. This point will be further discussed in a dedicated section below ([Section 4](#)). While efforts have been made to minimize the variability associated to the cloning process by using a clonal parental cell line, further functional studies are needed to confirm or disprove the regulatory role of Viperin in these pathways and processes.

A final major limitation intrinsic to most transcriptomic studies is that our study does not offer clues regarding the mechanisms of action underlying the regulatory role of Viperin. Now that Viperin's enzymatic activity is better known<sup>150</sup>, one question that arises is whether the production of ddhCTP and the regulation of cellular processes are two independent processes, or whether they are coupled. Indeed, ddhCTP generated by Viperin was initially described as a chain-terminating antiviral ribonucleotide for viral RdRp<sup>150</sup>. However, some authors have suggested that ddhCTP may have additional functions, including inhibition of NAD<sup>+</sup>-dependent dehydrogenases<sup>492</sup>, transcription regulation of mitochondrial genes<sup>467</sup> and promotion of ribosome collisions resulting in host translational arrest<sup>465</sup>. Further research into Viperin's regulatory role is needed to be able to identify possible control mechanisms. In particular, the analysis of interactome data may provide clues for future research.

### **3. Towards the use of knockout cell lines as virus production platforms?**

One of the objectives of my PhD project was to assess the potential of *pkr*<sup>-/-</sup> and *viperin*<sup>-/-</sup> cell lines as platforms to produce viral particles at higher yields than their wildtype counterparts. Indeed, the development and industrial production of inactivated vaccines, which still represent the main vaccine type currently available for the aquaculture market, is still limited by the relatively low yields of conventional viral particle production systems relying on permissive cell lines.

To address this issue, new manufacturing technologies are being investigated, including the optimization of cell culture media<sup>606</sup>, innovative bioreactor designs (*e.g.* roller bottles that allow higher cell densities or continuous systems)<sup>607,608</sup>, forced transition of adherent cells into suspension growth to increase cell densities<sup>609,610</sup>, selection of specific clones with enhanced functional

properties within a heterogeneous parental population <sup>611</sup>. Another technological approach is the engineering of cell lines using genome editing tools in order to improve viral titers. Based on the rational assumption that the innate immune response and more specifically the type I IFN response is a limiting factor for the production of viral particles in cell lines, one strategy is to invalidate specific *ISGs* involved in these pathways. The use of knockout cell lines defective for one or several components of the type I IFN pathway has proven successful for high-yield production in mammalian models. For instance, *Irf7*<sup>-/-</sup> MDCK cells were found to produce higher extracellular titers upon influenza virus infection than their wildtype counterparts <sup>612</sup>. Similarly, a ~2-log fold increase in influenza virus and VSV titers were reported in *Isg15*<sup>-/-</sup> Vero cells <sup>613</sup>. Importantly, engineered knockout cell lines are already used in industry for the production of specific viruses: for instance, Intervet (Merck/MSD) holds a patent for an *Irf3*<sup>-/-</sup> *Irf7*<sup>-/-</sup> MDBK cell line which is used for the production of bovine respiratory syncytial virus <sup>614</sup>.

Concerning our genes of interest, to the best of my knowledge, no specific *viperin* or *pkc* knockout cell lines were developed for virus production in mammalian models. Nonetheless, *viperin* knockdown was reported to increase influenza virus titers in MDCK cell line by ~1-log <sup>615</sup> and MEFs deriving from *viperin*<sup>-/-</sup> mice supported higher ZIKV and DENV replication rates and/or extracellular titers than WT MEFs <sup>410,472</sup>. Similarly, Sendai and Sindbis viruses were shown to replicate more efficiently in *PKR*<sup>-/-</sup> HeLa cell lines <sup>249</sup>. Despite these encouraging published results, our attempts to produce higher VHSV titers using *pkc*<sup>-/-</sup> and *viperin*<sup>-/-</sup> fish cell lines were unsuccessful and in the case of *pkc*<sup>-/-</sup> cell lines, titers were even slightly lower, presumably because VHSV takes advantage of PKR-mediated apoptosis to promote virion release.

Although our tests did not yield promising results with VHSV, it would be worth testing the ability of other viruses to replicate in the *pkc*<sup>-/-</sup> and *viperin*<sup>-/-</sup> cell lines. Indeed, the antiviral functions of Viperin and PKR are known to be virus-dependent and effects may drastically vary from one virus to another in mammalian models. For instance, Viperin knockdown and/or overexpression had no antiviral effects against flavivirus JEV <sup>456,462</sup>, Yellow fever virus <sup>462</sup>, paramyxovirus Shaan Virus <sup>463</sup>. Similarly, PKR-deficient MEFs infected with flavivirus DENV <sup>254</sup> and or measles virus <sup>255</sup> showed no detectable increase in virus yields.

### **Explaining the lack of improvement in viral yields from an evolutionary perspective?**

In the aforementioned mammalian models and in our fish cell lines, the lack of knockout effect on viral replication can typically be explained in two ways: (1) the virus has already developed strategies to counter the antiviral action of the protein of interest, making the knockout incidental; (2) the redundancy and robustness of the type I IFN response renders the loss of these specific ISGs negligible.

From an evolutionary perspective, both options likely play an equally important and concomitant role, as both viral and antiviral genes are under a strong evolutionary pressure, as postulated by the Red Queen hypothesis<sup>16</sup>. On this basis, it is not unreasonable to consider that the invalidation of a single ISG does not have a major impact on viral replication, when put back into a network as complex as the type I IFN system, with its hundreds of inducible ISGs and further backed by alternative IFN-independent antiviral pathways (e.g. IRF1-mediated pathways). This explanation is perhaps even more relevant of genes that are typically considered “effector” genes of the type I IFN response, such as *pkr* or *viperin*, as they may have a significant antiviral effect when co-expressed with other ISGs. In our study, the fact that the knockouts of *pkr* and *viperin* have no impact either on the replication of two different viruses, VHSV and GSV, or on the cells’ permissivity to other fish viruses (data not shown in this manuscript) suggests a predominant role of the second option.

In any case, more efficient CRISPR/Cas9-based strategies may be needed for the development of high-yield virus-producing cell lines.

#### **Alternative 1: targeting bottlenecks in signaling pathways?**

One alternative strategy could be to target genes that encode key proteins upstream in the type I IFN signaling cascade, including adaptor and signal transduction proteins (e.g. *trif*, *traf6*, *tbk1*), key receptors (e.g. *crfb5*) or key transcription factors (e.g. *irf1*, *irf3*, *irf7*, *stat1*, *stat2*, etc). In support of this strategy, the mammalian cell line developed by Intervet to produce bovine RSV is a double mutant for *Irf3* and *Irf7*<sup>614</sup>. Cell lines knocked out for some of these genes are currently being developed and/or characterized in our laboratory and may provide better platforms for the production of viral particles. Nonetheless, it should be noted the *stat2*<sup>-/-</sup> EC cell line previously developed in our laboratory only displayed moderately improved permissivity to EHNV, VHSV and SAV infections compared to WT cells, suggesting that this strategy may also have limits, likely due to alternative type I IFN-independent antiviral pathways<sup>136</sup>.

#### **Alternative 2: implementing a multiple gene knockout approach?**

In this regard, a second strategy could be to implement a multiple gene knockout approach. The rationale behind this approach is that different pathways and/or signaling bottlenecks need to be disrupted to circumvent the redundancy of the type I IFN system as well as IFN-independent pathways and effectively inhibit the antiviral innate response. In line with this reasoning, overexpression of one key ISG (e.g. *IRF1*, *IRF7*, *MDA5*, *RIG-I*) usually offered partial protection only against virus infection but co-expression of two ISGs improved inhibition of viral replication, suggesting that ISG-mediated antiviral effects are generally additive<sup>146</sup>. Consistently with these results, a combined effect of multiple gene knockdown on poliovirus titers compared to single gene

knockdown was also reported by Van der Sanden *et al.* (2016)<sup>616</sup>. Nonetheless, when implementing this approach, care should be taken to strike a balance between the disruption of specific pathways and cell survival/growth that can potentially be altered by the knockout.

### **Alternative 3: random screening of genes to invalidate?**

Alternatively, a third strategy could be to invalidate protein-coding genes at random and identify loss-of-function mutations promoting viral replication (without altering cell viability). This approach breaks away from this hypothesis that the type I IFN response is the main restricting factor for virus production and has the advantage of being unbiased, insofar as the targeted genes are not pre-selected. However, such a strategy requires to have or to develop genome-wide siRNA (RNAi technology) or sgRNA (CRISPR/Cas9 technology) libraries. Interestingly, this approach was proven successful using an siRNA library to identify genes for which knockdown increased poliovirus and rotavirus titers<sup>616,617</sup>. Surprisingly, most of these genes were not ISGs *per se* and were involved in other pathways, including CREB-dependent transcription pathway, ERK1/2 signaling pathway and apoptosis<sup>616</sup>. However, adapting this strategy to fish models is challenging: indeed, although premade lentivirus libraries for whole genome knockout screens are readily available for the human genome (*e.g.* LentiArray and LentiPool, Invitrogen), each fish species would require its own library to be developed. In addition, this approach primarily relies on a lentivirus-based delivery method, that needs to be optimized for fish cells<sup>558</sup>. Last but not least, the presence of numerous paralogous genes makes the task even more difficult and raises additional questions: should each paralog be invalidated one by one with the risk of compensatory effects, or should all paralogs be targeted all at once with the difficulty of developing sgRNAs that target several genes? In all cases, a great effort of research would be required.

### **Alternative 4: use of persistently infected cell lines?**

Last but not least, in the case of IPNV, another non-canonical option to be considered to produce viral particles is to take advantage of the persistently IPNV-infected cell lines presented in [Results 3](#). However, this would require several preliminary validation tests, including (1) to verify that the extracellular viral titers obtained are not lower than those classically obtained following acute infection, (2) to confirm that the viral particles are as antigenic as those obtained with an acute infection, and (3) to ensure that the potential presence of defective particles is not problematic. Regarding point 1, the data in [Results 3](#) are not encouraging insofar as even the highest titers are typically around  $10^7$ , *i.e.* 1-log lower than those classically obtained in case of acute infection on CHSE-214, suggesting that this strategy may not be as effective as the ones presented above.

#### 4. Challenges and limitations for the development of knockout fish cell lines

As mentioned earlier, my PhD project is part of a broader research project initiated in our laboratory and aiming at developing a “bank” of fish cell lines knocked-out for various *ISGs* to elucidate their function(s) and associated mechanisms of action. During the generation process of the *pkr*<sup>-/-</sup> CHSE-EC and *viperin*<sup>-/-</sup> EPC-EC cells, I was confronted with a number of challenges and limitations related to the development and characterization of knockout fish cell lines, which are worth discussing.

##### Challenges concerning the development of knockout fish cell lines

When considering the development of knockout fish cell lines, it is important to be aware that the process is not as straightforward as in mammalian *in vitro* models due to various difficulties at different development steps, including design of sgRNAs and knockout validation.

Firstly, the WGD events during the evolution of fish, including the teleost-specific and the salmonid-specific ones<sup>9-11</sup>, introduce another layer of complexity, making a thorough *in silico* study of the genome a pre-requisite to the design of sgRNAs. Importantly, whenever a new version of the genome of interest is released, care should be taken to check for the presence of previously unidentified paralogous genes that may become visible due to assembly improvements. To go even further, having a pangenome of the species considered, would provide insights into point and structural variants in the genes of interest and help the design of sgRNAs. In addition to having a proper (pan)genome assembly of the species of interest, it is also preferable to have the genome of the cell line itself, if possible. Indeed, in mammalian models, cell lines are known for their genetic instability over time leading to chromosomal rearrangement, aneuploidy, gain or loss of gene copies<sup>611,618</sup>. In fish, this phenomenon is not well documented, but the genotyping results of our *viperin*<sup>-/-</sup> EPC-EC clones suggest that the EPC-EC cell line has undergone local duplication event or (partial) chromosome gain during its development process (see Discussion from [Results 2](#) for more details). Having a well-characterized parental cell line at the genomic and chromosomal levels would help avoid some of these pitfalls.

Technical difficulties for the development and the validation of clonal knockout fish cell lines should also be taken into consideration. Indeed, most mammalian cell lines commonly used for CRISPR/Cas9-based genome editing have the advantage of having relatively short cell division times, high transfection efficiencies and they are often “clonable” (*i.e.* they have the ability to propagate from a single cell). In contrast, most fish cell lines have a much longer division time while others are not easily transfected (*e.g.* RTG-2 and derivatives)<sup>533</sup>. As a consequence, the cloning process is often time-consuming and laborious; for instance, 4 months were needed for individualized EPC-EC cells to grow sufficiently to be genotyped.

In addition, once clones with mutated genotypes have been obtained the knockout validation process can also be tricky. In mammalian models, it is recommended to validate the gene disruption using several methods, including western blots and RT-qPCR. In fish models, the scarcity of specific antibodies against the targeted protein makes the knockout validation at the protein level often laborious or impossible, if the gene of interest is a fast-evolving gene. In mammals, introduction of a premature stop codon following CRISPR/Cas9-mediated strand break can induce nonsense-mediated mRNA decay (NMD)<sup>619</sup>, which can be detected by RT-qPCR. However, not all mutated transcripts trigger NMD and the position of the premature stop codon within the transcript affect its susceptibility to NMD<sup>620,621</sup>. Curiously, in our fish cell lines no massive NMD was detected by RT-qPCR for the target genes, suggesting that the NMD rules described for mammals might not apply to fish models<sup>620</sup>. Nonetheless, a systematic study should be carried out to confirm this hypothesis.

### **Limitations of our workflow**

Besides these technical challenges specific to the development of knockout fish cell lines, our CRISPR/Cas9-based workflow has two important hurdles also found in mammalian models: (1) the risk of off-target mutations and (2) the clonal effect.

#### *Off-target mutations*

Off-targets are unwanted mutations in the genome resulting from the sgRNA binding to DNA sequences presenting mismatches<sup>622</sup>. The CRISPR/Cas9 technology (and other CRISPR/Cas approaches) is bound to lead to off-targets<sup>622</sup>. However, the risk of problematic off-targets can be minimized by implementing different strategies, including: (i) carefully designing sgRNAs using tools such as Crispor<sup>623</sup> or ChopChop<sup>624</sup>, which help identify the most likely off-targets and their location (exon, intron, intergenic region); (ii) using new generation Cas9 proteins (*e.g.* eSpCas9, HypaCas9) which have been engineered to have enhanced specificity<sup>625-627</sup>; (iii) using delivery methods that do not result in a prolonged or permanent expression of both Cas9 and sgRNA, which can favor off-target events (*e.g.* plasmid- or lentivirus-based delivery strategies)<sup>628</sup>; (iv) developing knockout clones obtained using different sgRNAs.

Our pipeline to develop knockout fish cell lines includes the use of Crispor for sgRNA design and the delivery method is based on the direct transfection of sgRNAs. It should be noted that CHSE-EC was initially developed to constitutively express Cas9<sup>555</sup>, but during my PhD, transfections of both recombinant Cas9 protein and sgRNAs were implemented, as the consistency of transfections with sgRNAs alone resulting in mutated bulks deteriorated for unknown reasons. Nonetheless, in both cases, sgRNAs were likely not present in the cells for a prolonged period of time, as sgRNAs have an estimated half-life of 1-3 hrs<sup>629,630</sup>. Concerning point (iv), for each targeted gene, I failed to obtain

different knockout clones generated with distinct sgRNAs: for the *pkr*<sup>-/-</sup> cell lines, although four different sgRNAs were tested, only one resulted in mutated bulks and for the *viperin*<sup>-/-</sup> cell line, only the bulks transfected with sgRNA-Vip1 and sgRNA-Vip2 gave rise to fully mutated clones. Nonetheless, even in this situation, we believe that the risk of off-target mutations is low. Indeed, independent empirical observations in our laboratory have shown that two distinct sgRNAs (targeting two very similar paralogs) differing by just 1 or 2 nucleotides do not cross-react. The development of single, double and triple *mx* knockout cell lines, presented in [Appendix 3](#), is another telling example of how very similar sgRNAs result in mutations only in the targeted gene, leaving the other paralogs untouched. Overall, although off-target effects cannot be completely ruled out, we believe that they are likely limited thanks to the efforts made to keep their negative effects to a minimum.

### *Clonal effect*

The so-called “clonal effect” refers to phenotypic variability between different clones generated from the same cell population that may arise from genetic drift or other non-genetic factors (*e.g.* transcriptional activity) during single cell clonal expansion. For the same reasons, subcloning from a clonally-derived population does not result in genetically identical and/or homogenous clonal populations either, highlighting the existence of an intra-clonal diversity<sup>611,631,632</sup>. In mammalian models, this clonal effect has been described in multiple studies<sup>611,631-635</sup>.

However, in knockout studies, clonal isolation from a genome-edited cell population is often a necessary step to generate a fully mutated cell line<sup>636</sup> and it is also implemented in our workflow. Nonetheless, it was recently pointed out that the phenotypic heterogeneity of parental cells is an important and often disregarded factor in knockout studies in cell lines, which can give rise to phenotypically different clones, without these differences being due to the knockout of the gene of interest<sup>635</sup>. In this study, the authors reported various cellular and biochemical differences between different WT clones and identified hundreds of DEGs ( $|\log_2FC| > 1$ ,  $p$ -value  $< 0.01$ ) between a population of the mouse mIMCD-3 cell line (originally established as a monoclonal cell line) and recently obtained WT clones deriving from this cell line<sup>635</sup>. In contrast, they showed that subclones deriving from a recent clonally-derived cell population showed similar transcriptomic profiles, suggesting that the generation of clonally-derived wild-type cells prior to genomic manipulation reduces variability<sup>635</sup>.

In our different studies, we believe that this “clonal effect” is limited, as the parental cell lines (CHSE-EC, EPC-EC) were already clonally-derived cell lines, which minimizes the variability associated to the cloning process. In addition, the CHSE-EC cell line appears to benefit from a high genomic stability, which might be linked to the initial method used to obtain the initial CHSE-214 (*i.e.* spontaneous immortalization instead of induced immortalization through inactivation of tumor

suppressor genes and/or expression of telomerase reverse transcriptase protein<sup>637</sup>). The genomic integrity of this CHSE-EC is currently being studied and characterized in detail in our laboratory. In any case, in the different subprojects presented in this manuscript, the use of different clones, wherever possible, helped rule out any clonal effect and prevent hasty conclusions.

Nonetheless, in addition to studying multiple clones, rescue experiments and/or knockout reversal could help eliminate false-positive results, including phenotypes resulting from both clonal effects and off-target effects.

## 5. Perspectives

### Towards the development of knock-in models?

As mentioned above, rescue experiments and reversal of genome-editing would help validate phenotypes obtained by comparing WT and knockout clones.

Rescue experiments consist of reintroducing the gene of interest into the genome of the knockout cell line and establishing a stable cell line, typically by transfection with a plasmid encoding the gene of interest, selection with antibiotics and cloning. Although easy to implement, this method is time-consuming and does not restore the native expression levels of the gene of interest, as its expression is under the control of the promoter present in the plasmid. Furthermore, it relies on the random integration of the plasmid into the cell's genome. In my PhD project, no rescue experiments were carried out *per se*, but transient transfections with plasmids encoding the gene of interest were performed resulting in opposite results (**Results 1**). Of note, for the PKR study, we failed to generate stable PKR-expressing clones from *pkrr*<sup>-/-</sup> cells transfected with PKR rescue plasmids, probably because of the cytotoxicity of PKR.

To take it a step further, it would be interesting to develop a protocol for knockout reversal in genome-edited clones in order to rescue the target gene and fully validate the gene function. In other words, the edited gene sequence is modified by targeted mutation in order to restore the native sequence. Contrary to rescue experiments, the gene of interest is still under the control of its native promoter and it does not require any genomic integration. In practical terms, this protocol would likely be based on a knock-in strategy. The term “knock-in” usually refers to both precise insertion/deletion or introduction of single or multiple transgenes. In case of knockout reversal, the first option would be typically considered. Contrary to knock-outs which are primarily obtained following the appearance of random indels at the targeted cut site *via* the NHEJ-mediated repair pathway, knock-ins primarily exploit the HDR-mediated repair pathway<sup>534</sup>. For this purpose, a homologous DNA sequence (*e.g.* ssDNA, dsDNA or plasmid) needs to be provided as a repair template to regenerate a matching DNA

sequence into the double-strand break<sup>534</sup>. By using a WT DNA template, it should be possible to reverse the loss-of-function mutation back to the WT sequence. This strategy was successfully developed in mammalian cell lines<sup>638,639</sup> but so far, no analogous work has been carried out in fish cell lines. Interestingly, this rescue strategy was successfully performed in albino zebrafish embryos, in which the *tyrosinase* gene (required for the conversion of tyrosine into melanin) had been knocked-out and then rescued by knock-in, thereby restoring the pigmentation<sup>640</sup>.

Preliminary knock-in tests are currently being conducted our laboratory to test whether this strategy could be implemented in fish cell lines.

### **Towards the understanding the functional specialization of paralogs?**

The development of fish knockout cell lines also offers great opportunities to investigate the functional specialization of paralogous genes in fish. This research avenue is particularly interesting for genes in extended families, which are a common occurrence in fish due to their evolution history<sup>14,79</sup>. I could not explore this research axis with my studies on *pkr* and *viperin* presented in this manuscript, as only one copy of the gene is present in the genome of the species considered. Nonetheless, I had the chance to develop CHSE-EC cell lines, in which 3 *mx* genes were invalidated using the same CRISPR/Cas9 approach: single, double and triple knockout clones could be generated and validated by western blots ([Appendix 3](#)). Preliminary results suggest that compensatory effects exist between different genes, with some paralogs being primarily expressed when others are knocked out. These cell lines provide an excellent model for studying these paralog-specific effects and their characterization is likely to yield exciting results.

## **6. Conclusion**

Overall, my research on the development and the characterization of *pkr*<sup>-/-</sup> and *viperin*<sup>-/-</sup> fish cell lines has provided novel insights into the molecular and regulatory functions of two key ISGs in fish, namely PKR and Viperin. This work further highlights the action potential of specific ISGs beyond the scope of the type I IFN response, as exemplified by Viperin's role in regulating specific metabolic pathways *a priori* unrelated to the antiviral response. The extension of this knockout approach to other ISGs combined with diverse characterization techniques will surely help in our understanding of this complex network.

---

# REFERENCES

---

## References

- (1) Ertl, H. C. J. Chapter 44: Response to Viruses. In *Paul's Fundamental Immunology*; Lippincott Williams & Wilkins, 2022.
- (2) Lindenmann, J.; Burke, D. C.; Isaacs, A. Studies on the Production, Mode of Action and Properties of Interferon. *Br J Exp Pathol* **1957**, *38* (5), 551–562.
- (3) Nagata, S.; Taira, H.; Hall, A.; Johnsrud, L.; Streuli, M.; Ecsödi, J.; Boll, W.; Cantell, K.; Weissmann, C. Synthesis in *E. Coli* of a Polypeptide with Human Leukocyte Interferon Activity. *Nature* **1980**, *284* (5754), 316–320. <https://doi.org/10.1038/284316a0>.
- (4) de Kinkelin, P.; Dorson, M. Interferon Production in Rainbow Trout (*Salmo Gairdneri*) Experimentally Infected with Egtved Virus. *J Gen Virol* **1973**, *19* (1), 125–127. <https://doi.org/10.1099/0022-1317-19-1-125>.
- (5) Altmann, S. M.; Mellon, M. T.; Distel, D. L.; Kim, C. H. Molecular and Functional Analysis of an Interferon Gene from the Zebrafish, *Danio Rerio*. *J Virol* **2003**, *77* (3), 1992–2002. <https://doi.org/10.1128/JVI.77.3.1992-2002.2003>.
- (6) Lutfalla, G.; Crollius, H. R.; Stange-thomann, N.; Jaillon, O.; Mogensen, K.; Monneron, D. Comparative Genomic Analysis Reveals Independent Expansion of a Lineage-Specific Gene Family in Vertebrates: The Class II Cytokine Receptors and Their Ligands in Mammals and Fish. *BMC Genomics* **2003**, *15*.
- (7) Robertsen, B.; Bergan, V.; Røkenes, T.; Larsen, R.; Albuquerque, A. Atlantic Salmon Interferon Genes: Cloning, Sequence Analysis, Expression, and Biological Activity. *Journal of Interferon & Cytokine Research* **2003**, *23* (10), 601–612. <https://doi.org/10.1089/107999003322485107>.
- (8) Nelson, J. S.; Grande, T.; Wilson, M. V. H.; Wilson, M. V. *Fishes of the World*, Fifth edition.; John Wiley & Sons: Hoboken, New Jersey, 2016.
- (9) Berthelot, C.; Brunet, F.; Chalopin, D.; Juanchich, A.; Bernard, M.; Noël, B.; Bento, P.; Da Silva, C.; Labadie, K.; Alberti, A.; Aury, J.-M.; Louis, A.; Dehais, P.; Bardou, P.; Montfort, J.; Klopp, C.; Cabau, C.; Gaspin, C.; Thorgaard, G. H.; Boussaha, M.; Quillet, E.; Guyomard, R.; Galiana, D.; Bobe, J.; Volff, J.-N.; Genêt, C.; Wincker, P.; Jaillon, O.; Crollius, H. R.; Guiguen, Y. The Rainbow Trout Genome Provides Novel Insights into Evolution after Whole-Genome Duplication in Vertebrates. *Nat Commun* **2014**, *5* (1), 3657. <https://doi.org/10.1038/ncomms4657>.
- (10) Lien, S.; Koop, B. F.; Sandve, S. R.; Miller, J. R.; Kent, M. P.; Nome, T.; Hvidsten, T. R.; Leong, J. S.; Minkley, D. R.; Zimin, A.; Grammes, F.; Grove, H.; Gjuvsland, A.; Walenz, B.; Hermansen, R. A.; von Schalburg, K.; Rondeau, E. B.; Di Genova, A.; Samy, J. K. A.; Olav Vik, J.; Vigeland, M. D.; Caler, L.; Grimholt, U.; Jentoft, S.; Inge Våge, D.; de Jong, P.; Moen, T.; Baranski, M.; Palti, Y.; Smith, D. R.; Yorke, J. A.; Nederbragt, A. J.; Tooming-Klunderud, A.; Jakobsen, K. S.; Jiang, X.; Fan, D.; Hu, Y.; Liberles, D. A.; Vidal, R.; Iturra, P.; Jones, S. J. M.; Jonassen, I.; Maass, A.; Omholt, S. W.; Davidson, W. S. The Atlantic Salmon Genome Provides Insights into Rediploidization. *Nature* **2016**, *533* (7602), 200–205. <https://doi.org/10.1038/nature17164>.
- (11) Macqueen, D. J.; Johnston, I. A. A Well-Constrained Estimate for the Timing of the Salmonid Whole Genome Duplication Reveals Major Decoupling from Species Diversification. *Proceedings of the Royal Society B: Biological Sciences* **2014**, *281* (1778), 20132881. <https://doi.org/10.1098/rspb.2013.2881>.
- (12) Pasquier, J.; Cabau, C.; Nguyen, T.; Jouanno, E.; Severac, D.; Braasch, I.; Journot, L.; Pontarotti, P.; Klopp, C.; Postlethwait, J. H.; Guiguen, Y.; Bobe, J. Gene Evolution and Gene Expression after Whole Genome Duplication in Fish: The PhyloFish Database. *BMC Genomics* **2016**, *17* (1), 368. <https://doi.org/10.1186/s12864-016-2709-z>.
- (13) Suurväli, J.; Garroway, C. J.; Boudinot, P. Recurrent Expansions of B30.2-Associated Immune Receptor Families in Fish. *Immunogenetics* **2022**, *74* (1), 129–147. <https://doi.org/10.1007/s00251-021-01235-4>.
- (14) Wang, T.; Liu, F.; Tian, G.; Secombes, C. J.; Wang, T. Lineage/Species-Specific Expansion of the Mx Gene Family in Teleosts: Differential Expression and Modulation of Nine Mx Genes in Rainbow Trout *Oncorhynchus Mykiss*. *Fish & Shellfish Immunology* **2019**, *90*, 413–430. <https://doi.org/10.1016/j.fsi.2019.04.303>.
- (15) Levraud, J.-P.; Jouneau, L.; Briolat, V.; Laghi, V.; Boudinot, P. IFN-Stimulated Genes in Zebrafish and Humans Define an Ancient Arsenal of Antiviral Immunity. *J Immunol* **2019**, *203* (12), 3361–3373. <https://doi.org/10.4049/jimmunol.1900804>.
- (16) tenOever, B. R. The Evolution of Antiviral Defense Systems. *Cell Host & Microbe* **2016**, *19* (2), 142–149. <https://doi.org/10.1016/j.chom.2016.01.006>.
- (17) Karki, R.; Kanneganti, T.-D. Chapter 12: Pattern Recognition Receptors and the IL-1 Family. In *Paul's Fundamental Immunology*; Lippincott Williams & Wilkins, 2022.
- (18) Mojzesz, M.; Rakus, K.; Chadzinska, M.; Nakagami, K.; Biswas, G.; Sakai, M.; Hikima, J. Cytosolic Sensors for Pathogenic Viral and Bacterial Nucleic Acids in Fish. *IJMS* **2020**, *21* (19), 7289. <https://doi.org/10.3390/ijms21197289>.
- (19) Jensen, S.; Thomsen, A. R. Sensing of RNA Viruses: A Review of Innate Immune Receptors Involved in Recognizing RNA Virus Invasion. *Journal of Virology* **2012**, *86* (6), 2900–2910. <https://doi.org/10.1128/JVI.05738-11>.
- (20) Gan, Z.; Chen, S. N.; Huang, B.; Zou, J.; Nie, P. Fish Type I and Type II Interferons: Composition, Receptor Usage, Production and Function. *Reviews in Aquaculture* **2019**, *32*.
- (21) Langevin, C.; Alekseejeva, E.; Passoni, G.; Palha, N.; Levraud, J.-P.; Boudinot, P. The Antiviral Innate Immune Response in Fish: Evolution and Conservation of the IFN System. *Journal of Molecular Biology* **2013**, *425* (24), 4904–4920. <https://doi.org/10.1016/j.jmb.2013.09.033>.
- (22) Nie, L.; Cai, S.-Y.; Shao, J.-Z.; Chen, J. Toll-Like Receptors, Associated Biological Roles, and Signaling Networks in Non-Mammals. *Front. Immunol.* **2018**, *9*, 1523. <https://doi.org/10.3389/fimmu.2018.01523>.
- (23) Poynter, S.; Lissner, G.; Monjo, A.; DeWitte-Orr, S. Sensors of Infection: Viral Nucleic Acid PRRs in Fish. *Biology* **2015**, *4* (3), 460–493. <https://doi.org/10.3390/biology4030460>.
- (24) Kawai, T.; Akira, S. The Roles of TLRs, RLRs and NLRs in Pathogen Recognition. *International Immunology* **2009**, *21* (4), 317–337. <https://doi.org/10.1093/intimm/dxp017>.
- (25) Matsumoto, M.; Funami, K.; Tanabe, M.; Oshiumi, H.; Shingai, M.; Seto, Y.; Yamamoto, A.; Seya, T. Subcellular Localization of Toll-like Receptor 3 in Human Dendritic Cells. *J Immunol* **2003**, *171* (6), 3154–3162. <https://doi.org/10.4049/jimmunol.171.6.3154>.
- (26) Pietretti, D.; Wiegertjes, G. F. Ligand Specificities of Toll-like Receptors in Fish: Indications from Infection Studies. *Developmental & Comparative Immunology* **2014**, *43* (2), 205–222. <https://doi.org/10.1016/j.dci.2013.08.010>.

## References

- (27) Quiniou, S. M. A.; Boudinot, P.; Bengtén, E. Comprehensive Survey and Genomic Characterization of Toll-like Receptors (TLRs) in Channel Catfish, *Ictalurus punctatus*: Identification of Novel Fish TLRs. *Immunogenetics* **2013**, *65* (7), 511–530. <https://doi.org/10.1007/s00251-013-0694-9>.
- (28) Avunje, S.; Kim, W.-S.; Park, C.-S.; Oh, M.-J.; Jung, S.-J. Toll-like Receptors and Interferon Associated Immune Factors in Viral Haemorrhagic Septicaemia Virus-Infected Olive Flounder (*Paralichthys Olivaceus*). *Fish & Shellfish Immunology* **2011**, *31* (3), 407–414. <https://doi.org/10.1016/j.fsi.2011.06.009>.
- (29) Avunje, S.; Oh, M.-J.; Jung, S.-J. Impaired TLR2 and TLR7 Response in Olive Flounder Infected with Viral Haemorrhagic Septicaemia Virus at Host Susceptible 15 °C but High at Non-Susceptible 20 °C. *Fish & Shellfish Immunology* **2013**, *34* (5), 1236–1243. <https://doi.org/10.1016/j.fsi.2013.02.012>.
- (30) Huang, R.; Dong, F.; Jang, S.; Liao, L.; Zhu, Z.; Wang, Y. Isolation and Analysis of a Novel Grass Carp Toll-like Receptor 4 (*Tlr4*) Gene Cluster Involved in the Response to Grass Carp Reovirus. *Developmental & Comparative Immunology* **2012**, *38* (2), 383–388. <https://doi.org/10.1016/j.dci.2012.06.002>.
- (31) Tyrkalska, S. D.; Martínez-López, A.; Pedoto, A.; Candel, S.; Cayuela, M. L.; Mulero, V. The Spike Protein of SARS-CoV-2 Signals via Tlr2 in Zebrafish. *Dev Comp Immunol* **2023**, *140*, 104626. <https://doi.org/10.1016/j.dci.2022.104626>.
- (32) Zhou, Z.; Zhang, B.; Sun, L. Poly(I:C) Induces Antiviral Immune Responses in Japanese Flounder (*Paralichthys Olivaceus*) That Require TLR3 and MDA5 and Is Negatively Regulated by Myd88. *PLoS One* **2014**, *9* (11), e112918. <https://doi.org/10.1371/journal.pone.0112918>.
- (33) Ji, J.; Rao, Y.; Wan, Q.; Liao, Z.; Su, J. Teleost-Specific TLR19 Localizes to Endosome, Recognizes dsRNA, Recruits TRIF, Triggers Both IFN and NF-κB Pathways, and Protects Cells from Grass Carp Reovirus Infection. *J.I.* **2018**, *200* (2), 573–585. <https://doi.org/10.4049/jimmunol.1701149>.
- (34) Matsuo, A.; Oshiumi, H.; Tsujita, T.; Mitani, H.; Kasai, H.; Yoshimizu, M.; Matsumoto, M.; Seya, T. Teleost TLR22 Recognizes RNA Duplex to Induce IFN and Protect Cells from Birnaviruses. *J Immunol* **2008**, *181* (5), 3474–3485. <https://doi.org/10.4049/jimmunol.181.5.3474>.
- (35) Brownlie, R.; Zhu, J.; Allan, B.; Mutwiri, G. K.; Babiuk, L. A.; Potter, A.; Griebel, P. Chicken TLR21 Acts as a Functional Homologue to Mammalian TLR9 in the Recognition of CpG Oligodeoxynucleotides. *Mol Immunol* **2009**, *46* (15), 3163–3170. <https://doi.org/10.1016/j.molimm.2009.06.002>.
- (36) Iliiev, D. B.; Skjæveland, I.; Jørgensen, J. B. CpG Oligonucleotides Bind TLR9 and RRM-Containing Proteins in Atlantic Salmon (*Salmo Salar*). *BMC Immunol* **2013**, *14*, 12. <https://doi.org/10.1186/1471-2172-14-12>.
- (37) Yeh, D.-W.; Liu, Y.-L.; Lo, Y.-C.; Yuh, C.-H.; Yu, G.-Y.; Lo, J.-F.; Luo, Y.; Xiang, R.; Chuang, T.-H. Toll-like Receptor 9 and 21 Have Different Ligand Recognition Profiles and Cooperatively Mediate Activity of CpG-Oligodeoxynucleotides in Zebrafish. *Proc Natl Acad Sci U S A* **2013**, *110* (51), 20711–20716. <https://doi.org/10.1073/pnas.1305273110>.
- (38) Invivogen. *InvivoGen's Posters & Pathways: TLRs & NLRs*; 2024. <https://www.invivogen.com/resources/posters-pathways> (accessed 2024-05-21).
- (39) van der Vaart, M.; van Soest, J. J.; Spaink, H. P.; Meijer, A. H. Functional Analysis of a Zebrafish Myd88 Mutant Identifies Key Transcriptional Components of the Innate Immune System. *Dis Model Mech* **2013**, *6* (3), 841–854. <https://doi.org/10.1242/dmm.010843>.
- (40) Phelan, P. E.; Mellon, M. T.; Kim, C. H. Functional Characterization of Full-Length TLR3, IRAK-4, and TRAF6 in Zebrafish (*Danio Rerio*). *Mol Immunol* **2005**, *42* (9), 1057–1071. <https://doi.org/10.1016/j.molimm.2004.11.005>.
- (41) Chow, K. T.; Gale, M.; Loo, Y.-M. RIG-I and Other RNA Sensors in Antiviral Immunity. *Annu Rev Immunol* **2018**, *36*, 667–694. <https://doi.org/10.1146/annurev-immunol-042617-053309>.
- (42) Kato, H.; Takeuchi, O.; Mikamo-Satoh, E.; Hirai, R.; Kawai, T.; Matsushita, K.; Hiiragi, A.; Dermody, T. S.; Fujita, T.; Akira, S. Length-Dependent Recognition of Double-Stranded Ribonucleic Acids by Retinoic Acid-Inducible Gene-1 and Melanoma Differentiation-Associated Gene 5. *J Exp Med* **2008**, *205* (7), 1601–1610. <https://doi.org/10.1084/jem.20080091>.
- (43) Pippig, D. A.; Hellmuth, J. C.; Cui, S.; Kirchhofer, A.; Lammens, K.; Lammens, A.; Schmidt, A.; Rothenfusser, S.; Hopfner, K.-P. The Regulatory Domain of the RIG-I Family ATPase LGP2 Senses Double-Stranded RNA. *Nucleic Acids Research* **2009**, *37* (6), 2014–2025. <https://doi.org/10.1093/nar/gkp059>.
- (44) Chen, S. N.; Zou, P. F.; Nie, P. Retinoic Acid-Inducible Gene I (RIG-I)-like Receptors (RLRs) in Fish: Current Knowledge and Future Perspectives. *Immunology* **2017**, *151* (1), 16–25. <https://doi.org/10.1111/imm.12714>.
- (45) Chang, M.; Collet, B.; Nie, P.; Lester, K.; Campbell, S.; Secombes, C. J.; Zou, J. Expression and Functional Characterization of the RIG-I-Like Receptors MDA5 and LGP2 in Rainbow Trout (*Oncorhynchus Mykiss*). *Journal of Virology* **2011**, *85* (16), 8403–8412. <https://doi.org/10.1128/JVI.00445-10>.
- (46) Poynter, S. J.; Herrington-Krause, S.; DeWitte-Orr, S. J. Two DExD/H-Box Helicases, DDX3 and DHX9, Identified in Rainbow Trout Are Able to Bind dsRNA. *Fish Shellfish Immunol* **2019**, *93*, 1056–1066. <https://doi.org/10.1016/j.fsi.2019.07.054>.
- (47) Chen, H.-Y.; Liu, W.; Wu, S.-Y.; Chiou, P. P.; Li, Y.-H.; Chen, Y.-C.; Lin, G.-H.; Lu, M.-W.; Wu, J.-L. RIG-I Specifically Mediates Group II Type I IFN Activation in Nervous Necrosis Virus Infected Zebrafish Cells. *Fish Shellfish Immunol* **2015**, *43* (2), 427–435. <https://doi.org/10.1016/j.fsi.2015.01.012>.
- (48) Huang, B.; Wang, Z. X.; Zhang, C.; Zhai, S. W.; Han, Y. S.; Huang, W. S.; Nie, P. Identification of a Novel RIG-I Isoform and Its Truncating Variant in Japanese Eel, *Anguilla Japonica*. *Fish Shellfish Immunol* **2019**, *94*, 373–380. <https://doi.org/10.1016/j.fsi.2019.09.037>.
- (49) Sun, F.; Zhang, Y.-B.; Liu, T.-K.; Shi, J.; Wang, B.; Gui, J.-F. Fish MITA Serves as a Mediator for Distinct Fish IFN Gene Activation Dependent on IRF3 or IRF7. *J Immunol* **2011**, *187* (5), 2531–2539. <https://doi.org/10.4049/jimmunol.1100642>.
- (50) Zou, P. F.; Chang, M. X.; Li, Y.; Huan Zhang, S.; Fu, J. P.; Chen, S. N.; Nie, P. Higher Antiviral Response of RIG-I through Enhancing RIG-I/MAVS-Mediated Signaling by Its Long Insertion Variant in Zebrafish. *Fish Shellfish Immunol* **2015**, *43* (1), 13–24. <https://doi.org/10.1016/j.fsi.2014.12.001>.
- (51) Biacchesi, S.; LeBerre, M.; Lamoureux, A.; Louise, Y.; Lauret, E.; Boudinot, P.; Brémont, M. Mitochondrial Antiviral Signaling Protein Plays a Major Role in Induction of the Fish Innate Immune Response against RNA and DNA Viruses. *J Virol* **2009**, *83* (16), 7815–7827. <https://doi.org/10.1128/JVI.00404-09>.

## References

- (52) Gong, X.-Y.; Zhang, Q.-M.; Gui, J.-F.; Zhang, Y.-B. SVCV Infection Triggers Fish IFN Response through RLR Signaling Pathway. *Fish Shellfish Immunol* **2019**, *86*, 1058–1063. <https://doi.org/10.1016/j.fsi.2018.12.063>.
- (53) Liu, J.; Huang, X.; Yu, Y.; Zhang, J.; Ni, S.; Hu, Y.; Huang, Y.; Qin, Q. Fish DDX3X Exerts Antiviral Function against Grouper Nervous Necrosis Virus Infection. *Fish & Shellfish Immunology* **2017**, *71*, 95–104. <https://doi.org/10.1016/j.fsi.2017.09.068>.
- (54) Zhao, J.-Z.; Xu, L.-M.; Ren, G.-M.; Shao, Y.-Z.; Lu, T.-Y. Identification and Characterization of DEAD-Box RNA Helicase DDX3 in Rainbow Trout (*Oncorhynchus Mykiss*) and Its Relationship with Infectious Hematopoietic Necrosis Virus Infection. *Dev Comp Immunol* **2022**, *135*, 104493. <https://doi.org/10.1016/j.dci.2022.104493>.
- (55) Invivogen. *InvivoGen's Posters & Pathways: CLR-RLR-CDS Pathways*; 2024. <https://www.invivogen.com/resources/posters-pathways> (accessed 2024-05-21).
- (56) Sun, L.; Wu, J.; Du, F.; Chen, X.; Chen, Z. J. Cyclic GMP-AMP Synthase Is a Cytosolic DNA Sensor That Activates the Type-I Interferon Pathway. *Science* **2013**, *339* (6121), 10.1126/science.1232458. <https://doi.org/10.1126/science.1232458>.
- (57) Zhang, Z.; Yuan, B.; Bao, M.; Lu, N.; Kim, T.; Liu, Y.-J. The Helicase DDX41 Senses Intracellular DNA Mediated by the Adaptor STING in Dendritic Cells. *Nat Immunol* **2011**, *12* (10), 959–965. <https://doi.org/10.1038/ni.2091>.
- (58) Fernandes-Alnemri, T.; Yu, J.-W.; Wu, J.; Datta, P.; Alnemri, E. S. AIM2 Activates the Inflammasome and Cell Death in Response to Cytoplasmic DNA. *Nature* **2009**, *458* (7237), 509–513. <https://doi.org/10.1038/nature07710>.
- (59) Unterholzner, L.; Keating, S. E.; Baran, M.; Horan, K. A.; Jensen, S. B.; Sharma, S.; Sirois, C. M.; Jin, T.; Latz, E.; Xiao, T. S.; Fitzgerald, K. A.; Paludan, S. R.; Bowie, A. G. IFI16 Is an Innate Immune Sensor for Intracellular DNA. *Nat Immunol* **2010**, *11* (11), 997–1004. <https://doi.org/10.1038/ni.1932>.
- (60) Chen, Q.; Sun, L.; Chen, Z. J. Regulation and Function of the cGAS-STING Pathway of Cytosolic DNA Sensing. *Nat Immunol* **2016**, *17* (10), 1142–1149. <https://doi.org/10.1038/ni.3558>.
- (61) Parvatiyar, K.; Zhang, Z.; Teles, R. M.; Ouyang, S.; Jiang, Y.; Iyer, S. S.; Zaver, S. A.; Schenk, M.; Zeng, S.; Zhong, W.; Liu, Z.-J.; Modlin, R. L.; Liu, Y.; Cheng, G. DDX41 Recognizes Bacterial Secondary Messengers Cyclic Di-GMP and Cyclic Di-AMP to Activate a Type I Interferon Immune Response. *Nat Immunol* **2012**, *13* (12), 1155–1161. <https://doi.org/10.1038/ni.2460>.
- (62) Chang, M. X. Emerging Mechanisms and Functions of Inflammasome Complexes in Teleost Fish. *Front Immunol* **2023**, *14*, 1065181. <https://doi.org/10.3389/fimmu.2023.1065181>.
- (63) Qin, X.-W.; Luo, Z.-Y.; Pan, W.-Q.; He, J.; Li, Z.-M.; Yu, Y.; Liu, C.; Weng, S.-P.; He, J.-G.; Guo, C.-J. The Interaction of Mandarin Fish DDX41 with STING Evokes Type I Interferon Responses Inhibiting Ranavirus Replication. *Viruses* **2022**, *15* (1), 58. <https://doi.org/10.3390/v15010058>.
- (64) Ma, Z.; Ni, G.; Damania, B. Innate Sensing of DNA Virus Genomes. *Annu. Rev. Virol.* **2018**, *5* (1), 341–362. <https://doi.org/10.1146/annurev-virology-092917-043244>.
- (65) Ablasser, A.; Schmid-Burgk, J. L.; Hemmerling, I.; Horvath, G. L.; Schmidt, T.; Latz, E.; Hornung, V. Cell Intrinsic Immunity Spreads to Bystander Cells via the Intercellular Transfer of cGAMP. *Nature* **2013**, *503* (7477), 530–534. <https://doi.org/10.1038/nature12640>.
- (66) Liu, Z.; Ji, J.; Jiang, X.; Shao, T.; Fan, D.; Jiang, X.; Lin, A.; Xiang, L.; Shao, J. Characterization of cGAS Homologs in Innate and Adaptive Mucosal Immunities in Zebrafish Gives Evolutionary Insights into cGAS-STING Pathway. *The FASEB Journal* **2020**, *34* (6), 7786–7809. <https://doi.org/10.1096/fj.201902833R>.
- (67) Zhang, L.; Zhang, X.; Liao, J.; Xu, L.; Kang, S.; Chen, H.; Sun, M.; Wu, S.; Xu, Z.; Wei, S.; Qin, Q.; Wei, J. Grouper cGAS Is a Negative Regulator of STING-Mediated Interferon Response. *Front Immunol* **2023**, *14*, 1092824. <https://doi.org/10.3389/fimmu.2023.1092824>.
- (68) Zhou, Y.; Lu, L.-F.; Lu, X.-B.; Li, S.; Zhang, Y.-A. Grass Carp cGASL Negatively Regulates Fish IFN Response by Targeting MITA. *Fish & Shellfish Immunology* **2019**, *94*, 871–879. <https://doi.org/10.1016/j.fsi.2019.10.010>.
- (69) Xu, X.; Li, M.; Deng, Z.; Jiang, Z.; Li, D.; Wang, S.; Hu, C. cGASa and cGASb from Grass Carp (*Ctenopharyngodon Idellus*) Play Opposite Roles in Mediating Type I Interferon Response. *Developmental & Comparative Immunology* **2021**, *125*, 104233. <https://doi.org/10.1016/j.dci.2021.104233>.
- (70) Zhou, Y.; Lu, L.-F.; Zhang, C.; Chen, D.-D.; Zhou, X.-Y.; Li, Z.-C.; Jiang, J.-Y.; Li, S.; Zhang, Y.-A. Grass Carp cGASL Negatively Regulates Interferon Activation through Autophagic Degradation of MAVS. *Dev Comp Immunol* **2021**, *115*, 103876. <https://doi.org/10.1016/j.dci.2020.103876>.
- (71) Liu, J.; Huang, Y.; Huang, X.; Li, C.; Ni, S. wei; Yu, Y.; Qin, Q. Grouper DDX41 Exerts Antiviral Activity against Fish Iridovirus and Nodavirus Infection. *Fish & Shellfish Immunology* **2019**, *91*, 40–49. <https://doi.org/10.1016/j.fsi.2019.05.019>.
- (72) Gan, Z.; Cheng, J.; Hou, J.; Xia, H.; Chen, W.; Xia, L.; Nie, P.; Lu, Y. Molecular and Functional Characterization of Tilapia DDX41 in IFN Regulation. *Fish Shellfish Immunol* **2020**, *99*, 386–391. <https://doi.org/10.1016/j.fsi.2020.02.031>.
- (73) Hornung, V.; Hartmann, R.; Ablasser, A.; Hopfner, K.-P. OAS Proteins and cGAS: Unifying Concepts in Sensing and Responding to Cytosolic Nucleic Acids. *Nat Rev Immunol* **2014**, *14* (8), 521–528. <https://doi.org/10.1038/nri3719>.
- (74) Malathi, K.; Saito, T.; Crochet, N.; Barton, D. J.; Gale, M.; Silverman, R. H. RNase L Releases a Small RNA from HCV RNA That Refolds into a Potent PAMP. *RNA* **2010**, *16* (11), 2108–2119. <https://doi.org/10.1261/rna.2244210>.
- (75) García, M. A.; Gil, J.; Ventoso, I.; Guerra, S.; Domingo, E.; Rivas, C.; Esteban, M. Impact of Protein Kinase PKR in Cell Biology: From Antiviral to Antiproliferative Action. *Microbiol Mol Biol Rev* **2006**, *70* (4), 1032–1060. <https://doi.org/10.1128/MMBR.00027-06>.
- (76) Chu, L.; Gong, Z.; Wang, W.; Han, G.-Z. Origin of the OAS–RNase L Innate Immune Pathway before the Rise of Jawed Vertebrates via Molecular Tinkering. *Proceedings of the National Academy of Sciences* **2023**, *120* (31), e2304687120. <https://doi.org/10.1073/pnas.2304687120>.
- (77) Allen, I. C.; Scull, M. A.; Moore, C. B.; Holl, E. K.; McElvania-TeKippe, E.; Taxman, D. J.; Guthrie, E. H.; Pickles, R. J.; Ting, J. P.-Y. The NLRP3 Inflammasome Mediates In Vivo Innate Immunity to Influenza A Virus through Recognition of Viral RNA. *Immunity* **2009**, *30* (4), 556–565. <https://doi.org/10.1016/j.immuni.2009.02.005>.
- (78) Sabbah, A.; Chang, T. H.; Harnack, R.; Frohlich, V.; Tominaga, K.; Dube, P. H.; Xiang, Y.; Bose, S. Activation of Innate Immune Antiviral Response by NOD2. *Nat Immunol* **2009**, *10* (10), 1073–1080. <https://doi.org/10.1038/ni.1782>.

## References

- (79) Howe, K.; Schiffer, P. H.; Zielinski, J.; Wiehe, T.; Laird, G. K.; Marioni, J. C.; Soylemez, O.; Kondrashov, F.; Leptin, M. Structure and Evolutionary History of a Large Family of NLR Proteins in the Zebrafish. *Open Biology* **2016**, *6* (4), 160009. <https://doi.org/10.1098/rsob.160009>.
- (80) Laing, K. J.; Purcell, M. K.; Winton, J. R.; Hansen, J. D. A Genomic View of the NOD-like Receptor Family in Teleost Fish: Identification of a Novel NLR Subfamily in Zebrafish. *BMC Evol Biol* **2008**, *8*, 42. <https://doi.org/10.1186/1471-2148-8-42>.
- (81) Chang, M. X.; Xiong, F.; Wu, X. M.; Hu, Y. W. The Expanding and Function of NLRC3 or NLRC3-like in Teleost Fish: Recent Advances and Novel Insights. *Developmental & Comparative Immunology* **2021**, *114*, 103859. <https://doi.org/10.1016/j.dci.2020.103859>.
- (82) Bermejo-Jambrina, M.; Eder, J.; Helgers, L. C.; Hertoghs, N.; Nijmeijer, B. M.; Stunnenberg, M.; Geijtenbeek, T. B. H. C-Type Lectin Receptors in Antiviral Immunity and Viral Escape. *Front Immunol* **2018**, *9*, 590. <https://doi.org/10.3389/fimmu.2018.00590>.
- (83) Oeckinghaus, A.; Ghosh, S. The NF- $\kappa$ B Family of Transcription Factors and Its Regulation. *Cold Spring Harb Perspect Biol* **2009**, *1* (4), a000034. <https://doi.org/10.1101/cshperspect.a000034>.
- (84) Pahl, H. L. Activators and Target Genes of Rel/NF-kappaB Transcription Factors. *Oncogene* **1999**, *18* (49), 6853–6866. <https://doi.org/10.1038/sj.onc.1203239>.
- (85) Taniguchi, T.; Ogasawara, K.; Takaoka, A.; Tanaka, N. IRF Family of Transcription Factors as Regulators of Host Defense. *Annu Rev Immunol* **2001**, *19*, 623–655. <https://doi.org/10.1146/annurev.immunol.19.1.623>.
- (86) Karin, M.; Liu, Z. g; Zandi, E. AP-1 Function and Regulation. *Curr Opin Cell Biol* **1997**, *9* (2), 240–246. [https://doi.org/10.1016/s0955-0674\(97\)80068-3](https://doi.org/10.1016/s0955-0674(97)80068-3).
- (87) Keegan, A. D.; Leonard, W. J. Chapter 9: Type I Cytokines, Interferons, and Their Receptors. In *Paul's Fundamental Immunology*; Lippincott Williams & Wilkins, 2022.
- (88) Zou, J.; Secombes, C. J. The Function of Fish Cytokines. *Biology (Basel)* **2016**, *5* (2), 23. <https://doi.org/10.3390/biology5020023>.
- (89) Pestka, S.; Krause, C. D.; Walter, M. R. Interferons, Interferon-like Cytokines, and Their Receptors. *Immunological Reviews* **2004**, *202* (1), 8–32. <https://doi.org/10.1111/j.0105-2896.2004.00204.x>.
- (90) Plataniias, L. C. Mechanisms of Type-I- and Type-II-Interferon-Mediated Signalling. *Nat Rev Immunol* **2005**, *5* (5), 375–386. <https://doi.org/10.1038/nri1604>.
- (91) Stark, G. R.; Kerr, I. M.; Williams, B. R.; Silverman, R. H.; Schreiber, R. D. How Cells Respond to Interferons. *Annu Rev Biochem* **1998**, *67*, 227–264. <https://doi.org/10.1146/annurev.biochem.67.1.227>.
- (92) Walter, M. R.; Windsor, W. T.; Nagabhushan, T. L.; Lundell, D. J.; Lunn, C. A.; Zauodny, P. J.; Narula, S. K. Crystal Structure of a Complex between Interferon-Gamma and Its Soluble High-Affinity Receptor. *Nature* **1995**, *376* (6537), 230–235. <https://doi.org/10.1038/376230a0>.
- (93) Valente, G.; Ozmen, L.; Novelli, F.; Geuna, M.; Palestro, G.; Forni, G.; Garotta, G. Distribution of Interferon-Gamma Receptor in Human Tissues. *Eur J Immunol* **1992**, *22* (9), 2403–2412. <https://doi.org/10.1002/eji.1830220933>.
- (94) Lazear, H. M.; Nice, T. J.; Diamond, M. S. Interferon- $\lambda$ : Immune Functions at Barrier Surfaces and Beyond. *Immunity* **2015**, *43* (1), 15–28. <https://doi.org/10.1016/j.immuni.2015.07.001>.
- (95) Schoenborn, J. R.; Wilson, C. B. Regulation of Interferon- $\gamma$  During Innate and Adaptive Immune Responses. In *Advances in Immunology*; Elsevier, 2007; Vol. 96, pp 41–101. [https://doi.org/10.1016/S0065-2776\(07\)96002-2](https://doi.org/10.1016/S0065-2776(07)96002-2).
- (96) Liu, F.; Bols, N. C.; Pham, P. H.; Secombes, C. J.; Zou, J. Evolution of IFN Subgroups in Bony Fish - 1: Group I-III IFN Exist in Early Ray-Finned Fish, with Group II IFN Subgroups Present in the Holostean Spotted Gar, *Lepisosteus Oculatus*. *Fish & Shellfish Immunology* **2019**, *95*, 163–170. <https://doi.org/10.1016/j.fsi.2019.10.032>.
- (97) Redmond, A. K.; Zou, J.; Secombes, C. J.; Macqueen, D. J.; Dooley, H. Discovery of All Three Types in Cartilaginous Fishes Enables Phylogenetic Resolution of the Origins and Evolution of Interferons. *Front Immunol* **2019**, *10*, 1558. <https://doi.org/10.3389/fimmu.2019.01558>.
- (98) Chen, S. N.; Gan, Z.; Hou, J.; Yang, Y. C.; Huang, L.; Huang, B.; Wang, S.; Nie, P. Identification and Establishment of Type IV Interferon and the Characterization of Interferon- $\nu$  Including Its Class II Cytokine Receptors IFN- $\nu$ R1 and IL-10R2. *Nat Commun* **2022**, *13* (1), 999. <https://doi.org/10.1038/s41467-022-28645-6>.
- (99) Boudinot, P.; Langevin, C.; Secombes, C.; Levraud, J.-P. The Peculiar Characteristics of Fish Type I Interferons. *Viruses* **2016**, *8* (11), 298. <https://doi.org/10.3390/v8110298>.
- (100) Maekawa, S.; Chiang, Y.-A.; Hikima, J.; Sakai, M.; Lo, C.-F.; Wang, H.-C.; Aoki, T. Expression and Biological Activity of Two Types of Interferon Genes in Medaka (*Oryzias Latipes*). *Fish Shellfish Immunol* **2016**, *48*, 20–29. <https://doi.org/10.1016/j.fsi.2015.11.036>.
- (101) Gao, F.-X.; Lu, W.-J.; Shi, Y.; Zhao, Z.-W.; Zhou, L.; Gui, J.-F.; Zhao, Z. Identification and Characterization of Type I and II IFN Genes in Obscure Puffer (*Takifugu Obscurus*). *Aquaculture Reports* **2022**, *23*, 101080. <https://doi.org/10.1016/j.aqrep.2022.101080>.
- (102) Aggad, D.; Mazel, M.; Boudinot, P.; Mogensen, K. E.; Hamming, O. J.; Hartmann, R.; Kotenko, S.; Herbolme, P.; Lutfalla, G.; Levraud, J.-P. The Two Groups of Zebrafish Virus-Induced Interferons Signal via Distinct Receptors with Specific and Shared Chains. *J Immunol* **2009**, *183* (6), 3924–3931. <https://doi.org/10.4049/jimmunol.0901495>.
- (103) Sun, B.; Robertsen, B.; Wang, Z.; Liu, B. Identification of an Atlantic Salmon IFN Multigene Cluster Encoding Three IFN Subtypes with Very Different Expression Properties. *Developmental & Comparative Immunology* **2009**, *33* (4), 547–558. <https://doi.org/10.1016/j.dci.2008.10.001>.
- (104) Quiniou, S. M. A.; Crider, J.; Felch, K. L.; Bengtén, E.; Boudinot, P. Interferons and Interferon Receptors in the Channel Catfish, *Ictalurus Punctatus*. *Fish & Shellfish Immunology* **2022**, *123*, 442–452. <https://doi.org/10.1016/j.fsi.2022.02.019>.
- (105) Zou, J.; Gorgoglione, B.; Taylor, N. G. H.; Summated, T.; Lee, P.-T.; Panigrahi, A.; Genet, C.; Chen, Y.-M.; Chen, T.-Y.; Ul Hassan, M.; Mughal, S. M.; Boudinot, P.; Secombes, C. J. Salmonids Have an Extraordinary Complex Type I IFN System: Characterization of the IFN Locus in Rainbow Trout *Oncorhynchus Mykiss* Reveals Two Novel IFN Subgroups. *J Immunol* **2014**, *193* (5), 2273–2286. <https://doi.org/10.4049/jimmunol.1301796>.

## References

- (106) Levraud, J.-P.; Boudinot, P.; Colin, I.; Benmansour, A.; Peyrieras, N.; Herbomel, P.; Lutfalla, G. Identification of the Zebrafish IFN Receptor: Implications for the Origin of the Vertebrate IFN System. *J Immunol* **2007**, *178* (7), 4385–4394. <https://doi.org/10.4049/jimmunol.178.7.4385>.
- (107) Hamming, O. J.; Lutfalla, G.; Levraud, J.-P.; Hartmann, R. Crystal Structure of Zebrafish Interferons I and II Reveals Conservation of Type I Interferon Structure in Vertebrates. *Journal of Virology* **2011**, *85* (16), 8181–8187. <https://doi.org/10.1128/JVI.00521-11>.
- (108) Zou, J.; Tafalla, C.; Truckle, J.; Secombes, C. J. Identification of a Second Group of Type I IFNs in Fish Sheds Light on IFN Evolution in Vertebrates. *J Immunol* **2007**, *179* (6), 3859–3871. <https://doi.org/10.4049/jimmunol.179.6.3859>.
- (109) Liu, F.; Wang, T.; Petit, J.; Forlenza, M.; Chen, X.; Chen, L.; Zou, J.; Secombes, C. J. Evolution of IFN Subgroups in Bony Fish - 2. Analysis of Subgroup Appearance and Expansion in Teleost Fish with a Focus on Salmonids. *Fish & Shellfish Immunology* **2020**, *98*, 564–573. <https://doi.org/10.1016/j.fsi.2020.01.039>.
- (110) Gan, Z.; Cheng, J.; Chen, S.; Hou, J.; Li, N.; Xia, H.; Xia, L.; Lu, Y.; Nie, P. Identification and Characterization of Tilapia CRFB1, CRFB2 and CRFB5 Reveals Preferential Receptor Usage of Three IFN Subtypes in Perciform Fishes. *Fish Shellfish Immunol* **2020**, *107* (Pt A), 194–201. <https://doi.org/10.1016/j.fsi.2020.10.002>.
- (111) Guan, Y.; Chen, J.; Guan, H.; Chen, T.-T.; Teng, Y.; Wei, Z.; Li, Z.; Ouyang, S.; Chen, X. Structural and Functional Characterization of a Fish Type I Subgroup d IFN Reveals Its Binding to Receptors. *J Immunol* **2024**, *212* (7), 1207–1220. <https://doi.org/10.4049/jimmunol.2300651>.
- (112) Chen, J.; Guan, Y.; Guan, H.; Mu, Y.; Ding, Y.; Zou, J.; Ouyang, S.; Chen, X. Molecular and Structural Basis of Receptor Binding and Signaling of a Fish Type I IFN with Three Disulfide Bonds. *The Journal of Immunology* **2022**, *209* (4), 806–819. <https://doi.org/10.4049/jimmunol.2200202>.
- (113) Igawa, D.; Sakai, M.; Savan, R. An Unexpected Discovery of Two Interferon Gamma-like Genes along with Interleukin (IL)-22 and -26 from Teleost: IL-22 and -26 Genes Have Been Described for the First Time Outside Mammals. *Molecular Immunology* **2006**, *43* (7), 999–1009. <https://doi.org/10.1016/j.molimm.2005.05.009>.
- (114) Milev-Milovanovic, I.; Long, S.; Wilson, M.; Bengten, E.; Miller, N. W.; Chinchar, V. G. Identification and Expression Analysis of Interferon Gamma Genes in Channel Catfish. *Immunogenetics* **2006**, *58* (1), 70–80. <https://doi.org/10.1007/s00251-006-0081-x>.
- (115) Chen, W. Q.; Xu, Q. Q.; Chang, M. X.; Zou, J.; Secombes, C. J.; Peng, K. M.; Nie, P. Molecular Characterization and Expression Analysis of the IFN-Gamma Related Gene (IFN-Gammarel) in Grass Carp Ctenopharyngodon Idella. *Vet Immunol Immunopathol* **2010**, *134* (3–4), 199–207. <https://doi.org/10.1016/j.vetimm.2009.09.007>.
- (116) Stolte, E. H.; Savelkoul, H. F. J.; Wiegertjes, G.; Flik, G.; Lidy Verburg-van Kemenade, B. M. Differential Expression of Two Interferon- $\gamma$  Genes in Common Carp (*Cyprinus Carpio* L.). *Developmental & Comparative Immunology* **2008**, *32* (12), 1467–1481. <https://doi.org/10.1016/j.dci.2008.06.012>.
- (117) Purcell, M. K.; Laing, K. J.; Woodson, J. C.; Thorgaard, G. H.; Hansen, J. D. Characterization of the Interferon Genes in Homozygous Rainbow Trout Reveals Two Novel Genes, Alternate Splicing and Differential Regulation of Duplicated Genes. *Fish & Shellfish Immunology* **2009**, *26* (2), 293–304. <https://doi.org/10.1016/j.fsi.2008.11.012>.
- (118) Zou, J.; Carrington, A.; Collet, B.; Dijkstra, J. M.; Yoshiura, Y.; Bols, N.; Secombes, C. Identification and Bioactivities of IFN-Gamma in Rainbow Trout *Oncorhynchus Mykiss*: The First Th1-Type Cytokine Characterized Functionally in Fish. *J Immunol* **2005**, *175* (4), 2484–2494. <https://doi.org/10.4049/jimmunol.175.4.2484>.
- (119) Aggad, D.; Stein, C.; Sieger, D.; Mazel, M.; Boudinot, P.; Herbomel, P.; Levraud, J.-P.; Lutfalla, G.; Leptin, M. In Vivo Analysis of Ifn-I1 and Ifn-I2 Signaling in Zebrafish. *The Journal of Immunology* **2010**, *185* (11), 6774–6782. <https://doi.org/10.4049/jimmunol.1000549>.
- (120) Shibasaki, Y.; Yabu, T.; Araki, K.; Mano, N.; Shiba, H.; Moritomo, T.; Nakanishi, T. Peculiar Monomeric Interferon Gammas, IFN $\gamma$ rel 1 and IFN $\gamma$ rel 2, in Ginbuna Crucian Carp. *The FEBS Journal* **2014**, *281* (4), 1046–1056. <https://doi.org/10.1111/febs.12666>.
- (121) Chen, L.; Liu, J.; Yan, J.; Pan, J.; Wu, H.; Xiao, J.; Feng, H. Cloning and Characterization of Type IV Interferon from Black Carp *Mylopharyngodon Piceus*. *Developmental & Comparative Immunology* **2023**, *140*, 104614. <https://doi.org/10.1016/j.dci.2022.104614>.
- (122) Chen, S. N.; Li, B.; Gan, Z.; Wang, K. L.; Li, L.; Pang, A. N.; Peng, X. Y.; Ji, J. X.; Deng, Y. H.; Li, N.; Liu, L. H.; Sun, Y. L.; Wang, S.; Huang, B.; Nie, P. Transcriptional Regulation and Signaling of Type IV IFN with Identification of the ISG Repertoire in an Amphibian Model, *Xenopus Laevis*. *The Journal of Immunology* **2023**, *210* (11), 1771–1789. <https://doi.org/10.4049/jimmunol.2300085>.
- (123) Pang, A. N.; Chen, S. N.; Liu, L. H.; Li, B.; Song, J. W.; Zhang, S.; Nie, P. IFN- $\nu$  and Its Receptor Subunits, IFN- $\nu$ R1 and IL10RB in Mallard *Anas Platyrhynchos*. *Poultry Science* **2024**, *103* (6), 103673. <https://doi.org/10.1016/j.psj.2024.103673>.
- (124) Honda, K.; Takaoka, A.; Taniguchi, T. Type I Interferon Gene Induction by the Interferon Regulatory Factor Family of Transcription Factors. *Immunity* **2006**, *25* (3), 349–360. <https://doi.org/10.1016/j.immuni.2006.08.009>.
- (125) Marié, I.; Durbin, J. E.; Levy, D. E. Differential Viral Induction of Distinct Interferon-Alpha Genes by Positive Feedback through Interferon Regulatory Factor-7. *EMBO J* **1998**, *17* (22), 6660–6669. <https://doi.org/10.1093/emboj/17.22.6660>.
- (126) Svingerud, T.; Solstad, T.; Sun, B.; Nyrud, M. L. J.; Kileng, Ø.; Greiner-Tollersrud, L.; Robertsen, B. Atlantic Salmon Type I IFN Subtypes Show Differences in Antiviral Activity and Cell-Dependent Expression: Evidence for High IFN $\beta$ /IFN $\epsilon$ -Producing Cells in Fish Lymphoid Tissues. *The Journal of Immunology* **2012**, *189* (12), 5912–5923. <https://doi.org/10.4049/jimmunol.1201188>.
- (127) Palha, N.; Guivel-Benhassine, F.; Briolat, V.; Lutfalla, G.; Sourisseau, M.; Ellett, F.; Wang, C.-H.; Lieschke, G. J.; Herbomel, P.; Schwartz, O.; Levraud, J.-P. Real-Time Whole-Body Visualization of Chikungunya Virus Infection and Host Interferon Response in Zebrafish. *PLoS Pathog* **2013**, *9* (9), e1003619. <https://doi.org/10.1371/journal.ppat.1003619>.
- (128) Bergan, V.; Steinsvik, S.; Xu, H.; Kileng, Ø.; Robertsen, B. Promoters of Type I Interferon Genes from Atlantic Salmon Contain Two Main Regulatory Regions. *The FEBS Journal* **2006**, *273* (17), 3893–3906. <https://doi.org/10.1111/j.1742-4658.2006.05382.x>.

## References

- (129) Feng, H.; Zhang, Y.-B.; Zhang, Q.-M.; Li, Z.; Zhang, Q.-Y.; Gui, J.-F. Zebrafish IRF1 Regulates IFN Antiviral Response through Binding to IFN $\beta$ 1 and IFN $\beta$ 3 Promoters Downstream of MyD88 Signaling. *J Immunol* **2015**, *194* (3), 1225–1238. <https://doi.org/10.4049/jimmunol.1402415>.
- (130) Chang, M.-X.; Zou, J.; Nie, P.; Huang, B.; Yu, Z.; Collet, B.; Secombes, C. J. Intracellular Interferons in Fish: A Unique Means to Combat Viral Infection. *PLoS Pathog* **2013**, *9* (11), e1003736. <https://doi.org/10.1371/journal.ppat.1003736>.
- (131) Long, S.; Milev-Milovanovic, I.; Wilson, M.; Bengten, E.; Clem, L. W.; Miller, N. W.; Chinchar, V. G. Identification and Expression Analysis of cDNAs Encoding Channel Catfish Type I Interferons. *Fish & Shellfish Immunology* **2006**, *21* (1), 42–59. <https://doi.org/10.1016/j.fsi.2005.10.008>.
- (132) Hou, Q.; Gong, R.; Liu, X.; Mao, H.; Xu, X.; Liu, D.; Dai, Z.; Wang, H.; Wang, B.; Hu, C. Poly I:C Facilitates the Phosphorylation of Ctenopharyngodon Idellus Type I IFN Receptor Subunits and JAK Kinase. *Fish & Shellfish Immunology* **2017**, *60*, 13–20. <https://doi.org/10.1016/j.fsi.2016.10.042>.
- (133) Skjesol, A.; Hansen, T.; Shi, C.-Y.; Thim, H. L.; Jørgensen, J. B. Structural and Functional Studies of STAT1 from Atlantic Salmon (*Salmo Salar*). *BMC Immunol* **2010**, *11* (1), 17. <https://doi.org/10.1186/1471-2172-11-17>.
- (134) Sobhkhhez, M.; Skjesol, A.; Thomassen, E.; Tollersrud, L. G.; Iliev, D. B.; Sun, B.; Robertsen, B.; Jørgensen, J. B. Structural and Functional Characterization of Salmon STAT1, STAT2 and IRF9 Homologs Sheds Light on Interferon Signaling in Teleosts. *FEBS Open Bio* **2014**, *4* (1), 858–871. <https://doi.org/10.1016/j.fob.2014.09.007>.
- (135) Laghari, Z. A.; Chen, S. N.; Li, L.; Huang, B.; Gan, Z.; Zhou, Y.; Huo, H. J.; Hou, J.; Nie, P. Functional, Signalling and Transcriptional Differences of Three Distinct Type I IFNs in a Perciform Fish, the Mandarin Fish *Siniperca Chuatsi*. *Developmental & Comparative Immunology* **2018**, *84*, 94–108. <https://doi.org/10.1016/j.dci.2018.02.008>.
- (136) Dehler, C. E.; Lester, K.; Della Pelle, G.; Jouneau, L.; Houel, A.; Collins, C.; Dovgan, T.; Machat, R.; Zou, J.; Boudinot, P.; Martin, S. A. M.; Collet, B. Viral Resistance and IFN Signaling in STAT2 Knockout Fish Cells. *J Immunol* **2019**, *203* (2), 465–475. <https://doi.org/10.4049/jimmunol.1801376>.
- (137) Grandvaux, N.; Servant, M. J.; tenOever, B.; Sen, G. C.; Balachandran, S.; Barber, G. N.; Lin, R.; Hiscott, J. Transcriptional Profiling of Interferon Regulatory Factor 3 Target Genes: Direct Involvement in the Regulation of Interferon-Stimulated Genes. *J Virol* **2002**, *76* (11), 5532–5539. <https://doi.org/10.1128/jvi.76.11.5532-5539.2002>.
- (138) Schneider, W. M.; Chevillotte, M. D.; Rice, C. M. Interferon-Stimulated Genes: A Complex Web of Host Defenses. *Annu Rev Immunol* **2014**, *32*, 513–545. <https://doi.org/10.1146/annurev-immunol-032713-120231>.
- (139) Thomas, E.; Saito, T. Special Issue “IFN-Independent ISG Expression and Its Role in Antiviral Cell-Intrinsic Innate Immunity.” *Viruses* **2019**, *11* (11), 981. <https://doi.org/10.3390/v11110981>.
- (140) Boudinot, P.; Massin, P.; Blanco, M.; Riffault, S.; Benmansour, A. *Vig-1*, a New Fish Gene Induced by the Rhabdovirus Glycoprotein, Has a Virus-Induced Homologue in Humans and Shares Conserved Motifs with the MxA Family. *J Virol* **1999**, *73* (3), 1846–1852. <https://doi.org/10.1128/JVI.73.3.1846-1852.1999>.
- (141) DeWitte-Orr, S. J.; Leong, J.-A. C.; Bols, N. C. Induction of Antiviral Genes, Mx and Vig-1, by dsRNA and Chum Salmon Reovirus in Rainbow Trout Monocyte/Macrophage and Fibroblast Cell Lines. *Fish & Shellfish Immunology* **2007**, *23* (3), 670–682. <https://doi.org/10.1016/j.fsi.2007.01.017>.
- (142) Langevin, C.; van der Aa, L. M.; Houel, A.; Torhy, C.; Briolat, V.; Lunazzi, A.; Harmache, A.; Bremont, M.; Levrud, J.-P.; Boudinot, P. Zebrafish ISG15 Exerts a Strong Antiviral Activity against RNA and DNA Viruses and Regulates the Interferon Response. *J Virol* **2013**, *87* (18), 10025–10036. <https://doi.org/10.1128/JVI.01294-12>.
- (143) Briolat, V.; Jouneau, L.; Carvalho, R.; Palha, N.; Langevin, C.; Herbomel, P.; Schwartz, O.; Spaink, H. P.; Levrud, J.-P.; Boudinot, P. Contrasted Innate Responses to Two Viruses in Zebrafish: Insights into the Ancestral Repertoire of Vertebrate IFN-Stimulated Genes. *J Immunol* **2014**, *192* (9), 4328–4341. <https://doi.org/10.4049/jimmunol.1302611>.
- (144) Verhelst, J.; Hulpiau, P.; Saelens, X. Mx Proteins: Antiviral Gatekeepers That Restrain the Uninvited. *Microbiol Mol Biol Rev* **2013**, *77* (4), 551–566. <https://doi.org/10.1128/MMBR.00024-13>.
- (145) Liu, S.-Y.; Aliyari, R.; Chikere, K.; Li, G.; Marsden, M. D.; Smith, J. K.; Pernet, O.; Guo, H.; Nusbaum, R.; Zack, J. A.; Freiberg, A. N.; Su, L.; Lee, B.; Cheng, G. Interferon-Inducible Cholesterol-25-Hydroxylase Broadly Inhibits Viral Entry by Production of 25-Hydroxycholesterol. *Immunity* **2013**, *38* (1), 92–105. <https://doi.org/10.1016/j.immuni.2012.11.005>.
- (146) Schoggins, J. W.; Wilson, S. J.; Panis, M.; Murphy, M. Y.; Jones, C. T.; Bieniasz, P.; Rice, C. M. A Diverse Array of Gene Products Are Effectors of the Type I Interferon Antiviral Response. *Nature* **2011**, *472* (7344), 481–485. <https://doi.org/10.1038/nature09907>.
- (147) Arimoto, K.-I.; Miyauchi, S.; Stoner, S. A.; Fan, J.-B.; Zhang, D.-E. Negative Regulation of Type I IFN Signaling. *J Leukoc Biol* **2018**. <https://doi.org/10.1002/JLB.2MIR0817-342R>.
- (148) Arimoto, K.; Takahashi, H.; Hishiki, T.; Konishi, H.; Fujita, T.; Shimotohno, K. Negative Regulation of the RIG-I Signaling by the Ubiquitin Ligase RNF125. *Proceedings of the National Academy of Sciences* **2007**, *104* (18), 7500–7505. <https://doi.org/10.1073/pnas.0611551104>.
- (149) Perng, Y.-C.; Lenschow, D. J. ISG15 in Antiviral Immunity and Beyond. *Nat Rev Microbiol* **2018**, *16* (7), 423–439. <https://doi.org/10.1038/s41579-018-0020-5>.
- (150) Gizzi, A. S.; Grove, T. L.; Arnold, J. J.; Jose, J.; Jangra, R. K.; Garforth, S. J.; Du, Q.; Cahill, S. M.; Dulyaninova, N. G.; Love, J. D.; Chandran, K.; Bresnick, A. R.; Cameron, C. E.; Almo, S. C. A Naturally Occurring Antiviral Ribonucleotide Encoded by the Human Genome. *Nature* **2018**, *558* (7711), 610–614. <https://doi.org/10.1038/s41586-018-0238-4>.
- (151) Ghosh, S.; Marsh, E. N. G. Viperin: An Ancient Radical SAM Enzyme Finds Its Place in Modern Cellular Metabolism and Innate Immunity. *J Biol Chem* **2020**, *295* (33), 11513–11528. <https://doi.org/10.1074/jbc.REV120.012784>.
- (152) Blasweiler, A.; Megens, H.-J.; Goldman, M. R. G.; Tadmor-Levi, R.; Lighten, J.; Groenen, M. A. M.; Dirks, R. P.; Jansen, H. J.; Spaink, H. P.; David, L.; Boudinot, P.; Wiegertjes, G. F. Symmetric Expression of Ohnologs Encoding Conserved Antiviral Responses in Tetraploid Common Carp Suggest Absence of Subgenome Dominance after Whole Genome Duplication. *Genomics* **2023**, *115* (6), 110723. <https://doi.org/10.1016/j.ygeno.2023.110723>.
- (153) Clark, T. C.; Naseer, S.; Gundappa, M. K.; Laurent, A.; Perquis, A.; Collet, B.; Macqueen, D. J.; Martin, S. A. M.; Boudinot, P. Conserved and Divergent Arms of the Antiviral Response in the Duplicated Genomes of Salmonid Fishes. *Genomics* **2023**, *115* (4), 110663. <https://doi.org/10.1016/j.ygeno.2023.110663>.

## References

- (154) Schlaak, J. F.; Hilken, C. M. U.; Costa-Pereira, A. P.; Strobl, B.; Aberger, F.; Frischauf, A.-M.; Kerr, I. M. Cell-Type and Donor-Specific Transcriptional Responses to Interferon- $\alpha$ : Use of Customized Gene Arrays. *Journal of Biological Chemistry* **2002**, *277* (51), 49428–49437. <https://doi.org/10.1074/jbc.M205571200>.
- (155) van Boxel-Dezaire, A. H. H.; Rani, M. R. S.; Stark, G. R. Complex Modulation of Cell Type-Specific Signaling in Response to Type I Interferons. *Immunity* **2006**, *25* (3), 361–372. <https://doi.org/10.1016/j.immuni.2006.08.014>.
- (156) Kerr, J. F. R.; Wyllie, A. H.; Currie, A. R. Apoptosis: A Basic Biological Phenomenon with Wideranging Implications in Tissue Kinetics. *Br J Cancer* **1972**, *26* (4), 239–257. <https://doi.org/10.1038/bjc.1972.33>.
- (157) Koyama, A. H.; Irie, H.; Fukumori, T.; Hata, S.; Iida, S.; Akari, H.; Adachi, A. Role of Virus-Induced Apoptosis in a Host Defense Mechanism against Virus Infection. *J Med Invest* **1998**, *45* (1–4), 37–45.
- (158) Elmore, S. Apoptosis: A Review of Programmed Cell Death. *Toxicol Pathol* **2007**, *35* (4), 495–516. <https://doi.org/10.1080/01926230701320337>.
- (159) Esposti, M. D. The Roles of Bid. *Apoptosis* **2002**, *7* (5), 433–440. <https://doi.org/10.1023/a:1020035124855>.
- (160) Li, H.; Zhu, H.; Xu, C. J.; Yuan, J. Cleavage of BID by Caspase 8 Mediates the Mitochondrial Damage in the Fas Pathway of Apoptosis. *Cell* **1998**, *94* (4), 491–501. [https://doi.org/10.1016/s0092-8674\(00\)81590-1](https://doi.org/10.1016/s0092-8674(00)81590-1).
- (161) Wani, A. K.; Akhtar, N.; Mir, T. ul G.; Singh, R.; Jha, P. K.; Mallik, S. K.; Sinha, S.; Tripathi, S. K.; Jain, A.; Jha, A.; Devkota, H. P.; Prakash, A. Targeting Apoptotic Pathway of Cancer Cells with Phytochemicals and Plant-Based Nanomaterials. *Biomolecules* **2023**, *13* (2), 194. <https://doi.org/10.3390/biom13020194>.
- (162) Chawla-Sarkar, M.; Lindner, D. J.; Liu, Y.-F.; Williams, B. R.; Sen, G. C.; Silverman, R. H.; Borden, E. C. Apoptosis and Interferons: Role of Interferon-Stimulated Genes as Mediators of Apoptosis. *Apoptosis* **2003**, *8* (3), 237–249. <https://doi.org/10.1023/a:1023668705040>.
- (163) Hay, S.; Kannourakis, G. A Time to Kill: Viral Manipulation of the Cell Death Program. *Journal of General Virology* **2002**, *83* (7), 1547–1564. <https://doi.org/10.1099/0022-1317-83-7-1547>.
- (164) Mi, J.; Li, Z. Y.; Ni, S.; Steinwaerder, D.; Lieber, A. Induced Apoptosis Supports Spread of Adenovirus Vectors in Tumors. *Hum Gene Ther* **2001**, *12* (10), 1343–1352. <https://doi.org/10.1089/104303401750270995>.
- (165) Guo, C. J.; He, J.; He, J. G. The Immune Evasion Strategies of Fish Viruses. *Fish & Shellfish Immunology* **2019**, *86*, 772–784. <https://doi.org/10.1016/j.fsi.2018.12.013>.
- (166) Banerjee, A. K. Transcription and Replication of Rhabdoviruses. *Microbiol Rev* **1987**, *51* (1), 66–87.
- (167) He, M.; Ding, N.-Z.; He, C.-Q. Novirhabdoviruses versus Fish Innate Immunity: A Review. *Virus Research* **2021**, *304*, 198525. <https://doi.org/10.1016/j.virusres.2021.198525>.
- (168) Kim, M. S.; Kim, K. H. Effects of NV Gene Knock-out Recombinant Viral Hemorrhagic Septicemia Virus (VHSV) on Mx Gene Expression in Epithelioma Papulosum Cyprini (EPC) Cells and Olive Flounder (*Paralichthys Olivaceus*). *Fish Shellfish Immunol* **2012**, *32* (3), 459–463. <https://doi.org/10.1016/j.fsi.2011.12.014>.
- (169) Chinchilla, B.; Encinas, P.; Estepa, A.; Coll, J. M.; Gomez-Casado, E. Transcriptome Analysis of Rainbow Trout in Response to Non-Virion (NV) Protein of Viral Haemorrhagic Septicaemia Virus (VHSV). *Appl Microbiol Biotechnol* **2015**, *99* (4), 1827–1843. <https://doi.org/10.1007/s00253-014-6366-3>.
- (170) Chinchilla, B.; Encinas, P.; Coll, J. M.; Gomez-Casado, E. Differential Immune Transcriptome and Modulated Signalling Pathways in Rainbow Trout Infected with Viral Haemorrhagic Septicaemia Virus (VHSV) and Its Derivative Non-Virion (NV) Gene Deleted. *Vaccines (Basel)* **2020**, *8* (1), 58. <https://doi.org/10.3390/vaccines8010058>.
- (171) Biacchesi, S.; Mérou, E.; Chevret, D.; Lamoureux, A.; Bernard, J.; Brémont, M. NV Proteins of Fish Novirhabdovirus Recruit Cellular PPM1Bb Protein Phosphatase and Antagonize RIG-I-Mediated IFN Induction. *Sci Rep* **2017**, *7*, 44025. <https://doi.org/10.1038/srep44025>.
- (172) Kesterson, S. P.; Ringies, J.; Vakharia, V. N.; Shepherd, B. S.; Leaman, D. W.; Malathi, K. Effect of the Viral Hemorrhagic Septicemia Virus Nonvirion Protein on Translation via PERK-eIF2 $\alpha$  Pathway. *Viruses* **2020**, *12* (5), 499. <https://doi.org/10.3390/v12050499>.
- (173) Kim, M. S.; Kim, K. H. The Role of Viral Hemorrhagic Septicemia Virus (VHSV) NV Gene in TNF- $\alpha$ - and VHSV Infection-Mediated NF- $\kappa$ B Activation. *Fish Shellfish Immunol* **2013**, *34* (5), 1315–1319. <https://doi.org/10.1016/j.fsi.2013.02.026>.
- (174) Wu, Y.; Guo, M.; Hua, X.; Duan, K.; Lian, G.; Sun, L.; Tang, L.; Xu, Y.; Liu, M.; Li, Y. The Role of Infectious Hematopoietic Necrosis Virus (IHNV) Proteins in the Modulation of NF- $\kappa$ B Pathway during IHNV Infection. *Fish Shellfish Immunol* **2017**, *63*, 500–506. <https://doi.org/10.1016/j.fsi.2017.02.041>.
- (175) Ammayappan, A.; Vakharia, V. N. Nonvirion Protein of Novirhabdovirus Suppresses Apoptosis at the Early Stage of Virus Infection. *J Virol* **2011**, *85* (16), 8393–8402. <https://doi.org/10.1128/JVI.00597-11>.
- (176) Collet, B.; Munro, E. S.; Gahlawat, S.; Acosta, F.; Garcia, J.; Roemelt, C.; Zou, J.; Secombes, C. J.; Ellis, A. E. Infectious Pancreatic Necrosis Virus Suppresses Type I Interferon Signalling in Rainbow Trout Gonad Cell Line but Not in Atlantic Salmon Macrophages. *Fish & Shellfish Immunology* **2007**, *22* (1), 44–56. <https://doi.org/10.1016/j.fsi.2006.03.011>.
- (177) Skjesol, A.; Aamo, T.; Hegseth, M. N.; Robertsen, B.; Jørgensen, J. B. The Interplay between Infectious Pancreatic Necrosis Virus (IPNV) and the IFN System: IFN Signaling Is Inhibited by IPNV Infection. *Virus Res* **2009**, *143* (1), 53–60. <https://doi.org/10.1016/j.virusres.2009.03.004>.
- (178) Lauksund, S.; Greiner-Tollersrud, L.; Chang, C.-J.; Robertsen, B. Infectious Pancreatic Necrosis Virus Proteins VP2, VP3, VP4 and VP5 Antagonize IFN $\alpha$ 1 Promoter Activation While VP1 Induces IFN $\alpha$ 1. *Virus Res* **2015**, *196*, 113–121. <https://doi.org/10.1016/j.virusres.2014.11.018>.
- (179) Rodríguez Saint-Jean, S.; de las Heras, A. I.; Pérez Prieto, S. I. The Persistence of Infectious Pancreatic Necrosis Virus and Its Influence on the Early Immune Response. *Veterinary Immunology and Immunopathology* **2010**, *136* (1–2), 81–91. <https://doi.org/10.1016/j.vetimm.2010.02.015>.
- (180) Melby, H. P.; Krogsrud, J.; Håstein, T.; Stenwig, H. All Commercial Atlantic Salmon Seawater Farms in Norway Harbour Carriers of Infectious Pancreatic Necrosis Virus (IPNV). In *Proceedings from the 2nd international symposium on viruses of lower vertebrates*; Oregon State University: Corvallis, 1991; pp 211–217.
- (181) Munro, E. S.; Gahlawat, S. K.; Acosta, F.; Ellis, A. E. In Infectious Pancreatic Necrosis Virus Carrier Atlantic Salmon, *Salmo Salar* L., Post-Smolts, Almost All Kidney Macrophages Ex Vivo Contain a Low Level of Non-Replicating Virus. *J Fish Dis* **2006**, *29* (1), 43–48. <https://doi.org/10.1111/j.1365-2761.2005.00680.x>.

## References

- (182) García-Rosado, E.; Markussen, T.; Kileng, O.; Baekkevold, E. S.; Robertsen, B.; Mjaaland, S.; Rimstad, E. Molecular and Functional Characterization of Two Infectious Salmon Anaemia Virus (ISAV) Proteins with Type I Interferon Antagonizing Activity. *Virus Res* **2008**, *133* (2), 228–238. <https://doi.org/10.1016/j.virusres.2008.01.008>.
- (183) Li, C.; Greiner-Tollersrud, L.; Robertsen, B. Infectious Salmon Anemia Virus Segment 7 ORF1 and Segment 8 ORF2 Proteins Inhibit IRF Mediated Activation of the Atlantic Salmon IFN $\alpha$ 1 Promoter. *Fish & Shellfish Immunology* **2016**, *52*, 258–262. <https://doi.org/10.1016/j.fsi.2016.03.038>.
- (184) McBeath, A. J. A.; Collet, B.; Paley, R.; Duraffour, S.; Aspehaug, V.; Biering, E.; Secombes, C. J.; Snow, M. Identification of an Interferon Antagonist Protein Encoded by Segment 7 of Infectious Salmon Anaemia Virus. *Virus Res* **2006**, *115* (2), 176–184. <https://doi.org/10.1016/j.virusres.2005.08.005>.
- (185) Thukral, V.; Varshney, B.; Ramly, R. B.; Ponia, S. S.; Mishra, S. K.; Olsen, C. M.; Banerjee, A. C.; Mukherjee, S. K.; Zaidi, R.; Rimstad, E.; Lal, S. K. s8ORF2 Protein of Infectious Salmon Anaemia Virus Is a RNA-Silencing Suppressor and Interacts with Salmon Salar Mov10 (SsMov10) of the Host RNAi Machinery. *Virus Genes* **2018**, *54* (2), 199–214. <https://doi.org/10.1007/s11262-017-1526-z>.
- (186) Schuster, S.; Miesen, P.; van Rij, R. P. Antiviral RNAi in Insects and Mammals: Parallels and Differences. *Viruses* **2019**, *11* (5), 448. <https://doi.org/10.3390/v11050448>.
- (187) Obbard, D. J.; Gordon, K. H. J.; Buck, A. H.; Jiggins, F. M. The Evolution of RNAi as a Defence against Viruses and Transposable Elements. *Philos Trans R Soc Lond B Biol Sci* **2009**, *364* (1513), 99–115. <https://doi.org/10.1098/rstb.2008.0168>.
- (188) Maillard, P. V.; van der Veen, A. G.; Poirier, E. Z.; Reis e Sousa, C. Slicing and Dicing Viruses: Antiviral RNA Interference in Mammals. *The EMBO Journal* **2019**, *38* (8), e100941. <https://doi.org/10.15252/embj.2018100941>.
- (189) Semple, S. L.; Au, S. K. W.; Jacob, R. A.; Mossman, K. L.; DeWitte-Orr, S. J. Discovery and Use of Long dsRNA Mediated RNA Interference to Stimulate Antiviral Protection in Interferon Competent Mammalian Cells. *Front Immunol* **2022**, *13*, 859749. <https://doi.org/10.3389/fimmu.2022.859749>.
- (190) Dixon, B.; Stafford, J. Honouring the Career of Miodrag (Mike) Belosevic. *Developmental & Comparative Immunology* **2023**, *149*, 105048. <https://doi.org/10.1016/j.dci.2023.105048>.
- (191) Roberts, W. K.; Hovanessian, A.; Brown, R. E.; Clemens, M. J.; Kerr, I. M. Interferon-Mediated Protein Kinase and Low-Molecular-Weight Inhibitor of Protein Synthesis. *Nature* **1976**, *264* (5585), 477–480. <https://doi.org/10.1038/264477a0>.
- (192) Hovanessian, A. G. Double-Stranded RNA Dependent Protein Kinase (s) in Rabbit Reticulocyte Lysates Analogous to Kinase from Interferon-Treated Cells. *Biochimie* **1980**, *62* (11–12), 775–778. [https://doi.org/10.1016/s0300-9084\(80\)80132-5](https://doi.org/10.1016/s0300-9084(80)80132-5).
- (193) Kimchi, A.; Zilberstein, A.; Schmidt, A.; Shulman, L.; Revel, M. The Interferon-Induced Protein Kinase PK-i from Mouse L Cells. *Journal of Biological Chemistry* **1979**, *254* (19), 9846–9853. [https://doi.org/10.1016/S0021-9258\(19\)83594-9](https://doi.org/10.1016/S0021-9258(19)83594-9).
- (194) Laurent, A. G.; Krust, B.; Galabru, J.; Svab, J.; Hovanessian, A. G. Monoclonal Antibodies to an Interferon-Induced Mr 68,000 Protein and Their Use for the Detection of Double-Stranded RNA-Dependent Protein Kinase in Human Cells. *Proc Natl Acad Sci U S A* **1985**, *82* (13), 4341–4345.
- (195) Samuel, C. E. Mechanism of Interferon Action: Phosphorylation of Protein Synthesis Initiation Factor eIF-2 in Interferon-Treated Human Cells by a Ribosome-Associated Kinase Processing Site Specificity Similar to Hemin-Regulated Rabbit Reticulocyte Kinase. *Proc Natl Acad Sci U S A* **1979**, *76* (2), 600–604. <https://doi.org/10.1073/pnas.76.2.600>.
- (196) Meurs, E.; Chong, K.; Galabru, J.; Thomas, N. S.; Kerr, I. M.; Williams, B. R.; Hovanessian, A. G. Molecular Cloning and Characterization of the Human Double-Stranded RNA-Activated Protein Kinase Induced by Interferon. *Cell* **1990**, *62* (2), 379–390. [https://doi.org/10.1016/0092-8674\(90\)90374-n](https://doi.org/10.1016/0092-8674(90)90374-n).
- (197) Clemens, M. J.; Hershey, J. W.; Hovanessian, A. C.; Jacobs, B. C.; Katze, M. G.; Kaufman, R. J.; Lengyel, P.; Samuel, C. E.; Sen, G. C.; Williams, B. R. PKR: Proposed Nomenclature for the RNA-Dependent Protein Kinase Induced by Interferon. *J Interferon Res* **1993**, *13* (3), 241. <https://doi.org/10.1089/jir.1993.13.241>.
- (198) Hu, C.-Y.; Zhang, Y.-B.; Huang, G.-P.; Zhang, Q.-Y.; Gui, J.-F. Molecular Cloning and Characterisation of a Fish PKR-like Gene from Cultured CAB Cells Induced by UV-Inactivated Virus. *Fish & Shellfish Immunology* **2004**, *17* (4), 353–366. <https://doi.org/10.1016/j.fsi.2004.04.009>.
- (199) Zhu, R.; Zhang, Y.-B.; Zhang, Q.-Y.; Gui, J.-F. Functional Domains and the Antiviral Effect of the Double-Stranded RNA-Dependent Protein Kinase PKR from *Paralichthys Olivaceus*. *J Virol* **2008**, *82* (14), 6889–6901. <https://doi.org/10.1128/JVI.02385-07>.
- (200) Rothenburg, S.; Deigendesch, N.; Dey, M.; Dever, T. E.; Tazi, L. Double-Stranded RNA-Activated Protein Kinase PKR of Fishes and Amphibians: Varying the Number of Double-Stranded RNA Binding Domains and Lineage-Specific Duplications. *BMC Biol* **2008**, *6* (1), 12. <https://doi.org/10.1186/1741-7007-6-12>.
- (201) Pakos-Zebrucka, K.; Koryga, I.; Mnich, K.; Ljujic, M.; Samali, A.; Gorman, A. M. The Integrated Stress Response. *EMBO Rep* **2016**, *17* (10), 1374–1395. <https://doi.org/10.15252/embr.201642195>.
- (202) Donnelly, N.; Gorman, A. M.; Gupta, S.; Samali, A. The eIF2 $\alpha$  Kinases: Their Structures and Functions. *Cell. Mol. Life Sci.* **2013**, *70* (19), 3493–3511. <https://doi.org/10.1007/s00018-012-1252-6>.
- (203) Rothenburg, S.; Deigendesch, N.; Dittmar, K.; Koch-Nolte, F.; Haag, F.; Lowenhaupt, K.; Rich, A. A PKR-like Eukaryotic Initiation Factor 2 Kinase from Zebrafish Contains Z-DNA Binding Domains Instead of dsRNA Binding Domains. *Proceedings of the National Academy of Sciences* **2005**, *102* (5), 1602–1607. <https://doi.org/10.1073/pnas.0408714102>.
- (204) Berlanga, J. J.; Ventoso, I.; Harding, H. P.; Deng, J.; Ron, D.; Sonenberg, N.; Carrasco, L.; de Haro, C. Antiviral Effect of the Mammalian Translation Initiation Factor 2 $\alpha$  Kinase GCN2 against RNA Viruses. *EMBO J* **2006**, *25* (8), 1730–1740. <https://doi.org/10.1038/sj.emboj.7601073>.
- (205) Cheng, G.; Feng, Z.; He, B. Herpes Simplex Virus 1 Infection Activates the Endoplasmic Reticulum Resident Kinase PERK and Mediates eIF-2 $\alpha$  Dephosphorylation by the  $\Gamma$ 134.5 Protein. *J Virol* **2005**, *79* (3), 1379–1388. <https://doi.org/10.1128/JVI.79.3.1379-1388.2005>.
- (206) Lee, E.-S.; Yoon, C.-H.; Kim, Y.-S.; Bae, Y.-S. The Double-Strand RNA-Dependent Protein Kinase PKR Plays a Significant Role in a Sustained ER Stress-Induced Apoptosis. *FEBS Letters* **2007**, *581* (22), 4325–4332. <https://doi.org/10.1016/j.febslet.2007.08.001>.
- (207) Cole, J. Activation of PKR: An Open and Shut Case? *Trends in Biochemical Sciences* **2007**, *32* (2), 57–62. <https://doi.org/10.1016/j.tibs.2006.12.003>.

## References

- (208) Letunic, I.; Khedkar, S.; Bork, P. SMART: Recent Updates, New Developments and Status in 2020. *Nucleic Acids Research* **2021**, *49* (D1), D458–D460. <https://doi.org/10.1093/nar/gkaa937>.
- (209) Letunic, I.; Bork, P. 20 Years of the SMART Protein Domain Annotation Resource. *Nucleic Acids Res* **2018**, *46* (Database issue), D493–D496. <https://doi.org/10.1093/nar/gkx922>.
- (210) Nanduri, S.; Carpick, B. W.; Yang, Y.; Williams, B. R.; Qin, J. Structure of the Double-Stranded RNA-Binding Domain of the Protein Kinase PKR Reveals the Molecular Basis of Its dsRNA-Mediated Activation. *EMBO J* **1998**, *17* (18), 5458–5465. <https://doi.org/10.1093/emboj/17.18.5458>.
- (211) Dar, A. C.; Dever, T. E.; Sicheri, F. Higher-Order Substrate Recognition of eIF2 $\alpha$  by the RNA-Dependent Protein Kinase PKR. *Cell* **2005**, *122* (6), 887–900. <https://doi.org/10.1016/j.cell.2005.06.044>.
- (212) St Johnston, D.; Brown, N. H.; Gall, J. G.; Jantsch, M. A Conserved Double-Stranded RNA-Binding Domain. *Proceedings of the National Academy of Sciences* **1992**, *89* (22), 10979–10983. <https://doi.org/10.1073/pnas.89.22.10979>.
- (213) Masliah, G.; Barraud, P.; Allain, F. H.-T. RNA Recognition by Double-Stranded RNA Binding Domains: A Matter of Shape and Sequence. *Cell Mol Life Sci* **2013**, *70* (11), 1875–1895. <https://doi.org/10.1007/s00018-012-1119-x>.
- (214) Patel, R. C.; Stanton, P.; Sen, G. C. Specific Mutations near the Amino Terminus of Double-Stranded RNA-Dependent Protein Kinase (PKR) Differentially Affect Its Double-Stranded RNA Binding and Dimerization Properties. *J Biol Chem* **1996**, *271* (41), 25657–25663. <https://doi.org/10.1074/jbc.271.41.25657>.
- (215) Romano, P. R.; Green, S. R.; Barber, G. N.; Mathews, M. B.; Hinnebusch, A. G. Structural Requirements for Double-Stranded RNA Binding, Dimerization, and Activation of the Human eIF-2 Alpha Kinase DAI in *Saccharomyces Cerevisiae*. *Mol Cell Biol* **1995**, *15* (1), 365–378.
- (216) Green, S. R.; Manche, L.; Mathews, M. B. Two Functionally Distinct RNA-Binding Motifs in the Regulatory Domain of the Protein Kinase DAI. *Mol Cell Biol* **1995**, *15* (1), 358–364.
- (217) Green, S. R.; Mathews, M. B. Two RNA-Binding Motifs in the Double-Stranded RNA-Activated Protein Kinase, DAI. *Genes Dev* **1992**, *6* (12B), 2478–2490. <https://doi.org/10.1101/gad.6.12b.2478>.
- (218) Herbert, A.; Alfken, J.; Kim, Y. G.; Mian, I. S.; Nishikura, K.; Rich, A. A Z-DNA Binding Domain Present in the Human Editing Enzyme, Double-Stranded RNA Adenosine Deaminase. *Proc Natl Acad Sci U S A* **1997**, *94* (16), 8421–8426. <https://doi.org/10.1073/pnas.94.16.8421>.
- (219) Kim, Y.-G.; Muralinath, M.; Brandt, T.; Percy, M.; Hauns, K.; Lowenhaupt, K.; Jacobs, B. L.; Rich, A. A Role for Z-DNA Binding in Vaccinia Virus Pathogenesis. *Proc Natl Acad Sci U S A* **2003**, *100* (12), 6974–6979. <https://doi.org/10.1073/pnas.0431131100>.
- (220) Kim, C. How Z-DNA/RNA Binding Proteins Shape Homeostasis, Inflammation, and Immunity. *BMB Rep* **2020**, *53* (9), 453–457. <https://doi.org/10.5483/BMBRep.2020.53.9.141>.
- (221) de Rosa, M.; Zacarias, S.; Athanasiadis, A. Structural Basis for Z-DNA Binding and Stabilization by the Zebrafish Z-DNA Dependent Protein Kinase PKZ. *Nucleic Acids Res* **2013**, *41* (21), 9924–9933. <https://doi.org/10.1093/nar/gkt743>.
- (222) Wu, C.; Zhang, Y.; Hu, C. PKZ, a Fish-Unique eIF2 $\alpha$  Kinase Involved in Innate Immune Response. *Front Immunol* **2020**, *11*. <https://doi.org/10.3389/fimmu.2020.00585>.
- (223) Wu, C.-X.; Wang, S.-J.; Lin, G.; Hu, C.-Y. The Zalpha Domain of PKZ from *Carassius Auratus* Can Bind to d(GC)(n) in Negative Supercoils. *Fish Shellfish Immunol* **2010**, *28* (5–6), 783–788. <https://doi.org/10.1016/j.fsi.2010.01.021>.
- (224) Hanks, S. K.; Quinn, A. M.; Hunter, T. The Protein Kinase Family: Conserved Features and Deduced Phylogeny of the Catalytic Domains. *Science* **1988**, *241* (4861), 42–52. <https://doi.org/10.1126/science.3291115>.
- (225) Romano, P. R.; Garcia-Barrio, M. T.; Zhang, X.; Wang, Q.; Taylor, D. R.; Zhang, F.; Herring, C.; Mathews, M. B.; Qin, J.; Hinnebusch, A. G. Autophosphorylation in the Activation Loop Is Required for Full Kinase Activity in Vivo of Human and Yeast Eukaryotic Initiation Factor 2alpha Kinases PKR and GCN2. *Mol Cell Biol* **1998**, *18* (4), 2282–2297. <https://doi.org/10.1128/MCB.18.4.2282>.
- (226) Cai, R.; Williams, B. R. G. Mutations in the Double-Stranded RNA-Activated Protein Kinase Insert Region That Uncouple Catalysis from eIF2 $\alpha$  Binding \*. *Journal of Biological Chemistry* **1998**, *273* (18), 11274–11280. <https://doi.org/10.1074/jbc.273.18.11274>.
- (227) Craig, A. W.; Cosentino, G. P.; Donzé, O.; Sonenberg, N. The Kinase Insert Domain of Interferon-Induced Protein Kinase PKR Is Required for Activity but Not for Interaction with the Pseudosubstrate K3L. *J Biol Chem* **1996**, *271* (40), 24526–24533. <https://doi.org/10.1074/jbc.271.40.24526>.
- (228) Rothenburg, S.; Seo, E. J.; Gibbs, J. S.; Dever, T. E.; Dittmar, K. Rapid Evolution of Protein Kinase PKR Alters Sensitivity to Viral Inhibitors. *Nat Struct Mol Biol* **2009**, *16* (1), 63–70. <https://doi.org/10.1038/nsmb.1529>.
- (229) Bergan, V.; Jagus, R.; Lauksund, S.; Kileng, Ø.; Robertsen, B. The Atlantic Salmon Z-DNA Binding Protein Kinase Phosphorylates Translation Initiation Factor 2 Alpha and Constitutes a Unique Orthologue to the Mammalian dsRNA-Activated Protein Kinase R. *The FEBS Journal* **2008**, *275* (1), 184–197. <https://doi.org/10.1111/j.1742-4658.2007.06188.x>.
- (230) Jeffrey, I. W.; Kadereit, S.; Meurs, E. F.; Metzger, T.; Bachmann, M.; Schwemmler, M.; Hovanessian, A. G.; Clemens, M. J. Nuclear Localization of the Interferon-Inducible Protein Kinase PKR in Human Cells and Transfected Mouse Cells. *Exp Cell Res* **1995**, *218* (1), 17–27. <https://doi.org/10.1006/excr.1995.1126>.
- (231) Wei, J.; Zang, S.; Li, C.; Zhang, X.; Gao, P.; Qin, Q. Grouper PKR Activation Inhibits Red-Spotted Grouper Nervous Necrosis Virus (RGNNV) Replication in Infected Cells. *Developmental & Comparative Immunology* **2020**, *111*, 103744. <https://doi.org/10.1016/j.dci.2020.103744>.
- (232) Xu, X.; Li, M.; Wu, C.; Li, D.; Jiang, Z.; Liu, C.; Cheng, B.; Mao, H.; Hu, C. The Fish-Specific Protein Kinase (PKZ) Initiates Innate Immune Responses via IRF3- and ISGF3-Like Mediated Pathways. *Front Immunol* **2019**, *10*, 582. <https://doi.org/10.3389/fimmu.2019.00582>.
- (233) Balachandran, S.; Roberts, P. C.; Brown, L. E.; Truong, H.; Pattnaik, A. K.; Archer, D. R.; Barber, G. N. Essential Role for the dsRNA-Dependent Protein Kinase PKR in Innate Immunity to Viral Infection. *Immunity* **2000**, *13* (1), 129–141. [https://doi.org/10.1016/S1074-7613\(00\)00014-5](https://doi.org/10.1016/S1074-7613(00)00014-5).
- (234) Goh, K. C.; deVeer, M. J.; Williams, B. R. The Protein Kinase PKR Is Required for P38 MAPK Activation and the Innate Immune Response to Bacterial Endotoxin. *EMBO J* **2000**, *19* (16), 4292–4297. <https://doi.org/10.1093/emboj/19.16.4292>.
- (235) Smyth, R.; Sun, J. Protein Kinase R in Bacterial Infections: Friend or Foe? *Frontiers in Immunology* **2021**, *12*.

## References

- (236) Wang, R.; Wang, J.; Paul, A. M.; Acharya, D.; Bai, F.; Huang, F.; Guo, Y.-L. Mouse Embryonic Stem Cells Are Deficient in Type I Interferon Expression in Response to Viral Infections and Double-Stranded RNA\*. *Journal of Biological Chemistry* **2013**, *288* (22), 15926–15936. <https://doi.org/10.1074/jbc.M112.421438>.
- (237) Cheng, X.; Jiang, Z.; Shanshan Zeng, null; Feng, Z.; Sun, Z.; Lu, S.; Xu, X.; Mao, H.; Hu, C. Grass Carp (Ctenopharyngodon Idella) Trans-Activation-Responsive RNA-Binding Protein 2 (TARBP2) Inhibits Apoptosis by Decreasing PKR Phosphorylation. *Dev Comp Immunol* **2022**, *133*, 104425. <https://doi.org/10.1016/j.dci.2022.104425>.
- (238) Hu, Y.-S.; Li, W.; Li, D.-M.; Liu, Y.; Fan, L.-H.; Rao, Z.-C.; Lin, G.; Hu, C.-Y. Cloning, Expression and Functional Analysis of PKR from Grass Carp (Ctenopharyngodon Idellus). *Fish & Shellfish Immunology* **2013**, *35* (6), 1874–1881. <https://doi.org/10.1016/j.fsi.2013.09.024>.
- (239) Liu, T.-K.; Zhang, Y.-B.; Liu, Y.; Sun, F.; Gui, J.-F. Cooperative Roles of Fish Protein Kinase Containing Z-DNA Binding Domains and Double-Stranded RNA-Dependent Protein Kinase in Interferon-Mediated Antiviral Response  $\tau$ . *J Virol* **2011**, *85* (23), 12769–12780. <https://doi.org/10.1128/JVI.05849-11>.
- (240) Pindel, A.; Sadler, A. The Role of Protein Kinase R in the Interferon Response. *Journal of Interferon & Cytokine Research* **2011**, *31* (1), 59–70. <https://doi.org/10.1089/jir.2010.0099>.
- (241) Das, S.; Ward, S. V.; Tacke, R. S.; Suske, G.; Samuel, C. E. Activation of the RNA-Dependent Protein Kinase PKR Promoter in the Absence of Interferon Is Dependent upon Sp Proteins. *J Biol Chem* **2006**, *281* (6), 3244–3253. <https://doi.org/10.1074/jbc.M510612200>.
- (242) Yoon, C.-H.; Lee, E.-S.; Lim, D.-S.; Bae, Y.-S. PKR, a P53 Target Gene, Plays a Crucial Role in the Tumor-Suppressor Function of P53. *Proc Natl Acad Sci U S A* **2009**, *106* (19), 7852–7857. <https://doi.org/10.1073/pnas.0812148106>.
- (243) Beretta, L.; Gabbay, M.; Berger, R.; Hanash, S. M.; Sonenberg, N. Expression of the Protein Kinase PKR in Modulated by IRF-1 and Is Reduced in 5q- Associated Leukemias. *Oncogene* **1996**, *12* (7), 1593–1596.
- (244) Kirchhoff, S.; Koromilas, A. E.; Schaper, F.; Grashoff, M.; Sonenberg, N.; Hauser, H. IRF-1 Induced Cell Growth Inhibition and Interferon Induction Requires the Activity of the Protein Kinase PKR. *Oncogene* **1995**, *11* (3), 439–445.
- (245) Liu, D.; Mao, H.; Gu, M.; Xu, X.; Sun, Z.; Lin, G.; Wang, H.; Xie, D.; Hou, Q.; Wang, X.; Mi, Y.; Liu, X.; Hu, C. The Transcription Regulation Analysis of Ctenopharyngodon Idellus PKR and PKZ Genes. *Gene* **2016**, *576* (1 Pt 3), 512–519. <https://doi.org/10.1016/j.gene.2015.10.070>.
- (246) Huang, Q.; Xie, D.; Mao, H.; Wang, H.; Wu, Z.; Huang, K.; Wan, Y.; Xu, Q.; Hu, C. Ctenopharyngodon Idella P53 Mediates between NF- $\kappa$ B and PKR at the Transcriptional Level. *Fish Shellfish Immunol* **2017**, *69*, 258–264. <https://doi.org/10.1016/j.fsi.2017.08.012>.
- (247) Der, S. D.; Lau, A. S. Involvement of the Double-Stranded-RNA-Dependent Kinase PKR in Interferon Expression and Interferon-Mediated Antiviral Activity. *Proc Natl Acad Sci U S A* **1995**, *92* (19), 8841–8845.
- (248) Flodström-Tullberg, M.; Hultcrantz, M.; Stotland, A.; Maday, A.; Tsai, D.; Fine, C.; Williams, B.; Silverman, R.; Sarvetnick, N. RNase L and Double-Stranded RNA-Dependent Protein Kinase Exert Complementary Roles in Islet Cell Defense during Coxsackievirus Infection. *J Immunol* **2005**, *174* (3), 1171–1177. <https://doi.org/10.4049/jimmunol.174.3.1171>.
- (249) Zuo, W.; Wakimoto, M.; Kozaiwa, N.; Shirasaka, Y.; Oh, S.-W.; Fujiwara, S.; Miyachi, H.; Kogure, A.; Kato, H.; Fujita, T. PKR and TLR3 Trigger Distinct Signals That Coordinate the Induction of Antiviral Apoptosis. *Cell Death Dis* **2022**, *13* (8), 1–15. <https://doi.org/10.1038/s41419-022-05101-3>.
- (250) Samuel, M. A.; Whitby, K.; Keller, B. C.; Marri, A.; Barchet, W.; Williams, B. R. G.; Silverman, R. H.; Gale, M.; Diamond, M. S. PKR and RNase L Contribute to Protection against Lethal West Nile Virus Infection by Controlling Early Viral Spread in the Periphery and Replication in Neurons. *J Virol* **2006**, *80* (14), 7009–7019. <https://doi.org/10.1128/JVI.00489-06>.
- (251) Durbin, R. K.; Mertz, S. E.; Koromilas, A. E.; Durbin, J. E. PKR Protection against Intranasal Vesicular Stomatitis Virus Infection Is Mouse Strain Dependent. *Viral Immunol* **2002**, *15* (1), 41–51. <https://doi.org/10.1089/088282402317340224>.
- (252) Smith, J. A.; Schmechel, S. C.; Williams, B. R. G.; Silverman, R. H.; Schiff, L. A. Involvement of the Interferon-Regulated Antiviral Proteins PKR and RNase L in Reovirus-Induced Shutoff of Cellular Translation. *J Virol* **2005**, *79* (4), 2240–2250. <https://doi.org/10.1128/JVI.79.4.2240-2250.2005>.
- (253) Willis, K. L.; Patel, S.; Xiang, Y.; Shisler, J. L. The Effect of the Vaccinia K1 Protein on the PKR-eIF2 $\alpha$  Pathway in RK13 and HeLa Cells. *Virology* **2009**, *394* (1), 73–81. <https://doi.org/10.1016/j.virol.2009.08.020>.
- (254) Diamond, M. S.; Harris, E. Interferon Inhibits Dengue Virus Infection by Preventing Translation of Viral RNA through a PKR-Independent Mechanism. *Virology* **2001**, *289* (2), 297–311. <https://doi.org/10.1006/viro.2001.1114>.
- (255) Toth, A. M.; Devaux, P.; Cattaneo, R.; Samuel, C. E. Protein Kinase PKR Mediates the Apoptosis Induction and Growth Restriction Phenotypes of C Protein-Deficient Measles Virus. *J Virol* **2009**, *83* (2), 961–968. <https://doi.org/10.1128/JVI.01669-08>.
- (256) Arnaud, N.; Dabo, S.; Maillard, P.; Budkowska, A.; Kalliampakou, K. I.; Mavromara, P.; Garcin, D.; Hugon, J.; Gatignol, A.; Akazawa, D.; Wakita, T.; Meurs, E. F. Hepatitis C Virus Controls Interferon Production through PKR Activation. *PLoS One* **2010**, *5* (5), e10575. <https://doi.org/10.1371/journal.pone.0010575>.
- (257) Xu, C.; Gamil, A. A. A.; Munang'andu, H. M.; Evensen, Ø. Apoptosis Induction by dsRNA-Dependent Protein Kinase R (PKR) in EPC Cells via Caspase 8 and 9 Pathways. *Viruses* **2018**, *10* (10), 526. <https://doi.org/10.3390/v10100526>.
- (258) Hu, Y.; Fan, L.; Wu, C.; Wang, B.; Sun, Z.; Hu, C. Identification and Function Analysis of the Three dsRBMs in the N Terminal dsRBD of Grass Carp (Ctenopharyngodon Idella) PKR. *Fish Shellfish Immunol* **2016**, *50*, 91–100. <https://doi.org/10.1016/j.fsi.2016.01.011>.
- (259) Hu, Z.; Du, H.; Lin, G.; Han, K.; Cheng, X.; Feng, Z.; Mao, H.; Hu, C. Grass Carp (Ctenopharyngodon Idella) PACT Induces Cell Apoptosis and Activates NF- $\kappa$ B via PKR. *Fish Shellfish Immunol* **2020**, *103*, 377–384. <https://doi.org/10.1016/j.fsi.2020.05.036>.
- (260) Wang, H.; Xu, Q.; Xu, X.; Hu, Y.; Hou, Q.; Zhu, Y.; Hu, C. Ctenopharyngodon Idella IKK $\beta$  Interacts with PKR and I $\kappa$ B $\alpha$ . *Acta Biochim Biophys Sin (Shanghai)* **2017**, *49* (8), 729–736. <https://doi.org/10.1093/abbs/gmx065>.
- (261) Wang, L.; Wu, Z.; Huang, Q.; Huang, K.; Qi, G.; Wu, C.; Mao, H.; Xu, X.; Wang, H.; Hu, C. Grass Carp (Ctenopharyngodon Idella) STAT3 Regulates the eIF2 $\alpha$  Phosphorylation through Interaction with PKR. *Dev Comp Immunol* **2018**, *78*, 26–34. <https://doi.org/10.1016/j.dci.2017.08.019>.

## References

- (262) Wu, C.; Hu, Y.; Fan, L.; Wang, H.; Sun, Z.; Deng, S.; Liu, Y.; Hu, C. Ctenopharyngodon Idella PKZ Facilitates Cell Apoptosis through Phosphorylating eIF2 $\alpha$ . *Molecular Immunology* **2016**, *69*, 13–23. <https://doi.org/10.1016/j.molimm.2015.11.006>.
- (263) Streiff, C.; He, B.; Morvan, L.; Zhang, H.; Delrez, N.; Fourrier, M.; Manfroid, I.; Suárez, N. M.; Betoulle, S.; Davison, A. J.; Donohoe, O.; Vanderplassen, A. Susceptibility and Permissivity of Zebrafish (*Danio Rerio*) Larvae to Cypriniviruses. *Viruses* **2023**, *15* (3), 768. <https://doi.org/10.3390/v15030768>.
- (264) Zenke, K.; Nam, Y. K.; Kim, K. H. Molecular Cloning and Expression Analysis of Double-Stranded RNA-Dependent Protein Kinase (PKR) in Rock Bream (*Oplegnathus Fasciatus*). *Veterinary Immunology and Immunopathology* **2010**, *133* (2–4), 290–295. <https://doi.org/10.1016/j.vetimm.2009.08.009>.
- (265) Gan, Z.; Cheng, J.; Hou, J.; Chen, S.; Xia, H.; Xia, L.; Kwok, K. W. H.; Lu, Y.; Nie, P. Tilapia dsRNA-Activated Protein Kinase R (PKR): An Interferon-Induced Antiviral Effector with Translation Inhibition Activity. *Fish Shellfish Immunol* **2021**, *112*, 74–80. <https://doi.org/10.1016/j.fsi.2021.02.016>.
- (266) del Castillo, C. S.; Hikima, J.; Ohtani, M.; Jung, T.-S.; Aoki, T. Characterization and Functional Analysis of Two PKR Genes in Fugu (*Takifugu Rubripes*). *Fish & Shellfish Immunology* **2012**, *32* (1), 79–88. <https://doi.org/10.1016/j.fsi.2011.10.022>.
- (267) Gamil, A. A. A.; Xu, C.; Mutoloki, S.; Evensen, Ø. PKR Activation Favors Infectious Pancreatic Necrosis Virus Replication in Infected Cells. *Viruses* **2016**, *8* (6). <https://doi.org/10.3390/v8060173>.
- (268) Yang, P.-J.; Wu, C.-X.; Li, W.; Fan, L.-H.; Lin, G.; Hu, C.-Y. Cloning and Functional Analysis of PKZ (PKR-like) from Grass Carp (*Ctenopharyngodon Idellus*). *Fish & Shellfish Immunology* **2011**, *31* (6), 1173–1178. <https://doi.org/10.1016/j.fsi.2011.10.012>.
- (269) Liu, Z.-Y.; Jia, K.-T.; Li, C.; Weng, S.-P.; Guo, C.-J.; He, J.-G. A Truncated *Danio Rerio* PKZ Isoform Functionally Interacts with eIF2 $\alpha$  and Inhibits Protein Synthesis. *Gene* **2013**, *527* (1), 292–300. <https://doi.org/10.1016/j.gene.2013.05.043>.
- (270) Su, J.; Zhu, Z.; Wang, Y. Molecular Cloning, Characterization and Expression Analysis of the PKZ Gene in Rare Minnow *Gobiocypris Rarus*. *Fish Shellfish Immunol* **2008**, *25* (1–2), 106–113. <https://doi.org/10.1016/j.fsi.2008.03.006>.
- (271) Ramnani, B.; Powell, S.; Shetty, A. G.; Manivannan, P.; Hibbard, B. R.; Leaman, D. W.; Malathi, K. Viral Hemorrhagic Septicemia Virus Activates Integrated Stress Response Pathway and Induces Stress Granules to Regulate Virus Replication. *Viruses* **2023**, *15* (2), 466. <https://doi.org/10.3390/v15020466>.
- (272) Gamil, A. A. A.; Mutoloki, S.; Evensen, Ø. A Piscine Birnavirus Induces Inhibition of Protein Synthesis in CHSE-214 Cells Primarily through the Induction of eIF2 $\alpha$  Phosphorylation. *Viruses* **2015**, *7* (4), 1987–2005. <https://doi.org/10.3390/v7041987>.
- (273) Arter, C.; Trask, L.; Ward, S.; Yeoh, S.; Bayliss, R. Structural Features of the Protein Kinase Domain and Targeted Binding by Small-Molecule Inhibitors. *J Biol Chem* **2022**, *298* (8), 102247. <https://doi.org/10.1016/j.jbc.2022.102247>.
- (274) Lemaire, P. A.; Lary, J.; Cole, J. L. Mechanism of PKR Activation: Dimerization and Kinase Activation in the Absence of Double-Stranded RNA. *J Mol Biol* **2005**, *345* (1), 81–90. <https://doi.org/10.1016/j.jmb.2004.10.031>.
- (275) Nanduri, S.; Rahman, F.; Williams, B. R. G.; Qin, J. A Dynamically Tuned Double-Stranded RNA Binding Mechanism for the Activation of Antiviral Kinase PKR. *EMBO J* **2000**, *19* (20), 5567–5574. <https://doi.org/10.1093/emboj/19.20.5567>.
- (276) Vattem, K. M.; Staschke, K. A.; Wek, R. C. Mechanism of Activation of the Double-Stranded-RNA-Dependent Protein Kinase, PKR. *European Journal of Biochemistry* **2001**, *268* (13), 3674–3684. <https://doi.org/10.1046/j.1432-1327.2001.02273.x>.
- (277) Gelev, V.; Aktas, H.; Marintchev, A.; Ito, T.; Frueh, D.; Hemond, M.; Rovnyak, D.; Debus, M.; Hyberts, S.; Usheva, A.; Halperin, J.; Wagner, G. Mapping of the Auto-Inhibitory Interactions of Protein Kinase R by Nuclear Magnetic Resonance. *J Mol Biol* **2006**, *364* (3), 352–363. <https://doi.org/10.1016/j.jmb.2006.08.077>.
- (278) Lemaire, P. A.; Tessmer, I.; Craig, R.; Erie, D. A.; Cole, J. L. Unactivated PKR Exists in an Open Conformation Capable of Binding Nucleotides. *Biochemistry* **2006**, *45* (30), 9074–9084. <https://doi.org/10.1021/bi060567d>.
- (279) Wang, D.; de Weerd, N. A.; Willard, B.; Polekhina, G.; Williams, B. R. G.; Sadler, A. J. Auto-Phosphorylation Represses Protein Kinase R Activity. *Sci Rep* **2017**, *7*, 44340. <https://doi.org/10.1038/srep44340>.
- (280) Cesaro, T.; Hayashi, Y.; Borghese, F.; Vertommen, D.; Wavreil, F.; Michiels, T. PKR Activity Modulation by Phosphomimetic Mutations of Serine Residues Located Three Aminoacids Upstream of Double-Stranded RNA Binding Motifs. *Sci Rep* **2021**, *11* (1), 9188. <https://doi.org/10.1038/s41598-021-88610-z>.
- (281) Lemaire, P. A.; Anderson, E.; Lary, J.; Cole, J. L. Mechanism of PKR Activation by dsRNA. *J Mol Biol* **2008**, *381* (2), 351–360. <https://doi.org/10.1016/j.jmb.2008.05.056>.
- (282) Ucci, J. W.; Kobayashi, Y.; Choi, G.; Alexandrescu, A. T.; Cole, J. L. Mechanism of Interaction of the Double-Stranded RNA (dsRNA) Binding Domain of Protein Kinase R with Short dsRNA Sequences. *Biochemistry* **2007**, *46* (1), 55–65. <https://doi.org/10.1021/bi061531o>.
- (283) Mayo, C. B.; Erlandsen, H.; Mouser, D. J.; Feinstein, A. G.; Robinson, V. L.; May, E. R.; Cole, J. L. Structural Basis of Protein Kinase R Autophosphorylation. *Biochemistry* **2019**, *58* (27), 2967–2977. <https://doi.org/10.1021/acs.biochem.9b00161>.
- (284) Dey, M.; Mann, B. R.; Anshu, A.; Mannan, M. A. Activation of Protein Kinase PKR Requires Dimerization-Induced Cis-Phosphorylation within the Activation Loop. *Journal of Biological Chemistry* **2014**, *289* (9), 5747–5757. <https://doi.org/10.1074/jbc.M113.527796>.
- (285) Jammi, N.; Beal, P. A. Phosphorylation of the RNA-Dependent Protein Kinase Regulates Its RNA-Binding Activity. *Nucleic Acids Res* **2001**, *29* (14), 3020–3029.
- (286) Rich, A. DNA Comes in Many Forms. *Gene* **1993**, *135* (1–2), 99–109. [https://doi.org/10.1016/0378-1119\(93\)90054-7](https://doi.org/10.1016/0378-1119(93)90054-7).
- (287) Davis, P. W.; Adamiak, R. W.; Tinoco, I. Z-RNA: The Solution NMR Structure of r(CGCGCG). *Biopolymers* **1990**, *29* (1), 109–122. <https://doi.org/10.1002/bip.360290116>.
- (288) Brown, B. A.; Lowenhaupt, K.; Wilbert, C. M.; Hanlon, E. B.; Rich, A. The Z $\alpha$  Domain of the Editing Enzyme dsRNA Adenosine Deaminase Binds Left-Handed Z-RNA as Well as Z-DNA. *Proc Natl Acad Sci U S A* **2000**, *97* (25), 13532–13536.
- (289) Tomé, A. R.; Kuš, K.; Correia, S.; Paulo, L. M.; Zacarias, S.; de Rosa, M.; Figueiredo, D.; Parkhouse, R. M. E.; Athanasiadis, A. Crystal Structure of a Poxvirus-like Z $\alpha$  Domain from Cyprinid Herpesvirus 3. *J Virol* **2013**, *87* (7), 3998–4004. <https://doi.org/10.1128/JVI.03116-12>.
- (290) Patel, C. V.; Handy, I.; Goldsmith, T.; Patel, R. C. PACT, a Stress-Modulated Cellular Activator of Interferon-Induced Double-Stranded RNA-Activated Protein Kinase, PKR \*. *Journal of Biological Chemistry* **2000**, *275* (48), 37993–37998. <https://doi.org/10.1074/jbc.M004762200>.

## References

- (291) Bennett, R. L.; Blalock, W. L.; May, W. S. Serine 18 Phosphorylation of RAX, the PKR Activator, Is Required for PKR Activation and Consequent Translation Inhibition. *J Biol Chem* **2004**, *279* (41), 42687–42693. <https://doi.org/10.1074/jbc.M403321200>.
- (292) Patel, R. C.; Sen, G. C. PACT, a Protein Activator of the Interferon-Induced Protein Kinase, PKR. *EMBO J* **1998**, *17* (15), 4379–4390. <https://doi.org/10.1093/emboj/17.15.4379>.
- (293) Liu, Y.; Wang, M.; Cheng, A.; Yang, Q.; Wu, Y.; Jia, R.; Liu, M.; Zhu, D.; Chen, S.; Zhang, S.; Zhao, X.-X.; Huang, J.; Mao, S.; Ou, X.; Gao, Q.; Wang, Y.; Xu, Z.; Chen, Z.; Zhu, L.; Luo, Q.; Liu, Y.; Yu, Y.; Zhang, L.; Tian, B.; Pan, L.; Rehman, M. U.; Chen, X. The Role of Host eIF2 $\alpha$  in Viral Infection. *Virology Journal* **2020**, *17* (1), 112. <https://doi.org/10.1186/s12985-020-01362-6>.
- (294) Kang, S.; Xu, Z.; Liu, S.; Wu, S.; Chen, H.; Xu, L.; Qin, Q.; Wei, J. Function Analysis of Fish PACT Gene in Response to Virus Infection. *Fish & Shellfish Immunology* **2024**, *144*, 109304. <https://doi.org/10.1016/j.fsi.2023.109304>.
- (295) Barber, G. N.; Tomita, J.; Hovanessian, A. G.; Meurs, E.; Katze, M. G. Functional Expression and Characterization of the Interferon-Induced Double-Stranded RNA Activated P68 Protein Kinase from Escherichia Coli. *Biochemistry* **1991**, *30* (42), 10356–10361. <https://doi.org/10.1021/bi00106a038>.
- (296) Hovanessian, A. G.; Galabru, J. The Double-Stranded RNA-Dependent Protein Kinase Is Also Activated by Heparin. *Eur J Biochem* **1987**, *167* (3), 467–473. <https://doi.org/10.1111/j.1432-1033.1987.tb13360.x>.
- (297) Li, S.; Peters, G. A.; Ding, K.; Zhang, X.; Qin, J.; Sen, G. C. Molecular Basis for PKR Activation by PACT or dsRNA. *Proceedings of the National Academy of Sciences* **2006**, *103* (26), 10005–10010. <https://doi.org/10.1073/pnas.0602317103>.
- (298) Srivastava, S. P.; Kumar, K. U.; Kaufman, R. J. Phosphorylation of Eukaryotic Translation Initiation Factor 2 Mediates Apoptosis in Response to Activation of the Double-Stranded RNA-Dependent Protein Kinase \*. *Journal of Biological Chemistry* **1998**, *273* (4), 2416–2423. <https://doi.org/10.1074/jbc.273.4.2416>.
- (299) Saelens, X.; Kalai, M.; Vandenabeele, P. Translation Inhibition in Apoptosis: Caspase-Dependent PKR Activation and eIF2-Alpha Phosphorylation. *J Biol Chem* **2001**, *276* (45), 41620–41628. <https://doi.org/10.1074/jbc.M103674200>.
- (300) Savill, J.; Fadok, V. Corpse Clearance Defines the Meaning of Cell Death. *Nature* **2000**, *407* (6805), 784–788. <https://doi.org/10.1038/35037722>.
- (301) Jackson, R. J.; Hellen, C. U. T.; Pestova, T. V. The Mechanism of Eukaryotic Translation Initiation and Principles of Its Regulation. *Nat Rev Mol Cell Biol* **2010**, *11* (2), 113–127. <https://doi.org/10.1038/nrm2838>.
- (302) Sonenberg, N.; Hinnebusch, A. G. Regulation of Translation Initiation in Eukaryotes: Mechanisms and Biological Targets. *Cell* **2009**, *136* (4), 731–745. <https://doi.org/10.1016/j.cell.2009.01.042>.
- (303) Kaufman, R. J. Double-Stranded RNA-Activated Protein Kinase Mediates Virus-Induced Apoptosis: A New Role for an Old Actor. *Proc Natl Acad Sci U S A* **1999**, *96* (21), 11693–11695.
- (304) Gil, J.; Alcamí, J.; Esteban, M. Induction of Apoptosis by Double-Stranded-RNA-Dependent Protein Kinase (PKR) Involves the Alpha Subunit of Eukaryotic Translation Initiation Factor 2 and NF-kappaB. *Mol Cell Biol* **1999**, *19* (7), 4653–4663. <https://doi.org/10.1128/MCB.19.7.4653>.
- (305) Lee, S. B.; Esteban, M. The Interferon-Induced Double-Stranded RNA-Activated Protein Kinase Induces Apoptosis. *Virology* **1994**, *199* (2), 491–496. <https://doi.org/10.1006/viro.1994.1151>.
- (306) Yeung, M. C.; Liu, J.; Lau, A. S. An Essential Role for the Interferon-Inducible, Double-Stranded RNA-Activated Protein Kinase PKR in the Tumor Necrosis Factor-Induced Apoptosis in U937 Cells. *Proc Natl Acad Sci U S A* **1996**, *93* (22), 12451–12455.
- (307) Der, S. D.; Yang, Y.-L.; Weissmann, C.; Williams, B. R. G. A Double-Stranded RNA-Activated Protein Kinase-Dependent Pathway Mediating Stress-Induced Apoptosis. *Proc Natl Acad Sci U S A* **1997**, *94* (7), 3279–3283.
- (308) Gil, J.; Esteban, M. The Interferon-Induced Protein Kinase (PKR), Triggers Apoptosis through FADD-Mediated Activation of Caspase 8 in a Manner Independent of Fas and TNF- $\alpha$  Receptors. *Oncogene* **2000**, *19* (32), 3665–3674. <https://doi.org/10.1038/sj.onc.1203710>.
- (309) Hsu, L.-C.; Park, J. M.; Zhang, K.; Luo, J.-L.; Maeda, S.; Kaufman, R. J.; Eckmann, L.; Guiney, D. G.; Karin, M. The Protein Kinase PKR Is Required for Macrophage Apoptosis after Activation of Toll-like Receptor 4. *Nature* **2004**, *428* (6980), 341–345. <https://doi.org/10.1038/nature02405>.
- (310) Guerra, S.; López-Fernández, L. A.; García, M. A.; Zaballos, A.; Esteban, M. Human Gene Profiling in Response to the Active Protein Kinase, Interferon-Induced Serine/Threonine Protein Kinase (PKR), in Infected Cells. *Journal of Biological Chemistry* **2006**, *281* (27), 18734–18745. <https://doi.org/10.1074/jbc.M511983200>.
- (311) Balachandran, S.; Kim, C. N.; Yeh, W. C.; Mak, T. W.; Bhalla, K.; Barber, G. N. Activation of the dsRNA-Dependent Protein Kinase, PKR, Induces Apoptosis through FADD-Mediated Death Signaling. *EMBO J* **1998**, *17* (23), 6888–6902. <https://doi.org/10.1093/emboj/17.23.6888>.
- (312) Gil, J.; Esteban, M. Induction of Apoptosis by the dsRNA-Dependent Protein Kinase (PKR): Mechanism of Action. *Apoptosis* **2000**, *5* (2), 107–114. <https://doi.org/10.1023/A:1009664109241>.
- (313) von Roretz, C.; Gallouzi, I.-E. Protein Kinase RNA/FADD/Caspase-8 Pathway Mediates the Proapoptotic Activity of the RNA-Binding Protein Human Antigen R (HuR). *J Biol Chem* **2010**, *285* (22), 16806–16813. <https://doi.org/10.1074/jbc.M109.087320>.
- (314) Gil, J.; García, M. A.; Esteban, M. Caspase 9 Activation by the dsRNA-Dependent Protein Kinase, PKR: Molecular Mechanism and Relevance. *FEBS Lett* **2002**, *529* (2–3), 249–255. [https://doi.org/10.1016/s0014-5793\(02\)03348-3](https://doi.org/10.1016/s0014-5793(02)03348-3).
- (315) Palam, L. R.; Baird, T. D.; Wek, R. C. Phosphorylation of eIF2 Facilitates Ribosomal Bypass of an Inhibitory Upstream ORF to Enhance CHOP Translation. *J Biol Chem* **2011**, *286* (13), 10939–10949. <https://doi.org/10.1074/jbc.M110.216093>.
- (316) Lu, P. D.; Harding, H. P.; Ron, D. Translation Reinitiation at Alternative Open Reading Frames Regulates Gene Expression in an Integrated Stress Response. *J Cell Biol* **2004**, *167* (1), 27–33. <https://doi.org/10.1083/jcb.200408003>.
- (317) Jiang, H.-Y.; Wek, S. A.; McGrath, B. C.; Lu, D.; Hai, T.; Harding, H. P.; Wang, X.; Ron, D.; Cavener, D. R.; Wek, R. C. Activating Transcription Factor 3 Is Integral to the Eukaryotic Initiation Factor 2 Kinase Stress Response. *Mol Cell Biol* **2004**, *24* (3), 1365–1377. <https://doi.org/10.1128/MCB.24.3.1365-1377.2004>.
- (318) Hu, H.; Tian, M.; Ding, C.; Yu, S. The C/EBP Homologous Protein (CHOP) Transcription Factor Functions in Endoplasmic Reticulum Stress-Induced Apoptosis and Microbial Infection. *Frontiers in Immunology* **2019**, *9*.

## References

- (319) Hua, B.; Tamamori-Adachi, M.; Luo, Y.; Tamura, K.; Morioka, M.; Fukuda, M.; Tanaka, Y.; Kitajima, S. A Splice Variant of Stress Response Gene ATF3 Counteracts NF- $\kappa$ B-Dependent Anti-Apoptosis through Inhibiting Recruitment of CREB-Binding Protein/P300 Coactivator\*. *Journal of Biological Chemistry* **2006**, *281* (3), 1620–1629. <https://doi.org/10.1074/jbc.M508471200>.
- (320) Liao, Y.; Fung, T. S.; Huang, M.; Fang, S. G.; Zhong, Y.; Liu, D. X. Upregulation of CHOP/GADD153 during Coronavirus Infectious Bronchitis Virus Infection Modulates Apoptosis by Restricting Activation of the Extracellular Signal-Regulated Kinase Pathway. *J Virol* **2013**, *87* (14), 8124–8134. <https://doi.org/10.1128/JVI.00626-13>.
- (321) Yuan, X.; Wu, H.; Gao, J.; Geng, X.; Xie, M.; Song, R.; Zheng, J.; Wu, Y.; Ou, D. Acute Deltamethrin Exposure Induces Oxidative Stress, Triggers Endoplasmic Reticulum Stress, and Impairs Hypoxic Resistance of Crucian Carp. *Comparative Biochemistry and Physiology Part C: Toxicology & Pharmacology* **2023**, *263*, 109508. <https://doi.org/10.1016/j.cbpc.2022.109508>.
- (322) Komoike, Y.; Matsuoka, M. Endoplasmic Reticulum Stress-Mediated Neuronal Apoptosis by Acrylamide Exposure. *Toxicol Appl Pharmacol* **2016**, *310*, 68–77. <https://doi.org/10.1016/j.taap.2016.09.005>.
- (323) Komoike, Y.; Matsuoka, M. Exposure to Tributyltin Induces Endoplasmic Reticulum Stress and the Unfolded Protein Response in Zebrafish. *Aquat Toxicol* **2013**, *142–143*, 221–229. <https://doi.org/10.1016/j.aquatox.2013.08.017>.
- (324) Xia, T.; Liao, Y.-Q.; Li, L.; Sun, L.-Y.; Ding, N.-S.; Wu, Y.-L.; Lu, K.-L. 4-PBA Attenuates Fat Accumulation in Cultured Spotted Seabass Fed High-Fat-Diet via Regulating Endoplasmic Reticulum Stress. *Metabolites* **2022**, *12* (12), 1197. <https://doi.org/10.3390/metabo12121197>.
- (325) Tsuchiya, Y.; Nakabayashi, O.; Nakano, H. FLIP the Switch: Regulation of Apoptosis and Necroptosis by cFLIP. *International Journal of Molecular Sciences* **2015**, *16* (12), 30321–30341. <https://doi.org/10.3390/ijms161226232>.
- (326) Sakamaki, K.; Iwabe, N.; Iwata, H.; Imai, K.; Takagi, C.; Chiba, K.; Shukunami, C.; Tomii, K.; Ueno, N. Conservation of Structure and Function in Vertebrate C-FLIP Proteins despite Rapid Evolutionary Change. *Biochem Biophys Res* **2015**, *3*, 175–189. <https://doi.org/10.1016/j.bbrep.2015.08.005>.
- (327) Grilli, M.; Chiu, J. J.; Lenardo, M. J. NF-Kappa B and Rel: Participants in a Multifunctional Transcriptional Regulatory System. *Int Rev Cytol* **1993**, *143*, 1–62. [https://doi.org/10.1016/s0074-7696\(08\)61873-2](https://doi.org/10.1016/s0074-7696(08)61873-2).
- (328) Kaltschmidt, B.; Kaltschmidt, C.; Hofmann, T. G.; Hehner, S. P.; Dröge, W.; Schmitz, M. L. The Pro- or Anti-Apoptotic Function of NF-kappaB Is Determined by the Nature of the Apoptotic Stimulus. *Eur J Biochem* **2000**, *267* (12), 3828–3835. <https://doi.org/10.1046/j.1432-1327.2000.01421.x>.
- (329) Tak, P. P.; Firestein, G. S. NF- $\kappa$ B: A Key Role in Inflammatory Diseases. *J Clin Invest* **2001**, *107* (1), 7–11.
- (330) Cuddihy, A. R.; Li, S.; Tam, N. W. N.; Wong, A. H.-T.; Taya, Y.; Abraham, N.; Bell, J. C.; Koromilas, A. E. Double-Stranded-RNA-Activated Protein Kinase PKR Enhances Transcriptional Activation by Tumor Suppressor P53. *Mol Cell Biol* **1999**, *19* (4), 2475–2484.
- (331) Bennett, R. L.; Pan, Y.; Christian, J.; Hui, T.; May, W. S. The RAX/PACT-PKR Stress Response Pathway Promotes P53 Sumoylation and Activation, Leading to G1 Arrest. *Cell Cycle* **2012**, *11* (2), 407–417. <https://doi.org/10.4161/cc.11.2.18999>.
- (332) Cuddihy, A. R.; Hoi-Tao Wong, A.; Wai Ning Tam, N.; Li, S.; Koromilas, A. E. The Double-Stranded RNA Activated Protein Kinase PKR Physically Associates with the Tumor Suppressor P53 Protein and Phosphorylates Human P53 on Serine 392 in Vitro. *Oncogene* **1999**, *18* (17), 2690–2702. <https://doi.org/10.1038/sj.onc.1202620>.
- (333) Aubrey, B. J.; Kelly, G. L.; Janic, A.; Herold, M. J.; Strasser, A. How Does P53 Induce Apoptosis and How Does This Relate to P53-Mediated Tumour Suppression? *Cell Death Differ* **2018**, *25* (1), 104–113. <https://doi.org/10.1038/cdd.2017.169>.
- (334) Aloni-Grinstein, R.; Charni-Natan, M.; Solomon, H.; Rotter, V. P53 and the Viral Connection: Back into the Future. *Cancers (Basel)* **2018**, *10* (6), 178. <https://doi.org/10.3390/cancers10060178>.
- (335) Rivas, C.; Aaronson, S. A.; Munoz-Fontela, C. Dual Role of P53 in Innate Antiviral Immunity. *Viruses* **2010**, *2* (1), 298–313. <https://doi.org/10.3390/v2010298>.
- (336) Morrison, D. K. MAP Kinase Pathways. *Cold Spring Harb Perspect Biol* **2012**, *4* (11), a011254. <https://doi.org/10.1101/cshperspect.a011254>.
- (337) Kumar, R.; Khandelwal, N.; Thachamvally, R.; Tripathi, B. N.; Barua, S.; Kashyap, S. K.; Maherchandani, S.; Kumar, N. Role of MAPK/MNK1 Signaling in Virus Replication. *Virus Res* **2018**, *253*, 48–61. <https://doi.org/10.1016/j.virusres.2018.05.028>.
- (338) Taghavi, N.; Samuel, C. E. Protein Kinase PKR Catalytic Activity Is Required for the PKR-Dependent Activation of Mitogen-Activated Protein Kinases and Amplification of Interferon Beta Induction Following Virus Infection. *Virology* **2012**, *427* (2), 208–216. <https://doi.org/10.1016/j.virol.2012.01.029>.
- (339) Zhang, P.; Langland, J. O.; Jacobs, B. L.; Samuel, C. E. Protein Kinase PKR-Dependent Activation of Mitogen-Activated Protein Kinases Occurs through Mitochondrial Adapter IPS-1 and Is Antagonized by Vaccinia Virus E3L. *J Virol* **2009**, *83* (11), 5718–5725. <https://doi.org/10.1128/JVI.00224-09>.
- (340) Silva, A. M.; Whitmore, M.; Xu, Z.; Jiang, Z.; Li, X.; Williams, B. R. G. Protein Kinase R (PKR) Interacts with and Activates Mitogen-Activated Protein Kinase Kinase 6 (MKK6) in Response to Double-Stranded RNA Stimulation. *J Biol Chem* **2004**, *279* (36), 37670–37676. <https://doi.org/10.1074/jbc.M406554200>.
- (341) Iordanov, M. S.; Paranjape, J. M.; Zhou, A.; Wong, J.; Williams, B. R. G.; Meurs, E. F.; Silverman, R. H.; Magun, B. E. Activation of P38 Mitogen-Activated Protein Kinase and c-Jun NH2-Terminal Kinase by Double-Stranded RNA and Encephalomyocarditis Virus: Involvement of RNase L, Protein Kinase R, and Alternative Pathways. *Mol Cell Biol* **2000**, *20* (2), 617–627.
- (342) Kumar, A.; Yang, Y. L.; Flati, V.; Der, S.; Kadereit, S.; Deb, A.; Haque, J.; Reis, L.; Weissmann, C.; Williams, B. R. Deficient Cytokine Signaling in Mouse Embryo Fibroblasts with a Targeted Deletion in the PKR Gene: Role of IRF-1 and NF-kappaB. *EMBO J* **1997**, *16* (2), 406–416. <https://doi.org/10.1093/emboj/16.2.406>.
- (343) McAllister, C. S.; Toth, A. M.; Zhang, P.; Devaux, P.; Cattaneo, R.; Samuel, C. E. Mechanisms of Protein Kinase PKR-Mediated Amplification of Beta Interferon Induction by C Protein-Deficient Measles Virus. *J Virol* **2010**, *84* (1), 380–386. <https://doi.org/10.1128/JVI.02630-08>.
- (344) McAllister, C. S.; Samuel, C. E. The RNA-Activated Protein Kinase Enhances the Induction of Interferon- $\beta$  and Apoptosis Mediated by Cytoplasmic RNA Sensors. *J Biol Chem* **2009**, *284* (3), 1644–1651. <https://doi.org/10.1074/jbc.M807888200>.

## References

- (345) Kumar, A.; Haque, J.; Lacoste, J.; Hiscott, J.; Williams, B. R. Double-Stranded RNA-Dependent Protein Kinase Activates Transcription Factor NF-Kappa B by Phosphorylating I Kappa B. *Proc Natl Acad Sci U S A* **1994**, *91* (14), 6288–6292.
- (346) Zamanian-Daryoush, M.; Mogensen, T. H.; DiDonato, J. A.; Williams, B. R. G. NF- $\kappa$ B Activation by Double-Stranded-RNA-Activated Protein Kinase (PKR) Is Mediated through NF- $\kappa$ B-Inducing Kinase and I $\kappa$ B Kinase. *Mol Cell Biol* **2000**, *20* (4), 1278–1290.
- (347) Bonnet, M. C.; Weil, R.; Dam, E.; Hovanessian, A. G.; Meurs, E. F. PKR Stimulates NF- $\kappa$ B Irrespective of Its Kinase Function by Interacting with the I $\kappa$ B Kinase Complex. *Mol Cell Biol* **2000**, *20* (13), 4532–4542.
- (348) Gil, J.; Rullas, J.; García, M. A.; Alcamí, J.; Esteban, M. The Catalytic Activity of dsRNA-Dependent Protein Kinase, PKR, Is Required for NF-kappaB Activation. *Oncogene* **2001**, *20* (3), 385–394. <https://doi.org/10.1038/sj.onc.1204109>.
- (349) Ishii, T.; Kwon, H.; Hiscott, J.; Mosialos, G.; Koromilas, A. E. Activation of the I Kappa B Alpha Kinase (IKK) Complex by Double-Stranded RNA-Binding Defective and Catalytic Inactive Mutants of the Interferon-Inducible Protein Kinase PKR. *Oncogene* **2001**, *20* (15), 1900–1912. <https://doi.org/10.1038/sj.onc.1204267>.
- (350) Gil, J.; García, M. A.; Gomez-Puertas, P.; Guerra, S.; Rullas, J.; Nakano, H.; Alcamí, J.; Esteban, M. TRAF Family Proteins Link PKR with NF- $\kappa$ B Activation. *Mol Cell Biol* **2004**, *24* (10), 4502–4512. <https://doi.org/10.1128/MCB.24.10.4502-4512.2004>.
- (351) Gao, L.; Tang, W.; Ding, Z.; Wang, D.; Qi, X.; Wu, H.; Guo, J. Protein-Binding Function of RNA-Dependent Protein Kinase Promotes Proliferation through TRAF2/RIP1/NF- $\kappa$ B/c-Myc Pathway in Pancreatic  $\beta$  Cells. *Mol Med* **2015**, *21* (1), 154–166. <https://doi.org/10.2119/molmed.2014.00235>.
- (352) Fullam, A.; Schröder, M. DEXD/H-Box RNA Helicases as Mediators of Anti-Viral Innate Immunity and Essential Host Factors for Viral Replication. *Biochim Biophys Acta Gene Regul Mech* **2013**, *1829* (8), 854–865. <https://doi.org/10.1016/j.bbagr.2013.03.012>.
- (353) Diebold, S. S.; Montoya, M.; Unger, H.; Alexopoulou, L.; Roy, P.; Haswell, L. E.; Al-Shamkhani, A.; Flavell, R.; Borrow, P.; Reis e Sousa, C. Viral Infection Switches Non-Plasmacytoid Dendritic Cells into High Interferon Producers. *Nature* **2003**, *424* (6946), 324–328. <https://doi.org/10.1038/nature01783>.
- (354) Schulz, O.; Pichlmair, A.; Rehwinkel, J.; Rogers, N. C.; Scheuner, D.; Kato, H.; Takeuchi, O.; Akira, S.; Kaufman, R. J.; Reis e Sousa, C. Protein Kinase R Contributes to Immunity against Specific Viruses by Regulating Interferon mRNA Integrity. *Cell Host Microbe* **2010**, *7* (5), 354–361. <https://doi.org/10.1016/j.chom.2010.04.007>.
- (355) Lee, J. H.; Park, E. J.; Kim, O. S.; Kim, H. Y.; Joe, E.-H.; Jou, I. Double-Stranded RNA-Activated Protein Kinase Is Required for the LPS-Induced Activation of STAT1 Inflammatory Signaling in Rat Brain Glial Cells. *Glia* **2005**, *50* (1), 66–79. <https://doi.org/10.1002/glia.20156>.
- (356) Arnaud, N.; Dabo, S.; Akazawa, D.; Fukasawa, M.; Shinkai-Ouchi, F.; Hugon, J.; Wakita, T.; Meurs, E. F. Hepatitis C Virus Reveals a Novel Early Control in Acute Immune Response. *PLoS Pathog* **2011**, *7* (10), e1002289. <https://doi.org/10.1371/journal.ppat.1002289>.
- (357) Pham, A. M.; Santa Maria, F. G.; Lahiri, T.; Friedman, E.; Marié, I. J.; Levy, D. E. PKR Transduces MDA5-Dependent Signals for Type I IFN Induction. *PLoS Pathog* **2016**, *12* (3), e1005489. <https://doi.org/10.1371/journal.ppat.1005489>.
- (358) Zhang, P.; Samuel, C. E. Induction of Protein Kinase PKR-Dependent Activation of Interferon Regulatory Factor 3 by Vaccinia Virus Occurs through Adapter IPS-1 Signaling. *J Biol Chem* **2008**, *283* (50), 34580–34587. <https://doi.org/10.1074/jbc.M807029200>.
- (359) Zhang, P.; Li, Y.; Xia, J.; He, J.; Pu, J.; Xie, J.; Wu, S.; Feng, L.; Huang, X.; Zhang, P. IPS-1 Plays an Essential Role in dsRNA-Induced Stress Granule Formation by Interacting with PKR and Promoting Its Activation. *J Cell Sci* **2014**, *127* (Pt 11), 2471–2482. <https://doi.org/10.1242/jcs.139626>.
- (360) Yoo, J.-S.; Takahashi, K.; Ng, C. S.; Ouda, R.; Onomoto, K.; Yoneyama, M.; Lai, J. C.; Lattmann, S.; Nagamine, Y.; Matsui, T.; Iwabuchi, K.; Kato, H.; Fujita, T. DHX36 Enhances RIG-I Signaling by Facilitating PKR-Mediated Antiviral Stress Granule Formation. *PLoS Pathog* **2014**, *10* (3), e1004012. <https://doi.org/10.1371/journal.ppat.1004012>.
- (361) Sen, A.; Pruijssers, A. J.; Dermody, T. S.; García-Sastre, A.; Greenberg, H. B. The Early Interferon Response to Rotavirus Is Regulated by PKR and Depends on MAVS/IPS-1, RIG-I, MDA-5, and IRF3. *J Virol* **2011**, *85* (8), 3717–3732. <https://doi.org/10.1128/JVI.02634-10>.
- (362) Fujita, T.; Kimura, Y.; Miyamoto, M.; Barsoumian, E. L.; Taniguchi, T. Induction of Endogenous IFN-Alpha and IFN-Beta Genes by a Regulatory Transcription Factor, IRF-1. *Nature* **1989**, *337* (6204), 270–272. <https://doi.org/10.1038/337270a0>.
- (363) Pflugheber, J.; Fredericksen, B.; Sumpter, R.; Wang, C.; Ware, F.; Sodora, D. L.; Gale, M. Regulation of PKR and IRF-1 during Hepatitis C Virus RNA Replication. *Proc Natl Acad Sci U S A* **2002**, *99* (7), 4650–4655. <https://doi.org/10.1073/pnas.062055699>.
- (364) Chung, H.; Calis, J. J. A.; Wu, X.; Sun, T.; Yu, Y.; Sarbanes, S. L.; Dao Thi, V. L.; Shilvock, A. R.; Hoffmann, H.-H.; Rosenberg, B. R.; Rice, C. M. Human ADAR1 Prevents Endogenous RNA from Triggering Translational Shutdown. *Cell* **2018**, *172* (4), 811–824.e14. <https://doi.org/10.1016/j.cell.2017.12.038>.
- (365) Thomis, D. C.; Samuel, C. E. Mechanism of Interferon Action: Autoregulation of RNA-Dependent P1/eIF-2 Alpha Protein Kinase (PKR) Expression in Transfected Mammalian Cells. *Proc Natl Acad Sci U S A* **1992**, *89* (22), 10837–10841.
- (366) Abraham, N.; Jaramillo, M. L.; Duncan, P. I.; Méthot, N.; Icely, P. L.; Stojdl, D. F.; Barber, G. N.; Bell, J. C. The Murine PKR Tumor Suppressor Gene Is Rearranged in a Lymphocytic Leukemia. *Experimental Cell Research* **1998**, *244* (2), 394–404. <https://doi.org/10.1006/excr.1998.4201>.
- (367) Kawakubo, K.; Kuhnen, K. L.; Vessey, J. W.; George, C. X.; Samuel, C. E. Alternative Splice Variants of the Human PKR Protein Kinase Possessing Different 5'-Untranslated Regions: Expression in Untreated and Interferon-Treated Cells and Translational Activity. *Virology* **1999**, *264* (1), 106–114. <https://doi.org/10.1006/viro.1999.9995>.
- (368) Park, S.-H.; Choi, J.; Kang, J.-I.; Choi, S.-Y.; Hwang, S.-B.; Kim, J.; Ahn, B.-Y. Attenuated Expression of Interferon-Induced Protein Kinase PKR in a Simian Cell Devoid of Type I Interferons. *Molecules and Cells* **2006**, *21* (1), 21–28.
- (369) Li, S.; Koromilas, A. E. Dominant Negative Function by an Alternatively Spliced Form of the Interferon-Inducible Protein Kinase PKR\*. *Journal of Biological Chemistry* **2001**, *276* (17), 13881–13890. <https://doi.org/10.1074/jbc.M008140200>.

## References

- (370) Kimball, S. R.; Horetsky, R. L.; Ron, D.; Jefferson, L. S.; Harding, H. P. Mammalian Stress Granules Represent Sites of Accumulation of Stalled Translation Initiation Complexes. *Am J Physiol Cell Physiol* **2003**, *284* (2), C273-284. <https://doi.org/10.1152/ajpcell.00314.2002>.
- (371) Protter, D. S. W.; Parker, R. Principles and Properties of Stress Granules. *Trends Cell Biol* **2016**, *26* (9), 668–679. <https://doi.org/10.1016/j.tcb.2016.05.004>.
- (372) Hofmann, S.; Kedersha, N.; Anderson, P.; Ivanov, P. Molecular Mechanisms of Stress Granule Assembly and Disassembly. *Biochim Biophys Acta Mol Cell Res* **2021**, *1868* (1), 118876. <https://doi.org/10.1016/j.bbamcr.2020.118876>.
- (373) Miller, C. L. Stress Granules and Virus Replication. *Future Virol* **2011**, *6* (11), 1329–1338. <https://doi.org/10.2217/fvl.11.108>.
- (374) Onomoto, K.; Jogi, M.; Yoo, J.-S.; Narita, R.; Morimoto, S.; Takemura, A.; Sambhara, S.; Kawaguchi, A.; Osari, S.; Nagata, K.; Matsumiya, T.; Namiki, H.; Yoneyama, M.; Fujita, T. Critical Role of an Antiviral Stress Granule Containing RIG-I and PKR in Viral Detection and Innate Immunity. *PLoS One* **2012**, *7* (8), e43031. <https://doi.org/10.1371/journal.pone.0043031>.
- (375) Reineke, L. C.; Lloyd, R. E. The Stress Granule Protein G3BP1 Recruits Protein Kinase R to Promote Multiple Innate Immune Antiviral Responses. *J Virol* **2015**, *89* (5), 2575–2589. <https://doi.org/10.1128/JVI.02791-14>.
- (376) Sun, M.; Wu, S.; Kang, S.; Liao, J.; Zhang, L.; Xu, Z.; Chen, H.; Xu, L.; Zhang, X.; Qin, Q.; Wei, J. Critical Roles of G3BP1 in Red-Spotted Grouper Nervous Necrosis Virus-Induced Stress Granule Formation and Viral Replication in Orange-Spotted Grouper (*Epinephelus Coioides*). *Front Immunol* **2022**, *13*, 931534. <https://doi.org/10.3389/fimmu.2022.931534>.
- (377) Cesaro, T.; Michiels, T. Inhibition of PKR by Viruses. *Front Microbiol* **2021**, *12*, 757238. <https://doi.org/10.3389/fmicb.2021.757238>.
- (378) Fenner, B. J.; Goh, W.; Kwang, J. Sequestration and Protection of Double-Stranded RNA by the Betanodavirus B2 Protein. *J Virol* **2006**, *80* (14), 6822–6833. <https://doi.org/10.1128/JVI.00079-06>.
- (379) Ou, M.-C.; Chen, Y.-M.; Jeng, M.-F.; Chu, C.-J.; Yang, H.-L.; Chen, T.-Y. Identification of Critical Residues in Nervous Necrosis Virus B2 for dsRNA-Binding and RNAi-Inhibiting Activity through by Bioinformatic Analysis and Mutagenesis. *Biochem Biophys Res Commun* **2007**, *361* (3), 634–640. <https://doi.org/10.1016/j.bbrc.2007.07.075>.
- (380) Olsen, C. M.; Markussen, T.; Thiede, B.; Rimstad, E. Infectious Salmon Anaemia Virus (ISAV) RNA Binding Protein Encoded by Segment 8 ORF2 and Its Interaction with ISAV and Intracellular Proteins. *Viruses* **2016**, *8* (2), 52. <https://doi.org/10.3390/v8020052>.
- (381) Song, L.; Wang, H.; Wang, T.; Lu, L. Sequestration of RNA by Grass Carp Ctenopharyngodon Idella TIA1 Is Associated with Its Positive Role in Facilitating Grass Carp Reovirus Infection. *Fish Shellfish Immunol* **2015**, *46* (2), 442–448. <https://doi.org/10.1016/j.fsi.2015.07.018>.
- (382) Rothenburg, S.; Chinchar, V. G.; Dever, T. E. Characterization of a Ranavirus Inhibitor of the Antiviral Protein Kinase PKR. *BMC Microbiol* **2011**, *11*, 56. <https://doi.org/10.1186/1471-2180-11-56>.
- (383) Langland, J. O.; Jacobs, B. L. The Role of the PKR-Inhibitory Genes, E3L and K3L, in Determining Vaccinia Virus Host Range. *Virology* **2002**, *299* (1), 133–141. <https://doi.org/10.1006/viro.2002.1479>.
- (384) Zhu, H.; Cong, J.-P.; Shenk, T. Use of Differential Display Analysis to Assess the Effect of Human Cytomegalovirus Infection on the Accumulation of Cellular RNAs: Induction of Interferon-Responsive RNAs. *Proc Natl Acad Sci U S A* **1997**, *94* (25), 13985–13990.
- (385) Boudinot, P.; Riffault, S.; Salhi, S.; Carrat, C.; Sedlik, C.; Mahmoudi, N.; Charley, B.; Benmansour, A. Vesicular Stomatitis Virus and Pseudorabies Virus Induce a Vig1/Cig5 Homologue in Mouse Dendritic Cells via Different Pathways. *J Gen Virol* **2000**, *81* (Pt 11), 2675–2682. <https://doi.org/10.1099/0022-1317-81-11-2675>.
- (386) Grewal, T. S.; Genever, P. G.; Brabbs, A. C.; Birch, M.; Skerry, T. M. *Best5*: A Novel Interferon-inducible Gene Expressed during Bone Formation. *FASEB j* **2000**, *14* (3), 523–531. <https://doi.org/10.1096/fasebj.14.3.523>.
- (387) Chin, K. C.; Cresswell, P. Viperin (Cig5), an IFN-Inducible Antiviral Protein Directly Induced by Human Cytomegalovirus. *Proc Natl Acad Sci U S A* **2001**, *98* (26), 15125–15130. <https://doi.org/10.1073/pnas.011593298>.
- (388) Sofia, H. J.; Chen, G.; Hetzler, B. G.; Reyes-Spindola, J. F.; Miller, N. E. Radical SAM, a Novel Protein Superfamily Linking Unresolved Steps in Familiar Biosynthetic Pathways with Radical Mechanisms: Functional Characterization Using New Analysis and Information Visualization Methods. *Nucleic Acids Res* **2001**, *29* (5), 1097–1106.
- (389) Oberg, N.; Precord, T. W.; Mitchell, D. A.; Gerlt, J. A. RadicalSAM.Org: A Resource to Interpret Sequence-Function Space and Discover New Radical SAM Enzyme Chemistry. *ACS Bio Med Chem Au* **2022**, *2* (1), 22–35. <https://doi.org/10.1021/acsbiochemau.1c00048>.
- (390) Landgraf, B. J.; McCarthy, E. L.; Booker, S. J. Radical S -Adenosylmethionine Enzymes in Human Health and Disease. *Annu. Rev. Biochem.* **2016**, *85* (1), 485–514. <https://doi.org/10.1146/annurev-biochem-060713-035504>.
- (391) Schwarz, G.; Mendel, R. R. Molybdenum Cofactor Biosynthesis and Molybdenum Enzymes. *Annu Rev Plant Biol* **2006**, *57*, 623–647. <https://doi.org/10.1146/annurev.arplant.57.032905.105437>.
- (392) Cronan, J. E. Assembly of Lipoic Acid on Its Cognate Enzymes: An Extraordinary and Essential Biosynthetic Pathway. *Microbiol Mol Biol Rev* **2016**, *80* (2), 429–450. <https://doi.org/10.1128/MMBR.00073-15>.
- (393) Hunt, R. D. Radical S -Adenosyl Methionine Domain Containing-1 (Rsd1): A Novel Gene Essential for Cell Survival during Vertebrate Development" (2006). Texas Medical Center Dissertations (via ProQuest). AAI3328246., The University of Texas Graduate School of Biomedical Sciences at Houston, 2006. <https://digitalcommons.library.tmc.edu/dissertations/AAI3328246/>.
- (394) Fenwick, M. K.; Li, Y.; Cresswell, P.; Modis, Y.; Ealick, S. E. Structural Studies of Viperin, an Antiviral Radical SAM Enzyme. *Proc Natl Acad Sci U S A* **2017**, *114* (26), 6806–6811. <https://doi.org/10.1073/pnas.1705402114>.
- (395) Rivera-Serrano, E. E.; Gizzi, A. S.; Arnold, J. J.; Grove, T. L.; Almo, S. C.; Cameron, C. E. Viperin Reveals Its True Function. *Annu Rev Virol* **2020**, *7* (1), 421–446. <https://doi.org/10.1146/annurev-virology-011720-095930>.
- (396) Jiang, D.; Guo, H.; Xu, C.; Chang, J.; Gu, B.; Wang, L.; Block, T. M.; Guo, J.-T. Identification of Three Interferon-Inducible Cellular Enzymes That Inhibit the Replication of Hepatitis C Virus. *J Virol* **2008**, *82* (4), 1665–1678. <https://doi.org/10.1128/JVI.02113-07>.
- (397) Milic, N. L.; Davis, S.; Carr, J. M.; Isberg, S.; Beard, M. R.; Helbig, K. J. Sequence Analysis and Characterisation of Virally Induced Viperin in the Saltwater Crocodile (*Crocodylus Porosus*). *Developmental & Comparative Immunology* **2015**, *51* (1), 108–115. <https://doi.org/10.1016/j.dci.2015.03.001>.

## References

- (398) Shah, M.; Bharadwaj, M. S. K.; Gupta, A.; Kumar, R.; Kumar, S. Chicken Viperin Inhibits Newcastle Disease Virus Infection *in Vitro*: A Possible Interaction with the Viral Matrix Protein. *Cytokine* **2019**, *120*, 28–40. <https://doi.org/10.1016/j.cyto.2019.04.007>.
- (399) Shanaka, K. a. S. N.; Jung, S.; Madushani, K. P.; Wijerathna, H. M. S. M.; Neranjan Tharuka, M. D.; Kim, M.-J.; Lee, J. Generation of Viperin-Knockout Zebrafish by CRISPR/Cas9-Mediated Genome Engineering and the Effect of This Mutation under VHSV Infection. *Fish Shellfish Immunol* **2022**, *131*, 672–681. <https://doi.org/10.1016/j.fsi.2022.10.040>.
- (400) Fenwick, M. K.; Su, D.; Dong, M.; Lin, H.; Ealick, S. E. Structural Basis of the Substrate Selectivity of Viperin. *Biochemistry* **2020**, *59* (5), 652–662. <https://doi.org/10.1021/acs.biochem.9b00741>.
- (401) Eslamloo, K.; Ghorbani, A.; Xue, X.; Inkpen, S. M.; Larijani, M.; Rise, M. L. Characterization and Transcript Expression Analyses of Atlantic Cod Viperin. *Front Immunol* **2019**, *10*, 311. <https://doi.org/10.3389/fimmu.2019.00311>.
- (402) Wang, B.; Zhang, Y.-B.; Liu, T.-K.; Gui, J.-F. Sequence Analysis and Subcellular Localization of Crucian Carp *Carassius Auratus* Viperin. *Fish & Shellfish Immunology* **2014**, *39* (2), 168–177. <https://doi.org/10.1016/j.fsi.2014.04.025>.
- (403) McMahon, H. T.; Gallop, J. L. Membrane Curvature and Mechanisms of Dynamic Cell Membrane Remodelling. *Nature* **2005**, *438* (7068), 590–596. <https://doi.org/10.1038/nature04396>.
- (404) Helbig, K. J.; Eyre, N. S.; Yip, E.; Narayana, S.; Li, K.; Fiches, G.; McCartney, E. M.; Jangra, R. K.; Lemon, S. M.; Beard, M. R. The Antiviral Protein Viperin Inhibits Hepatitis C Virus Replication via Interaction with Nonstructural Protein 5A. *Hepatology* **2011**, *54* (5), 1506–1517. <https://doi.org/10.1002/hep.24542>.
- (405) Hinson, E. R.; Cresswell, P. The N-Terminal Amphipathic  $\alpha$ -Helix of Viperin Mediates Localization to the Cytosolic Face of the Endoplasmic Reticulum and Inhibits Protein Secretion. *Journal of Biological Chemistry* **2009**, *284* (7), 4705–4712. <https://doi.org/10.1074/jbc.M807261200>.
- (406) Hinson, E. R.; Cresswell, P. The Antiviral Protein, Viperin, Localizes to Lipid Droplets via Its N-Terminal Amphipathic Alpha-Helix. *Proc Natl Acad Sci U S A* **2009**, *106* (48), 20452–20457. <https://doi.org/10.1073/pnas.0911679106>.
- (407) Helbig, K. J.; Carr, J. M.; Calvert, J. K.; Wati, S.; Clarke, J. N.; Eyre, N. S.; Narayana, S. K.; Fiches, G. N.; McCartney, E. M.; Beard, M. R. Viperin Is Induced Following Dengue Virus Type-2 (DENV-2) Infection and Has Anti-Viral Actions Requiring the C-Terminal End of Viperin. *PLoS Negl Trop Dis* **2013**, *7* (4), e2178. <https://doi.org/10.1371/journal.pntd.0002178>.
- (408) Upadhyay, A. S.; Vonderstein, K.; Pichlmair, A.; Stehling, O.; Bennett, K. L.; Dobler, G.; Guo, J.-T.; Superti-Furga, G.; Lill, R.; Överby, A. K.; Weber, F. Viperin Is an Iron-Sulfur Protein That Inhibits Genome Synthesis of Tick-Borne Encephalitis Virus via Radical SAM Domain Activity. *Cell Microbiol* **2014**, *16* (6), 834–848. <https://doi.org/10.1111/cmi.12241>.
- (409) Fang, J.; Wang, H.; Bai, J.; Zhang, Q.; Li, Y.; Liu, F.; Jiang, P. Monkey Viperin Restricts Porcine Reproductive and Respiratory Syndrome Virus Replication. *PLoS One* **2016**, *11* (5), e0156513. <https://doi.org/10.1371/journal.pone.0156513>.
- (410) Van der Hoek, K. H.; Eyre, N. S.; Shue, B.; Khantisithiporn, O.; Glab-Ampi, K.; Carr, J. M.; Gartner, M. J.; Jolly, L. A.; Thomas, P. Q.; Adikusuma, F.; Jankovic-Karasoulos, T.; Roberts, C. T.; Helbig, K. J.; Beard, M. R. Viperin Is an Important Host Restriction Factor in Control of Zika Virus Infection. *Sci Rep* **2017**, *7*, 4475. <https://doi.org/10.1038/s41598-017-04138-1>.
- (411) Teng, T.-S.; Foo, S.-S.; Simamarta, D.; Lum, F.-M.; Teo, T.-H.; Lulla, A.; Yeo, N. K. W.; Koh, E. G. L.; Chow, A.; Leo, Y.-S.; Merits, A.; Chin, K.-C.; Ng, L. F. P. Viperin Restricts Chikungunya Virus Replication and Pathology. *J Clin Invest* **2012**, *122* (12), 4447–4460. <https://doi.org/10.1172/JCI63120>.
- (412) Tharuka, M. D. N.; Priyathilaka, T. T.; Yang, H.; Pavithiran, A.; Lee, J. Molecular and Transcriptional Insights into Viperin Protein from Big-Belly Seahorse (*Hippocampus abdominalis*), and Its Potential Antiviral Role. *Fish & Shellfish Immunology* **2019**, *86*, 599–607. <https://doi.org/10.1016/j.fsi.2018.12.006>.
- (413) Mou, C.-Y.; Li, S.; Lu, L.-F.; Wang, Y.; Yu, P.; Li, Z.; Tong, J.-F.; Zhang, Q.-Y.; Wang, Z.-W.; Zhang, X.-J.; Wang, G.-X.; Zhou, L.; Gui, J.-F. Divergent Antiviral Mechanisms of Two Viperin Homeologs in a Recurrent Polyploid Fish. *Front Immunol* **2021**, *12*, 702971. <https://doi.org/10.3389/fimmu.2021.702971>.
- (414) Duschene, K. S.; Broderick, J. B. The Antiviral Protein Viperin Is a Radical SAM Enzyme. *FEBS Lett* **2010**, *584* (6), 1263–1267. <https://doi.org/10.1016/j.febslet.2010.02.041>.
- (415) Shaveta, G.; Shi, J.; Chow, V. T. K.; Song, J. Structural Characterization Reveals That Viperin Is a Radical S-Adenosyl-L-Methionine (SAM) Enzyme. *Biochem Biophys Res Commun* **2010**, *391* (3), 1390–1395. <https://doi.org/10.1016/j.bbrc.2009.12.070>.
- (416) Lachowicz, J. C.; Gizzi, A. S.; Almo, S. C.; Grove, T. L. Structural Insight into the Substrate Scope of Viperin and Viperin-like Enzymes from Three Domains of Life. *Biochemistry* **2021**, *60* (26), 2116–2129. <https://doi.org/10.1021/acs.biochem.0c00958>.
- (417) Lu, X.; Yi, M.; Hu, Z.; Yang, T.; Zhang, W.; Marsh, E. N. G.; Jia, K. Feedback Loop Regulation between Viperin and Viral Hemorrhagic Septicemia Virus through Competing Protein Degradation Pathways. *bioRxiv* **2024**, 2024.01.09.574905. <https://doi.org/10.1101/2024.01.09.574905>.
- (418) Seo, J.-Y.; Yaneva, R.; Cresswell, P. Viperin: A Multifunctional, Interferon-Inducible Protein That Regulates Virus Replication. *Cell Host Microbe* **2011**, *10* (6), 534–539. <https://doi.org/10.1016/j.chom.2011.11.004>.
- (419) Upadhyay, A. S.; Stehling, O.; Panayiotou, C.; Rösser, R.; Lill, R.; Överby, A. K. Cellular Requirements for Iron–Sulfur Cluster Insertion into the Antiviral Radical SAM Protein Viperin. *J Biol Chem* **2017**, *292* (33), 13879–13889. <https://doi.org/10.1074/jbc.M117.780122>.
- (420) Haldar, S.; Paul, S.; Joshi, N.; Dasgupta, A.; Chattopadhyay, K. The Presence of the Iron-Sulfur Motif Is Important for the Conformational Stability of the Antiviral Protein, Viperin. *PLoS One* **2012**, *7* (2), e31797. <https://doi.org/10.1371/journal.pone.0031797>.
- (421) Broderick, J. B.; Duffus, B. R.; Duschene, K. S.; Shepard, E. M. Radical S-Adenosylmethionine Enzymes. *Chem. Rev.* **2014**, *114* (8), 4229–4317. <https://doi.org/10.1021/cr4004709>.
- (422) Makins, C.; Ghosh, S.; Román-Meléndez, G. D.; Malec, P. A.; Kennedy, R. T.; Marsh, E. N. G. Does Viperin Function as a Radical S-Adenosyl-L-Methionine-Dependent Enzyme in Regulating Farnesylpyrophosphate Synthase Expression and Activity? *J Biol Chem* **2016**, *291* (52), 26806–26815. <https://doi.org/10.1074/jbc.M116.751040>.

## References

- (423) Patel, A. M.; Koebke, K. J.; Grunkemeyer, T. J.; Riordan, C. M.; Kim, Y.; Bailey, R. C.; Marsh, E. N. G. Purification of the Full-Length, Membrane-Associated Form of the Antiviral Enzyme Viperin Utilizing Nanodiscs. *Sci Rep* **2022**, *12*, 11909. <https://doi.org/10.1038/s41598-022-16233-z>.
- (424) Kambara, H.; Niazi, F.; Kostadinova, L.; Moonka, D. K.; Siegel, C. T.; Post, A. B.; Carnero, E.; Barriocanal, M.; Fortes, P.; Anthony, D. D.; Valadkhan, S. Negative Regulation of the Interferon Response by an Interferon-Induced Long Non-Coding RNA. *Nucleic Acids Res* **2014**, *42* (16), 10668–10680. <https://doi.org/10.1093/nar/gku713>.
- (425) Hover, B. M.; Lokszejn, A.; Ribeiro, A. A.; Yokoyama, K. Identification of a Cyclic Nucleotide as a Cryptic Intermediate in Molybdenum Cofactor Biosynthesis. *J Am Chem Soc* **2013**, *135* (18), 7019–7032. <https://doi.org/10.1021/ja401781t>.
- (426) Grunkemeyer, T. J.; Ghosh, S.; Patel, A. M.; Sajja, K.; Windak, J.; Basrur, V.; Kim, Y.; Nesvizhskii, A. I.; Kennedy, R. T.; Marsh, E. N. G. The Antiviral Enzyme Viperin Inhibits Cholesterol Biosynthesis. *Journal of Biological Chemistry* **2021**, *297* (1). <https://doi.org/10.1016/j.jbc.2021.100824>.
- (427) Zhang, Y.-B.; Jiang, J.; Chen, Y.-D.; Zhu, R.; Shi, Y.; Zhang, Q.-Y.; Gui, J.-F. The Innate Immune Response to Grass Carp Hemorrhagic Virus (GCHV) in Cultured Carassius Auratus Blastulae (CAB) Cells. *Dev Comp Immunol* **2007**, *31* (3), 232–243. <https://doi.org/10.1016/j.dci.2006.05.015>.
- (428) Sun, B. J.; Nie, P. Molecular Cloning of the Viperin Gene and Its Promoter Region from the Mandarin Fish Siniperca Chuatsi. *Veterinary Immunology and Immunopathology* **2004**, *101* (3–4), 161–170. <https://doi.org/10.1016/j.vetimm.2004.04.013>.
- (429) Lee, S.-H.; Peng, K.-C.; Lee, L.-H.; Pan, C.-Y.; Hour, A.-L.; Her, G. M.; Hui, C.-F.; Chen, J.-Y. Characterization of Tilapia (*Oreochromis Niloticus*) Viperin Expression, and Inhibition of Bacterial Growth and Modulation of Immune-Related Gene Expression by Electroporation of Viperin DNA into Zebrafish Muscle. *Veterinary Immunology and Immunopathology* **2013**, *151* (3–4), 217–228. <https://doi.org/10.1016/j.vetimm.2012.11.010>.
- (430) Zhang, Y.; Lv, S.; Zheng, J.; Huang, X.; Huang, Y.; Qin, Q. Grouper Viperin Acts as a Crucial Antiviral Molecule against Iridovirus. *Fish Shellfish Immunol* **2019**, *86*, 1026–1034. <https://doi.org/10.1016/j.fsi.2018.12.038>.
- (431) Lei, M.; Liu, H.; Liu, S.; Zhang, Y.; Zhang, S. Identification and Functional Characterization of Viperin of Amphioxus Branchiostoma Japonicum: Implications for Ancient Origin of Viperin-Mediated Antiviral Response. *Developmental & Comparative Immunology* **2015**, *53* (2), 293–302. <https://doi.org/10.1016/j.dci.2015.07.008>.
- (432) Lewandowska, M.; Sharoni, T.; Admoni, Y.; Aharoni, R.; Moran, Y. Functional Characterization of the Cnidarian Antiviral Immune Response Reveals Ancestral Complexity. *Mol Biol Evol* **2021**, *38* (10), 4546–4561. <https://doi.org/10.1093/molbev/msab197>.
- (433) Green, T. J.; Speck, P.; Geng, L.; Raftos, D.; Beard, M. R.; Helbig, K. J. Oyster Viperin Retains Direct Antiviral Activity and Its Transcription Occurs via a Signalling Pathway Involving a Heat-Stable Haemolymph Protein. *J Gen Virol* **2015**, *96* (12), 3587–3597. <https://doi.org/10.1099/jgv.0.000300>.
- (434) Chakravarti, A.; Selvadurai, K.; Shahoei, R.; Lee, H.; Fatma, S.; Tajkhorshid, E.; Huang, R. H. Reconstitution and Substrate Specificity for Isopentenyl Pyrophosphate of the Antiviral Radical SAM Enzyme Viperin. *J Biol Chem* **2018**, *293* (36), 14122–14133. <https://doi.org/10.1074/jbc.RA118.003998>.
- (435) Bernheim, A.; Millman, A.; Ofir, G.; Meitav, G.; Avraham, C.; Shomar, H.; Rosenberg, M. M.; Tal, N.; Melamed, S.; Amitai, G.; Sorek, R. Prokaryotic Viperins Produce Diverse Antiviral Molecules. *Nature* **2021**, *589* (7840), 120–124. <https://doi.org/10.1038/s41586-020-2762-2>.
- (436) Honarmand Ebrahimi, K.; Rowbotham, J. S.; McCullagh, J.; James, W. S. Mechanism of Diol Dehydration by a Promiscuous Radical-SAM Enzyme Homologue of the Antiviral Enzyme Viperin (RSAD2). *ChemBiochem* **2020**, *21* (11), 1605–1612. <https://doi.org/10.1002/cbic.201900776>.
- (437) Honarmand Ebrahimi, K.; Carr, S. B.; McCullagh, J.; Wickens, J.; Rees, N. H.; Cantley, J.; Armstrong, F. A. The Radical-SAM Enzyme Viperin Catalyzes Reductive Addition of a 5'-Deoxyadenosyl Radical to UDP-Glucose in Vitro. *FEBS Lett* **2017**, *591* (16), 2394–2405. <https://doi.org/10.1002/1873-3468.12769>.
- (438) Dukhovny, A.; Shlomai, A.; Sklan, E. H. The Antiviral Protein Viperin Suppresses T7 Promoter Dependent RNA Synthesis—Possible Implications for Its Antiviral Activity. *Sci Rep* **2018**, *8* (1), 8100. <https://doi.org/10.1038/s41598-018-26516-z>.
- (439) Eom, J.; Kim, J. J.; Yoon, S. G.; Jeong, H.; Son, S.; Lee, J. B.; Yoo, J.; Seo, H. J.; Cho, Y.; Kim, K. S.; Choi, K. M.; Kim, I. Y.; Lee, H.-Y.; Nam, K. T.; Cresswell, P.; Seong, J. K.; Seo, J.-Y. Intrinsic Expression of Viperin Regulates Thermogenesis in Adipose Tissues. *Proc Natl Acad Sci U S A* **2019**, *116* (35), 17419–17428. <https://doi.org/10.1073/pnas.1904480116>.
- (440) Saitoh, T.; Satoh, T.; Yamamoto, N.; Uematsu, S.; Takeuchi, O.; Kawai, T.; Akira, S. Antiviral Protein Viperin Promotes Toll-like Receptor 7- and Toll-like Receptor 9-Mediated Type I Interferon Production in Plasmacytoid Dendritic Cells. *Immunity* **2011**, *34* (3), 352–363. <https://doi.org/10.1016/j.immuni.2011.03.010>.
- (441) Helbig, K. J.; Teh, M. Y.; Crosse, K. M.; Monson, E. A.; Smith, M.; Tran, E. N.; Standish, A. J.; Morona, R.; Beard, M. R. The Interferon Stimulated Gene Viperin, Restricts Shigella. Flexneri in Vitro. *Sci Rep* **2019**, *9* (1), 15598. <https://doi.org/10.1038/s41598-019-52130-8>.
- (442) Zhou, X.; Xu, H.; Li, Q.; Wang, Q.; Liu, H.; Huang, Y.; Liang, Y.; Lie, L.; Han, Z.; Chen, Y.; Huang, Y.; Zhou, W.; Wen, Q.; Zhou, C.; Hu, S.; Ma, L. Viperin Deficiency Promotes Dendritic Cell Activation and Function via NF-kappaB Activation during Mycobacterium Tuberculosis Infection. *Inflamm Res* **2023**, *72* (1), 27–41. <https://doi.org/10.1007/s00011-022-01638-3>.
- (443) Mattijssen, S.; Hinson, E. R.; Onnekink, C.; Hermanns, P.; Zabel, B.; Cresswell, P.; Puijijn, G. J. M. Viperin mRNA Is a Novel Target for the Human RNase MRP/RNase P Endoribonuclease. *Cell Mol Life Sci* **2011**, *68* (14), 2469–2480. <https://doi.org/10.1007/s00018-010-0568-3>.
- (444) Wang, X.; Hinson, E. R.; Cresswell, P. The Interferon-Inducible Protein Viperin Inhibits Influenza Virus Release by Perturbing Lipid Rafts. *Cell Host & Microbe* **2007**, *2* (2), 96–105. <https://doi.org/10.1016/j.chom.2007.06.009>.
- (445) Wang, B.; Zhang, Y.-B.; Liu, T.-K.; Shi, J.; Sun, F.; Gui, J.-F. Fish Viperin Exerts a Conserved Antiviral Function through RLR-Triggered IFN Signaling Pathway. *Developmental & Comparative Immunology* **2014**, *47* (1), 140–149. <https://doi.org/10.1016/j.dci.2014.07.006>.
- (446) Shanaka, K. a. S. N.; Jung, S.; Madushani, K. P.; Kim, M.-J.; Lee, J. Viperin Mutation Is Linked to Immunity, Immune Cell Dynamics, and Metabolic Alteration during VHSV Infection in Zebrafish. *Front Immunol* **2023**, *14*, 1327749. <https://doi.org/10.3389/fimmu.2023.1327749>.

## References

- (447) Wang, F.; Jiao, H.; Liu, W.; Chen, B.; Wang, Y.; Chen, B.; Lu, Y.; Su, J.; Zhang, Y.; Liu, X. The Antiviral Mechanism of Viperin and Its Splice Variant in Spring Viremia of Carp Virus Infected Fathead Minnow Cells. *Fish & Shellfish Immunology* **2019**, *86*, 805–813. <https://doi.org/10.1016/j.fsi.2018.12.012>.
- (448) Gao, Y.; Li, C.; Shi, L.; Wang, F.; Ye, J.; Lu, Y.-A.; Liu, X.-Q. Viperin<sub>sv1</sub> Promotes RIG-I Expression and Suppresses SVCV Replication through Its Radical SAM Domain. *Developmental & Comparative Immunology* **2021**, *123*, 104166. <https://doi.org/10.1016/j.dci.2021.104166>.
- (449) Dang, W.; Zhang, M.; Hu, Y.; Sun, L. Differential Regulation of *Sciaenops Ocellatus* Viperin Expression by Intracellular and Extracellular Bacterial Pathogens. *Fish Shellfish Immunol* **2010**, *29* (2), 264–270. <https://doi.org/10.1016/j.fsi.2010.04.015>.
- (450) Zhang, B.; Zhang, J.; Xiao, Z.; Sun, L. Rock Bream (*Oplegnathus Fasciatus*) Viperin Is a Virus-Responsive Protein That Modulates Innate Immunity and Promotes Resistance against Megalocytivirus Infection. *Developmental & Comparative Immunology* **2014**, *45* (1), 35–42. <https://doi.org/10.1016/j.dci.2014.02.001>.
- (451) Zhang, J.; Liu, C.; Zhao, S.; Guo, S.; Shen, B. Molecular Characterization and Expression Analyses of the Viperin Gene in *Larimichthys Crocea* (Family: Sciaenidae). *Developmental & Comparative Immunology* **2018**, *79*, 59–66. <https://doi.org/10.1016/j.dci.2017.10.013>.
- (452) Raji Sathyan, K.; Premraj, A.; Thavarool Puthiyedathu, S. Antiviral Radical SAM Enzyme Viperin Homologue from Asian Seabass (*Lates Calcarifer*): Molecular Characterisation and Expression Analysis. *Dev Comp Immunol* **2022**, *136*, 104499. <https://doi.org/10.1016/j.dci.2022.104499>.
- (453) Huang, L.; Zhu, X.; Kuang, J.; Li, B.; Yu, Q.; Liu, M.; Li, B.; Guo, H.; Li, P. Molecular and Functional Characterization of Viperin in Golden Pompano, *Trachinotus Ovatus*. *Fish Shellfish Immunol* **2023**, *142*, 109098. <https://doi.org/10.1016/j.fsi.2023.109098>.
- (454) Madushani, K. P.; Shanaka, K. a. S. N.; Yang, H.; Lim, C.; Jeong, T.; Tharuka, M. D. N.; Lee, J. Molecular Characterization, Expression Profile, and Antiviral Activity of Redlip Mullet (*Liza Haematocheila*) Viperin. *Comp Biochem Physiol B Biochem Mol Biol* **2022**, *258*, 110699. <https://doi.org/10.1016/j.cbpb.2021.110699>.
- (455) Shanaka, K. A. S. N.; Tharuka, M. D. N.; Priyathilaka, T. T.; Lee, J. Molecular Characterization and Expression Analysis of Rockfish (*Sebastes Schlegelii*) Viperin, and Its Ability to Enervate RNA Virus Transcription and Replication in Vitro. *Fish & Shellfish Immunology* **2019**, *92*, 655–666. <https://doi.org/10.1016/j.fsi.2019.06.015>.
- (456) Chan, Y.-L.; Chang, T.-H.; Liao, C.-L.; Lin, Y.-L. The Cellular Antiviral Protein Viperin Is Attenuated by Proteasome-Mediated Protein Degradation in Japanese Encephalitis Virus-Infected Cells. *J Virol* **2008**, *82* (21), 10455–10464. <https://doi.org/10.1128/JVI.00438-08>.
- (457) Severa, M.; Coccia, E. M.; Fitzgerald, K. A. Toll-like Receptor-Dependent and -Independent Viperin Gene Expression and Counter-Regulation by PRDI-Binding Factor-1/BLIMP1\*. *Journal of Biological Chemistry* **2006**, *281* (36), 26188–26195. <https://doi.org/10.1074/jbc.M604516200>.
- (458) Duschene, K. S.; Broderick, J. B. Viperin: A Radical Response to Viral Infection. *BioMolecular Concepts* **2012**, *3* (3), 255–266. <https://doi.org/10.1515/bmc-2011-0057>.
- (459) Stirnweiss, A.; Ksienzyk, A.; Klages, K.; Rand, U.; Grashoff, M.; Hauser, H.; Kröger, A. IFN Regulatory Factor-1 Bypasses IFN-Mediated Antiviral Effects through Viperin Gene Induction. *J Immunol* **2010**, *184* (9), 5179–5185. <https://doi.org/10.4049/jimmunol.0902264>.
- (460) Hee, J. S.; Cresswell, P. Viperin Interaction with Mitochondrial Antiviral Signaling Protein (MAVS) Limits Viperin-Mediated Inhibition of the Interferon Response in Macrophages. *PLoS ONE* **2017**, *12* (2), e0172236. <https://doi.org/10.1371/journal.pone.0172236>.
- (461) Seo, J.-Y.; Yaneva, R.; Hinson, E. R.; Cresswell, P. Human Cytomegalovirus Directly Induces the Antiviral Protein Viperin to Enhance Infectivity. *Science* **2011**, *332* (6033), 1093–1097. <https://doi.org/10.1126/science.1202007>.
- (462) Panayiotou, C.; Lindqvist, R.; Kurhade, C.; Vonderstein, K.; Pasto, J.; Edlund, K.; Upadhyay, A. S.; Överby, A. K. Viperin Restricts Zika Virus and Tick-Borne Encephalitis Virus Replication by Targeting NS3 for Proteasomal Degradation. *J Virol* **2018**, *92* (7), e02054-17. <https://doi.org/10.1128/JVI.02054-17>.
- (463) Lim, H. A.; Noh, J. Y.; Jang, S. S.; Kim, M. C.; Moon, S. H.; Kim, H. Y.; Mun, D. Y.; Kim, H. K. Innate Antiviral Responses against Shaan Virus Infection in HEK293, A549 and MARC-145 Cells and Limited Role of Viperin against Shaan Virus Replication. *Heliyon* **2023**, *9* (12), e22597. <https://doi.org/10.1016/j.heliyon.2023.e22597>.
- (464) Gao, Y.; Xiang, Y.-H.; Wang, F.; Ye, J.; Lu, Y.-A.; Ashraf, U.; Liu, X.-Q. The N Protein of Spring Viremia of Carp Virus Promotes the Ubiquitination and Degradation of Viperin<sub>sv1</sub> to Escape from the Fish Innate Immunity. *Aquaculture* **2021**, *538*, 736583. <https://doi.org/10.1016/j.aquaculture.2021.736583>.
- (465) Hsu, J. C.-C.; Laurent-Rolle, M.; Pawlak, J. B.; Xia, H.; Kunte, A.; Hee, J. S.; Lim, J.; Harris, L. D.; Wood, J. M.; Evans, G. B.; Shi, P.-Y.; Grove, T. L.; Almo, S. C.; Cresswell, P. Viperin Triggers Ribosome Collision-Dependent Translation Inhibition to Restrict Viral Replication. *Mol Cell* **2022**, *82* (9), 1631–1642.e6. <https://doi.org/10.1016/j.molcel.2022.02.031>.
- (466) Arnold, J. J.; Smidansky, E. D.; Moustafa, I. M.; Cameron, C. E. Human Mitochondrial RNA Polymerase: Structure–Function, Mechanism and Inhibition. *Biochimica et Biophysica Acta (BBA) - Gene Regulatory Mechanisms* **2012**, *1819* (9), 948–960. <https://doi.org/10.1016/j.bbagr.2012.04.002>.
- (467) Dumbrepatil, A. B.; Zegalia, K. A.; Sajja, K.; Kennedy, R. T.; Marsh, E. N. G. Targeting Viperin to the Mitochondrion Inhibits the Thiolase Activity of the Trifunctional Enzyme Complex. *Journal of Biological Chemistry* **2020**, *295* (9), 2839–2849. <https://doi.org/10.1074/jbc.RA119.011526>.
- (468) Ebrahimi, K. H.; Howie, D.; Rowbotham, J. S.; McCullagh, J.; Armstrong, F. A.; James, W. S. Viperin, through Its Radical-SAM Activity, Depletes Cellular Nucleotide Pools and Interferes with Mitochondrial Metabolism to Inhibit Viral Replication. *FEBS Letters* **2020**, *594* (10), 1624–1630. <https://doi.org/10.1002/1873-3468.13761>.
- (469) Ghosh, S.; Patel, A. M.; Grunkemeyer, T. J.; Dumbrepatil, A. B.; Zegalia, K.; Kennedy, R. T.; Marsh, E. N. G. Interactions between Viperin, Vesicle-Associated Membrane Protein A, and Hepatitis C Virus Protein NS5A Modulate Viperin Activity and NS5A Degradation. *Biochemistry* **2020**, *59* (6), 780–789. <https://doi.org/10.1021/acs.biochem.9b01090>.
- (470) Wang, S.; Wu, X.; Pan, T.; Song, W.; Wang, Y.; Zhang, F.; Yuan, Z. Viperin Inhibits Hepatitis C Virus Replication by Interfering with Binding of NS5A to Host Protein hVAP-33. *J Gen Virol* **2012**, *93* (Pt 1), 83–92. <https://doi.org/10.1099/vir.0.033860-0>.

## References

- (471) Crosse, K. M.; Monson, E. A.; Dumbrepasil, A. B.; Smith, M.; Tseng, Y.-Y.; Van der Hoek, K. H.; Revill, P. A.; Saker, S.; Tschärke, D. C.; G Marsh, E. N.; Beard, M. R.; Helbig, K. J. Viperin Binds STING and Enhances the Type-I Interferon Response Following dsDNA Detection. *Immunology & Cell Biology* **2021**, *99* (4), 373–391. <https://doi.org/10.1111/imcb.12420>.
- (472) Al Shujairi, W.-H.; Kris, L. P.; van der Hoek, K.; Cowell, E.; Bracho-Granado, G.; Woodgate, T.; Beard, M. R.; Carr, J. M. Viperin Is Anti-Viral in Vitro but Is Dispensable for Restricting Dengue Virus Replication or Induction of Innate and Inflammatory Responses in Vivo. *J Gen Virol* **2021**, *102* (10), 001669. <https://doi.org/10.1099/jgv.0.001669>.
- (473) Khantisitthiporn, O.; Shue, B.; Eyre, N. S.; Nash, C. W.; Turnbull, L.; Whitchurch, C. B.; Van der Hoek, K. H.; Helbig, K. J.; Beard, M. R. Viperin Interacts with PEX19 to Mediate Peroxisomal Augmentation of the Innate Antiviral Response. *Life Sci Alliance* **2021**, *4* (7), e202000915. <https://doi.org/10.26508/lsa.202000915>.
- (474) Kim, J. J.; Kim, K. S.; Eom, J.; Lee, J. B.; Seo, J.-Y. Viperin Differentially Induces Interferon-Stimulated Genes in Distinct Cell Types. *Immune Netw* **2019**, *19* (5), e33. <https://doi.org/10.4110/in.2019.19.e33>.
- (475) Dumbrepasil, A. B.; Ghosh, S.; Zegalia, K. A.; Malec, P. A.; Hoff, J. D.; Kennedy, R. T.; Marsh, E. N. G. Viperin Interacts with the Kinase IRAK1 and the E3 Ubiquitin Ligase TRAF6, Coupling Innate Immune Signaling to Antiviral Ribonucleotide Synthesis. *J Biol Chem* **2019**, *294* (17), 6888–6898. <https://doi.org/10.1074/jbc.RA119.007719>.
- (476) Bai, L.; Dong, J.; Liu, Z.; Rao, Y.; Feng, P.; Lan, K. Viperin Catalyzes Methionine Oxidation to Promote Protein Expression and Function of Helicases. *Sci Adv* **2019**, *5* (8), eaax1031. <https://doi.org/10.1126/sciadv.aax1031>.
- (477) Qiu, L.-Q.; Cresswell, P.; Chin, K.-C. Viperin Is Required for Optimal Th2 Responses and T-Cell Receptor-Mediated Activation of NF- $\kappa$ B and AP-1. *Blood* **2009**, *113* (15), 3520–3529. <https://doi.org/10.1182/blood-2008-07-171942>.
- (478) Gao, X.; Gao, L.-F.; Zhang, Y.-N.; Kong, X.-Q.; Jia, S.; Meng, C.-Y. Huc-MSCs-Derived Exosomes Attenuate Neuropathic Pain by Inhibiting Activation of the TLR2/MyD88/NF- $\kappa$ B Signaling Pathway in the Spinal Microglia by Targeting Rsad2. *Int Immunopharmacol* **2023**, *114*, 109505. <https://doi.org/10.1016/j.intimp.2022.109505>.
- (479) Eom, J.; Yoo, J.; Kim, J. J.; Lee, J. B.; Choi, W.; Park, C. G.; Seo, J.-Y. Viperin Deficiency Promotes Polarization of Macrophages and Secretion of M1 and M2 Cytokines. *Immune Netw* **2018**, *18* (4), e32. <https://doi.org/10.4110/in.2018.18.e32>.
- (480) Zhong, Z.; Liang, S.; Sanchez-Lopez, E.; He, F.; Shalapur, S.; Lin, X.; Wong, J.; Ding, S.; Seki, E.; Schnabl, B.; Hevener, A. L.; Greenberg, H. B.; Kisseleva, T.; Karin, M. New Mitochondrial DNA Synthesis Enables NLRP3 Inflammasome Activation. *Nature* **2018**, *560* (7717), 198–203. <https://doi.org/10.1038/s41586-018-0372-z>.
- (481) Tang, H.-B.; Lu, Z.-L.; Wei, X.-K.; Zhong, T.-Z.; Zhong, Y.-Z.; Ouyang, L.-X.; Luo, Y.; Xing, X.-W.; Liao, F.; Peng, K.-K.; Deng, C.-Q.; Minamoto, N.; Luo, T. R. Viperin Inhibits Rabies Virus Replication via Reduced Cholesterol and Sphingomyelin and Is Regulated Upstream by TLR4. *Sci Rep* **2016**, *6*, 30529. <https://doi.org/10.1038/srep30529>.
- (482) Nasr, N.; Maddocks, S.; Turville, S. G.; Harman, A. N.; Woolger, N.; Helbig, K. J.; Wilkinson, J.; Bye, C. R.; Wright, T. K.; Rambukwelle, D.; Donaghy, H.; Beard, M. R.; Cunningham, A. L. HIV-1 Infection of Human Macrophages Directly Induces Viperin Which Inhibits Viral Production. *Blood* **2012**, *120* (4), 778–788. <https://doi.org/10.1182/blood-2012-01-407395>.
- (483) Vonderstein, K.; Nilsson, E.; Hubel, P.; Nygård Skalmann, L.; Upadhyay, A.; Pasto, J.; Pichlmair, A.; Lundmark, R.; Överby, A. K. Viperin Targets Flavivirus Virulence by Inducing Assembly of Noninfectious Capsid Particles. *J Virol* **2017**, *92* (1), e01751-17. <https://doi.org/10.1128/JVI.01751-17>.
- (484) Steinbusch, M. M. F.; Caron, M. M. J.; Surtel, D. A. M.; van den Akker, G. G. H.; van Dijk, P. J.; Friedrich, F.; Zabel, B.; van Rhijn, L. W.; Peffers, M. J.; Welting, T. J. M. The Antiviral Protein Viperin Regulates Chondrogenic Differentiation via CXCL10 Protein Secretion. *J Biol Chem* **2019**, *294* (13), 5121–5136. <https://doi.org/10.1074/jbc.RA119.007356>.
- (485) Komander, D. The Emerging Complexity of Protein Ubiquitination. *Biochem Soc Trans* **2009**, *37* (Pt 5), 937–953. <https://doi.org/10.1042/BST0370937>.
- (486) Yau, R.; Rape, M. The Increasing Complexity of the Ubiquitin Code. *Nat Cell Biol* **2016**, *18* (6), 579–586. <https://doi.org/10.1038/ncb3358>.
- (487) Yuan, Y.; Miao, Y.; Qian, L.; Zhang, Y.; Liu, C.; Liu, J.; Zuo, Y.; Feng, Q.; Guo, T.; Zhang, L.; Chen, X.; Jin, L.; Huang, F.; Zhang, H.; Zhang, W.; Li, W.; Xu, G.; Zheng, H. Targeting UBE4A Revives Viperin Protein in Epithelium to Enhance Host Antiviral Defense. *Molecular Cell* **2020**, *77* (4), 734-747.e7. <https://doi.org/10.1016/j.molcel.2019.11.003>.
- (488) Shen, G.; Wang, S.; Wang, S.; Cai, M.; Li, M.; Zheng, C. Herpes Simplex Virus 1 Counteracts Viperin via Its Virion Host Shutoff Protein UL41. *J Virol* **2014**, *88* (20), 12163–12166. <https://doi.org/10.1128/JVI.01380-14>.
- (489) Seo, J.-Y.; Cresswell, P. Viperin Regulates Cellular Lipid Metabolism during Human Cytomegalovirus Infection. *PLoS Pathog* **2013**, *9* (8), e1003497. <https://doi.org/10.1371/journal.ppat.1003497>.
- (490) Choi, K. M.; Kim, J. J.; Yoo, J.; Kim, K. S.; Gu, Y.; Eom, J.; Jeong, H.; Kim, K.; Nam, K. T.; Park, Y. S.; Chung, J.-Y.; Seo, J.-Y. The Interferon-Inducible Protein Viperin Controls Cancer Metabolic Reprogramming to Enhance Cancer Progression. *J Clin Invest* **2022**, *132* (24), e157302. <https://doi.org/10.1172/JCI157302>.
- (491) Weinstein, A. G.; Godet, I.; Gilkes, D. M. The Rise of Viperin: The Emerging Role of Viperin in Cancer Progression. *J Clin Invest* **2022**, *132* (24), e165907. <https://doi.org/10.1172/JCI165907>.
- (492) Honarmand Ebrahimi, K.; Vowles, J.; Browne, C.; McCullagh, J.; James, W. S. ddhCTP Produced by the Radical-SAM Activity of RSAD2 (Viperin) Inhibits the NAD<sup>+</sup>-Dependent Activity of Enzymes to Modulate Metabolism. *FEBS Lett* **2020**, *594* (10), 1631–1644. <https://doi.org/10.1002/1873-3468.13778>.
- (493) Lee, J. H.; Wood, J. M.; Almo, S. C.; Evans, G. B.; Harris, L. D.; Grove, T. L. Chemoenzymatic Synthesis of 3'-Deoxy-3',4'-Didehydro-Cytidine Triphosphate (ddhCTP). *ACS Bio Med Chem Au* **2023**, *3* (4), 322–326. <https://doi.org/10.1021/acsbiochemau.3c00014>.
- (494) Amanatullah, D. F.; Yamane, S.; Reddi, A. H. Distinct Patterns of Gene Expression in the Superficial, Middle and Deep Zones of Bovine Articular Cartilage. *J Tissue Eng Regen Med* **2014**, *8* (7), 505–514. <https://doi.org/10.1002/term.1543>.
- (495) Liu, C.; Hou, L.; Zhao, Q.; Zhou, W.; Liu, K.; Liu, Q.; Zhou, T.; Xu, B.; Li, P.; Huang, R. The Selected Genes NR6A1, RSAD2-CMPK2, and COL3A1 Contribute to Body Size Variation in Meishan Pigs through Different Patterns. *Journal of Animal Science* **2023**, *101*, skad304. <https://doi.org/10.1093/jas/skad304>.
- (496) Dong, Y.; Song, C.; Wang, Y.; Lei, Z.; Xu, F.; Guan, H.; Chen, A.; Li, F. Inhibition of PRMT5 Suppresses Osteoclast Differentiation and Partially Protects against Ovariectomy-Induced Bone Loss through Downregulation of CXCL10 and RSAD2. *Cell Signal* **2017**, *34*, 55–65. <https://doi.org/10.1016/j.cellsig.2017.03.004>.

## References

- (497) FAO. *The State of World Fisheries and Aquaculture 2022*; FAO, 2022. <https://doi.org/10.4060/cc0461en>.
- (498) Cain, K. The Many Challenges of Disease Management in Aquaculture. *Journal of the World Aquaculture Society* **2022**, *53* (6), 1080–1083. <https://doi.org/10.1111/jwas.12936>.
- (499) World Bank. *Reducing Disease Risks in Aquaculture*; World Bank Report; 88257-GLB; World Bank, 2014.
- (500) Rodger, H. D. Fish Disease Causing Economic Impact in Global Aquaculture. In *Fish Vaccines*; Adams, A., Ed.; Birkhäuser Advances in Infectious Diseases; Springer Basel: Basel, 2016; pp 1–34. [https://doi.org/10.1007/978-3-0348-0980-1\\_1](https://doi.org/10.1007/978-3-0348-0980-1_1).
- (501) Sommerset, I.; Wiik-Nielsen, J.; Moldal, T.; Oliveira, V. H. S. de; Svendsen, J. C.; Haukaas, A.; Brun, E. *Norwegian Fish Health Report 2024*; Norwegian Veterinary Institute Report; #8a/2024; Norwegian Veterinary Institute, 2024.
- (502) Rimstad, E.; Dale, O. B.; Dannevig, B. H.; Falk, K. Infectious Salmon Anaemia. In *Fish Diseases and Disorders*; Viral, Bacterial and Fungal Infections; CAB International, 2011; Vol. 3, pp 143–165.
- (503) Godoy, M. G.; Aedo, A.; Kibenge, M. J.; Groman, D. B.; Yason, C. V.; Grothusen, H.; Lisperguer, A.; Calbucura, M.; Avendaño, F.; Imilán, M.; Jarpa, M.; Kibenge, F. S. First Detection, Isolation and Molecular Characterization of Infectious Salmon Anaemia Virus Associated with Clinical Disease in Farmed Atlantic Salmon (*Salmo Salar*) in Chile. *BMC Vet Res* **2008**, *4* (1), 28. <https://doi.org/10.1186/1746-6148-4-28>.
- (504) Alvia, A.; Kibenge, F.; Forster, J.; Burgos, J. M.; Ibarra, R.; St-Hilaire, S. *The Recovery of the Chilean Salmon Industry*; Global Aquaculture Alliance (GAA), 2012.
- (505) Bandín, I.; Souto, S. Betanodavirus and VER Disease: A 30-Year Research Review. *Pathogens* **2020**, *9* (2), 106. <https://doi.org/10.3390/pathogens9020106>.
- (506) Chen, J.; Toh, X.; Ong, J.; Wang, Y.; Teo, X.-H.; Lee, B.; Wong, P.-S.; Khor, D.; Chong, S.-M.; Chee, D.; Wee, A.; Wang, Y.; Ng, M.-K.; Tan, B.-H.; Huangfu, T. Detection and Characterization of a Novel Marine Birnavirus Isolated from Asian Seabass in Singapore. *Virology Journal* **2019**, *16* (1), 71. <https://doi.org/10.1186/s12985-019-1174-0>.
- (507) Haugland, Ø.; Mikalsen, A. B.; Nilsen, P.; Lindmo, K.; Thu, B. J.; Eliassen, T. M.; Roos, N.; Rode, M.; Evensen, Ø. Cardiomyopathy Syndrome of Atlantic Salmon (*Salmo Salar* L.) Is Caused by a Double-Stranded RNA Virus of the Totiviridae Family. *J Virol* **2011**, *85* (11), 5275–5286. <https://doi.org/10.1128/JVI.02154-10>.
- (508) Kibenge, F. S. Emerging Viruses in Aquaculture. *Current Opinion in Virology* **2019**, *34*, 97–103. <https://doi.org/10.1016/j.coviro.2018.12.008>.
- (509) WOA. Diseases of Fish. In *Aquatic Animal Health Code*; World Organisation for Animal Health, 2023.
- (510) Mugimba, K. K.; Byarugaba, D. K.; Mutoloki, S.; Evensen, Ø.; Munang'andu, H. M. Challenges and Solutions to Viral Diseases of Finfish in Marine Aquaculture. *Pathogens* **2021**, *10* (6), 673. <https://doi.org/10.3390/pathogens10060673>.
- (511) Houston, R. D.; Haley, C. S.; Hamilton, A.; Guy, D. R.; Tinch, A. E.; Taggart, J. B.; McAndrew, B. J.; Bishop, S. C. Major Quantitative Trait Loci Affect Resistance to Infectious Pancreatic Necrosis in Atlantic Salmon (*Salmo Salar*). *Genetics* **2008**, *178* (2), 1109–1115. <https://doi.org/10.1534/genetics.107.082974>.
- (512) Moen, T.; Baranski, M.; Sonesson, A. K.; Kjøglum, S. Confirmation and Fine-Mapping of a Major QTL for Resistance to Infectious Pancreatic Necrosis in Atlantic Salmon (*Salmo Salar*): Population-Level Associations between Markers and Trait. *BMC Genomics* **2009**, *10*, 368. <https://doi.org/10.1186/1471-2164-10-368>.
- (513) Sommerset, I.; Wiik-Nielsen, J.; Oliveira, V. H. S. de; Moldal, T.; Bornø, G.; Haukaas, A.; Brun, E. *Norwegian Fish Health Report 2023*; Norwegian Veterinary Institute Report; #5a/2023; Norwegian Veterinary Institute, 2023.
- (514) Godoy, M.; Kibenge, M. J. T.; Montes de Oca, M.; Pontigo, J. P.; Coca, Y.; Caro, D.; Kusch, K.; Suarez, R.; Burbulis, I.; Kibenge, F. S. B. Isolation of a New Infectious Pancreatic Necrosis Virus (IPNV) Variant from Genetically Resistant Farmed Atlantic Salmon (*Salmo Salar*) during 2021–2022. *Pathogens* **2022**, *11* (11), 1368. <https://doi.org/10.3390/pathogens11111368>.
- (515) Hillestad, B.; Johannessen, S.; Melingen, G. O.; Moghadam, H. K. Identification of a New Infectious Pancreatic Necrosis Virus (IPNV) Variant in Atlantic Salmon (*Salmo Salar* L.) That Can Cause High Mortality Even in Genetically Resistant Fish. *Front Genet* **2021**, *12*, 635185. <https://doi.org/10.3389/fgene.2021.635185>.
- (516) Håstein, T.; Gudding, R.; Evensen, O. Bacterial Vaccines for Fish—an Update of the Current Situation Worldwide. *Dev Biol (Basel)* **2005**, *121*, 55–74.
- (517) Ma, J.; Bruce, T. J.; Jones, E. M.; Cain, K. D. A Review of Fish Vaccine Development Strategies: Conventional Methods and Modern Biotechnological Approaches. *Microorganisms* **2019**, *7* (11), 569. <https://doi.org/10.3390/microorganisms7110569>.
- (518) Mondal, H.; Thomas, J. A Review on the Recent Advances and Application of Vaccines against Fish Pathogens in Aquaculture. *Aquacult Int* **2022**, *30* (4), 1971–2000. <https://doi.org/10.1007/s10499-022-00884-w>.
- (519) WOA. Infectious Hematopoietic Necrosis Virus. In *Manual of Diagnostic Tests for Aquatic Animals*; World Organisation for Animal Health, 2021.
- (520) Escobar, L. E.; Escobar-Dodero, J.; Phelps, N. B. D. Infectious Disease in Fish: Global Risk of Viral Hemorrhagic Septicemia Virus. *Rev Fish Biol Fisheries* **2018**, *28* (3), 637–655. <https://doi.org/10.1007/s11160-018-9524-3>.
- (521) WOA. Salmonid Alphavirus. In *Manual of Diagnostic Tests for Aquatic Animals*; World Organisation for Animal Health, 2021.
- (522) WOA. Infection with HRP-Deleted or HPR0 Infectious Salmon Anemia Virus. In *Manual of Diagnostic Tests for Aquatic Animals*; World Organisation for Animal Health, 2022.
- (523) WOA. Spring Viremia Carp Virus. In *Manual of Diagnostic Tests for Aquatic Animals*; World Organisation for Animal Health, 2021.
- (524) WOA. Epizootic Hematopoietic Necrosis Virus. In *Manual of Diagnostic Tests for Aquatic Animals*; World Organisation for Animal Health, 2023.
- (525) WOA. Koi Herpesvirus. In *Manual of Diagnostic Tests for Aquatic Animals*; World Organisation for Animal Health, 2022.
- (526) WOA. Red Seabream Iridovirus. In *Manual of Diagnostic Tests for Aquatic Animals*; World Organisation for Animal Health, 2021.
- (527) WOA. Tilapia Lake Virus. In *Manual of Diagnostic Tests for Aquatic Animals*; World Organisation for Animal Health, 2023.
- (528) Pham, P. H.; Misk, E.; Papazotos, F.; Jones, G.; Polinski, M. P.; Contador, E.; Russell, S.; Garver, K. A.; Lumsden, J. S.; Bols, N. C. Screening of Fish Cell Lines for Piscine Orthoreovirus-1 (PRV-1) Amplification: Identification of the Non-Supportive PRV-1 In Vitro. *Pathogens* **2020**, *9* (10), 833. <https://doi.org/10.3390/pathogens9100833>.

## References

- (529) Goswami, M.; Yashwanth, B. S.; Trudeau, V.; Lakra, W. S. Role and Relevance of Fish Cell Lines in Advanced in Vitro Research. *Molecular Biology Reports* **2022**, *49* (3), 2393. <https://doi.org/10.1007/s11033-021-06997-4>.
- (530) WOA. General Information on Diagnostic Tests for Aquatic Animals. In *Manual of Diagnostic Tests for Aquatic Animals*; World Organisation for Animal Health, 2023.
- (531) Lorenzen, E.; Carstensen, B.; Olesen, N. J. Inter-Laboratory Comparison of Cell Lines for Susceptibility to Three Viruses: VHSV, IHNV and IPNV. *Dis Aquat Organ* **1999**, *37* (2), 81–88. <https://doi.org/10.3354/dao037081>.
- (532) Dong, C.; Shuang, F.; Weng, S.; He, J. Cloning of a New Fibroblast Cell Line from an Early Primary Culture from Mandarin Fish (*Siniperca chuatsi*) Fry for Efficient Proliferation of Megalocytiviruses. *Cytotechnology* **2014**, *66* (6), 883–890. <https://doi.org/10.1007/s10616-013-9642-7>.
- (533) Collet, B.; Collins, C.; Lester, K. Engineered Cell Lines for Fish Health Research. *Developmental & Comparative Immunology* **2018**, *80*, 34–40. <https://doi.org/10.1016/j.dci.2017.01.013>.
- (534) Gaj, T.; Gersbach, C. A.; Barbas, C. F. ZFN, TALEN, and CRISPR/Cas-Based Methods for Genome Engineering. *Trends in Biotechnology* **2013**, *31* (7), 397–405. <https://doi.org/10.1016/j.tibtech.2013.04.004>.
- (535) Wyman, C.; Kanaar, R. DNA Double-Strand Break Repair: All's Well That Ends Well. *Annu. Rev. Genet.* **2006**, *40* (1), 363–383. <https://doi.org/10.1146/annurev.genet.40.110405.090451>.
- (536) Gupta, R. M.; Musunuru, K. Expanding the Genetic Editing Tool Kit: ZFNs, TALENs, and CRISPR-Cas9. *J Clin Invest* **2014**, *124* (10), 4154–4161. <https://doi.org/10.1172/JCI72992>.
- (537) Carroll, D. Genome Engineering With Zinc-Finger Nucleases. *Genetics* **2011**, *188* (4), 773–782. <https://doi.org/10.1534/genetics.111.131433>.
- (538) Bogdanove, A. J.; Voytas, D. F. TAL Effectors: Customizable Proteins for DNA Targeting. *Science* **2011**, *333* (6051), 1843–1846. <https://doi.org/10.1126/science.1204094>.
- (539) Deltcheva, E.; Chylinski, K.; Sharma, C. M.; Gonzales, K.; Chao, Y.; Pirzada, Z. A.; Eckert, M. R.; Vogel, J.; Charpentier, E. CRISPR RNA Maturation by Trans-Encoded Small RNA and Host Factor RNase III. *Nature* **2011**, *471* (7340), 602–607. <https://doi.org/10.1038/nature09886>.
- (540) Sander, J. D.; Joung, J. K. CRISPR-Cas Systems for Genome Editing, Regulation and Targeting. *Nat Biotechnol* **2014**, *32* (4), 347–355. <https://doi.org/10.1038/nbt.2842>.
- (541) Chavez, M.; Chen, X.; Finn, P. B.; Qi, L. S. Advances in CRISPR Therapeutics. *Nat Rev Nephrol* **2023**, *19* (1), 9–22. <https://doi.org/10.1038/s41581-022-00636-2>.
- (542) Janik, E.; Niemcewicz, M.; Ceremuga, M.; Krzowski, L.; Saluk-Bijak, J.; Bijak, M. Various Aspects of a Gene Editing System—CRISPR—Cas9. *Int J Mol Sci* **2020**, *21* (24), 9604. <https://doi.org/10.3390/ijms21249604>.
- (543) Wang, H.; Yang, H.; Shivalila, C. S.; Dawlaty, M. M.; Cheng, A. W.; Zhang, F.; Jaenisch, R. One-Step Generation of Mice Carrying Mutations in Multiple Genes by CRISPR/Cas-Mediated Genome Engineering. *Cell* **2013**, *153* (4), 910–918. <https://doi.org/10.1016/j.cell.2013.04.025>.
- (544) Jinek, M.; Chylinski, K.; Fonfara, I.; Hauer, M.; Doudna, J. A.; Charpentier, E. A Programmable Dual RNA-Guided DNA Endonuclease in Adaptive Bacterial Immunity. *Science* **2012**, *337* (6096), 816–821. <https://doi.org/10.1126/science.1225829>.
- (545) Jiang, W.; Bikard, D.; Cox, D.; Zhang, F.; Marraffini, L. A. CRISPR-Assisted Editing of Bacterial Genomes. *Nat Biotechnol* **2013**, *31* (3), 233–239. <https://doi.org/10.1038/nbt.2508>.
- (546) DiCarlo, J. E.; Norville, J. E.; Mali, P.; Rios, X.; Aach, J.; Church, G. M. Genome Engineering in *Saccharomyces cerevisiae* Using CRISPR-Cas Systems. *Nucleic Acids Res* **2013**, *41* (7), 4336–4343. <https://doi.org/10.1093/nar/gkt135>.
- (547) Cho, S. W.; Kim, S.; Kim, J. M.; Kim, J.-S. Targeted Genome Engineering in Human Cells with the Cas9 RNA-Guided Endonuclease. *Nat Biotechnol* **2013**, *31* (3), 230–232. <https://doi.org/10.1038/nbt.2507>.
- (548) Jinek, M.; East, A.; Cheng, A.; Lin, S.; Ma, E.; Doudna, J. RNA-Programmed Genome Editing in Human Cells. *eLife* **2013**, *2*, e00471. <https://doi.org/10.7554/eLife.00471>.
- (549) Hwang, W. Y.; Fu, Y.; Reyon, D.; Maeder, M. L.; Tsai, S. Q.; Sander, J. D.; Peterson, R. T.; Yeh, J.-R. J.; Joung, J. K. Efficient In Vivo Genome Editing Using RNA-Guided Nucleases. *Nat Biotechnol* **2013**, *31* (3), 227–229. <https://doi.org/10.1038/nbt.2501>.
- (550) Li, J.-F.; Aach, J.; Norville, J. E.; McCormack, M.; Zhang, D.; Bush, J.; Church, G. M.; Sheen, J. Multiplex and Homologous Recombination-Mediated Plant Genome Editing via Guide RNA/Cas9. *Nat Biotechnol* **2013**, *31* (8), 688–691. <https://doi.org/10.1038/nbt.2654>.
- (551) Nidhi, S.; Anand, U.; Oleksak, P.; Tripathi, P.; Lal, J. A.; Thomas, G.; Kuca, K.; Tripathi, V. Novel CRISPR—Cas Systems: An Updated Review of the Current Achievements, Applications, and Future Research Perspectives. *Int J Mol Sci* **2021**, *22* (7), 3327. <https://doi.org/10.3390/ijms22073327>.
- (552) Addgene. *CRISPR History and Development for Genome Engineering*. <https://www.addgene.org/crispr/history/> (accessed 2024-04-03).
- (553) Edvardsen, R. B.; Leininger, S.; Kleppe, L.; Skafnesmo, K. O.; Wargelius, A. Targeted Mutagenesis in Atlantic Salmon (*Salmo salar* L.) Using the CRISPR/Cas9 System Induces Complete Knockout Individuals in the F0 Generation. *PLOS ONE* **2014**, *9* (9), e108622. <https://doi.org/10.1371/journal.pone.0108622>.
- (554) Chakrapani, V.; Patra, S. K.; Panda, R. P.; Rasal, K. D.; Jayasankar, P.; Barman, H. K. Establishing Targeted Carp TLR22 Gene Disruption via Homologous Recombination Using CRISPR/Cas9. *Developmental & Comparative Immunology* **2016**, *61*, 242–247. <https://doi.org/10.1016/j.dci.2016.04.009>.
- (555) Dehler, C. E.; Boudinot, P.; Martin, S. A. M.; Collet, B. Development of an Efficient Genome Editing Method by CRISPR/Cas9 in a Fish Cell Line. *Mar Biotechnol (NY)* **2016**, *18* (4), 449–452. <https://doi.org/10.1007/s10126-016-9708-6>.
- (556) Kim, M. S.; Kim, K. H. CRISPR/Cas9-Mediated Knockout of HIF-1 $\alpha$  Gene in Epithelioma Papulosum Cyprini (EPC) Cells Inhibited Apoptosis and Viral Hemorrhagic Septicemia Virus (VHSV) Growth. *Arch Virol* **2018**, *163* (12), 3395–3402. <https://doi.org/10.1007/s00705-018-4018-0>.
- (557) Liu, Q.; Yuan, Y.; Zhu, F.; Hong, Y.; Ge, R. Efficient Genome Editing Using CRISPR/Cas9 Ribonucleoprotein Approach in Cultured Medaka Fish Cells. *Biol Open* **2018**, *7* (8). <https://doi.org/10.1242/bio.035170>.

## References

- (558) Gratacap, R. L.; Jin, Y. H.; Mantsopoulou, M.; Houston, R. D. Efficient Genome Editing in Multiple Salmonid Cell Lines Using Ribonucleoprotein Complexes. *Mar Biotechnol (NY)* **2020**, *22* (5), 717–724. <https://doi.org/10.1007/s10126-020-09995-y>.
- (559) van der Wal, Y. A.; Nordli, H.; Akandwanaho, A.; Greiner-Tollersrud, L.; Kool, J.; Jørgensen, J. B. CRISPR-Cas- Induced IRF3 and MAVS Knockouts in a Salmonid Cell Line Disrupt PRR Signaling and Affect Viral Replication. *Front Immunol* **2023**, *14*, 1214912. <https://doi.org/10.3389/fimmu.2023.1214912>.
- (560) Strømsnes, T. A. H.; Schmidke, S. E.; Azad, M.; Singstad, Ø.; Grønsberg, I. M.; Dalmo, R. A.; Okoli, A. S. CRISPR/Cas9-Mediated Gene Editing in Salmonids Cells and Efficient Establishment of Edited Clonal Cell Lines. *Int J Mol Sci* **2022**, *23* (24), 16218. <https://doi.org/10.3390/ijms232416218>.
- (561) Kim, M. S.; Shin, M. J.; Kim, K. H. Increase of Viral Hemorrhagic Septicemia Virus Growth by Knockout of IRF9 Gene in Epithelioma Papulosum Cyprini Cells. *Fish Shellfish Immunol* **2018**, *83*, 443–448. <https://doi.org/10.1016/j.fsi.2018.09.025>.
- (562) Hamar, J.; Kültz, D. An Efficient Vector-Based CRISPR/Cas9 System in an Oreochromis Mossambicus Cell Line Using Endogenous Promoters. *Sci Rep* **2021**, *11* (1), 7854. <https://doi.org/10.1038/s41598-021-87068-3>.
- (563) Hamar, J.; Cnaani, A.; Kültz, D. Effects of CRISPR/Cas9 Targeting of the Myo-Inositol Biosynthesis Pathway on Hyper-Osmotic Tolerance of Tilapia Cells. *Genomics* **2024**, *116* (3), 110833. <https://doi.org/10.1016/j.ygeno.2024.110833>.
- (564) Ma, J.; Fan, Y.; Zhou, Y.; Liu, W.; Jiang, N.; Zhang, J.; Zeng, L. Efficient Resistance to Grass Carp Reovirus Infection in JAM-A Knockout Cells Using CRISPR/Cas9. *Fish Shellfish Immunol* **2018**, *76*, 206–215. <https://doi.org/10.1016/j.fsi.2018.02.039>.
- (565) Helbig, K. J.; Lau, D. T.-Y.; Semendric, L.; Harley, H. A. J.; Beard, M. R. Analysis of ISG Expression in Chronic Hepatitis C Identifies Viperin as a Potential Antiviral Effector. *Hepatology* **2005**, *42* (3), 702–710. <https://doi.org/10.1002/hep.20844>.
- (566) Dorson, M.; Torhy, C.; Billard, R.; Saudrais, C.; Maise, G.; Haffray, P.; Hollebecq, M. G. Nécrose pancréatique infectieuse des salmonidés : évaluation de méthodes destinées à couper la transmission par l'oeuf. *Bull. Fr. Pêche Piscic.* **1996**, No. 340, 1–14. <https://doi.org/10.1051/kmae:1996001>.
- (567) Evensen, Ø.; Santi, N. Infectious Pancreatic Necrosis Virus. In *Encyclopedia of Virology (Third Edition)*; Mahy, B. W. J., Van Regenmortel, M. H. V., Eds.; Academic Press: Oxford, 2008; pp 83–89. <https://doi.org/10.1016/B978-012374410-4.00772-X>.
- (568) Dobos, P. The Molecular Biology of Infectious Pancreatic Necrosis Virus (IPNV). *Annual Review of Fish Diseases* **1995**, *5*, 25–54. [https://doi.org/10.1016/0959-8030\(95\)00003-8](https://doi.org/10.1016/0959-8030(95)00003-8).
- (569) Hong, J.-R.; Gong, H.-Y.; Wu, J.-L. IPNV VP5, a Novel Anti-Apoptosis Gene of the Bcl-2 Family, Regulates Mcl-1 and Viral Protein Expression. *Virology* **2002**, *295* (2), 217–229. <https://doi.org/10.1006/viro.2001.1336>.
- (570) Petit, S.; Lejal, N.; Huet, J.-C.; Delmas, B. Active Residues and Viral Substrate Cleavage Sites of the Protease of the Birnavirus Infectious Pancreatic Necrosis Virus. *Journal of Virology* **2000**, *74* (5), 2057. <https://doi.org/10.1128/jvi.74.5.2057-2066.2000>.
- (571) Galloux, M.; Chevalier, C.; Henry, C.; Huet, J.-C.; Costa, B. D.; Delmas, B. Peptides Resulting from the pVP2 C-Terminal Processing Are Present in Infectious Pancreatic Necrosis Virus Particles. *J Gen Virol* **2004**, *85* (Pt 8), 2231–2236. <https://doi.org/10.1099/vir.0.80012-0>.
- (572) Levican, J.; Miranda-Cárdenas, C.; Soto-Rifo, R.; Aguayo, F.; Gaggero, A.; León, O. Infectious Pancreatic Necrosis Virus Enters CHSE-214 Cells via Macropinocytosis. *Sci Rep* **2017**, *7* (1), 3068. <https://doi.org/10.1038/s41598-017-03036-w>.
- (573) Delmas, B. Birnaviruses. In *Encyclopedia of Life Sciences*; John Wiley & Sons, Ltd, 2015; pp 1–8. <https://doi.org/10.1002/9780470015902.a0001009.pub2>.
- (574) Galloux, M.; Libersou, S.; Morellet, N.; Bouaziz, S.; Da Costa, B.; Ouldali, M.; Lepault, J.; Delmas, B. Infectious Bursal Disease Virus, a Non-Enveloped Virus, Possesses a Capsid-Associated Peptide That Deforms and Perforates Biological Membranes. *J Biol Chem* **2007**, *282* (28), 20774–20784. <https://doi.org/10.1074/jbc.M701048200>.
- (575) Brodrick, A. J.; Broadbent, A. J. The Formation and Function of Birnaviridae Virus Factories. *Int J Mol Sci* **2023**, *24* (10), 8471. <https://doi.org/10.3390/ijms24108471>.
- (576) Reddy, V. R. A. P.; Campbell, E. A.; Wells, J.; Simpson, J.; Nazki, S.; Hawes, P. C.; Broadbent, A. J. Birnaviridae Virus Factories Show Features of Liquid-Liquid Phase Separation and Are Distinct from Paracrystalline Arrays of Virions Observed by Electron Microscopy. *J Virol* **2022**, *96* (6), e02024-21. <https://doi.org/10.1128/jvi.02024-21>.
- (577) Villanueva, R. A.; Galaz, J. L.; Valdés, J. A.; Jashés, M. M.; Sandino, A. M. Genome Assembly and Particle Maturation of the Birnavirus Infectious Pancreatic Necrosis Virus. *J Virol* **2004**, *78* (24), 13829–13838. <https://doi.org/10.1128/JVI.78.24.13829-13838.2004>.
- (578) Bootland, L.; Dobos, P.; Stevenson, R. The IPNV Carrier State and Demonstration of Vertical Transmission in Experimentally Infected Brook Trout. *Dis. Aquat. Org.* **1991**, *10*, 13–21. <https://doi.org/10.3354/dao010013>.
- (579) Johansen, L.-H.; Sommer, A.-I. Multiplication of Infectious Pancreatic Necrosis Virus (IPNV) in Head Kidney and Blood Leucocytes Isolated from Atlantic Salmon, *Salmo Salar* L. *Journal of Fish Diseases* **1995**, *18* (2), 147–156. <https://doi.org/10.1111/j.1365-2761.1995.tb00272.x>.
- (580) Hedrick, R. P.; Leong, J. C.; Fryer, J. L. Persistent Infections in Salmonid Fish Cells with Infectious Pancreatic Necrosis Virus (IPNV). *J Fish Diseases* **1978**, *1* (4), 297–308. <https://doi.org/10.1111/j.1365-2761.1978.tb00034.x>.
- (581) Hedrick, R. P.; Fryer, J. L. Persistent Infection of Three Salmonid Cell Lines with Infectious Pancreatic Necrosis Virus (IPNV). *Fish Pathol.* **1981**, *15* (3–4), 163–172. <https://doi.org/10.3147/jspf.15.163>.
- (582) MacDonald, R. D.; Kennedy, J. C. Infectious Pancreatic Necrosis Virus Persistently Infects Chinook Salmon Embryo Cells Independent of Interferon. *Virology* **1979**, *95* (1), 260–264. [https://doi.org/10.1016/0042-6822\(79\)90428-8](https://doi.org/10.1016/0042-6822(79)90428-8).
- (583) Marjara, I. S.; Thu, B. J.; Evensen, Ø. Differentially Expressed Genes Following Persistent Infection with Infectious Pancreatic Necrosis Virus in Vitro and in Vivo. *Fish & Shellfish Immunology* **2010**, *28* (5–6), 845–853. <https://doi.org/10.1016/j.fsi.2010.02.001>.
- (584) Jurado, M. T.; García-Valtanen, P.; Estepa, A.; Perez, L. Antiviral Activity Produced by an IPNV-Carrier EPC Cell Culture Confers Resistance to VHSV Infection. *Vet Microbiol* **2013**, *166* (3–4), 412–418. <https://doi.org/10.1016/j.vetmic.2013.06.022>.

## References

- (585) Kim, H. J.; Cho, J.-K.; Hwang, H.-K.; Oh, M.-J.; Nishizawa, T. Establishment and Characterization of the Epithelioma Papulosum Cyprini (EPC) Cell Line Persistently Infected with Infectious Pancreatic Necrosis Virus (IPNV), an Aquabirnavirus. *J Microbiol* **2012**, *50* (5), 821–826. <https://doi.org/10.1007/s12275-012-2364-2>.
- (586) Rima, R. K.; Martín, S. J. Persistent Infection of Tissue Culture Cells by RNA Viruses. *Med Microbiol Immunol* **1976**, *162* (2), 89–119. <https://doi.org/10.1007/BF02121320>.
- (587) Kennedy, J. C.; Macdonald, R. D. Persistent Infection with Infectious Pancreatic Necrosis Virus Mediated by Defective-Interfering (DI) Virus Particles in a Cell Line Showing Strong Interference but Little DI Replication. *J Gen Virol* **1982**, *58* (Pt 2), 361–371. <https://doi.org/10.1099/0022-1317-58-2-361>.
- (588) Macqueen, D. J.; Kristjánsson, B. K.; Johnston, I. A. Salmonid Genomes Have a Remarkably Expanded Akirin Family, Coexpressed with Genes from Conserved Pathways Governing Skeletal Muscle Growth and Catabolism. *Physiol Genomics* **2010**, *42* (1), 134–148. <https://doi.org/10.1152/physiolgenomics.00045.2010>.
- (589) Vázquez, D.; Cutrín, J. M.; Oliveira, J. G.; Dopazo, C. P. Design and Validation of a RT-qPCR Procedure for Diagnosis and Quantification of Most Types of Infectious Pancreatic Necrosis Virus Using a Single Pair of Degenerated Primers. *J Fish Dis* **2017**, *40* (9), 1155–1167. <https://doi.org/10.1111/jfd.12590>.
- (590) Lannan, C. N.; Winton, J. R.; Fryer, J. L. Fish Cell Lines: Establishment and Characterization of Nine Cell Lines from Salmonids. *In Vitro* **1984**, *20* (9), 671–676. <https://doi.org/10.1007/BF02618871>.
- (591) Cave, D. R.; Hendrickson, F. M.; Huang, A. S. Defective Interfering Virus Particles Modulate Virulence. *J Virol* **1985**, *55* (2), 366–373.
- (592) Kawai, A.; Matsumoto, S.; Tanabe, K. Characterization of Rabies Viruses Recovered from Persistently Infected BHK Cells. *Virology* **1975**, *67* (2), 520–533. [https://doi.org/10.1016/0042-6822\(75\)90452-3](https://doi.org/10.1016/0042-6822(75)90452-3).
- (593) Palma, E. L.; Huang, A. Cyclic Production of Vesicular Stomatitis Virus Caused by Defective Interfering Particles. *J Infect Dis* **1974**, *129* (4), 402–410. <https://doi.org/10.1093/infdis/129.4.402>.
- (594) Julin, K.; Johansen, L.-H.; Sommer, A.-I.; Jørgensen, J. B. Persistent Infections with Infectious Pancreatic Necrosis Virus (IPNV) of Different Virulence in Atlantic Salmon, *Salmo Salar* L. *J Fish Dis* **2015**, *38* (11), 1005–1019. <https://doi.org/10.1111/jfd.12317>.
- (595) Vignuzzi, M.; López, C. B. Defective Viral Genomes Are Key Drivers of the Virus–Host Interaction. *Nat Microbiol* **2019**, *4* (7), 1075–1087. <https://doi.org/10.1038/s41564-019-0465-y>.
- (596) Huang, A. S.; Baltimore, D. Defective Viral Particles and Viral Disease Processes. *Nature* **1970**, *226* (5243), 325–327. <https://doi.org/10.1038/226325a0>.
- (597) Stauffer Thompson, K. A.; Rempala, G. A.; Yin, J. Multiple-Hit Inhibition of Infection by Defective Interfering Particles. *J Gen Virol* **2009**, *90* (Pt 4), 888–899. <https://doi.org/10.1099/vir.0.005249-0>.
- (598) Stauffer Thompson, K. A.; Yin, J. Population Dynamics of an RNA Virus and Its Defective Interfering Particles in Passage Cultures. *Viral J* **2010**, *7*, 257. <https://doi.org/10.1186/1743-422X-7-257>.
- (599) Nicholson, B. L.; Dunn, J. Homologous Viral Interference in Trout and Atlantic Salmon Cell Cultures Infected with Infectious Pancreatic Necrosis Virus. *J Virol* **1974**, *14* (1), 180–182. <https://doi.org/10.1128/JVI.14.1.180-182.1974>.
- (600) Conant, D.; Hsiao, T.; Rossi, N.; Oki, J.; Maures, T.; Waite, K.; Yang, J.; Joshi, S.; Kelso, R.; Holden, K.; Enzmann, B. L.; Stoner, R. Inference of CRISPR Edits from Sanger Trace Data. *CRISPR J* **2022**, *5* (1), 123–130. <https://doi.org/10.1089/crispr.2021.0113>.
- (601) Chang, H. W.; Watson, J. C.; Jacobs, B. L. The E3L Gene of Vaccinia Virus Encodes an Inhibitor of the Interferon-Induced, Double-Stranded RNA-Dependent Protein Kinase. *Proc Natl Acad Sci U S A* **1992**, *89* (11), 4825–4829.
- (602) Shors, T.; Kibler, K. V.; Perkins, K. B.; Seidler-Wulff, R.; Banaszak, M. P.; Jacobs, B. L. Complementation of Vaccinia Virus Deleted of the E3L Gene by Mutants of E3L. *Virology* **1997**, *239* (2), 269–276. <https://doi.org/10.1006/viro.1997.8881>.
- (603) Kuš, K.; Rakus, K.; Boutier, M.; Tsigkri, T.; Gabriel, L.; Vanderplasschen, A.; Athanasiadis, A. The Structure of the Cyprinid Herpesvirus 3 ORF112- $\alpha$ -Z-DNA Complex Reveals a Mechanism of Nucleic Acids Recognition Conserved with E3L, a Poxvirus Inhibitor of Interferon Response. *J Biol Chem* **2015**, *290* (52), 30713–30725. <https://doi.org/10.1074/jbc.M115.679407>.
- (604) Bogunovic, D.; Byun, M.; Durfee, L. A.; Abhyankar, A.; Sanal, O.; Mansouri, D.; Salem, S.; Radovanovic, I.; Grant, A. V.; Adimi, P.; Mansouri, N.; Okada, S.; Bryant, V. L.; Kong, X.-F.; Kreins, A.; Velez, M. M.; Boisson, B.; Khalilzadeh, S.; Ozcelik, U.; Darazam, I. A.; Schoggins, J. W.; Rice, C. M.; Al-Muhsen, S.; Behr, M.; Vogt, G.; Puel, A.; Bustamante, J.; Gros, P.; Huibregtse, J. M.; Abel, L.; Boisson-Dupuis, S.; Casanova, J.-L. Mycobacterial Disease and Impaired IFN- $\gamma$  Immunity in Humans with Inherited ISG15 Deficiency. *Science* **2012**, *337* (6102), 1684–1688. <https://doi.org/10.1126/science.1224026>.
- (605) Wilson, M. R.; Harkins, S.; Reske, J. J.; Siwicki, R. A.; Adams, M.; Bae-Jump, V. L.; Teixeira, J. M.; Chandler, R. L. PIK3CA Mutation in Endometriotic Epithelial Cells Promotes Viperin-Dependent Inflammatory Response to Insulin. *Reprod Biol Endocrinol* **2023**, *21*, 43. <https://doi.org/10.1186/s12958-023-01094-6>.
- (606) Trabelsi, K.; Majoul, S.; Rourou, S.; Kallel, H. Process Intensification for an Enhanced Replication of a Newly Adapted RM-65 Sheep Pox Virus Strain in Vero Cells Grown in Stirred Bioreactor. *Biochemical Engineering Journal* **2014**, *90*, 131–139. <https://doi.org/10.1016/j.bej.2014.06.001>.
- (607) Fontana, D.; Marsili, F.; Garay, E.; Battagliotti, J.; Etcheverrigaray, M.; Kratje, R.; Prieto, C. A Simplified Roller Bottle Platform for the Production of a New Generation VLPs Rabies Vaccine for Veterinary Applications. *Comparative Immunology, Microbiology and Infectious Diseases* **2019**, *65*, 70–75. <https://doi.org/10.1016/j.cimid.2019.04.009>.
- (608) Tapia, F.; Vázquez-Ramírez, D.; Genzel, Y.; Reichl, U. Bioreactors for High Cell Density and Continuous Multi-Stage Cultivations: Options for Process Intensification in Cell Culture-Based Viral Vaccine Production. *Appl Microbiol Biotechnol* **2016**, *100*, 2121–2132. <https://doi.org/10.1007/s00253-015-7267-9>.
- (609) Graham, F. L. Growth of 293 Cells in Suspension Culture. *Journal of General Virology* **1987**, *68* (3), 937–940. <https://doi.org/10.1099/0022-1317-68-3-937>.
- (610) Schwarz, H.; Zhang, Y.; Zhan, C.; Malm, M.; Field, R.; Turner, R.; Sellick, C.; Varley, P.; Rockberg, J.; Chotteau, V. Small-Scale Bioreactor Supports High Density HEK293 Cell Perfusion Culture for the Production of Recombinant Erythropoietin. *J Biotechnol* **2020**, *309*, 44–52. <https://doi.org/10.1016/j.jbiotec.2019.12.017>.

## References

- (611) Davies, S. L.; Lovelady, C. S.; Grainger, R. K.; Racher, A. J.; Young, R. J.; James, D. C. Functional Heterogeneity and Heritability in CHO Cell Populations. *Biotech & Bioengineering* **2013**, *110* (1), 260–274. <https://doi.org/10.1002/bit.24621>.
- (612) Mayuramart, O.; Poomipak, W.; Rattanaburi, S.; Khongnomnan, K.; Anuntakarun, S.; Saengchoowong, S.; Chavalit, T.; Chantaravisoot, N.; Payungporn, S. IRF7-Deficient MDCK Cell Based on CRISPR/Cas9 Technology for Enhancing Influenza Virus Replication and Improving Vaccine Production. *PeerJ* **2022**, *10*, e13989. <https://doi.org/10.7717/peerj.13989>.
- (613) Sène, M.; Xia, Y.; Kamen, A. A. From Functional Genomics of Vero Cells to CRISPR-based Genomic Deletion for Improved Viral Production Rates. *Biotechnol Bioeng* **2022**, *119* (10), 2794–2805. <https://doi.org/10.1002/bit.28190>.
- (614) Langereis, A. M.; Groof, A. de; Simmelink, W. B.; Vermeij, P. Mdbk Irf3/Irf7 Knock out Mutant Cell and Its Use for Vaccine Production. US20220315953A1, October 6, 2022. <https://patents.google.com/patent/US20220315953A1/en> (accessed 2024-04-30).
- (615) Qiao, Z.; Liao, Y.; Pei, M.; Qiu, Z.; Liu, Z.; Jin, D.; Zhang, J.; Ma, Z.; Yang, X. RSAD2 Is an Effective Target for High-Yield Vaccine Production in MDCK Cells. *Viruses* **2022**, *14* (11), 2587. <https://doi.org/10.3390/v14112587>.
- (616) van der Sanden, S. M. G.; Wu, W.; Dybdahl-Sissoko, N.; Weldon, W. C.; Brooks, P.; O'Donnell, J.; Jones, L. P.; Brown, C.; Tompkins, S. M.; Oberste, M. S.; Karpilow, J.; Tripp, R. A. Engineering Enhanced Vaccine Cell Lines To Eradicate Vaccine-Preventable Diseases: The Polio End Game. *J Virol* **2016**, *90* (4), 1694–1704. <https://doi.org/10.1128/JVI.01464-15>.
- (617) Wu, W.; Orr-Burks, N.; Karpilow, J.; Tripp, R. A. Development of Improved Vaccine Cell Lines against Rotavirus. *Sci Data* **2017**, *4*, 170021. <https://doi.org/10.1038/sdata.2017.21>.
- (618) Stepanenko, A. A.; Dmitrenko, V. V. HEK293 in Cell Biology and Cancer Research: Phenotype, Karyotype, Tumorigenicity, and Stress-Induced Genome-Phenotype Evolution. *Gene* **2015**, *569* (2), 182–190. <https://doi.org/10.1016/j.gene.2015.05.065>.
- (619) Popp, M. W.; Maquat, L. E. Leveraging Rules of Nonsense-Mediated mRNA Decay for Genome Engineering and Personalized Medicine. *Cell* **2016**, *165* (6), 1319–1322. <https://doi.org/10.1016/j.cell.2016.05.053>.
- (620) Lindeboom, R. G. H.; Vermeulen, M.; Lehner, B.; Supek, F. The Impact of Nonsense-Mediated mRNA Decay on Genetic Disease, Gene Editing and Cancer Immunotherapy. *Nat Genet* **2019**, *51* (11), 1645–1651. <https://doi.org/10.1038/s41588-019-0517-5>.
- (621) Reber, S.; Mechttersheimer, J.; Nasif, S.; Benitez, J. A.; Colombo, M.; Domanski, M.; Jutzi, D.; Hedlund, E.; Ruepp, M.-D. CRISPR-Trap: A Clean Approach for the Generation of Gene Knockouts and Gene Replacements in Human Cells. *Mol Biol Cell* **2018**, *29* (2), 75–83. <https://doi.org/10.1091/mbc.E17-05-0288>.
- (622) Hsu, P. D.; Scott, D. A.; Weinstein, J. A.; Ran, F. A.; Konermann, S.; Agarwala, V.; Li, Y.; Fine, E. J.; Wu, X.; Shalem, O.; Cradick, T. J.; Marraffini, L. A.; Bao, G.; Zhang, F. DNA Targeting Specificity of RNA-Guided Cas9 Nucleases. *Nat Biotechnol* **2013**, *31* (9), 827–832. <https://doi.org/10.1038/nbt.2647>.
- (623) Concordet, J.-P.; Haeussler, M. CRISPOR: Intuitive Guide Selection for CRISPR/Cas9 Genome Editing Experiments and Screens. *Nucleic Acids Research* **2018**, *46* (W1), W242–W245. <https://doi.org/10.1093/nar/gky354>.
- (624) Labun, K.; Montague, T. G.; Krause, M.; Torres Cleuren, Y. N.; Tjeldnes, H.; Valen, E. CHOPCHOP v3: Expanding the CRISPR Web Toolbox beyond Genome Editing. *Nucleic Acids Research* **2019**, *47* (W1), W171–W174. <https://doi.org/10.1093/nar/gkz365>.
- (625) Chen, J. S.; Dagdas, Y. S.; Kleinstiver, B. P.; Welch, M. M.; Sousa, A. A.; Harrington, L. B.; Sternberg, S. H.; Joung, J. K.; Yildiz, A.; Doudna, J. A. Enhanced Proofreading Governs CRISPR-Cas9 Targeting Accuracy. *Nature* **2017**, *550* (7676), 407–410. <https://doi.org/10.1038/nature24268>.
- (626) Schmid-Burgk, J. L.; Gao, L.; Li, D.; Gardner, Z.; Strecker, J.; Lash, B.; Zhang, F. Highly Parallel Profiling of Cas9 Variant Specificity. *Mol Cell* **2020**, *78* (4), 794–800.e8. <https://doi.org/10.1016/j.molcel.2020.02.023>.
- (627) Slaymaker, I. M.; Gao, L.; Zetsche, B.; Scott, D. A.; Yan, W. X.; Zhang, F. Rationally Engineered Cas9 Nucleases with Improved Specificity. *Science* **2016**, *351* (6268), 84–88. <https://doi.org/10.1126/science.aad5227>.
- (628) Campenhout, C. V.; Cabochette, P.; Veillard, A.-C.; Laczik, M.; Zelisko-Schmidt, A.; Sabatel, C.; Dhainaut, M.; Vanhollenbeke, B.; Gueydan, C.; Kruys, V. Guidelines for Optimized Gene Knockout Using CRISPR/Cas9. *Biotechniques* **2019**, *66* (6), 295–302. <https://doi.org/10.2144/btn-2018-0187>.
- (629) Finn, J. D.; Smith, A. R.; Patel, M. C.; Shaw, L.; Youniss, M. R.; van Heteren, J.; Dirstine, T.; Ciullo, C.; Lescarbeau, R.; Seitzer, J.; Shah, R. R.; Shah, A.; Ling, D.; Growe, J.; Pink, M.; Rohde, E.; Wood, K. M.; Salomon, W. E.; Harrington, W. F.; Dombrowski, C.; Strapps, W. R.; Chang, Y.; Morrissey, D. V. A Single Administration of CRISPR/Cas9 Lipid Nanoparticles Achieves Robust and Persistent *In Vivo* Genome Editing. *Cell Reports* **2018**, *22* (9), 2227–2235. <https://doi.org/10.1016/j.celrep.2018.02.014>.
- (630) Ma, H.; Tu, L.-C.; Naseri, A.; Huisman, M.; Zhang, S.; Grunwald, D.; Pederson, T. CRISPR-Cas9 Nuclear Dynamics and Target Recognition in Living Cells. *Journal of Cell Biology* **2016**, *214* (5), 529–537. <https://doi.org/10.1083/jcb.201604115>.
- (631) Kim, N. S.; Kim, S. J.; Lee, G. M. Clonal Variability within Dihydrofolate Reductase-Mediated Gene Amplified Chinese Hamster Ovary Cells: Stability in the Absence of Selective Pressure. *Biotechnol Bioeng* **1998**, *60* (6), 679–688.
- (632) Pilbrough, W.; Munro, T. P.; Gray, P. Intracolon Protein Expression Heterogeneity in Recombinant CHO Cells. *PLoS One* **2009**, *4* (12), e8432. <https://doi.org/10.1371/journal.pone.0008432>.
- (633) Barnes, L. M.; Moy, N.; Dickson, A. J. Phenotypic Variation during Cloning Procedures: Analysis of the Growth Behavior of Clonal Cell Lines. *Biotechnol Bioeng* **2006**, *94* (3), 530–537. <https://doi.org/10.1002/bit.20856>.
- (634) Scarcelli, J. J.; Hone, M.; Beal, K.; Ortega, A.; Figueroa, B.; Starkey, J. A.; Anderson, K. Analytical Subcloning of a Clonal Cell Line Demonstrates Cellular Heterogeneity That Does Not Impact Process Consistency or Robustness. *Biotechnol Prog* **2018**, *34* (3), 602–612. <https://doi.org/10.1002/btpr.2646>.
- (635) Westermann, L.; Li, Y.; Göcmen, B.; Niedermoser, M.; Rhein, K.; Jahn, J.; Cascante, I.; Schöler, F.; Moser, N.; Neubauer, B.; Hofherr, A.; Behrens, Y. L.; Göhring, G.; Köttgen, A.; Köttgen, M.; Busch, T. Wildtype Heterogeneity Contributes to Clonal Variability in Genome Edited Cells. *Sci Rep* **2022**, *12* (1), 18211. <https://doi.org/10.1038/s41598-022-22885-8>.
- (636) Giuliano, C. J.; Lin, A.; Girish, V.; Sheltzer, J. M. Generating Single Cell-Derived Knockout Clones in Mammalian Cells with CRISPR/Cas9. *Current Protocols in Molecular Biology* **2019**, *128* (1), e100. <https://doi.org/10.1002/cpmb.100>.
- (637) Irfan Maqsood, M.; Matin, M. M.; Bahrami, A. R.; Ghasroldasht, M. M. Immortality of Cell Lines: Challenges and Advantages of Establishment. *Cell Biology International* **2013**, *37* (10), 1038–1045. <https://doi.org/10.1002/cbin.10137>.

## References

- (638) Jin, J.; Xu, Y.; Huo, L.; Ma, L.; Scott, A. W.; Pizzi, M. P.; Li, Y.; Wang, Y.; Yao, X.; Song, S.; Ajani, J. A. An Improved Strategy for CRISPR/Cas9 Gene Knockout and Subsequent Wildtype and Mutant Gene Rescue. *PLoS One* **2020**, *15* (2), e0228910. <https://doi.org/10.1371/journal.pone.0228910>.
- (639) Richardson, C. D.; Ray, G. J.; DeWitt, M. A.; Curie, G. L.; Corn, J. E. Enhancing Homology-Directed Genome Editing by Catalytically Active and Inactive CRISPR-Cas9 Using Asymmetric Donor DNA. *Nat Biotechnol* **2016**, *34* (3), 339–344. <https://doi.org/10.1038/nbt.3481>.
- (640) Bai, H.; Liu, L.; An, K.; Lu, X.; Harrison, M.; Zhao, Y.; Yan, R.; Lu, Z.; Li, S.; Lin, S.; Liang, F.; Qin, W. CRISPR/Cas9-Mediated Precise Genome Modification by a Long ssDNA Template in Zebrafish. *BMC Genomics* **2020**, *21*, 67. <https://doi.org/10.1186/s12864-020-6493-4>.
- (641) Grunkemeyer, T. J.; Ghosh, S.; Patel, A. M.; Sajja, K.; Windak, J.; Basrur, V.; Kim, Y.; Nesvizhskii, A. I.; Kennedy, R. T.; Marsh, E. N. G. The Antiviral Enzyme Viperin Inhibits Cholesterol Biosynthesis. *J Biol Chem* **2021**, *297* (1), 100824. <https://doi.org/10.1016/j.jbc.2021.100824>.
- (642) Haller, O.; Staeheli, P.; Schwemmler, M.; Kochs, G. Mx GTPases: Dynamins-like Antiviral Machines of Innate Immunity. *Trends in Microbiology* **2015**, *23* (3), 154–163. <https://doi.org/10.1016/j.tim.2014.12.003>.
- (643) Gao, S.; von der Malsburg, A.; Dick, A.; Faelber, K.; Schröder, G. F.; Haller, O.; Kochs, G.; Daumke, O. Structure of Myxovirus Resistance Protein A Reveals Intra- and Intermolecular Domain Interactions Required for the Antiviral Function. *Immunity* **2011**, *35* (4), 514–525. <https://doi.org/10.1016/j.immuni.2011.07.012>.
- (644) Solbakken, M. H.; Rise, M. L.; Jakobsen, K. S.; Jentoft, S. Successive Losses of Central Immune Genes Characterize the Gadiformes' Alternate Immunity. *Genome Biol Evol* **2016**, *8* (11), 3508–3515. <https://doi.org/10.1093/gbe/evw250>.
- (645) Yap, W. H.; Tay, A.; Brenner, S.; Venkatesh, B. Molecular Cloning of the Pufferfish (*Takifugu rubripes*) Mx Gene and Functional Characterization of Its Promoter. *Immunogenetics* **2003**, *54* (10), 705–713. <https://doi.org/10.1007/s00251-002-0525-x>.
- (646) Robertsen, B.; Greiner-Tollersrud, L.; Jørgensen, L. G. Analysis of the Atlantic Salmon Genome Reveals a Cluster of Mx Genes That Respond More Strongly to IFN Gamma than to Type I IFN. *Developmental & Comparative Immunology* **2019**, *90*, 80–89. <https://doi.org/10.1016/j.dci.2018.09.004>.
- (647) Larsen, R.; Røkenes, T. P.; Robertsen, B. Inhibition of Infectious Pancreatic Necrosis Virus Replication by Atlantic Salmon Mx1 Protein. *J Virol* **2004**, *78* (15), 7938–7944. <https://doi.org/10.1128/JVI.78.15.7938-7944.2004>.
- (648) Lester, K.; Hall, M.; Urquhart, K.; Gahlawat, S.; Collet, B. Development of an in Vitro System to Measure the Sensitivity to the Antiviral Mx Protein of Fish Viruses. *Journal of Virological Methods* **2012**, *182* (1), 1–8. <https://doi.org/10.1016/j.jviromet.2012.01.014>.
- (649) Trobridge, G. D.; Chiou, P. P.; Leong, J. A. Cloning of the Rainbow Trout (*Oncorhynchus mykiss*) Mx2 and Mx3 cDNAs and Characterization of Trout Mx Protein Expression in Salmon Cells. *J Virol* **1997**, *71* (7), 5304–5311.
- (650) Biacchesi, S.; Lamoureux, A.; Mérour, E.; Bernard, J.; Brémont, M. Limited Interference at the Early Stage of Infection between Two Recombinant Novirhabdoviruses: Viral Hemorrhagic Septicemia Virus and Infectious Hematopoietic Necrosis Virus. *J Virol* **2010**, *84* (19), 10038–10050. <https://doi.org/10.1128/JVI.00343-10>.

---

# **SUPPLEMENTARY MATERIAL**

---

---

# APPENDIX 1

## List of publications and presentations

---

### Publications

- **Chaumont, L.**, Collet, B., & Boudinot, P. (2023). Double-stranded RNA-dependent protein kinase (PKR) in antiviral defence in fish and mammals. *Developmental & Comparative Immunology*, 145, 104732. <https://doi.org/10.1016/j.dci.2023.104732>
- **Chaumont, L.**, Peruzzi, M., Huetz, F., Raffy, C., Le Hir, J., Minke, J., Boudinot, P., & Collet, B. (2024). Salmonid Double-stranded RNA-Dependent Protein Kinase Activates Apoptosis and Inhibits Protein Synthesis. *Journal of immunology (Baltimore, Md. : 1950)*, 213(5), 700–717. <https://doi.org/10.4049/jimmunol.2400076>
- **Chaumont, L.**, Jouneau, L., Huetz, F., van Muilekom, D. R., Peruzzi, M., Raffy, C., Le Hir, J., Minke, J., Boudinot, P., & Collet, B. (2024). Unexpected regulatory functions of cyprinid Viperin on inflammation and metabolism. *BMC genomics*, 25(1), 650. <https://doi.org/10.1186/s12864-024-10566-x>
- Collins, C., **Chaumont, L.**, Peruzzi, M., Jamak, N., Boudinot, P., Béjar, J., Moreno, P., Alvarez Torres, D., Collet, B. Effect of a loss of the *mda5/ifih1* gene on the antiviral resistance in a Chinook salmon *Oncorhynchus tshawytscha* cell line. [Manuscript submitted to *Plos One* on 2024/05/23, currently under review].

### Oral presentations

- “Functional characterization of a Viperin knockout fish cell line”, 15<sup>th</sup> ISDCI Congress, Wageningen, The Netherlands, August 28-31, 2023.

### Posters

- “Development and characterization of a Pkr knockout fish cell line and assessment of its permissivity to viral infections”, Fish Immunology and Vaccination Workshop, Wageningen, The Netherlands, April 24-28, 2022.
- “Understanding the role of Chinook salmon PKR in the antiviral response during Viral Hemorrhagic Septicemia Virus (VHSV) infection”, 21<sup>st</sup> EAFP Congress, Aberdeen, UK, September 11-14, 2023.

### Supervision activities

- Co-supervision of Camille REGARD, Master 1, AgroParisTech, 2022

---

## APPENDIX 2 - RÉSUMÉ EN FRANÇAIS

### « Étude fonctionnelle de gènes stimulés par l'interféron par une approche *in vitro* d'invalidation génique en lignées cellulaires de poisson : de l'immunologie comparée à l'intérêt pour la production de vaccins »

---

#### 1. État de l'art

##### 1. 1. Vue d'ensemble de la réponse interféron chez les mammifères et les poissons

Lors d'une infection microbienne, causée par un virus, une bactérie, un champignon ou un parasite, les vertébrés déclenchent une réponse immunitaire pour lutter contre le pathogène et endiguer l'infection. Chez les poissons, comme chez tous les vertébrés, cette réponse immunitaire repose sur deux piliers : la réponse immunitaire innée et la réponse immunitaire adaptative. La réponse immunitaire innée est la première ligne de défense contre les agents pathogènes. Il s'agit d'une réponse à action rapide initiée par un réseau de senseurs spécialisés, appelés PRRs (*pattern recognition receptors* en anglais), qui sont exprimés par un grand nombre de cellules de l'hôte. Au cours d'une infection virale, la détection de motifs moléculaires spécifique du pathogène, appelés PAMPs (*pathogen-associated molecular patterns* en anglais), déclenche une cascade de signalisation qui conduit à la production de molécules de défense de l'hôte, principalement des interférons (IFNs) de type I et II, des cytokines pro-inflammatoires et des chimiokines. Ces cytokines activent des mécanismes de défense, amplifient la réponse immunitaire innée et régulent la réponse adaptative par le biais d'actions autocrines et paracrines. En particulier, les IFNs de type I induisent la transcription de centaines de gènes appelés ISGs (*IFN-stimulated genes* en anglais), y compris des gènes effecteurs, qui ont une action antivirale directe ou modulent la physiologie cellulaire dans le but d'inhiber la propagation virale <sup>1</sup> (**Figure 43**).

De façon générale, les mécanismes immunitaires innés sont relativement bien conservés chez les vertébrés à mâchoires. Cependant, le répertoire des gènes codant les IFNs et les ISGs est bien plus diversifié chez les poissons que chez les mammifères, en raison de leur histoire évolutive complexe et de leurs spécificités anatomiques et physiologiques. En effet, au cours de leur évolution, les poissons téléostéens ont subi un événement de duplication de génome entier il y a 320-350 millions d'années ; les salmonidés, quant à eux, ont subi un second événement de duplication du génome il y a ~ 80-100 millions d'années <sup>9-11</sup>. En conséquence, pour chaque gène unique chez les tétrapodes, il existe, en théorie, deux copies localisées sur des loci distincts chez les cyprinidés diploïdes et jusqu'à quatre copies chez les salmonidés. En réalité, les gènes dupliqués peuvent être perdus, pseudogénisés,

sous- ou néo-fonctionnalisés, et des événements de duplication en tandem supplémentaires peuvent également avoir lieu <sup>12</sup>. Chez les salmonidés, il a été estimé que près de la moitié des gènes dupliqués devenaient des pseudogènes <sup>9</sup> ; néanmoins, certaines familles géniques présentent une grande diversité de membres <sup>13,14</sup>. Dans le cas des gènes impliqués dans les réponses immunitaires antivirales, il a été suggéré que cette diversification a été favorisée par la pression évolutive et la nécessité de contrer des mécanismes viraux impliqués dans l'évasion immunitaire, comme le postule l'hypothèse de la Reine Rouge <sup>15,16</sup>. Par conséquent, en raison des événements de néo-fonctionnalisation et de sous-fonctionnalisation, la/les fonction(s) de nombreux gènes immunitaires de poissons et leurs mécanismes d'action restent encore nébuleux.

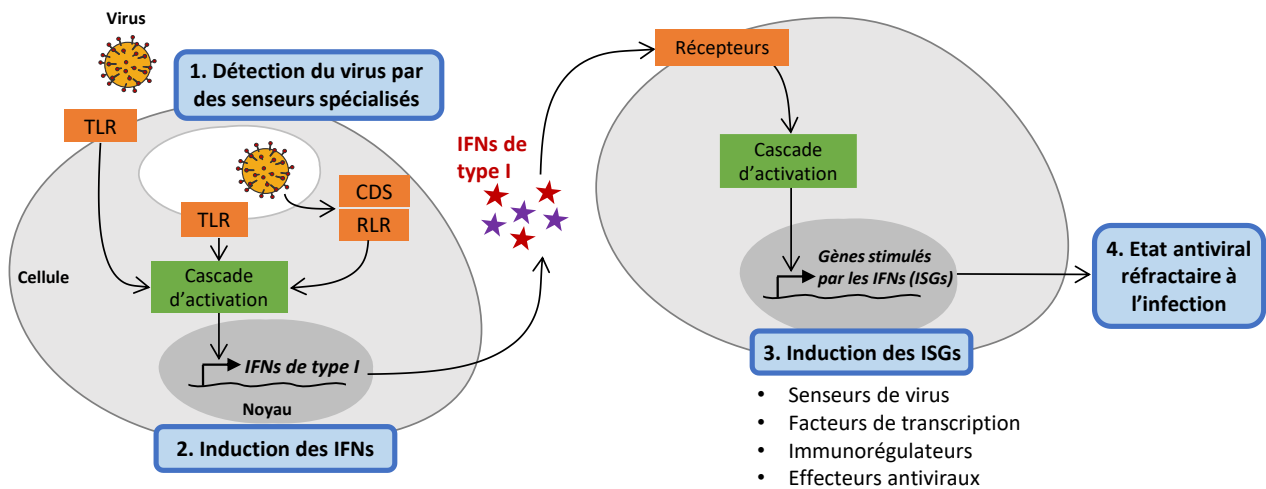


**Figure 43: Schéma simplifié de la réponse IFN de type I**

Les senseurs et récepteurs sont représentés en orange (TLR : Toll-like receptors – famille de récepteurs membranaires reconnaissant divers PAMPs viraux, dont des protéines et des acides nucléiques viraux ; RLR : RIG-I-like receptors – famille de récepteurs cytosoliques reconnaissant de ARNdb viraux ; CDS : cytosolic DNA sensors – famille hétérogène de récepteurs cytosoliques reconnaissances des ADNs viraux). Les cascades de transduction du signal sont représentées en vert : elles comprennent notamment des molécules adaptatrices et des facteurs de transcription, permettant l'induction de gènes spécifiques.

## 1. 2. Le rôle de la PKR dans les défenses antivirales des mammifères et poissons

La protéine EIF2AK2 (*eukaryotic translation initiation factor 2 alpha kinase 2* en anglais), mieux connue sous le nom de protéine kinase dépendante de l'ARN double-brin (ARNdb) (PKR, *dsRNA-dependent protein kinase* en anglais) fait partie des protéines codées par un ISG les plus étudiées. Elle est reconnue comme un facteur clé multifonctionnel de l'immunité innée, en agissant à la fois comme un senseur de virus et un effecteur à activité antivirale.

### 1. 2. 1. Expression, structure et activité antivirale de la PKR

Chez les mammifères, la PKR est exprimée de manière constitutive et ubiquitaire à de faibles niveaux dans tous les tissus et son expression est induite par une variété de réponses à des stress, y compris un traitement à l'IFN de type I ou des infections virales <sup>196</sup>.

Structurellement, la PKR est composée d'une région N-terminale régulatrice présentant deux motifs de liaison à l'ARNdb (dsRBM, *dsRNA binding motif* en anglais) et un domaine C-terminal à activité kinase <sup>196,211</sup>. Cette structure conservée chez la plupart des vertébrés, bien que le nombre de dsRBMs varie de un à trois en fonction des espèces <sup>200</sup>.

Son action antivirale a été démontrée contre un large spectre de virus à ARN <sup>75</sup> et son importance dans la réponse immunitaire de l'hôte est également mise en évidence par les nombreuses stratégies de subversion développées par les virus pour contrer ses effets antiviraux <sup>377</sup>.

### 1. 2. 2. Inhibition de la traduction médiée par PKR

La PKR nécessite une étape d'activation pour être catalytiquement fonctionnelle <sup>274,281</sup>. Cette activation est notamment médiée par liaison à l'ARNdb, qui est généré pendant les cycles de réplication des virus à ARN. Les interactions avec l'ARNdb sont orchestrées par les dsRBMs et induisent la dimérisation de PKR ainsi que son autophosphorylation <sup>211,283</sup>. Une fois activée, la PKR catalyse la phosphorylation la sous-unité  $\alpha$  du complexe eIF2, qui est impliquée dans l'initiation de la traduction de l'ARN messenger. La phosphorylation de eIF2 $\alpha$  conduit à un blocage général de la traduction cellulaire dans la cellule, ce qui inhibe la réplication virale, qui nécessite la machinerie cellulaire de l'hôte pour avoir lieu <sup>75,202</sup>.

### 1. 2. 3. Activation de l'apoptose médiée par PKR

Outre son action inhibitrice sur la traduction cellulaire, la PKR est également impliquée dans d'autres mécanismes antiviraux, notamment l'activation de l'apoptose. Cette dernière est un type de mort cellulaire programmée conduisant à l'autodestruction des cellules sous forme de corps apoptotiques qui sont alors phagocytés par des cellules immunitaires <sup>156</sup>. Au cours d'une infection virale, le déclenchement de l'apoptose à un stade précoce de l'infection permet de limiter la propagation virale en empêchant le virus de terminer son cycle de vie dans les cellules infectées <sup>157</sup>.

Les mécanismes moléculaires qui sous-tendent l'activation de l'apoptose par la PKR sont divers. Plusieurs études ont montré que ce processus dépendait de la phosphorylation de l'eIF2 $\alpha$ , qui limite la traduction de régulateurs anti-apoptotiques et favorise l'expression de gènes spécifiques impliqués dans les voies de réponse au stress, telles que la voie ATF4/CHOP <sup>206,249,309,310,320</sup>. Par ailleurs,

l'apoptose médiée par la PKR peut aussi être déclenchée par l'activation du facteur de transcription NF- $\kappa$ B<sup>342,343</sup>. Dans tous les cas, le déclenchement de l'apoptose par la PKR se traduit par l'activation de la cascade caspase, qui constitue la phase exécutive de l'apoptose<sup>158</sup>.

#### 1. 2. 4. Modulation des réponses inflammatoires et IFNs par PKR

La PKR potentialise également les réponses inflammatoires et IFN, en modulant certaines voies de signalisation MAPK- et NF- $\kappa$ B-dépendantes<sup>338–340,346</sup> et en stimulant la production d'IFN de type I lors de certaines infections virales<sup>344,354,357</sup>. Néanmoins, le rôle précis de la PKR dans l'activation de ces différentes voies reste encore à élucider.

Il a néanmoins été montré que la PKR interagissait avec certains composants des voies de signalisation RIG-I et MDA5 – tous les deux des senseurs cytosoliques d'ARNdb – ce qui suggère que la PKR agit comme une protéine adaptatrice dans la transduction du signal. Parmi d'autres mécanismes d'action, il a été proposé que PKR stabilise les transcrits *IFNB*<sup>354</sup> et active certaines voies IRF-1-dépendantes<sup>342</sup>.

#### 1. 2. 5. La PKR des poissons

Des orthologues de la PKR mammalienne ont été identifiés dans le génome de poissons cartilagineux (Chondrichthyes) et osseux (Osteichthyes). Dans le cas des poissons téléostéens (*i.e.* la plus grande infraclasse des poissons osseux), le gène codant la PKR a été cloné et caractérisé chez des espèces appartenant à différents ordres taxonomiques, dont les Tétraodontiformes (*e.g.* fugu<sup>266</sup>), les Perciformes (*e.g.* brème de roche<sup>264</sup>, tilapia du Nil<sup>265</sup>, mérou taches oranges<sup>231</sup>), les Pleuronectiformes (*e.g.* cardeau hirame<sup>199</sup>) et les Cypriniformes (*e.g.* carassin doré<sup>239</sup>, carpe de roseau<sup>238</sup>, poisson zèbre<sup>200</sup>). Par ailleurs, certaines familles de poissons téléostéens, dont les cyprinidés, les salmonidés et les clupéidés, possèdent également un paralogue de *pkz*, appelé *pkz*, codant une protéine kinase dépendante de l'ADN-Z<sup>198,200,229</sup>. L'ADN-Z correspond à une conformation non-canonique d'acides nucléiques<sup>286</sup>. Sa fonction précise biologique n'a pas encore identifiée mais il a été suggéré qu'elle était générée au cours de certaines infections virales<sup>220,289</sup>.

La plupart des études sur la PKR (et la PKZ) des poissons n'ont pas disséqué ses mécanismes d'action de manière aussi approfondie que chez les mammifères. Elles indiquent, néanmoins, que plusieurs fonctions antivirales attribuées à la PKR des mammifères sont conservées dans ces organismes. En particulier, plusieurs études ont montré que les PKRs (et la PKZ) des poissons pouvaient phosphoryler eIF2 $\alpha$  et inhiber la synthèse protéique *de novo*<sup>199,238,257,265,266</sup>. En outre, l'activation de l'apoptose médiée par la PKR/PKZ a également été décrite chez certains cyprinidés<sup>238,257,262</sup>. D'autres travaux

suggèrent également que la PKR de poissons est capable de moduler la voie de signalisation NF- $\kappa$ B<sup>260,266</sup> ainsi que la production d'IFN de type I<sup>231,271</sup>.

### 1. 3. Le rôle de la Viperin dans les défenses antivirales des mammifères et poissons

#### 1. 3. 1. Expression, structure et activité antivirale

La Viperin (*virus inhibitory protein, endoplasmic reticulum associated, IFN inducible* en anglais), également appelée RSAD2 (*radical S-adenosyl-methionine (SAM) domain-containing protein 2* en anglais) figure parmi les ISGs les plus fortement induits lors de la stimulation par les IFNs et les infections virales<sup>396,418</sup>. Le gène codant la Viperin fait partie des rares ISGs à avoir été initialement identifiés et étudiés dans un modèle non-mammalien : en effet, la Viperin a tout d'abord été caractérisée dans des leucocytes de truite arc-en-ciel (*Oncorhynchus mykiss*) infectés par le virus de la septicémie hémorragique virale (VSHV)<sup>140</sup>, avant d'être clonée chez l'Homme<sup>387</sup>.

Structurellement, la Viperin est composée de 3 domaines distincts : un domaine N-terminal comportant une hélice  $\alpha$  amphipathique nécessaire à sa localisation au niveau de face cytosolique du réticulum endoplasmique et des gouttelettes lipidiques<sup>405,406</sup> ; un domaine central conservé portant le motif canonique CX<sub>3</sub>CX<sub>2</sub>C, caractéristique de la superfamille à radical SAM et nécessaire à son activité enzymatique, et un domaine C-terminal conservé impliqué dans des interactions protéine-protéine et dans la reconnaissance de substrats<sup>394,400,418</sup>. Cette structure est largement conservée chez les vertébrés<sup>396,398,399</sup> ainsi que chez les invertébrés<sup>433</sup>. Par ailleurs, des gènes apparentés à la Viperin ont été récemment identifiés chez les champignons, les bactéries et les archées, ce qui suggère que la Viperin fait partie d'un arsenal très ancien de mécanismes de défense antivirale<sup>394,416,434</sup>.

Chez les mammifères, la Viperin inhibe un large spectre de virus à ADN et à ARN<sup>151</sup>, bien que sa capacité à limiter la réplication virale puisse radicalement différer d'un virus à l'autre<sup>456,462</sup>. D'un point de vue mécanistique, la Viperin exerce son action antivirale par différents moyens, impliquant son activité enzymatique et/ou des interactions protéine-protéine<sup>151</sup>.

#### 1. 3. 2. Effet antiviral du ddhCTP généré par la Viperin

Bien qu'il ait été identifié très tôt que la Viperin nécessitait d'être catalytiquement active pour exercer son action antivirale dans la majorité des cas<sup>396,461</sup>, son substrat est resté inconnu pendant de nombreuses années. Des études biochimiques ont récemment démontré qu'elle était capable de catalyser la conversion de la cytidine triphosphate (CTP) en son analogue 3'-deoxy-3',4'-didehydro-cytidine triphosphate (ddhCTP) par le biais d'un mécanisme radicalaire dépendant de SAM<sup>150,394</sup>. Il a, par la suite, été montré que le ddhCTP inhibait la réplication de certains virus à ARN en agissant comme un terminateur de chaîne pour les ARN polymérases ARN dépendantes<sup>150</sup>.

### 1. 3. 3. Interactions protéine-protéine

La Viperin exerce également son action antivirale en interagissant avec un large éventail de protéines virales et cellulaires. En particulier, il a été rapporté qu'elle se lie aux protéines virales et qu'elle favorise leur dégradation par la voie du protéasome <sup>462,469</sup>.

En outre, la Viperin interagit avec les médiateurs cellulaires impliqués dans la signalisation immunitaire innée, notamment la voie TLR7 impliquée dans la détection des ARN à simple brin, la voie TLR9 spécialisée dans la détection de l'ADN CpG non méthylé <sup>440,475</sup> et la voie cGAS-STING activée par l'ADNdb cytosolique <sup>471</sup>, renforçant ainsi la réponse IFN.

Plusieurs études suggèrent également que la Viperin module certaines voies métaboliques exploitées au cours des cycles viraux, notamment la biosynthèse du cholestérol <sup>422,444,641</sup> et la sécrétion de protéines solubles <sup>405,483</sup>.

Par ailleurs, quelques études indiquent un rôle de la Viperin dans la régulation des processus métaboliques dans des conditions non infectieuses, y compris la formation des os et du cartilage <sup>386,484</sup>, la réduction de la  $\beta$ -oxydation des acides gras <sup>439,475,490</sup> et la régulation du métabolisme mitochondrial <sup>492</sup>. Cependant, les mécanismes d'action sous-jacents restent encore à étudier en détails.

### 1. 3. 4. La Viperin de poissons

Chez les poissons, des orthologues du gène *viperin* ont été identifiés chez de nombreuses espèces et présentent une activité antivirale <sup>140,413,430,447,450,455</sup>.

En ce qui concerne les mécanismes d'action moléculaires de la Viperin de poisson, aucune étude ne s'est penchée sur la génération du ddhCTP, vraisemblablement en raison des difficultés techniques associées à ce type d'expérience (*e.g.* conditions anaérobiques). Néanmoins, des études de surexpression en cellules de poisson montrent que les Viperins de poisson sont capable de moduler l'expression des gènes impliqués dans les réponses inflammatoires et IFN <sup>430,447,448,450</sup>, d'interagir avec des protéines virales pour promouvoir leur dégradation *via* les voies du protéasome et/ou de l'autophagosome <sup>413</sup> et de moduler le métabolisme du cholestérol <sup>446</sup>.

## 2. Objectifs

La majorité des études fonctionnelles visant à caractériser les ISGs de poissons, dont la PKR et la Viperin, sont principalement basées sur des approches de surexpression et, dans une moindre mesure, de knock-down ou d'inhibition chimique. Bien qu'informatives, ces approches présentent des biais intrinsèques, notamment des niveaux anormalement élevés ou au contraire rémanents de la protéine d'intérêt et une spécificité discutable des inhibiteurs chimiques, respectivement. Cependant,

l'expansion des technologies d'édition du génome associée au séquençage massif de génomes de nombreuses espèces de poisson est actuellement en train de révolutionner le domaine de l'immunologie des poissons, en rendant les études fonctionnelles par invalidation génique possibles.

Dans ce contexte, l'objectif principal de mon projet de doctorat était de développer et de caractériser des lignées cellulaires de poissons, dans lesquelles ces deux ISGs majeurs ont été invalidés à l'aide du système CRISPR/Cas9, afin de comprendre leur contribution respective à la réponse immunitaire antivirale. À cet égard, les objectifs de mon projet étaient triples :

- (1) Développer et valider des cellules de poisson *pkr*<sup>-/-</sup> et *viperin*<sup>-/-</sup>, en utilisant la lignée cellulaire CHSE-EC de saumon Chinook (salmonidé) et la lignée cellulaire EPC-EC du poisson tête-de-boule (cyprinidé) comme lignées cellulaires parentales, respectivement ;
- (2) Caractériser fonctionnellement ces lignées cellulaires, afin d'identifier leurs mécanismes d'action respectifs et leur(s) rôle(s) potentiel(s) dans la régulation de la réponse IFN de type I par des boucles de rétroaction ;
- (3) Évaluer l'impact des invalidations géniques sur la capacité des cellules à produire des particules virales à des plus hauts rendements que ceux de leurs homologues de type sauvage.

### 3. Résultats

#### 3.1. Caractérisation des fonctions moléculaires de la PKR de salmonidés par des approches de surexpression et d'invalidation génique

Dans cette première étude, nous avons souhaité approfondir les connaissances sur la PKR de salmonidés, en caractérisant les fonctions moléculaires de la PKR de saumon Chinook (*Oncorhynchus tshawytscha*) par des approches complémentaires de surexpression et d'invalidation génique. Nous nous sommes ainsi penchés sur les problématiques suivantes : (1) la PKR de saumon Chinook active-t-elle l'apoptose ? (2) Inhibe-t-elle la traduction des protéines de l'hôte ? (3) Est-elle impliquée dans l'inhibition de la réplication virale ?

Dans un premier temps, nous avons identifié et cloné trois différents transcrits du gène *pkr* exprimé dans une lignée cellulaire de saumon Chinook CHSE-EC infectée par le VSHV : une forme longue (PKR-FL), présentant des domaines structuraux (3 motifs de liaison à l'ARN db, domaine kinase) conservés, une forme intermédiaire (PKR-ML), comportant des domaines N-terminal et C-terminal tronqués et une forme courte (PKR-SL), uniquement composée d'un motif de liaison à l'ARNdb et aucun domaine kinase (**Figure 44A**). Des études de RT-qPCR et western blot ont montré que la PKR-FL était prédominante et fortement inductible par l'IFN de type I mais pas durant l'infection par le VSHV.

En parallèle, nous avons également développé et validé la première lignée cellulaire clonale de poisson invalidée pour le gène *pkc* en utilisant la technologie d'édition du génome CRISPR/Cas9 (**Figure 44B**).

Dans un deuxième temps, nous avons étudié le rôle de la PKR de saumon Chinook dans l'activation de l'apoptose. Des expériences de surexpression ont permis de démontrer que seule la PKR-FL était impliquée dans le déclenchement de l'apoptose par activation de la cascade caspase (**Figure 44C**). De même, nous avons montré par des expériences de perte de fonction que la PKR endogène activait la cascade caspase durant l'infection par le VSHV (**Figure 44D**).

Dans un troisième temps, nous nous sommes intéressés au rôle de la PKR dans l'inhibition de la traduction cellulaire. Nos résultats ont confirmé que la PKR de saumon Chinook jouait un rôle majeur dans l'arrêt de la traduction en cas de surexpression ou de transfection avec du poly(I:C), un analogue synthétique de l'ARNdb (**Figure 44E,F**). En revanche, il est apparu que la PKR endogène n'était pas responsable de l'arrêt de la synthèse protéique durant l'infection par le VSHV (**Figure 44G**).

Nos données indiquent également que la PKR n'affecte pas la réplication du VSHV en tant que telle mais favorise la libération des virions dans le surnageant à un stade infectieux tardif, probablement en déclenchant l'apoptose (**Figure 44H**).

En résumé, nos résultats suggèrent que le VSHV a développé une stratégie pour échapper à l'action antivirale de la PKR, en limitant son induction précoce, en évitant l'arrêt de la traduction médié par la PKR et en tirant partie de l'activation de l'apoptose par la PKR à un stade tardif de l'infection pour favoriser la propagation du virus. Notre étude illustre ainsi les stratégies de subversion développées par les virus pour contrarier ou détourner les mécanismes antiviraux médiés par la PKR décrits chez les mammifères.

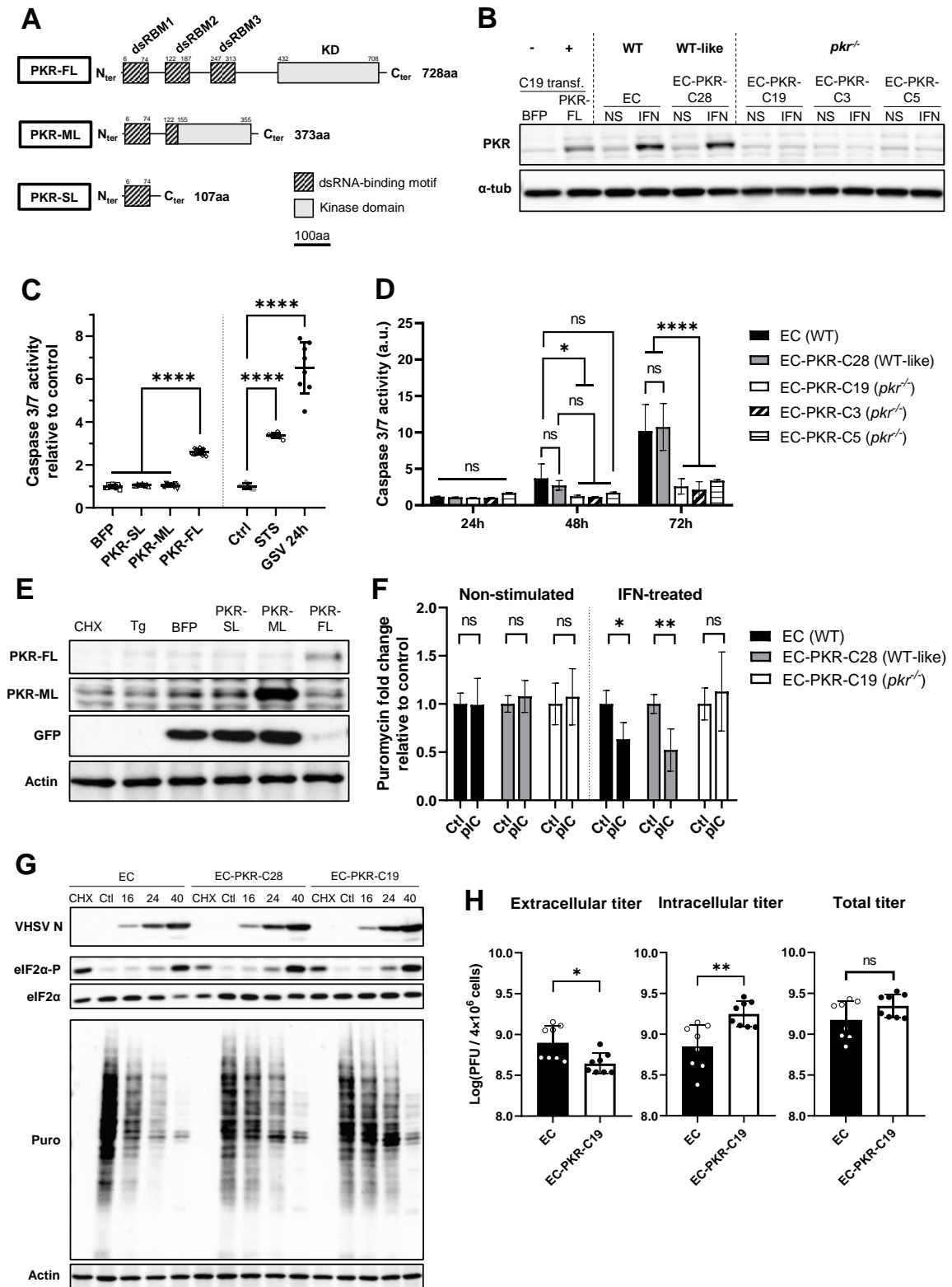


**Figure 44: La PKR de saumon Chinook présente des fonctions moléculaires conservées**

(A) Représentation schématique des trois isoformes de PKR exprimées par les cellules EC. dsRBM = motif de liaison à l'ARNdb, KD = domaine kinase. (B) Validation des lignées EC *pkr*<sup>-/-</sup> par western blot. Les cellules EC (sauvages) et EC-PKR (*pkr*<sup>-/-</sup>) ont été stimulées avec de l'IFNA2 de *S. salar* pendant 72h ; les contrôles positifs et négatifs sont des cellules transfectées avec les vecteurs d'expression pcDNA3.1-Zeo-BFP et pcDNA3.1-Zeo-BFP-P2A-PKR-FL, respectivement. Les lysats cellulaires ont été séparés par SDS-PAGE et incubés avec des anticorps contre la PKR et l'α-tubuline (protéine de ménage). (C, D) Activité enzymatique de la caspase 3/7. (C) Les cellules EC-PKR-C19 *pkr*<sup>-/-</sup> ont été transfectées avec des plasmides codant la BFP ou différentes isoformes de PKR (PKR-SL, -ML, -FL) et l'activité enzymatique de la caspase 3/7 a été mesurée à 72hpt. Des cellules stimulées avec de la staurosporine (STS, 1 μM, 24h), infectées par le GSV (MOI

1, 24-48h) ou sans traitement sont des contrôles positifs et négatifs, respectivement. Les graphiques représentent la moyenne  $\pm$  ET de deux expériences indépendantes (n=8 pour les expériences de transfection ; n=4 pour les expériences d'infection) ; ns, non significatif ( $p > 0,05$ ), \*\*\*\*,  $p < 0,0001$ , ANOVA un facteur avec tests post-hoc de Tukey. **(D)** Les cellules ont été infectées avec du rVSHV-Tomato (MOI 0.1) et l'activité enzymatique de la caspase 3/7 a été mesurée à 24, 48 et 72 hpi. Les graphiques représentent la moyenne  $\pm$  ET de deux expériences indépendantes (n=4 pour chaque expérience) ; ns, non significatif ( $p > 0,05$ ), \*,  $p < 0,05$ , \*\*,  $p < 0,01$ , \*\*\*\*,  $p < 0,0001$ , ANOVA deux facteurs avec tests post-hoc de Tukey. **(E)** Les cellules EC-PKR-C19 *pk<sup>r</sup>-/-* ont été cotransfectées avec le plasmide pcDNA3.1-Hyg-mEGFP et des vecteurs d'expression codant la BFP ou différentes isoformes de PKR (PKR-SL, -ML, -FL). À 8 hpt, les cellules contrôles ont été traitées avec du cycloheximide (CHX, 50  $\mu\text{g}/\text{mL}$ ) ou de la thapsigargin (Tg, 2  $\mu\text{M}$ , 45 min). À 30 hpt, les lysats cellulaires ont été analysés par western blot des anticorps contre la PKR, la GFP ou l'actine (protéine de ménage). **(F)** Des cellules non-stimulées ou prétraitées avec de l'IFN $\alpha 2$  ont été transfectées avec ou sans poly(I:C). A 24 hpt, les cellules ont été pulsées avec de la puromycine (5  $\mu\text{g}/\text{mL}$ , 15 min), un marqueur de la synthèse protéique *de novo*, et les lysats cellulaires ont été analysés par western blot. Le graphique représente la moyenne  $\pm$  ET de deux expériences indépendantes (n=3 pour chaque expérience) ; ns, non significatif ( $p > 0,05$ ) ; \*,  $p < 0,05$  ; \*\*,  $p < 0,01$ , ANOVA à deux facteurs avec tests post-hoc de Bonferroni. **(G)** Les cellules ont été infectées avec du rVSHV-Tomato (MOI 1), laissées sans traitement (Ctrl) ou stimulées avec du cycloheximide (CHX, 50  $\mu\text{g}/\text{mL}$ ) for 24h. A 16, 24 ou 40 hpi, les cellules ont été pulsées avec de la puromycine (5  $\mu\text{g}/\text{mL}$ , 15 min) et les lysats cellulaires ont été analysés par western blot avec des anticorps contre la protéine N du VSHV, eIF2 $\alpha$ -P, eIF2 $\alpha$ , puromycine et actine. **(H)** Les cellules ont été infectées avec le rVHSV-Tomato (MOI 1) ; les surnageants ont été collectés à 96 hpi et les cellules restantes ont été récupérées et soniquées ; les surnageants et les soniquats ont été titrés. Les graphiques représentent la moyenne  $\pm$  ET de deux expériences indépendantes (n=4 pour chaque expérience), \*,  $p < 0,05$  ; \*\*,  $p < 0,01$ , test de Kruskal-Wallis avec tests post-hoc de Dunn sur les données log-transformées.

### 3. 2. Caractérisation de la Viperin de cyprinidés par étude transcriptomique en lignées cellulaires *viperin*<sup>-/-</sup>

Dans cette seconde étude, nous avons souhaité étudier la contribution de la Viperin de poisson à la réponse antivirale et notamment son rôle régulateur à l'échelle transcriptionnelle. Nous avons ainsi abordé les questions suivantes : (1) La Viperin de poisson contribue-t-elle à la régulation de la réponse IFN de type I ? (2) La Viperin de poisson est-elle impliquée dans la régulation d'autres voies métaboliques/fonctionnelles ?

Pour répondre à ces interrogations, nous avons développé et validé une lignée cellulaire clonale de type épithélial, dérivant du poisson tête-de-boule (*Pimephales promelas*), dans laquelle le gène *viperin* a été invalidé par édition du génome.

Afin d'obtenir une vue d'ensemble de la réponse transcriptionnelle différentielle entre les lignées cellulaires *viperin*<sup>-/-</sup> et sauvages, nous avons effectué une analyse comparative du transcriptome des deux lignées cellulaires avec ou sans une stimulation de 24h avec de l'IFN de type I recombinant du poisson tête-de-boule. Notre analyse transcriptomique montre que, dans ce type cellulaire, la Viperin n'est pas impliquée dans la régulation de la réponse IFN de type I canonique, ce qui laisse supposer que, dans ce type cellulaire, la Viperin est essentiellement un effecteur du système IFN. En revanche, nos données indiquent que la Viperin agit comme un régulateur négatif de la réponse inflammatoire, en limitant l'expression de gène pro-inflammatoires spécifiques en cas de stimulation par l'IFN de type I et en promouvant l'expression de régulateurs négatifs de l'activation de NF- $\kappa$ B en conditions contrôles. En outre, il semblerait que la Viperin ait une fonction régulatrice dans d'autres processus

métaboliques tels que l'organisation de la matrice extracellulaire, l'adhésion cellulaire, la formation osseuse et le métabolisme un carbone et ce, même en conditions non-induites (**Figure 45**). Ces résultats soutiennent la notion émergente selon laquelle la Viperin pourrait jouer un rôle dans les processus métaboliques au-delà de la réponse antivirale.

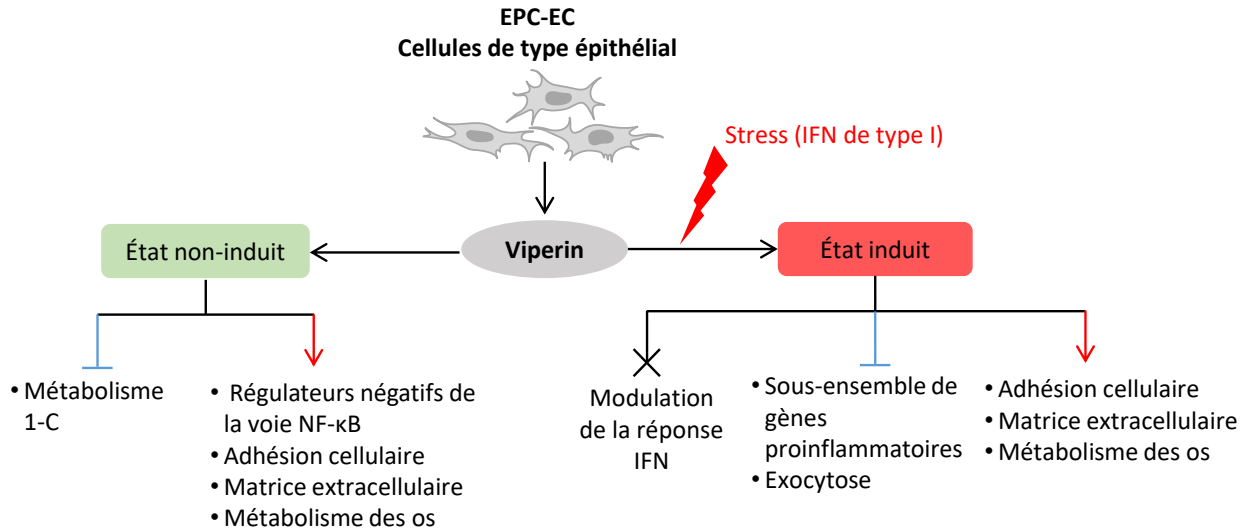


**Figure 45 :** Schéma-bilan des différentes voies régulées par la Viperin à l'échelle transcriptionnelle dans les cellules de poisson tête-de-boule de type épithélial

### 3. 3. Caractérisation de lignées cellulaires infectées de façon persistante avec l'IPNV

Au cours du processus de développement de lignées cellulaires *pkr*<sup>-/-</sup> initiales, deux lignées de saumon Chinook se sont révélées être infectées de façon persistante par le virus de la nécrose pancréatique infectieuse (VNPI), vraisemblablement suite à une contamination accidentelle. Nous avons donc entrepris de caractériser ces lignées cellulaires infectées au cours de 40 passages. Notre étude indique que les deux lignées cellulaires présentent toutes les caractéristiques canoniques des cellules infectées de manière persistante, à savoir une morphologie similaire aux cellules exemptes de virus, une croissance continue, une production continue de virions infectieux au cours des passages, une résistance à une surinfection avec différentes souches de virus homologues tout en restant susceptibles à une infection par des virus hétérologues.

Nous avons également observé la présence d'oscillations périodiques des titres viraux extracellulaires et des niveaux intracellulaires d'ARN viral au cours des passages (**Figure 46**). Nos résultats suggèrent en outre que la réponse IFN de type I de l'hôte n'est pas déclenchée pendant l'infection persistante. Il semblerait donc que le VNPI persistant ait développé des stratégies pour échapper à la réponse immunitaire innée de l'hôte, tout en maintenant un faible niveau de réplication.

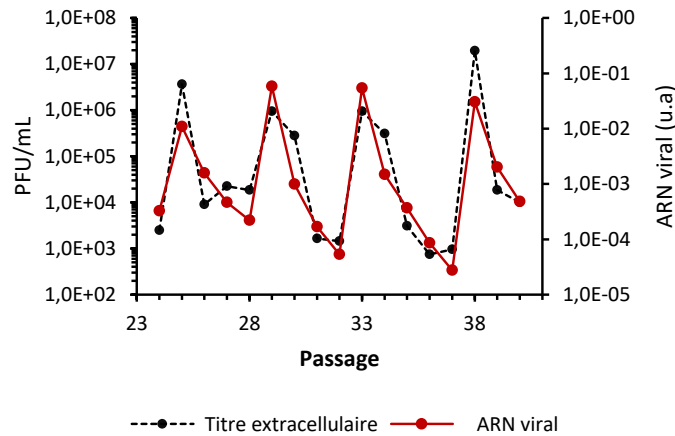


**Figure 46: Le niveau intracellulaire d'ARN viral dans les cellules infectées de façon persistante avec le VNPI corrèle avec les titres extracellulaires**

Graphique montrant les titres extracellulaires et le niveau intracellulaire d'ARN viral au cours de 15 passages d'une flasque individuelles de EC<sup>IPNV</sup>. Ce graphique est représentatif des données obtenues avec d'autres flasques individuelles suivies en parallèle.

Ces lignées cellulaires constituent ainsi un modèle idéal pour étudier l'impact d'une infection persistante sur le transcriptome cellulaire et identifier des mécanismes sous-jacents de la persistance virale, mais également explorer la présence de particules défectives interférentes, qui sont peut-être à l'origine des oscillations périodiques observées.

#### 4. Conclusion

Mes travaux de recherche sur le développement et la caractérisation des lignées cellulaires de poissons *pkr*<sup>-/-</sup> et *viperin*<sup>-/-</sup> ont apporté de nouvelles connaissances sur les fonctions moléculaires et régulatrices de deux ISGs clés chez les poissons, à savoir la PKR et la Viperin. Ce travail met également en lumière le potentiel d'action de certains ISGs au-delà de la réponse à l'IFN de type I, comme le montre le rôle de la Viperin dans la modulation de voies métaboliques spécifiques, *a priori* sans rapport avec la réponse antivirale. L'extension de cette approche d'inactivation génique à d'autres ISGs, combinée à diverses techniques de caractérisation, contribuera certainement à approfondir notre compréhension de ce réseau complexe.

---

## APPENDIX 3

# Development and validation of three Chinook salmon *mx* knockout cell lines

---

### 1. Introduction

During the four years of my thesis, in addition to the *pkr*<sup>-/-</sup> and *viperin*<sup>-/-</sup> cell lines, I successfully developed additional knockout cell lines for other ISGs, in particular *mx*<sup>-/-</sup> cell lines.

*Mx* (myxovirus resistance) is another key antiviral effector ISG. *Mx* genes encode IFN-inducible dynamin-like GTPases that have an antiviral effect against a wide array of RNA viruses as well as some DNA viruses<sup>144,642</sup>. Mechanistically, Mx proteins were found to inhibit viral replication *via* distinct mechanisms of action depending on the virus<sup>642</sup>. According to the current mechanistic model, Mx proteins oligomerize around viral nucleocapsids, leading to sequestration of targeted components into aggregates, blockade of nuclear translocation and/or disruption of their functional integrity<sup>642,643</sup>.

Two *mx* genes are usually present in the genome of mammalian species<sup>144</sup>. In fish, the number of *mx* paralogs dramatically varies from one species to another: while *mx* genes appear to be lost in Gadiformes fish<sup>644</sup>, only one *mx* gene was found in Tetraodontiformes fish<sup>14,645</sup>. In contrast, diploid cyprinids, such as zebrafish, have up to 8 *mx* paralogs, while 6 to 10 *mx* genes have been found in salmonids<sup>14</sup>. In salmonids, the *mx* genes reside in four distinct chromosomal loci, that cluster together into separate phylogenetic clades (**Figure 47**). Interestingly, Atlantic salmon *mx* genes seem to respond differently to IFNs, with *mx1-3* (Chr12) and *mx4-8* (Chr25) being primarily induced by type I and type II IFNs, respectively<sup>646</sup>. Wang *et al.* (2019) further confirmed that *mx* genes can be induced in a cytokine- and cell line-dependent manner<sup>14</sup>. In addition, the antiviral activity of salmonid Mx proteins was established for Atlantic salmon Mx1 against IPNV<sup>647</sup> and rainbow trout Mx1<sup>648</sup>.

During my thesis, I was able to develop all the tools needed to study the function of Chinook salmon *mx1-3* genes, which are all clustered together on Chr2. The purpose of this additional chapter is to summarize the development and validation processes of Chinook salmon *mx1-3* expression vectors as well as a collection of *mx*<sup>-/-</sup> cell lines (single, double, triple mutants).



The sgRNAs were synthesized using the T7 RiboMAX™ Express Large Scale RNA Production System kit (Promega) using 0.5 µg of each primer, incubated with 1 µL of RQ1 DNase (Promega) for 1h at 37°C and purified using TRIzol™ reagent (Invitrogen), according to the manufacturers' instructions. The sgRNAs were resuspended in RNase- and DNase-free water and quantified using a Nanodrop spectrophotometer. The purity of the sgRNAs was checked on a 2% agarose-EtBr gel before or after a 30 min treatment with RNase A (Qiagen) at room temperature. Each sgRNA was mixed with recombinant TrueCut™ Cas9 Protein v2 (Invitrogen) at a 1:1 molar ratio (0.2 µg sgRNA and 1 µg rCas9 *i.e.* 6.1 pmol each in 2 µL) and incubated at room temperature for 20 min. For single mutants, the sgRNA-mEGFP/Cas9 complex was mixed with each sgRNA-Mx/Cas9 complex at 1:1 volume ratio in resuspension buffer R (Neon™ Transfection System kit, Invitrogen); for double or triple mutants, the sgRNA-mEGFP/Cas9 complex was mixed with combinations of sgRNA-Mx/Cas9 complex at 2:1:1 volume ratio in resuspension buffer R. The mix was transfected into EC cells using the Neon™ Transfection System (Invitrogen): EC cells were prepared as described in [Section 2. 4](#) and 5 µL of cell suspension at  $2 \times 10^7$  cells/mL was mixed with 5 µL of sgRNA/Cas9 complex. The cells were transfected using the same conditions established for plasmids, as described in [Section 2. 4](#). All transfected cells ( $\sim 5 \times 10^5$  cells) were mixed in 5 mL L-15+10% FBS+P/S in a 25 cm<sup>2</sup> flask (Sarstedt) and incubated at 20°C for 3-4 weeks.

Once the cell population reached confluency, the transfected cells were passaged (surface ratio 1:4), and  $\sim 2 \times 10^6$  cells were used for genomic DNA extraction using NucleoSpin Tissue Mini kit (Macherey-Nagel), according to the manufacturer's instructions. Genomic DNA segments containing the targeted sites were amplified by PCR using GoTaq® G2 Flexi DNA Polymerase (Promega) using the following genotyping primers: Mx1-gen-F/Mx1-gen-R for *mx1*, and Mx2ab-gen-F/Mx2ab-gen-R for *mx2a* and *mx2b*, and Mx3-gen-F/Mx3-gen-R for *mx3* ([Table X](#)). The PCR cycling program was performed in a thermal cycler (Eppendorf) and was as follows: 94°C for 3 min then 35 cycles of 94°C for 15 s, 56°C for 15 sec, 72°C for 40 sec, and a final extension of 72°C for 5 min. The PCR products were purified using NucleoSpin Gel and PCR Clean-up Mini kit (Macherey-Nagel) and directly sequenced (Sanger sequencing service, Eurofins) using the same amplification primers ([Table X](#)). Sequences were analyzed using Synthego ICE analysis tool v3 (Synthego)<sup>600</sup> to assess the percentage of mutated cells in the transfected cell populations (bulks). sgRNA-Mx2d, sgRNA-Mx2d, sgRNA-Mx3b, sgRNA-Mx123 failed to yield genome-edited cells at the targeted sites so only the bulks transfected with sgRNA-Mx1a, sgRNA-Mx3a, sgRNA-Mx12, sgRNA-Mx1a+sgRNA3a and sgRNA-Mx12+sgRNA-Mx3a were further used for clonal isolation.

Transfected cells were manually isolated except cells transfected with sgRNA-Mx3a; which were sorted by FACS. For manual isolation,  $\sim 1 \times 10^5$  cells were seeded in a 6-well plate and serially diluted

(6-fold dilutions) in duplicates. Three to four weeks post-seeding, clonal cell patches were marked, analyzed under a fluorescent Axio Observer Z1 microscope (Zeiss, Oberkochen, Germany) and for each condition, ~50 mEGFP-deficient clones were selected, detached mechanically by scraping with a pipette tip and sub-cultured into 48-well plates. After 3-4 weeks, ~20 clones were sub-cultured and propagated in 25 cm<sup>2</sup> flasks and their genotype was characterized as described above. For FACS-sorted clones, cells were detached by trypsin-EDTA action and mEGFP-deficient single cells at a density of ~4 x 10<sup>6</sup> cells/mL were individualized by a BD FACSAria™ Fusion Flow Cytometer (Institut Pasteur, Paris, France) using a 100 µm duct into a 96-well plate (Sarstedt) in L-15 supplemented with 10% FBS, penicillin (200 U/mL)-streptomycin (200 µg/mL), 500 µg/mL G418 and 30 µg/mL hygromycin B Gold. Four weeks later, clones were sub-cultured and propagated in 25 cm<sup>2</sup> flasks and their genotype was characterized as described above.

The following clones were kept for knockout validation by western blot and further study: *mx1*<sup>-/-</sup> EC-Mx1a-C8 and -C13; *mx3*<sup>-/-</sup> EC-Mx3a-C12 and -C18, *mx1*<sup>-/-</sup> *mx2ab*<sup>-/-</sup> EC-Mx12-C7 and -C16, *mx1*<sup>-/-</sup> *mx3*<sup>-/-</sup> EC-Mx1a+3a-C15, *mx1*<sup>-/-</sup> *mx2ab*<sup>-/-</sup> *mx3*<sup>-/-</sup> EC-Mx12-C7-C7, EC-Mx12-C16-C18 and EC-Mx12+3a-C21. Of note, EC-Mx12-C7-C7 and EC-Mx12-C16-C18 were developed by transfecting EC-Mx12-C7 and EC-Mx12-C16 with sgRNA-Mx3a previously obtained and blindly screening manually isolated clones. An mGFP-deficient WT clone, EC-Mx12-C6, presenting no mutation for *mx1*, *mx2* or *mx3*, was also kept as an additional control. The mutated sequences and corresponding chromatograms are available in as supplementary material.

### 2. 3. Plasmid constructions

The Chinook salmon *mx* open reading frame (ORF) sequences were identified *in silico* using NCBI Reference Otsh\_v2.0 Primary Assembly and the following predicted transcripts were used for molecular cloning: XM\_024415949.2 for *mx1* (LOC112247236), XM\_042295559.1 for *mx2a* (LOC112247237), XM\_042295553.1 for *mx2b* (LOC121839060), XM\_024415946.2 for *mx3* (LOC112247235).

Total RNA from 1.5 x 10<sup>6</sup> EC cells stimulated for 48h with *Salmo salar* ssIFNA2 supernatant diluted to 1:10 in L-15+2% FBS+P/S or left untreated in triplicates was extracted using the QiaShredder and RNeasy mini kits (Qiagen) according to the manufacturer's instructions. RNA (1 µg) was used as template for reverse transcription and generation of cDNA using the QuantiTect Reverse Transcription kit (Qiagen) with random primers.

The cDNA was diluted two-fold with RNase-free water, triplicates were pooled and used as template to amplify the CDS sequences of *mx1*, *mx2ab* and *mx3*. Nested PCR amplifications were performed using Q5 2X High-Fidelity mastermix (New England Biolabs) and 2 sets of specific primers

according to the manufacturer's instructions: for the first PCR round, OtMx1-R0-F/ OtMx1-R0-R, OtMx2-R0-F/OtMx2-R0-R and OtMx3-R0-F/OtMx3-R0-R were used to amplify *mx1*, *mx2ab* and *mx3*, respectively; for the second PCR round, OtMx1-P2A-F/OtMx13-HindIII-R, OtMx2-P2A-F/OtMx2-HindIII-R and OtMx3-P2A-F/OtMx13-HindIII-R were used to amplify *mx1*, *mx2ab* and *mx3* (**Table X**). The PCR cycling programs were performed in a thermal cycler (Eppendorf) and were as follows: 98°C for 30 sec followed by 40 cycles of 98°C for 10 s, 65°C for 10 sec (1<sup>st</sup> round) or 60°C for 15 sec (2<sup>nd</sup> round), 72°C for 90 sec (1<sup>st</sup> round) or 75 sec (2<sup>nd</sup> round), and a final extension of 72°C for 2 min. DNA fragments of interest were excised from agarose gel and purified with NucleoSpin Gel and PCR Clean-up Mini kit (Macherey-Nagel). Purified PCR products were digested with HindIII enzymes (ThermoFisher), cloned into HindIII/EcoRV-digested pcDNA3.1-Pur-BFP vectors using T4 DNA ligase (New England Biolabs) according to the manufacturer's instructions and fully sequenced. It should be noted that only *mx2a* (LOC112247237) was amplified by PCR, although the primers were designed for both *mx3a* and *mx2b*, suggesting that *mx2b* is not expressed or not induced following IFNA2 stimulation in EC cells. All plasmids were produced in Stellar<sup>TM</sup> Competent Cells (Takara) and were purified using NucleoBond Xtra Maxi EF (Macherey-Nagel) according to the manufacturer's instructions.

## 2. 4. Transfections

Transfections were performed by electroporation using the Neon<sup>TM</sup> Transfection System (Invitrogen) as described in **Results 1**. Briefly, the cells were washed in DPBS (Sigma-Aldrich), detached by trypsin-EDTA action, resuspended in L-15+10% FBS+P/S and centrifuged at 400 g for 5 min. The cell pellet was drained, resuspended in L-15 without Phenol Red (Gibco), centrifuged at 13 000g for 30 sec, and resuspended again in L-15 without Phenol Red. The cell concentration was adjusted to  $2 \times 10^7$  cells/mL. The cell suspension was mixed with *mx1*-, *mx2* or *mx3*-rescue plasmids to reach a final concentration of 0.5  $\mu$ g/ $1 \times 10^5$  cells/10  $\mu$ L of transfection reaction. A fluorescent vector (pcDNA3.1-Hyg-RFP-KDEL) was added to verify transfection efficiency between each condition. Transfections were carried out in an electroporator MPK5000 (Neon<sup>TM</sup> Transfection System, Invitrogen) using either the 100  $\mu$ L transfection kit (Neon<sup>TM</sup> Transfection System, Invitrogen) set to two pulses for 20 ms at 1300 V. All transfected cells were mixed in L-15+10% FBS+P/S, split into plates and incubated at 20°C for 48h.

## 2. 5. Immunoblotting

*mx*<sup>-/-</sup> clones and the WT EC cell line were seeded into 6-well plates at a density of  $1.2 \times 10^6$  cells/well in L-15+2% FBS+P/S and incubated at 20°C overnight. The next day, cells were stimulated in triplicates with *Salmo salar* IFNA2 supernatant diluted to 1:10 in L-15+2% FBS+P/S or left untreated

and incubated at 20°C. At 72h post-stimulation, medium was removed, cells were washed once with ice-cold DPBS, scraped in 1 mL ice-cold DPBS supplemented with 2.5 mM EDTA and centrifuged at 1500 g at 4°C for 5 min. The cell pellets were drained, resuspended in 100 µL NP-40 lysis buffer (50 mM Tris-HCl pH 7.4, 150 mM NaCl, 2 mM EDTA, 0.5% NP40, 1 mM DTT, 10% glycerol, cOmplete™ protease inhibitor (Merck)) and lysed for 45 min at 4°C under gentle shaking. The cell lysates were clarified by centrifugation at 5000 g at 4°C for 5 min and stored at -80°C until use.

Aliquots of 60 µL of cell lysates were mixed with 30 µL Laemmli buffer (45 mM Tris, 345 mM glycine, 38% glycerol, 4.8% SDS, 20% β-mercaptoethanol, 0.04% bromophenol blue) and incubated at 100°C for 5 min. A volume of 8 µL of cell lysates was loaded onto 10% polyacrylamide gels and protein samples were separated by electrophoresis in Tris-glycine buffer (25 mM Tris, 192 mM glycine, pH 8,3). Proteins were then transferred onto a nitrocellulose membrane (BioRad) using the mixed molecular weight program from the Trans-Blot® Turbo™ Transfer System (BioRad). The blots were blocked with 5% non-fat milk in TBST (10 mM Tris pH 7.4, 150 mM NaCl, 0.1% Tween 20) for 1h at room temperature and then incubated with rabbit anti-Mx123 antiserum (1:2000, TBST+5% non-fat milk) overnight at 4°C. Rabbit anti-Mx123 antibody was a generous gift from Dr. Marta Alonso-Hearn (Department of Animal Health, NEIKER-Basque Institute for Agricultural Research and Development, Basque Research and Technology Alliance, Derio, Spain) and Pr. Jorunn Jorgensen (UiT The Arctic University of Norway, Tromsø, Norway). The blots were washed 5 times in TBST, incubated with horseradish peroxidase (HRP)-conjugated anti-rabbit (1:4000) secondary antibodies (SeraCare), washed 4 times in TBST and once in PBS. Western blots were developed using Clarity™ Western ECL substrate (BioRad) and detected using ChemiDoc Touch Imaging System (BioRad). After the first detection, the membrane was washed twice with TBST, stripped for 15 min at 37°C using Restore™ Plus buffer (Thermo Scientific), washed twice in TBST, saturated with TBST-5% non-fat milk for 1h and re-probed with mouse monoclonal anti-α-tubulin antibody (1:3000, TBST+5% non-fat milk, T9026, Sigma Aldrich) for 2.5h-3h and developed as described above.

## 2. 6. rVHSV-Tomato fluorescence monitoring

The replication of rVHSV-Tomato in infected cell lines was monitored by sequential fluorescence measurement. WT EC, *mx1*<sup>-/-</sup> *mx2*<sup>-/-</sup> *mx3*<sup>-/-</sup> EC-Mx12-C7-Mx3a-C7, EC-Mx12-C16-Mx3a-C18 and EC-Mx12+3a-C21 cells were seeded in 96-well plates to a final density of 5 x 10<sup>4</sup> cells/well in L-15+2% heat-inactivated FBS+P/S and incubated overnight at 20°C. The next day, the medium was removed and the cells were infected in octuplicates with 100 µL of rVHSV-Tomato diluted in L-15 without Phenol Red (Gibco)+2% heat-inactivated FBS+P/S to reach MOI 0.1, 1 or 10 or left uninfected. At 24, 32, 48, 56, 72, 80 and 96h post-infection, the tomato red fluorescence was

measured using a fluorometer (Tecan Infinite M200PRO) with excitation and emission wavelengths of 548 and 593 nm, respectively. The fluorescence values were corrected by subtracting the mean values obtained from the non-infected wells.

### 3. Results

#### 3.1. Mx1-3 are expressed in EC cells following IFNA2 stimulation

The expression of *mx1-3* genes was examined in EC cells following IFNA2 stimulation for 30h using RNA-Seq data from Dehler *et al.*<sup>136</sup>. In this study, reads were mapped onto rainbow trout genome (NCBI RefSeq assembly GCF\_002163495.1, Omyk\_1.0) so rainbow trout orthologs of Chinook salmon *mx1-3* were used to search the data (Figure 48A). It appeared that *mx1*, *mx2* and *mx3* were all induced following IFNA2 stimulation, *mx3* being the one with the highest fold change (Figure 48B).

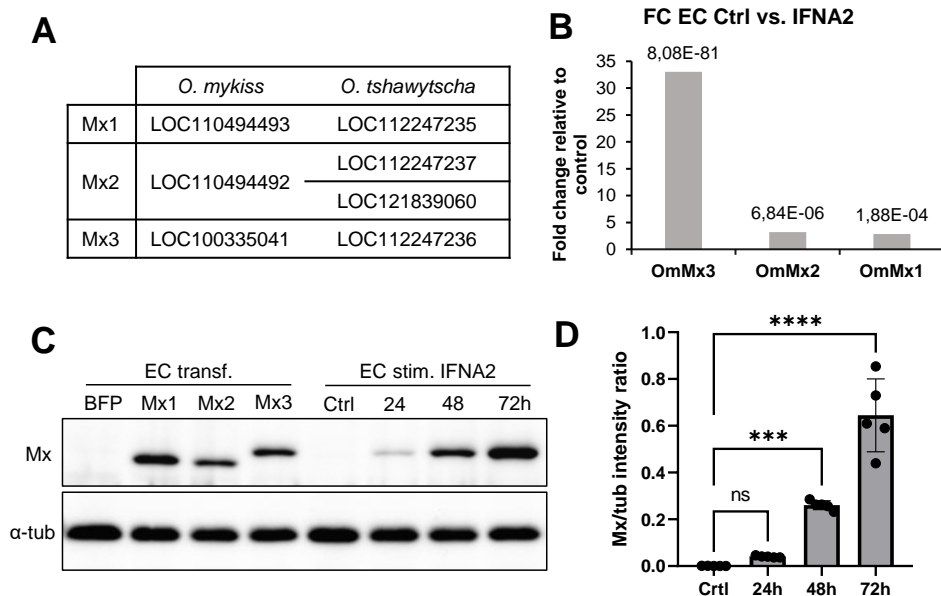


**Figure 48: mx1-3 genes are induced in EC cells following IFNA2 stimulation.**

(A) *mx1-3* genes in rainbow trout (*O. mykiss*) and the corresponding orthologs in Chinook salmon (*O. tshawytscha*) based on the nomenclature from Wang *et al.*<sup>14</sup>. (B) Expression fold change of *mx1-3* genes in EC cells stimulated with IFNA2 for 30h, retrieved by searching RNA-Seq data from Dehler *et al.*<sup>136</sup>. (C) EC cells were stimulated with *S. salar* IFNA2 supernatant for (24-72h) left untreated (Ctrl). Negative and positive controls are EC cells transfected with pcDNA3.1-Pur-BFP or plasmids encoding *mx1*, *mx2* or *mx3*, respectively. Cell lysates were separated by SDS-PAGE and immunoblotted with antibodies against *O. mykiss* Mx1-3 and  $\alpha$ -tubulin ( $\alpha$ -tub). (D) Densitometric quantification of (C). Mx signal intensity normalized to  $\alpha$ -tubulin signal intensity. Bars show means  $\pm$  SD from 3 pooled independent experiments (n=1 or n=3 for each experiment); ns, non-significant, \*\*\*,  $p < 0.001$ , \*\*\*\*,  $p < 0.0001$ , ordinary one-way ANOVA with Tukey's post-hoc multiple comparison tests.

The expression profile of Mx1-3 proteins was characterized by western blot in EC cells stimulated with recombinant *Salmo salar* IFNA2 supernatant (Figure 48C,D). Detection of Mx1-3 proteins was

performed using a custom-made rabbit polyclonal antibody raised against a 115-aa polypeptide from *O. mykiss* Mx3<sup>649</sup>. Importantly, the fragment is located in a highly conserved region of Mx1-3 proteins and differs by only 2 aa from Mx1 and by 9 aa from Mx2; in addition, it was reported to detect all three *O. mykiss* Mx1-3 proteins<sup>649</sup>. Similarly, recombinant Mx1-3 proteins expressed in EC cells were detected by western blot, as shown in **Figure 48C**. The expression of endogenous Mx proteins was also significantly induced in IFNA2-stimulated cells at 48h and 72h post-stimulation. Interestingly, it seems that Mx3 is primarily detected in these cells, which is consistent with *mx3* transcript expression fold change from the RNA-Seq data.

Taken together, these data confirm the ISG status of *mx1-3* genes in EC cells and support the use of this cell line for the development of *mx*<sup>-/-</sup> cell lines.

### 3. 2. Genotyping of EC-Mx clones

We developed single, double or triple *mx* KO cell lines, by disrupting *mx1* (LOC112247236), *mx2ab* (LOC112247237, LOC121839060) and/or *mx3* (LOC112247235) genes in EC cells, using CRISPR/Cas9 technology (**Table IX**).

The following clones were kept for further study: *mx1*<sup>-/-</sup> EC-Mx1a-C8 and EC-Mx1a-C13, both presenting a 1-nt insertion (48\_49insA) in at the targeted cut site in *mx1* resulting in a frameshift and the introduction of a premature stop codon at position 63 (N17fsX63); *mx3*<sup>-/-</sup> EC-Mx3a-C12 and EC-Mx3a-C18, presenting a 1-nt insertion (48\_49insA, N17fsX94) and a 2-nt deletion in *mx3* (49\_50delAT, R17fsX93), respectively, respectively; *mx1*<sup>-/-</sup> *mx2ab*<sup>-/-</sup> EC-Mx12-C7, presenting a 1-nt deletion in *mx1* (75delC, A27fsX28) and a 1-nt deletion in *mx2ab* (75delC, A27fsX28); *mx1*<sup>-/-</sup> *mx2ab*<sup>-/-</sup> EC-Mx12-C16, presenting a 5-nt deletion in *mx1* (71\_75delGCTCC, P24fsX61) and a heterozygous 1-nt/10-nt deletion in *mx2ab* (75delC, A27fsX28 / 67\_76delCTACGCTCCC, A24fsX25); *mx1*<sup>-/-</sup> *mx3*<sup>-/-</sup> EC-Mx1a+3a-C15, presenting a 1-nt insertion in *mx1* (48\_49insA, N17fsX63) and a heterozygous indel in *mx3* (49\_50delAT, R17fsX93 / 48\_49insA, N17fsX94); *mx1*<sup>-/-</sup> *mx2ab*<sup>-/-</sup> *mx3*<sup>-/-</sup> EC-Mx12+3a-C21, presenting a 1-nt deletion in *mx1* (75delC, A27fsX28), a heterozygous indel in *mx2ab* (72\_76delCTCCC, P24fsX92 / 74\_75insCA H25fsX29) and a 1-nt insertion in *mx3* (48\_49insA, N17fsX94). Two additional *mx1*<sup>-/-</sup> *mx2ab*<sup>-/-</sup> *mx3*<sup>-/-</sup> cell lines were also developed, using *mx1*<sup>-/-</sup> *mx2ab*<sup>-/-</sup> EC-Mx12-C7 and EC-Mx12-C16 as parental cell lines, respectively: EC-Mx12-C7-Mx3a-C7 and EC-Mx12-C16-Mx3a-C18, presenting the same genotype as EC-Mx12-C7 or -C16 for *mx1* and *mx2ab*, respectively, as well as a 2-nt deletion (49\_50delAT, R17fsX93) in *mx3*. One last clone, named EC-Mx12-C6, exhibiting no mutation for *mx1*, *mx2* or *mx3*, was also kept as an additional WT control.

**Table IX: Genotypes of EC-Mx clones isolated and characterized in this study.**

The mutated sequences and corresponding chromatograms are available in as supplementary material.

Type	Cell line	Clone	Indel		
			Mx1	Mx2ab	Mx3
WT	WT	EC-Mx12-C6	WT	WT	WT
Single mutants	EC-Mx1	EC-Mx1a-C8	+1 48_49insA N17fsX63	WT	WT
		EC-Mx1a-C13	+1 48_49insA N17fsX63	WT	WT
	EC-Mx3	EC-Mx3a-C12	WT	WT	+1 48_49insA N17fsX94
		EC-Mx3a-C18	WT	WT	-2 49_50delAT R17fsX93
Double mutants	EC-Mx12	EC-Mx12-C7	-1 75delC A27fsX28	-1 75delC A27fsX28	WT
		EC-Mx12-C16	-5 71_75delGCTC C P24fsX61	-1/-10 75delC 67_76delCTACGCTCC C A27fsX28 A24fsX25	WT
	EC-Mx13	EC-Mx1a+3a-C15	+1 48_49insA N17fsX63	WT	-2/+1 49_50delAT 48_49insA R17fsX93 N17fsX94
Triple mutants	EC-Mx123	EC-Mx12-C7-Mx3a-C7	-1 75delC A27fsX28	-1 75delC A27fsX28	-2 49_50delAT R17fsX93
		EC-Mx12-C16-Mx3a-C18	-5 71_75delGCTC C P24fsX61	-1/-10 75delC 67_76delCTACGCTCC C A27fsX28 A24fsX25	-2 49_50delAT R17fsX93
		EC-Mx12+3a-C21	-1 75delC A27fsX28	-5/+2 72_76delCTCCC 74_75insCA P24fsX92 H25fsX29	+1 48_49insA N17fsX94

### 3. 3. Validation of Mx1, Mx2 and Mx3 expression disruption by western blot

Previous experiments (Figure 48) showed that IFNA2 was a fast and potent inducer of Mx in EC cells. The expression status of Mx in each  $mx^{-/-}$  clone was therefore assessed by western blot using recombinant *Salmo salar* IFNA2 supernatant as an inducer. Our results indicate that a band the size of Mx3 was strongly expressed in WT EC cells, as well as in  $mx1^{-/-}$  EC-Mx1a-C13,  $mx1^{-/-} mx2ab^{-/-}$  EC-Mx12-C7 and -C16, to a lesser extent. A band corresponding to Mx1 was detected in  $mx3^{-/-}$  cell lines, while a band the size of Mx2 was expressed in  $mx1^{-/-} mx3^{-/-}$  EC-Mx1a+3a-C15 cells. No expression of Mx1-3 was detected in  $mx1^{-/-} mx2ab^{-/-} mx3^{-/-}$  cells (Figure 49). These results suggest the existence of compensatory expression patterns of the *mx* genes, with the following expression order: Mx3 > Mx1 > Mx2.

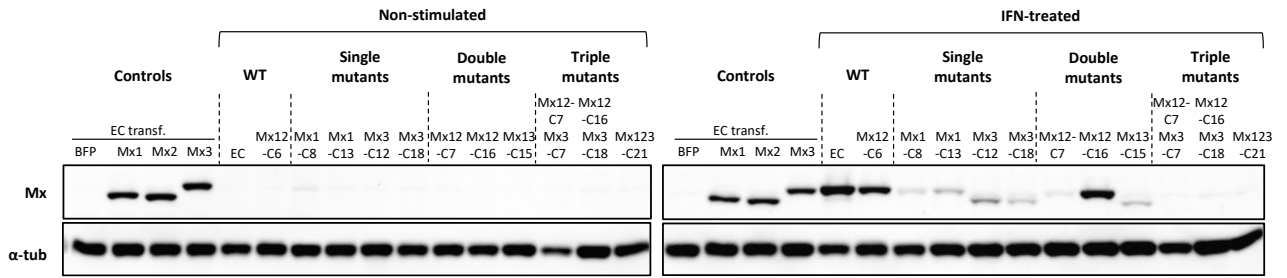


**Figure 49: Development and validation of *mx*<sup>-/-</sup> cell lines**

EC and EC-Mx clones were stimulated with *S. salar* IFNA2 supernatant for 72h; positive and negative controls are EC cells transfected with pcDNA3.1-Pur-BFP or pcDNA3.1-Pur-BFP-P2A-Mx1, -Mx2 and -Mx3, respectively. Cell lysates were separated by SDS-PAGE and immunoblotted with antibodies against Mx and  $\alpha$ -tubulin ( $\alpha$ -tub).

### 3. 4. Preliminary tests suggest that triple Mx mutants are more permissive to rVHSV-Tomato infection

The antiviral role of endogenous Mx against VHSV was investigated by monitoring the replication of rVHSV-Tomato. This recombinant virus contains an tdTomato-encoding expression cassette inserted in its genome<sup>650</sup>. The tdTomato protein is only expressed during its replication cycle and the tdTomato fluorescence can be used as a non-invasive marker of viral replication. The fluorescence intensity was sequentially measured in WT EC cells and in three *mx1*<sup>-/-</sup> *mx2ab*<sup>-/-</sup> *mx3*<sup>-/-</sup> clones from 24h to 96h post-infection. The fluorescence signal was higher in *mx*<sup>-/-</sup> cell lines compared to WT EC cells, particularly at MOI 1 and MOI 0.1, suggesting that the triple *mx* knockout favored the replication of rVHSV-Tomato (Figure 50).

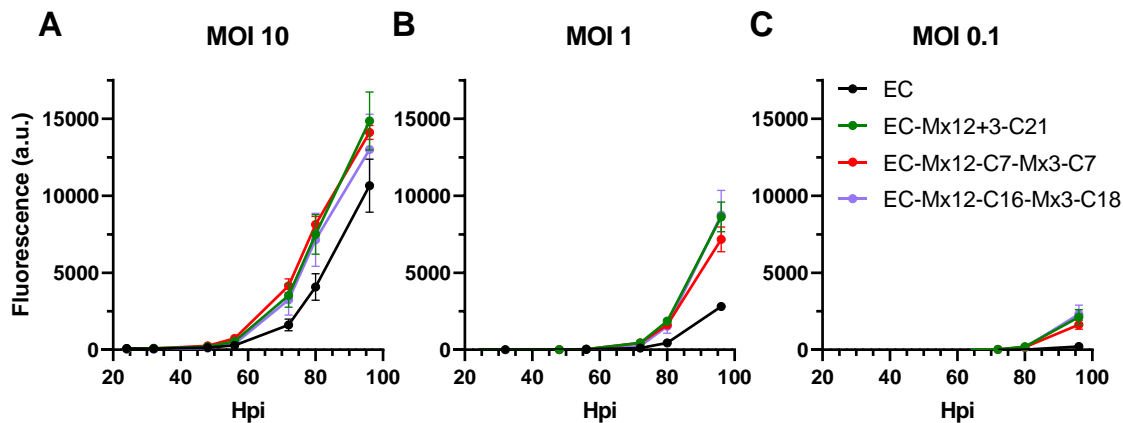


**Figure 50: rVHSV-Tomato replicates better in *mx1*<sup>-/-</sup> *mx2*<sup>-/-</sup> *mx3*<sup>-/-</sup> cell lines than WT EC cell line**

EC (WT), EC-Mx12+3a-C21, EC-Mx12-C7-Mx3-C7 and EC-Mx12-C16-Mx3-C18 (*mx1*<sup>-/-</sup> *mx2*<sup>-/-</sup> *mx3*<sup>-/-</sup>) cells were infected with rVHSV-Tomato at (A) MOI 10, (B) MOI 1 or (C) MOI 0.1 and fluorescence was measured at different time points post-infection. Graphs show means  $\pm$  SD from one experiment (n=8).

## 4. Conclusion and perspectives

During my thesis, I was able to develop all the tools needed to study the role of 3 Mx genes using overexpression and knockout approaches. The next step will be to functionally characterize these cell lines, in particular their permissivity to various viral infections. The single, double or triple *mx* KO cell lines are also a good tool for studying in detail the additive and/or complementary effects of different paralogous genes.

## 5. Supplementary data

**Table X: Primers used in this study**

Green boxes indicate sgRNAs that gave rise to mutated bulks while orange boxes indicate the ones that failed and were not further used.

Primer name	Sequence (5'→3')	Source reference	or	Specificities	Worked ?
<b>sgRNA:</b>					
sgRNA-mEGFP-S	<u>TCCTAATACGACTCACTATA</u> GGCGAGGGCG ATGCCACCTAGTTTTAGAGCTAGAAATAGC AAGTTAAAATAAGGCTAGTCCGTTATCAAC TTGAAAAAGTGGCACCAGTCCGGTGCTTTT	555		T7 promoter sgRNA target Scaffold	Yes
sgRNA-mEGFP-AS	AAAAGCACCGACTCGGTGCCACTTTTTCAA GTTGATAACGGACTAGCCTTATTTAACTT GCTATTTCTAGCTCTAAAACCTAGGTGGCAT CGCCCTCGCC <u>TATAGTGAGTCGTATTAGGA</u>	555		T7 promoter sgRNA target Scaffold	Yes
sgRNA-Mx1a-S	<u>TCCTAATACGACTCACTATA</u> AGAGTCGATGA GGTCGATACAGTTTTAGAGCTAGAAATAGC AAGTTAAAATAAGGCTAGTCCGTTATCAAC TTGAAAAAGTGGCACCAGTCCGGTGCTTTT	LOC112247236		T7 promoter sgRNA target Scaffold	Yes
sgRNA-Mx1a-AS	AAAAGCACCGACTCGGTGCCACTTTTTCAA GTTGATAACGGACTAGCCTTATTTAACTT GCTATTTCTAGCTCTAAAACCTGTATCGACC TCATCGACTC <u>TATAGTGAGTCGTATTAGGA</u>	LOC112247236		T7 promoter sgRNA target Scaffold	Yes
sgRNA-Mx1b-S	<u>TCCTAATACGACTCACTATA</u> TTCCGGGGAAG AGCTCCGTGTGTTTTAGAGCTAGAAATAGC AAGTTAAAATAAGGCTAGTCCGTTATCAAC TTGAAAAAGTGGCACCAGTCCGGTGCTTTT	LOC112247236		T7 promoter sgRNA target Scaffold	No
sgRNA-Mx1b-AS	AAAAGCACCGACTCGGTGCCACTTTTTCAA GTTGATAACGGACTAGCCTTATTTAACTT GCTATTTCTAGCTCTAAAACACACGGAGCT CTTCCCGAA <u>TATAGTGAGTCGTATTAGGA</u>	LOC112247236		T7 promoter sgRNA target Scaffold	No
sgRNA-Mx2d-S	<u>TCCTAATACGACTCACTATA</u> TGGCTTTGCC AAGTTGTCCGGTTTTAGAGCTAGAAATAGC AAGTTAAAATAAGGCTAGTCCGTTATCAAC TTGAAAAAGTGGCACCAGTCCGGTGCTTTT	LOC112247237 LOC121839060		T7 promoter sgRNA target Scaffold	No
sgRNA-Mx2d-AS	AAAAGCACCGACTCGGTGCCACTTTTTCAA GTTGATAACGGACTAGCCTTATTTAACTT GCTATTTCTAGCTCTAAAACCCGACAACCT GGCAAAGCCA <u>TATAGTGAGTCGTATTAGGA</u>	LOC112247237 LOC121839060		T7 promoter sgRNA target Scaffold	No
sgRNA-Mx2e-S	<u>TCCTAATACGACTCACTATA</u> TTCCGGGAAAG AGCTCCGTGCGTTTTAGAGCTAGAAATAGC AAGTTAAAATAAGGCTAGTCCGTTATCAAC TTGAAAAAGTGGCACCAGTCCGGTGCTTTT	LOC112247237 LOC121839060		T7 promoter sgRNA target Scaffold	No
sgRNA-Mx2e-AS	AAAAGCACCGACTCGGTGCCACTTTTTCAA GTTGATAACGGACTAGCCTTATTTAACTT GCTATTTCTAGCTCTAAAACGCACGGAGCT CTTTCCCGAA <u>TATAGTGAGTCGTATTAGGA</u>	LOC112247237 LOC121839060		T7 promoter sgRNA target Scaffold	No
sgRNA-Mx3a-S	<u>TCCTAATACGACTCACTATA</u> AGAGTCGATAA GGTCTATACAGTTTTAGAGCTAGAAATAGC	LOC112247235		T7 promoter sgRNA target	Yes

Supplementary material – Appendix 3

	AAGTTAAAATAAGGCTAGTCCGTTATCAAC TTGAAAAAGTGGCACCAGTCGGTGCTTTT		<i>Scaffold</i>	
<b>sgRNA-Mx3a-AS</b>	AAAAGCACCGACTCGGTGCCACTTTTTTCAA GTTGATAACGGACTAGCCTATTTTAACTT GCTATTTCTAGCTCTAAAAGTGTATAGACC TTATCGACTCTATAGTGAGTCGTATTAGGA	LOC112247235	<b>T7 promoter</b> <u>sgRNA target</u> <i>Scaffold</i>	<b>Yes</b>
<b>sgRNA-Mx3b-S</b>	TCCTAATACGACTCACTATAATTCGGGAAAG AGCTCGGTGCGTTTTAGAGCTAGAAATAGC AAGTTAAAATAAGGCTAGTCCGTTATCAAC TTGAAAAAGTGGCACCAGTCGGTGCTTTT	LOC112247235	<b>T7 promoter</b> <u>sgRNA target</u> <i>Scaffold</i>	<b>No</b>
<b>sgRNA-Mx3b-AS</b>	TCCTAATACGACTCACTATAATTCGGGAAAG AGCTCGGTGCGTTTTAGAGCTAGAAATAGC AAGTTAAAATAAGGCTAGTCCGTTATCAAC TTGAAAAAGTGGCACCAGTCGGTGCTTTT	LOC112247235	<b>T7 promoter</b> <u>sgRNA target</u> <i>Scaffold</i>	<b>No</b>
<b>sgRNA-Mx12-S</b>	TCCTAATACGACTCACTATAATTCGACTCTC TACGCTCCCTGTTTTAGAGCTAGAAATAGC AAGTTAAAATAAGGCTAGTCCGTTATCAAC TTGAAAAAGTGGCACCAGTCGGTGCTTTT	LOC112247236 LOC112247237 LOC121839060	<b>T7 promoter</b> <u>sgRNA target</u> <i>Scaffold</i>	<b>Yes</b>
<b>sgRNA-Mx12-AS</b>	AAAAGCACCGACTCGGTGCCACTTTTTCAA GTTGATAACGGACTAGCCTATTTTAACTT GCTATTTCTAGCTCTAAAACAGGGAGCGTA GAGAGTCGATATATAGTGAGTCGTATTAGGA	LOC112247236 LOC112247237 LOC121839060	<b>T7 promoter</b> <u>sgRNA target</u> <i>Scaffold</i>	<b>Yes</b>
<b>sgRNA-Mx123-S</b>	TCCTAATACGACTCACTATAATCGCCGTGAT AGGGACCAGGTTTTAGAGCTAGAAATAGC AAGTTAAAATAAGGCTAGTCCGTTATCAAC TTGAAAAAGTGGCACCAGTCGGTGCTTTT	LOC112247236 LOC112247237 LOC121839060 LOC112247235	<b>T7 promoter</b> <u>sgRNA target</u> <i>Scaffold</i>	<b>No</b>
<b>sgRNA-Mx123-AS</b>	AAAAGCACCGACTCGGTGCCACTTTTTCAA GTTGATAACGGACTAGCCTATTTTAACTT GCTATTTCTAGCTCTAAAACCTGGTCCCT ATCACGGCGATATATAGTGAGTCGTATTAGGA	LOC112247236 LOC112247237 LOC121839060 LOC112247235	<b>T7 promoter</b> <u>sgRNA target</u> <i>Scaffold</i>	<b>No</b>
<b>Plasmid constructs:</b>				
<b>OtMx1-R0-F</b>	ATCCAGCTTCAGCACTAACTTTC	LOC112247236		
<b>OtMx1-R0-R</b>	AGACTAGCTGCTTGCGTTC	XM_024415949.2		
<b>OtMx2-R0-F</b>	GATCTTGTACAGCCAGTAGTCAG	LOC112247237		
<b>OtMx2-R0-R</b>	CAAACCCCAATGCCTACTTC	XM_042295559.1 LOC121839060 XM_042295553.1		
<b>OtMx3-R0-F</b>	ACGTAAAATCTCCTGTATCGGAGA	LOC112247235		
<b>OtMx3-R0-R</b>	GACCAATCCATCTGGCATTAGTC	XM_024415946.2		
<b>OtMx1-P2A-F</b>	GGAAGCGGAGCTACTAACTTCAGCCTGCTG AAGCAGGCTGGAGACGTGGAGGAGAACCCT GGACCTATGAATAATACGCTGAACCAACAT TAC	LOC112247236 XM_024415949.2	<u>P2A</u>	
<b>OtMx13-HindIII-R</b>	CTGCTGCTGAAGCTTCTAGAACTCCAC TAGGTAGCTG		<u>HindIII</u>	
<b>OtMx2-P2A-F</b>	GGAAGCGGAGCTACTAACTTCAGCCTG CTGAAGCAGGCTGGAGACGTGGAGGAG AACCCCTGGACCTATGAATTATACGCTG AACCAACATTATG	LOC112247237 XM_042295559.1 LOC121839060 XM_042295553.1	<u>P2A</u>	
<b>OtMx2-HindIII-R</b>	CTGCTGCTGAAGCTTCTAGAACTCCAC TAGATAGTTGCG		<u>HindIII</u>	
<b>OtMx3-P2A-F</b>	GGAAGCGGAGCTACTAACTTCAGCCTG CTGAAGCAGGCTGGAGACGTGGAGGAG AACCCCTGGACCTATGAATAACACTCTA AACCAACATTATGAG	LOC112247235 XM_024415946.2	<u>P2A</u>	
<b>Genotyping:</b>				
<b>Mx1-gen-F</b>	CCCAGGAATGATACTCCCTCCG	LOC112247236		
<b>Mx1-gen-R</b>	CCGCTACCCTTGGCAAAGCCAC	LOC112247236		
<b>Mx2ab-gen-F</b>	ATCGCAAATCATGAATTATACGC	LOC112247237 LOC121839060		
<b>Mx2ab-gen-R</b>	ACAGACACTGTGAACACTATAAAC	LOC112247237 LOC121839060		
<b>Mx3-gen-F</b>	ACCGCTTAAGATTCGATTCCCA	LOC112247235		
<b>Mx3-gen-R</b>	TGCATATAAAATGGGTGAACTTCCT	LOC112247235		





**B.**

EC-WT-mx1	MNNTLNQHYEEKVRPCIDLIDSLRSLGVEKDLALPAIAVIGDQSSGKSSVLEALSGVALPRGSGIVTRCPLELKMKRKKEGEEHWGKISYQDREEEIEDPSDVEKKIREAQD (...)	112
EC-Mx12-C6-mx1	MNNTLNQHYEEKVRPCIDLIDSLRSLGVEKDLALPAIAVIGDQSSGKSSVLEALSGVALPRGSGIVTRCPLELKMKRKKEGEEHWGKISYQDREEEIEDPSDVEKKIREAQD (...)	112
EC-Mx1-C8-mx1	MNNTLNQHYEEKVRPCIDLRPHRLSTLPWRREGPCAASHRRDRGPEFGHEELRVGGAVWGGFAKG*	
EC-Mx1-C13-mx1	MNNTLNQHYEEKVRPCIDLRPHRLSTLPWCGEGPCASHRRDRGPEFGHEELRVGGAVWGGFAKG*	
EC-Mx3-C12-mx1	MNNTLNQHYEEKVRPCIDLIDSLRSLGVEKDLALPAIAVIGDQSSGKSSVLEALSGVALPRGSGIVTRCPLELKMKRKKEGEEHWGKISYQDREEEIEDPSDVEKKIREAQD (...)	112
EC-Mx3-C18-mx1	MNNTLNQHYEEKVRPCIDLIDSLRSLGVEKDLALPAIAVIGDQSSGKSSVLEALSGVALPRGSGIVTRCPLELKMKRKKEGEEHWGKISYQDREEEIEDPSDVEKKIREAQD (...)	112
EC-Mx12-C7-mx1	MNNTLNQHYEEKVRPCIDLIDSLRSLA*	
EC-Mx12-C16-mx1	MNNTLNQHYEEKVRPCIDLIDSLA*--WCGEGPCASHRRDRGPEFGHEELRVGGAVWGGFAKG*	
EC-Mx13-C15-mx1	MNNTLNQHYEEKVRPCIDLRPHRLSTLPWCGEGPCASHRRDRGPEFGHEELRVGGAVWGGFAKG*	
EC-Mx123-C7-mx1	MNNTLNQHYEEKVRPCIDLIDSLRSLA*	
EC-Mx123-C18-mx1	MNNTLNQHYEEKVRPCIDLIDSLA*--WCGEGPCASHRRDRGPEFGHEELRVGGAVWGGFAKG*	
EC-Mx123-C21-mx1	MNNTLNQHYEEKVRPCIDLIDSLRSLA*	
	*****	
EC-WT-mx2	MNYTLNQHYYEEKVRPSIDLIDSLRSLGVEKDLALPAIAVIGDQSSGKSSVLEALSGVALPRGSGIVTRCPLELKMKRKKEGEEHWGKISYQDREEEIEDPSDVENKIRKAQD (...)	112
EC-Mx12-C6-mx2	MNYTLNQHYYEEKVRPSIDLIDSLRSLGVEKDLALPAIAVIGDQSSGKSSVLEALSGVALPRGSGIVTRCPLELKMKRKKEGEEHWGKISYQDREEEIEDPSDVENKIRKAQD (...)	112
EC-Mx1-C8-mx2	MNYTLNQHYYEEKVRPSIDLIDSLRSLGVEKDLALPAIAVIGDQSSGKSSVLEALSGVALPRGSGIVTRCPLELKMKRKKEGEEHWGKISYQDREEEIEDPSDVENKIRKAQD (...)	112
EC-Mx1-C13-mx2	MNYTLNQHYYEEKVRPSIDLIDSLRSLGVEKDLALPAIAVIGDQSSGKSSVLEALSGVALPRGSGIVTRCPLELKMKRKKEGEEHWGKISYQDREEEIEDPSDVENKIRKAQD (...)	112
EC-Mx3-C12-mx2	MNYTLNQHYYEEKVRPSIDLIDSLRSLGVEKDLALPAIAVIGDQSSGKSSVLEALSGVALPRGSGIVTRCPLELKMKRKKEGEEHWGKISYQDREEEIEDPSDVENKIRKAQD (...)	112
EC-Mx3-C18-mx2	MNYTLNQHYYEEKVRPSIDLIDSLRSLGVEKDLALPAIAVIGDQSSGKSSVLEALSGVALPRGSGIVTRCPLELKMKRKKEGEEHWGKISYQDREEEIEDPSDVENKIRKAQD (...)	112
EC-Mx12-C7-mx2	MNYTLNQHYYEEKVRPSIDLIDSLRSLA*	
EC-Mx12-C16-mx2-hpt1	MNYTLNQHYYEEKVRPSIDLIDSLRSLA*	
EC-Mx12-C16-mx2-hpt2	MNYTLNQHYYEEKVRPSIDLIDSLA*	
EC-Mx13-C15-mx2	MNYTLNQHYYEEKVRPSIDLIDSLRSLGVEKDLALPAIAVIGDQSSGKSSVLEALSGVALPRGSGIVTRCPLELKMKRKKEGEEHWGKISYQDREEEIEDPSDVENKIRKAQD (...)	112
EC-Mx123-C7-mx2	MNYTLNQHYYEEKVRPSIDLIDSLRSLA*	
EC-Mx123-C18-mx2-hpt1	MNYTLNQHYYEEKVRPSIDLIDSLRSLA*	
EC-Mx123-C18-mx2-hpt2	MNYTLNQHYYEEKVRPSIDLIDSLA*	
EC-Mx123-C21-mx2-hpt1	MNYTLNQHYYEEKVRPSIDLIDSLA*PWRREGPCACHRRDRGPEFGKELRAGGAVWGGFAKGEWYCNTPPRAEDEKEERRRGMARNQLPGP*	
EC-Mx123-C21-mx2-hpt2	MNYTLNQHYYEEKVRPSIDLIDSLRHTLA*	
	*****	
EC-WT-mx3	MNNTLNQHYEEKVRPCIDLIDSLRSLGVEKDLALPAIAVIGDQSSGKSSVLEALSGVALPRGSGIVTRCPLELKMKRKKEGEEHWGKISYQDHEEEIEDPSDVEKKIREAQD (...)	112
EC-Mx12-C6-mx3	MNNTLNQHYEEKVRPCIDLIDSLRSLGVEKDLALPAIAVIGDQSSGKSSVLEALSGVALPRGSGIVTRCPLELKMKRKKEGEEHWGKISYQDHEEEIEDPSDVEKKIREAQD (...)	112
EC-Mx1-C8-mx3	MNNTLNQHYEEKVRPCIDLIDSLRSLGVEKDLALPAIAVIGDQSSGKSSVLEALSGVALPRGSGIVTRCPLELKMKRKKEGEEHWGKISYQDHEEEIEDPSDVEKKIREAQD (...)	112
EC-Mx1-C13-mx3	MNNTLNQHYEEKVRPCIDLIDSLRSLGVEKDLALPAIAVIGDQSSGKSSVLEALSGVALPRGSGIVTRCPLELKMKRKKEGEEHWGKISYQDHEEEIEDPSDVEKKIREAQD (...)	112
EC-Mx3-C12-mx3	MNNTLNQHYEEKVRPCIDLRPYRLPALPWCGEGPCAACHRRDRGPEFGKELGAGGAVWGGFAKGEWYCNTPMSRAEDEEEERRRRMAWKNQLPRP*	
EC-Mx3-C18-mx3	MNNTLNQHYEEKVRPCIDLRPYRLPALPWCGEGPCAACHRRDRGPEFGKELGAGGAVWGGFAKGEWYCNTPMSRAEDEEEERRRRMAWKNQLPRP*	
EC-Mx12-C7-mx3	MNNTLNQHYEEKVRPCIDLIDSLRSLGVEKDLALPAIAVIGDQSSGKSSVLEALSGVALPRGSGIVTRCPLELKMKRKKEGEEHWGKISYQDHEEEIEDPSDVEKKIREAQD (...)	112
EC-Mx12-C16-mx3	MNNTLNQHYEEKVRPCIDLIDSLRSLGVEKDLALPAIAVIGDQSSGKSSVLEALSGVALPRGSGIVTRCPLELKMKRKKEGEEHWGKISYQDHEEEIEDPSDVEKKIREAQD (...)	112
EC-Mx13-C15-mx3-hpt1	MNNTLNQHYEEKVRPCIDLRPYRLPALPWRREGPCAACHRRDRGPEFGKELGAGGAVWGGFAKGEWYCNTPMSRAEDEEEERRRRMAWKNQLPRP*	
EC-Mx13-C15-mx3-hpt2	MNNTLNQHYEEKVRPCIDLRPYRLPALPWRREGPCAACHRRDRGPEFGKELGAGGAVWGGFAKGEWYCNTPMSRAEDEEEERRRRMAWKNQLPRP*	
EC-Mx123-C7-mx3	MNNTLNQHYEEKVRPCIDLRPYRLPALPWCGEGPCAACHRRDRGPEFGKELGAGGAVWGGFAKGEWYCNTPMSRAEDEEEERRRRMAWKNQLPRP*	
EC-Mx123-C18-mx3	MNNTLNQHYEEKVRPCIDLRPYRLPALPWCGEGPCAACHRRDRGPEFGKELGAGGAVWGGFAKGEWYCNTPMSRAEDEEEERRRRMAWKNQLPRP*	
EC-Mx123-C21-mx3	MNNTLNQHYEEKVRPCIDLRPYRLPALPWCGEGPCAACHRRDRGPEFGKELGAGGAVWGGFAKGEWYCNTPMSRAEDEEEERRRRMAWKNQLPRP*	
	*****	

**Figure 52: Genotype of EC cells (WT) and EC-Mx clones obtained from sequencing of purified PCR products amplified from genomic DNA from each cell line (A) and corresponding protein sequences (B)**

(A) The locations of the sgRNA-Mx1a, sgRNA-Mx12 and sgRNA-Mx3a are highlighted in pink, blue and green, respectively; the protospacer adjacent motif is in light grey, the start codon is highlighted red and indels in mutated sequences are in red highlighted in yellow. (B) The first amino acids affected by a frameshift are in black and the premature end of the polypeptides are represented by a purple star.

**A.**

Clones	Geno- typing	Indel	ICE deconvoluted sequences
EC-Mx12-C6	Mx1-gen1-F	WT	<p>EDITED SAMPLE 237 TO 302 BP</p> <p>2000 C G G C C C T G T A T C G A C C T C A T C G A C T C T C T A C C C T C C C T T G G T G T G C A G A A G G A C C T T G C C C T G C C A</p> <p>CONTROL SAMPLE 234 TO 299 BP</p> <p>3000 C G G C C C T G T A T C G A C C T C A T C G A C T C T C T A C C C T C C C T T G G T G T G C A G A A G G A C C T T G C C C T G C C A</p>
	Mx1-gen1-R	WT	<p>EDITED SAMPLE 52 TO 117 BP</p> <p>2000 T G G C T G G C A G G G C A A G G T C C T T T C T C C A C A C C A A G G C A G C C T A G A G A C T C G A T G A G G T C G A T A C A G G</p> <p>CONTROL SAMPLE 50 TO 115 BP</p> <p>2000 T G G C T G G C A G G G C A A G G T C C T T T C T C A C A C C A A G G C A G C C T A G A G A C T C G A T G A G G T C G A T A C A G G</p>
	Mx22bis-gen-R	WT	<p>EDITED SAMPLE 116 TO 181 BP</p> <p>2000 T G G C A G C C A G C C C A A G G T C C T T T C T C T A C C C C A A G G C A G C C T A G A G A C T C G A T G A C T C A A T A C T A G</p> <p>CONTROL SAMPLE 126 TO 191 BP</p> <p>2000 T G G C A G C C A G C C C A A G G T C C T T T C T C T A C C C C A A G G C A G C C T A G A G A C T C G A T G A C T C A A T A C T A G</p>
	Mx3-gen2-F	WT	<p>EDITED SAMPLE 186 TO 251 BP</p> <p>2000 C G T C C C T G T A T A G A C C T T A T G A C T C C C T G C G C T C C C T T G C G T A G A C A A G G A C C T T G C G C T G C C T</p> <p>CONTROL SAMPLE 188 TO 253 BP</p> <p>2000 C G T C C C T G T A T A G A C C T T A T G A C T C C C T G C G C T C C C T T G C G T A G A C A A G G A C C T T G C G C T G C C T</p>
	Mx3-gen2-R	WT	<p>EDITED SAMPLE 200 TO 265 BP</p> <p>1500 T G G C A G C C C A G C C G C A A G G T C C T T T C T C T A C C C A A G G C A G C C C A G G C A G T C G A T A A G C T C T A T A C A G G</p> <p>CONTROL SAMPLE 202 TO 267 BP</p> <p>1500 T G G C A G C C C A G C C G C A A G G T C C T T T C T C T A C C C A A G G C A G C C C A G G C A G T C G A T A A G C T C T A T A C A G G</p>

**B.**

Clones	Geno- typing	Indel	ICE deconvoluted sequences
EC-Mx1a-C8	Mx1-gen1-F	+1	<p>EDITED SAMPLE 209 TO 274 BP</p> <p>T G A A C C A A C A T T A C G A A G A G A A G G T G C G G C C C T G T A T C G A C C T C A T C G A C T C T C T A G C C T C C C T T</p> <p>CONTROL SAMPLE 210 TO 275 BP</p> <p>T G A A C C A A C A T T A C G A A G A G A A G G T G C G G C C C T G T A T C G A C C T C A T C G A C T C T C T A G C C T C C C T T G</p>
	Mx1-gen1-R	+1	<p>EDITED SAMPLE 81 TO 148 BP</p> <p>A C C C C A A G G G A G C G T A G A G A G T C G A T C A G C T C G A T A C A G G G C C C C A C C T T C T C T T C G T A A T G T T G</p> <p>CONTROL SAMPLE 65 TO 130 BP</p> <p>A C C C C A A G G G A G C G T A G A G A G T C G A T C A G C T C G A T A C A G G G C C C C A C C T T C T C T T C G T A A T G T T G C</p>
	Mx22bis-gen-R	WT	<p>EDITED SAMPLE 146 TO 211 BP</p> <p>A C C C C A A G G G A G C G T A G A G A G T C G A T G A G G T C A A T A C T A G G A C G C A C C T T C T C C T C A T A A T G T T G C</p> <p>CONTROL SAMPLE 149 TO 214 BP</p> <p>A C C C C A A G G G A G C G T A G A G A G T C G A T G A G G T C A A T A C T A G G A C G C A C C T T C T C C T C A T A A T G T T G C</p>
	Mx3-gen2-F	WT	<p>EDITED SAMPLE 159 TO 224 BP</p> <p>T A A A C C A A C A T T A T G A G G A G A A G G T G C G T C C C T G T A T A G A C C T T A T C G A C T C C C T G C G C T C C C T T G</p> <p>CONTROL SAMPLE 164 TO 229 BP</p> <p>T A A A C C A A C A T T A T G A G G A G A A G G T G C G T C C C T G T A T A G A C C T T A T C G A C T C C C T G C G C T C C C T T G</p>

C.

Clones	Geno- typing	Indel	ICE deconvoluted sequences
EC-Mx1a-C13	Mx1-gen1-F	+1	<p>EDITED SAMPLE 211 TO 276 BP</p> <p>T G A A C C A A C A T T A C G A A G A G A A G G T G C G C C C T G <b>A</b> T C G A C C T C A T C G A C T C T C T A C G C T C C C T T</p> <p>CONTROL SAMPLE 210 TO 275 BP</p> <p>T G A A C C A A C A T T A C G A A G A G A A G G T G C G C C C C C T G A T C G A C C T C A T C G A C T C T C T A C G C T C C C T T G</p>
	Mx1-gen1-R	+1	<p>EDITED SAMPLE 79 TO 144 BP</p> <p>A C A C C A A G G G A G C T A G A G A C T C G A T G A G G T C C A T <b>A</b> C A G C G C C C G C A C C T T C T C T T C G T A A T G T T G</p> <p>CONTROL SAMPLE 65 TO 130 BP</p> <p>A C A C C A A G G G A G C T A G A G A G T C G A T G A G G T C C A T A C A G C C C C G C A C C T T C T C T T C G T A A T G T T G G</p>
	Mx22bis-gen-R	WT	<p>EDITED SAMPLE 148 TO 213 BP</p> <p>A C G C C A A G G G A G C C T A G A G A C T C G A T G A G C T C A A T <b>A</b> C T A G A C C C A C C T T C T C C T C A T A A T G T T G G</p> <p>CONTROL SAMPLE 149 TO 214 BP</p> <p>A C G C C A A G G G A G C C T A G A G A G T C G A T G A G C T C A A T A C T A G A C C C A C C T T C T C C T C A T A A T G T T G G</p>
	Mx3-gen2-F	WT	<p>EDITED SAMPLE 158 TO 223 BP</p> <p>T A A C C A A C A T T A T G A G G A G A A G G T G C G T C C C T G <b>A</b> T A G A C C T T A T C G A C T C C C T G C G C T C C C T T G</p> <p>CONTROL SAMPLE 164 TO 229 BP</p> <p>T A A C C A A C A T T A T G A G G A G A A G G T G C G T C C C T G A T A G A C C T T A T C G A C T C C C T G C G C T C C C T T G</p>

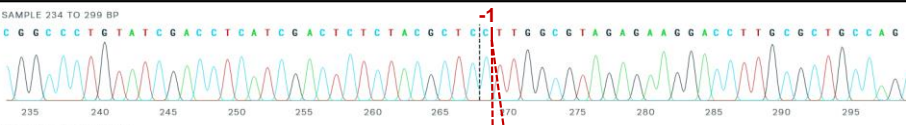
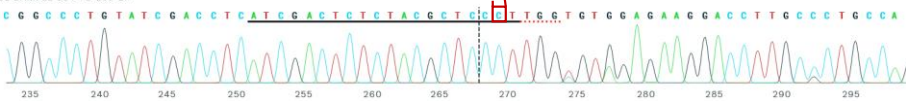
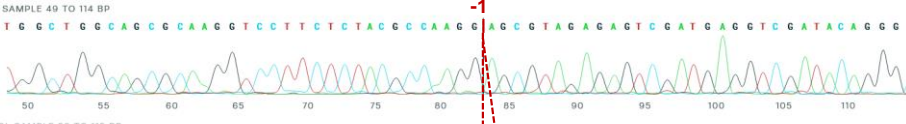
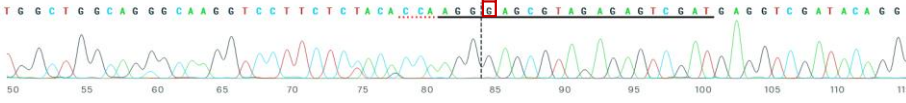
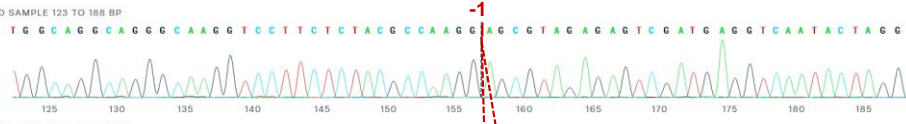
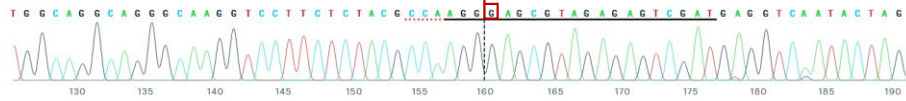
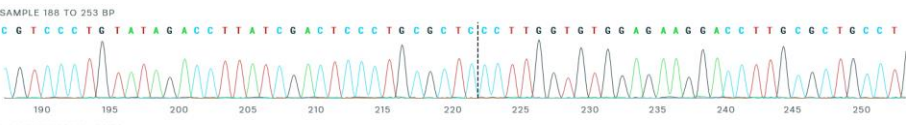
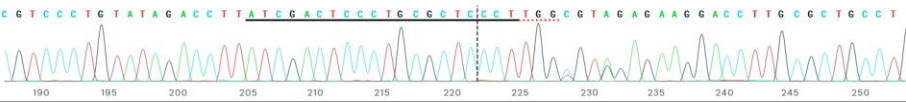
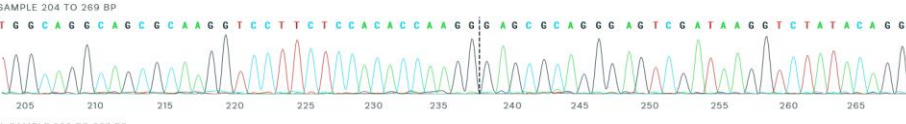
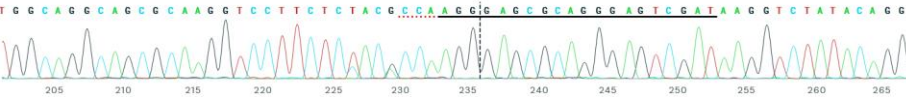
D.

Clones	Geno-typing	Indel	ICE deconvoluted sequences
EC-Mx3a-C12	Mx1-gen1-F	WT	<p>EDITED SAMPLE 206 TO 271 BP</p> <p>CONTROL SAMPLE 209 TO 274 BP</p>
	Mx1-gen1-R	WT	<p>EDITED SAMPLE 76 TO 141 BP</p> <p>CONTROL SAMPLE 65 TO 130 BP</p>
Mx22bis-gen-R	WT	WT	<p>EDITED SAMPLE 147 TO 212 BP</p> <p>CONTROL SAMPLE 149 TO 214 BP</p>
Mx3-gen2-F	+1	+1	<p>EDITED SAMPLE 159 TO 224 BP</p> <p>CONTROL SAMPLE 162 TO 227 BP</p>
Mx3-gen2-R	+1	+1	<p>EDITED SAMPLE 222 TO 287 BP</p> <p>CONTROL SAMPLE 224 TO 289 BP</p>

E.

Clones	Geno- typing	Indel	ICE deconvoluted sequences
EC-Mx3a-C18	Mx1-gen1-F	WT	<p>EDITED SAMPLE 205 TO 270 BP</p> <p>T G A A C C A A C A T T A C G A A G A G A A G G T G C G G C C C T G T A T C G A C C T C A T C G A C T C T C T A C G C T C C C T T G</p> <p>CONTROL SAMPLE 209 TO 274 BP</p> <p>T G A A C C A A C A T T A C G A A G A G A A G G T G C G G C C C T G T A T C G A C C T C A T C G A C T C T C T A C G C T C C C T T G</p>
	Mx1-gen1-R	WT	<p>EDITED SAMPLE 78 TO 143 BP</p> <p>A C A C C A A G C G A G C G T A G A G A G T C G A T G A G G T C G A T A C A C G G C C G C A C C T T C T C T T C G T A A T G T T G G</p> <p>CONTROL SAMPLE 65 TO 130 BP</p> <p>A C A C C A A G C G A G C G T A G A G A G T C G A T G A G G T C G A T A C A C G G C C G C A C C T T C T C T T C G T A A T G T T G G</p>
Mx22bis-gen-R	WT	WT	<p>EDITED SAMPLE 144 TO 209 BP</p> <p>A C G C C A A G C G A G C G T A G A G A G T C G A T G A G G T C A A T A C T A G G A C G C A C C T T C T C C T C A T A A T G T T G G</p> <p>CONTROL SAMPLE 149 TO 214 BP</p> <p>A C G C C A A G C G A G C G T A G A G A G T C G A T G A G G T C A A T A C T A G G A C G C A C C T T C T C C T C A T A A T G T T G G</p>
Mx3-gen2-F	-2	-2	<p>EDITED SAMPLE 165 TO 230 BP</p> <p>T A A A C C A A C A T T A T C A G G A G A A G G T G C G T C C C T G T A G A C C T T A T C G A C T C C C T G C G C T C C C T T G G T</p> <p>CONTROL SAMPLE 162 TO 227 BP</p> <p>T A A A C C A A C A T T A T C A G G A G A A G G T G C G T C C C T G T A G A C C T T A T C G A C T C C C T G C G C T C C C T T G G T</p>
Mx3-gen2-R	-2	-2	<p>EDITED SAMPLE 230 TO 295 BP</p> <p>A C A C C A A G C G A G C G C A G C G A T A A G G T C T A C A G G G A C G C A C C T T C T C C T C A T A A T G T T G T T</p> <p>CONTROL SAMPLE 224 TO 289 BP</p> <p>A C A C C A A G C G A G C G C A G C G A T A A G G T C T A C A G G G A C G C A C C T T C T C C T C A T A A T G T T G T T</p>

F.

Clones	Geno- typing	Indel	ICE deconvoluted sequences
EC-Mx12-C7	Mx1-gen1-F	-1	<p>EDITED SAMPLE 234 TO 299 BP</p> <p>2000   </p> <p>CONTROL SAMPLE 234 TO 299 BP</p> <p>3000   </p>
	Mx1-gen1-R	-1	<p>EDITED SAMPLE 49 TO 114 BP</p> <p>2000   </p> <p>CONTROL SAMPLE 50 TO 115 BP</p> <p>2000   </p>
	Mx22bis-gen-R	-1	<p>EDITED SAMPLE 123 TO 188 BP</p> <p>2000   </p> <p>CONTROL SAMPLE 126 TO 191 BP</p> <p>2000   </p>
	Mx3-gen2-F	WT	<p>EDITED SAMPLE 188 TO 253 BP</p> <p>2000   </p> <p>CONTROL SAMPLE 188 TO 253 BP</p> <p>2000   </p>
	Mx3-gen2-R	WT	<p>EDITED SAMPLE 204 TO 269 BP</p> <p>1500   </p> <p>CONTROL SAMPLE 202 TO 267 BP</p> <p>1500   </p>

G.

Clones	Geno-typing	Indel	ICE deconvoluted sequences
EC-Mx12-C16	Mx1-gen1-F	-5	<p>EDITED SAMPLE 235 TO 300 BP</p> <p>CONTROL SAMPLE 236 TO 301 BP</p>
	Mx1-gen1-R	-5	<p>EDITED SAMPLE 51 TO 116 BP</p> <p>CONTROL SAMPLE 39 TO 104 BP</p>
Mx22bis-gen-R	-1/-10		<p>EDITED SAMPLE 119 TO 184 BP</p> <p>CONTROL SAMPLE 123 TO 188 BP</p>
Mx3-gen2-F	WT		<p>EDITED SAMPLE 185 TO 250 BP</p> <p>CONTROL SAMPLE 180 TO 255 BP</p>
Mx3-gen2-R	WT		<p>EDITED SAMPLE 198 TO 263 BP</p> <p>CONTROL SAMPLE 207 TO 272 BP</p>

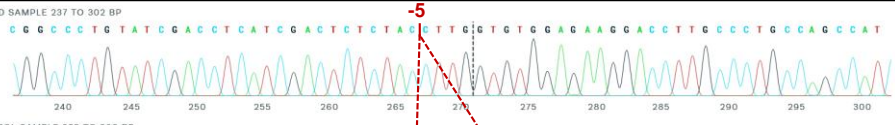
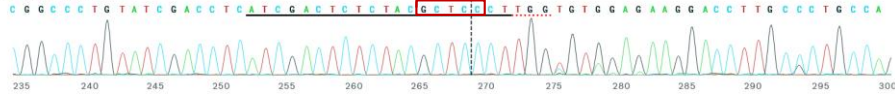
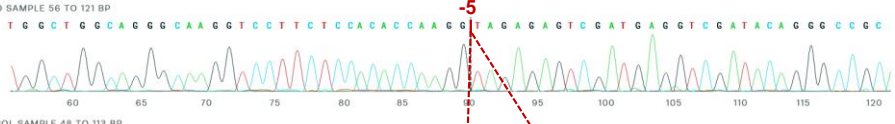
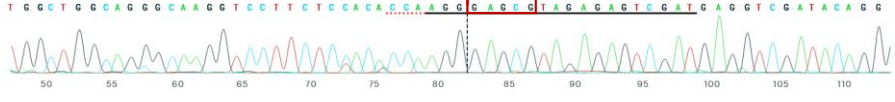
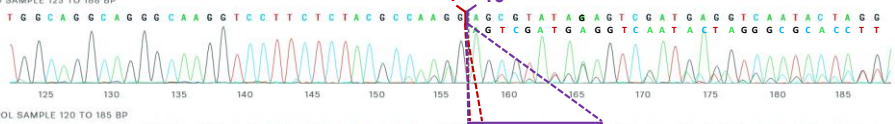
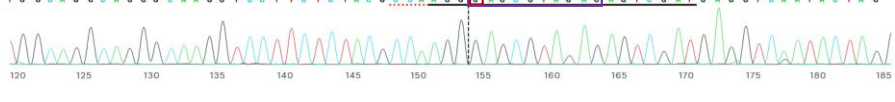
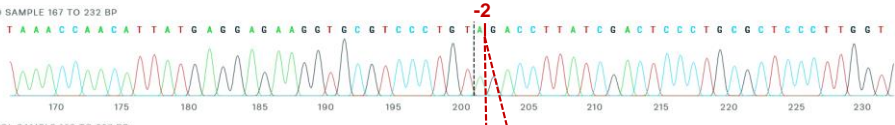
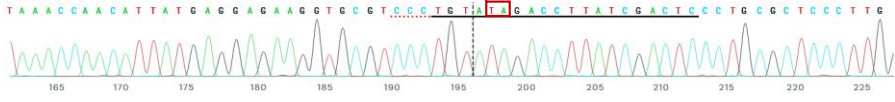
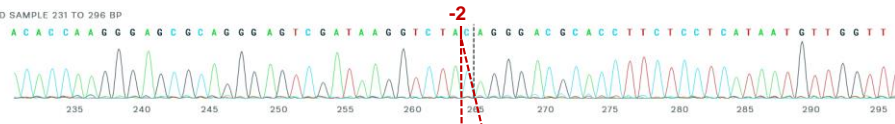
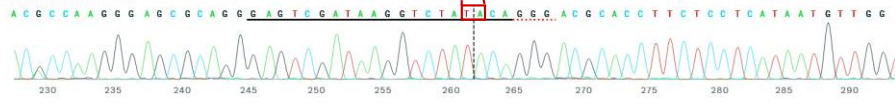
H.

Clones	Geno- typing	Indel	ICE deconvoluted sequences
EC-Mx1a+3a- mi-C15	Mx1-gen1- F	+1	<p>EDITED SAMPLE 212 TO 277 BP</p> <p>CONTROL SAMPLE 208 TO 273 BP</p>
	Mx1-gen1- R	+1	<p>EDITED SAMPLE 79 TO 144 BP</p> <p>CONTROL SAMPLE 76 TO 141 BP</p>
Mx22bis- gen-R	WT	WT	<p>EDITED SAMPLE 150 TO 215 BP</p> <p>CONTROL SAMPLE 140 TO 205 BP</p>
Mx3-gen2- F	Mx3-gen2- R	-2/+1	<p>EDITED SAMPLE 170 TO 235 BP</p> <p>CONTROL SAMPLE 162 TO 227 BP</p>
		-2/+1	<p>EDITED SAMPLE 230 TO 295 BP</p> <p>CONTROL SAMPLE 228 TO 293 BP</p>

I.

Clones	Geno-tying	Indel	ICE deconvoluted sequences
EC-Mx12-C7-Mx3a-C7	Mx1-gen1-F	-1	<p>EDITED SAMPLE 236 TO 301 BP</p> <p>2000  </p> <p>CONTROL SAMPLE 235 TO 300 BP</p> <p>2000  </p>
	Mx1-gen1-R	-1	<p>EDITED SAMPLE 52 TO 117 BP</p> <p>2000  </p> <p>CONTROL SAMPLE 48 TO 113 BP</p> <p>2000  </p>
	Mx22bis-gen-R	-1	<p>EDITED SAMPLE 123 TO 188 BP</p> <p>2000  </p> <p>CONTROL SAMPLE 120 TO 185 BP</p> <p>2000  </p>
	Mx3-gen2-F	-2	<p>EDITED SAMPLE 167 TO 232 BP</p> <p>2000  </p> <p>CONTROL SAMPLE 162 TO 227 BP</p> <p>2000  </p>
	Mx3-gen2-R	-2	<p>EDITED SAMPLE 229 TO 294 BP</p> <p>1500  </p> <p>CONTROL SAMPLE 228 TO 293 BP</p> <p>1500  </p>

J.

Clones	Geno- typing	Indel	ICE deconvoluted sequences
EC-Mx12-C16- Mx3a-C18	Mx1-gen1- F	-5	<p>EDITED SAMPLE 237 TO 302 BP</p> <p>2000   </p> <p>CONTROL SAMPLE 235 TO 300 BP</p> <p>2000   </p>
	Mx1-gen1- R	-5	<p>EDITED SAMPLE 56 TO 121 BP</p> <p>2000   </p> <p>CONTROL SAMPLE 48 TO 113 BP</p> <p>2000   </p>
	Mx22bis- gen-R	-1/-10	<p>EDITED SAMPLE 123 TO 188 BP</p> <p>2000   </p> <p>CONTROL SAMPLE 120 TO 185 BP</p> <p>2000   </p>
	Mx3-gen2- F	-2	<p>EDITED SAMPLE 167 TO 232 BP</p> <p>2000   </p> <p>CONTROL SAMPLE 162 TO 227 BP</p> <p>2000   </p>
	Mx3-gen2- R	-2	<p>EDITED SAMPLE 231 TO 296 BP</p> <p>1500   </p> <p>CONTROL SAMPLE 228 TO 293 BP</p> <p>1500   </p>

**K.**

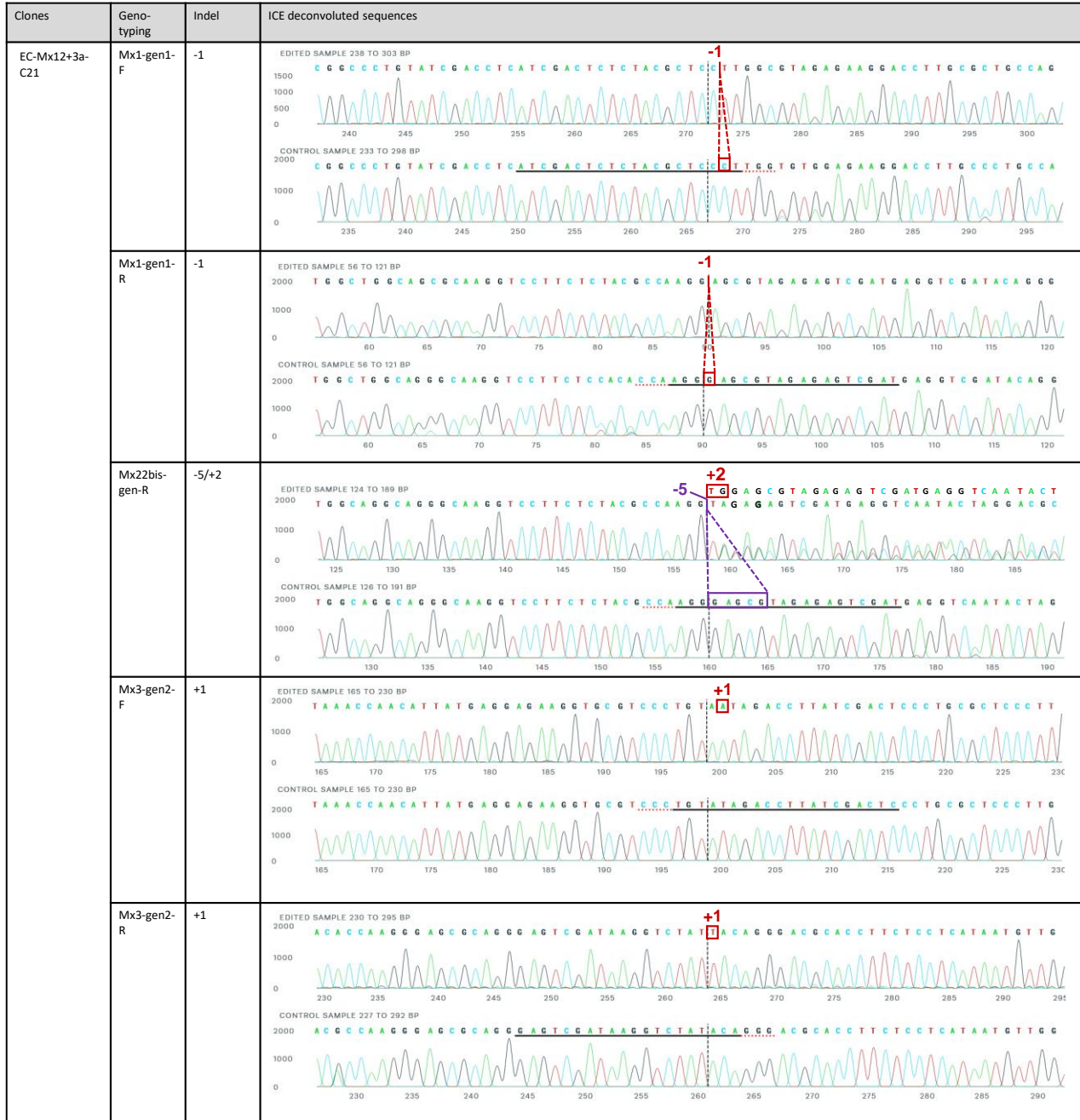


**Figure 53: Alignment of chromatograms from EC-Mx clones with EC (WT) cell line**

Chromatograms showing edited and wild-type (control) sequences in the region around the sequence targeted by sgRNAs from (A) EC-Mx12-C6 (WT), (B) EC-Mx1a-C8 (*mx1*<sup>-/-</sup>), (C) EC-Mx1a-C13 (*mx1*<sup>-/-</sup>), (D) EC-Mx3a-C12 (*mx3*<sup>-/-</sup>), (E) EC-Mx3a-C18 (*mx3*<sup>-/-</sup>), (F) EC-Mx12-C7 (*mx1*<sup>-/-</sup> *mx2*<sup>-/-</sup>), (G) EC-Mx12-C16 (*mx1*<sup>-/-</sup> *mx2*<sup>-/-</sup>), (H) EC-Mx1a+3a-C15 (*mx1*<sup>-/-</sup> *mx3*<sup>-/-</sup>), (I) EC-Mx12-C7-Mx3a-C7 (*mx1*<sup>-/-</sup> *mx2*<sup>-/-</sup> *mx3*<sup>-/-</sup>), (J) EC-Mx12-C16-Mx3a-C18 (*mx1*<sup>-/-</sup> *mx2*<sup>-/-</sup> *mx3*<sup>-/-</sup>), (K) EC-Mx12+3a-C21 (*mx1*<sup>-/-</sup> *mx2*<sup>-/-</sup> *mx3*<sup>-/-</sup>) clones. The horizontal black line represents the guide sequence; the horizontal red dotted line corresponds to the PAM site; the vertical black dotted line represents the theoretical cut site. The red or purple boxes show the inserted or deleted nucleotides in each edited clone. Alignments were obtained using Synthego ICE Analysis tool.

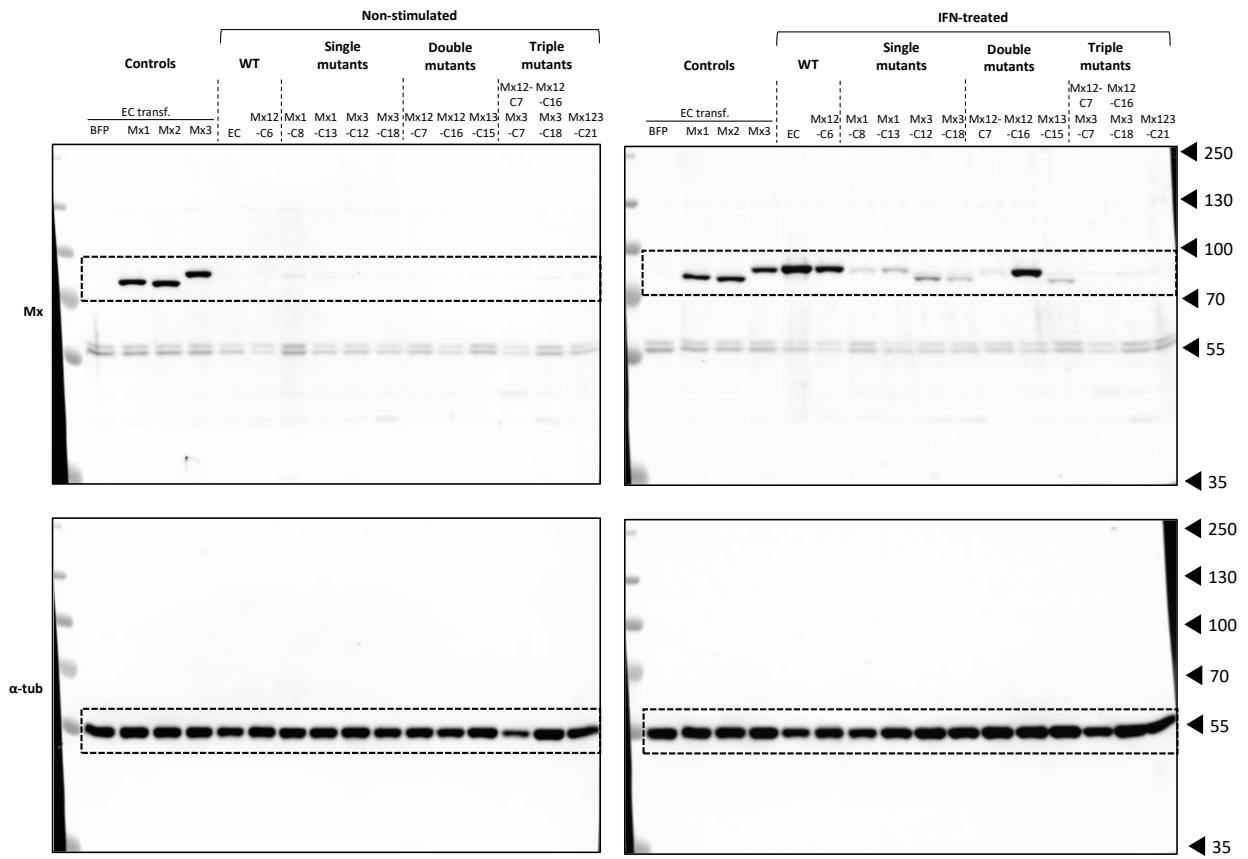


**Figure 54: Original full-length blots used in Figure 49**

Regions corresponding to the cropped images are surrounded by a dotted line.

---

## **APPENDIX 4**

### **Review article**

---

Chaumont, L., Collet, B., & Boudinot, P. (2023). Double-stranded RNA-dependent protein kinase (PKR) in antiviral defence in fish and mammals. *Developmental & Comparative Immunology*, 145, 104732. <https://doi.org/10.1016/j.dci.2023.104732>

## **Protein Kinase double-stranded RNA-dependent (PKR) in antiviral defence in fish and mammals**

Lise Chaumont<sup>1</sup>, Bertrand Collet<sup>1</sup> and Pierre Boudinot<sup>1</sup>

<sup>1</sup> Université Paris-Saclay, INRAE, UVSQ, VIM, Jouy-en-Josas, 78350, France

Corresponding author:

Pierre Boudinot

Université Paris-Saclay, INRAE, UVSQ, VIM, Jouy-en-Josas, 78350, France

[Pierre.Boudinot@inrae.fr](mailto:Pierre.Boudinot@inrae.fr)

Phone : 0033 1 34 65 25 85

## Abstract

The interferon-inducible double-stranded RNA-dependent protein kinase (PKR) is one of the key antiviral arms of the innate immune system. Upon binding of viral double stranded RNA, a viral Pattern Associated Molecular Pattern (PAMP), PKR gets activated and phosphorylates the eukaryotic initiation factor 2 $\alpha$  (eIF2 $\alpha$ ) resulting in a protein shut-down that limits viral replication. Since its discovery in the mid-seventies, PKR has been shown to be involved in multiple important cellular processes including apoptosis, proinflammatory and innate immune responses. Viral subversion mechanisms of PKR underline its importance in the antiviral response of the host. PKR activation pathways and its mechanisms of action were previously identified and characterised mostly in mammalian models. However, fish Pkr and fish-specific paralogue Z-DNA-dependent protein kinase (Pgz) also play key role in antiviral defence. This review gives an update on the current knowledge on fish Pkr/Pgz, their conditions of activation and their implication in the immune responses to viruses, in comparison to their mammalian counterparts.

## Introduction

In 1976, the research group of Ian M. Kerr at the National Institute for Medical Research, London, United Kingdom, discovered that lysates from interferon (IFN)-treated human and mouse cells displayed an enhanced protein kinase activity upon exposure to double-stranded RNA (dsRNA) (Roberts et al., 1976). This activity was attributed to a 68-kDa protein in human cells, which was shown to phosphorylate the  $\alpha$ -subunit of the eukaryotic initiation factor 2 (eIF2), leading to the inhibition of protein synthesis (Content et al., 1975; Hovanessian, 1980; Laurent et al., 1985; Samuel, 1979). Cloned in 1990 (Meurs et al., 1990), this protein, initially called p68 kinase, was later named dsRNA-dependent protein kinase (PKR) (Clemens et al., 1993). It is now also referred to as the eukaryotic translation initiation factor 2 $\alpha$  (eIF2 $\alpha$ ) kinase 2 (EIF2AK2) by the HGNC-approved nomenclature.

The human PKR comprises a C-terminal kinase domain, and a N-terminal regulatory region with two dsRNA binding motifs (dsRBMs) (VanOudenhove et al., 2009). Binding of dsRNA generated during viral infection to these dsRBMs triggers PKR activation via dimerisation and autophosphorylation (Meurs et al., 1990). Once activated, PKR exerts its antiviral function through several pathways, including inhibition of the cell translation machinery and activation of apoptosis. In addition, PKR plays a role in signal transduction of the proinflammatory response and the innate immune signalling pathways (García et al., 2006). Of note, a growing body of evidence suggests that PKR is also involved in the regulation of cell growth, proliferation and differentiation (Jagus et al., 1999; Samuel et al., 1997), although this function will not be further discussed in this review.

Several reviews focusing on PKR mechanisms of action have been published during the past 25 years (Cesaro and Michiels, 2021; Clemens and Elia, 1997; Cole, 2007; Gal-Ben-Ari et al., 2019; García et al., 2006). In this review, we first present the evolution of PKR and related eIF2 $\alpha$  kinases; we then discuss its main antiviral functions, including PKR-mediated phosphorylation of eIF2 $\alpha$  and activation of apoptosis, the role of PKR in transduction of inflammatory and IFN responses. Finally, we summarise the antiviral activity of PKR and its modulation during viral infections.

Although PKR mechanisms of action have mainly been studied in mammalian models, this review aims to provide an analysis of the current knowledge on the implication of fish Pkr and fish-specific paralogue Z-DNA-dependent protein kinase (P<sub>kz</sub>) in antiviral defences. In this regard, a systematic comparison of mammalian and fish PKR has been conducted of each antiviral function.

## 1. Evolution of PKR and related eIF2 $\alpha$ kinases

### 1.1. eIF2 $\alpha$ kinase family

In response to various extrinsic and intrinsic stress stimuli (e.g. hypoxia, nutrient deprivation, endoplasmic reticulum (ER) stress, viral infection), eukaryotic cells activate a signalling pathway, termed integrated stress response (ISR), in order to restore cellular homeostasis (Cesaro & Michiels, 2021; Donnelly et al., 2013; Pakos-Zebrucka et al., 2016). ISR results in the phosphorylation of eIF2 $\alpha$ , which leads to the shut-down of the cell translation machinery and the induction of specific stress-induced gene sets, which can promote two opposite cell fates: survival/recovery or apoptosis (Pakos-Zebrucka et al., 2016).

eIF2 $\alpha$  can be phosphorylated by a family of five kinases, including: (1) PERK (PKR-like ER kinase; EIF2AK3); (2) GCN2 (general control non-derepressible 2; EIF2AK4), (3) HRI (heme-regulated inhibitor; EIF2AK1), (4) PKR (double-stranded RNA-dependent protein kinase, EIF2AK2), (5) fish specific P<sub>kz</sub> (Z-DNA-dependent protein kinase) (Donnelly et al., 2013; Hu, 2004; Rothenburg et al., 2005). Each kinase possesses unique regulatory domains allowing them to respond to distinct type of stress stimuli (Dey et al., 2007; Donnelly et al., 2013): PERK senses misfolded proteins in the ER and transduces this signal to attenuate protein synthesis; GCN2 is activated under amino acid starvation conditions through binding of uncharged tRNAs; HRI is activated under conditions of heme deprivation and coordinates globin chain synthesis in erythroid cells. PKR and fish P<sub>kz</sub> are the main members of the family that are activated during viral infections. Interestingly, although eIF2 $\alpha$  kinases primarily respond to specific stresses, a few studies suggest that they may have cooperative functions (reviewed in Pakos-Zebrucka et al., 2016). For instance, eIF2 $\alpha$  phosphorylation can be mediated by PKR but also PERK and GCN2 during viral infections (Berlanga et al., 2006; Cheng et al., 2005). Conversely, PKR was shown to play a significant role in the ER-stress signalling pathway

along with PERK (Lee et al., 2007). It is noteworthy that this cooperative phenomenon has also been reported with fish viruses such as Viral Hemorrhagic Septicemia Virus (VHSV) (Kesterson et al., 2020).

### 1.2. Fish Pkr

*pkr* genes are present across jawed vertebrates from sharks (e.g., in the great white shark *Carcharodon carcharias*, ENSCHSG00020012606/LOC121278105), to bony fish and tetrapods. Only one copy is present in Zebrafish and salmonids, but two or more paralogues are often present next to each other in a head-to-tail orientation in percomorph species (for example, tongue sole (*Cynoglossus semilaevis*), Japanese medaka (*Oryzias latipes*) and green spotted puffer fish (*Tetraodon nigroviridis*)). Similar to their mammalian counterparts, fish Pkr contain a N-terminal dsRNA-binding domain and a C-terminal kinase domain. Interestingly, while mammalian PKR consists of two tandem dsRNA binding motifs (dsRBMs), this number varies from one to three in fish Pkr (Rothenburg et al., 2008) (Figure 1A). A detailed phylogenetic analysis revealed an accelerated evolution of the kinase domain of PKR, compared to other related kinases (Rothenburg et al., 2009). This domain showed a robust signature of diversifying (positive) selection, with variations at positively selected sites altering the sensitivity to viral inhibitors involved in immune evasion. These observations highlight the importance of PKR in antiviral immunity.

### 1.3. Pkz

*pkz* gene was initially identified in Crucian carp (*Carassius auratus*) (Hu et al., 2004), Zebrafish (*Danio rerio*) (Rothenburg et al., 2005) and in Atlantic salmon (*Salmon salar*) (Bergan et al., 2008). Although it seems to be absent from many fish groups, it is not restricted to cyprinids and salmonids. It also found in clupeids (herrings) as well as in *Paramorpyrops kingsleyae* and *Scleropages formosus* (osteoglossomorphs). *pkz* genes, in species in which they are present, are located next to *pkr*, but encode a kinase in which the dual dsRNA-binding domain is replaced by two or more Z $\alpha$  motifs (Figure 1A). These domains, which are also found in adenosine deaminase RNA-specific binding protein 1 (ADAR1, an RNA editing enzyme) and in a number of proteins from dsDNA viruses, such as pox or herpesvirus, specifically bind dsDNA and dsRNA in the left-handed Z conformation (Kim, 2020).

Phylogenetic analyses showed that fish *pkr* genes are more closely related to fish *pkz* than to their mammalian counterparts (Rothenburg et al., 2008). This suggests that *pkr* and *pkz* are paralogous genes that derive from an ancestral kinase gene, which was duplicated after the divergence from the tetrapod lineage. It was proposed that the existence of Pkz in certain fish species reflects an adaptation to specific fish viruses (Zou et al., 2016).

## 1.4. Other eIF2 $\alpha$ kinases

In contrast, PERK is found across metazoans (Mori, 2022) and has been extensively studied in *Drosophila* (Sood et al., 2000) in which it is involved in Toll signalling (Zhu et al., 2022). PERK controls ER stress, blocking the entry of new polypeptides into the lumen and thus promoting refolding of misfolded proteins. GCN2 is widely found across metazoans, while HIR is present in vertebrates including Agnathans.

## 2. Main functions of PKR and its implication in fish antiviral immunity

The following section summarises the main functions of PKR and Pkz in a context of viral infection and shed light on the underlying molecular mechanisms identified in mammals and in fish. Figure 2 provides an overview of the mechanisms of action of PKR identified in mammals during viral infections.

### 2.1. Activation of PKR

*eIF2ak2*, the gene encoding PKR, is constitutively expressed at low levels in mammalian cells and is then further induced by a variety of stress associated responses, including viral infection and IFN (Meurs et al., 1990). This distinctive feature is also found in fish *in vivo* as well as *in vitro* in fish cell lines (Table 1). Furthermore, mammalian PKR mainly localises in the cytoplasm but it has also been detected in the nucleus (Jeffrey et al., 1995). Similarly, cytoplasmic localisation of Pkr but also Pkz has been described in fish (Wei et al., 2020; Xu et al., 2019).

In the cytoplasm, mammalian PKR is predicted to exist in a weak monomer-dimer equilibrium, the latent monomeric state being predominant (Cole, 2007; Donnelly et al., 2013; Lemaire et al., 2005). In a similar fashion to the other eIF2 $\alpha$  kinases, it requires dimerisation and auto-phosphorylation to be fully active.

#### 2.1.1. Double-stranded RNA-mediated activation

**Mammalian PKR.** The canonical and best-characterised PKR substrate is dsRNA, which is primarily generated during the replication cycle of RNA viruses. PKR activation is triggered by viral dsRNA binding to the N-terminal dsRNA-binding domain. Interestingly, activation by dsRNA is length-dependent and requires a minimum of 30 pb (Lemaire et al., 2008). dsRNA binding results in back-to-back homodimer formation which is mediated by the C-terminal kinase domain (Dey et al., 2005; Lavoie et al., 2014). Recent crystallographic studies suggest that the PKR dimer catalysed, *in trans*, the phosphorylation of the activation loop of another ‘substrate’ PKR (as a monomer or dimer) docked in a front-to-front geometry (Mayo et al., 2019). The phosphorylation of the kinase domain enhances

dimer stability (Dey et al., 2014; Lemaire et al., 2005) and reduces dsRNA binding affinity (Jammi & Beal, 2001). Eventually, the phosphorylated PKR dimer dissociates from dsRNA (Cole, 2007; Dzananovic et al., 2018). It is believed that the PKR dimer represents the active enzyme form that phosphorylates eIF2 $\alpha$  (Cole, 2007).

**Fish Pkr.** In fish, the dsRNA binding capacity of the N-terminal dsRBMs was demonstrated for Japanese flounder (*Paralichthys olivaceus*) PoPkr (Zhu et al., 2008), Zebrafish DrPkr (Liu et al., 2011) as well as Grass Carp (*Ctenopharyngodon idellus*) CiPkr (Hu et al., 2016) via poly(I:C) (a synthetic analogue of double-stranded RNA)-sepharose pull-down assays. Interestingly, dsRBMs from Japanese flounder could bind poly(I:C) separately (Zhu et al., 2008) while dsRBMs from Grass Carp needed two or three dsRBMs to cooperate *in vitro* (Hu et al., 2016). This activity was never directly demonstrated for other fish PKR but the systematic presence of double or triple dsRBMs (Rothenburg et al., 2008) along with functional analysis suggest that fish Pkr activation is similar to its mammalian counterparts.

**Fish Pkz.** Z-DNA binding domains (ZBDs) of Pkz bind tightly and specifically to Z-DNA (Liu et al., 2011; Rothenburg et al., 2005) and the ZBDs of Crucian carp have been found to interact with poly(dG:dC) and form a complex with Z-DNA *in vitro* and to facilitate efficient B-to-Z transition of bound nucleic acid ligand (Kim et al., 2014, 2009). Subsequently, binding of Pkz to Z-DNA induces its activation through homodimerisation and autophosphorylation (Liu et al., 2011; Rothenburg et al., 2005). The involvement of Pkz in detection of viral nucleic acids during infections is strongly supported by the capacity of the Z $\alpha$  protein encoded by the cyprinid herpesvirus 3 (CyHV-3) ORF112 to outcompete the binding of PKZ to Z-DNA (Tomé et al., 2013); recent results about ORF112 suggest a complex interplay between this Z $\alpha$  protein, Pkz and possibly other nucleic acid sensors involving competition for Z-DNA binding, conversion from A- to Z-DNA and induction of liquid phase separation by two Z $\alpha$  domains (Diallo et al., 2023).

## 2.1.2. Alternative activation pathways

Other studies have suggested that PKR can be activated in the absence of dsRNA binding, under specific conditions, including ER stress and artificially high concentrations of PKR.

### 2.1.2.1. Protein activator of PKR (PACT)

**Mammalian PKR.** Mammalian PKR can be activated in a seemingly dsRNA-independent manner by protein activator of PKR (PACT) in response to diverse stress stimuli including serum starvation, peroxide, arsenite or thapsigargin (ER stress) treatment (Lee et al., 2007; Patel et al., 2000). Exposure to these stress stimuli leads to PACT phosphorylation and activation (Bennett et al., 2004; Lee et al.,

2007; Patel et al., 2000). Once activated, PACT interacts with PKR through its dsRBMs, leading to PKR activation (Patel et al., 2000; Peters et al., 2001). PACT binding to the same region as dsRNA would result in conformational changes necessary for PKR activation (Patel & Sen, 1998). Although the primary signals inducing endogenous PACT-mediated PKR activation remain unclear (Chukwurah et al., 2021), it is possible that PACT potentiates PKR activation in viral infections, insofar as viral proteins induce ER stress (Liu et al., 2020).

**Fish Pkr.** PACT-Pkr interaction was also described *in vitro* in HEK293T transfected with Grass Carp CiPact and CiPkr (Hu et al., 2020). Furthermore, similarly to their mammalian counterparts, overexpression of CiPact increased the phosphorylation of CiPkr.

#### 2.1.2.2. High protein concentration

**Mammalian PKR.** PKR was found in a phosphorylated state when overexpressed in *Escherichia coli* (Barber et al., 1991). Although the presence of dsRNA or structured ssRNA of bacterial origin could not be ruled out, it was suggested that the high intracellular concentration of PKR was enough to induce 337imerization and subsequent autophosphorylation. This hypothesis was later supported by *in vitro* studies (Lemaire et al., 2005). In both cases, the PKR dimers were able to catalyse eIF2 $\alpha$  phosphorylation (Barber et al., 1991; Cole, 2007; Lemaire et al., 2005). In a similar fashion, PKR autophosphorylation was observed when incubated with heparin (Hovanessian and Galabru, 1987; Li et al., 2006) or other polyanions (reviewed in García et al., 2006). Although such concentrations are unlikely to happen in physiological conditions, it was suggested that this mode of PKR activation is mediated by monomers coming into close proximity in a similar manner to 337imerization of PKR via dsRNA binding (Lemaire et al., 2005).

**Fish Pkr.** A few observations suggest that autophosphorylation of fish Pkr at high concentrations might occur: firstly, Xu et al. have reported that only catalytically inactive mutated Pkr could be detected by Western blot when the proteins were overexpressed in EPC cells (Xu et al., 2018), likely because of the shut-off induced by active Pkr; secondly, overexpression of both mammalian and fish PKR can induce apoptosis in transfected cells (Srivastava et al., 1998; Xu et al., 2018). Altogether, these results suggest that overexpressed fish Pkr are seemingly functionally active even in the absence of dsRNA substrate.

#### 2.1.2.3. Caspases

Mammalian PKR can also be activated during apoptosis triggered by diverse stimuli (including tumour necrosis factor  $\alpha$  (TNF- $\alpha$ ), anti-FAS and staurosporine) via proteolysis as Asp251 by caspases (3, 7 and 8). This cleavage-mediated release of PKR kinase domain leads to eIF2 $\alpha$  phosphorylation resulting in translation inhibition during apoptosis (Saelens et al., 2001). It was suggested that inhibition of *de novo* protein synthesis during apoptosis might be of importance to prevent inadvertent

synthesis of proinflammatory molecules allowing safe clearance once phagocytosed (Savill and Fadok, 2000). Whether this phenomenon exists with fish Pkr is currently not known.

## 2.2. Phosphorylation of eIF2 $\alpha$ and inhibition of protein synthesis

### 2.2.1. Mammalian PKR

Like all members of the eIF2 $\alpha$  kinase family, activated PKR catalyses the phosphorylation of eIF2 $\alpha$  (on Ser51 in human eIF2 $\alpha$ ). eIF2 $\alpha$  is the main regulatory subunit of the eIF2 complex, which consists of 3 subunits (eIF2 $\alpha$ , eIF2 $\beta$ , and eIF2 $\gamma$ ). Under normal stress-free conditions, the eIF2 complex plays a key role in the initiation of mRNA translation: eIF2 forms a ternary complex by binding the initiator tRNA (Met-tRNA<sub>i</sub>) in a GTP-dependent manner. The eIF2-tRNA complex then joins the 40S ribosome subunit, which forms the 43S pre-initiation complex with other initiation factors (Jackson et al., 2010; Sonenberg & Hinnebusch, 2009). As initiation proceeds, GTP on eIF2 is hydrolysed upon binding of the Met-tRNA<sub>i</sub> anticodon with the AUG start codon. This results in the dissociation of the eIF2-GDP complex from the 40S ribosome subunit. Inactive eIF2-GDP complexes are continuously recycled for further rounds of mRNA translation initiation in a process catalysed by the GTP exchange factor eIF2B. Eventually, this results in the return of eIF2 to its active form (Jackson et al., 2010; Sonenberg & Hinnebusch, 2009).

Under stress conditions, Ser51-phosphorylated eIF2 $\alpha$  blocks the eIF2B-mediated exchange of GDP by sequestering eIF2B into a tight complex (Sudhakar et al., 2000). This inhibition of eIF2B activity results in a deficient eIF2 recycling preventing formation of new 43S pre-initiation complex. This leads to the attenuation of protein synthesis, thereby limiting the production of virions in the infected cells (García et al., 2006; Pakos-Zebrucka et al., 2016). In mammals, the inhibition of protein translation via PKR-mediated eIF2 $\alpha$  during viral infection is a well-known antiviral mechanism that has been described for a wide array of viruses (reviewed by Liu et al., 2020).

### 2.2.2. Fish Pkr

#### 2.2.2.1. Pkr-mediated phosphorylation of eIF2 $\alpha$

Several studies have demonstrated that fish Pkr catalyses the phosphorylation of eIF2 $\alpha$  both *in vitro* and *in vivo*. For instance, co-immuno-precipitation assays showed that Japanese flounder PoPkr physically interacts with eIF2 $\alpha$  during *Scophthalmus maximus* rhabdovirus (SMRV) infection *in vitro* (in FEC cells) and *in vivo* (in liver) leading to increased levels of phosphorylated eIF2 $\alpha$  bound to PoPkr (Zhu et al., 2008). Further evidence comes from overexpression studies: eIF2 $\alpha$  phosphorylation was increased in FEC cells transiently transfected with wildtype PoPkr and subsequently infected with SMRV. This was not the case with the catalytically inactive mutant K421R, suggesting that

eIF2 $\alpha$  results from the catalytic activity of PoPkr (Zhu et al., 2008). Similarly, overexpression of wildtype CaPkr but not catalytically inactive mutant CaPkr K419R in EPC cells resulted in phosphorylation of eIF2 $\alpha$  (Xu et al., 2018). Likewise, transfection of CO cells with Grass carp CiPkr resulted in phosphorylation of eIF2 $\alpha$  compared to control (Hu et al., 2016). Interestingly, it was reported that overexpression of Zebrafish DrPkr in yeast led to phosphorylation of yeast eIF2 $\alpha$  (Rothenburg et al., 2008).

Knockdown studies further corroborate the hypothesis that fish Pkr is able to phosphorylate eIF2 $\alpha$ : knockdown of CiPkr leads to reduced levels of phosphorylated eIF2 $\alpha$  upon poly(I:C) stimulation in CIK cells (Hu et al., 2020; Wang et al., 2018). In a similar fashion, knockdown of CaPkr and PoPkr also resulted in inhibition of eIF2 $\alpha$  phosphorylation upon Grass Carp Reovirus (GCRV) and SMRV infections, respectively (Liu et al., 2011; Zhu et al., 2008), thereby confirming that eIF2 $\alpha$  phosphorylation is catalysed by Pkr.

#### 2.2.2.2. *Pkr-mediated inhibition of protein synthesis*

Inhibition of *de novo* protein synthesis is probably one of the best studied functions of fish Pkr (Table 1). This function has been established with *in vitro* overexpression studies combined with luciferase assays. It was reported that Japanese flounder PoPkr (Zhu et al., 2008), Crucian carp CaPkr (Liu et al., 2011), Grass carp CiPkr (Hu et al., 2016, 2013), Fugu (*Takifugu rubripes*) TrPkr1 and TrPkr2 (del Castillo et al., 2012), and Nile tilapia OnPkr (Gan et al., 2021) can decrease luciferase activity upon transient transfection in mammalian and/or fish cells, and that this activity is dependent on a functional kinase domain. Interestingly, Liu et al. showed that co-transfection of both CiPkr and CiPkrz potentiated this effect using the same reporter system (Liu et al., 2011).

#### 2.2.3. Fish Pkz

Several studies suggest that Pkz can phosphorylate eIF2 $\alpha$  in a similar fashion as Pkr. It was demonstrated that Grass carp CiPkrz could phosphorylate eIF2 $\alpha$  *in vitro* when incubated with Z-DNA but not poly(I:C) (Yang et al., 2011). Wu et al. also confirmed Grass carp CiPKZ capacity to phosphorylate eIF2 $\alpha$ , as Pkz knockdown CIK cells that were transiently transfected with CiPkrz displayed increased level of phosphorylated eIF2 $\alpha$ , contrary to catalytically inactive mutant (Wu et al., 2016). Similarly, Atlantic Salmon SsPkrz was also able to phosphorylate recombinant human eIF2 $\alpha$  and rabbit eIF2 *in vitro* but not the non-phosphorylatable mutant eIF2 $\alpha$  (Bergan et al., 2008). Zebrafish DrPkrz and Crucian carp CaPkrz were also reported to interact with endogenous eIF2 $\alpha$  when overexpressed in mammalian cell lines or in yeast leading to its phosphorylation (Liu et al., 2011, 2013; Rothenburg et al., 2008). These results were, however, not confirmed by another study in human PKR-deficient cells, in which DrPkrz was unable to mediate eIF2 $\alpha$  phosphorylation when

overexpressed in mammalian cells (unlike mammalian PKR) (Taghavi and Samuel, 2013). The authors argued that the observed increase in the other studies might be due to PKR presence in the transfected cells. Knock-down of CaPkc also led to reduced levels of phosphorylated eIF2 $\alpha$  upon GCRV infection although to a lesser extent than CaPkr (Liu et al., 2011).

Similar to Pkr, fish Pkc has the capacity to inhibit protein synthesis and this function requires a functional kinase domain, as described for DrPkc (Liu et al., 2013; Rothenburg et al., 2005; Taghavi and Samuel, 2013), CiPkc (Yang et al., 2011) and SsPkc (Bergan et al., 2008).

### 2.3. PKR-mediated activation of apoptosis

PKR is known for limiting viral replication not only through inhibition of global protein synthesis (aka. viral “shutoff”) but also by inducing apoptosis (Kaufman, 1999).

#### 2.3.1. Activation of apoptosis

Apoptosis, also known as programmed cell death, is a highly regulated biological process, whereby cells undergo systematic self-destruction in response to diverse stimuli, including exposure to pathogens (Kerr et al., 1972). Unlike necrotic cells, apoptotic cells do not spill out their cellular contents but produce apoptotic bodies that can be phagocytosed without initiating an inflammatory response. The molecular mechanisms resulting in apoptosis are complex and involve two main pathways: (1) the “extrinsic pathway” aka. “death receptor pathway” is triggered by binding of extracellular ligands (TNF- $\alpha$ , FAS ligand (FASL), TNF related apoptosis inducing ligand (TRAIL)) to transmembrane death receptors (TNF receptor 1 (TNFR1), FAS receptor (FASR)) linked to adaptor proteins such as FAS-associated death domain protein (FADD); (2) the “intrinsic pathway” aka. “mitochondrial pathway” mediated by B-cell lymphoma 2 (BCL-2)–associated X protein (BAX)/BCL-2 homologous antagonist killer (BAK) insertion into mitochondrial membrane with subsequent cytochrome *c* released which associates with apoptotic peptidase activating factor 1 (APAF-1) and procaspase-9 to produce the apoptosome. Both of these pathways result in the activation of the caspase cascade, which constitutes the execution phase of apoptosis (Elmore, 2007).

##### 2.3.1.1. Apoptosis triggered by PKR overexpression

Several studies have reported that overexpression of PKR is sufficient to induce apoptosis in transfected mammalian cells (Lee and Esteban, 1994; Srivastava et al., 1998; Yeung et al., 1996). Furthermore, it was reported that *Pkr*<sup>-/-</sup> mouse embryonic fibroblasts (MEFs) were resistant to apoptosis in response to dsRNA, TNF- $\alpha$ , or lipopolysaccharide (LPS) (Der et al., 1997; Gil & Esteban, 2000a).

Similar results were obtained in fish cell lines transfected with fish Pkr: for instance, overexpression of wild-type Crucian carp CaPkr, but not catalytically inactive mutant, was sufficient to induce apoptosis in EPC cells (Xu et al., 2018). A comparable response was observed for both Grass carp CiPkr and CiPpz when overexpressed in CIK cells (Hu et al., 2016, 2013; Wu et al., 2016).

### 2.3.1.2. Induction of apoptosis-related genes

The role of PKR in apoptosis is also supported by transcriptional analysis of HeLa cells overexpressing wild-type PKR or catalytically inactive mutant PKR: pro-apoptotic genes (e.g. *CASP9*) were upregulated in PKR-expressing cells while anti-apoptotic genes (e.g. heat-shock protein *HSP70*, that inhibits mitochondrial release of cytochrome *c* and blocks procaspase-9 recruitment), were downregulated (Guerra et al., 2006).

Interestingly, overexpression of grass carp CiPkr also leads to upregulation of pro-apoptotic *bax* and down-regulation of antiapoptotic *bcl-2* while its knockdown resulted in opposite effects (Hu et al., 2020).

### 2.3.1.3. Activation of caspase cascade

Furthermore, a few studies showed that PKR is able to activate the FADD/caspase-8/caspase-3 pathway, independently from FAS/FASL and TNF- $\alpha$ /TNFR1 interaction (Gil and Esteban, 2000a; von Roretz and Gallouzi, 2010). PKR overexpression can also trigger the intrinsic pathway via activation of caspase 9, leading to BAX translocation into the mitochondria and subsequent release of cytochrome *c* to the cytoplasm (Gil et al., 2002). Conversely, poly(I:C) transfection results in reduced levels of apoptotic markers (cleaved PARP, and caspases 8 and 9) in *PKR*<sup>-/-</sup> HeLa cells, compared to wildtype cells (Zuo et al., 2022). Similarly, caspase-8 and -9 were also activated in EPC transfected with Crucian carp CaPkr (Xu et al., 2018).

## 2.3.2. Underlying mechanism: PKR/eIF2 $\alpha$ mediated apoptosis

Several studies have demonstrated that PKR-mediated apoptosis is a process dependent on eIF2 $\alpha$  phosphorylation.

### 2.3.2.1. PKR/ATF4/CHOP pathway

**Mammalian PKR.** Although the translation of most cell mRNAs is inhibited by PKR-mediated eIF2 $\alpha$ -phosphorylation, it also induces the translation of specific host genes involved in the stress response, such as activating transcription factor 4 (*ATF4*), *ATF3* and C/EBP homologous protein (*CHOP*) (Guerra et al., 2006; Palam et al., 2011). CHOP is known for regulating the expression of many anti-apoptotic and pro-apoptotic genes, including genes encoding the BCL-2-family proteins and the death receptors DR4 and DR5, which trigger the intrinsic and extrinsic apoptotic pathways (Hu et al., 2019; Puthalakath et al., 2007).

Current understanding of eIF2 $\alpha$ /ATF4/CHOP signalling pathway comes largely from studies on ER stress and amino acid starvation involving the eIF2 $\alpha$  phosphorylation by PERK and GCN2, respectively. Nevertheless, it has been shown that PKR also can induce apoptosis under ER stress conditions through PACT leading to the activation of eIF2 $\alpha$ /ATF4/CHOP signalling pathway in a PERK-independent manner (Lee et al., 2007). Furthermore, ATF3 was reported to be induced upon overexpression of wildtype PKR but not the catalytically inactive mutant (Guerra et al., 2006). Further investigation revealed that the absence of ATF3 decreased PKR-induced apoptosis when PKR was overexpressed in cell lines (Guerra et al., 2006). Interestingly, PKR overexpression also upregulated the expression of an alternative spliced isoform of ATF3, called ATF3 $\Delta$ Zip2, which promotes apoptosis via competition for the binding with the 65kDa subunit of the Nuclear Factor  $\kappa$ B (NF- $\kappa$ B) complex (Guerra et al., 2006). ATF3 $\Delta$ Zip2 was reported to suppress the NF- $\kappa$ B-dependent transcription of survival genes, referred to as cellular inhibitors of apoptosis, thereby indirectly making the cells more sensitive to apoptosis (Hua et al., 2006).

Viral infections can induce also apoptosis through the eIF2 $\alpha$ /ATF4/CHOP pathway (reviewed by Liu et al., 2020), although the kinase which phosphorylates eIF2 $\alpha$  may vary from one virus to another. While many studies have reported the activation of the PERK/eIF2 $\alpha$ /ATF4/CHOP pathway in virus-infected cells, a few others mention PKR as one of the kinase activators. For instance, knockdown of both PKR and PERK inhibited CHOP upregulation and apoptosis in infectious bronchitis virus (IBV)-infected cells (Liao et al., 2013).

**Fish Pkr.** The Pkr/eIF2 $\alpha$ /Atf4/Chop axis has not been directly investigated in fish. However, unique orthologues of *atf3*, *atf4* and *chop* are present in most fish genomes, suggesting that this pathway is likely functional in these organisms. Binding experiments of recombinant Grass carp CiAtf4 to the promoter of *prkra* (*interferon-inducible double-stranded RNA-dependent protein kinase activator A*) suggested it may reduce the transcription of this gene involved in adaptation to ER stress (Huang et al., 2017a). Several studies have also reported the activation the eIF2 $\alpha$ /Atf4/Chop pathway in case of ER stress *in vivo* in Crucian carp (Yuan et al., 2023), Zebrafish (Komoike & Matsuoka, 2016, 2013), Spotted seabass (*Lateolabrax maculatus*) (Xia et al., 2022), although in most cases, PERK was identified as the initiator kinase.

#### 2.3.2.2. PKR-mediated inhibition of translation promotes apoptosis

**Mammalian PKR.** A recent study suggested that PKR-mediated translational arrest indirectly promotes apoptosis by downregulating cFLIP (cellular FLICE (FADD-like IL-1 $\beta$ -converting enzyme)-inhibitory protein) (Zuo et al., 2022), known as a key anti-apoptotic regulator (Safa, 2012). Mechanistically, not only do cFLIP isoforms bind caspase-8 via homophilic interactions and thereby regulate the activation of apoptosis (reviewed by Tsuchiya et al., 2015), they also induce NF- $\kappa$ B

activation via interaction with TNF receptor-associated factor 2 (TRAF2) (Kataoka et al., 2000; Kataoka and Tschopp, 2004). Zuo et al. observed that coumermycin A1-mediated activation of PKR led to decreased cFLIP levels, while apoptosis markers including caspases 8 and 9 were upregulated (Zuo et al., 2022). Conversely, in poly(I:C) transfected wildtype HeLa cells but not *PKR*<sup>-/-</sup> cells, cFLIP expression was decreased and proapoptotic markers became apparent. As cycloheximide, a potent translation inhibitor, displayed a similar response to PKR activation, the authors suggested that PKR-driven inhibition of cFLIP was mediated by translational arrest (Zuo et al., 2022).

**Fish Pkr.** The functional role of cFlip in Pkr-mediated apoptosis has not been investigated in fish. Nevertheless, Sakamaki et al. showed cFlip proteins retain a relatively conserved structure across vertebrates. Further investigation revealed that Zebrafish cFlip, along with other non-mammalian cFlip proteins, had the ability to inhibit the extrinsic apoptotic pathway when overexpressed in mammalian HeLa cells and to interact with endogenous TRAF2 and FADD, in a similar fashion as their mammalian counterparts (Sakamaki et al., 2015). Furthermore, cFlip proteins from Zebrafish and Medaka and were able to induce NF- $\kappa$ B activation (Sakamaki et al., 2015). These results provide evidence that cFlip proteins have conserved functions from fish to mammals.

### 2.3.3. Underlying mechanism: eIF2 $\alpha$ -independent apoptosis

PKR can also induce apoptosis independently of eIF2 $\alpha$  phosphorylation via activation of transcription factors NF- $\kappa$ B (see below) and p53 (reviewed in García et al., 2006).

NF- $\kappa$ B controls the transcription of a large number of genes involved in immune and inflammatory responses, cell growth, cell survival (Grilli et al., 1993). NF- $\kappa$ B is commonly known for controlling development, survival and inflammation programmes, but numerous reports have also linked NF- $\kappa$ B activation to apoptosis (Kaltschmidt et al., 2000; Tak et Firestein, 2001). Indeed, under certain conditions including viral infections, NF- $\kappa$ B is known for inducing several pro-apoptotic transcription genes (e.g. *P53*, *CMYC*, *FAS*, *FASL*) (Gil and Esteban, 2000b). The molecular mechanisms by which PKR activates the NF- $\kappa$ B pathway will be discussed in a dedicated section hereinbelow.

The p53 tumor suppressor plays a key role in cellular homeostasis through the modulation of cell-cycle arrest, DNA repair, senescence, and apoptosis (Yoon et al., 2009). Studies using *Pkr*<sup>-/-</sup> MEFs also suggest that PKR might modulate p53 function (Cuddihy et al., 1999). The underlying mechanism involves the activation of PACT/PKR stress signalling pathway, resulting in the sumoylation-dependent p53 phosphorylation, translational activation and stability leading to G1 cell cycle arrest (Bennett et al., 2012). Since p53 transcription factor activates several effector processes, including the intrinsic apoptotic pathway (Aubrey et al., 2018), it was suggested that PACT/PKR-

mediated p53 stabilisation could result in apoptosis, thereby highlighting its role in antiviral innate immunity (Aloni-Grinstein et al., 2018).

## 2.4. PKR as a transducer of the inflammatory and interferon responses

In addition to inhibiting cellular translation and to promoting apoptosis, PKR was reported to be involved in various signal transduction pathways of the inflammatory response and the IFN response, which are both triggered upon viral infection. Activation of those responses leads to cytokine production and promotion of a systemic immune response, thereby preventing spreading of the viral infection. Nevertheless, in most cases, the precise role of PKR in the activation of these pathways remains elusive and whether PKR acts directly or indirectly has not been fully clarified.

### 2.4.1. PKR role in mitogen-activated protein kinase (MAPK) signalling

The mitogen-activated protein kinases (MAPKs) are a family of highly conserved serine-threonine protein kinases, involved in signal transduction pathways that regulate mitosis, cell differentiation, metabolism and cell death in eukaryotes (Morrison, 2012). The MAPKs can be classified into 3 groups: (1) ERKs (extracellular-signal-regulated kinases), responding primarily to growth factors and mitogens; (2) JNKs (Jun amino-terminal kinases), activated by environmental stress stimuli, inflammatory cytokines and growth factors; and (3) p38/SAPKs (stress-activated protein kinases), which are strongly activated in response to stress stimuli and inflammatory cytokines (Morrison, 2012). Importantly, the MAPK cascade participates in regulating the immune response and apoptosis upon viral infection (Kumar et al., 2018; Mohanta et al., 2020). In particular, downstream targets of the MAPK pathway include transcriptional factors as NF- $\kappa$ B p65, c-Jun, c-Fos, ATF1/2/6, CHOP, p53, signal transducer and activator of transcription 1 (STAT1), STAT3 which modulate the expression of genes involved in proliferation, apoptosis and immune and inflammatory responses (Kumar et al., 2018).

Interestingly, *Pkr*<sup>-/-</sup> MEFs were shown to be defective in activating p38 and JNK MAPKs in response to proinflammatory signals including poly(I:C), LPS, interleukin 1 $\beta$  (IL-1 $\beta$ ), and TNF- $\alpha$  (Goh et al., 2000). Furthermore, PKR knock-down in HeLa cells impaired the phosphorylation of JNK and p38 in response to dsRNA or a mutant strain of vaccinia virus (Zhang et al., 2009). Similarly, *PKR*<sup>-/-</sup> HeLa cells demonstrated a lack of p38, JNK, and ATF2 phosphorylation upon infection with the measles virus, which was restored upon transfection with wild-type human PKR (Taghavi & Samuel, 2012). From a mechanistic point of view, it was discovered that p38 MAPK activator MKK6 was efficiently phosphorylated by PKR *in vitro* and that activated PKR is able to directly regulate MKK6 activity *in vivo* upon poly(I:C) treatment (Silva et al., 2004). Nevertheless, other studies demonstrated that although dsRNA-mediated activation of the JNK pathway was greatly reduced in cells lacking

RnaseL and PKR, activation of the p38 pathway happened in a RnaseL- and PKR-independent manner, suggesting existence of alternative dsRNA-triggered signalling pathways (Jordanov et al., 2000).

#### 2.4.2. PKR role in NF- $\kappa$ B signalling

Besides activating the MAPK signalling pathway, PKR is also known for regulating the inflammatory response by modulating NF- $\kappa$ B signalling pathway.

Under normal conditions, NF- $\kappa$ B dimers are held inactive in the cell cytosol through association with inhibitors of NF- $\kappa$ B (I $\kappa$ B), which block NF- $\kappa$ B nuclear localization signal (Hayden and Ghosh, 2012; Oeckinghaus and Ghosh, 2009). Upon stress stimuli, the I $\kappa$ B kinase complex (IKK) is activated, leading to phosphorylation, ubiquitination and subsequent degradation of I $\kappa$ B proteins. Released NF- $\kappa$ B translocates to the nucleus and binds specific regulatory elements, thereby inducing the transcription of its target genes (Liu et al., 2017).

In *Pkr*<sup>-/-</sup> MEFs dsRNA treatment was unable to activate NF- $\kappa$ B (Kumar et al., 1997). Furthermore, PKR knock-down assays combined with NF- $\kappa$ B electrophoretic-mobility shift assay and I $\kappa$ B $\alpha$  detection by western blot showed that PKR was required for maximal NF- $\kappa$ B activation upon poly(I:C) transfection as well as during measles virus infection. NF- $\kappa$ B activation was dependent on MAVS but not TRIF (McAllister et al., 2010; McAllister and Samuel, 2009). Early studies showed that PKR could phosphorylate I $\kappa$ B $\alpha$  and induce NF- $\kappa$ B DNA-binding *in vitro* (Kumar et al., 1994), although evidence for a direct phosphorylation of I $\kappa$ B $\alpha$  by PKR *in vivo* was not demonstrated. It was later discovered that PKR acts upstream of IKK and NF- $\kappa$ B inducing kinase (NIK), leading to the degradation of the inhibitors I $\kappa$ B $\alpha$  and I $\kappa$ B $\beta$  and the concomitant release of NF- $\kappa$ B (Kumar et al., 1994; Zamanian-Daryoush et al., 2000). It is still unclear whether the PKR-driven activation of IKK involves PKR catalytic domain or not, as discrepancies can be found in the literature (Bonnet et al., 2000; Gil et al., 2001; Ishii et al., 2001). Another hypothesis is that PKR provides a signalling platform via its dsRNA-binding domain, which recruits signalling molecules such as members of the TRAF family, which are well-known signal transducers of NF- $\kappa$ B signalling pathway (Gil et al., 2004).

To date, the exact relationship between PKR and NF- $\kappa$ B and their downstream targets still remains elusive. This is particularly evident in fish models, where the studies tackling this question are scarce. Nevertheless, co-immuno-precipitation and GST-pull down assays showed that Grass carp CiPkr binds to Ikk $\beta$  and that Ikk $\beta$  interacts with I $\kappa$ B $\alpha$  (Wang et al., 2017). Furthermore, Fugu TrPkr1 and TrPkr2 induced transcriptional activity of a mammalian NF- $\kappa$ B luciferase reporter upon transfection in HINAE cells (del Castillo et al., 2012). This pathway of action of PKR is therefore likely functional in fish.

### 2.4.3. PKR role in type I IFN response

#### 2.4.3.1. PKR potentiates the production of type I IFN

The importance of PKR for type I IFN production has been strongly debated over the years (Fullam and Schröder, 2013) and it is suggested that PKR might potentiate the type I IFN response upon viral infections (as reviewed in Pfaller et al., 2011).

Der and Lau initially showed that induction of *IFNA* and *IFNB* genes was impaired in PKR deficient U-937 cells (a human lymphoma) upon exposure to several inducers including LPS and encephalomyocarditis virus (EMCV) (Der and Lau, 1995; Schulz et al., 2010). PKR knock-down reduces IFN- $\beta$  and/or IFN- $\alpha$  induction upon transfection with dsRNA (Diebold et al., 2003; McAllister and Samuel, 2009) but also during infection with a measles virus vaccine strain (McAllister et al., 2010). Interestingly, PKR silencing or inhibition with pharmacological inhibitors both led to increased induction levels of IFN- $\beta$  upon Hepatitis C Virus (HCV) infection (Arnaud et al., 2010).

Taken together, these results suggest that PKR can act as an enhancer for IFN- $\beta$  production for some but not all viruses. It has been suggested that PKR is not required for IFN- $\alpha/\beta$  production in cells infected with RIG-I dependent viruses (Sendai virus, influenza), while it promotes IFN- $\alpha/\beta$  production to MDA5-dependent viruses (EMCV, rotavirus, West Nile virus, Semliki Forest virus) (Schulz et al., 2010).

#### 2.4.3.2. Underlying mechanisms

PKR-dependent enhancement of IFN- $\beta$  induction may involve several pathways. The *IFNB* promoter contains NF- $\kappa$ B as well as IFN-regulatory factor (IRF)-binding sites (Garoufalidis et al., 1994). PKR may also act as a stabiliser of *IFNB* transcripts, as an activator of the IRF1 pathway, or as a STAT regulator.

**Activation of NF- $\kappa$ B.** IFN- $\beta$  induction involves the PKR-dependent activation of ATF2 and NF- $\kappa$ B activation whereas IRF3 activation was a PKR-independent process during measles virus infection (McAllister et al., 2010). Another study showed that LPS stimulation also led to induction of IFN- $\beta$  through PKR-mediated activation of NF- $\kappa$ B, resulting in STAT1 phosphorylation and STAT1-dependent transcription of inflammatory cytokines and chemokines (Lee et al., 2005). Chemical inhibition of PKR activity and/or PKR knock-down resulted in inhibition of STAT1 phosphorylation and subsequent STAT-mediated transcription of inflammatory genes, as well as suppression of nuclear factors binding activity to GAS/ IFN-stimulated response elements (ISRE) in the context of stimulation with LPS (Lee et al., 2005). Nevertheless, as mentioned above, the molecular mechanisms by which PKR activates NF- $\kappa$ B are still poorly understood.

***PKR as an adaptor in RIG-I/MDA5 signalling pathway.*** PKR was shown to directly interact with components of the retinoic acid-inducible gene I (RIG-I)/ melanoma differentiation-associated protein 5 (MDA5) signalling pathway, which stimulates IFN- $\beta$  production. For example, knockdown and co-immuno-precipitation studies showed that upon HCV infection PKR interacts with mitochondrial antiviral-signalling protein (MAVS) and TRAF3 but not RIG-I leading to a strong induction of protein ISG15 as well as other IRF3-dependent IFN simulated genes (ISGs) (Arnaud et al., 2011). These associations required dsRBMs but not the kinase activity of PKR, suggesting that PKR acts as an adaptor protein in this pathway (Arnaud et al., 2011). PKR was also reported to associate with MDA5 and to stimulate IFN- $\beta$  production in a kinase-dependent manner after vaccinia virus infection without eIF2 $\alpha$  phosphorylation requirement (Pham et al., 2016). Further investigation revealed that PKR was required for IRF3 phosphorylation and nuclear translocation during vaccinia virus or EMCV infection (Pham et al., 2016; Zhang and Samuel, 2008). Furthermore, it was shown that activation of PKR resulted in IFN- $\beta$  upregulation even in the absence of MDA5, but required MAVS, suggesting that PKR acts as a signal transducer between these two elements of the pathway (Pham et al., 2016). Consistent with this hypothesis, a direct interaction between PKR and MAVS has also been reported (Zhang et al., 2014).

Direct interaction between PKR and RIG-I upon influenza or vaccinia virus infections has also been recently reported (Pham et al., 2016; Yoo et al., 2014) but PKR activation was not required in RIG-I signalling pathway, suggesting that PKR role downstream of RIG-I might be redundant with other signals.

***PKR as a stabiliser of IFNB transcripts.*** Schulz et al. reported that EMCV infection strongly induced *IFNB* transcription in PKR-deficient cells, but little or no IFN- $\beta$  protein was produced (Schulz et al., 2010). Similarly, Sen et al. reported low IFN- $\beta$  secretion in *Pkr*<sup>-/-</sup> MEFs infected with rotavirus compared to wildtype MEFs although the transcript levels were not reduced (Sen et al., 2011). Further investigation revealed that *IFNB* mRNAs produced in EMCV-infected PKR-deficient cells lacked a polyA-tail, suggesting that PKR is required for the integrity and stability of *IFNB* transcripts (Schulz et al., 2010). However, the regulation of this mechanism by PKR is currently not known.

***PKR as component of IRF1 pathway.*** IRF1 regulates the expression of *IFNA* and *IFNB* genes and is strongly induced upon viral infections (Fujita et al., 1989). Activation of IRF1 promoter in response to dsRNA exposure is defective in *Pkr*<sup>-/-</sup> MEFs, suggesting that PKR acts as a signal transducer for IRF1-dependent gene induction (Kumar et al., 1997). This hypothesis is also supported by another study showing that HCV inhibits PKR, thereby suppressing IRF1 activation and IRF1-dependent gene expression (Pflugheber et al., 2002). The mechanisms by which PKR promotes IRF1 activation are poorly understood.

**PKR as a STAT regulator.** PKR might also play a role downstream of the IFN pathway, as a few studies reports its interaction with STATs proteins. PKR associates with STAT1 in mammalian cells independently from its kinase activity (Wong et al., 1997, 2001). This interaction takes place in unstimulated cells but stimulation with IFNs or dsRNA leads to the dissociation of the PKR-STAT1 complex. Furthermore, increased levels of PKR-STAT1 complex have a negative effect on STAT1 DNA binding capacity, thereby impairing STAT1 transcriptional function (Wong et al., 1997). This suggests that PKR functions as a negative regulator of STAT1.

Very few studies have focused on Pkr role in type I Ifn production in fish. Nevertheless, chemical inhibition of Pkr (but also Perk) resulted in reduced mRNA levels of *ifn* and *mx1* in RTG2 and RTgill cells upon VHSV infection (Ramnani et al., 2023). Overexpression studies in fish showed that *irf1-3-7*, *isg15*, *isg56*, and *mx* were all significantly increased in cells overexpressing orange-spotted grouper (*Epinephelus coioides*) EcPkr (Wei et al., 2020). In addition, reporter studies showed that EcPkr overexpression led to increased activity of *ifnb* and *nfkB* promoters compared to the cells transfected with the empty vector (Wei et al., 2020). Similarly, overexpression of Grass carp CiPkr leads to enhanced activity of *ifn* promoter in CIK and CO cells, and CiPkr knock-down results in reduced induction of type I *ifn* mRNA upon poly(G:C) stimulation (Xu et al., 2019). Co-immunoprecipitation assays showed that CiPkr can separately interact with Irf3, Sting, Zdhhc1, eIF2 $\alpha$ , Irf9, and Stat2 (Xu et al., 2019). Another recent study demonstrated that STAT3 binds the catalytic domain of human PKR, thereby inhibiting its capacity to phosphorylate eIF2 $\alpha$  and to mediate starvation-induced autophagy (Shen et al., 2012). Physical interaction between cytoplasmic grass carp CiStat3 and CiPkr was also reported, *in vivo* and *in vitro* (Wang et al., 2018). Overexpression of CiStat3 in CIK cells reduced the levels of eIF2 $\alpha$  phosphorylation, while knockdown led to opposite results (Wang et al., 2018).

#### **2.4.4. Reconciling two antagonist PKR-mediated programmes via sequential activation**

PKR is involved in two seemingly antagonist programmes upon viral infections: (1) protein translation shut-off in individual virally infected cells and initiation of apoptosis; (2) a survival pathway mediated by NF- $\kappa$ B leading to cytokine production and promotion of a systemic immune response, thereby preventing spreading of the viral infection.

Some authors have proposed that PKR can activate those two programmes in a sequential manner during the course of a viral infection, leading to a chronological activation of the survival and apoptosis responses (Donzé et al., 2004). This hypothesis is supported by the observation that NF- $\kappa$ B and anti-apoptotic signals (e.g., cellular inhibitors of apoptosis (cIAPs), A20) are activated by PKR overexpression several hours prior to the beginning of eIF2 $\alpha$ -mediated cell death. It was suggested

that the interplay between kinase-independent (NF- $\kappa$ B pathway) and kinase-dependent (eIF2 $\alpha$ ) strategies allows fine-tuning of two opposite cellular programmes, namely cell survival to delay cell death in order to alert naive cells by producing antiviral cytokines, and apoptosis to eliminate infected cells (Donzé et al., 2004). It is not known if fish Pkr and Pkz may show this temporal control.

### 3. PKR antiviral activity and modulation of PKR during viral infection

#### 3.1. PKR antiviral activity

##### 3.1.1. Mammalian PKR

PKR constitutes a fast defence mechanism against viral infections and depletion of PKR often lead to increased viral titres *in vitro* and *in vivo*.

In mammals, several studies have shown that viruses tend to replicate more efficiently in PKR-deficient MEFs or cell lines, such as EMCV (Der & Lau, 1995), Sendai and Sindbis viruses (Zuo et al., 2022). Similarly, mice lacking PKR showed increased mortality following vesicular stomatitis virus infection (Durbin et al., 2002), coxsackievirus (Flodström-Tullberg et al., 2005) or West Nile virus (Samuel et al., 2006).

In some cases, however, PKR-deficient MEFs show no detectable increase in virus yield, as for dengue virus (Diamond and Harris, 2001), or display reduced titres, as for HCV (Arnaud et al., 2010).

##### 3.1.2. Fish Pkr and Pkz

In fish, studies focused on the antiviral activity of Pkr and Pkz are scarce (Table 2): Liu et al. showed that overexpression of either Grass carp CiPkr or CiPkz lead to inhibition of GCRV; this antiviral activity was enhanced when both kinases were overexpressed (Liu et al., 2011). Conversely, knock-down assays of either or both kinases made fish cells more permissive to virus infection, although the antiviral ability of CiPkz seemed weaker than CiPkr, which correlated with its lower ability to phosphorylate eIF2 $\alpha$  (Liu et al., 2011). Recent overexpression studies showed that overexpressed Nile tilapia OnPkr leads to reduced GCRV in FHM cells (Gan et al., 2021). Similar results were obtained with orange spotted grouper EcPkr in GS cells infected with red-spotted grouper nervous necrosis virus (RGNNV) (Wei et al., 2020). Interestingly, although chemical inhibition of OmPkr in RTG2 and RTGill resulted in increased VHSV N mRNA levels, it did not have any impact on viral titres in comparison to untreated cells (Ramnani et al., 2023). An *in vivo* study in Zebrafish larvae infected with CyHV-3 also showed that *pkr* KO had no effect on viral levels while *pkz* KO larvae displayed higher viral levels during 1-4 dpi but not afterwards (Streiff et al., 2023).

Curiously, treatment with pharmaceutical inhibitors of Pkr resulted in reduced infectious pancreatic necrosis virus (IPNV) titre in CHSE214 (Gamil et al., 2016). Although IPNV infection in CHSE214

induces phosphorylation of eIF2 $\alpha$  and protein synthesis inhibition, PKR transcript and protein were not induced over the course of IPNV infection (Gamil et al., 2016, 2015). It was suggested protein inhibition might be part of IPNV strategy to evade the host antiviral response.

### 3.2. Modulation of PKR at the transcriptional and translational level

#### 3.2.1. Transcriptional regulation of PKR expression

Transcription factor binding sites in the 5'-untranslated region of mammalian PKR gene include an ISRE, a kinase-conserved sequence (KCS) response element, as well as a p53 response elements (reviewed in Pindel and Sadler, 2011). Yoon et al. confirmed with *p53* KO cell lines that p53 induces the expression of PKR under IFN stimulation or genotoxic stress. Furthermore, luciferase reporter assay showed that p53 activates the *PKR* promoter independently from ISRE (Yoon et al., 2009).

In fish, it was also found that Grass carp Cip53 can bind to CiPkr promoter with high affinity. Interestingly, when Cip53 was knocked down in CIK cells, the mRNA levels of CiPkr were decreased, suggesting an effect on *pkcr* transcription (Huang et al., 2017b).

#### 3.2.2. Translational autoregulation

Activated PKR autoregulates the expression of its own mRNA via the inhibition of protein translation initiation (Thomis and Samuel, 1992). Similar results were suggested in fish, as non-functional CaPkr but not catalytically active CaPkr can be detected by western blot in transfected EPC cells (Xu et al., 2018).

### 3.3. Inhibitors of PKR functions

The list of PKR cellular inhibitors has been extensively reviewed by Garcia et al (2006). Cellular inhibitors of PKR include: 58-kDa inhibitor of PKR (P58<sup>IPK</sup>), trans-activation response RNA-binding protein (TRBP), 67kDa-glycoprotein (p67), nucleophosmin (NPM), MDA7, HSP90 and HSP70 (García et al., 2006). Except P58<sup>IPK</sup> and TRBP, the role of these inhibitors during viral infection has not been always elucidated and will not be further discussed in this review. Importantly, those inhibitors have been identified in mammalian systems and it is currently not known if their fish counterparts exist and/or function in a similar fashion.

#### 3.3.1. P58<sup>IPK</sup>

P58<sup>IPK</sup> belongs to the tetratricopeptide repeat family of proteins and is recruited by influenza virus to block PKR antiviral functions (Lee et al., 1994). Mechanistically, it inhibits PKR autophosphorylation and the subsequent phosphorylation of eIF2 $\alpha$  (Lee et al., 1994). P58<sup>IPK</sup> knockout

mice infected with influenza displayed increased lung pathology and mortality rate, which correlated with PKR activation and eIF2 $\alpha$  phosphorylation (Goodman et al., 2009).

### 3.3.2. trans-activation response RNA-binding protein (TRBP)

The trans-activation response RNA-binding protein (TRBP) inhibits PKR function by direct interaction as well as by binding PKR activators, namely dsRNA and PACT, thereby sequestering them away from PKR (Benkirane et al., 1997; Daher et al., 2009). Interestingly, MAPK-mediated phosphorylation of TRBP potentiates TRBP ability to inhibit PKR during oxidative stress (Chukwurah and Patel, 2018). Unique orthologues of *trbp* can be found in fish genomes, including Zebrafish and Pufferfish (Murphy et al., 2008), suggesting that this pathway might be functional in fish.

## 3.4. PKR modulation in stress granules (SGs)

### 3.4.1. SGs in mammals

PKR-mediated inhibition of the translation machinery results in the accumulation of stalled translation pre-initiation complexes, which assemble into cytoplasmic ribonucleoprotein complexes called stress granules (SGs) (Kedersha et al., 2002; Kimball et al., 2003; Protter & Parker, 2016). Importantly, SG formation is induced in response to environmental stress conditions, including heat/cold shock, oxidative and osmotic stress, UV irradiation but also viral infections (Hofmann et al., 2021).

Substantial evidence indicates that PKR plays a key role in the SG formation as well as in their antiviral activity. SG formation often occurs in an eIF2 $\alpha$  phosphorylation-dependent manner upon viral infections (reviewed by Miller, 2011). Overexpression and KO studies demonstrated that PKR is necessary for formation of SGs upon transfection with poly(I:C) and infection with Influenza A virus, and plays a key role in the induction of *IFNB* gene and the production of IFN- $\beta$  protein (Onomoto et al., 2012). It was also recently discovered that DEAH-Box Helicase 36 (DHX36):RIG-I complex facilitates the activation of PKR upon dsRNA exposure or viral infection (influenza, Newcastle disease virus), resulting in subsequent SG formation (Yoo et al., 2014). The newly formed SGs provide a platform for antiviral signalling pathways by recruiting PKR as well as other RNA-binding proteins (MDA5, RIG-I, oligoadenylate synthetase (OAS)) thereby potentiating eIF2 $\alpha$  phosphorylation and promoting transcription of type I IFNs and inflammatory cytokines via MAVS-driven activation of IRF3/7 and NF- $\kappa$ B transcription factors (Onomoto et al., 2012; Reineke and Lloyd, 2015).

### 3.4.2. SGs in fish

A recent study showed that SG formation is triggered by Perk and not Pkr upon VHSV infection in EPC cells but also RTG-2 and RTGill (Ramnani et al., 2023). This is consistent with previous studies reporting that VHSV infection in EPC cells regulates translation by activating the Perk/eIF2 $\alpha$  pathway rather than by Pkr (Kesterson et al., 2020). Similar results were obtained in a GS cell lines upon RGNNV infection: chemical inhibition of Pkr had little effect on the formation of SGs, whereas inhibition of Perk significantly limited the formation of SGs and decreased the phosphorylation of eIF2 $\alpha$  (Sun et al., 2022). In contrast, measles virus infection induces SG formation in Pkr-deficient cells complemented by transfection with Zebrafish DrPkr but not DrPkz (Taghavi and Samuel, 2013). The possible role of fish Pkz in the formation of SG induced by fish viruses has, however, not been studied.

### 3.5. Viral subversion of PKR activation in fish

PKR subversion mechanisms were recently reviewed for mammalian viruses by Cesaro et Michiels in 2021. No specific studies, however, were conducted in fish. There are a few reports demonstrating the ability of some fish viral protein to sequester dsRNA and therefore, prevent optimal activation of PKR and other dsRNA receptors. The betanodavirus B2 is capable of binding its own dsRNA (Fenner et al., 2006; Ou et al., 2007) and prevent dsRNA-dependent processes. The ORF2 protein encoded by the segment 8 of the infectious salmon anaemia virus (ISAV) has been described as a type I IFN suppressor (McBeath et al., 2006) with some dsRNA binding properties (García-Rosado et al., 2008; Olsen et al., 2016). Some viruses can also subvert sequestration of cellular proteins to allow full replication in infected cells. This is the case for GCRV, where the cellular CiTia1 binds dsRNA, depleting it for efficient activation of Pkr (Song et al., 2015). These are indirect observations and further specific studies would be required to evaluate the limitation of PKR activation. Finally, the vIF2 $\alpha$  protein from *Rana catesbeiana* iridovirus Z is a functional inhibitor of human PKR and Zebrafish DrPkr, and probably functions as a pseudosubstrate inhibitor of PKR (Rothenburg et al., 2011).

## Conclusion

As presented in this review, PKR is a versatile kinase at the crossroads of virus sensing, stress response and innate immune signalling pathways: once activated, it initiates inhibition and protein translation and promotes apoptosis, but it also acts as a transducer in the inflammatory and IFN responses. Its crucial role in the antiviral response is further supported by the finding that many viruses evolved subversion strategies to antagonise PKR-mediated antiviral mechanisms. Although

studies focusing on fish Pkr are relatively scarce, it seems that the antiviral functions attributed to mammalian PKR are also relatively conserved in these organisms. The existence of a fish specific Pkr-like protein, namely Pkz, raises further questions about their respective and/or cooperative roles in fish antiviral response. This opens many interesting avenues for future investigation to provide insights into fish Pkr and Pkz mode of action. The generation of KO mutants, guided by transcriptomic data, will help to provide an integrated picture of this complex network.

## Acknowledgements

This work has been funded by the projects ANR LipofishVac (ANR-21-CE35-0019) and ERANET ICRAD nucnanofish, and by institutional funding from INRAE.

## References

- Aloni-Grinstein, R., Charni-Natan, M., Solomon, H., Rotter, V., 2018. p53 and the Viral Connection: Back into the Future. *Cancers (Basel)* 10, 178. <https://doi.org/10.3390/cancers10060178>
- Arnaud, N., Dabo, S., Akazawa, D., Fukasawa, M., Shinkai-Ouchi, F., Hugon, J., Wakita, T., Meurs, E.F., 2011. Hepatitis C Virus Reveals a Novel Early Control in Acute Immune Response. *PLoS Pathog* 7, e1002289. <https://doi.org/10.1371/journal.ppat.1002289>
- Arnaud, N., Dabo, S., Maillard, P., Budkowska, A., Kalliampakou, K.I., Mavromara, P., Garcin, D., Hugon, J., Gagnon, A., Akazawa, D., Wakita, T., Meurs, E.F., 2010. Hepatitis C Virus Controls Interferon Production through PKR Activation. *PLoS One* 5, e10575. <https://doi.org/10.1371/journal.pone.0010575>
- Aubrey, B.J., Kelly, J., Janic, A., Herold, M.J., Strasser, A., 2018. How does p53 induce apoptosis and how does this relate to p53-mediated tumour suppression? *Cell Death Differ* 25, 104–113. <https://doi.org/10.1038/cdd.2017.169>
- Barber, G.N., Tomita, J., Hovanessian, A.G., Meurs, E., Katze, M.G., 1991. Functional expression and characterization of the interferon-induced double-stranded RNA activated P68 protein kinase from *Escherichia coli*. *Biochemistry* 30, 10356–10361. <https://doi.org/10.1021/bi00106a038>
- Benkirane, M., Neuveut, C., Chun, R.F., Smith, S.M., Samuel, C.E., Gagnon, A., Jeang, K.T., 1997. Oncogenic potential of TAR RNA binding protein TRBP and its regulatory interaction with RNA-dependent protein kinase PKR. *EMBO J* 16, 611–624. <https://doi.org/10.1093/emboj/16.3.611>
- Bennett, R.L., Blalock, W.L., May, W.S., 2004. Serine 18 phosphorylation of RAX, the PKR activator, is required for PKR activation and consequent translation inhibition. *J Biol Chem* 279, 42687–42693. <https://doi.org/10.1074/jbc.M403321200>
- Bennett, R.L., Pan, Y., Christian, J., Hui, T., May, W.S., 2012. The RAX/PACT-PKR stress response pathway promotes p53 sumoylation and activation, leading to G1 arrest. *Cell Cycle* 11, 407–417. <https://doi.org/10.4161/cc.11.2.18999>
- Bergan, V., Jagus, R., Lauksund, S., Kileng, Ø., Robertsen, B., 2008. The Atlantic salmon Z-DNA binding protein kinase phosphorylates translation initiation factor 2 alpha and constitutes a unique orthologue to the mammalian dsRNA-activated protein kinase R. *The FEBS Journal* 275, 184–197. <https://doi.org/10.1111/j.1742-4658.2007.06188.x>
- Berlanga, J.J., Ventoso, I., Harding, H.P., Deng, J., Ron, D., Sonenberg, N., Carrasco, L., de Haro, C., 2006. Antiviral effect of the mammalian translation initiation factor 2 $\alpha$  kinase GCN2 against RNA viruses. *EMBO J* 25, 1730–1740. <https://doi.org/10.1038/sj.emboj.7601073>
- Bonnet, M.C., Weil, R., Dam, E., Hovanessian, A.G., Meurs, E.F., 2000. PKR Stimulates NF- $\kappa$ B Irrespective of Its Kinase Function by Interacting with the I $\kappa$ B Kinase Complex. *Mol Cell Biol* 20, 4532–4542.
- Cesaro, T., Michiels, T., 2021. Inhibition of PKR by Viruses. *Front Microbiol* 12, 757238. <https://doi.org/10.3389/fmicb.2021.757238>
- Cheng, G., Feng, Z., He, B., 2005. Herpes Simplex Virus 1 Infection Activates the Endoplasmic Reticulum Resident Kinase PERK and Mediates eIF-2 $\alpha$  Dephosphorylation by the  $\gamma$ 134.5 Protein. *J Virol* 79, 1379–1388. <https://doi.org/10.1128/JVI.79.3.1379-1388.2005>
- Chukwurah, E., Farabaugh, K.T., Guan, B.-J., Ramakrishnan, P., Hatzoglou, M., 2021. A tale of two proteins: PACT and PKR and their roles in inflammation. *The FEBS Journal* 288, 6365–6391. <https://doi.org/10.1111/febs.15691>
- Chukwurah, E., Patel, R.C., 2018. Stress-induced TRBP phosphorylation enhances its interaction with PKR to regulate cellular survival. *Sci Rep* 8, 1020. <https://doi.org/10.1038/s41598-018-19360-8>
- Clemens, M.J., Elia, A., 1997. The double-stranded RNA-dependent protein kinase PKR: structure and function. *J Interferon Cytokine Res* 17, 503–524. <https://doi.org/10.1089/jir.1997.17.503>
- Clemens, M.J., Hershey, J.W., Hovanessian, A.C., Jacobs, B.C., Katze, M.G., Kaufman, R.J., Lengyel, P., Samuel, C.E., Sen, G.C., Williams, B.R., 1993. PKR: proposed nomenclature for the RNA-dependent protein kinase induced by interferon. *J Interferon Res* 13, 241. <https://doi.org/10.1089/jir.1993.13.241>
- Cole, J., 2007. Activation of PKR: an open and shut case? *Trends in Biochemical Sciences* 32, 57–62. <https://doi.org/10.1016/j.tibs.2006.12.003>

- Content, J., Lebleu, B., Nudel, U., Zilberstein, A., Berissi, H., Revel, M., 1975. Blocks in elongation and initiation of protein synthesis induced by interferon treatment in mouse L cells. *Eur J Biochem* 54, 1–10. <https://doi.org/10.1111/j.1432-1033.1975.tb04106.x>
- Cuddihy, A.R., Li, S., Tam, N.W.N., Wong, A.H.-T., Taya, Y., Abraham, N., Bell, J.C., Koromilas, A.E., 1999. Double-Stranded-RNA-Activated Protein Kinase PKR Enhances Transcriptional Activation by Tumor Suppressor p53. *Mol Cell Biol* 19, 2475–2484.
- Daher, A., Laraki, G., Singh, M., Melendez-Peña, C.E., Bannwarth, S., Peters, A.H.F.M., Meurs, E.F., Braun, R.E., Patel, R.C., Gatignol, A., 2009. TRBP Control of PACT-Induced Phosphorylation of Protein Kinase R Is Reversed by Stress. *Mol Cell Biol* 29, 254–265. <https://doi.org/10.1128/MCB.01030-08>
- del Castillo, C.S., Hikima, J., Ohtani, M., Jung, T.-S., Aoki, T., 2012. Characterization and functional analysis of two PKR genes in fugu (*Takifugu rubripes*). *Fish & Shellfish Immunology* 32, 79–88. <https://doi.org/10.1016/j.fsi.2011.10.022>
- Der, S.D., Lau, A.S., 1995. Involvement of the double-stranded-RNA-dependent kinase PKR in interferon expression and interferon-mediated antiviral activity. *Proc Natl Acad Sci U S A* 92, 8841–8845.
- Der, S.D., Yang, Y.-L., Weissmann, C., Williams, B.R.G., 1997. A double-stranded RNA-activated protein kinase-dependent pathway mediating stress-induced apoptosis. *Proc Natl Acad Sci U S A* 94, 3279–3283.
- Dey, M., Cao, C., Dar, A.C., Tamura, T., Ozato, K., Sicheri, F., Dever, T.E., 2005. Mechanistic Link between PKR Dimerization, Autophosphorylation, and eIF2 $\alpha$  Substrate Recognition. *Cell* 122, 901–913. <https://doi.org/10.1016/j.cell.2005.06.041>
- Dey, M., Cao, C., Sicheri, F., Dever, T.E., 2007. Conserved intermolecular salt bridge required for activation of protein kinases PKR, GCN2, and PERK. *J Biol Chem* 282, 6653–6660. <https://doi.org/10.1074/jbc.M607897200>
- Dey, M., Mann, B.R., Anshu, A., Mannan, M.A., 2014. Activation of Protein Kinase PKR Requires Dimerization-induced cis-Phosphorylation within the Activation Loop. *Journal of Biological Chemistry* 289, 5747–5757. <https://doi.org/10.1074/jbc.M113.527796>
- Diallo, M.A., Pirotte, S., Hu, Y., Morvan, L., Rakus, K., Suárez, N.M., PoTsang, L., Saneyoshi, H., Xu, Y., Davison, A.J., Tompa, P., Sussman, J.L., Vanderplassen, A., 2023. A fish herpesvirus highlights functional diversities among Za domains related to phase separation induction and A-to-Z conversion. *Nucleic Acids Res* 51, 806–830. <https://doi.org/10.1093/nar/gkac761>
- Diamond, M.S., Harris, E., 2001. Interferon inhibits dengue virus infection by preventing translation of viral RNA through a PKR-independent mechanism. *Virology* 289, 297–311. <https://doi.org/10.1006/viro.2001.1114>
- Diebold, S.S., Montoya, M., Unger, H., Alexopoulou, L., Roy, P., Haswell, L.E., Al-Shamkhani, A., Flavell, R., Borrow, P., Reis e Sousa, C., 2003. Viral infection switches non-plasmacytoid dendritic cells into high interferon producers. *Nature* 424, 324–328. <https://doi.org/10.1038/nature01783>
- Donnelly, N., Gorman, A.M., Gupta, S., Samali, A., 2013. The eIF2 $\alpha$  kinases: their structures and functions. *Cell. Mol. Life Sci.* 70, 3493–3511. <https://doi.org/10.1007/s00018-012-1252-6>
- Donzé, O., Deng, J., Curran, J., Sladek, R., Picard, D., Sonenberg, N., 2004. The protein kinase PKR: a molecular clock that sequentially activates survival and death programs. *EMBO J* 23, 564–571. <https://doi.org/10.1038/sj.emboj.7600078>
- Durbin, R.K., Mertz, S.E., Koromilas, A.E., Durbin, J.E., 2002. PKR protection against intranasal vesicular stomatitis virus infection is mouse strain dependent. *Viral Immunol* 15, 41–51. <https://doi.org/10.1089/088282402317340224>
- Dzananovic, E., McKenna, S.A., Patel, T.R., 2018. Viral proteins targeting host protein kinase R to evade an innate immune response: a mini review. *Biotechnology and Genetic Engineering Reviews* 34, 33–59. <https://doi.org/10.1080/02648725.2018.1467151>
- Elmore, S., 2007. Apoptosis: A Review of Programmed Cell Death. *Toxicol Pathol* 35, 495–516. <https://doi.org/10.1080/01926230701320337>
- Fenner, B.J., Goh, W., Kwang, J., 2006. Sequestration and Protection of Double-Stranded RNA by the Betanodavirus B2 Protein. *J Virol* 80, 6822–6833. <https://doi.org/10.1128/JVI.00079-06>
- Flodström-Tullberg, M., Hultcrantz, M., Stotland, A., Maday, A., Tsai, D., Fine, C., Williams, B., Silverman, R., Sarvetnick, N., 2005. RNase L and double-stranded RNA-dependent protein kinase exert complementary roles in islet cell defense during coxsackievirus infection. *J Immunol* 174, 1171–1177. <https://doi.org/10.4049/jimmunol.174.3.1171>
- Fujita, T., Kimura, Y., Miyamoto, M., Barsoumian, E.L., Taniguchi, T., 1989. Induction of endogenous IFN- $\alpha$  and IFN- $\beta$  genes by a regulatory transcription factor, IRF-1. *Nature* 337, 270–272. <https://doi.org/10.1038/337270a0>
- Fullam, A., Schröder, M., 2013. DExD/H-box RNA helicases as mediators of anti-viral innate immunity and essential host factors for viral replication. *Biochim Biophys Acta Gene Regul Mech* 1829, 854–865. <https://doi.org/10.1016/j.bbagr.2013.03.012>
- Gal-Ben-Ari, S., Barrera, I., Ehrlich, M., Rosenblum, K., 2019. PKR: A Kinase to Remember. *Front Mol Neurosci* 11, 480. <https://doi.org/10.3389/fnmol.2018.00480>
- Gamil, A.A.A., Mutoloki, S., Evensen, Ø., 2015. A Piscine Birnavirus Induces Inhibition of Protein Synthesis in CHSE-214 Cells Primarily through the Induction of eIF2 $\alpha$  Phosphorylation. *Viruses* 7, 1987–2005. <https://doi.org/10.3390/v7041987>
- Gamil, A.A.A., Xu, C., Mutoloki, S., Evensen, Ø., 2016. PKR Activation Favors Infectious Pancreatic Necrosis Virus Replication in Infected Cells. *Viruses* 8. <https://doi.org/10.3390/v8060173>
- Gan, Z., Cheng, J., Hou, J., Chen, S., Xia, H., Xia, L., Kwok, K.W.H., Lu, Y., Nie, P., 2021. tilapia dsRNA-activated protein kinase R (PKR): An interferon-induced antiviral effector with translation inhibition activity. *Fish Shellfish Immunol* 112, 74–80. <https://doi.org/10.1016/j.fsi.2021.02.016>
- García, M.A., Gil, J., Ventoso, I., Guerra, S., Domingo, E., Rivas, C., Esteban, M., 2006. Impact of Protein Kinase PKR in Cell Biology: from Antiviral to Antiproliferative Action. *Microbiol Mol Biol Rev* 70, 1032–1060. <https://doi.org/10.1128/MMBR.00027-06>
- García-Rosado, E., Markussen, T., Kileng, O., Baekkevold, E.S., Robertsen, B., Mjaaland, S., Rimstad, E., 2008. Molecular and functional characterization of two infectious salmon anaemia virus (ISAV) proteins with type I interferon antagonizing activity. *Virus Res* 133, 228–238. <https://doi.org/10.1016/j.virusres.2008.01.008>
- Garoufalos, E., Kwan, I., Lin, R., Mustafa, A., Pepin, N., Roulston, A., Lacoste, J., Hiscott, J., 1994. Viral induction of the human beta interferon promoter: modulation of transcription by NF- $\kappa$ B/rel proteins and interferon regulatory factors. *J Virol* 68, 4707–4715.

- Gil, J., Esteban, M., 2000a. The interferon-induced protein kinase (PKR), triggers apoptosis through FADD-mediated activation of caspase 8 in a manner independent of Fas and TNF- $\alpha$  receptors. *Oncogene* 19, 3665–3674. <https://doi.org/10.1038/sj.onc.1203710>
- Gil, J., Esteban, M., 2000b. Induction of apoptosis by the dsRNA-dependent protein kinase (PKR): Mechanism of action. *Apoptosis* 5, 107–114. <https://doi.org/10.1023/A:1009664109241>
- Gil, J., García, M.A., Esteban, M., 2002. Caspase 9 activation by the dsRNA-dependent protein kinase, PKR: molecular mechanism and relevance. *FEBS Lett* 529, 249–255. [https://doi.org/10.1016/s0014-5793\(02\)03348-3](https://doi.org/10.1016/s0014-5793(02)03348-3)
- Gil, J., García, M.A., Gomez-Puertas, P., Guerra, S., Rullas, J., Nakano, H., Alcamí, J., Esteban, M., 2004. TRAF Family Proteins Link PKR with NF- $\kappa$ B Activation. *Mol Cell Biol* 24, 4502–4512. <https://doi.org/10.1128/MCB.24.10.4502-4512.2004>
- Gil, J., Rullas, J., García, M.A., Alcamí, J., Esteban, M., 2001. The catalytic activity of dsRNA-dependent protein kinase, PKR, is required for NF- $\kappa$ B activation. *Oncogene* 20, 385–394. <https://doi.org/10.1038/sj.onc.1204109>
- Goh, K.C., deVeer, M.J., Williams, B.R., 2000. The protein kinase PKR is required for p38 MAPK activation and the innate immune response to bacterial endotoxin. *EMBO J* 19, 4292–4297. <https://doi.org/10.1093/emboj/19.16.4292>
- Goodman, A.G., Fornek, J.L., Medigeshi, G.R., Perrone, L.A., Peng, X., Dyer, M.D., Proll, S.C., Knoblaugh, S.E., Carter, V.S., Korth, M.J., Nelson, J.A., Tumpey, T.M., Katze, M.G., 2009. P58IPK: A Novel “CIHD” Member of the Host Innate Defense Response against Pathogenic Virus Infection. *PLOS Pathogens* 5, e1000438. <https://doi.org/10.1371/journal.ppat.1000438>
- Grilli, M., Chiu, J.J., Lenardo, M.J., 1993. NF- $\kappa$ B and Rel: participants in a multifunctional transcriptional regulatory system. *Int Rev Cytol* 143, 1–62. [https://doi.org/10.1016/s0074-7696\(08\)61873-2](https://doi.org/10.1016/s0074-7696(08)61873-2)
- Guerra, S., López-Fernández, L.A., García, M.A., Zaballos, A., Esteban, M., 2006. Human Gene Profiling in Response to the Active Protein Kinase, Interferon-induced Serine/threonine Protein Kinase (PKR), in Infected Cells. *Journal of Biological Chemistry* 281, 18734–18745. <https://doi.org/10.1074/jbc.M511983200>
- Harding, H.P., Zhang, Y., Zeng, H., Novoa, I., Lu, P.D., Calfon, M., Sadri, N., Yun, C., Popko, B., Paules, R., Stojdl, D.F., Bell, J.C., Hettmann, T., Leiden, J.M., Ron, D., 2003. An Integrated Stress Response Regulates Amino Acid Metabolism and Resistance to Oxidative Stress. *Molecular Cell* 11, 619–633. [https://doi.org/10.1016/S1097-2765\(03\)00105-9](https://doi.org/10.1016/S1097-2765(03)00105-9)
- Hayden, M.S., Ghosh, S., 2012. NF- $\kappa$ B, the first quarter-century: remarkable progress and outstanding questions. *Genes Dev.* 26, 203–234. <https://doi.org/10.1101/gad.183434.111>
- Hofmann, S., Kedersha, N., Anderson, P., Ivanov, P., 2021. Molecular mechanisms of stress granule assembly and disassembly. *Biochim Biophys Acta Mol Cell Res* 1868, 118876. <https://doi.org/10.1016/j.bbamcr.2020.118876>
- Hovanessian, A.G., 1980. Double-stranded RNA dependent protein kinase (s) in rabbit reticulocyte lysates analogous to kinase from interferon-treated cells. *Biochimie* 62, 775–778. [https://doi.org/10.1016/s0300-9084\(80\)80132-5](https://doi.org/10.1016/s0300-9084(80)80132-5)
- Hovanessian, A.G., Galabru, J., 1987. The double-stranded RNA-dependent protein kinase is also activated by heparin. *Eur J Biochem* 167, 467–473. <https://doi.org/10.1111/j.1432-1033.1987.tb13360.x>
- Hu, C., 2004. Molecular cloning and characterisation of a fish PKR-like gene from cultured CAB cells induced by UV-inactivated virus\*1. *Fish & Shellfish Immunology* 17, 353–366. <https://doi.org/10.1016/j.fsi.2004.04.009>
- Hu, C.-Y., Zhang, Y.-B., Huang, G.-P., Zhang, Q.-Y., Gui, J.-F., 2004. Molecular cloning and characterisation of a fish PKR-like gene from cultured CAB cells induced by UV-inactivated virus. *Fish & Shellfish Immunology* 17, 353–366. <https://doi.org/10.1016/j.fsi.2004.04.009>
- Hu, H., Tian, M., Ding, C., Yu, S., 2019. The C/EBP Homologous Protein (CHOP) Transcription Factor Functions in Endoplasmic Reticulum Stress-Induced Apoptosis and Microbial Infection. *Frontiers in Immunology* 9.
- Hu, Y., Fan, L., Wu, C., Wang, B., Sun, Z., Hu, C., 2016. Identification and function analysis of the three dsRBMs in the N terminal dsRBD of grass carp (*Ctenopharyngodon idella*) PKR. *Fish Shellfish Immunol* 50, 91–100. <https://doi.org/10.1016/j.fsi.2016.01.011>
- Hu, Y.-S., Li, W., Li, D.-M., Liu, Y., Fan, L.-H., Rao, Z.-C., Lin, G., Hu, C.-Y., 2013. Cloning, expression and functional analysis of PKR from grass carp (*Ctenopharyngodon idellus*). *Fish & Shellfish Immunology* 35, 1874–1881. <https://doi.org/10.1016/j.fsi.2013.09.024>
- Hu, Z., Du, H., Lin, G., Han, K., Cheng, X., Feng, Z., Mao, H., Hu, C., 2020. Grass carp (*Ctenopharyngodon idella*) PACT induces cell apoptosis and activates NF- $\kappa$ B via PKR. *Fish Shellfish Immunol* 103, 377–384. <https://doi.org/10.1016/j.fsi.2020.05.036>
- Hua, B., Tamamori-Adachi, M., Luo, Y., Tamura, K., Morioka, M., Fukuda, M., Tanaka, Y., Kitajima, S., 2006. A Splice Variant of Stress Response Gene ATF3 Counteracts NF- $\kappa$ B-dependent Anti-apoptosis through Inhibiting Recruitment of CREB-binding Protein/p300 Coactivator\*. *Journal of Biological Chemistry* 281, 1620–1629. <https://doi.org/10.1074/jbc.M508471200>
- Huang, K., Qi, G., Sun, Z., Liu, X., Xu, X., Wang, H., Wu, Z., Wan, Y., Hu, C., 2017. *Ctenopharyngodon idella* IRF2 and ATF4 down-regulate the transcriptional level of PRKRA. *Fish & Shellfish Immunology* 64, 155–164. <https://doi.org/10.1016/j.fsi.2017.03.002>
- Huang, Q., Xie, D., Mao, H., Wang, H., Wu, Z., Huang, K., Wan, Y., Xu, Q., Hu, C., 2017. *Ctenopharyngodon idella* p53 mediates between NF- $\kappa$ B and PKR at the transcriptional level. *Fish Shellfish Immunol* 69, 258–264. <https://doi.org/10.1016/j.fsi.2017.08.012>
- Iordanov, M.S., Paranjape, J.M., Zhou, A., Wong, J., Williams, B.R.G., Meurs, E.F., Silverman, R.H., Magun, B.E., 2000. Activation of p38 Mitogen-Activated Protein Kinase and c-Jun NH2-Terminal Kinase by Double-Stranded RNA and Encephalomyocarditis Virus: Involvement of RNase L, Protein Kinase R, and Alternative Pathways. *Mol Cell Biol* 20, 617–627.
- Ishii, T., Kwon, H., Hiscott, J., Mosialos, G., Koromilas, A.E., 2001. Activation of the I kappa B alpha kinase (IKK) complex by double-stranded RNA-binding defective and catalytic inactive mutants of the interferon-inducible protein kinase PKR. *Oncogene* 20, 1900–1912. <https://doi.org/10.1038/sj.onc.1204267>
- Jackson, R.J., Hellen, C.U.T., Pestova, T.V., 2010. The Mechanism of Eukaryotic Translation Initiation and Principles of its Regulation. *Nat Rev Mol Cell Biol* 11, 113–127. <https://doi.org/10.1038/nrm2838>
- Jagus, R., Joshi, B., Barber, G.N., 1999. PKR, apoptosis and cancer. *The International Journal of Biochemistry & Cell Biology* 31, 123–138. [https://doi.org/10.1016/S1357-2725\(98\)00136-8](https://doi.org/10.1016/S1357-2725(98)00136-8)
- Jammi, N., Beal, P.A., 2001. Phosphorylation of the RNA-dependent protein kinase regulates its RNA-binding activity. *Nucleic Acids Res* 29, 3020–3029.

- Jeffrey, I.W., Kadereit, S., Meurs, E.F., Metzger, T., Bachmann, M., Schwemmle, M., Hovanessian, A.G., Clemens, M.J., 1995. Nuclear localization of the interferon-inducible protein kinase PKR in human cells and transfected mouse cells. *Exp Cell Res* 218, 17–27. <https://doi.org/10.1006/excr.1995.1126>
- Kaltschmidt, B., Kaltschmidt, C., Hofmann, T.G., Hehner, S.P., Dröge, W., Schmitz, M.L., 2000. The pro- or anti-apoptotic function of NF-kappaB is determined by the nature of the apoptotic stimulus. *Eur J Biochem* 267, 3828–3835. <https://doi.org/10.1046/j.1432-1327.2000.01421.x>
- Kataoka, T., Budd, R.C., Holler, N., Thome, M., Martinon, F., Imler, M., Burns, K., Hahne, M., Kennedy, N., Kovacovics, M., Tschopp, J., 2000. The caspase-8 inhibitor FLIP promotes activation of NF-kappaB and Erk signaling pathways. *Curr Biol* 10, 640–648. [https://doi.org/10.1016/s0960-9822\(00\)00512-1](https://doi.org/10.1016/s0960-9822(00)00512-1)
- Kataoka, T., Tschopp, J., 2004. N-Terminal Fragment of c-FLIP(L) Processed by Caspase 8 Specifically Interacts with TRAF2 and Induces Activation of the NF-κB Signaling Pathway. *Mol Cell Biol* 24, 2627–2636. <https://doi.org/10.1128/MCB.24.7.2627-2636.2004>
- Kaufman, R.J., 1999. Double-stranded RNA-activated protein kinase mediates virus-induced apoptosis: A new role for an old actor. *Proc Natl Acad Sci U S A* 96, 11693–11695.
- Kedersha, N., Chen, S., Gilks, N., Li, W., Miller, I.J., Stahl, J., Anderson, P., 2002. Evidence that ternary complex (eIF2-GTP-tRNA(i)(Met))-deficient preinitiation complexes are core constituents of mammalian stress granules. *Mol Biol Cell* 13, 195–210. <https://doi.org/10.1091/mbc.01-05-0221>
- Kerr, J.F.R., Wyllie, A.H., Currie, A.R., 1972. Apoptosis: A Basic Biological Phenomenon with Widespread Implications in Tissue Kinetics. *Br J Cancer* 26, 239–257. <https://doi.org/10.1038/bjc.1972.33>
- Kesterson, S.P., Ringiesn, J., Vakharia, V.N., Shepherd, B.S., Leaman, D.W., Malathi, K., 2020. Effect of the Viral Hemorrhagic Septicemia Virus Nonvirion Protein on Translation via PERK-eIF2α Pathway. *Viruses* 12, 499. <https://doi.org/10.3390/v12050499>
- Kim, C., 2020. How Z-DNA/RNA binding proteins shape homeostasis, inflammation, and immunity. *BMB Rep* 53, 453–457. <https://doi.org/10.5483/BMBRep.2020.53.9.141>
- Kim, D., Hur, J., Park, K., Bae, S., Shin, D., Ha, S.C., Hwang, H.-Y., Hohng, S., Lee, J.-H., Lee, S., Kim, Y.-G., Kim, K.K., 2014. Distinct Z-DNA binding mode of a PKR-like protein kinase containing a Z-DNA binding domain (PKZ). *Nucleic Acids Res* 42, 5937–5948. <https://doi.org/10.1093/nar/gku189>
- Kim, D., Hwang, H.Y., Kim, Y.G., Kim, K.K., 2009. Crystallization and preliminary X-ray crystallographic studies of the Z-DNA-binding domain of a PKR-like kinase (PKZ) in complex with Z-DNA. *Acta Crystallogr Sect F Struct Biol Cryst Commun* 65, 267–270. <https://doi.org/10.1107/S1744309109002504>
- Kimball, S.R., Horetsky, R.L., Ron, D., Jefferson, L.S., Harding, H.P., 2003. Mammalian stress granules represent sites of accumulation of stalled translation initiation complexes. *Am J Physiol Cell Physiol* 284, C273–284. <https://doi.org/10.1152/ajpcell.00314.2002>
- Komoike, Y., Matsuoka, M., 2016. Endoplasmic reticulum stress-mediated neuronal apoptosis by acrylamide exposure. *Toxicol Appl Pharmacol* 310, 68–77. <https://doi.org/10.1016/j.taap.2016.09.005>
- Komoike, Y., Matsuoka, M., 2013. Exposure to tributyltin induces endoplasmic reticulum stress and the unfolded protein response in Zebrafish. *Aquat Toxicol* 142–143, 221–229. <https://doi.org/10.1016/j.aquatox.2013.08.017>
- Kumar, A., Haque, J., Lacoste, J., Hiscott, J., Williams, B.R., 1994. Double-stranded RNA-dependent protein kinase activates transcription factor NF-kappa B by phosphorylating I kappa B. *Proc Natl Acad Sci U S A* 91, 6288–6292.
- Kumar, A., Yang, Y.L., Flati, V., Der, S., Kadereit, S., Deb, A., Haque, J., Reis, L., Weissmann, C., Williams, B.R., 1997. Deficient cytokine signaling in mouse embryo fibroblasts with a targeted deletion in the PKR gene: role of IRF-1 and NF-kappaB. *EMBO J* 16, 406–416. <https://doi.org/10.1093/emboj/16.2.406>
- Kumar, R., Khandelwal, N., Thachamvally, R., Tripathi, B.N., Barua, S., Kashyap, S.K., Maherchandani, S., Kumar, N., 2018. Role of MAPK/MNK1 signaling in virus replication. *Virus Res* 253, 48–61. <https://doi.org/10.1016/j.virusres.2018.05.028>
- Laurent, A.G., Krust, B., Galabru, J., Svab, J., Hovanessian, A.G., 1985. Monoclonal antibodies to an interferon-induced Mr 68,000 protein and their use for the detection of double-stranded RNA-dependent protein kinase in human cells. *Proc Natl Acad Sci U S A* 82, 4341–4345.
- Lavoie, H., Li, J.J., Thevakumaran, N., Therrien, M., Sicheri, F., 2014. Dimerization-induced allostery in protein kinase regulation. *Trends in Biochemical Sciences* 39, 475–486. <https://doi.org/10.1016/j.tibs.2014.08.004>
- Lee, E.-S., Yoon, C.-H., Kim, Y.-S., Bae, Y.-S., 2007. The double-strand RNA-dependent protein kinase PKR plays a significant role in a sustained ER stress-induced apoptosis. *FEBS Letters* 581, 4325–4332. <https://doi.org/10.1016/j.febslet.2007.08.001>
- Lee, J.H., Park, E.J., Kim, O.S., Kim, H.Y., Joe, E.-H., Jou, I., 2005. Double-stranded RNA-activated protein kinase is required for the LPS-induced activation of STAT1 inflammatory signaling in rat brain glial cells. *Glia* 50, 66–79. <https://doi.org/10.1002/glia.20156>
- Lee, S.B., Esteban, M., 1994. The interferon-induced double-stranded RNA-activated protein kinase induces apoptosis. *Virology* 199, 491–496. <https://doi.org/10.1006/viro.1994.1151>
- Lee, T.G., Tang, N., Thompson, S., Miller, J., Katze, M.G., 1994. The 58,000-dalton cellular inhibitor of the interferon-induced double-stranded RNA-activated protein kinase (PKR) is a member of the tetratricopeptide repeat family of proteins. *Mol Cell Biol* 14, 2331–2342. <https://doi.org/10.1128/mcb.14.4.2331-2342.1994>
- Lemaire, P.A., Anderson, E., Lary, J., Cole, J.L., 2008. Mechanism of PKR Activation by dsRNA. *J Mol Biol* 381, 351–360. <https://doi.org/10.1016/j.jmb.2008.05.056>
- Lemaire, P.A., Lary, J., Cole, J.L., 2005. Mechanism of PKR activation: dimerization and kinase activation in the absence of double-stranded RNA. *J Mol Biol* 345, 81–90. <https://doi.org/10.1016/j.jmb.2004.10.031>
- Letunic, I., Bork, P., 2018. 20 years of the SMART protein domain annotation resource. *Nucleic Acids Res* 46, D493–D496. <https://doi.org/10.1093/nar/gkx922>
- Letunic, I., Khedkar, S., Bork, P., 2021. SMART: recent updates, new developments and status in 2020. *Nucleic Acids Research* 49, D458–D460. <https://doi.org/10.1093/nar/gkaa937>
- Li, S., Peters, G.A., Ding, K., Zhang, X., Qin, J., Sen, G.C., 2006. Molecular basis for PKR activation by PACT or dsRNA. *Proceedings of the National Academy of Sciences* 103, 10005–10010. <https://doi.org/10.1073/pnas.0602317103>

- Liao, Y., Fung, T.S., Huang, M., Fang, S.G., Zhong, Y., Liu, D.X., 2013. Upregulation of CHOP/GADD153 during Coronavirus Infectious Bronchitis Virus Infection Modulates Apoptosis by Restricting Activation of the Extracellular Signal-Regulated Kinase Pathway. *J Virol* 87, 8124–8134. <https://doi.org/10.1128/JVI.00626-13>
- Liu, T., Zhang, L., Joo, D., Sun, S.-C., 2017. NF- $\kappa$ B signaling in inflammation. *Sig Transduct Target Ther* 2, 1–9. <https://doi.org/10.1038/sigtrans.2017.23>
- Liu, T.-K., Zhang, Y.-B., Liu, Y., Sun, F., Gui, J.-F., 2011. Cooperative Roles of Fish Protein Kinase Containing Z-DNA Binding Domains and Double-Stranded RNA-Dependent Protein Kinase in Interferon-Mediated Antiviral Response  $\nu$ . *J Virol* 85, 12769–12780. <https://doi.org/10.1128/JVI.05849-11>
- Liu, Yuanzhi, Wang, M., Cheng, A., Yang, Q., Wu, Y., Jia, R., Liu, M., Zhu, D., Chen, S., Zhang, S., Zhao, X.-X., Huang, J., Mao, S., Ou, X., Gao, Q., Wang, Y., Xu, Z., Chen, Z., Zhu, L., Luo, Q., Liu, Yunya, Yu, Y., Zhang, L., Tian, B., Pan, L., Rehman, M.U., Chen, X., 2020. The role of host eIF2 $\alpha$  in viral infection. *Virology Journal* 17, 112. <https://doi.org/10.1186/s12985-020-01362-6>
- Liu, Z.-Y., Jia, K.-T., Li, C., Weng, S.-P., Guo, C.-J., He, J.-G., 2013. A truncated Danio rerio PKZ isoform functionally interacts with eIF2 $\alpha$  and inhibits protein synthesis. *Gene* 527, 292–300. <https://doi.org/10.1016/j.gene.2013.05.043>
- Mayo, C.B., Erlandsen, H., Mouser, D.J., Feinstein, A.G., Robinson, V.L., May, E.R., Cole, J.L., 2019. Structural basis of protein kinase R autophosphorylation. *Biochemistry* 58, 2967–2977. <https://doi.org/10.1021/acs.biochem.9b00161>
- McAllister, C.S., Samuel, C.E., 2009. The RNA-activated Protein Kinase Enhances the Induction of Interferon- $\beta$  and Apoptosis Mediated by Cytoplasmic RNA Sensors. *J Biol Chem* 284, 1644–1651. <https://doi.org/10.1074/jbc.M807888200>
- McAllister, C.S., Toth, A.M., Zhang, P., Devaux, P., Cattaneo, R., Samuel, C.E., 2010. Mechanisms of protein kinase PKR-mediated amplification of beta interferon induction by C protein-deficient measles virus. *J Virol* 84, 380–386. <https://doi.org/10.1128/JVI.02630-08>
- McBeath, A.J.A., Collet, B., Paley, R., Duraffour, S., Aspehaug, V., Biering, E., Secombes, C.J., Snow, M., 2006. Identification of an interferon antagonist protein encoded by segment 7 of infectious salmon anaemia virus. *Virus Res* 115, 176–184. <https://doi.org/10.1016/j.virusres.2005.08.005>
- Meurs, E., Chong, K., Galabru, J., Thomas, N.S., Kerr, I.M., Williams, B.R., Hovanessian, A.G., 1990. Molecular cloning and characterization of the human double-stranded RNA-activated protein kinase induced by interferon. *Cell* 62, 379–390. [https://doi.org/10.1016/0092-8674\(90\)90374-n](https://doi.org/10.1016/0092-8674(90)90374-n)
- Miller, C.L., 2011. Stress Granules and Virus Replication. *Future Virol* 6, 1329–1338. <https://doi.org/10.2217/fvl.11.108>
- Mohanta, T.K., Sharma, N., Arina, P., Defilippi, P., 2020. Molecular Insights into the MAPK Cascade during Viral Infection: Potential Crosstalk between HCQ and HCQ Analogues. *BioMed Research International* 2020, e8827752. <https://doi.org/10.1155/2020/8827752>
- Mori, K., 2022. Evolutionary Aspects of the Unfolded Protein Response. *Cold Spring Harb Perspect Biol* 14, a041262. <https://doi.org/10.1101/cshperspect.a041262>
- Morrison, D.K., 2012. MAP Kinase Pathways. *Cold Spring Harb Perspect Biol* 4, a011254. <https://doi.org/10.1101/cshperspect.a011254>
- Murphy, D., Dancis, B., Brown, J.R., 2008. The evolution of core proteins involved in microRNA biogenesis. *BMC Evol Biol* 8, 92. <https://doi.org/10.1186/1471-2148-8-92>
- Oeckinghaus, A., Ghosh, S., 2009. The NF- $\kappa$ B Family of Transcription Factors and Its Regulation. *Cold Spring Harb Perspect Biol* 1, a000034. <https://doi.org/10.1101/cshperspect.a000034>
- Olsen, C.M., Markussen, T., Thiede, B., Rimstad, E., 2016. Infectious Salmon Anaemia Virus (ISAV) RNA Binding Protein Encoded by Segment 8 ORF2 and Its Interaction with ISAV and Intracellular Proteins. *Viruses* 8, 52. <https://doi.org/10.3390/v8020052>
- Onomoto, K., Jogi, M., Yoo, J.-S., Narita, R., Morimoto, S., Takemura, A., Sambhara, S., Kawaguchi, A., Osari, S., Nagata, K., Matsumiya, T., Namiki, H., Yoneyama, M., Fujita, T., 2012. Critical role of an antiviral stress granule containing RIG-I and PKR in viral detection and innate immunity. *PLoS One* 7, e43031. <https://doi.org/10.1371/journal.pone.0043031>
- Ou, M.-C., Chen, Y.-M., Jeng, M.-F., Chu, C.-J., Yang, H.-L., Chen, T.-Y., 2007. Identification of critical residues in nervous necrosis virus B2 for dsRNA-binding and RNAi-inhibiting activity through by bioinformatic analysis and mutagenesis. *Biochem Biophys Res Commun* 361, 634–640. <https://doi.org/10.1016/j.bbrc.2007.07.075>
- Pakos-Zebrucka, K., Koryga, I., Mnich, K., Ljujic, M., Samali, A., Gorman, A.M., 2016. The integrated stress response. *EMBO Rep* 17, 1374–1395. <https://doi.org/10.15252/embr.201642195>
- Palam, L.R., Baird, T.D., Wek, R.C., 2011. Phosphorylation of eIF2 Facilitates Ribosomal Bypass of an Inhibitory Upstream ORF to Enhance CHOP Translation. *J Biol Chem* 286, 10939–10949. <https://doi.org/10.1074/jbc.M110.216093>
- Patel, C.V., Handy, I., Goldsmith, T., Patel, R.C., 2000. PACT, a Stress-modulated Cellular Activator of Interferon-induced Double-stranded RNA-activated Protein Kinase, PKR \*. *Journal of Biological Chemistry* 275, 37993–37998. <https://doi.org/10.1074/jbc.M004762200>
- Patel, R.C., Sen, G.C., 1998. PACT, a protein activator of the interferon-induced protein kinase, PKR. *EMBO J* 17, 4379–4390. <https://doi.org/10.1093/emboj/17.15.4379>
- Peters, G.A., Hartmann, R., Qin, J., Sen, G.C., 2001. Modular Structure of PACT: Distinct Domains for Binding and Activating PKR. *Mol Cell Biol* 21, 1908–1920. <https://doi.org/10.1128/MCB.21.6.1908-1920.2001>
- Pfaller, C.K., Li, Z., George, C.X., Samuel, C.E., 2011. Protein Kinase PKR and RNA Adenosine Deaminase ADAR1: New Roles for Old Players as Modulators of the Interferon Response. *Curr Opin Immunol* 23, 573–582. <https://doi.org/10.1016/j.coi.2011.08.009>
- Pflugheber, J., Fredericksen, B., Sumpter, R., Wang, C., Ware, F., Sodora, D.L., Gale, M., 2002. Regulation of PKR and IRF-1 during hepatitis C virus RNA replication. *Proc Natl Acad Sci U S A* 99, 4650–4655. <https://doi.org/10.1073/pnas.062055699>
- Pham, A.M., Santa Maria, F.G., Lahiri, T., Friedman, E., Marié, I.J., Levy, D.E., 2016. PKR Transduces MDA5-Dependent Signals for Type I IFN Induction. *PLoS Pathog* 12, e1005489. <https://doi.org/10.1371/journal.ppat.1005489>
- Pindel, A., Sadler, A., 2011. The Role of Protein Kinase R in the Interferon Response. *Journal of Interferon & Cytokine Research* 31, 59–70. <https://doi.org/10.1089/jir.2010.0099>
- Protter, D.S.W., Parker, R., 2016. Principles and Properties of Stress granules. *Trends Cell Biol* 26, 668–679. <https://doi.org/10.1016/j.tcb.2016.05.004>

- Puthalakath, H., O'Reilly, L.A., Gunn, P., Lee, L., Kelly, P.N., Huntington, N.D., Hughes, P.D., Michalak, E.M., McKimm-Breschkin, J., Motoyama, N., Gotoh, T., Akira, S., Bouillet, P., Strasser, A., 2007. ER stress triggers apoptosis by activating BH3-only protein Bim. *Cell* 129, 1337–1349. <https://doi.org/10.1016/j.cell.2007.04.027>
- Ramrani, B., Powell, S., Shetty, A.G., Manivannan, P., Hibbard, B.R., Leaman, D.W., Malathi, K., 2023. Viral Hemorrhagic Septicemia Virus Activates Integrated Stress Response Pathway and Induces Stress Granules to Regulate Virus Replication. *Viruses* 15, 466. <https://doi.org/10.3390/v15020466>
- Reineke, L.C., Lloyd, R.E., 2015. The stress granule protein G3BP1 recruits protein kinase R to promote multiple innate immune antiviral responses. *J Virol* 89, 2575–2589. <https://doi.org/10.1128/JVI.02791-14>
- Rivas, C., Aaronson, S.A., Munoz-Fontela, C., 2010. Dual Role of p53 in Innate Antiviral Immunity. *Viruses* 2, 298–313. <https://doi.org/10.3390/v2010298>
- Roberts, W.K., Hovanessian, A., Brown, R.E., Clemens, M.J., Kerr, I.M., 1976. Interferon-mediated protein kinase and low-molecular-weight inhibitor of protein synthesis. *Nature* 264, 477–480. <https://doi.org/10.1038/264477a0>
- Rothenburg, S., Chinchar, V.G., Dever, T.E., 2011. Characterization of a ranavirus inhibitor of the antiviral protein kinase PKR. *BMC Microbiol* 11, 56. <https://doi.org/10.1186/1471-2180-11-56>
- Rothenburg, S., Deigendesch, N., Dey, M., Dever, T.E., Tazi, L., 2008. Double-stranded RNA-activated protein kinase PKR of fishes and amphibians: Varying the number of double-stranded RNA binding domains and lineage-specific duplications. *BMC Biol* 6, 12. <https://doi.org/10.1186/1741-7007-6-12>
- Rothenburg, S., Deigendesch, N., Dittmar, K., Koch-Nolte, F., Haag, F., Lowenhaupt, K., Rich, A., 2005. A PKR-like eukaryotic initiation factor 2 kinase from Zebrafish contains Z-DNA binding domains instead of dsRNA binding domains. *Proceedings of the National Academy of Sciences* 102, 1602–1607. <https://doi.org/10.1073/pnas.0408714102>
- Saelens, X., Kalai, M., Vandenabeele, P., 2001. Translation inhibition in apoptosis: caspase-dependent PKR activation and eIF2-alpha phosphorylation. *J Biol Chem* 276, 41620–41628. <https://doi.org/10.1074/jbc.M103674200>
- Safa, A.R., 2012. c-FLIP, a Master anti-apoptotic Regulator. *Exp Oncol* 34, 176–184.
- Sakamaki, K., Iwabe, N., Iwata, H., Imai, K., Takagi, C., Chiba, K., Shukunami, C., Tomii, K., Ueno, N., 2015. Conservation of structure and function in vertebrate c-FLIP proteins despite rapid evolutionary change. *Biochem Biophys Rep* 3, 175–189. <https://doi.org/10.1016/j.bbrep.2015.08.005>
- Samuel, C.E., 1979. Mechanism of interferon action: phosphorylation of protein synthesis initiation factor eIF-2 in interferon-treated human cells by a ribosome-associated kinase processing site specificity similar to hemin-regulated rabbit reticulocyte kinase. *Proc Natl Acad Sci U S A* 76, 600–604. <https://doi.org/10.1073/pnas.76.2.600>
- Samuel, C.E., Kuhlen, K.L., George, C.X., Ortega, L.G., Rende-Fournier, R., Tanaka, H., 1997. The PKR protein kinase--an interferon-inducible regulator of cell growth and differentiation. *Int J Hematol* 65, 227–237. [https://doi.org/10.1016/s0925-5710\(96\)00544-0](https://doi.org/10.1016/s0925-5710(96)00544-0)
- Samuel, M.A., Whitby, K., Keller, B.C., Marri, A., Barchet, W., Williams, B.R.G., Silverman, R.H., Gale, M., Diamond, M.S., 2006. PKR and RNase L Contribute to Protection against Lethal West Nile Virus Infection by Controlling Early Viral Spread in the Periphery and Replication in Neurons. *J Virol* 80, 7009–7019. <https://doi.org/10.1128/JVI.00489-06>
- Savill, J., Fadok, V., 2000. Corpse clearance defines the meaning of cell death. *Nature* 407, 784–788. <https://doi.org/10.1038/35037722>
- Schulz, O., Pichlmair, A., Rehwinkel, J., Rogers, N.C., Scheuner, D., Kato, H., Takeuchi, O., Akira, S., Kaufman, R.J., Reis e Sousa, C., 2010. Protein kinase R contributes to immunity against distinct specific viruses by regulating interferon mRNA integrity. *Cell Host Microbe* 7, 354–361. <https://doi.org/10.1016/j.chom.2010.04.007>
- Sen, A., Puijssers, A.J., Dermody, T.S., García-Sastre, A., Greenberg, H.B., 2011. The Early Interferon Response to Rotavirus Is Regulated by PKR and Depends on MAVS/IPS-1, RIG-I, MDA-5, and IRF3. *J Virol* 85, 3717–3732. <https://doi.org/10.1128/JVI.02634-10>
- Shen, S., Niso-Santano, M., Adjemian, S., Takehara, T., Malik, S.A., Minoux, H., Souquere, S., Mariño, G., Lachkar, S., Senovilla, L., Galluzzi, L., Kepp, O., Pierron, G., Maiuri, M.C., Hikita, H., Kroemer, R., Kroemer, G., 2012. Cytoplasmic STAT3 represses autophagy by inhibiting PKR activity. *Mol Cell* 48, 667–680. <https://doi.org/10.1016/j.molcel.2012.09.013>
- Silva, A.M., Whitmore, M., Xu, Z., Jiang, Z., Li, X., Williams, B.R.G., 2004. Protein kinase R (PKR) interacts with and activates mitogen-activated protein kinase kinase 6 (MKK6) in response to double-stranded RNA stimulation. *J Biol Chem* 279, 37670–37676. <https://doi.org/10.1074/jbc.M406554200>
- Sonenberg, N., Hinnebusch, A.G., 2009. Regulation of Translation Initiation in Eukaryotes: Mechanisms and Biological Targets. *Cell* 136, 731–745. <https://doi.org/10.1016/j.cell.2009.01.042>
- Song, L., Wang, H., Wang, T., Lu, L., 2015. Sequestration of RNA by grass carp *Ctenopharyngodon idella* TIA1 is associated with its positive role in facilitating grass carp reovirus infection. *Fish Shellfish Immunol* 46, 442–448. <https://doi.org/10.1016/j.fsi.2015.07.018>
- Sood, R., Porter, A.C., Ma, K., Quilliam, L.A., Wek, R.C., 2000. Pancreatic eukaryotic initiation factor-2alpha kinase (PEK) homologues in humans, *Drosophila melanogaster* and *Caenorhabditis elegans* that mediate translational control in response to endoplasmic reticulum stress. *Biochem J* 346 Pt 2, 281–293.
- Srivastava, S.P., Kumar, K.U., Kaufman, R.J., 1998. Phosphorylation of Eukaryotic Translation Initiation Factor 2 Mediates Apoptosis in Response to Activation of the Double-stranded RNA-dependent Protein Kinase \*. *Journal of Biological Chemistry* 273, 2416–2423. <https://doi.org/10.1074/jbc.273.4.2416>
- Streiff, C., He, B., Morvan, L., Zhang, H., Delrez, N., Fourrier, M., Manfroid, I., Suárez, N.M., Betoulle, S., Davison, A.J., Donohoe, O., Vanderplasschen, A., 2023. Susceptibility and Permissivity of Zebrafish (*Danio rerio*) Larvae to Cypriniviruses. *Viruses* 15, 768. <https://doi.org/10.3390/v15030768>
- Su, J., Zhu, Z., Wang, Y., 2008. Molecular cloning, characterization and expression analysis of the PKZ gene in rare minnow *Gobiocypris rarus*. *Fish Shellfish Immunol* 25, 106–113. <https://doi.org/10.1016/j.fsi.2008.03.006>
- Sudhakar, A., Ramachandran, A., Ghosh, S., Hasnain, S.E., Kaufman, R.J., Ramaiah, K.V.A., 2000. Phosphorylation of Serine 51 in Initiation Factor 2α (eIF2α) Promotes Complex Formation between eIF2α(P) and eIF2B and Causes Inhibition in the Guanine Nucleotide Exchange Activity of eIF2B. *Biochemistry* 39, 12929–12938. <https://doi.org/10.1021/bi0008682>

- Sun, M., Wu, S., Kang, S., Liao, J., Zhang, L., Xu, Z., Chen, H., Xu, L., Zhang, X., Qin, Q., Wei, J., 2022. Critical Roles of G3BP1 in Red-Spotted Grouper Nervous Necrosis Virus-Induced Stress Granule Formation and Viral Replication in Orange-Spotted Grouper (*Epinephelus coioides*). *Front Immunol* 13, 931534. <https://doi.org/10.3389/fimmu.2022.931534>
- Taghavi, N., Samuel, C.E., 2013. RNA-dependent Protein Kinase PKR and the Z-DNA Binding Orthologue PKZ Differ in their Capacity to Mediate Initiation Factor eIF2 $\alpha$ -dependent Inhibition of Protein Synthesis and Virus-induced Stress Granule Formation. *Virology* 443, 48–58. <https://doi.org/10.1016/j.virol.2013.04.020>
- Taghavi, N., Samuel, C.E., 2012. Protein Kinase PKR Catalytic Activity is Required for the PKR-dependent Activation of Mitogen-activated Protein Kinases and Amplification of Interferon Beta Induction following Virus Infection. *Virology* 427, 208–216. <https://doi.org/10.1016/j.virol.2012.01.029>
- Tak, P.P., Firestein, G.S., 2001. NF- $\kappa$ B: a key role in inflammatory diseases. *J Clin Invest* 107, 7–11.
- Thomis, D.C., Samuel, C.E., 1992. Mechanism of interferon action: autoregulation of RNA-dependent P1/eIF-2 alpha protein kinase (PKR) expression in transfected mammalian cells. *Proc Natl Acad Sci U S A* 89, 10837–10841.
- Tomé, A.R., Kuš, K., Correia, S., Paulo, L.M., Zacarias, S., de Rosa, M., Figueiredo, D., Parkhouse, R.M.E., Athanasiadis, A., 2013. Crystal structure of a poxvirus-like zalpha domain from cyprinid herpesvirus 3. *J Virol* 87, 3998–4004. <https://doi.org/10.1128/JVI.03116-12>
- Tsuchiya, Y., Nakabayashi, O., Nakano, H., 2015. FLIP the Switch: Regulation of Apoptosis and Necroptosis by cFLIP. *International Journal of Molecular Sciences* 16, 30321–30341. <https://doi.org/10.3390/ijms161226232>
- VanOudenhove, J., Anderson, E., Kreuger, S., Cole, J.L., 2009. Analysis of PKR structure by small angle scattering. *J Mol Biol* 387, 910–920. <https://doi.org/10.1016/j.jmb.2009.02.019>
- von Roretz, C., Gallouzi, I.-E., 2010. Protein Kinase RNA/FADD/Caspase-8 Pathway Mediates the Proapoptotic Activity of the RNA-binding Protein Human Antigen R (HuR). *J Biol Chem* 285, 16806–16813. <https://doi.org/10.1074/jbc.M109.087320>
- Wang, H., Xu, Q., Xu, X., Hu, Y., Hou, Q., Zhu, Y., Hu, C., 2017. Ctenopharyngodon idella IKK $\beta$  interacts with PKR and I $\kappa$ B $\alpha$ . *Acta Biochim Biophys Sin (Shanghai)* 49, 729–736. <https://doi.org/10.1093/abbs/gmx065>
- Wang, L., Wu, Z., Huang, Q., Huang, K., Qi, G., Wu, C., Mao, H., Xu, X., Wang, H., Hu, C., 2018. Grass carp (*Ctenopharyngodon idella*) STAT3 regulates the eIF2 $\alpha$  phosphorylation through interaction with PKR. *Dev Comp Immunol* 78, 26–34. <https://doi.org/10.1016/j.dci.2017.08.019>
- Wei, J., Zang, S., Li, C., Zhang, X., Gao, P., Qin, Q., 2020. Grouper PKR activation inhibits red-spotted grouper nervous necrosis virus (RGNNV) replication in infected cells. *Developmental & Comparative Immunology* 111, 103744. <https://doi.org/10.1016/j.dci.2020.103744>
- Wong, A.H., Tam, N.W., Yang, Y.L., Cuddihy, A.R., Li, S., Kirchhoff, S., Hauser, H., Decker, T., Koromilas, A.E., 1997. Physical association between STAT1 and the interferon-inducible protein kinase PKR and implications for interferon and double-stranded RNA signaling pathways. *EMBO J* 16, 1291–1304. <https://doi.org/10.1093/emboj/16.6.1291>
- Wong, A.H.-T., Durbin, J.E., Li, S., Dever, T.E., Decker, T., Koromilas, A.E., 2001. Enhanced Antiviral and Antiproliferative Properties of a STAT1 Mutant Unable to Interact with the Protein Kinase PKR\*. *Journal of Biological Chemistry* 276, 13727–13737. <https://doi.org/10.1074/jbc.M011240200>
- Wu, C., Hu, Y., Fan, L., Wang, H., Sun, Z., Deng, S., Liu, Y., Hu, C., 2016. Ctenopharyngodon idella PKZ facilitates cell apoptosis through phosphorylating eIF2 $\alpha$ . *Molecular Immunology* 69, 13–23. <https://doi.org/10.1016/j.molimm.2015.11.006>
- Xia, T., Liao, Y.-Q., Li, L., Sun, L.-Y., Ding, N.-S., Wu, Y.-L., Lu, K.-L., 2022. 4-PBA Attenuates Fat Accumulation in Cultured Spotted Seabass Fed High-Fat-Diet via Regulating Endoplasmic Reticulum Stress. *Metabolites* 12, 1197. <https://doi.org/10.3390/metabo12121197>
- Xu, C., Gamil, A.A.A., Munang'andu, H.M., Evensen, Ø., 2018. Apoptosis Induction by dsRNA-Dependent Protein Kinase R (PKR) in EPC Cells via Caspase 8 and 9 Pathways. *Viruses* 10, 526. <https://doi.org/10.3390/v10100526>
- Xu, X., Li, M., Wu, C., Li, D., Jiang, Z., Liu, C., Cheng, B., Mao, H., Hu, C., 2019. The Fish-Specific Protein Kinase (PKZ) Initiates Innate Immune Responses via IRF3- and ISGF3-Like Mediated Pathways. *Front Immunol* 10, 582. <https://doi.org/10.3389/fimmu.2019.00582>
- Yang, P.-J., Wu, C.-X., Li, W., Fan, L.-H., Lin, G., Hu, C.-Y., 2011. Cloning and functional analysis of PKZ (PKR-like) from grass carp (*Ctenopharyngodon idellus*). *Fish & Shellfish Immunology* 31, 1173–1178. <https://doi.org/10.1016/j.fsi.2011.10.012>
- Yeung, M.C., Liu, J., Lau, A.S., 1996. An essential role for the interferon-inducible, double-stranded RNA-activated protein kinase PKR in the tumor necrosis factor-induced apoptosis in U937 cells. *Proc Natl Acad Sci U S A* 93, 12451–12455.
- Yoo, J.-S., Takahashi, K., Ng, C.S., Ouda, R., Onomoto, K., Yoneyama, M., Lai, J.C., Lattmann, S., Nagamine, Y., Matsui, T., Iwabuchi, K., Kato, H., Fujita, T., 2014. DHX36 Enhances RIG-I Signaling by Facilitating PKR-Mediated Antiviral Stress Granule Formation. *PLoS Pathog* 10, e1004012. <https://doi.org/10.1371/journal.ppat.1004012>
- Yoon, C.-H., Lee, E.-S., Lim, D.-S., Bae, Y.-S., 2009. PKR, a p53 target gene, plays a crucial role in the tumor-suppressor function of p53. *Proc Natl Acad Sci U S A* 106, 7852–7857. <https://doi.org/10.1073/pnas.0812148106>
- Yuan, X., Wu, H., Gao, J., Geng, X., Xie, M., Song, R., Zheng, J., Wu, Y., Ou, D., 2023. Acute deltamethrin exposure induces oxidative stress, triggers endoplasmic reticulum stress, and impairs hypoxic resistance of crucian carp. *Comparative Biochemistry and Physiology Part C: Toxicology & Pharmacology* 263, 109508. <https://doi.org/10.1016/j.cbpc.2022.109508>
- Zamanian-Daryoush, M., Mogensen, T.H., DiDonato, J.A., Williams, B.R.G., 2000. NF- $\kappa$ B Activation by Double-Stranded-RNA-Activated Protein Kinase (PKR) Is Mediated through NF- $\kappa$ B-Inducing Kinase and I $\kappa$ B Kinase. *Mol Cell Biol* 20, 1278–1290.
- Zenke, K., Nam, Y.K., Kim, K.H., 2010. Molecular cloning and expression analysis of double-stranded RNA-dependent protein kinase (PKR) in rock bream (*Oplegnathus fasciatus*). *Veterinary Immunology and Immunopathology* 133, 290–295. <https://doi.org/10.1016/j.vetimm.2009.08.009>
- Zhang, P., Langland, J.O., Jacobs, B.L., Samuel, C.E., 2009. Protein kinase PKR-dependent activation of mitogen-activated protein kinases occurs through mitochondrial adapter IPS-1 and is antagonized by vaccinia virus E3L. *J Virol* 83, 5718–5725. <https://doi.org/10.1128/JVI.00224-09>
- Zhang, P., Samuel, C.E., 2008. Induction of Protein Kinase PKR-dependent Activation of Interferon Regulatory Factor 3 by Vaccinia Virus Occurs through Adapter IPS-1 Signaling. *J Biol Chem* 283, 34580–34587. <https://doi.org/10.1074/jbc.M807029200>

- Zhang, Peifen, Li, Y., Xia, J., He, J., Pu, J., Xie, J., Wu, S., Feng, L., Huang, X., Zhang, Ping, 2014. IPS-1 plays an essential role in dsRNA-induced stress granule formation by interacting with PKR and promoting its activation. *J Cell Sci* 127, 2471–2482. <https://doi.org/10.1242/jcs.139626>
- Zhu, R., Zhang, Y.-B., Zhang, Q.-Y., Gui, J.-F., 2008. Functional Domains and the Antiviral Effect of the Double-Stranded RNA-Dependent Protein Kinase PKR from *Paralichthys olivaceus*. *J Virol* 82, 6889–6901. <https://doi.org/10.1128/JVI.02385-07>
- Zhu, Y., Liu, L., Zhang, Chuchu, Zhang, Chao, Han, T., Duan, R., Jin, Y., Guo, H., She, K., Xiao, Y., Goto, A., Cai, Q., Ji, S., 2022. Endoplasmic reticulum-associated protein degradation contributes to Toll innate immune defense in *Drosophila melanogaster*. *Front Immunol* 13, 1099637. <https://doi.org/10.3389/fimmu.2022.1099637>
- Zuo, W., Wakimoto, M., Kozaiwa, N., Shirasaka, Y., Oh, S.-W., Fujiwara, S., Miyachi, H., Kogure, A., Kato, H., Fujita, T., 2022. PKR and TLR3 trigger distinct signals that coordinate the induction of antiviral apoptosis. *Cell Death Dis* 13, 1–15. <https://doi.org/10.1038/s41419-022-05101-3>

## Figures

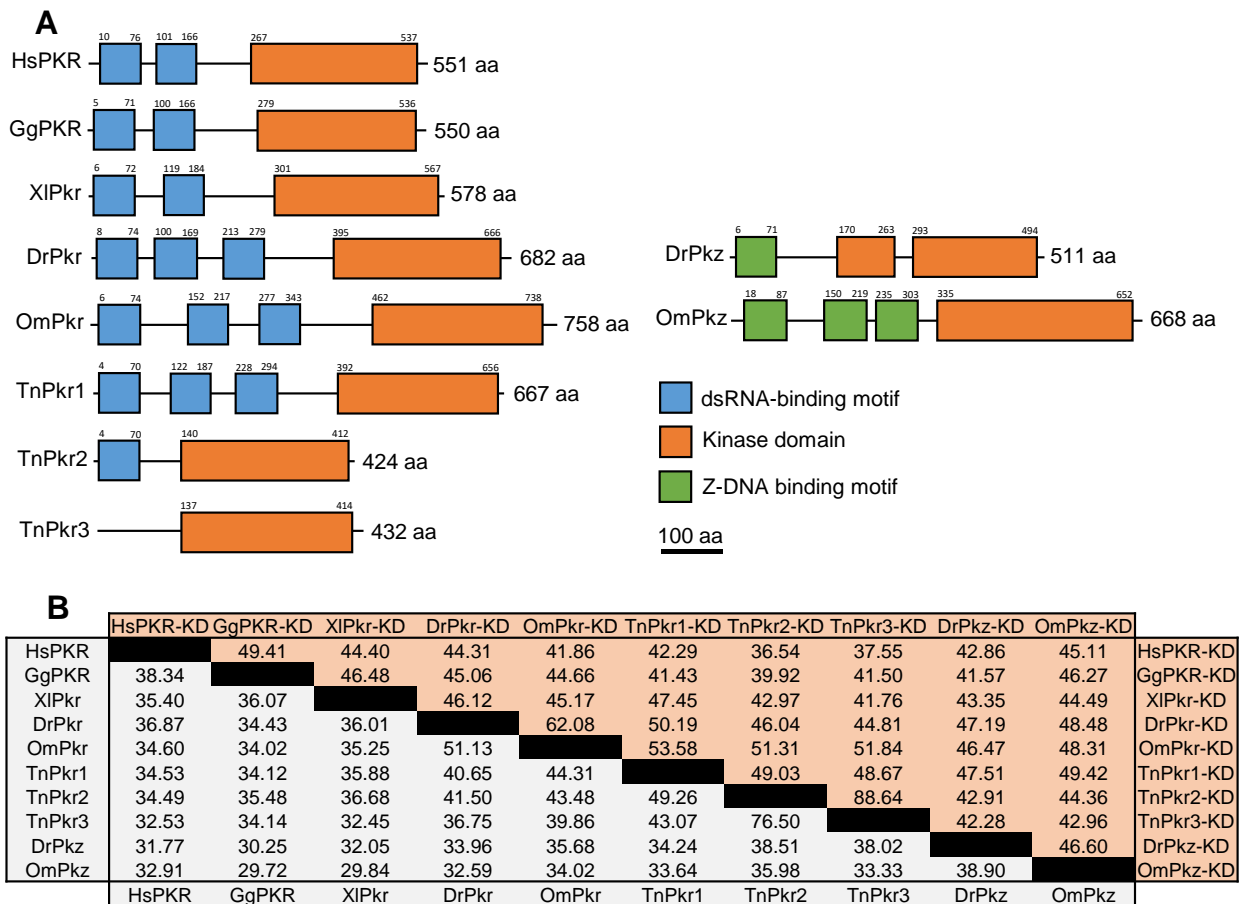


**Figure 1: Mammalian and fish PKR and fish Pkz proteins.**

(A) Schematic representation of domain organisation of PKR and Pkz proteins from *Homo sapiens* (Hs) (NP\_001129123.1/5610), *Gallus gallus* (Gg) (NP\_989818.3/395147), *Xenopus laevis* (Xl) (NP\_001091256.1/100037060), *Danio rerio* (Dr) (DrPKR: NP\_001107942.1/100001092; DrPz: NP\_001035466.1/503703), *Onchorhynchus mykiss* (Om) (OmPKR: NP\_001139363.1/100271898; OmPz: XP\_036801832.1/110491201) and *Tetraodon nigroviridis* (Tn) (TnPKR1: CAM07147.1; TnPKR2: CAM07148.1; TnPKR3: CAM07149.1). The localisation of predicted domains and motifs was obtained using SMART (Simple Modular Architecture Research Tool) (Letunic et al., 2021; Letunic and Bork, 2018) (B) Percent identity matrix of full length Pkr and Pkz proteins (in grey) and their respective kinase domains (KD) (in orange).

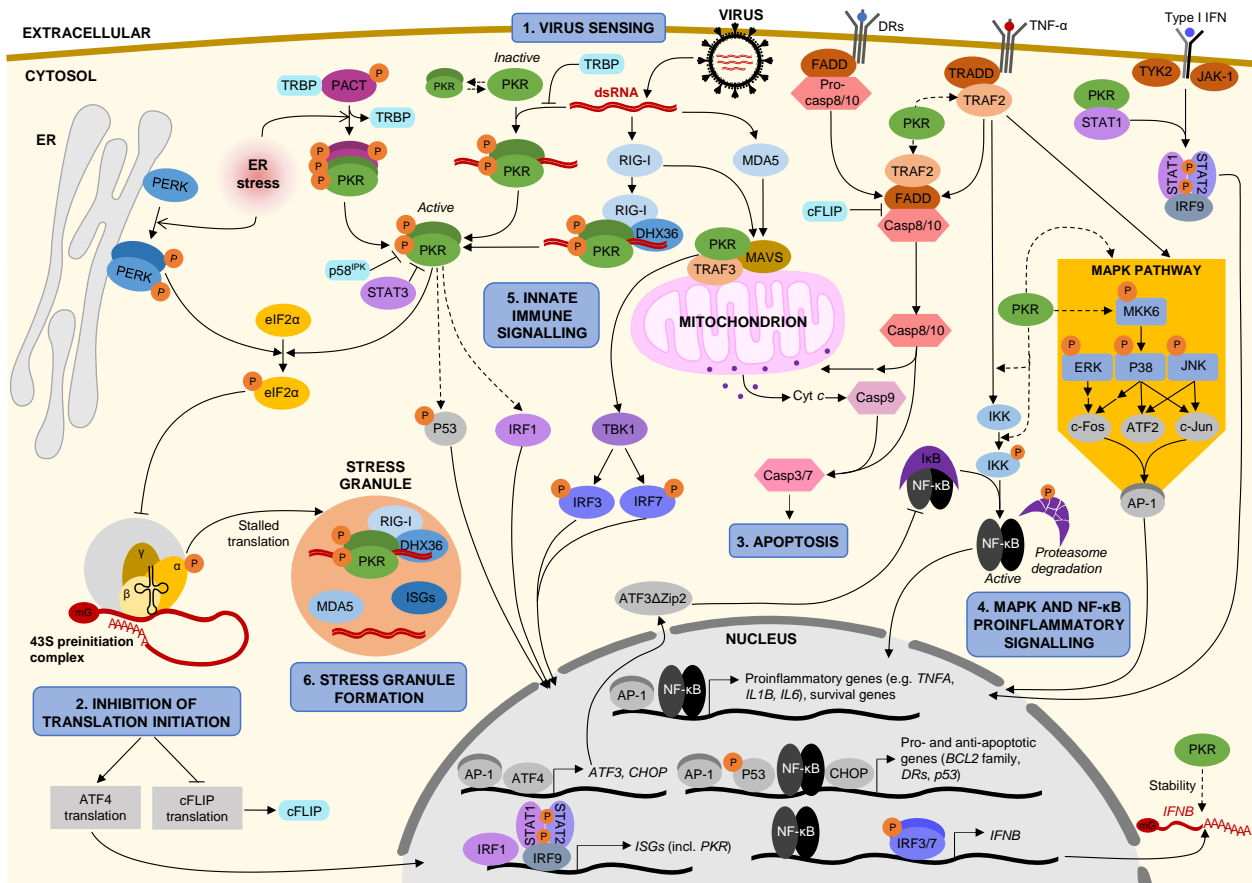


**Figure 2: Overview of mammalian PKR mechanisms of action during viral infection.**

**(1) Virus sensing.** PKR can be activated either by virus-derived double-stranded RNA (dsRNA) or protein activator of PKR (PACT) in response to endoplasmic reticulum (ER) stress (misfolded proteins), which can be caused by virus infection. DEAH-box helicase 36(DHX36):RIG-I complex also facilitates PKR activation upon dsRNA exposure. PKR activation is modulated by cellular inhibitors p58<sup>IPK</sup> (58-kDa inhibitor of protein kinase) which inhibits PKR autophosphorylation, and transactivation response RNA-binding protein (TRBP), which sequesters dsRNA and PACT.

**(2) Inhibition of translation initiation.** Both PKR-like ER kinase (PERK) and activated PKR can phosphorylate eukaryotic translation initiation factor 2  $\alpha$  (eIF2 $\alpha$ ). This results in the inhibition of translation initiation and a global shutdown of protein synthesis.

**(3) Activation of apoptosis.** PKR also triggers apoptosis via several pathways: inhibition of protein synthesis leads to (1) upregulation of transcription factors such as activating transcription factor 4 (ATF4), ATF3 and C/EBP homologous protein (CHOP) and activation of p53, resulting in the induction of proapoptotic genes, including B-cell lymphoma 2 (*BCL2*) family and death receptors (*DRs*); (2) downregulation of antiapoptotic regulators, such as cellular FADD-like interleukin (IL)-1 $\beta$ -converting enzyme inhibitory protein (cFLIP). Apoptosis is triggered by a signalling cascade involving FAS-associated protein with death domain (FADD), tumor necrosis factor (TNF) receptor type 1-associated death domain (TRADD), TNF receptor-associated factor 2 (TRAF2), resulting in activation of the caspase (casp) cascade, involving upstream initiator casp8, 10 and 9 and downstream executioner casp3 and 7.

**(4) MAPK and NF- $\kappa$ B proinflammatory signalling.** PKR stimulates mitogen-activated protein kinases (MAPK) mediated proinflammatory signalling pathway involving MAPK kinase 6 (MKK6), extracellular signal-regulated kinases (ERK), c-Jun N-terminal kinases (JNK), p38 and their downstream targets such as c-Fos, c-Jun, which form together activator protein 1 (AP-1) and ATF2. PKR also activates the nuclear factor- $\kappa$ B (NF- $\kappa$ B) signalling pathway by acting upstream of inhibitor of NF- $\kappa$ B (I $\kappa$ B) kinase (IKK) and/or by recruiting signal transducers such as members of the TRAF family. Both pathways converge on the induction of proinflammatory genes, such as *TNFA*, *IL6* and *IL1B*.

**(5) Innate immune signalling.** PKR interacts with cytosolic nucleic acid sensors retinoic acid-inducible gene I (RIG-I) and melanoma differentiation-associated protein 5 (MDA5). This enhances downstream signaling pathways involving mitochondrial antiviral signalling protein (MAVS), TRAF3, TANK-binding kinase 1 (TBK1), interferon regulatory factor 1 (IRF1), IRF3, IRF7, resulting in induction of interferon (IFN). Subsequent activation of the JAK/STAT cascade occurs involving janus kinase 1 (JAK1), tyrosine kinase 2 (TYK2), signal transducer and activator of transcription 1 (STAT1), STAT2 and IRF9. This eventually leads to the induction of IFN-stimulated genes (ISGs). PKR is also involved in stabilising of *IFNB* transcripts via an unknown mechanism.

**(6) Formation of stress granules.** Stalled protein synthesis promotes the formation of stress granules, which function as a platform for dsRNA sensing and for potentiating proinflammatory and IFN responses. Solid arrows represent direct interactions or actions; while dashed arrows indicate speculated interactions or unknown mechanisms.